



AVERTISSEMENT

Ce document est le fruit d'un long travail approuvé par le jury de soutenance et mis à disposition de l'ensemble de la communauté universitaire élargie.

Il est soumis à la propriété intellectuelle de l'auteur. Ceci implique une obligation de citation et de référencement lors de l'utilisation de ce document.

D'autre part, toute contrefaçon, plagiat, reproduction illicite encourt une poursuite pénale.

Contact : ddoc-theses-contact@univ-lorraine.fr

LIENS

Code de la Propriété Intellectuelle. articles L 122. 4

Code de la Propriété Intellectuelle. articles L 335.2- L 335.10

http://www.cfcopies.com/V2/leg/leg_droi.php

<http://www.culture.gouv.fr/culture/infos-pratiques/droits/protection.htm>



Nancy-Université
Université
Henri Poincaré



Ecole Doctorale RP2E
Ressources, Produits, Procédés et Environnement

Thèse
présentée pour l'obtention du titre de
Docteur de l'Université Henri Poincaré
en Géosciences

par
Alexander SHURILOV

Métallogénèse de l'uranium dans la région de Ladoga
(Karélie, Russie)

Soutenance publique le 28 Avril 2008

Membres du jury :

Président : **Maurice PAGEL**, *Professeur, Université de Paris Sud*

Rapporteurs : **Tapani RÄMÖ**, *Professeur, Université d'Helsinki*
Maurice PAGEL, *Professeur, Université de Paris Sud*

Directeur de thèse : **Michel CUNEY**, *Directeur de Recherche CNRS, UMR G2R-CREGU, Nancy*

Codirecteur de thèse : **Vladimir KUSHNERENKO**, *Chef Geologue, l'entreprise RGEC*
Marc LESPINASSE, *Professeur, Université Henri Poincaré Nancy*

Examineur : **Claude CAILLAT**, *Ingénieur AREVA*

REMERCIEMENTS

Ce travail a été mené dans le cadre d'une collaboration entre AREVA, financeur de cette thèse, la société CREGU et l'Université Henri Poincaré de Nancy et l'Université de Saint Péterbourg. Le travail a été réalisé en partie à l'Université de Nancy et en partie à l'Université de Saint Péterbourg. Je tiens donc à adresser ma reconnaissance à **Claude Caillat** (AREVA NC) pour sa bienveillance et son intérêt envers Russie et **Michel Cathelineau** pour son accueil dans ce laboratoire.

Je remercie tout particulièrement **Michel Cuney**, mon directeur de thèse, qui a toujours répondu à mes interrogations et m'a fait bénéficier de ses expériences et compétences. Il a su me faire partager sa connaissance de la métallogénie de l'uranium, de la géochimie des granites et la grammaire français et anglaise. Merci beaucoup pour la direction de cette thèse !

Je remercie beaucoup **Marc Lespinasse**, mon codirecteur de thèse, pour sa bienveillance immuable et l'aide avec tous les difficultés administratives.

Je remercie également **Yury Stepanovich Polekhovsky** (Université d'Etat de Saint-Pétersbourg), mon codirecteur de thèse, qui a su m'intéresser à la minéralogie de l'uranium et me faire partager ses connaissances profondes.

Un grand merci à **Vladimir Konstantinovich Kushnereko** (de l'entreprise géologique Nevskgeologia), un autre codirecteur de ma thèse, pour son accueil dans les archives de Nevskgeologia et ses conseils prévisionnels.

Je remercie tout particulièrement **Philippe Kister** (AREVA NC) pour son aide très diverse : lors des missions de terrain, les interprétations des données isotopiques, la correction de ma thèse en premier lieu pour son amitié constante !

Mes remerciements vont également aux rapporteuses qui me font l'honneur d'examiner ce travail : **Maurice Pagel** (Université de Paris Sud), **Tapani Rämö** (Université d'Helsinki).

Je remercie tous les G2Riens et Cregusiens (actuels et anciens) : **Pierre Schumacher** (spécialement pour le français intensif), **Christine Leonard**, **Marc Brouand**, **Roland Mairet**, **Patrick Lagrange**, **Marie Odile**, **Laurence Moine** et **Alam Ibrahim** (bon courage en la

patrie !).

Je remercie également **Bernard Poty** pour son introduction générale dans la culture française.

Mes remerciements vont également au personnel d'AREVA NC : **Joseph Roux** pour son introduction aux méthodes géophysiques, **Benoit Magrina** pour sa connaissance des Alpes (bon courage !), **Gwenelle Potet** pour son introduction aux projets SIG et sa sympathie.

Je remercie le Service commun d'analyse de l'UHP : **Frédéric Diot**, **Alain Kholer** et **Jacqueline Joffrin** pour leur aide et leur disponibilité quant aux analyses à la microsonde électronique et au MEB.

Je remercie également **Denis Mangin** et **Claire Rollion-Bard** (CRPG) pour leur encadrement à la sonde ionique.

Mes remerciements vont **Jean-Jacques Royer** et **Christian Le Carlier de Veslud** pour leur aide avec les modèles GOCAD.

Mes remerciements vont également les géologues finnois **Olli Äikäs** et **Peter Sorjonen-Ward** (GTK) et **Laura Lauri** (AREVA Finlande) pour l'introduction à la géologie de la Finlande et leur grande bienveillance.

Je remercie tous de Nevskgeologia qui m'ont accompagné pendant les travaux: **Boris Shustov**, **Viktor Belyaev**, **Alexander Apanasevich**, **Natalya Roman**, **Alexander Sokolov**, **Yury Petrov**, **Viktor Kudrinski**, **Yury Vorobiev** et les autres.

Je remercie **Anna Saltykova**, **Vitalii Mikhailov**, **Elena Afanasieva**, **Alexander Larionov** (tout – VSEGEI), **Irina Tarasova**, **Alexei Borozdin**, **Irina Bugrova**, **Igor Buldakov** (tout – SPbGU), **Vyacheslav Golubev** et **Alexei Aleshin** (IGEM), **Vladimir Bogachev** et **Olga Tomilina** (Mineral) pour leur aide et sympathies.

Enfin, je remercie du fond du cœur mes parents et ma famille.

Merci beaucoup !

RÉSUMÉ

La région de Ladoga est une des plus intéressantes du bouclier Baltique pour la métallogénèse de l'uranium. Des minéralisations uranifères sont connues dans tous les niveaux stratigraphiques de la région. Les principaux gisements sont : celui de Karku associé à une discordance localisé dans les grès Mésoprotérozoïques (Riphéen) du bassin Pasha Ladoga, ceux de type grès et de type schistes noirs dans les dépôts de plateforme paléozoïques inférieurs, les minéralisations localisées dans les granites anatectique et dans des roches carbonatées riches en phosphore métamorphosées appartenant au socle cristallin Archéen-Paléoprotérozoïque de la zone de Raahe-Ladoga; des minéralisations de type filonien dans le socle et les formations riphéennes. Une croissance graduelle des teneurs en U des formations géologiques et des ressources minières en U est mise en évidence pendant de l'évolution géologique depuis l'Archéen jusqu'au Paléozoïque. Trois stades principaux de la métallogénèse de l'uranium ont été déterminés : le Svécofennien (1.97-1.77 Ga), le Mésoprotérozoïque (1.6-1.2 Ga) et de l'Ordovicien au Devonien (0.45-0.38 Ga). Il est montré que les gisements de type discordance, grès et filonien sont les plus prospectifs pour de découverte de gisements d'U de dimension économique dans la région de Ladoga. La plupart d'entre eux sont localisés le long de la zone Raahe-Ladoga.

Mots clé: Uranium, Ladoga, Discordance, Gisements, Métallogénèse.

ABSTRACT

The Ladoga region is one of the most interesting areas of the Baltic Shield with respect to U metallogenesis. U mineralization occurs at all stratigraphic levels of the geological succession in the region. The main U occurrences are: the unconformity-related Karku deposit in the Mesoproterozoic (Riphean) sandstones of the Pasha Ladoga basin, those of sandstone and black-shale type in the Lower Paleozoic platform sediments, the mineralization located in anatectic granites and metamorphosed phosphorites in the Archaean-Palaeoproterozoic crystalline basement of the Raahe-Ladoga zone, vein type U mineralization hosted in the basement and in the Riphean. U content in the geological formations and U ore resources gradually increase during the geological evolution of the Ladoga region from Archaean to Paleozoic. Three main stages of U metallogenesis have been identified: Svecofennian (1.97-1.77 Ga), Mesoproterozoic (1.6-1.2 Ga) and Ordovician-Devonian (0.45-0.38 Ga). Unconformity-related, sandstone and vein types represent the most prospective ones for the discovery of economic-grade U deposits in the Ladoga region. Most of the promising areas are located along the Raahe-Ladoga zone.

Key words: Uranium, Ladoga, Unconformity, Deposits, Metallogenesis.

CONTENTS

REMERCIEMENTS.....	3
RESUME AND ABSTRACT.....	7
CONTENTS.....	9
LIST OF FIGURES.....	15
LIST OF TABLES.....	27
<u>GENERAL INTRODUCTION</u>	31
1. Object and aim of the study.....	33
2. Structure of the manuscript.....	35
3. Terminological aspects.....	35
4. Methodology.....	39
<u>PART 1. REGIONAL GEOLOGICAL REVIEW</u>	43
1. Geological structure of the Ladoga region.....	45
1.1. The Karelian domain.....	46
1.2. The Raahe-Ladoga domain.....	48
1.2.1. Tectonic and metamorphic structure.....	48
1.2.2. Lithology.....	52
1.3. The Svecofennian domain.....	55
1.4. The Riphean basins.....	59
1.5. The platform cover.....	62
1.6. Quaternary.....	63
1.7. Magmatism.....	63
1.8. Fault zones.....	87
1.9. Non-radioactive metallogeny.....	91
2. Evolution of geological structure and uranium abundance of the Ladoga region.....	93
Appendix to Part 1.....	105
<u>PART 2. URANIUM OCCURRENCES OF THE LADOGA REGION</u>	123
Introduction.....	125
Chapter 1. Basement-hosted uranium occurrences.....	127

Introduction.....	129
Paragraph 1.1. Granite-hosted uranium occurrences.....	131
Introduction.....	131
1. U-Th-REE occurrences in anatectic granites.....	131
1.1. Uranium mineralization in the pegmatoids.....	133
1.2. Uranium mineralization in the migmatites.....	138
1.3. Other uranium occurrences in the anatexites.....	151
1.4. Generalized geological parameters characterizing the anatexite-hosting uranium mineralization of the Northern Ladoga area.....	151
1.5. Remarks to genesis of the anatexite-hosted uranium occurrences of the Northern Ladoga area.....	152
1. U-Th occurrences hosted by intrusive granites	159
2.1. U-Th-REE-rare metal late-Svecofennian pegmatites of the Impilakhti-Pitkjaranta area.....	160
2.2. Others granite-hosted uranium occurrences.....	161
Conclusion.....	163
Paragraph 1.2. Th-U anomalies in the Jatulian quartzites.....	165
Introduction.....	165
1. Geological structure of the Kuhilaslampi area.....	165
2. Th-U mineralization in the Jatulian quartzites.....	168
Conclusion.....	171
Paragraph 1.3. U-P occurrences in the Ludicovian carbonate rocks.....	173
Introduction.....	173
1. U-P occurrences of the Northern Ladoga area.....	173
1.1. The Mramornaya Gora ore-showing.....	173
1.2. The Ruskeala group of uranium ore-showings.....	195
1.3. The Impilakhti group of uranium ore-showings.....	199
2. Generalized characteristic features of the U-P occurrences.....	202
3. Remarks to origin of the U-P occurrences.....	204
Conclusion.....	206
Paragraph 1.4. Vein-type uranium occurrences.....	207
Introduction.....	207

1. Uranium as a principal ore mineralization in quartz-carbonate veins.....	207
<i>1.1. The Varalakhti uranium ore-showing.....</i>	207
<i>1.2. Vein-type uranium mineralization of the Latvasurje area.....</i>	216
<i>1.3. Vein-type uranium and thorium mineralization of the Kuhilaslampi area.....</i>	222
2. Uranium as a by-product of complex-ore occurrences.....	229
<i>2.1. The Jalonvara complex ore deposit.....</i>	229
<i>2.2. The Prolonvara complex ore-showing.....</i>	231
<i>2.3. The Faddein-Kelya complex ore deposit.....</i>	231
<i>2.4. Uranium ore-showings of the Pitkjaranta-Kitelya ore knot.....</i>	232
3. Late vein-type uranium mineralization in other type uranium occurrences.....	233
4. Generalized geological characteristics of vein-type uranium mineralization of the Northern Ladoga area.....	234
Conclusion.....	237
Conclusion to Chapter 1.....	239
Appendix to Chapter 1.....	245
Chapter 2. Uranium occurrences hosted by the Riphean formations.....	255
Introduction.....	257
1. The Salmi depression.....	257
<i>1.1. Geological environment.....</i>	257
<i>1.2. Bedrock petrology.....</i>	258
<i>1.3. Metallogenic characteristic of the bedrocks.....</i>	271
2. The Karku uranium deposit.....	272
<i>2.1. Geological environment.....</i>	272
<i>2.2. Characteristics of the deposit.....</i>	273
<i>2.3. Host rocks alterations.....</i>	278
3. Other uranium occurrences in the Riphean formations of the Salmi depression.....	286
4. Characteristics of the radioactive mineralization.....	288

4.1. <i>Texture types of the mineralization</i>	288
4.2. <i>Radioactive mineragraphy</i>	290
4.3. <i>Isotopic study of the uranium mineralization of the Salmi depression uranium occurrences</i>	303
4.4. <i>Succession of uranium metallogenesis in the Karku deposit area</i>	310
4.5. <i>Particularities of the epigenetic uranium mineralization in the Salmi depression</i>	313
5. Factors controlling uranium mineralization in the Salmi depression.....	314
6. Typology of the Karku deposit.....	317
6.1. <i>Comments on origin of the Karku deposit and unconformity-type deposits of the Athabasca basin</i>	318
6.2. <i>Generalized comparison of the Karku deposit with unconformity-related deposits of the Athabasca basin</i>	322
Conclusion.....	324
Appendix to Chapter 2.....	327
Chapter 3. Uranium occurrences hosted by Vendian-Palaeozoic platform sediments	339
Introduction.....	341
3.1. Uranium occurrences in the Upper Vendian sandstones.....	342
3.2. Uranium occurrences in the Lower Ordovician formations.....	347
3.2.1. <i>P-U anomalies in the Lower Ordovician Obolus sandstones</i> ...	347
3.2.2. <i>V-Mo-Pd-U occurrences in the Lower Ordovician Dictyonema black shales</i>	348
3.2.3. <i>Origin and typology of U occurrences in the Lower Ordovician sediments</i>	349
Conclusion.....	349
Conclusion to Part 2.....	351
<u>PART 3. URANIUM PROSPECTS OF THE LADOGA REGION</u>	363
Introduction.....	365
1. <i>Uranium source</i>	365
2. <i>Extraction and transport</i>	368
3. <i>Trap</i>	369

1. Unconformity type.....	370
<i>1.1. Unconformity-type exploration criteria applied to the Ladoga region</i>	370
<i>1.2. Prospects</i>	376
2. Sandstone-type.....	380
<i>2.1. Sandstone-type exploration criteria applied to the Ladoga region</i>	380
<i>2.2. Prospects</i>	381
3. Vein-type.....	382
<i>3.1. Vein-type exploration criteria applied to the Ladoga region</i>	382
<i>3.2. Prospects</i>	384
Conclusion to Part 3.....	385
 GENERAL CONCLUSION.....	 387
 REFERENCES.....	 393
 GENERAL APPENDIX 1. FIGURES.....	 423
GENERAL APPENDIX 2. TABLES.....	437

LIST OF FIGURES

PART 1. REGIONAL GEOLOGICAL REVIEW

Figure 1.1. Map of metamorphic zoning of the Northern Ladoga area.....	49
Figure 1.2. U and Th contents in the rocks of the granite-gneiss domes of the Northern Ladoga area.....	65
Figure 1.3. A/CNK diagrams for the granitoids of the Ladoga region.....	68
Figure 1.4. Uranium and thorium distribution in the different granite phases of the Wiborg and Salmi massifs.....	83
Figure 1.5. AFM diagram for the Salmisky complex basalts.....	85
Figure 1.6. TAS diagram for the rocks of the Salminsky and Valaam magmatic complexes.....	87
Figure 1.7. Map of non-radioactive mineral resources of the Northern Ladoga area...	91
Figure 1.8. Scheme of the geodynamic evolution of the Ladoga region during the Svecofennian tectonic-magmatic event.....	96
Figure 1.9. Evolution of metamorphic conditions in the Ladoga region crust during the Svecofennian orogeny.....	97
Figure 1.10. Evolution of uranium contents in the bedrocks of the Ladoga region.....	104

APPENDIX TO THE PART 1.

Figure 1. Generalized map of the tectonic zoning of the Baltic Shield.....	107
Figure 2 a. Map of the regional tectonic zoning of the Ladoga region.....	108
Figure 2 b. Map of the detailed tectonic zoning of the Ladoga region.....	109
Figure 2 c. Map of the magmatic formations of the Ladoga region.....	110
Figure 2 d. Map of the major fault zones of the Ladoga region.....	111
Figure 2 e. Legend to the set of maps of the Ladoga region.....	112
Figure 3. Column of pre-Vendian geological formations of the Ladoga region.....	113
Figure 4. Map and section of the deep structure of the Ladoga region.....	114
Figure 5. Map of the gravity field anomalies of the Ladoga region.....	115
Figure 6. Geological column of the Pasha-Ladoga basin.....	116

PART 2. URANIUM OCCURRENCES OF THE LADOGA REGION

Chapter 1. Basement-hosted uranium occurrences

Paragraph 1.1. Granite-hosted uranium occurrences

Figure 2.1.1.1. Svecofennian ptigmatites hosted by Kalevian micaschist in the Pitkjaranta area.....	132
Figure 2.1.1.2. Uranium-mineralized pegmatoid granite body. Sjuskinsaari area.....	134
Figure 2.1.1.3. Biotite aggregates in uranium-mineralized pegmatoid. Sjuskinsaari area.....	134
Figure 2.1.1.4. Impregnated uraninite mineralization in pegmatoid from the Sjuskinsaari are.....	135
Figure 2.1.1.5. Idiomorphic uraninite crystals in biotite aggregates in the pegmatoid from the Sjuskinsaari area.....	135
Figure 2.1.1.6. Development of pitchblende and coffinite after uraninite. The Sjuskinsaari area.....	136
Figure 2.1.1.7. Secondary uranium mineralization in pegmatoids of the Sjuskinsaari area.....	136
Figure 2.1.1.8. Concordia diagram for the uraninite from the Sjuskinsaari area, sample Sju-1.....	137
Figure 2.1.1.9. Chondrite-normalized REE patterns of uraninite from the Sjuskinsaari area.....	138
Figure 2.1.1.10. Rose-diagram of fractures in the Puttummyaki ore-showing area.....	140
Figure 2.1.1.11. Tectonized migmatites hosting uranium mineralization of the Puttummyaki ore-showing. Part of the Outcrop 23.....	140
Figure 2.1.1.12. Outcrop 23 of the Puttummyaki ore-showing.....	141
Figure 2.1.1.13. Chained pitchblende mineralization from the Hirsimyaki ore-showing; sample and autoradiography.....	142
Figure 2.1.1.14. Pitchblende segregation in the quartz-feldspar “metasomatite”. The Hirsimyaki ore-showing; optical photo of a thick section.....	143
Figure 2.1.1.15. Different types of development of pitchblende-2 after pitchblende-1, the Puttummyaki ore-showing, BSE photos.....	143
Figure 2.1.1.16. Development of coffinite after pitchblende. Galena crystal occurs at the periphery. The Puttummyaki ore-showing. BSE photo.....	143

Figure 2.1.1.17. Concordia diagram for pitchblende from the Puttummyaki ore-showing, sample Pt-1.....	144
Figure 2.1.1.18. Outcrop of the Korennoye ore-showing.....	146
Figure 2.1.1.19. Autoradiography of chained impregnations of pitchblende in the Korennoye ore-showing.....	148
Figure 2.1.1.20. Fracture-bound pitchblende mineralization in the Korennoye ore-showing, sample, autoradiography and optical photos of polished sections.....	148
Figure 2.1.1.21. First possible interpretation of U-Pb isotopic data in a Concordia diagram for the pitchblende from the Korennoye ore-showing.....	149
Figure 2.1.1.22. Second possible interpretation of U-Pb isotopic data in a Concordia diagram for the pitchblende from the Korennoye ore-showing.....	150
Figure 2.1.1.23. Chondrite-normalized REE patterns of uranium oxides from late vein type mineralization of the Korennoye and Särkijärvi occurrences.....	150
Figure 2.1.1.24. Boudin-like segregation of pitchblende in tectonized migmatites from the Sumeria ore-showing. Optical photo of a polished section.....	156
Figure 2.1.1.25. Th-bearing minerals from Archaean granites from the Kuhilaslampi area. BSE photos.....	162
Figure 2.1.1.26. The Matkaselka massif, radioactive anomaly related to muscovite segregation in coarse-grained granite.....	163
Paragraph 1.2. Th-U anomalies in the Jatulian quartzites	
Figure 2.1.2.1. Jatulian quartzite from the Kuhilaslampi area.....	167
Figure 2.1.2.2. Jatulian quartzite with radioactive conglomerate from the Kuhilaslampi area.....	169
Figure 2.1.2.3. Th-bearing mineral phases from the Jatulian quartzites.....	170
Figure 2.1.2.4. Ferrithorite segregations in the quartzite.....	170
Figure 2.1.2.5. Radioactive anomaly in the Jatulian quartzite.....	171
Paragraph 1.3. U-P occurrences in the Ludicovian carbonate rocks	
Figure 2.1.3.1. Geological map of the Mramornaya Gora ore-showing area.....	174
Figure 2.1.3.2. Geological map of the Mramornaya Gora ore-showing.....	177
Figure 2.1.3.3. Geological section of the Mramornaya Gora ore-showing.....	178

Figure 2.1.3.4. The outcrop of the Mramornaya Gora ore-showing.....	180
Figure 2.1.3.5. Microstructure of Ludicovian dolomite marble hosting the Mramornaya Gora ore-showing.....	181
Figure 2.1.3.6. Uranium ore-hosting brecciated dolomitic marble cemented by calcitic marble in the Mramornaya Gora ore-showing.....	182
Figure 2.1.3.7. Early silicification of uranium ore hosting marbles in the Mramornaya Gora ore-showing; pitchblende and sulphide mineralization occur in lower left corners of the images. Sample MG-5, thin section optical photos.....	182
Figure 2.1.3.8. Folded quartz vein in the marble hosting the Mramornaya Gora ore-showing.....	183
Figure 2.1.3.9. Late quartz-sulphide veinlet cutting silicified marble of the Mramornaya Gora ore-showing.....	183
Figure 2.1.3.10. High-radioactive spot (over 1300 μ R/h) in brecciated marbles associated with local enrichment in oxidized sulphides; the Mramornaya Gora ore-showing.....	184
Figure 2.1.3.11. Different texture types of uranium ore of the Mramornaya Gora ore-showing.....	184
Figure 2.1.3.12. Uraninite mineralization associated with carbonaceous phase and different generations of pyrrhotite in the Mramornaya Gora ore-showing.....	185
Figure 2.1.3.13. Diverse distribution of uranium mineralization in the brecciated marbles of the Mramornaya Gora ore-showing, samples (and corresponding autoradiographies.....	186
Figure 2.1.3.14. Characteristic spectrum photos of the Mramornaya Gora ore-showing early uranium mineralization associated with apatite, carbonaceous phase, sulphides and arsenides.....	187
Figure 2.1.3.15. Early pitchblende from the Mramornaya Gora ore-showing associated with carbonaceous phase.....	188
Figure 2.1.3.16. Uranium-bearing cement of late breccias from the Mramornaya Gora ore-showing.....	189
Figure 2.1.3.17. Different types of late pitchblende from the Mramornaya Gora ore-showing.....	190

Figure 2.1.3.18. Heterogeneous structure of the pitchblende-2 spherulites from the Mramornaya Gora ore-showing.....	191
Figure 2.1.3.19. Concordia diagram for late pitchblende-2 from the Mramornaya Gora ore-showing.....	192
Figure 2.1.3.20. Pattern of chondrite-normalized REE contents in uraninite from the Sjuskinsaari area; sample MG-6.....	192
Figure 2.1.3.21. Coffinite (Coff) replacing pitchblende-2 (Pbl-2); pyrite (Py-1), galena (Gl-2); Mo-phase (Mo).....	194
Figure 2.1.3.22. Late calcite veinlet with coffinite mineralization cutting early pitchblende ores in the Mramornaya Gora ore-showing.....	194
Figure 2.1.3.23. Development of pitchblende-2 after rutile-1 with intermediate cryptocrystalline Ti-U phase.....	195
Figure 2.1.3.24. Development of late rutile after pitchblende-2.....	195
Figure 2.1.3.25. Geological map of the Ruskeala area.....	196
Figure 2.1.3.26. Folded marbles in a quarry of the Ruskeala area.....	197
Figure 2.1.3.27. Autoradiographies of drill core samples with U mineralization from the Severnaya Ruskeala U ore-showing.....	198
Figure 2.1.3.28. Outcropped U-mineralized tremolite-pyroxene-carbonate rocks in the Centralno-Impilakhtinskoye ore-showing.....	200
Figure 2.1.3.29. Tremolite-pyroxene-carbonate rocks from the Centralno-Impilakhtinskoye ore-showing and its autoradiography.....	200
Figure 2.1.3.30. Geological map of the Centralno-Impilakhtinskoye ore-showing area.....	201
Figure 2.1.3.31. Pitchblende (Pbl) mineralization from the Vostochno-Impilakhtinskoye ore-showing, optical photos, reflected light.....	202
Paragraph 1.4. Vein-type uranium occurrences	
Figure 2.1.4.1. Geological map and sections of the Varalakhti ore-showing area.....	209
Figure 2.1.4.2. Geological map the Varalakhti ore-showing.....	210
Figure 2.1.4.3. Quartz breccias cemented by calcite and ankerite from the breccias zone hosting the Varalakhti ore-showing.....	210
Figure 2.1.4.4. U mineralized breccias from the Varalakhti ore-showing; sample Va-6 and its autoradiography.....	211

Figure 2.1.4.5. Quartz deformations in the U mineralized breccias of the Varalakhti ore-showing.....	211
Figure 2.1.4.6. U mineralized zone inside of the adit.....	212
Figure 2.1.4.7. Pitchblende mineralization of the Varalakhti ore-showing, optical photos.....	213
Figure 2.1.4.8. Pitchblende fragments cemented by late gangue and sulphide minerals.....	214
Figure 2.1.4.9. Two types of coffinite mineralization.....	214
Figure 2.1.4.10. Two possible interpretations of isotopic U-Pb data for pitchblende from the Varalakhti ore-showing.....	216
Figure 2.1.4.11. Two generations of late Svecofennian leucogranites veins cutting the Ladoga group mica schists in the Latvasurje area.....	217
Figure 2.1.4.12. Outcrop of the Karinmyaki ore-showing.....	218
Figure 2.1.4.13. U-mineralized breccias from the Karinmyaki ore-showing.....	219
Figure 2.1.4.14. Karinmyaki ore-showing uraninite crystals partly replaced by pitchblende, coffinite, kasolite and hydropitchblende.....	220
Figure 2.1.4.15. Karinmyaki ore-showing; development of kasolite in fractures in sphalerite.....	220
Figure 2.1.4.16. Geological map of the Razlomnaya anomaly area.....	224
Figure 2.1.4.17. Fracture-bound U mineralization of the Razlomnaya anomaly.....	224
Figure 2.1.4.18. Razlomnaya anomaly; relic of a pitchblende spherulite replaced by coffinite and rutile associated with magnetite replaced by hematite.....	225
Figure 2.1.4.19. Geological scheme of the southern flank of the Dyke anomaly.....	226
Figure 2.1.4.20. Altered gabbro-diorite from the Dyke anomaly; sample and autoradiography.....	227
Figure 2.1.4.21. Thorite mineralization from the Dyke anomaly.....	228
Figure 2.1.4.22. Secondary uranium mineralization from the Jalonvara deposit, BSE photos.....	230
Figure 2.1.4.23. Low-grade ferrithorite mineralization from the Hopunvaara complex-ore deposit.....	233

Figure 2.1.4.24. Ferrithorite impregnations associated with pyrite, marcasite and magnetite from the Hopunvaara deposit.....	233
Figure 2.1.4.25. Diagrams of striking of brittle tectonic structures controlling vein-type uranium occurrences in the Northern Ladoga area.....	234
Figure 2.1.4.26. Distribution of different type uranium occurrences of 20 vein-type uranium occurrences of the Northern Ladoga area according to the host rocks.....	235
Conclusion to Chapter 1	
Figure 2.1.5.1. Distribution of basement-hosted uranium ore resources of the Northern Ladoga area according to the host rocks.....	240
Figure 2.1.5.2. Typological distribution of the basement-hosted uranium ore resources of the Northern Ladoga area.....	242
Appendix to the Chapter 1	
Figure 1. Geological map of the Impilakhti-Pitkjaranta area.....	246
Figure 2. Geological map and section of the Puttummyaki uranium occurrence.	247
Figure 3.1. Geological map and section of the Korennoye uranium occurrence.....	248
Figure 3 (continued). Legend to geological map and section of the Korennoye uranium occurrence.....	249
Figure 4. Geological map and section of the Maloye Janisjarvi area.....	250
Figure 5. Geological map of the Kuhilaslampi area.....	251
Figure 6. Geological map of the Latvasurje area.....	252
Figure 6 (continued). Legend to geological map of the Latvasurje area.....	253
Chapter 2. Uranium occurrences hosted by the Riphean formations	
Figure 2.2.1. Biotite granite-gneiss cut by a granophyre vein from the Salmi depression.....	259
Figure 2.2.2. Graphite/sulphide- bearing biotite schist of the Impilakhti suite from the Karku deposit.....	260
Figure 2.2.3. Blastocataclasite of graphite-bearing biotite schist of the Impilakhti suite from the Salmi depression.....	260
Figure 2.2.4. Newly formed graphite and pyrite in tectonized biotite schist of the Impilakhti suite from the Karku deposit area.....	260
Figure 2.2.5. Rapakivi granite of the Salmi massif from the Salmi depression.	261

Figure 2.2.6. Contact of the Priozersk suite gritstone and physical weathering crust of the basement from the Karku deposit.....	262
Figure 2.2.7. Shale from the physical zone of the regolith of the basement from the Karku deposit.....	263
Figure 2.2.8. Contact of the physical altered shale with the chemically altered quartz-microcline gneiss of the Impilakhti suite from the Karku deposit.....	264
Figure 2.2.9. Altered graphite-bearing biotite schist of the Impilakhti suite from the chemical alteration zone from the Karku deposit.....	265
Figure 2.2.10. Non-altered graphite-bearing biotite gneiss from the bottom of the borewell from the Karku deposit.....	265
Figure 2.2.11. The Priozersk suite quartz-feldspar sandstone, gritstone and conglomerate from the Karku deposit.....	266
Figure 2.2.12. The Priozersk suite polymictic conglomerate with soft pebbles (mud rolls) from the Karku deposit.....	267
Figure 2.2.13. The Priozersk suite sandstone from the Salmi depression; quartz and feldspar clasts are cemented with kaolinite and hydromicas.....	267
Figure 2.2.14. Heavy mineral concentration in the leached sandstone of the Priozersk suite from the Karku deposit.....	267
Figure 2.2.15. The Priozersk suite mafic effusives of the lower subsuite from the Salmi depression.....	269
Figure 2.2.16. Different types of agates from the Salmi suite basalts.....	270
Figure 2.2.17. The Salmi suite polymictic conglomerate from the Karku deposit.....	270
Figure 2.2.18. Conglomerates with agate fragments from the basal horizon of the Salmi suite sedimentary interlayer from the Karku deposit.....	271
Figure 2.2.19. Geological map and sections of Karku deposit Ore body 3.....	275
Figure 2.2.20. Development of graphite in tectonized biotite schist of the Impilakhti suite.....	276
Figure 2.2.21. Cataclasis of the ore-hosting sulphide-chlorite-carbonate Priozersk suite rock.....	276
Figure 2.2.22. Brecciated graphite-bearing biotite schist of the Impilakhti suite from the Karku deposit area.....	277

Figure 2.2.23. Brecciated basalt of the Salmi suite lower subsuite from the Karku deposit area.....	278
Figure 2.2.24. Generalized geological section of the Karku deposit ore body...	279
Figure 2.2.25. Samples of ore-hosting altered sandstones from the Karku deposit.....	280
Figure 2.2.26. Detrital quartz overgrowth on epigenetic quartz.....	280
Figure 2.2.27. Poikilitic calcite cement in a sulphide-carbonate altered rock of the Priozersk suite sandstone.....	282
Figure 2.2.28. Composition of chlorites from the Karku and Shea-Creek deposits in Al ^{VI} -Mg-Fe ternary diagram.....	283
Figure 2.2.29. MgO/FeO diagram of the chlorites versus whole rock U in the Karku deposit.....	284
Figure 2.2.30. Bitumen aggregates associated with Mo phase in sulphide-carbonate metasomatite.....	284
Figure 2.2.31. The mineral and element behavior in the different zones of the Karku deposit alteration halo.....	286
Figure 2.2.32. Geological section of the Kotalakhti ore-showing.....	287
Figure 2.2.33. Autoradiographies and corresponding samples of different textural types of the radioactive mineralization.....	289
Figure 2.2.34. Pitchblende as a cement of the high-grade mineralized sandstone in the Karku deposit.....	291
Figure 2.2.35. Intergranular aggregates of two pitchblende generations.....	291
Figure 2.2.36. Mineralogical particularities of the pitchblendes from the high-grade ores from the Karku deposit.....	292
Figure 2.2.37. Carbonate overgrowths and replacement of different mineral phases.....	292
Figure 2.2.38. High-grade pitchblende mineralization of the Karku deposit....	293
Figure 2.2.39. Pitchblende cement of the altered quartz sandstone; galena impregnations occur in the pitchblende.....	294
Figure 2.2.40. Vein-type U mineralization in the Salmi suite basalts.....	294
Figure 2.2.41. Coffinite mineralization in altered sulphide-carbonate Priozersk suite sandstone.....	295

Figure 2.2.42. Coffinite replaces quartz; sphalerite and pyrite develop in the intergranular space of the Priozersk suite sandstone.....	296
Figure 2.2.43. Coffinite-carbonate cement of the quartz-feldspar sandstone.....	296
Figure 2.2.44. Diverse types of coffinite development.....	297
Figure 2.2.45. Coffinite replacement of zircon.....	297
Figure 2.2.46. Coffinite veinlets in the quartz-feldspar sandstone.....	298
Figure 2.2.47. Coffinite-like phase in cement of the Priozersk suite sandstone.	298
Figure 2.2.48. Carnotite and V-bearing seladonite in the Priozersk suite sandstone cement and in the fractures of quartz grains.....	299
Figure 2.2.49. Microstructure of carnotite; the Matala ore-showing.....	300
Figure 2.2.50. Carnotite, V-bearing celadonite and hollandite in the cement of the Priozersk suite sandstone.....	300
Figure 2.2.51. Replacement of brannerite fragments by pitchblende and late rutile in altered quartz sandstone of the Priozersk suite.....	301
Figure 2.2.52. Natural heavy concentration in the Priozersk suite sandstone of the Salmi depression.....	302
Figure 2.2.53. Romanechite veinlet cutting the Priozersk suite quartz-feldspar sandstone.....	302
Figure 2.2.54. Spectra of radioactive isotopes of sample 929 from the Matala ore-showing.....	303
Figure 2.2.55. Different interpretations of U-Pb isotopic data in Concordia diagrams for the pitchblendes from the Karku deposit and Kotalakhti ore-showing.....	305
Figure 2.2.56. Chondrite-normalized REE patterns of pitchblendes from the Kotalakhti ore-showing and the Karku deposit.....	307
Figure 2.2.57. Chondrite-normalized REE patterns of two generations of uraninites from the Sue deposit (Athabasca Basin).....	308
Figure 2.2.58. Chondrite-normalized REE patterns of uranium oxides from the Kotalakhti ore-showing and the Karku deposit in comparison with those of the Särkijärvi, Luthi and Alho vein-type occurrences of Finland.....	309
Figure 2.2.59. Succession of the epigenetic mineral parageneses of the Karku deposit, Matala and Kotalakhti ore-showings.....	310
Figure 2.2.60. Diagram of the geochemical zoning in the Karku deposit area..	317

Figure 2.2.61. Sandstone-hosted and basement-hosted subtypes of unconformity-type deposits.....	318
Figure 2.2.62. Comparative geological sections of the Karku and Cigar-Lake deposits.....	319
Appendix to the Chapter 2.	
Figure 1. Geological map and section of the Salmi depression.....	329
Figure 2. Geological map of the Central Block area.....	330
Figure 3. Map of the basement surface in the Central Block area.....	331
Figure 4. Map of thickness of the Priozersk suite in the Central Block area.....	332
Figure 5. Geological map of the Karku deposit Ore body 3 area.....	333
Figure 6. Map of the basement surface of the Karku deposit Ore body 3 area..	334
Figure 7. Map of thickness of the Priozersk suite in the Karku deposit Ore body 3 area.....	335
Figure 8. Map of metasomatic alterations in the Karku deposit Ore body 3 area.....	336
Figure 9. Drill core samples of the ore-hosting sulphide-chlorite-carbonate metasomatites after the Priozersk suite sandstone and corresponding autoradiographies.....	337
Figure 10. Sections with U and Th contents in the Karku deposit Ore body 1..	338
Chapter 3. Uranium occurrences hosted by Vendian-Palaeozoic platform sediments	
Figure 2.3.1. Geological map of the Nevsko-Volkhovskiy uranium ore district	341
Figure 2.3.2. Geological map of the Slavyanskoye deposit.....	344
Figure 2.3.3. Geological section of the Slavyanskoye deposit.....	344
Conclusion to the Part 2	
Figure 2.1. Typological distribution of uranium ore resources of the Ladoga region.....	353
Figure 2.2. Distribution of different type uranium occurrences in the Ladoga region.....	354
Figure 2.3. Schematic geological section and column of the Ladoga region with position of uranium occurrences.....	356
Figure 2.4. Ages of uranium mineralization discovered in the Ladoga region..	357
Figure 2.5. Evolution of uranium enrichment in the Ladoga region.....	360

PART 3. URANIUM PROSPECTS OF THE LADOGA REGION

Figure 3.1. Comparative geological maps of the Athabasca and Ladoga regions.....	370
--	-----

GENERAL APPENDIX 1

Figure 1.1. Geological map of the Northern Ladoga area.....	426
Figure 1.2. Prognostic geological map of the Northern Ladoga area.....	427
Figure 2.1. Geological map of the South-Eastern Ladoga area.....	428
Figure 2.2. Prognostic geological map of the South-Eastern Ladoga area.....	429
Figure 3.1. Geological map of the Western Ladoga area.....	430
Figure 3.2. Prognostic geological map of the Western Ladoga area.....	431
Figure 4. Legend to geological and prognostic maps of the Northern Ladoga, South-Eastern Ladoga and Western Ladoga areas.....	432
Figure 5. Map of location of uranium occurrences in the Northern Ladoga area.....	436

LIST OF TABLES

GENERAL INTRODUCTION

Table 1. General chronostratigraphic scale of Precambrian of Russia and its correlation with the International geochronological scale.....	36
Table 2. Russian classification of grade of uranium mineralization.....	37

APPENDIX TO THE PART 1

Table.1.1.1. Accessory minerals of the potassic granitoids of the Ladoga region.....	117
Table 1.2. Average chemical composition of Svecofennian potassic granites of the Ladoga region.	118
Table 1.3. Succession of the geological events in the Ladoga region.	119

PART 2. URANIUM OCCURRENCES OF THE LADOGA REGION

Chapter 1. Basement-hosted uranium occurrences

Paragraph 1.1. Granite-hosted uranium occurrences

Table 2.1.1.1. Quartz-microcline metasomatic alteration paragenesis for different types of host rocks.....	153
Table 2.1.1.2. Geochemical characteristics of the quartz-microcline metasomatites developed from different protoliths.....	154
Table 2.1.1.3. Sericite-quartz-albite metasomatic alterations for various host rocks.....	155
Table 2.1.1.4. Isotopic age constrains of U mineralization hosted by anatexitites of the Northern Ladoga area.....	158

Paragraph 1.2. Th-U anomalies in the Jatulian quartzites

Table 2.1.2.1. Chemical compositions of Th and U containing minerals from the Jatulian quartzites of the Kuhilaslampi area.....	168
---	-----

Paragraph 1.3. U-P occurrences in the Ludicovian carbonate rocks

Table 2.1.3.1. Ore mineral paragenesis of the Mramornaya Gora ore-showing.....	193
Table 2.1.3.2. Isotopic age constrains of U mineralization hosted by Ludicovian carbonate rocks of the Northern Ladoga area.....	204

Paragraph 1.4. Vein-type uranium occurrences.....

Table 2.1.4.1. Ore paragenesises of the Varalakhti ore-showing.....	215
Table 2.1.4.2. Ore paragenesis of the Karinmyaki ore-showing.....	221

Table 2.1.4.3. Ore paragenesis of the Razlomnaya anomaly.....	223
Table 2.1.4.4. Ore paragenesis of the Dyke anomaly.....	228
Table 2.1.4.5. Chemical composition of vein-type thorite mineralization in the Dyke anomaly. Sample Jn-8.....	229
Table 2.1.4.6. The Jalonvara complex ore deposit. Vein-type uranium mineralization.....	230
Table 2.1.4.7. The Hopunvaara complex ore deposit. Vein-type ferrithorite. Sample BV-1.....	233
Table 2.1.4.8. Isotopic age constrains of vein-type U mineralization of the Northern Ladoga area.....	236
Chapter 2. Uranium occurrences hosted by the Riphean formations	
Table 2.2.1. Chemical composition of the Priozersk suite rocks.....	285
Table 2.2.2. Isotopic age constrains of Riphean-hosted uranium mineralization.....	304
Table 2.2.3. U (IV), U (V) and U (VI) contents in pitchblendes of the Karku deposit.....	309
Table 2.2.4. Location of epigenetic uranium mineral phases in the different rock types and types of the uranium mineralization.....	314
Table 2.2.5. Average uranium abundance in rocks of the Karku deposit area.....	316
Conclusion to the Part 2.	
Table 2.1. Principal types of uranium occurrences of the Ladoga region.....	352
Table 2.2. Typology of the Ladoga region uranium occurrences in the IAEA classification.....	351

PART 3. URANIUM PROSPECTS OF THE LADOGA REGION

Table. 3.1. Applications of unconformity-type deposits exploration criteria to the different part of the Ladoga region.....	375
---	-----

GENERAL APPENDIX 2.

2.1. Table of radiogeochemical characteristics of the geological formations of the Ladoga region.....	439
2.2. U and Th contents in Svecofennian syn-, late- and post-orogenic intrusions of	

the Ladoga region.....	442
2.3. Tables of chemical composition of uranium and thorium bearing mineral phases. Analyzed with the ABT-55 Akashi electron microprobe, St-Petersburg.....	448
2.4. Tables of chemical composition of uranium mineral phases. Analyzed with Cameca SX-100, Nancy.....	456
2.5. Table of chemical composition of pitchblendes from the Karku deposit. Analyzed with ABT-55 Akashi electron microprobe, St-Petersburg.....	460
2.6. Table of chemical composition of pitchblende from the Karku deposit and the Kotalakhti ore-showing. Analyzed with Cameca SX-100, Nancy.....	462
2.7. Tables of chondrite-normalized REE and Y content in the uranium oxides.....	463

GENERAL INTRODUCTION

GENERAL INTRODUCTION

1. Object and aim of the study.

Several peripheral areas of the Baltic Shield are considered as potential area for the location of uranium deposits similar to the huge uranium deposits of Athabasca (Canada) and Pine-Creek (Australia) related to Proterozoic unconformities.

The Ladoga region is especially prospective for the discovery of unconformity-type uranium deposits for the following reasons:

1) it contains the largest Mesoproterozoic (Riphean) intracontinental sedimentary basin of the Baltic shield – the Pasha-Ladoga basin that unconformably overlays the Archaean-Palaeoproterozoic (AR-PR₁) metamorphic and granitoidic basement;

2) it is located at the intersection of two trans-regional tectonic belts controlling various types of uranium mineralization in adjacent areas: the Raahe-Ladoga and Baltic-Mezen zones;

3) there are many uranium-bearing formations and numerous uranium occurrences of different types in the Ladoga region;

4) there are good evidences for the existence of unconformity-related U accumulation – the Karku deposit, localized in basal horizon of Riphean sediments of the Pasha-Ladoga basin.

Geological exploration has been carried out in the Ladoga region since the XVIIIth century. U exploration started in 1945. Because of the low level of knowledge about the factors controlling U mineralization, the first works were global with no specific prospecting targets and any kind of radioactive anomalies were investigated. In 1945-1948 a series of U deposits in the Ordovician Dictyonema shales were discovered. Diverse U occurrences in crystalline formations of the Northern Ladoga area were also discovered by the exploration work of “Nevskgeologia” from 1948 to 1981. First, the Vendian-hosted deposit of Slavyanovskoye was found in 1957, others were discovered later. In the middle of 1980th, exploration directed toward the discovery of unconformity-type deposits started in the Riphean Pasha-Ladoga basin. As a result the Karku deposit related to the Mesoproterozoic unconformity was discovered in 1989.

Initially uranium exploration in the Ladoga region have started by an operative group attached to the Leningrad geological directorate (LGGU).

Since 1947, another enterprise was the exclusive executor of all uranium specialized explorations. Its name changed many times. In 2007 it has been named SZSP “Nevskgeologia” of SE “Urango”. To be short this enterprise will be called “Nevskgeologia”. More limited

uranium exploration was carried out by: “Sevzapgeologia”, Severnoye (Northern) and Pyatoye (Fifth) geological directorates, ZGT, “Sevmorgeo”, “Hydrospecegeologia”, “Aerogeologia” and others. Accompanying scientific researches have been undertaken by specialists of VSEGEI, St-Petersburg State University (SPbGU, previous name LGU), VIRG, VIMS, CNIIGRI, IGEM, KNC etc. Unfortunately, 99 % of the information on uranium mineralization of the Ladoga region is unpublished. Until 2004 all reports have been accumulated in archives of “Nevskgeologia” and SE “Urango”. This process is still continuing but since 2004, an independent compilation of information about U started in the ZAO Novaya Lekhta (joint-stock company established by AREVA, VSEGEI, SE “Urango” and “Geologorazvedka”).

Until now only a few theses deal with uranium in the Ladoga region: Russian Candidate degree thesis of A.V. Krasnyh “Structural conditions of the localization of high-grade uranium ores of the “unconformity type” in the Karku deposit (Karelia) and foreign objects” 2003, at VIMS; thesis for PhD degree of the Henri Poincaré University of V.M. Lobaev “Mineralogical and petrogeochemical characteristics of the Mesoproterozoic Pasha-Ladoga volcanic-sedimentary basin and its basement (Baltic shield, Russia)”, in 2005; Russian Candidate degree thesis of A.V. Shurilov – “Geological-structural position of Karku uranium deposit (North-Eastern Ladoga)” SPbGU, 2006. The main targets of all of these researches were focused on different aspects of the unconformity-type Karku deposit.

The aim of the present thesis is a comprehensive review of the uranium metallogenesis of the Ladoga region. As unconformity-type deposits are suggested as the most attractive economic target in the region, the main attention has been concentrated on uranium occurrences related to the Riphean unconformity and pre-Riphean basement formations. They are available for sampling, whereas uranium mineralization in V-PZ platform sediments does not outcrop and mineralized drill core had been lost long ago.

For the basement-hosted and Riphean-hosted uranium occurrences of the Ladoga region complex analysis has been undertaken. Different geological parameters controlling the uranium mineralization such as petrologic, structural and geochemical features have been studied. Special attention was paid to the ore mineralogy.

General evolution of the uranium fractionation in the Ladoga region is proposed.

Prospective of the Ladoga region for the discovery of economic-grade U mineralization will be defined as a major outcome of the detailed analysis of old and newly-obtained data.

2. Structure of the manuscript.

Part 1.

Part 1 is devoted to the presentation of the metallogenic diversity of the Ladoga region in relation with its specific location in the structures of the Baltic Shield. It includes the description of tectonic zoning, of the sedimentary and magmatic complexes, the evolution of geological structure and of the uranium abundance in the region.

Part 2.

The different uranium occurrences of the Ladoga region are described in Part 2. Their geological, structural, geochemical and mineralogical characteristics, the parameters controlling the uranium mineralization and grade are considered. Their classification and an estimation of their economic attractivity will be proposed.

Part 3.

The third part comprises an attempt to propose the most prospective areas for discovering economic uranium deposits in the Ladoga region.

Conclusion.

It summarizes the major results obtained during the present research work and introduces unresolved problems requiring additional investigations.

Appendixes.

The Appendixes to Part 1, Part 2 and the General Appendix contain graphics and tables too large to be inserted directly in the text or being referred in different chapters.

3. Terminological aspects.

There are many differences in the understanding of major geological processes and in the corresponding terminology between the Russian and Western geological literature. Some of them should be first discussed to avoid confusions as much as possible.

1. Stratigraphic aspects.

Since 1980th in USSR and now in Russia a specific chronostratigraphic scale is in use (Table 1). The principal formal difference of it from the international geochronological scale is

the subdivision of the Archaean and Proterozoic into two periods. In this thesis the international terminology for global subdivisions is used as much as possible.

Table 1. General chronostratigraphic scale of Precambrian of Russia and its correlation with the International geochronological scale
(compiled from Glebovitsky and Shemyakin, 1996, Mitrofanov and Negruța, 2002).

Acro theme	Eontheme	Eratheme /System	Subdivision	Limits, Ma	International version
Proterozoic	Upper Proterozoic	Vendian, V	Upper	620±15	Neoproterozoic
			Lower	650±20	
		Riphean, R	Upper	1000±50	
			Middle	1350±50	
			Lower	1650±50	
	Lower Proterozoic (Karelian, K)	Upper, K ₂	Vepsian, Vp	1800	Palaeoproterozoic
			Kalevian, Kl	1920	
			Ludicovian, Ld	2100	
		Lower, K ₁	Jatulian, Jt	2300	
			Sariolian, Sr	2400	
Sumian, Sm			2500		
Archaean	Upper Archaean (Lopian, L)	Upper, L ₃	2800	Neoarchaeon	
		Middle, L ₂	3000	Mesoarchaeon	
		Lower, L ₁	3200		
	Lower Archaean (Saamian, S)		3600	Palaeoarchaeon	

Sometimes Vendian is included into Palaeozoic. Although the platform sequence of the Eastern Europe plate (Russian Platform) starts from Upper Vendian and the correspondence of the last system to Palaeozoic seems quite reasonable, official subdivision is used in this thesis – with a lower limit of Palaeozoic corresponding to the Cambrian (cca 540 Ma).

Some local subdivisions are in use only for Russian part of the Baltic Shield.

So, a term Ludicovian was proposed by Sokolov in 1979 (Sokolov, 1984) for metamorphosed carbonaceous terrigenous and carbonate formations associated with mafic volcanites. They overlap the Upper Jatulian dolomites. The Ludicovian stratotype is described in the Onega Lake area. The Ludicovian sequence of the Ladoga region can be correlated with the marine formations the upper part of the Upper Jatulian and the Lower Kalevian of adjacent areas of Finland, but this parallelism is not well established.

The Vepsian subdivision has been proposed by Krats (1963) for weakly-metamorphosed terrigene-dominated sequence of the Onega depression. Such kind of rocks does not exist in other parts of the Baltic Shield where this period is only represented by igneous formations.

The Riphean stratotype was defined for Mesoproterozoic formations of the Ural region. The Riphean sequence of the Pasha-Ladoga basin can be correlated with the Jotnian one of Finland (the Satakunta and Muhos grabens).

Subdivision and age reference for the different units of the Riphean sequence of the Pasha-Ladoga basin are still not definitively fixed. There is contradiction between the traditional scheme and newly obtained isotopic constraints. This problem will be specially discussed in Part 1 (paragraph 1.4. Riphean sedimentary basin).

2. Problem of granite petrogenesis.

There are also different theories on the origin of U-hosted granites of the Northern Ladoga granite-gneiss domes. Either intrusive emplacement or in-situ partial melting or high-temperature metasomatism have been proposed. I try to adopt a neutral terminology as much as possible in the present work.

3. Problem of evaluation of deposit resource.

There are different classifications of uranium ore resources in the world mining industry. As the descriptions the uranium occurrences described in this thesis are based on Russian reports, the Russian terminology will be used.

Table 2. Russian classification of grade of uranium mineralization (after Skorospelkin, 2002).

Content, ppm								Grade of deposit, kt			
Increased			Ore					small	median	large	very large
incr. bcgrd	geoch. anom.	showing	out of balance	low (poor)	ordinary	high (rich)	very high				
5	50	100	300	500	1000	3000	10000	0,5	10	50	100

incr. bcgrd. – increased background;

geoch. anom. – relevant geochemical anomaly.

Classification of uranium occurrences:

Anomaly – mineralized spot of small size (few meters); *low-grade* – if uranium content is below 300 ppm.

Ore-showing – extended U-mineralized zone with average uranium content over 300 ppm and evaluated or presumed resource less 500 kt.

Deposit – evaluated occurrence with resource over 500 kt for a 300 ppm U cut-off.

Unfortunately, information about uranium occurrence resources in the Ladoga region is often uncertain. Only the unconformity-related Karku deposit and sandstone-type deposits have been studied sufficiently for Identified Resource evaluation including Reasonably Assured Resources according the IAEA classification system. Grade of other occurrences in better case can be estimated as Inferred Resources only. Sometimes the information is controversial and the same occurrences are ranged as ore-showing or as deposits in different reports.

4. Radiometric measurements.

Different units are used for radiometric measurements during uranium explorations. For Russia the most common is micro-Roentgen per hour ($\mu\text{R/h}$) measured by radiometer, whereas in France scintillometer measurements of counts per second (cps) are used. For approximate correlation between them the following ratio can be used: $1 \mu\text{R/h} / 1 \text{ cps} = 4.8$.

$\mu\text{R/h}$ units will be used for the preservation of the original numbers compiled from old reports. Also they are used in some figures made by the present author, because radiometers SRP-68-1 and dosimeter “Bella” ($1 \mu\text{Sv/h} = 100 \mu\text{R/h}$) were used during work in the Karku deposit and field first trip of this thesis (in 2005). During following field works a scintillometer SPP- γ was used and radioactivity is given in cps.

5. Linguistic problems.

Since most of the information used in this thesis is from Russian published and archive sources, problems caused by transformation of the names from Cyrillic to Latin alphabet should be considered. It concerns mainly archive topographic names, never published, hence never before translated into English. Although translations of these words have been done according to special grammatical rules, some alternative version exists.

Another problem is diverse description in Latin some of Russian topographic names used in different publications in other languages. In this text the most common versions will be used.

Special mention should be done for a word “Выборг” – a name of the city at the frontier with Finland. In the European literature it is often translated as Vyborg according to above mentioned rules, but for the rapakivi batholith with the same name in Russian, a German name

“Wiborg” is usually used (see for example Rämö, 2001). Here the rapakivi batholith is called “Wiborg”, whereas a word “Vyborg” is used for one of blocks of the Svecofennian domain – the Vyborg block.

References to Russian publications and archives are translated into English, but the original names are given in brackets.

4. Methodology.

The research has been carried out at the G2R laboratory of the University of Henri Poincaré (UHP, Nancy, France) and at the Saint-Petersburg State University (SPbGU, St-Petersburg, Russia). Several successive and synchronous activities have been undertaken:

- 1) compilation of old published and archive data;
- 2) field works including mapping of ore-hosting geological structures and sampling of mineralized rocks;
- 3) mineralogical studies on mineralized rocks;
- 4) interpretation of old and newly-obtained information
- 5) writing and design of the manuscript.

1) Compilation of previous data.

This study is based on information obtained during long-term geological and especially uranium investigations carried out in the Ladoga region. As published as archive data of “Nevskgeologia”, VSEGEI, “Sevzapgeologia”, SPbGU, “Mineral”, IGGD and ZAO “Novaya Lekhta” were used.

The geological structure of the Ladoga region is quite well studied, but this knowledge is not uniform. The outcropping northern part was well studied by Finnish geologist before 1940th (O. Trustedt, P. Eskola et al). More detailed studies were carried out by many Soviet and Russian geologists (K.O. Krats, N.G. Sudovikov, A.N. Kairyak, L.V. Grigorieva, R.A. Khazov, V.Z. Negrutza et al). There are many publications on this matter and they have been used during this research. More detailed archive reports of “Sevzapgeologia”, “Nevskgeologia”, “Mineral”, VSEGEI, SPbGU and IGGD have been used as well.

The structure of the southern part of the region concealed under the V-PZ platform cover is not well studied. Geophysics and drillings give a very general geological image of this area.

Detailed works were local and many important features are still uncertain. Most of the information on this area is unpublished. Archives of “Nevskgeologia” have been used here.

There is lack of open publications on the U occurrences of the Ladoga region. The Karku deposit, Vendian- and Ordovician-hosted occurrences have been described in several periodicals and special editions, but information on others is only available in archives. Descriptions of U occurrences presented in the thesis are based on unpublished reports of “Nevskgeologia”, less of VSEGEI. An additional difficulty of the compilation was caused by the strictly confidential character of the information concerning U in the former Soviet Union. A “top-secret” degree of archive reports has been abolished just a few years ago and now are available for commercial use, but because of long storage and disturbance of 1990th lot of primary information is lost.

2) *Field works.*

Author observations obtained during field work in the Ladoga region represent a major part of the thesis. From 2000 to 2003 the author has worked as a geologist of “Nevskgeologia” in the Karku deposit. Materials obtained during this period give the base of the Chapter 2 of this thesis devoted to the Riphean-hosted U mineralization.

Three field trips have been accomplished in 2005-2007 specifically for the thesis. Two additional excursions to the most representative areas have been organized by the author for visits of French and Finnish geologists in 2005 and 2006.

Mapping and sampling of the most representative uranium occurrences have been undertaken during the field works. Some key geological objects have been observed in addition.

3) *Mineralogical studies.*

A collaboration project between the Saint-Petersburg State University (SPbGU, Russia) and the Centre de Recherche sur la Géologie des Matières Premières Minérales et Énergétiques (CREGU, France) has been established for the study of uranium ore parageneses of several U occurrences. A group of geologists of the Faculty of SPbGU, IGGD, “Hypronickel” and VSEGEI under the direction of professor Yu. S. Polekhovskiy (SPbGU) was also involved in this research project. Significant part of work including electron-microprobe and isotopic researches was done at the UHP and the CRPG in Nancy.

Mineralogical studies were preceded and accompanied by autoradiographies made with 18×24 cm Roentgen film (Sterling Diagnostic Imaging, USA). Macro images of the samples have been obtained with Epson Perfection 3200 Photo scanner. Optical microscope studies and micro-photos were achieved with Polam P312, Leica DM 2500 P, Olympus BX51 microscopes.

Chemical compositions of the ore minerals were determined with following electronic microprobes (EMP):

- 1) ABT-55 “Akashi” (IGGD, St.-Petersburg, Russia);
- 2) CAMECA SX 100 (UHP, Nancy, France);
- 3) CamScan-4 (Hypronickel, St.-Petersburg, Russia).

U, Pb isotopic compositions and REE abundance in the uranium oxides were measured by Second Ion Mass Spectrometry (SIMS) using the CAMECA IMS-3F ion-microprobe at CRPG-CNRS (Nancy, France).

Uraninite from Katanga (Zambia) dated at 540±4 Ma was used as a standard for U-Pb analysis. Analytic protocol was according to Holliger (1988).

Determination of the REE distribution in uranium oxides is useful for identification of a uranium source, chemical composition of the ore-producing fluids, process of deposition and type of ore occurrence. A uraninite from Mistamisk Valley in Canada (Kish and Cuney, 1981) was used as a standard for analysis of REE content in uranium oxides from the Ladoga region. REE composition of the standard has been independently determined by ICP-MS (Bonhoure et al., 2007). Results were normalized to chondrite REE content after Evenson et al., 1978.

The main results of the mineralogical studies are included in this manuscript. A full version is presented as an independent report “Ore parageneses of radioactive mineralization of the Northern Ladoga area (Karelia)” (Polekhovsky et al., 2007).

4) Interpretation of the obtained data.

All figures of the thesis were compiled from publications, archives and from results obtained during this study. Results of a new interpretation of satellite images (Landsat-7) were used for mapping the tectonic structure of the Ladoga region. The interpretation was carried out with *Arc-View 3.2* and *Map-Info 7.8* software with the help of Zakharov V.I. (SPbGU).

Interpretation of U-Pb isotopic data was carried out with the help of Kister Ph.

(AREVA), Golubev V. (IGEM) and Larionov A. (VSEGEI). The concordia diagrams were built with the ISOPLOT software (Ludwig, 1999).

Interpretation of the geochemical data was done with *Microsoft Excel XP* and *Minpet* software with the help of Saltykova A. (VSEGEI).

5) Design of the manuscript.

The text was written with *Microsoft Word 2000* and *XP*. Tables and some diagrams were compiled with *Microsoft Excel 2000* and *XP*. Some diagrams and all other figures were drawn and designed with *Corel Draw 11* and *13*, *ACDSee 7.0* and *Photoshop CS*. Final compilation and publication of the manuscript was released with *Adobe Acrobat Professional 7.0*.

PART 1
REGIONAL GEOLOGICAL
REVIEW

PART 1. REGIONAL GEOLOGICAL REVIEW.

1. Geological structure of the Ladoga region.

The Baltic (Fennoscandian) Shield is an exposed part of the East-European craton, and represents an assemblage of Precambrian domains that show a generally decreasing age from Archaean in the northeast to Neoproterozoic/Riphean to the southwest. The oldest known rocks are 3.5 Ga granulite facies trondhjemitic gneisses in the Pudasjarvi Complex in Finland (Huhma et al, 2004) and the Vodlozero domain in Russia (Gorbatshev and Bogdanova, 1993; Glebovitsky, 2005). The last major crustal forming event took place in the Upper Riphean (about 0.9 Ga) in the southeastern part of the Scandinavian Peninsula, although the Paleozoic Caledonian Orogeny caused significant tectonometamorphic reworking of the western margin of the Shield.

The Ladoga region is of particular interest in that occupies a key position at the intersection of two regional tectonic zones – the Raahe-Ladoga zone and the Baltic-Mezen belt (Appendix to the Part 1, fig. 1). The first one corresponds to the boundary between the Archaean Karelian and the Palaeoproterozoic Svecofennian cratons, the second – to the southern part of the Baltic Shield.

Because of its location, the Ladoga region is geologically very complex, with multiple crust-forming and reactivation events since Archaean time. The extensive Mesoproterozoic (Riphean) Pasha-Ladoga basin occurs in the central part of the Ladoga region. To the south the older basement is covered by gently dipping Vendian-Palaeozoic sediments of the East-European platform.

The crystalline basement of the Ladoga region can be divided into three zones related to different geological units of the Baltic Shield (Appendix to Part 1, fig. 2 a):

- the Karelian domain of Archaean age basement, locally overlapped with Palaeoproterozoic syncline formations;
- the heterogeneous Raahe-Ladoga zone composed of Archaean-Palaeoproterozoic formations;
- the Palaeoproterozoic Svecofennian domain.

Inasmuch as the region considered here includes only parts of these geological units, they will be referred to in this study as the Karelian, Raahe-Ladoga and Svecofennian “domains” respectively. As the Karelian domain is located towards the northern margin of the study area and is essentially devoid of interesting uranium anomalies, it will be described here

only briefly, while the Svecofennian domain and in particular the Raahe-Ladoga domain, which represents the main focus of research, will be treated more extensively.

Generalized geological column of the Ladoga region is presented in the figure 3 of Appendix to Part 1.

1.1. The Karelian domain.

According to geophysical data (Sharov, 1993; Khazov et al., 2004; Shustova, 1997; Isanina, 1988; Isanina, 2001), the thickness of the crust in the Russian part of the Karelian craton is 40 km on average, with a general tendency to increase towards the SE. Near the Raahe-Ladoga domain the crust is up to 45 km thick (Luosto, 1997) and consists of a predominantly granitic upper crustal layer 10-12 km thick, underlain by a dioritic layer 15-25 km thick, and a lower crustal mafic layer from 10-15 km in thickness (Appendix to Part 1, fig. 4). The south-eastern limit of the Karelian craton is defined by the NW-SE trending Janisjarvi fault zone.

The oldest rocks in the Karelian craton are within the Vodlozero domain, located to NE and the Iisalmi and Koitelainen domains, to the NW of the study area. These oldest rocks consist of Mesoarchaeon, locally Palaeoarchaeon (Saamian), high metamorphosed amphibolites and calc-alkaline tonalite and trondhjemite gneisses with ages greater than 3.2 Ga. Gneisses from the Vodlozero domain have yielded an age of 3500 ± 90 Ma (Sergeev et al., 1990). The Palaeoarchaeon and Mesoarchaeon rocks are generally only weakly mineralized, and uranium concentrations are only 0.5 ppm on average (Mikhailov et al., 1999).

Neoarchaeon (Lopian) rocks typically form elongated N-S trending greenstone belts consisting of mica-quartz-feldspar schists and amphibolites, intruded by various granitoids with ages between 2.89-2.74 Ga (Rybakov and Golubev, 1999). The southern parts of two such greenstone belts lie within the studied area, namely the Ilomantsi-Jalonvara and Hautavaara belts, while the Segozero trough is located some distance to the northwest (Appendix to Part 1, fig. 2.b).

The Jalonvara (or Ilomasi-Jalonvara) greenstone belt consists mainly of metasediments and metavolcanics of andesitic-basaltic and dacitic composition, with some komatiites in the northernmost part (Sorjonen-Ward, 1993). Reported ages for the Jalonvara rocks are between 2995-2865 Ma (Rybakov and Golubev, 1999), while volcanic and plutonic rocks in the Ilomantsi part of the belt are mostly in the age range 2755-2725 Ma (Vaasjoki et al., 1993). Polymetallic mineral deposits are present in the Jalonvara area, including several occurrences of Mo, W, Cu, Au mineralization associated with granitoids intruding the volcanic rocks.

The *Hautavaara greenstone belt* is composed mainly of metavolcanics belonging to the komatiite-basalt and andesite-dacite series, dated at 2995 ± 20 , 2921 ± 55 and 2854 ± 14 Ma (Svetov, 2004). Subordinate metasediments (sometimes graphite-bearing) occur as well.

The Archaean structure of the Karelian craton is both partially obscured and complicated by unconformably overlying sequences of Paleoproterozoic sedimentary and volcanic rocks, occurring as erosional outliers and fault-bounded basin remnants. These Sariolian, Jatulian and Ludicovian sedimentary and volcanogenic units were metamorphosed from greenschist up to amphibolite facies during the Paleoproterozoic Svecofennian Orogeny. The largest of these Paleoproterozoic structures is the *Zaonegskaya Synclinorium*, located to the northeast of the study area. The northern part of the *Zaonegskaya Synclinorium* contains numerous deposits enriched in noble metals, uranium and vanadium, including the Padma group deposits, Czarevskoye and Kosmozerskoe. These deposits show a distinct structural localization within ductile and brittle dislocations – so-called “SDD (structure-discontinuity dislocation) zones” - in narrow NW-SE trending anticlinal hinge zones. In the southeastern part of the Onega area Ludicovian and Archaean formations are overlain by Kalevian-Vepsian sediments and mafic volcanics of the *Prionejskaya depression*. All these formations are in turn intruded by the Ropruchei mafic sill, which has been dated at 1.77 Ga (Bogdanov et al., 2000). Carbonaceous Vepsian sandstones host the small Pticefabrika uranium deposit and the Rybreka uranium ore-showing, which is located within fractures in the mafic volcanics. The southern part of the Prionejskaya depression is covered by younger, unmetamorphosed platform sandstones of uncertain, though probably Riphean, age.

The Paleoproterozoic *Tulomozero depression* occurs at the margin between the Karelian craton and the Raahe-Ladoga zone (fig. 1.2.b) and lies along the continuation of the N-S trending Murto-Kudongupskaya tectonic zone, which is considered to have been episodically active between at least 2.7-1.2 Ga, and was the presumed locus of a Svecofennian aulacogen. The Tulomozero depression is filled with mafic volcanics, carbonates and metapelites of Jatulian and Ludicovian age, with uranium contents varying from 1.3 to 2.4 ppm. An E-W striking fault zone cutting the Archaean and Jatulian formations of the western limb of the Tulomozero inlier hosts the small and complex (Au, Cu, Pb, Zn) Faddein-Kelya deposit of complex ores (Au, Cu, Pb, Zn) with superimposed uranium mineralization.

A number of Proterozoic intrusions cut the Archaean basement of the Karelian craton. Near the Raahe-Ladoga domain, small mafic intrusions are mostly of Jatulian and Ludicovian

age. Apophyses of the Lower Riphean Rapakivi Salmi massif intrude the Karelian craton as well as the adjacent Raahe-Ladoga domain; the Ulalegi massif is the latest of these intrusions.

Farther to the south the Precambrian rocks of the Karelian craton are concealed by the Vendian-Paleozoic sediments of the East-European platform.

1.2. The Raahe-Ladoga domain.

1.2.1. Tectonic and metamorphic structure.

The Raahe-Ladoga Zone (known variously as the Ladoga-Bothnian belt or zone, the Svecokarelian fault zone, or in Sweden as the Luleå-Jokkmokk zone) is an elongated narrow tectonic belt between the Archaean Karelian and the Paleoproterozoic Svecofennian cratons (Appendix to Part 1, fig. 1). The zone can evidently be traced southeastward from the Caledonian thrust front in Norway, as far as the southeastern Ladoga region, where it disappears beneath the East-European platform cover. However, Raahe-Ladoga Zone can be traced by geophysical means both further to the NW beneath the Caledonides and to the SE as far as the Rybinskoe reservoir. The width of the Raahe-Ladoga zone varies, but in the Ladoga region it reaches 70-90 km. In the northern Ladoga region, the northeastern boundary of the Zone is defined by the Janisjarvi fault, while the southeastern margin corresponds to the Meeri Thrust. In the southeastern part of the Ladoga area the precise location of the boundary is uncertain, due to deep burial beneath Riphean-Paleozoic sediments. It is worth noting here that Skorospelkin (2002) proposed locating this margin further to the west, to including the Pasha Graben entirely within the Raahe-Ladoga domain.

The deep crustal structure beneath the Raahe-Ladoga zone in the Ladoga region is characterized by steep NE-dipping features, beneath the Karelian domain. Isotopic indications of contamination of different intrusions located in the Northern Ladoga area (the Salmi massif, the Valaam sill) by Archaean material suggest that the Archaean lithosphere underlies Palaeoproterozoic one in this area (Rämö, 1991 and 2001; Amantov et al., 1996).

The crustal thickness is 45 km in average, with a tendency to thicken westwards. Instead of a granitic composition, the upper crust is mainly dioritic (Appendix to Part 1, fig. 4), while a mafic layer is distinguished below 35 km (Shustova, 1997).

The upper 15-20 km is composed of heterogeneous metamorphosed rock units of Archaean and Palaeoproterozoic age. In the Raahe-Ladoga domain, the metamorphic grade of the basement units tends to increase from greenschist facies (quartzites) in the Janisjarvi pericratonic depression to upper amphibolite facies (garnet-cordierite gneiss), close to the Meeri

thrust zone at the border of the Svecofennian domain (fig. 1.1). The following characteristic mineral parageneses have been distinguished within the different metamorphic zones of the Northern Ladoga area (Baltybaev et al., 2000):

- 1) greenschist facies – $Bt+Chl+Qtz+Pl\pm KFsp\pm Ms\pm Grt$;
- 2) staurolite subfacies – $Bt+Qtz+Pl+Ms\pm St\pm And\pm Grt\pm Cum$;
- 3) biotite-sillimanite subfacies – $Grt+Bt+Qtz+Pl+Sil\pm Ms$;
- 4) garnet-cordierite subfacies – $Grt+Bt+Qtz+Pl+Crd+Sil$.

The Raahe-Ladoga domain can be subdivided into several structural units as follows, each with its own specific geological features: the Janisjarvi syncline, the Ruskeala anticline, the Salmi massif, the Sortavala, Ljaskelja, Impilakhti-Pitkjaranta and Svir blocks (Appendix to Part 1, fig. 2 b).

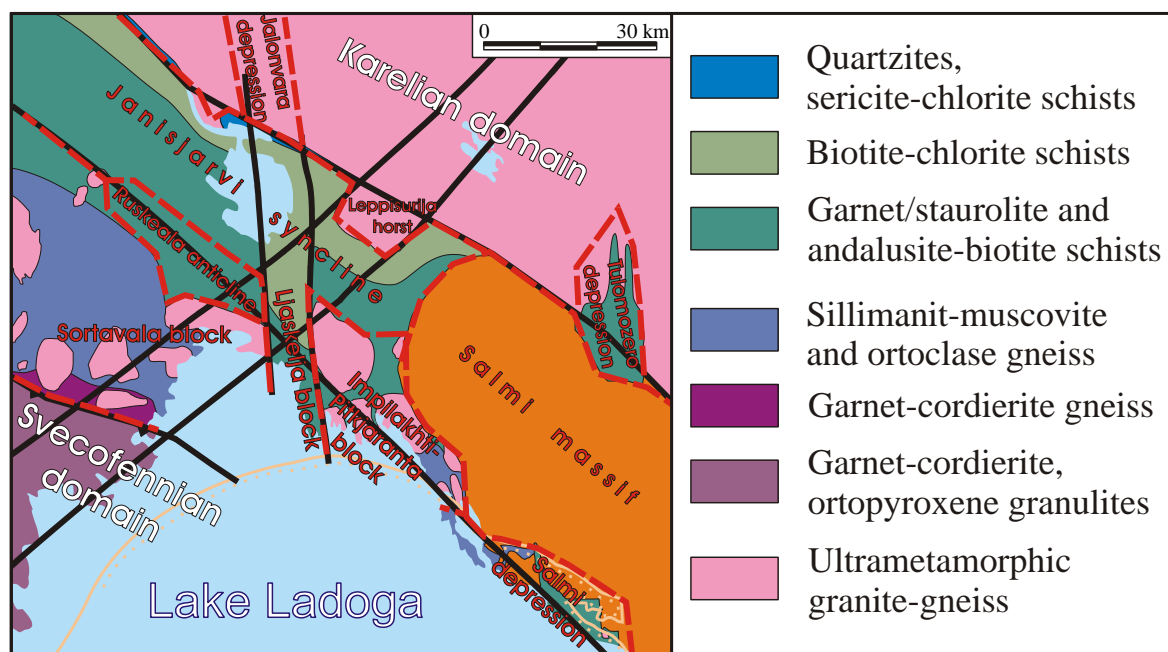


Figure 1.1. Map of metamorphic zoning of the Northern Ladoga area.

The Janisjarvi syncline (depression) is a pericratonic trough between the Ruskeala and Janisjarvi fault zones, at the southwestern margin of the Karelian domain. It consists mainly of Kalevian sediments of low- to intermediate metamorphic grade (Ladoga group, Kontiosaari, Naatselka, Pyalkjarvi, Hunukki, Velimyaki suites). In the pericratonic zone several separate depressions occur, separated by domal axial culminations exposing basement gneisses and granitoids. The cover rocks within the Vyartselya, Maloye Janisjarvi and Leppyasurja depressions consist of Jatulian (Jangozero and Tulomozero suites) and Ludicovian (Sortavala group, Soanlakhti suite) terrigenous and shallow marine deposits and mafic volcanogenic rocks,

with relatively low metamorphic grade. The axis of the trough generally trends NW-SE with an increasing thickness towards the SE, with some deflection in its southeastern part around the basement uplift between the Kokkoselka dome and the Leppyasurja horst of the Karelian domain. East from this uplift, the axis of the trough dips towards the south-east until it is truncated by the Salmi granite intrusion. The NE limb of the syncline dips to the SW at an angle of 70-80°, and is complicated against the Leppyasurja domal culmination, where dips are less steep, being to the south at angles from 45° to 70°. The SE limb is steeply overturned, with a dip of 60-80° to the southwest. There are many local elongated synclinal and anticlinal folds of different size (up to 1×10 km) along the trough, mostly trending NW-SE. A large N-S trending syncline (5-7 km across) occurs in the vicinity of the eastern shore of Janisjarvi Lake. East from the Kokkoselka-Leppyasurja uplift, the wavelength of local folds increases and strike trends become more E-W. In the vicinity of the Salmi massif, the folding is very complex, with strong variations in fold trend and plunge.

The Ljaskelja block is a tectonic inlier located along the continuation of the Jalonvara greenstone belt of the Karelian craton and is bounded to the west by the meridional Janisjoki Fault, and to the east by the Kokkoselka Fault. Where outcropping the block is composed of Ladoga group flysch formations (mainly metaturbidites, with some additional taphrogenic material). Metamorphic grade increases towards the shore of Ladoga Lake, and mafic to intermediate volcanics with increased alkalinity occur, including the Velimyaki gabbro-monzonite-diorite and the Impiniemi granitoid massifs in the southern part of the block.

The Ruskeala anticline strikes NW-SE along the fault zone of the same name with a southwards deflection in its southern part. The hinge zone is structurally complex, although plunges are generally to the NW. The anticline is steeply overturned, with both limbs dipping 60-80° to the south-west. The anticline has a length of about 35 km and a width of 1.5-6 km. Its core is composed of Ludicovian carbonate and volcanogenic formations (Archaean gneisses are inferred to be present at the base), with overlying Kalevian sediments and volcanics preserved on the limbs. Some narrow smaller synclines (mainly striking NW-SE, with limbs dipping 10-80°) composed of Kalevian sediments occur in the central part of the Ruskeala anticline. The Kalevian sediments on the anticline limbs are intensively tectonized and folded in the vicinity of the Matkaselka and Kaalamo intrusive complexes.

The *Sortavala* and *Impilakhti-Pitkjaranta* blocks are characterized by the presence of numerous domal structures composed of Archaean-Palaeoproterozoic gneisses and amphibolites. There are a total of about 20 domes in the Northern Ladoga area, varying in size from 0.3-0.5 to 8-10 km²; the domes tend to decrease in size and become more closely spaced towards the SE. With a few exceptions, notably Kirjavalakhti and Jokiranta, the domes are elongated in a meridional direction. NE-directed stresses during convergent deformation resulted in inverted (60-85°) dips of the northern contacts of many of the domes, particularly within the Sortavala block. Conversely, southern contacts usually dip to the south at highly variable angles (40 to 85°).

Dome uplifts are surrounded by Ludicovian strata (Sortavala group, Pitkjaranta suite carbonate, volcanogenic and subordinate terrigenous rocks). The Kalevian terrigenous formations (Ladoga group) occupy the interdome synformal depressions. In the Impilakhti-Pitkjaranta block they comprise a rather monotonous rock association of metapelite and metapsammities with rare intercalations of carbonate schist (Impilakhti suite). In the Sortavala block, the Kalevian association is complicated by late folding and metamorphism and its subdivision is tentative. In the present work they are therefore classified as an undefined Ladoga group. Metamorphic grade increases from NE to SW in both blocks, but in the Sortavala block the grade is higher, up to garnet-cordierite gneiss near the Meeri thrust zone. Ductile deformation in the Impilakhti-Pitkjaranta block is manifest as synclinal-anticlinal fold pairs concordant with the domes and by complex deformations in other tectonic zones. Within the Sortavala block, isoclinal folds and other cover structures with a general NE vergence are typical, and not merely restricted to the vicinity of domes.

There are numerous small intrusions of the Svecofennian synorogenic granodiorite at Impiniemi and of the late-orogenic leucogranitic Pitkjaranta complexes in the Impilakhti-Pitkjaranta block. Moreover, the eastern part of this area is occupied by the Lower Riphean Salmi granite intrusion, with numerous related pegmatites, skarns and greisen. The Lower-Middle Riphean Hopunvaara gabbro-diabase stock also occurs in the eastern part of this block. Numerous Svecofennian orogenic intrusions of varying composition are present within the Sortavala block, the most significant being the Kaalamo pyroxenite-gabbro-diorite complex and the Matkaselka and Latvasursky granite complexes. A Riphean gabbro-diabase dyke complex occurs in the Sortavala area. Migmatization and granitic veins are widespread in both blocks, but are more typical of the southern part of the Sortavala block, within a zone of high-temperature metamorphism near the Meeri thrust.

The *Salmi basin* occurs in the southeastern part of the Impilakhti-Pitkjaranta block. The basement of this depression consists of the same kinds of metamorphic rock units described above, in part intruded by the Lower Riphean Salmi rapakivi granite massif. Volcanogenic and sedimentary basin fill will be described in the section below devoted to the Riphean basin and in Chapter 2 devoted to the Karku deposit.

The Svir block is covered with Vendian and in part Palaeozoic sediments and consequently its structure is uncertain. It is supposed to be similar to the Impilakhti-Pitkjaranta block, differing only in that Ludicovian rocks are more extensively developed. The Riphean Pasha graben is present in the southwestern part of the block. According to geophysical and drilling data, crystalline units beneath the Pasha graben sediments are partly cut by the Oyat granite intrusion, which is assumed to correlate with the Lower Riphean rapakivi intrusions. The southern part of the Svir block corresponds to a fault zone concealed by the Riphean and Vendian and Paleozoic sediments. According to Skorospelkin (2002) the boundary between the Raahe-Ladoga and the Svecofennian domains in the southern Ladoga area would be 20-30 km to the southwest of the Pasha graben.

The Salmi rapakivi massif, which occupies a significant part of the north-eastern part of the Ladoga region, will be described below, in the section devoted to the magmatism.

1.2.2. Lithology.

The lowermost structural levels of the Raahe-Ladoga domain are represented by specific granite-gneiss domes. The most typical rock types within the domes are gray plagiogranite-gneisses and pink plagioclase-microcline granite-gneiss. Archaean isotopic ages of 2.7 Ga have been obtained for zircons from gneisses within the domes (Tugarinov and Bibikova, 1977). There are also diverse Palaeoproterozoic rocks within the domes, including abundant concordant and discordant amphibolite bodies; Svecofennian granites and migmatites are widespread as well. The proportion of Archaean to Palaeoproterozoic material varies from dome to dome and has not been quantitatively defined. Therefore the granite-gneisses of the domes are usually referred as undifferentiated *Archaean-Palaeoproterozoic*.

The lowermost Palaeoproterozoic crystalline units occur along the pericratonic Janisjarvi fault zone where they overlie Archaean basement of the Karelian domain, either unconformably or with tectonic contact. In the study area they are present in several separate depressions,

namely (from NW to SE) the Vyartselya, Maloye Janisjarvi, Leppyasurja and Tulomozero depressions. At the very base of the succession, a thin layer (< 50 m) of conglomerates, inferentially of *Sariolian* age (Seletskaya suite) is locally present. These rocks are overlain by *Jatulian* formations of the Onega group, which in this area consists of two units: the lower Jangozero and upper Tulomozero suites. The *Jangozero suite* (thickness up to 800 m) is composed of quartz conglomerates, quartzites, and in the upper part, arkoses. The *Tulomozero suite* (up to 200 m thickness) consists of dolomites, dolomitic marbles, phyllites and tholeiitic basalts.

Ludicovian units of the Raahe-Ladoga domain are presented by the Soanlakhti and Pitkjaranta suites of the Sortavala group. These suites are considered as coeval and lateral correlatives, but represent different facies and compositions, deposited in different areas.

The Soanlakhti suite overlaps eroded *Jatulian* formations in the pericratonic zone along the Janisjarvi fault. It consists of chlorite-mica schists with dolomitic interlayers. Carbonaceous (graphite) schist intercalated with mafic lavas occurs in its upper part. The total thickness of the suite is up to 950 m.

The Pitkjaranta suite occurs to the south of the Janisjarvi syncline, surrounding the granite-gneiss domes and forming the core of the Ruskeala anticline. It tends to decrease southwards in thickness, from a maximum of more than 1900 m to the north of the Kokkoselka dome and in the central parts of the Ruskeala anticline, but less than 600 m along the northern shore of Lake Ladoga. Further south, in the area surrounding the Karku deposit, the Pitkjaranta suite has a thickness of about 180 m only. Four subsuites have been recognized, (Akromovskii et al., 2000), the first of which directly overlies the Archaean-Palaeoproterozoic gneisses of the domes. However, due to overprinting by deformation and metamorphism, the precise nature of the contact is obscure, although the lowermost sediments consist of arkosic metapsammites. The uppermost part of the first subsuite is composed of carbonate rocks (also referred to as the “lower carbonate horizon”), with some volcanoclastic intercalations. The second and third subsuites are composed of volcanogenic rocks (ortho-amphibolites), separated from one another by an interval of carbonate schist. Rare intercalations of siliceous and graphite-bearing rocks occur between volcanogenic units. The fourth, uppermost subsuite is composed of carbonate rocks interbedded with mica-amphibole and biotite-quartz schists, locally containing graphite (“upper carbonate horizon”).

The *Kalevian* formations are represented by terrigenous sediments of the Ladoga group. Sedimentation occurred during lower Kalevian, until about 1.89 Ga, when orogenic deformation commenced, followed by uplift. According to different estimates, the total thickness of the Kalevian supergroup varies from 3 000 (Akromovskii et al., 2000) to 10 000 m (Ojakangas et al., 2001). The sediments occupy synformal depressions between domes and are generally interpreted as metaturbidites. Basal conglomerates of the pericratonic depression on the northeastern limb of the Janisjarvi syncline indicate a cratonic source for the Kalevian sediments and their deposition at a rifted or passive continental margin.

There are two different types of Kalevian sedimentary sequences in the Ladoga group: the Janisjarvi and the Impilakhti (Bogdanov et al., 2000) sequences. Correlation between them is uncertain.

The *Janisjarvi* sequence was mapped mainly in the Janisjarvi syncline and in the Ljaskelja block and consists of, in ascending order:

1. *The Kontiosaari suite*: quartz conglomerates, quartzites, overlain by quartz-biotite schist, phyllite; total thickness = 400 m.
2. *The Naatselka suite*: coarsely rhythmic two mica schists, rarely quartzites; thickness = 1000-1150 m.
3. *The Pyalkjarvi suite*: finely rhythmic quartz-biotite schist. Garnet, staurolite, andalusite, sillimanite and cordierite appear in the south with increasing metamorphic grade. The thickness of the suite is 1150-1250 m.

The *Impilakhti* sequence was mapped between the gneiss domes in the Impilakhti-Pitkjaranta block and consists of:

1. *The Impilakhti suite* with quartz-biotite, biotite schists (usually graphite-bearing), quartzites with garnet-biotite schist interlayers. Rocks of this suite usually lack distinct rhythmic layering. The thickness of the suite is 600-800 m.
2. *The Hunukki suite* with coarsely rhythmic quartzite-sandstones (coarse/fine grained variations), with sporadic trachyandesite intercalations; the latter have been dated at 1883 ± 6.7 (Bogachev, 1999). The thickness of the suite is 1000 m.
3. *The Velimyaki suite* is composed of metaturbidites, with variable grain size, from gritstone to siltstone and argillite, metamorphosed to garnet- and staurolite-bearing schists. Typically, rocks of the suite show graded bedding, with cross bedding, and slumping features. Syngenetic breccias, neptunic dykes and metamorphosed limestone concretions are also present. The thickness of the suite is 1200 m.

Subdivision of Kalevian of northwestern part of the area is the subject of considerable debate and is therefore classified in the present work as undifferentiated Ladoga group.

1.3. The Svecofennian domain.

The Meeri thrust zone defines the northeastern boundary of the Svecofennian domain in the northwestern part of the Ladoga area; in the southern Ladoga area this boundary is buried beneath a thick Riphean to Paleozoic sedimentary cover sequence. This boundary also coincides with a change in structural style, with the typical domal structure of the Raahe-Ladoga zone being absent from the Svecofennian domain. The continental crust in the Svecofennian domain is entirely of Palaeoproterozoic age and no Archaean rocks have been found (Huhma, 1986). The crust of the Svecofennian domain in the study area has a thickness of 45 km on average, but is about 40 km thick beneath the Wiborg rapakivi massif (Haapala et al., 2005). There is no sharply defined transition between the granitic and dioritic crustal layers, but it is considered that the thickness of the granite layer is less in the northern part of the domain (Isanina et al., 2001). Mantle upwelling, recognized in the northwestern part of the Ladoga Lake depression (Gintov et al., 1987; Khazov et al., 2004), is responsible for the anomalous heat flow, occurring in the Valaam archipelago area. Farther to the SW, a large part of the upper crust consists of the rapakivi granites of the Wiborg massif.

In contrast to the metamorphic zoning of the Raahe-Ladoga domain, the regional metamorphism associated with the Svecofennian domain is rather monotonous and corresponds to high-grade amphibolite and granulite facies. Variations in metamorphic grade are however locally present in local tectonically controlled retrograde deformation zones. Migmatized garnet-bearing gneisses are the most typical rock types of the Svecofennian domain, with typical prograde mineral paragenesis being: Grt+Bt+Pl±Kfsp±Qtz, Grt±Crld+Sil+Bt+Pl±Kfsp±Qtz±Sp, Grt+Opx+Bt+Pl±Kfsp±Qtz. Retrograde assemblages typically contain Ms, And, Cm and Chl.. Less common rock types include hypersthene and two-pyroxene gneisses with biotite, hornblende and (or) cummingtonite, hornblende and hornblende-cummingtonite amphibolites, and calcareous rocks with variable paragenesis: Calc±Hbl±Cpx±Ca±Grt±Sc±Ep±Tit±Bt±Pl(Lb-Byt)±Qtz (Baltybaev et al., 2000).

Because of strong metamorphism and migmatization, the identification of the nature of the protoliths and their stratigraphic position are very difficult. It is presumed that the crystalline formations of the Svecofennian domain are related to Kalevian sedimentation (not earlier than 1.89 Ga) (Shuldiner et al., 1999).

Based on observed differences in basement lithological composition, the Svecofennian domain can be subdivided into two parts: the northern and the southern parts, usually referred to as the Lahdenpokhya and Priozersk subdomains correspondingly, separated by the NW-trending Priozersk fault (Shuldiner et al., 1999; Baltybaev et al., 2000). Because the present review also includes the Southern Ladoga area, which is covered by more than 250 m of Vendian and Paleozoic sediments, different terminology will be used here; accordingly the northern subdomain is called Lahdenpokhya-Hiitola, while the southern is the Petersburg subdomain.

The Lahdenpokhya-Hiitola subdomain

The northern boundary of the Lahdenpokhya-Hiitola subdomain corresponds to the Meeri thrust zone. Svecofennian formations have been overthrust onto the heterogeneous basement of the Raahe-Ladoga domain and underwent intensive migmatization. The southern boundary of the Lahdenpokhya-Hiitola subdomain is the Priozersk fault. According to the deep seismic data, there is a mantle upwelling under this subdomain (Gintov et al., 1987; Khazov et al., 2004). The basement in the southwestern margin of the Pasha graben and in the Southern Ladoga region may also possibly be correlated with the Lahdenpokhya-Hiitola subdomain.

The Lahdenpokhya-Hiitola subdomain is composed of undifferentiated Ludicovian-Kalevian Lahdenpokhya gneisses and migmatites. On this basis of lithological similarities, these rock units are considered to mainly correlate with the Kalevian Ladoga group of the Raahe-Ladoga; relict rhythmic sedimentary layering can be distinguished and subordinate calc-alkaline volcanics occur. The main differences are the higher grade of metamorphism (up to low-pressure granulite facies) and predominance of greywacke with a calcic-sodic trend (Baltybaev et al., 2000). Intensively folded metabasalts discovered in the southern part of the subdomain have been interpreted as belonging to an ophiolite complex (Ivanikov et al., 1999). Migmatization is widespread, especially close to the Meeri thrust zone. A sodic composition for the migmatites is typical. Svecofennian early- and syn-orogenic I-type intrusions are more abundant in the Lahdenpokhya-Hiitola subdomain, whereas late- and post-orogenic intrusions are more common in the Petersburg subdomain (Baltybaev et al., 2000).

Based on variations in rock composition, the Lahdenpokhya-Hiitola subdomain is subdivided into two blocks: the Lahdenpokhya (southeastern) and the Isojarvi (northwestern) blocks (Appendix to Part 1, fig. 2 b). They are also well differentiated in gravimetric field: the Isojarvi block has a lower density (“felsic”) character, whereas the Lahdenpokhya block is more heterogeneous with high-density domains corresponding to the North-Western Ladoga mantle

upwelling and a more localized local low-density anomaly corresponding to the Tervus granite massif (Appendix to Part 1, fig. 5). The NE-SW trending Elisenvaara fault separates these two blocks.

The metamorphic complex of the *Lahdenpokhya block* is subdivided into 5 granulite-gneiss suites, based on the diagnostic presence of: biotite, garnet, diopside-biotite, diopside-garnet, cordierite and hypersthene-garnet. Biotite and garnet gneisses are derived from terrigenous clastic rocks and subordinate felsic volcanics; from the latter rocks, an isotopic age of 1883.3 ± 6.6 was obtained (Baltybaev et al., 2004). Diopside-bearing gneisses have had terrigenous and carbonate protoliths. The cordierite-bearing suite is composed of peraluminous gneisses, always with two feldspars and variable contents of cordierite, garnet, sillimanite and biotite. Hypersthene-bearing rocks correspond to metamorphosed volcanics of mafic and intermediate composition, and subordinate metagreywackes. It is assumed that the hypersthene-garnet suite is composed of younger rocks compared to the Northern Ladoga Kalevian formations, since it mainly consists of metavolcanics, for which no analogous rocks are found in the classical Ladoga group (Bogachev, 1999).

The Isojarvi block is the less studied because of poor exposure and its proximity to the national frontier. In contrast to the rock units of the Lahdenpokhya block, those of the Isojarvi block are less metamorphosed and migmatized and include sandstones, volcanoclastic deposits, carbonaceous aleurolite and quartzite, skarns, basalts and andesites, metamorphosed in upper amphibolite facies. In the southern part of the Isojarvi block metabasalts have been attributed to an ophiolite complex. In the adjacent Finnish territory, mica schist and gneiss alternating with amphibolite, felsic volcanics and graphitic schists have been mapped (Bogachev, 1999).

The Petersburg subdomain.

This subdomain occupies the western and southern parts of the Ladoga region and continues into Finland (the Tampere zone).

Although crystalline rocks of this subdomain are considered as of Kalevian age, rock characteristics differ from the contemporaneous sequences of the Northern Ladoga domain. The metamorphic grade in general corresponds to upper amphibolite and granulite facies with local evidence of diaphoresis. Primary depositional features are no longer preserved and highly calcareous rocks and metavolcanics are absent. Typical rocks are metapelites and moderately aluminous metapsammities with distinctly potassic compositional trends. An isolated occurrence of marble is present near the NE contact of the Wiborg rapakivi massif. In contrast to the

Lahdenpokhya-Hiitola subdomain, migmatites in the Petersburg subdomain are predominantly of potassic composition. A characteristic feature of this subdomain is the abundance of Svecofennian late-orogenic S-type granite intrusions. Post-orogenic intrusions are also common in the Petersburg subdomain, whereas early- and syn-orogenic I-type Svecofennian intrusions are less typical (Baltybaev et al., 2000). The extensive Lower Riphean Wiborg rapakivi massif occupies the southwestern part of this subdomain, intruding and underlying Palaeoproterozoic rock units for a distance up to 20 km from its exposed contact. The Riphean Priozersk and Simagina depressions occur in the western part of the subdomain, while the Pasha graben is located further to the southeast.

The Petersburg Subdomain can be subdivided into three blocks separated by E-W striking fault zones which are from the north to the south: the Priozersk, Vyborg and Southern blocks.

Adjacent to the Lahdenpokhya-Hiitola subdomain the *Priozersk block* is characterized by a high metamorphism grade (high temperature and low pressure granulites), the presence of short but thick bodies of orthopyroxene gneisses near its northern border and the prevalence of late-Svecofennian potassic granites.

The metamorphic grade of the basement rocks decreases toward the south; in the *Vyborg block* it corresponds to upper amphibolite facies. It is assumed that this block was downfaulted relative to the Priozersk one by the E-W striking Sukhodolje tectonic zone. Another indication of this displacement is the lower degree of erosion of the granite intrusions in the Vyborg and Southern blocks; the upper contacts have been recognized in drill cores in these areas (Caillat et al., 2002).

The *Southern block* is completely covered with a thick (> 250 m) succession of Vendian to Paleozoic sediments and its geological structure is therefore less well studied. Crystalline rock units resemble those of the Vyborg block and mainly consist of greywacke and pelite metamorphosed to upper amphibolite facies. The easternmost part of the block (east of the SE continuation of the Priozersk fault) is composed of less metamorphosed biotite schists. Late Svecofennian potassic granite intrusions in this area are represented by the Polyany and Chaplinsky complexes, the former being an analog of the Kuznechensky complex. The Chaplinsky granites, located further to the east, are more leucocratic and are comprise small intrusive bodies, probably analogous to the intrusions of the Matkaselsky complex. Gravimetric data show that they represent apophysis of deeper intrusions (Skorospelkin and Dolgushina, 2004). Correlation with other blocks is difficult. Its western part is assumed to be an analog of

the Vyborg block whereas the eastern part has been considered as either a continuation of its western part (i.e. Vyborg block), or as the western margin of the Raahe-Ladoga zone (Skorospelkin, 2002).

1.4. The Riphean basins.

A key geological object of the region is the vast (120×200 km) *Pasha-Ladoga sedimentary basin*, located at the intersection of the NW-SE and NE-SW trending faults of the Raahe-Ladoga zone and the Baltic-Mezen belt respectively. The basin is elongated parallel to the NW-SE trending faults which divide it into several uplifted and down-faulted blocks (grabens). The NE-SW trending Vaskelovo fault separates the basin into two parts which coincide with changes in the present day topography beneath Lake Ladoga as well as the basement morphology beneath the Riphean sediments. In the northern part of Lake Ladoga, the Quaternary surface topography is more dissected: numerous uplifts corresponding to islands (mostly resulting from the Vallaam sill gabbro) are separated by deep (down to 230 m) depressions with a NW trend (Rumyantsev, 2002). In general this relief reflects the Riphean unconformity surface in the Northern Ladoga region. Topographic relief beneath the southern part of the Lake Ladoga, which is underlain by Vendian to Cambrian sediments, is more subdued, with water depths less than 70 m. The most significant elongated depressions coincide to reactivated fault zones, mainly striking NW, representing continuations of the Priozersk, Sortavala, Ruskeala and other faults of the Northern Ladoga region, although some have N-S trends, being continuations of the Hautavaara and Jalonvara tectonic belts. The Riphean unconformity surface in the Southern Ladoga area is more complex (Amantov et al., 1996), including various steep down-faulted and locally uplifted blocks resulting from a combination of faults with predominantly NW and NE trends. There are three trough-like depressions striking NW beneath the eastern part of the lake; these combine further south into the Pasha graben, which continues under the platform cover for about 70 km to the south (the exact SE boundary of the graben is unknown). According to geophysical data, the total thickness of Riphean basin formations in the southern part of the Lake Ladoga is up to 2000 m, whereas in its northern part it is only 400-500 m.

The basin is filled with non-metamorphosed Riphean sediments and volcanites, lying unconformably over eroded basement formations. Lobaev (2005) has given a detailed description of the mineralogical and lithogeochemical characteristics of the Pasha-Ladoga basin formations and some of the underlying rocks, therefore only brief summary will be given here.

Most of the Riphean basin formations are either under Lake Ladoga, or concealed by Quaternary till and Vendian-Palaeozoic cover, and are not exposed, except for a single outcrop of Riphean basalts in the Tulema river rapids and several outcrops of sediments and volcanics or sills on islands within Lake Ladoga (Amantov et al., 1996)

There are five land occurrences of Riphean sediments in the Ladoga region:

- three sub-basins within the Pasha-Ladoga basin: the Priozersk, Salmi, and Pasha, sub-basins (depressions) located to the NW, NE and SE from the Ladoga Lake;
- the Ulja-Risti and Simagino depressions (basins), separated from the major basin and located to the NE and W respectively.

All these depressions, except the Pasha graben, are quite shallow, with the total thickness of the Riphean sequence being less than 400 m. The Pasha graben is a steeply bounded trough 60 km in width (the widest part being at the Ladoga Lake coastline) and about 70 km length (from the Ladoga Lake coastline to the poorly defined south-eastern margin). The graben is bounded by the Ruskeala and Priozersk faults, with a total preserved thickness of the Riphean sequence up to 1600 m. There is a local narrow tectonic uplift in the axial part of the graben.

It is probable that the original extent of the Riphean sedimentary basin was much greater; evidence to support this idea is given by the apparent parallelism of the Riphean layers imaged in the seismic data (Amantov et al., 1996). Indirect evidence for an initial upper level of erosion is the existence of swarms of Middle Riphean dykes in northeastern (Salmi massif) and northwestern (Sortavala area) parts of the Ladoga region.

Before describing the Riphean basin sequence, it is necessary to clarify some uncertainties with respect to stratigraphy. Traditionally (Bogdanov et al., 2000; Caillat et al., 2002; Skorospelkin, 2002), formations of the Pasha-Ladoga basin have been regarded as of Middle-Upper Riphean age, which means that sedimentation took place between 650 and 1350 Ma. However, age determinations from basaltic flows within the Salmi depression (1499±68 Ma, Sm-Nd analysis, Bogdanov, 2003) and of gabbro from the Vallaam sill, which intrudes basin sediments (1457±2 Ma, U-Pb dating of baddeleyite by Rämö et al., 2001) demonstrate that most of the sediments were instead deposited during the Lower Riphean. Accordingly, the present study adopts this revised age for the Riphean sequence, based the above results, as well as new data reported below from Riphean-hosted uranium mineralization. The previous stratigraphic subdivision will nevertheless be referred to as well.

The oldest Riphean sediments of this region are found in the *Simagino depression* (it is a conventional name proposed by author, because of absence of an official one). It is a narrow

trough located to the west of the area and closely related to a NW-trending fault. According to data from several drillholes, the trough is filled with quartzose sandstones and tuffaceous shales of uncertain stratigraphic affinity. Some researchers correlate these rocks with the *Hoagland suite*, which is, in turn considered to be Lower Riphean (Akromovskii et al., 2000) or Vepsian (Skorospelkin, 2002). Alternatively, it may be correlated with the Priozersk suite (Caillat et al., 2002). The former alternative is preferred here because the Simagino depression rocks differ from all other units in the Pasha-Ladoga basin yet seem to resemble stratotype of the Hoagland suite on, which takes its name from the island in the Gulf of Finland (Suursaari island in Finnish). The quartz- and feldspar phyric porphyry at the base of the Hoagland island sequence has an age of 1640 ± 11 and 1638 ± 4 Ma (Belyaev et al., 1998). The sediments referred to the Hoagland suite locally overlie the Wiborg rapakivi massif and consequently were deposited after 1615 Ma (Puura and Flodén, 1999).

The basal unit of the Riphean sequence of the Pasha-Ladoga basin is known as the *Priozersk suite* (traditionally attributed to Middle Riphean) (Appendix to Part 1, fig. 6). It consists of pink or beige quartz-feldspar coarse-grained sandstones, some gritstones, with local basal conglomerates and rare lenses of siltstone and mudstone. The thickness of the Priozersk suite varies from up to 250 m in the Priozersk depression in the Western Ladoga area, to over 450 m in the Pasha graben, while in the Salmi depression it is less than 80 m thick. The Ulja-Risti depression, located to the NW of the Salmi depression is very small (less than 2 km² in areal extent) and is inferred to contain Priozersk suite sediments, although the paucity of drill hole data make this difficult to confirm. The mean uranium content of the Priozersk suite sediments is 3.6 ppm, although it varies considerably at different localities, being 5.2 ppm in the Salmi depression, 2.5 ppm in the Priozersk depression, and 2 ppm in the Pasha graben (Skorospelkin, 2002).

In the Salmi and Pasha depressions, the Priozersk suite is overlain by the *Salmi* volcanogenic and sedimentary *suite* of Lower Riphean age (previously assigned to the Middle Riphean). The Salmi suite consists of two horizons of sub-alkaline basalts (the lower layer has also been assigned to the Priozersk suite, Skorospelkin, 2002), separated by a layer of quartz-feldspar sandstone. The total thickness of the suite in the Salmi depression is up to 250 m; in the Pasha depression the thickness is less certain, presumably about 300 m. Uranium abundances in Salmi sediments are on average 4 ppm, compared to 1 ppm in the basalts (Skorospelkin, 2002).

The Salmi suite is overlain by the *Pasha* terrigenous *suite*, which attains a thickness of 290 m in the Salmi depression, compared to only 150 m in the Pasha graben. In the Salmi

depression the sequence consists of interbedded quartz-feldspar sandstones, siltstones and mudstones with fine-grained varieties predominating. Coarse-grained sediments are more typical in the Pasha graben. The average content of uranium in the Pasha suite sediments is 3.6 ppm with enrichment up to 5.6 ppm in argillite layers (Skorospelkin, 2002).

In the Priozersk depression the *Priladojskaya suite* overlies the Priozersk sandstones and has a thickness up to 250 m. The age of the suite is uncertain, though more likely Middle than Upper Riphean. The lower part of the suite starts with a thick layer of basal conglomerates, followed by interbedded quartz-feldspar sandstone, siltstone and mudstone. The middle part of the sequence is composed of carbonate rocks (limestone and dolomite) with terrigenous interlayers, while the upper part of the suite is composed of sulfide-bearing gray-green siltstone and mudstone.

The Jablonovskaya suite overlies the *Priladojskaya suite*. In addition to the Priozersk depression, this unit is also locally present at the bottom of E-W trending depressions (corresponding to fault zones) in the western and central part of Lake Ladoga (Amantov, 1992). The sequence is composed of coarse-grained polymictic sandstones and tillite-like rocks. The age of the sedimentation is tentative, being either Upper Riphean (Caillat et al., 2002; Mikhailov, 2004), or more probably Lower Vendian, and was in part deposited during a glacial episode (V₁ Volyn series) (Amantov et al., 1996; Akromovskii et al., 2000). Such sediments are also quite typical in the late Precambrian depressions of the Eastern European platform.

1.5. The platform cover.

The southern half of the region is covered by sediments of the East European platform, which form a monocline sequence dipping gently to the SE. The boundary between the uplifted Baltic Shield and the downfaulted East European platform occurs along the Baltic-Mezen tectonic belt, although no evident post Lower Vendian displacements have been identified along this zone – the platform sediments are essentially flat and undisturbed here (Amantov et al., 1993).

The lower unit of the platform cover sequence is composed of Upper Vendian sediments. They unconformably overlie lateritic paleoregoliths that developed over the basement and the Riphean formations. The basal unit is named the Redkino horizon (Akromovskii et al., 2000), although it is also sometimes known as the Gdov horizon (Skorospelkin, 2002). The lower part of the horizon consists of polymictic sandstone (up to 7 m thick), which is enriched in uranium to values of up to 1900 ppm. This sandstone is overlain by clays, which are sometimes

bituminous and pyrite-bearing (thickness 20-40 m). The Kotlin horizon overlies the Redkinsky unit; it has a similar composition but is up to 225 m thick.

The Palaeozoic sequence in the study area comprises Cambrian, Ordovician, Devonian and Carboniferous sediments. Lower Cambrian sediments conformably overlie Upper Vendian rocks and are mainly composed of clays with subordinate sandstone intercalations, and have a total thickness up to 140 m. There was a brief hiatus before deposition of Middle and Upper Cambrian sandstones, with intercalated clay layers. The thickness of these sediments is up to 30 m. The Lower Ordovician sequence is up to 32 m thick and is composed of sandstone and uranium-bearing *Dictyonema* shales (Tremadoc stage, Pakerortsky horizon), overlain by with glauconitic sandstone, clay, marl and limestone (Arenigian stage). The Middle Ordovician (Llandeilo stage) is represented by clay, marl and limestone with a thickness of up to 12 m. Upper Devonian sediments unconformably overlie the Ordovician rocks and consist of sandstone, clay, limestone, marl and dolomite of the Frasnian age. Carboniferous sandstone, siltstone, clay, limestone and bauxite occur in the very SE of the considered area.

1.6. Quaternary.

Quaternary sediments cover about 80% of the northern part of the Ladoga region and the entire southern part, with an average thickness of 30-35 m (up to 200 m in local depressions). There are no natural outcrops of Vendian or Paleozoic sediments, but basement rock units are relatively well exposed in the Northern Ladoga area. There are also a few outcrops of the Pasha-Ladoga basin Riphean formations in the Northern Ladoga area.

The Quaternary sequence consists of two layers of glacial and lake-glacial sediments separated by an interglacial horizon of bituminous clay and sand. The last moraine is dated at $21\ 880 \pm 110$ and $21\ 140 \pm 150$ years (Ekman et al., 1991). Recent soil formation has occurred on top of the moraine deposits.

1.7. Magmatism.

Magmatic rock units preceding the Svecofennian orogeny are confined to the Karelian and Raahe-Ladoga domains.

The earliest well-preserved record of magmatic activity occurs in the granite-greenstone belts of the Karelian craton. Andesite-basalt and dacite metavolcanics of the *Jalonvara trough* (2995-2865 Ma, Rybakov and Golubev, 1999) were intruded by the *Jalonvara granitoid massif*,

which is dated at 2600 ± 90 Ma (Ivaschenko and Ovchinnikova, 1988) and forms a NW-oriented elongate stock about 15 km^2 in extent, accompanied by numerous NW-striking granite dykes. The intrusion consists of multiphase and composed of: diorite and granodiorite, granite, porphyritic leucogranite, dacite and rhyolite (Ivaschenko and Lavrov, 1994).

The granite-gneiss domes of the Northern Ladoga region represent a specific group of rock units of with uncertain origin. Traditionally, all granite-gneiss domes of the Northern Ladoga area have been interpreted as autochthonous Archaean basement windows (Trustedt, 1907; Krats, 1963) or as allochthonous thrust sheets of Archaean basement (Sudovikov, 1954). Eskola (1948) proposed a the conception of diapir-like domal uplifts consisting of remobilized ancient granitoids. The youngest granites in the domes were attributed to syn-orogenic Svecofennian granitization (Saranchina, 1972; Nikolskaya and Gordienko, 1977). According to the research in recent decades, the central cluster of domes (Kirjavalakhti, Jokiranta, Kokkoselka, Impilakhti etc) are composed predominantly of Archaean protoliths (60-70 %), whereas those in the domes of the NW part of the study region (NW of Sortavala block) and Pitkjaranta district (Luppico, Ristiniemi, Uuksa etc) have greater proportions of Palaeoproterozoic components (Bogachev, 1999). In the present study, the domes to the NW of the Sortavala block are correlated with the early-orogenic Svecofennian Jakkima intrusive complex (see below), as also indicated on the most recent edition of the geological map of this area (Stepanov et al., 2006). The domes of the NW Ladoga area are nevertheless still classified as an undifferentiated Neoproterozoic-Palaeoproterozoic (AR₂-PR₁) granite-gneiss complex comprising tonalitic and plagioclase-microcline granitic gneisses, gneissic granites and subordinate amphibolites. Intensive migmatization is typical. Pegmatites and pegmatoids are widespread especially in the domes at the periphery of the Northern Ladoga area. Granitoids of the domes of this area include migmatites and anatectic granites combined under the name: *Kokkaselsky granite-migmatite complex* and referred to a formation. There are two main rock types in this complex:

- Pinkish gray to gray fine- to medium-grained, occasionally porphyritic biotite plagioclase-microcline gneissic granites, strongly recrystallized, sometimes blastomylonitic, with patches of pink pegmatoid granites in which biotite has altered to chlorite.

- Light-red medium-grained granites with less evidence of recrystallization and containing segregations of pink-gray and gray granites, with ovoid enclaves (skyalithes) of gneiss. Pegmatoid granite segregations and coarse-grained pegmatite veins are also typical.

A trend towards U and Th enrichment in the gneisses and granitoids has been distinguished toward from the central set of domes to its periphery (fig. 1.2). This might be due to the different intensity of anatexis during the Svecofennian orogeny, which was stronger in the peripheral domes, as is evident from the abundance of anatectic granites. It is significant too, that the Th-U ratio increases in the Impilakhti, Korinoya-Pitkjaranta and especially Mursula domes. Because these domes (and notably the Mursula dome) contain abundant uranium occurrences (mostly related to the intradome granites), this can be interpreted as result of the uranium redistribution during anatexis.

The earliest generation of pegmatites distinguished in the Northern Ladoga area is also considered to predate Svecofennian orogenic processes, occurring. They form thick veins inside the granite-gneiss domes, folded concordantly with enclosing metamorphic host rocks.

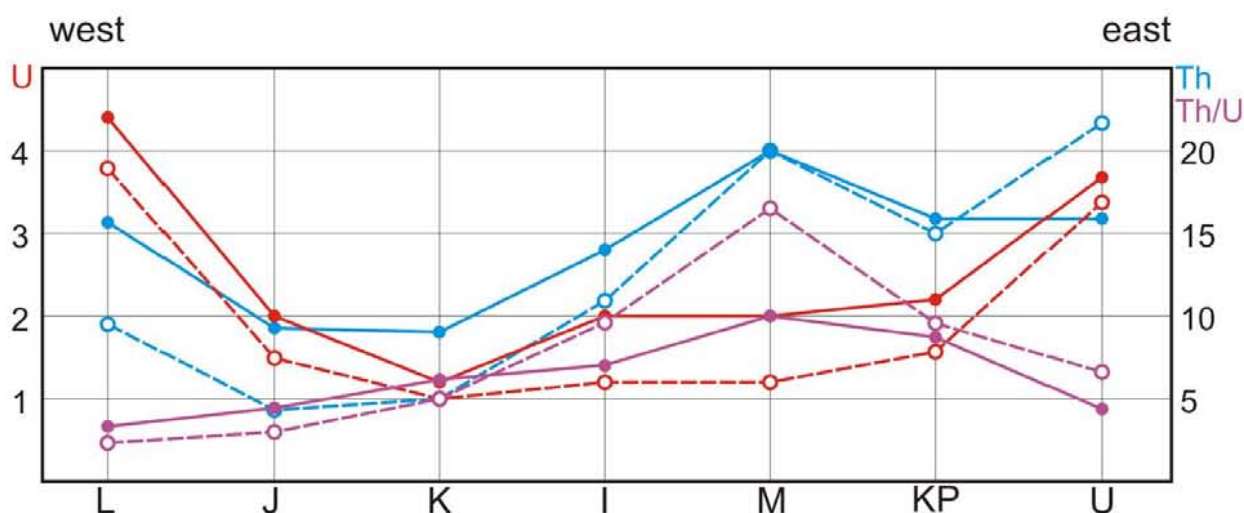


Figure 1.2. U and Th contents in the rocks of the granite-gneiss domes of the Northern Ladoga area (compiled from Gavrilenco, 1990; Grigorieva, 1977; Korotaev et al., 1978).

Empty circles – granite-gneiss, filled ones – granite. Names of the domes: L – Latvasurje, J – Jokiranta, K – Kirjavalakhti, I – Impilakhti, M – Mursula, KP – Korinoya-Pitkjaranta, U – Uuksa. Location of the domes see in the Appendix to Part 1, fig. 2 b.

The *Jatulian* magmatic rocks occur along the pericratonic Janisjarvi fault zone and are called the Vyartsilya-Kiihtelusvaara belt (Pekkarinen, 1979; Kolbantsev, 1994). They are represented by the mafic volcanites of the Tulomozero suite and gabbro-dolerite dykes. These dykes are mostly of Upper Jatulian age – 2150 ± 60 Ma (Akromovskii et al., 2000), although it is possible that the latest ones could be Ludicovian, Kalevian and, perhaps, Riphean too. Some of the dykes that are restricted to the Karelian craton may also be older, of Sumian and Sariolian age.

The *Ludicovian* magmatism is related to the rifting and extensional events that preceded Svecofennian orogenic deformation. Three magmatic complexes are distinguished (Bogachev, 1999):

- 1) trap metabasalts;
- 2) high-magnesium basalts and picrites;
- 3) ophiolite gabbro-basalts.

Metabasalts (orthoamphibolites) form the major part of the Sortavala group and consist predominantly of Fe-rich tholeiites, with magnesian basalts being less common. More silicic differentiates, corresponding to andesites, have been found at the northern margin of the Kirjavalakhti dome. Mafic sills and dykes co-magmatic with the basalts occur inside the granite-gneiss domes. Their primitive composition, relatively low REE content and uniformly negative ϵ_{Nd} demonstrate that these basalts were derived from depleted mantle magmas contaminated with Archaean crust (Bogachev, 1999). Trachyandesite from basal horizons of the Sortavala group volcanites was dated at 2000 ± 25 (Bogdanov et al., 2000).

Metabasalts and picrites related to the rifting and breakup of the Karelian craton, prior to the Svecofennian orogeny, have been mapped in the southern part the Sortavala block, close to the Meeri thrust zone (Svetov et al., 1990). They have predominantly high-Mg compositions and are enriched in LIL- and HFS- and LRE-elements that indicates their derivation from primitive mantle sources. A picrite dyke cutting the Sortavala granite-gneiss dome has been dated at 1995 Ma (Bogachev, 1999).

A gabbro-dolerite and pillow basalt complex was mapped locally around the Kirjavalakhti dome, including lava flows, dykes and sills with gradual contacts. The metabasalts discovered in southern part of the Isojarvi block are assigned to the same complex (Stepanov et al., 2006). The chemical composition and uniformly positive ϵ_{Nd} of these rocks correspond to low K-Ti tholeiites of MORB origin and in this respect they are analogous to volcanic rocks associated with the Jormua-Outokumpu ophiolite complex in Finland. An isotopic age of 1963 ± 19 Ma was obtained for a metadolerite dyke cutting the Sortavala dome, (Baltybaev et al., 2000). The same type of material within the Ludicovian amphibolites was dated at 1942 ± 12 Ma (Stepanov et al., 2006).

The Svecofennian orogenic event culminated in Upper Kalevian was very rich in respect of magmatic manifestations in the Ladoga region. The Raahe-Ladoga and Svecofennian

domains are saturated with numerous intrusions referred to this period (Appendix to Part 1, fig. 2 c).

The 1.9-1.89 Ga tonalite and granodiorite complex. The *Jakkima complex* is considered to be an analog of the early-orogenic Svecofennian tonalite-trondhjemite complexes in southern and central Finland. It consists partly of domal uplifts in both the NW Ladoga (Lahdenpohkya-Hiitola subdomain, Sortavala block) and NE Ladoga (Impilakhti-Pitkjaranta block) areas. The complex consists of two phases:

1) hypersthene-amphibole-biotite diorite, quartz diorite and tonalite forming the main part of the massifs;

2) porphyritic biotite tonalite-leucoplagiogranite, which occur as thick dykes

Granitoids of the Jakkima complex are referred to peraluminous field in the A/CNK diagram (fig. 1.3 a). For diorite of the Jakkima complex an isotopic U-Pb age of 1893 ± 5.2 Ma was obtained (Bogachev, 1999).

The 1.89-1.88 Ga gabbro, norite, pyroxenite, diorite, monzodiorite, tonalite complex. The clinopyroxenite-gabbro-norite-diorite-monzodiorite *Kaalamo complex* comprises a pluton some 70 km² in area, a series of smaller satellite intrusions and several isolated small plutonic bodies throughout the northwestern and northern Ladoga area, the Ruskeala anticline, the southern part of the Janisjarvi syncline, and the Isojarvi, Sortavala and Ljaskelja blocks.

The Kaalamo massif is located to the southwest of the northwestern part of the Ruskeala anticline. On the gravimetric map it corresponds to a high-density anomaly, consistent with a deep-rooted structure of mafic composition (Appendix to Part 1, fig. 5). The intrusion is discordant relative to the earliest folding event, but was apparently affected by later deformations and metamorphism (rocks are partly altered to amphibolites).

The earliest magmatic phases of the massif are olivine clinopyroxenites and melanocratic gabbros; they mainly occur as xenoliths in leucocratic gabbro-norite or in subordinate diorite and tonalite intruded during the subsequent phase. The latest phase is a plagiogranite-porphyry dyke complex, which transects all earlier rock types.

Enrichment of the mafic rocks of the main phase in LIL-elements, particularly Ba and Sr, and conversely, their depletion in Ti, Ta and Nb, are features characteristic of arc-related calc-alkaline basalts and andesites in active continental margins (Pearce, 1983). The age of the diorite in the Kaalamo intrusion is 1888 ± 5.2 Ma (Bogachev et al., 1999).

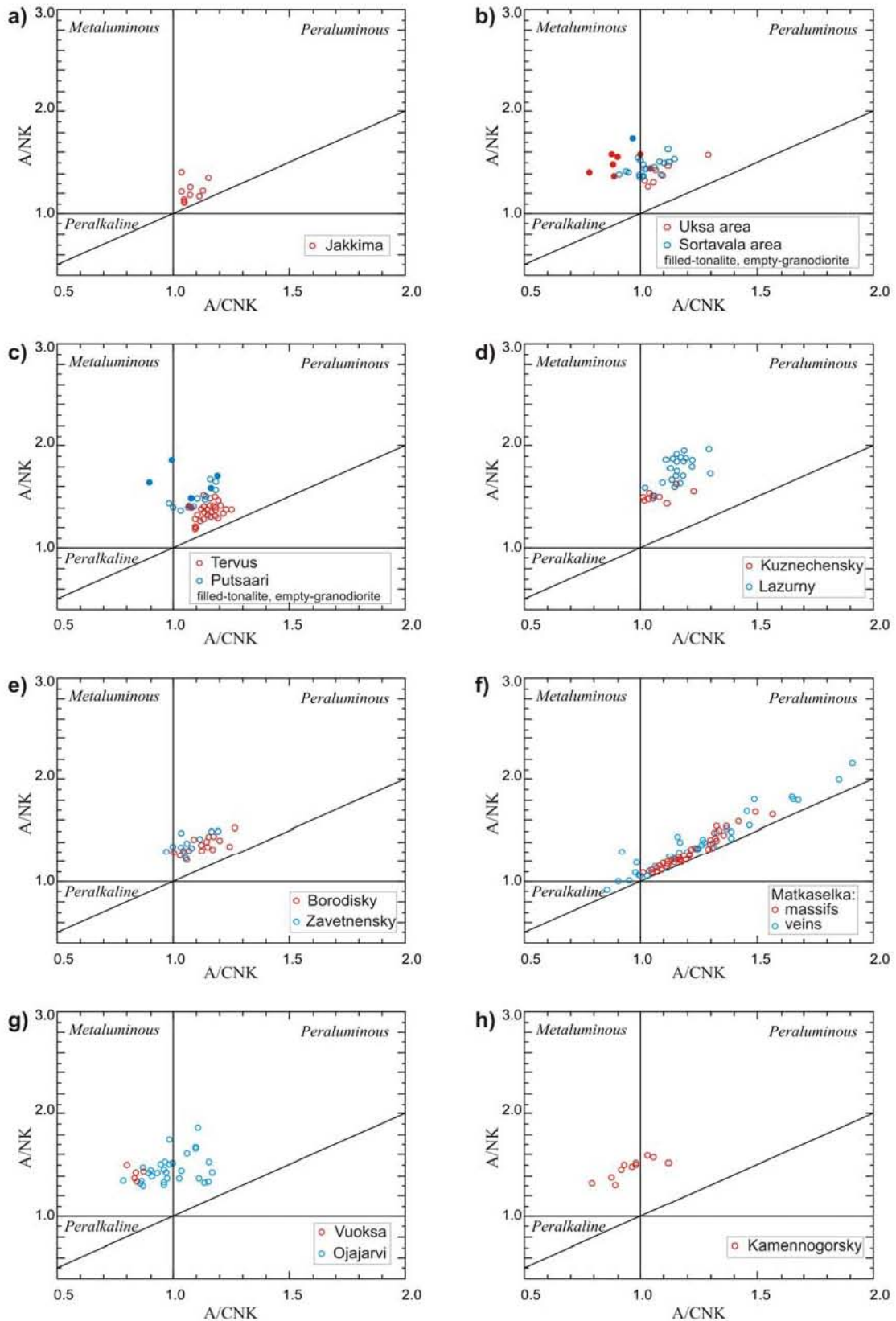


Figure 1.3. A/CNK diagrams (Manjar and Piccoli, 1987) for the granitoids of the Ladoga region (based on Bogachev, 1999 and Stepanov, 2006), plutonic complexes: a-Jakkima, b-Lavutsaari-Impiniemi, c-Tervus and Putsaari, d-Kuznechenoe, e-Borodinsky, f-Matkaselka, g-Elisenvaarsko-Vuoksinsky, h-Kamennogorsky.

The earliest magmatic phases of the massif are olivine clinopyroxenites and melanocratic gabbros; they mainly occur as xenoliths in leucocratic gabbro-norite or in subordinate diorite and tonalite intruded during the subsequent phase. The latest phase is a plagiogranite-porphry dyke complex, which transects all earlier rock types.

Enrichment of the mafic rocks of the main phase in LIL-elements, particularly Ba and Sr, and conversely, their depletion in Ti, Ta and Nb, are features characteristic of arc-related calc-alkaline basalts and andesites in active continental margins (Pearce, 1983). The age of the diorite in the Kaalamo intrusion is 1888 ± 5.2 Ma (Bogachev et al., 1999).

Another relatively large (10 km^2) intrusion of the Kaalamo complex, the Velimyaki massif, is located in the southern part of the Ljaskelja block. It is composed of wide spectra of rocks – from ultramafites to monzonites. The main part of the massif consists of monzodiorites and monzonites dated at 1891.7 ± 4.9 Ma (Bogachev et al., 1999). A subordinated gabbro has an age of 1893 ± 6 Ma (Lokhov et al., 2004). A small deposit of magnetite is related to the ultramafic sequence.

There are numerous hypabyssal dykes and small massifs of dominantly plagiogranite composition occurring from the south-eastern part of the Sortavala block (south of Sortavala city) to the central part of the Janisjarvi syncline (southern coast of lake Janisjarvi). These are known as the Suistamo complex of intrusions, with rock composition varying from gabbro-diorite to tonalite (porphyritic plagiogranite). It is remarkable however, that dioritic compositions (SiO_2 53-58 %) are absent from the sequence, thus imparting a bimodal character to the complex (Bogachev 1999). The tonalite from the Janis massif was dated at 1872 ± 13 Ma (Stepanov et al., 2006) and the gabbro-diorite from the Alattu stock was dated at 1884.8 ± 3.3 Ma (Pb-Pb dating of the zircons, Bogachev, 1999). Gabbro-diorite and porphyritic tonalite belonging to this age group host hydrothermal gold mineralization (the Alattu occurrence).

Intrusions of the Kaalamo complex have been correlated with basic and ultrabasic rocks of the Kotalakhti ore belt of Finland (Glebovitsky et al., 1996).

The 1.89-1.88 Ga andesite-basalt complex. Rare occurrences of volcanic rocks have been found intercalated with Kalevian metasediments of the Hunukki suite (Svetov et al., 1991). They have been also mapped to the north of the Kirjavalakhti dome. These rocks are fine-grained amphibolites and amphibole-biotite plagioclase schists, sometimes garnet-bearing. They are often enriched in apatite (up to 2 %) and titanite. According to their lithochemical characteristics these rocks are classified as trachy-andesibasalt-trachy-andesites of K-Na type (Artamonova,

1989) and resemble rocks of the Velimyaki massif. They have been dated at 1883 ± 6.7 Ma (Bogachev, 1999).

The 1.88 Ga pyroxene granitoid complexes. Norite-enderbite intrusive massifs such as the *Kurkijoki complex* are mainly confined to the Lahdenpohya-Hiitola subdomain of the Svecofennian domain but also occur in the northern part of the Petersburg subdomain. They underwent intense deformation during later orogenic events. According to interpretations of geophysical data, they represent apophysis of the North-Western Ladoga mantle upwelling (Khazov et al., 2004).

These massifs consist of multiple phases, the earliest phase being of noritic and gabbro-noritic composition, the second of dioritic and enderbite composition, while the third, youngest phase consists of hypersthene-biotite plagioclarnockite and plagiogranite. Granites of the complex are low-K, high-Ca rocks belonging to the I-type calc-alkaline series, reflecting a mixture of mantle-derived and crustal material in an active continental margin setting. The isotopic age of the Kurkijoki intrusive complex is 1883 ± 2 Ma (U-Pb method, Bogachev et al. 1999).

The 1.88-1.865 Ga tonalite and diorite complex. Intrusions of this age are grouped under the name of the *Lauvatsaari-Impiniemi complex*. Such intrusions are widespread throughout the Ladoga region. They are usually relatively small (3-10 km² in area), the largest plutons being the Priozersk (50-70 km², NE part of the Priozersk block of the Petersburg subdomain) and Lauvatsaari intrusions (20-25 km², covering the islands and shoreline of Lake Ladoga in the southern part of the Lahdenpohya block of the Lahdenpohya-Hiitola subdomain). Tonalite, biotite-hornblende diorites and quartz diorites predominate. Early gabbroic intrusions, sometimes occur very close to the tonalite and diorite massifs, and have also been assigned to the Lauvatsaari-Impiniemi complex (Glebovitsky, 2005), although it is more probable that they belong to the Kaalamo complex (Bogachev et al., 1999). Leucogranites occur in late phases of the Lauvatsaari-Impiniemi complex in the Impilakhti-Pitkjaranta block.

Rocks of this complex share similarities with those of the Kurkijoki complex and are interpreted as the product of crystallization of high-Ca magma of calc-alkaline type. The tonalites are also considered to represent I-type magmatism, although the most leucocratic varieties may correspond to S-type granites (Bogachev, 1999). A peraluminous-metaluminous trend is observed from granodiorite to tonalite (fig 1.3 b). A U-Pb isotopic age of 1878.5 ± 3.3

Ma has been obtained for tonalite from the Lauvatsaari massif (Stepanov et al., 2006), and 1864 ± 13 Ma for the granite (Kotov et al., 1992). The Impiniemi granite massif, located at the southern edge of the Ljaskelja block of the Raahe-Ladoga domain, was dated at about the same age: 1871 ± 12 Ma (Baltybaev et al., 2000).

The *muscovite-tourmaline apatite- and garnet-bearing pegmatite complex* in the Raahe-Ladoga domain was presumably emplaced contemporaneous with or shortly after the Lauvatsaari-Impiniemi intrusions. Large and typically zoned pegmatite dykes cut the gneisses of the domes. In Ludicovian and Kalevian crystalline rocks, these pegmatites are concordantly folded and form thick layered veins (Grodnitsky, 1982). Radioactive mineralization (orthite, viikite etc) occurs in these pegmatites.

The 1.87-1.8 Ga group of biotite granites. Such granites are only known to occur in the Svecofennian domain. In the Northern Ladoga part of the Raahe-Ladoga domain they are absent. To the south, under the Vendian and Paleozoic cover, Svecofennian granites have not been sufficiently studied for classification with certainty. Biotite granite plutons have crosscutting, sometimes tectonic contacts with enclosing crystalline rocks and were evidently intruded during late collisional deformation.

Granites of this group have often been grouped together under the name: Kuznechensky complex, but differences in mineralogy (especially accessory minerals), geochemistry and age of emplacement allow subdivision into four complexes: 1) Kuznechensky, 2) Borodinsky, 3) Tervussky, 4) Putsaarsky. Poorly studied biotite granites of southern Ladoga area are referred to the Polyansky complex. Accessory mineral set and geochemistry of the potassic granites of the Ladoga region are presented in the tables 1.1 and 1.2 of Appendix to Part 1.

Plutons of the *Kuznechensky complex* are located in the Svecofennian domain (mostly the Petersburg subdomain and in Isojarvi block of the Lahdenpohkya-Hiitola subdomain), and are confined to the north of the Petersburg subdomain. In Western Ladoga the largest intrusions are the Kuznechnoye (55 km^2) and Lazurny (300 km^2) plutons, located in the Priozersk block.

The Kuznechnoye massif is composed of porphyritic medium- to coarse-grained biotite-amphibole garnet-bearing granites, and more leucocratic medium-grained and pegmatoid biotite-oligoclase granites. The intrusion has a dome-like shape. The massif is cut by rare thick dykes of

fine-grained mafic rocks (Bt-Hbl-Pl) and a 2 km long swarm of carbonatite (phlogopite-Qtz-Calcite) dykes striking NW in the central part of the massif. The age of these dykes is unknown.

The Lazurny (sometimes it is called Lazurninsky) massif is a concentrically zoned funnel-like intrusion. The central part is composed of massive coarse-grained and porphyritic biotite granite with locally coarse-grained to pegmatoid leucogranites. At its periphery a trachytoid granodiorite occurs, containing numerous xenoliths of the surrounding crystalline host rocks occurs. The transition between these rocks is gradual. Rocks in the central part are characterized by a predominance of potassium feldspar over plagioclase. Typical minerals are garnet, ilmenite, apatite, monazite and zircon. The trachytoid granodiorite has more plagioclase than potassium feldspar, a high content of biotite and lower content of quartz. Accessory minerals in these intrusions are: garnet, ilmenite, apatite, monazite and zircon with increasing garnet, monazite and zircon content in the marginal facies. (Appendix to Part 1, table 1.1). Zircons of the Kuznechnoye massif granite have given a U-Pb age of 1873.6 ± 4.1 Ma and those of the small un-named massif of garnet leucogranites, which also belonging to the Kuznechensky complex have given an age of 1866.9 ± 4.4 Ma (Bogachev et al., 1999).

The *Borodinsky complex* comprises the Borodino (100 km²), Zavetny (37 km², sometimes called Zavetnensky) massifs and several small intrusions (the largest one being Gory with an area of 2 km²) located in the Priozersk block. As a rule, the locations of the massifs are controlled by the intersection of NE and NW striking fault zones. Tectonic controls also determined the irregular and complex shape of the intrusions, and the occurrence of protoclastic textures, cataclasis and mylonitization especially at the edges of the massifs. Enclaves of host rocks are abundant especially in the endocontact zone. Injection of the magma into the frame rocks occurred quite often. Large massifs have concentric zone structure with a central part consisting of trachytoid granite with a coarse-grained ground mass, gradually becoming massive and porphyry granites with fine medium-grained matrix. The abundance of granite and aplite veins increases from the center to the periphery of the structure. At the south-western edge of the Borodino massif, medium-grained granites contain enclaves of trachytoid granodiorite of the Lazurny massif; indicating a later origin for the Borodino massif. The trachytoid granite is composed of K-feldspar (40-50 %), oligoclase, quartz (20-35 %), biotite (2-5 %) and garnet. The mineral composition of the external zone and of the porphyry granite is similar, only the quartz content is lower. Accessory minerals are the same for all rock varieties: garnet, ilmenite

(strongly replaced by leucoxene), monazite, apatite and zircon (Appendix to Part 1, table 1.1). The Borodino massif is dated at 1799 ± 4 Ma (Konopelko and Eklund, 2003).

The *Tervusky complex* is located in the Lahdenpokhya block. It represents a dense cluster of intrusions concentrated near by the main Tervus massif (50 km^2), which occupies the Tervus peninsula and surrounding area. The complex is composed of three varieties of microcline granites. The central part of the Tervus massif consists of trachytoid microcline granites with a NE-striking fabric alignment of feldspar crystals. They are surrounded by a zone of leucocratic medium-grained granites up to 250 m thick, which are usually equigranular, rarely porphyritic. Coarse-grained granite forms the matrix to magmatic breccias of Lahdenpokhya gneiss and Lauvatsaari tonalite at the periphery of the massif. Accessory minerals are: garnet, ilmenite, apatite, zircon, pyrite, thorite, and rarely titanite. A specific feature of granites of the Tervusky complex is the presence of muscovite, which is not typical of the biotite granites of the Svecofennian domain, but is well-known in leucogranites from the Raahe-Ladoga domain (see below). The Tervus granites have been dated at 1859 ± 2 Ma (Glebovitsky et al., 2001).

The *Putsaarsky complex* is composed of a main Putsaari massif and several smaller satellite bodies in the Lahdenpokhya block, on Putsaari island and along the adjoining coastline. The Putsaari complex is composed of a suite containing gabbro, diorite, monzonite and granite suite. Nikolskaya and Gordienko (1977) and Saranchina (1972) have distinguished two different magmatic complexes: K-enriched moderately mafic rock, altered by later emplaced granites, whereas Jdanov (1972) proposed the existence of only one multiphased intrusion from the same deep source. The latter interpretation appears more realistic in view of new geochemical and geochronological data. U-Pb isotopic analyses of zircons give about the same age for the mafic and felsic varieties: 1869 ± 7.7 Ma and 1867.2 ± 5.6 Ma respectively, suggesting a coeval emplacement and crystallization of all the rocks of the Putsaari massif (Konopelko and Eklund, 2003). The different phases of this massif are also geochemically similar to other complexes of the Ladoga region: the mafic rocks are comparable to the monzodiorite of the early-orogenic Velimyaki massif, the diorite to early mafic phase of the post-orogenic Elisenvaara, and the granite to the Tervusky granites (Stepanov et al., 2006).

The Putsaarsky granites are rich in magnetite (up to 3 %), but poor in other accessories, which include: pyrite, ilmenite, apatite and zircon. Garnet and monazite are not common. Allanite is also present but it is not typical for the other complexes of the group.

The *Migmatite-anatectite-granite* complex occurs in the Svecofennian subdomain and in the domes of the Raahe-Ladoga domain. Rocks of this complex are often difficult to recognize and distinguish due to complex relations with its granite-gneiss hosts rocks. Contacts are typically transitional rather than sharp, with zones of garnet-bearing migmatites enclosing host rock relics. Microcline-plagioclase and plagioclase-microcline varieties, often with large microcline crystals, are associated with granites of above mentioned group of intrusions and have similar chemical composition. The U-Pb age of the leucosome of the migmatites from the Petersburg subdomain is 1873-1869 Ma (Baltybaev et al., 2002)

The biotite granites of this group are peraluminous (fig. 1.3 c, d, e; Appendix to Part 1, table 1.2). The Tervusky, Lazurny and Borodino granites are strongly peraluminous ($A/CNK > 1.1$), alkali-rich ($Na_2O + K_2O = 7.5-9.5\%$), with high $K_2O/(K_2O+Na_2O) = 0.42-0.65$, high SiO_2 and low Mg, Ti and Ca contents. The Tervusky granite richer in Na. The Zavetny granite has higher Mg-content and is less peraluminous. The Lazurny massif is richer in Ca. The Borodino massif is characterized high K_2O contents – up to 7%.

All of these granites have low abundance of the trace elements, F and Cl. Negative Eu anomalies are also typical of all granites of the Svecofennian domain (except Putsaarsky). REE patterns tend to be specific for each complex. The Kuznechensky complex granites are poor in LREE and rich in HREE (up to 7 ppm Yb), whereas the Borodino granites are rich in LREE (La up to 250 ppm) and poor in HREE (Yb – 0.5 ppm). The Tervusky granites have intermediate characteristics.

The Putsaarsky granites have distinctive features: they tend to be less peraluminous, more magnesian, they have a higher Fe oxidation state with magnetite prevailing over ilmenite, lower Th and U, but higher Ca and Mg contents. REE abundances are but highly fractionated ($[La/Yb]_n = 60$ in average) and, unlike other peraluminous granites of the Svecofennian domain, the Putsaarsky granites have no negative Eu anomaly (Bogachev, 1999).

Biotite granites of the Svecofennian domain have very similar accessory mineral paragenesis with Grt-Ilm-Mzt (Appendix to Part 1, table 1.1). However the Tervusky granite is poor in monazite and contains thorite and magnetite, which are rare in other granites of the group, and sometimes titanite. The Borodino granite is rich in monazite (high Th and LREE) and the Kuznechensky in garnet (high Y).

The Kuznechensky, Borodinsky and Tervusky granite accessory minerals and REE patterns correspond to S-type granites, whereas the Putsaarsky granite has characteristics closer to I-type (Chappel and White, 1974). Unlike other massifs of the group, Putsaari is located on a positive gravimetric anomaly (Appendix to Part 1, fig. 5), which is another indication of its relation to magmas with a primitive source.

In general, all Svecofennian granites of the Priozersk block are poor in U and enriched in Th (especially the Borodinsky complex). Average contents of U and Th are presented in the table 1.2 of Appendix to Part 1. U and Th abundance in some derivatives of syn-, late- and post-orogenic Svecofennian granitoids rocks see in General Appendix 2.2.

Direct comparisons between the Ladoga region biotite-granite and those of the Southern Finland migmatite-granite belt have been made (Glebovitsky, 2005 and others) but are not necessary justified because of their different emplacement ages. The Ladoga region granites have been mainly intruded between 1.86 and 1.87 Ga, whereas the Finnish potassium granites are younger (1.84-1.82 Ga) (Bedrock Map of Finland, 1997). The southern Finland granites are more comparable with the leucogranites of Northern Ladoga (see below), but this problem demands further investigation.

1.8 Ga two-mica leucogranites.

Granites of this group are conventionally grouped under the name the *Matkaselsky complex* (Bogachev, 1999; Skorospelkin, 2002). It includes three occurrences located in Northern Ladoga Raahe-Ladoga domain: Matkaselka, Latvasursky and Pitkjarantsky complexes (Bogachev, 1999). The leucogranites of the south-eastern part of the Svecofennian domain (so called "Chaplinsky complex", Skorospelkin, 2002) may belong to this group, but they have not been sufficiently studied to support such an interpretation.

Common features of all these intrusions are: post-metamorphic and post-kinematic emplacement, discordant relationships with respect to all metamorphic rock units (including late-kinematic migmatites); control by NW-SE and NE-SW faults; diversity of petrologic and geochemical characteristics, and enrichment in accessory minerals and in particular the trace elements U, Th, Nb, Y, and Ti. No precise age determination is available for these intrusions although indirect estimations lead to an age between 1.73-1.82 Ga (Grodnitsky, 1982), or about 1.8 Ga (Konopelko and Eklund, 2003).

The intrusions of the *Matkaselka complex* are confined to an area between the Ruskeala anticline and the Janisjarvi syncline, where they intrude mica schists of the Kalevian Ladoga

group. The complex is composed of four relatively large massifs: Kurenlampi (10 km²), Vahvajarvi (8 km²), Matkaselka (6.5 km²), Jakkima (2 km²) and numerous bodies of pegmatites. They are localized along an E-W trending negative gravimetric anomaly extending from the Janisjarvi lake to the Kitee and Puruvesi massifs on the Finnish territory.

On the eroded surface intrusions of the Matkaselka complex have lens shape and are localized within the Ruskeala tectonic zone. According to geophysical data, massifs forms system of harpolith bodies located one above another. Veins and dykes of pegmatite are common in the vicinity of the main intrusive bodies, but also occur separately.

The other main types of the rocks of the Matkaselka complex are:

- 1) Fine- to medium-grained garnet-muscovite albite-oligoclase leucogranite (leucoplagiogranite);
- 2) Medium- to coarse-grained tourmaline-bearing two mica granite (microcline-plagioclase pegmatoid granite);
- 3) Fine-grained garnet- and tourmaline-bearing muscovite and two-mica granite (aplite);
- 4) Two-mica microcline and muscovite- tourmaline-albite-microcline pegmatite;
- 5) Quartz-muscovite- tourmaline-microcline pegmatoid;
- 6) Rare metal albite granite with beryl, columbite, tantalite and cassiterite.

The *Latvasursky complex* is located to the SW of the Sortavala block, surrounding the northern and eastern margins of the Latvasursky dome. Numerous small intrusive bodies occur within the granite-gneisses of the dome, and within the Ludicovian Pitkjaranta suite carbonates and amphibole schist, and Kalevian Ladoga group quartz-biotite schists and gneisses. A N-S strike is typical for these intrusive bodies. Three types of rocks are recognized: (i) fine- to medium-grained biotite leucogranites, (ii) garnet-biotite pegmatite, (iii) zoned muscovite pegmatite. They occur as two types of intrusions, the first being stock-like bodies of even-grained leucogranites (varying from 20×30 m² to 3×3 km² in size.. Another (probably later) type is presented by N-S-elongated lenticular or vein-like bodies (up to 150×1000 m² in extent, consisting of even-grained and pegmatoid plagioclase, microcline-plagioclase granites. The Latvasursky granites have a general resemblance to the granites of the Matkaselka complex but are less differentiated, have less plagioclase, are poor in apatite, tourmaline and muscovite and lack rare-metal mineralization.

The *Pitkjarantsky* (other names – Impilakhtinsky, Mursulsky) complex is composed of pegmatite dykes and veins, and small intrusions of leucogranite located in the Impilakhti-Pitkjaranta block. In the literature it is often referred to as the Pitkjaranta field of ceramic pegmatites. Two mineralogical-geochemical groups are recognized:

(i) Muscovite-albite-microcline rare metal pegmatites and leucogranites, usually intruding the Ludicovian Pitkjaranta formations and more rarely the Kalevian Impilakhti schists. They occur as dykes, lenses, stocks and irregular bodies, varying in length from 10 to 600 m, with thicknesses up to 35 m. They are typically homogenous and consist of coarse-grained two-mica Qtz-Pl-Mcl pegmatoids, sometimes with graphic pegmatite, aplite and quartz cores, although medium- to coarse-grained two-mica leucogranite bodies are also common. The most extremely differentiated varieties are usually coarsely zoned, with an outer medium- to coarse-grained Qtz-Fsp zone, an intermediate coarse-grained Qtz-Pl-Mcl pegmatoidal zone, locally with graphic textures and quartz, and a central zone composed of blocky microcline and coarse-graphic pegmatite. Sometimes late-crystallized clevelandite and albite are present. Typical accessory minerals are: beryl, apatite, magnetite, pyrite, chalcopyrite, molybdenite, and more rarely titanite, monazite and xenotime. Pegmatites of this group are similar to the rare-metal pegmatites of the Matkaselka complex.

(ii) REE-rare metal pegmatites usually occur inside the granite-gneiss domes (especially within the Mursula dome), but more rarely in the Palaeoproterozoic schists and amphibolites between domes. They occur as dykes and lenses with sharp contacts and can be up to 700 m long and up to 15 m thick, although in exceptional cases as much as 25 m thick. Most veins however are 25-40 m in length with a thickness of 2-4 m. Zoned structure is typical, from a fine- to medium-grained granitic marginal zone, through a Qtz-Mcl-Pl pegmatite, locally with graphic texture and large biotite laths, finely graphic pegmatite, then a zone of blocky microcline and large biotite laths and finally a quartz core with biotite laths. A characteristic feature of this group of the pegmatites is the abundance of the accessory minerals of U, Th, Nb, Y, REE and Ti. Besides accessory magnetite, ilmenite, hematite, rutile, tourmaline, titanite, orthite, monazite, apatite, xenotime, zircon, cyrtolite, pyrite, chalcopyrite, arsenopyrite, molybdenite, bismuthinite and galena, there are also REE and rare-metal minerals: evkensenite, samarskite, columbite, tantalite, fergusonite and U-Y-bearing Ti-Ta-niobates (obruchevite, Y-gatchettolite, Y-betafite, Ta-betafite). All these minerals occur in the block microcline zone, more rarely in the quartz core.

Geochemically, the Matkaselka complex comprises K-Na peraluminous leucogranites with subordinated metaluminous and peralkaline terms (fig. 1.3 f; Appendix to Part 1, table 1.2). Mineralogically their peraluminous character is reflected by the presence of garnet, muscovite and corundum. In most rocks $K_2O/(K_2O+Na_2O) < 0,5$. Leucogranites of the Matkaselka complex are rich in Al and Fe, and poor in K, Ca, Mg, Ti compared to the Latvasursky and Pitkjarantsky granites. Peraluminous leucogranites and non-differentiated Bt-Mcl pegmatites are rich in Rb, U (10 ppm), Pb and poor in F, Ba, Sr, Ti, Zr, Cr, Th, REE. There is a trend towards increased U, F, S, Cs, P, Li, Pb, Nb, Sn, Be and a concomitant decrease in Ba, Zr, Y, Th, and Pb when comparing early fractionated and late derivatives of the Matkaselka complex, although Sr behaves independently. Mus-Ab-Mcl rare-metal pegmatites are enriched in F, B, Li, Cs, Nb, U (up to 65 ppm), Sn, and Be but are relatively depleted in Ba, Zr, Th and have the lowest K/Rb, K/Cs and highest Rb/Ba ratios. The Latvasursky complex is less differentiated than the Matkaselka complex, with lower P, F, Li, Cs, U, Sn, Be and higher Zr, Th, Ba contents. Pitkjaranta granites have geochemical characteristics intermediate between those of Latvasursky and Matkaselka (Bogachev, 1999).

The Matkaselka complex is characterized by differentiation, from homogenous biotite and two-mica leucogranites in its center, to biotite microcline pegmatites with simple texture and finally to differentiated muscovite albite-microcline pegmatites with rare-metal mineralization at its margin. The proportion leucoplagioaplite and quartz-muscovite rock increase in the same direction, Rare Metal-bearing albite appears. In general, albite, muscovite, tourmaline, apatite abundance increase towards the margin as well. The Matkaselka complex represents a complete compositional range. On the basis of this observed trend, and taking in account geophysical data, the Puruvesi massif of Finland (1797 ± 19 Ma, Huhma, 1986) may represent the deeper parts of a similar intrusive body, while the other massifs are later derivatives, becoming younger from west to east.

In contrast with biotite-granites of the Svecofennian domain, two-mica granites of the Raahe-Ladoga domain are enriched in U and Th content is low. The most uranium-bearing are pegmatites of the Pitkjaranta area – 12.5 ppm in average (General Appendix 2.2).

The highly differentiated granites of the Matkaselka complex are fertile for concentration of rare metals and ore minerals. The Matkaselka lepidolite-albite rare-metal pegmatite hosts Li-Be-Sn-Nb-Ta mineralization. Sn, Be, Li, Nb, Ta mineralization (up to economic grade) occurs in

skarns associated with the Matkaselka and Pitkjarantsky granites. Tungsten mineralization also occurs in skarns associated with the Latvasursky granites (Ivanikov et al., 1984).

The 1.81-1.77 Ga gabbro-monzonite-syenite-granite complex.

There is a series of multiphase hypabyssal intrusions intruded within the Svecofennian domain during the post-kinematics stage of the Svecofennian orogeny. In the present study area they are regrouped under the name Elisenvaarsko-Vuoksinsky complex. They cut discordantly across all other Palaeoproterozoic rock units, are not metamorphosed and do not show any ductile deformation overprint. These massifs are related to the intersection of deep NW- and NE-trending faults. The *Vuoksa and Oja-Jarvi massifs* in the Priozersk block are relatively large, while the *Elisenvaara complex* comprises 12 small intrusions in the Lahdenpokhya block. The swarm of lamprophyre dykes on the Kalto island to the NE of the Lahdenpokhya block also belong to this magmatic group. In general, they consist of two intrusive series: (i) ultramafic-mafic dykes with widely varying composition (from ultramafic, calc-alkaline, apatite-rich potassium lamprophyres to quartz diorites, monzodiorites and monzosyenites), and (ii) leucocratic felsic rocks (leucosyenites, quartz monzonites, granodiorites, and granites). They are considered to be the eastern continuation of an elongated belt of shoshonitic intrusions, extending from the Ladoga region through, southern Finland to the Aland islands (Eklund et al., 1998).

Shoshonitic rocks are characterized by $K_2O+Na_2O>5$ wt %, $K_2O/Na_2O>0.5$, $Al_2O_3>9$ wt % and wide variations in SiO_2 content (32-78 wt %). Granites are metaluminous to peraluminous (fig. 1.3 g; Appendix to the Part 1, table 1.2) and mafic rocks are extremely enriched in P, F, Ba, Sr. REE contents are also very high and the patterns are highly fractionated. Abundances of La in Vuoksa mafic rocks are 1000 times higher and for Elisenvaara up to 10000 times higher than chondrite values. $(Ce/Yb)_n$ is up to 100 and more. The main LREE bearing minerals are orthite and monazite. Uranium abundances vary from 1 to 8 ppm ($m=4.5$ ppm), the most U-rich being the lamprophyre derivatives; Th contents are 25 ppm on average. The most typical accessory mineral paragenesis is Mt-Tit-All (Bogachev, 1999).

The apatite-bearing ultramafites of the Vuoksa have an age of 1802 ± 17 Ma (Ivanikov et al., 1996) and the Elisenvaara syenite is dated at 1801 ± 4 Ma (Andersson et al., 2006).

The small gabbroic-dioritic Ostrovsky and Kamennogorsky complexes in the Priozersk block differ from the other post-orogenic intrusions. They are located close to the northern contact of the Lazurny massif and controlled by an E-W fracture zone.

Mafic rocks of the *Ostrovsky complex* (includes mafic facies of the Kamennogorsky massifs) unlike those of the Elisenvaarsko-Vuoksinsky complex, contain OPx, have no alkali feldspar, are much richer in mafic minerals and ilmenite prevails over magnetite. Mineralogically these rocks are similar to the gabbro-anorthosite of the early phase of the rapakivi complex. Geochemically they have continental tholeiitic signatures, in contrast to the calc-alkaline character of the Elisenvaarsko-Vuoksinsky complex (Bogachev, 1999). Zircons from the mafic rocks of the Ostrovsky massif have given an age of 1785 ± 5 Ma (Bogachev V.A., personal communication).

The amphibole-biotite trachytic granitoids of the *Kamennogorsky complex* (felsic facies of the Ostrovsky and Kamennogorsky massifs, Prudinsky massif) from the northern part of the Lazurny massif were originally considered as part of its marginal facies. However, recent mineralogical and geochemical studies have led to its being classified separately. These hornblende-bearing medium-grained rocks correspond to monzodiorites and granodiorites. When compared with the Lazurny granites, the Kamennogorsky complex granitoids are found to have similar silica content, are less aluminous, richer in K and Fe (fig. 1.3 h; Appendix to Part 1, table 1.2). LIL-element patterns are similar to crustally derived peraluminous potassic granites. Their HFSE (Nb, Ta, Y and esp. Zr and Hf) and F abundances are the highest of all late- and post-orogenic granites, and approach those of the rapakivi-granites.

Their accessory mineral paragenesis is quite distinct: ilmenite > magnetite, titanite, apatite, zircon, allanite, \pm fluorite and molybdenite. The most typical accessory mineral association for the Kamennogorsky granite complex is Ilm-Tit-All.

The 1.67-1.5 Ga gabbro-anorthosite-granite rapakivi complex.

Lower Riphean anorogenic intrusions of rapakivi type occur throughout the southern part of the Baltic Shield (Fennoscandian Rapakivi Province) and have been recognized by drilling and geophysics under the platform cover (Appendix to Part 1, fig. 1). Several intrusions of this type occur in the study area: the large multiphase Wiborg and Salmi batholiths, the small Ulalegi and Svir massifs, the Oyat massif, whose presence is only presumed from geophysical data, and a series of small bodies of fault-related leucocratic granites and pegmatites.

The Wiborg massif is situated in the center of the Fennoscandian Rapakivi Province, south of Lake Ladoga, on the northern coast and under the Gulf of Finland. The total surface

area of the pluton is about 30 000 km², 16 000 km² being on land. There are two satellite bodies north of the main intrusion: Ahvenisto and Suomenniemi. According to geophysical data, the batholith transects much of the crust, being composed of several phases with a total thickness about 30 km (Elo and Korja, 1993). A positive gravimetric anomaly to a depth of 10-16 km beneath the pluton is interpreted as a gabbro-anorthosite phase, similar to the Ahvenisto massif. Depth to Moho beneath the batholith is about 41 km, which is 10-20 km less than in surrounding areas (Sharkov, 1999). In the Western Ladoga area, gravimetric surveys demonstrate that the upper surface of the batholith has a dip of 40-55° below Palaeoproterozoic metamorphic rock units at a distance of over 10-30 km from the surface contact (Appendix to Part 1, fig. 5).

The Wiborg massif is composed of several intrusive phases. Gabbro-anorthosites are exposed in the Ahvenisto massif (Finland), whereas only rare xenoliths of these rocks occur within the granites. Four groups of granites have been recognized (Velikoslavinsky et al., 1978):

(i) Biotite-amphibole quartz syenites (local name – lappee-granites) occur in the northern periphery of the pluton representing its uppermost part, near the roof of the intrusion.

(ii) Ovoid hornblende-biotite rapakivi granites (“wiborgite”) is the main phase (76% of the total surface area). These rocks are characterized by large (2-5 cm) phenocrysts of K-Na Fsp with concentric-zonal structure, often with oligoclase rims, set within a coarse-grained groundmass. NW-elongated bodies of ovoid granites with a fine-grained groundmass represent the residual melts of this phase. Veins of fine-grained ovoid granites are related to orthogonal fracture systems.

(iii) Medium- coarse-grained and porphyritic trachytic biotite granites with black quartz form bodies of variable size intruding the wiborgites and including them as xenoliths. Rare fine-grained biotite granite dykes also occur along orthogonal fracture sets.

(iv) Biotite-muscovite-topaz granites occur as a 3×5 km² stock in the western part of the massif. The central part of the stock is a fine-grained porphyritic rock and the outer fine-grained zone has a width of 0.5 km. Greisenised pegmatite stockscheider is developed at the contact with the wiborgite and Sn-rare metal mineralization occurs in the biotite-muscovite granites.

The emplacement of the Wiborg batholith occurred from 1615 to 1645 Ma, and was preceded by mafic dykes at 1665 Ma (Vaasjoki et al., 1991).

The *Salmi massif* is located to the east of Lake Ladoga and is partly covered by it. It is an irregular-shaped intrusive body, elongated in a NW-SE direction, parallel to the main structural

trend of the Raahe-Ladoga zone. At the basement surface it has a length of about 130 km and a width of 40-50 km, making a total area of about 4200 km². The southern part of the Salmi massif is sometime considered as a separate intrusion, referred to as the Olonetsky massif (Caillat et al., 2002). The elongated shape of the Salmi massif is not typical for rapakivi plutons but results from its emplacement along the Janisjarvi fault zone and reactivation of NW-SE faults.

According to geophysical data, the Salmi massif is a sheet-like body with a thickness increasing from 2 to 12 km towards the south-east where a feeder channel has been inferred (Sharkov, 1999). The north-eastern contact of the massif is generally sharp and related to the Janisjarvi fault zone. Only in its central part is a satellite body emplaced into the Karelian domain: the *Ulalegi massif*. To the north-west, the roof of the Salmi massif dips gently under Archaean and Palaeoproterozoic (AR-PR₁) basement rocks and can be traced by geophysical means for a distance up to 8 km from the exposed contact. In that area, crystalline rocks are intruded by pegmatite apophysis of the Salmi massif and hydrothermally altered. To the south, the massif is cut by the E-W trending Podporoje fault zone.

The Salmi massif is composed of six successively emplaced phases (Amelin et al., 1997):

(i) gabbro-norite, labrodorite and anorthosite, occurring in central southeastern part of the massif above the proposed feeder channel, dated at 1546.7 Ma,

(ii) monzonite, quartz syenites, syenites, locally observed to the north of the first phase, dated at 1543.7 Ma;

(iii) biotite-amphibole syenogranite, composing the easternmost part of the Salmi massif and the main part of the Ulalegi satellite intrusion, dated at 1543.4 Ma;

(iv) amphibole-biotite rapakivi granite, with wiborgite, pyterlite and rare-ovoid varieties, which is the most widespread rock type, dated at 1540.6-1537.9 Ma for Salmi and 1529.9 for Ulalegi,

(v) biotite granite with porphyritic and even-grained varieties, comprising the northwestern part of the massif, dated at 1538.4-1535.0 Ma,

(vi) albite - Li-siderophyllite topaz-bearing granite, occurring very locally at the western edge of the massif (Pitkjaranta area), dated at 1538.0 Ma.

The latest generation of pegmatites is related to the youngest major phase of the massif. The pegmatite bodies occur both within the plutons and in their immediate vicinity.

There is trend towards increasing U and Th contents from the early to the late phases of Salmi and Wiborg massifs (fig. 1.4). Mineral hosts for the radioactive elements are orthite, viikite (a mixture of euxenite and obruchevite), monazite and zircon.

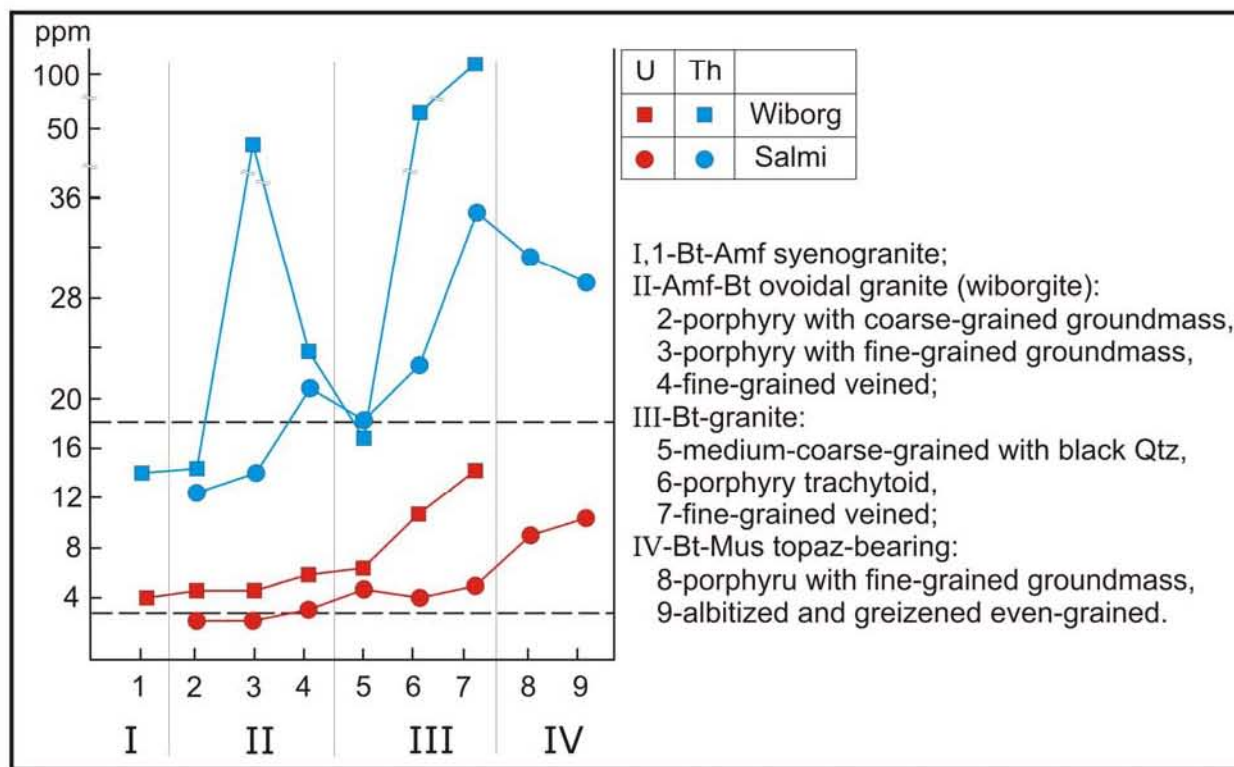


Figure 1.4. Uranium and thorium distribution in the different granite phases of the Wiborg and Salmi massifs (after Ivanikov et al., 1984).

Differences in source rock composition influence the geochemistry of the rapakivi granites. It is proposed that the Wiborg intrusion originated by about 20 % partial melting of intermediate-felsic Svecofennian lower crust, whereas the Salmi granites have an Archaean crust component (Rämö, 1991). This observation can explain the relative enrichment of the Wiborg granites in U in comparison with the Salmi ones.

The *Svir rapakivi granite massif* is located SE of the Salmi massif. It is a dome-like intrusive body with gently dipping contacts under the enclosing Palaeoproterozoic rock units of the Raahe-Ladoga domain. At the present erosion level it covers 50 km² and has a regular ellipsoid shape with an E-W trending long axis. The intrusion represents another apophysis of the Salmi massif. The Svir massif has not been studied in detail because it is totally covered by Vendian sediments. However, a predominantly wiborgite composition is assumed on the basis of rare drill holes data (Skorospelkin, 2002). Two small intrusions assigned to the rapakivi type are located to the SW of the Svir massif.

According to geophysical data, a large low density region is present in the basement beneath the northeastern part of the Pasha graben and also further to the northwest, under Lake Ladoga (Appendix to the Par1, fig. 5); this anomaly is attributed to another rapakivi-granite intrusion, referred to here as the *Oyat massif*.

Rapakivi complexes cannot be related to any known orogenic event, but their emplacement is considered as an important event in the construction of continental crust. A predominantly crustal source is inferred for the rapakivi magmas and they are classified as A-type granitoids. Globally, ages of rapakivi granites generally fall between 1.0-1.8 Ga, but there are also Phanerozoic analogs as well (Rämö and Haapala, 1996; Calzia and Rämö, 2005; Haapala et al., 2005). It is supposed that rapakivi provinces could be formed under the influence of large mantle upwellings, such as plumes or hot spots) in an anomalously thick continental crust environment (Sharkov, 1999). Local crustal thinning has been detected beneath large rapakivi intrusions, such as the Wiborg batholith (Elo and Korja, 1993). The Fennoscandian Rapakivi Province has a radiating shape (Appendix to Part 1, fig. 1) similar to the classical configuration of pre-rifting intracratonic break-up above a plume. The oldest ancient rapakivi intrusions are located in the central part of this configuration, becoming younger towards the periphery, along the radial axes. Although there have been attempts to relate the formation of the rapakivi magmatism to an intermittent subduction event on the SW flank of the Shield (Åhäll et al., 2000), the plume hypothesis seems more tenable (Haapala and Rämö, 1992; Rämö and Korja, 2000). Taking into account the spatial coincidence of the Fennoscandian Rapakivi Province and late Lower-Middle Riphean intracratonic rifting, such magmatism can be considered as an integral part of the pre-rifting stage during crust extension.

The 1.46-1.35 Ga gabbro-dolerite and basalts

The Pasha-Ladoga basin comprises not only a sedimentary sequence but also contemporaneous volcanic units. The *Salmi trap complex* is located between clastic sedimentary units and is composed of two horizons of tholeiitic trachybasalts with a total thickness up to 350 m. The basaltic units are known in both the Salmi and Pasha depressions and have been detected by geophysical techniques under the Ladoga lake. The basalts are characterized by SiO₂ contents of 45-50 %, high Fe (up to 15-17 wt %), Ti (up to 3-3.5 wt %), alkali (Na > K), P, Zr, Sr contents and a high oxidation state of Fe (Scheglov et al., 1993) and are assigned to the tholeiitic series (fig. 1.5). The eruption of the lavas took place in a subaerial environment, as indicated by the absence of pillow lavas and intense oxidation of upper parts of the lava flows (Frank-

Kamenetsky, 1996). A Sm-Nd age 1499 ± 68 Ma was obtained for these rocks (Bogdanov et al., 2003).

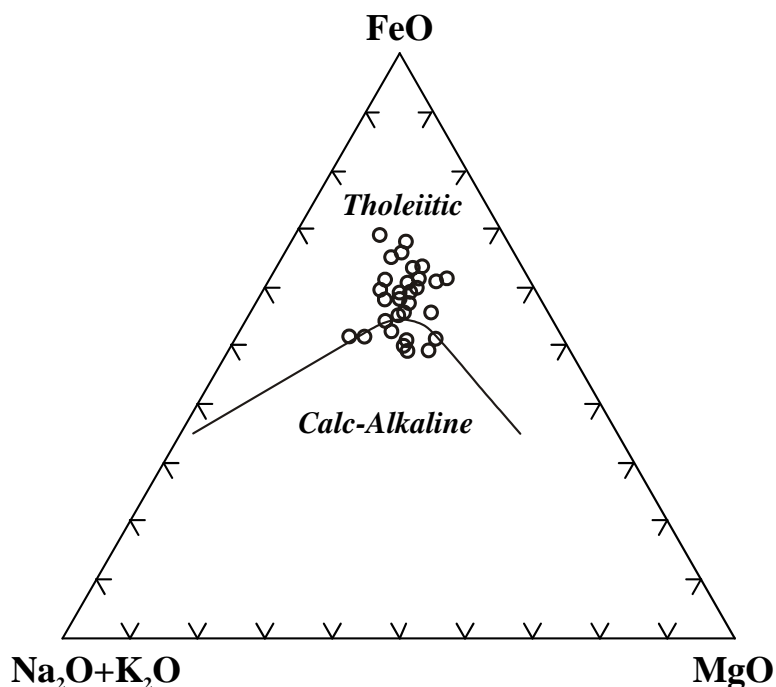


Figure 1.5. AFM diagram for the Salminsky complex basalts (after Frank-Kamenetsky, 1998).

Two other centers of mafic magmatism are present in the Northern Ladoga area: the well preserved Valaam sill and the Hopunvaara intrusion (stock), which has been eroded to a depth exposing its feeding channel. Together with the Sortavala group of dykes they are regrouped under the name *Valaam intrusive complex*.

The *Valaam sill* forms a flat intrusive body extending over 2000 km^2 , exposed on the pre-Quaternary surface of the Valaam archipelago in the northern part of the Ladoga Lake and on islands of the north-eastern shore of the lake. It cuts the sediments of the Salmi depression and is composed of two compositional rock series: (i) one ranging from subalkaline gabbroids through monzonites to syenogranites, and (ii) another from alkaline granites to alkaline leucogranites. The main bulk of the sill consists of subalkaline ferro-gabbro-dolerites, while more felsic rocks occur in the uppermost part of the intrusion; granophyre aplite veins are the latest phase of the intrusion. The gabbros and dolerites have high Ti, Fe, P, K, Ba, Rb, LIL, HFS and LREE contents and low Mg, Cr, Ni, Co contents. They are considered as derivatives of continental tholeiitic basalts, which underwent differentiation in magmatic reservoirs in the middle crust, and show evidence of contamination by continental crust including admixture of

Archaean material (Amantov et al., 1996; Bogachev, 1999 Rämö et al., 2001). The U-Pb age of the intrusion is 1457 ± 2 Ma (Rämö et al., 2001).

The *Hopunvaara stock*, consisting of augite porphyrites, is located in the Pitkjaranta area 7 km from the north-eastern shore of the Ladoga Lake and 40 km north of the Salmi depression. Svetov (1979) interpreted it as a feeder zone to the Salmi basalts, but Frank-Kamenetsky (1998), based on petrologic analysis and spatial analysis has rejected this hypothesis. The feeder zone hypothesis is also inconsistent with the 1325 ± 52 Ma Rb-Sr age of the intrusion (Larin and Kutuyavin, 1993) but this age needs to be rechecked.

According to some maps (Skorospelkin, 2002), a dyke swarm also cuts the Salmi rapakivi massif. The dykes have not been dated, but are presumed to be Riphean, contemporaneous with the Valaam sill. Their location along a N-S trending continuation of the Palaeoproterozoic Tulomozero tectonic trough indicates a reactivation of this structure during a Riphean event. Dyke swarms have also been found cutting all formations of the Prionejskaya depression to the east of the present study area. The age of these dykes is unknown, but they are also presumed to be Riphean (Skorospelkin, 2002).

Mafic dykes also occur to the NE of Lake Ladoga, in the Sortavala city area. The dykes are up to 10m wide and 300 m long and mainly strike NW-SE. Their composition corresponds to subalkaline diabase porphyrites and hyalobasalts called “sortavalites” (Nazimova, 1986).

Volcanic and subvolcanic formations define a trend from the trachydolerites of the Sortavala dykes to the late alkaline leucogranites of the Valaam sill (fig. 1.6). Their similar geochemical compositions (high Ti, P, Zr, Y, Ba, Nb, Rb contents and low Cr and Ni contents, high Fe/Mg ratios, uniform K_2O/Na_2O) suggest derivation from a common source (Amantov et al., 1996; Frank-Kamenetsky, 1998) during Lower Riphean intracratonic rifting.

The 0.77-0.72 Ga tagamite complex

The latest traces of magmatic activity in the Ladoga region were discovered on islands and very locally on the western coast (Leppyaniemi cape) of the Janisjarvi Lake. The origin of the lake depression is considered as an Upper Riphean cryptoexplosion structure. It is filled by allogenic breccias, zuvites, tagamites and andesite-litites. The age of the impact event and associated magmatic activity is estimated at 770 (Khazov et al., 1999) or 730-720 Ma (Bogdanov et al., 2000). Andesite-litites are enriched in U – up to 7 ppm (Grigorieva, 1977).

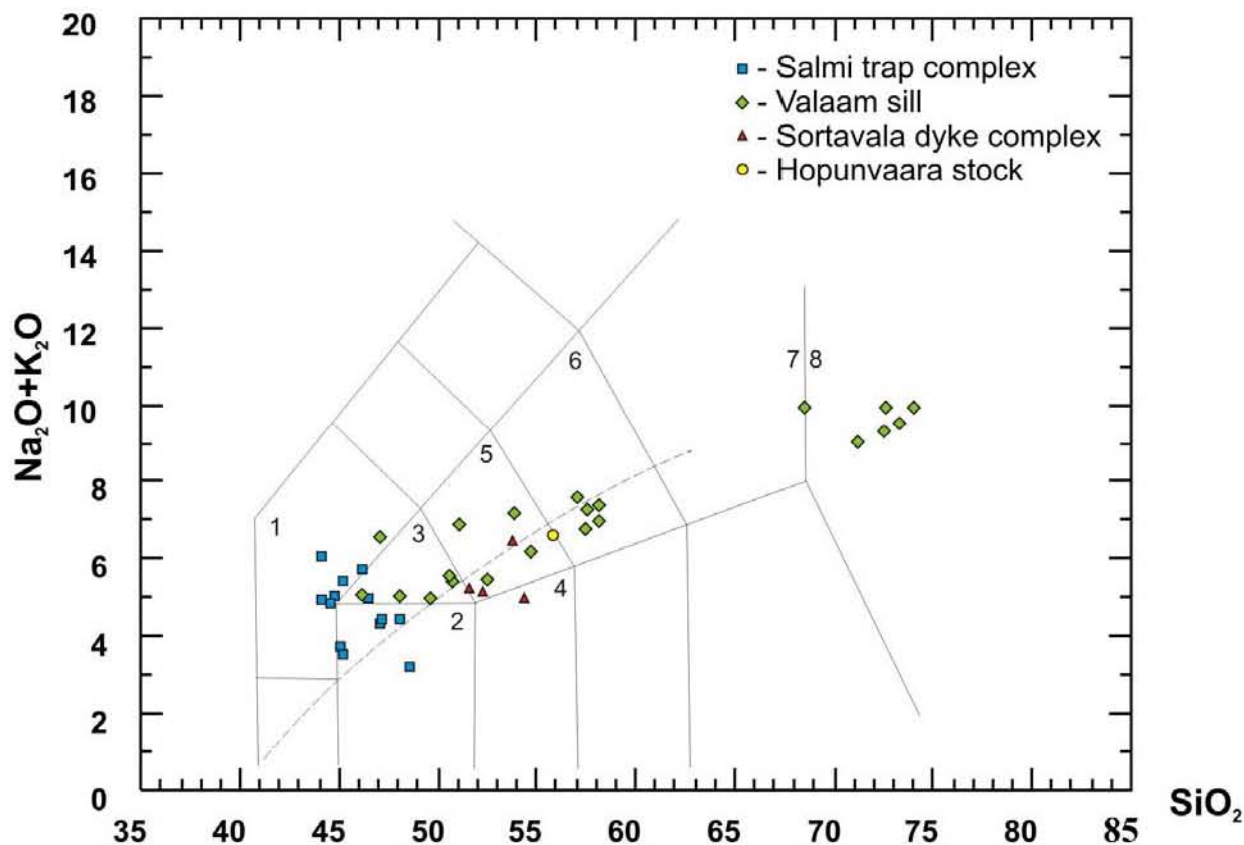


Figure 1.6. TAS diagram for the rocks of the Salminsky and Valaam magmatic complexes (after Frank-Kamenetsky, 1998). Fields according to Le Maitre et al., 1989: 1 – phoydogabbro, 2 – gabbro, 3 – monzogabbro, 4 – gabbro-diorite, 5 – monzodiorite, 6 – monzonite, 7 – syenite/qtz-monzonite, 8 – granite-tonalite. The dotted line separates alkali and calc-alkali fields.

1.8. Fault zones

Interpretation of satellite images and gravimetric data allows orthogonal and diagonal tectonic systems in the Ladoga region to be recognized (Appendix to Part 1, fig. 2 d). The orthogonal trends (especially the meridional faults) are more typical of the Archaean Karelian craton, whereas in the Proterozoic crust the diagonal system predominates. Arcuate and concentric structures of variable size are widespread. Many of these correspond to domal uplifts and intrusions, but the circular Janisjarvi astrobleme is a distinctive feature in the northern part of the region. The higher density of tectonic structures in the northern part of the area compared to the southern one is explained by the burial of ancient structures beneath Vendian and Paleozoic platform sediments such that only the most significant faults, reactivated after sedimentation, can be distinguished in the southern part of the area. Many of the tectonic structures of the Ladoga region were subjected to repeated tectonic reactivations from

Palaeoproterozoic until recent times, so that the early kinematics of these faults usually is quite obscure.

The most significant faults of Ladoga region are striking NW-SE, parallel to the general trend of the Raahe-Ladoga zone. The Janisjarvi, Ruskeala, Priozersk and Vuoksa faults are the largest fault zones and can be traced by geophysical methods to the upper mantle, down to a depth of 110 km. The Sortavala and Lahdenpokhya faults are intracrustal and appear to terminate at a depth of about 40 km. The Svecofennian rock units have been thrust onto the heterogeneous basement of the Raahe-Ladoga domain along the flat-lying Meeri thrust zone, which also generally trends NW-SE. All large tectonic dislocations striking NW-SE consist of a series of parallel and en *echelon* structures with a total thickness up to 7 km. For the Ruskeala, Sortavala, Priozersk and Vuoksa fault zones, it is usually possible to distinguish a main fault surrounded by smaller ones, whereas the Janisjarvi and Meeri zones are typically composed of a series of equal-sized faults. Most of the faults dip steeply towards the NE, subparallel to the overall trend of the Raahe-Ladoga zone, which likewise shows a steep contact with the Karelian domain. The Ruskeala and Meeri tectonic zones are exceptions; the Ruskeala fault dips steeply (80-85°) to the SW (Khazov et al., 2004) as a result of Riphean reactivation. The Meeri thrust zone is very distinctive, since it comprises numerous faults overprinted by high grade metamorphism and migmatization. This flat-lying to gently dipping tectonic zone has a true thickness of some 6-8 km, but because of its orientation, it is exposed over an area 20 km in width. It is interpreted as a zone of combined ductile and brittle deformation related to the thrusting of the Svecofennian domain over the Raahe-Ladoga zone (Baltybaev et al., 2000).

Generally, reverse displacements and thrust faults and strike-slip displacements characterized deformation along NW-SE-trending structures during the Svecofennian orogeny. During late Cenozoic time, some of the earlier dextral NW-SE trending faults were reactivated, mostly with dextral and normal sense of displacement (Chuvardinsky, 2000).

Dykes of diabases and granodiorites, and pegmatites of Jatulian, Svecofennian and Lower-Middle Riphean age are often oriented parallel to NW-SE trending structures.

Tectonic zones striking NW-SE correspond to schistose zones, mylonites and breccias. Metasomatic alteration in these rocks is widespread. Medium- to low-temperature conditions prevailed, as indicated by alteration paragenesis consisting of sericite-quartz and sericite-albite-quartz (often accompanied by sulphides), and the presence of quartz-carbonate veins and breccias zones filled with a hematite-albite-quartz-carbonate cement. High-temperature microcline-quartz metasomatic rocks occur sporadically in the east part of the Janisjarvi fault

zone in the granite-gneisses of the Karelian domain (Grigorieva, 1977). Numerous U occurrences of different types and grades are associated with the Janisjarvi and especially the Ruskeala fault zones.

NE-SW trending faults in the Ladoga area form part of the Baltic-Mezen tectonic belt, which overall has a convex shape toward the east, with orientations changing from E-W along the Baltic Sea, to NNE in White Sea area. At regional scale, there is a fault-controlled mosaic of uplifted blocks and downfaulted depressions, the latter corresponding to the present Baltic Sea, Ladoga and Onega lakes, and the Dvinsky and Mezen gulf areas of the White Sea. Uplifted areas correspond to the Karelian isthmus, Podporojskaya upland, Vetrenny belt and the Belomorian-Kuloiskoe plateau. The Baltic-Mezen belt controls the location of many of the granite-rapakivi intrusions (Aland, Laitila, Wiborg, Svir, Salmi and Ulalegi). The Migmatite Belt of Southern Finland, which can be traced as far as the Ladoga region, is also located within the limits of the Baltic-Mezen belt. Most of the Riphean sedimentary basins preserved on land (Muhos, Pasha-Ladoga, Lemsky, Onegozersky and Severoberegny) also lie within the belt.

The NE-SW tectonic zones are composed of fault systems up to 2-5 km in total width. Generally, these dislocations are strike-slip faults, the largest of which are the Elisenvaara and Ruokojarvi fault zones, observed north and northwest of Ladoga. They are discernible in seismic images to a depth of 40 km, and can generally be traced for many kilometers along strike. In the NE-SW trending brecciated zones, low- to medium- temperature hydrothermal alteration is evident (Grigorieva, 1977). The Southern Ladoga tectonic system (Svir fault, etc) is concealed beneath the Vendian and Paleozoic cover and has been identified on the basis of geophysical signatures, although interpretations are mostly of a tentative nature.

Many of the meridional faults of the area correspond to ancient structures of the Karelian basement. Thus, the Jalonvara granite-greenstone belt continues into the Raahe-Ladoga domain as the Ljaskelja downlifted block and further south to the Svecofennian domain (southern Ladoga Petrokrepost bay). The southern continuation of the Hautavaara belt can be recognized under the platform cover as the Volkhov river fault. These meridional structures differ markedly depending on whether they traverse Archaean or Palaeoproterozoic terrain: in the first case they are composed of numerous faults and can be traced through the crust to the upper mantle, while their continuations into the Palaeoproterozoic domains are not so deep and are represented by several intracrustal dislocations and expressed as a major fault. The north-south extension of most of the granite-gneiss domes of Northern Ladoga and local occurrences of syn- to late-orogenic granitoid intrusions along the meridional faults (Latvasurje area) indicate the

importance of this tectonic direction in controlling the emplacement of anatectic melts during the Svecofennian orogeny. Meridional faults of the pericratonic Tulomozero depression continued into the Salmi massif, accompanied by a swarm of mafic dykes of Lower-Middle Riphean age.

The meridional dislocations had different kinematics at different times. However, it is considered that strike-slip faults were the most typical during the Svecofennian orogeny. Among neotectonic dislocations, N-S and NW uplifts and dextral displacements occur that correspond to moderate horizontal compression (Chuvardinsky, 2000).

Several generations of deformation and alteration are related to intradome meridional structures (Grigorieva, 1977). The earliest deformation place soon after the consolidation of the granite-gneiss domes and is represented by intense small-scale folding, development of augen structures in the gneisses, layered migmatites, agmatites and boudinage structures. During the second stage, contemporaneous with Svecofennian late-orogenic leucogranite formation, microcline-quartz metasomatic rocks with REE mineralization, and abundant blastomylonites and blastocataclasites were developed. The third event is represented by zones of cataclasis and fine mylonitic and fracture systems and, sericite-quartz and sericite-albite-quartz metasomatism often hosting uranium mineralization. Lastly, Neogene-Quaternary reactivation of the meridional faults is responsible for the formation of the numerous fjord-like gulfs of the Northern Ladoga coastline.

The E-W trending fault system is less significant in the Ladoga region, being mainly represented by local short fault segments with small depth extent. Individual structures usually have a length of less than 10 km, although they can combine to form swarms that can be followed for distances up to 55 km (Grigorieva, 1977). One of the most significant E-W trending fault systems is the Sukhodolje system, which disrupts metamorphic rocks and the Wiborg granite massif and can be traced beneath the lake to the Podporoje faults in the Eastern Ladoga region. The Valaam archipelago, which is composed of uplifted Valaam sill formations, is partly controlled by an E-W trending fault with a reverse throw on the southern limb of 100-150 m (Amantov, 1992). The Gulf of Finland is likewise formed by the E-W trending Baltic tectonic trough. The Kitelya fault can be followed from the Ljaskelja block of the Raahe-Ladoga domain into the Salmi massif. Usually the kinematics of E-W trending dislocations corresponds to small-amplitude normal and reverse faults, with small horizontal displacement.

The E-W trending faults are not usually accompanied by significant alteration: fractures are “dry”, and only rarely associated with mylonitization and fine-grained breccias cemented

with chalcedony and carbonate. Ore mineralization is absent as a rule; an exception however, is the Kitelya fault, which is intensively mineralized in the vicinity of the Salmi massif (Kitelya Sn-polymetallic deposit with overprinting U mineralization).

1.9. Non-radioactive metallogeny.

All ore deposits of the region are located in the Northern Ladoga part of the Raahe-Ladoga zone (fig. 1.7), in the other areas mineralization only corresponds to anomaly range.

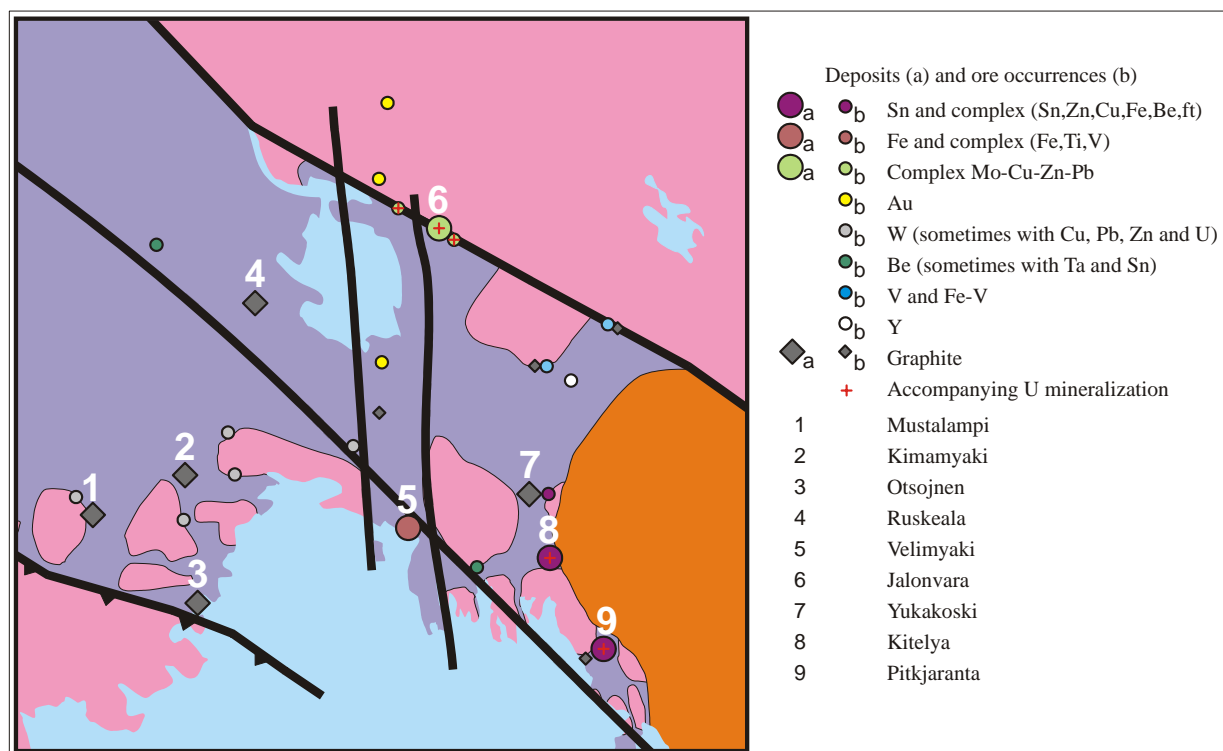


Figure 1.7. Map of non-radioactive mineral resources of the Northern Ladoga area.

The most significant mineralized areas is at Pitkjaranta-Kitelya, surrounding the Salmi granite massif, where there are numerous medium- to small-sized complex ore deposits (Sn, Zn, Cu, Fe, Be, fluorite). Late U mineralization in fractures accompanies these ores. . Mineralization is hosted mainly in skarns and greisens in enclosing metamorphic rocks, but also as veins within the Salmi granites. A Palaeoproterozoic age was obtained for molybdenite from these deposits (1750-1820 Ma by Re-Os analysis, Stem et al., 1996), but Sm-Nd analyses of ore-hosting skarn and greisen give Lower Riphean ages (1546±28 and 1492±25 Ma , Larin et al., 1991). These deposits are related to granite formation in the domes during the Svecofennian orogeny and to the Lower Riphean Salmi massif. They were mined from 1814 to 1904.

In the Salmi depression under the Riphean sediments two complex-ore occurrences similar to ones of the Pitkjaranta-Kitelya ore knot are located – Salmi and Karkunlampi ore-showings.

The small deposit at Jalonvara and several occurrences of Mo-polymetallic ores are located at the intersection of the Janisjarvi and Elisenvaara fault zones and the Jalonvara greenstone belt. The more significant Mo mineralization is related to metasomatically altered Lower Lopian silicic metavolcanic rock and the Upper-Lopian Jalonvara granite massif. The Mo ores are often associated with Cu, Zn, Pb, W, Au, Ag, S, while U mineralization has been found in late fracture zones.

The small Velimyaki Fe-Ti deposit is localized in pyroxenites of the Velimyaki intrusion, while Fe ores also occur in lacustrine sediments east of Lake Janisjarvi.

Gold ore-showings were discovered to the north within the Jalonvara and Hautavaara greenstone belts and also in their southern continuation at Alattu, in greenschist formations of the Ladoga group, south of the Janisjarvi Lake. The Au mineralization is related to beresite alteration of Palaeoproterozoic granite and gabbro-dolerite dykes and hosting quartzose sandstones.

Tungsten mineralization has been found in the Sortavala block. Scheelite mineralization is also associated with the magnesium skarns after carbonate rocks (Pitkjaranta suite), accompanied by molybdenite, wolframite, cassiterite, bismuthine, native bismuth, sulphides. The ore-showings are considered as analogs of the occurrences of the Begslagen area of Sweden (Ohlson, 1979).

Vanadium mineralization is present within the Ludicovian carbonaceous rocks of the pericratonic depression along the Janisjarvi fault zone.

Beryllium mineralization occurs in skarns (with Sn) and in pegmatites (with Ta).

Occurrences of Ta, Nb and REE are related to pegmatites of Palaeoproterozoic and Lower Riphean age (late phases of the Ulalegi rapakivi massif). REE mineralization was also discovered in the exocontact of the Wiborg granite massif.

The Ladoga region also contains other, non-metallic mineral resources; there are many deposits of dimension stone in both the Raahe-Ladoga domain and the Svecofennian domain: Svecofennian and Riphean intrusive rocks, Ruskeala marbles, Putilovo limestone etc. There are five small deposits and numerous occurrences of graphite in the Kalevian schists of the Northern Ladoga area, while Ladoga group schists host the small Kitelya garnet deposit in the Northern Ladoga region.

There are also numerous uranium occurrences in the Ladoga area. In general, according to their stratigraphic position, they may be subdivided into three groups:

- I. basement hosted,
- II. Riphean hosted,
- III. Vendian-Palaeozoic platform sediment hosted.

Each of these types will be considered in detail in the subsequent chapters.

2. Evolution of geological structures and uranium abundance of the Ladoga region.

The present Baltic Shield was formed mainly as a result of accretionary growth during several successive tectono-magmatic cycles: i.e. Lopian (3.0-2.6 Ga), Karelian (2.5-2.1 Ga), Svecofennian (2.0-1.8 Ga), Sveconorwegian (1.5-0.85 Ga) and Caledonian (0.53-0.39 Ga). This prolonged and complex evolution from Archaean to recent times is recorded in the geological structures of the Ladoga region (Appendix to Part 1, table 1.3). The formation of the continental crust was accompanied by a gradual enrichment in uranium.

Archaean geologic processes occurred in the Karelian craton and locally in the Raahe-Ladoga zone. During the Mesoarchaeon (Saamian: < 3.15 Ga) the earliest sialic cratonic nuclei formed, the largest of them being the Vodlozersky domain, located to the north-east of the Ladoga area. Processes of continental crust break up, riftogenesis, subduction and collision during the Lopian (3.15-2.5 Ga) led to the formation of linear greenstone belts with a submeridional strike. The amalgamation of the present Kola-Karelian craton occurred as a result of the Late Lopian or Rebol orogeny.

Economic uranium concentrations are not very typical of Archaean terrains (De Vivo et al., 1988). However, the first significant U-enrichment event in the Karelian crust is related to the late- (2.8-2.7 Ga) and post-collision (2.7-2.6 Ga) granites of the Rebol orogeny, with the formation of U-rich granites and pegmatoids (U content 5 ppm) (Voinov and Polekhovsky, 1985).

The regional U clark value for Mesoarchaeon rocks in the Ladoga region is 0.5 ppm, compared to 1.4 ppm for Neoarchaeon rocks. Increasing U abundances occurs in the late Lopian silicic metavolcanics (up to 3.5 ppm) of the Jalonvara belt and in the Jalonvara granite intrusion (up to 6.1 ppm).

After a long (about 100 Ma) period of tectonic stability, at the beginning of the Palaeoproterozoic, the Kola-Karelian continent was subjected to tectonic reactivation. During the Early Sumian (after 2.5 Ga), extension and incipient break up of the continental crust

occurred. Rifts formed, mostly in the northern and central parts of Karelia, often due to reactivation of earlier structures in the Lopian greenstone belts. Deposition of volcanogenic and sedimentary sequences occurred in these fault troughs. Rifting of the northern part of the craton and emplacement of layered dunite-peridotite-gabbro-norite plutons and dyke swarms took place during Sumian-Sariolian time (2.5-2.3 Ga). It is presumed that the northern part of the Palaeocraton was rifted and an ocean was formed. The southern part of the Karelian craton during that period was relatively stable and traces of early Palaeoproterozoic tectonic as a rule are not recognized in the considered area. Sumian and Sariolian formations of the Karelian craton are poor in U, containing only 1.1 ppm on average.

During Lower Jatulian time (2.3-2.15 Ga), a vast basin with continental and transgressing shallow-marine sedimentation covered much of Karelia (Ojakangas et al., 2001, Heiskanen, 1990). Orthoquartzites, from the pericratonic depression of the north-eastern limb of the Janisjarvi syncline, derived from weathering and aeolian erosion of the Archaean craton, while respective clay fractions were mainly removed to depocenters which are not preserved in the Ladoga region. Mechanical separation of detrital material, in the absence of organic reductants, led to the formation of Th-U placers, well-known in the nearby Koli-Eno area in Finland. Similar types of sediments are preserved in the pericratonic depression at the north-eastern limb of the Janisjarvi syncline. Uranium and thorium abundances in these rocks are on average 2.8 ppm and 49 ppm respectively. Numerous Th anomalies (up to 450 ppm Th, with a value of 7000 ppm) with subordinate U enrichments occur in the quartz conglomerate interbeds.

Towards the end of the Early Jatulian, tectonic activity increased, reflected by an increasing abundance of detritus in the basal quartzites layers and arkoses. The first record of stromatolite colonies also appears in the Jatulian. In the Upper Jatulian (2.15-2.06 Ga), rifting commenced at the southern edge of the Karelian craton, reflected by thick basaltic flows and numerous dyke swarms (mostly striking NW-SE), intruded along pre-existing structural trends, and also shallow marine sediments. This Jatulian extensional event did not however proceed to continental break up, but only formed aulacogen depressions (Glebovitsky, 2005). Sometimes this rifting event is referred to as part of Svecokarelian tectonic-magmatic cycle. However, Heiskanen (1990) proposed that a complete tectonic cycle took place and that an ocean basin opened and closed during the Upper Jatulian. There are no proves of this conception in the Ladoga region because the earth crust of this area had been formed or strongly reworked during the Svecofennian orogeny.

Upper Jatulian formations are relatively poor in uranium (up to 2.3 ppm in dolomite and 0.8 ppm in basalts), but some epigenetic concentrations hosted by these rocks probably represent endogenic reactivation, as in Finland (Laverov et al., 1983).

Ludicovian (2.1 or 2.06-1.92 Ga) and Kalevian (1.92-1.8 Ga) geodynamic processes played a key role in the geological structural evolution and U enrichment of the basement in the Ladoga region. Juvenile crust of the Svecofennian domain was formed during the latter period (fig. 1.8).

At the beginning of Ludicovian, intensive, predominantly basaltic magmatism occurred in the Raahe-Ladoga domain. The earliest tholeiitic basalts of the Sortavala series derive from a depleted mantle, were contaminated with Archaean crust material and represent the pre-rift stage of crustal extension. The picritic composition of the next stage of magmatism corresponds to an enriched mantle source and is consistent with continental break up. Prolonged and episodic rifting culminated in the opening of the Svecofennian ocean basin at about 1.97 Ga (Glebovitsky, 2005).

The oceanic rift axis had a NW-SE trend, with NE-SW trending transform faults. Subsequent convergent deformation reworked the Karelian craton margin, which also presumably gave rise to the orthogneiss domes. Dolomite, limestone and subordinate arkoses were deposited in rather shallow marine basins between the craton and a belt of accreted terrains – possibly an ensialic island arc complex. The presence of organic- and sulfide-rich rocks indicates an oxygen free environment, which was apparently normal for the upper Palaeoproterozoic. Phosphatic iron formations occurring in carbonate layers precipitated from upwelling waters at the shelf margin (Ojakangas et al., 2001). Deposition of carbonaceous and phosphatic marine sediments was associated with uranium accumulation, resulting in an average abundance of 11 ppm, whereas. Average uranium content in the Ludicovian sequence is only 2.4 ppm, due to its predominantly mafic volcanic composition.

Dating of the earliest volcanics of the bimodal series and primitive tonalites of the Ladoga region, indicate that the beginning of subduction and juvenile island arc formation occurred at 1.91-1.92 Ga. Kalevian sedimentation continued in the marginal basins. Conglomerate and sandstone occur in the pericratonic depression of the northern limb of the Janisjarvi syncline (Kontiosaari suite). Mature metapelites and subordinate metavolcanics (Hunukki suite) are interpreted as distal facies of a back-arc basin, but in the Raahe-Ladoga domain flyschoid facies derived from the adjacent Karelian craton predominate. Essentially greywacke metasediments of the Svecofennian domain, often associated with mafic and

intermediate metavolcanics, are presumed to represent fragments of a primitive ensimatic arc system. As a whole, this domain is considered to be a proximal facies of a back-arc basin (Bogachev, 1999; Stepanov et al., 2006). Precipitation of U by organic matter led to its enrichment in graphite-bearing rocks of the Raahe-Ladoga domain with 5.6 ppm U, in contrast with an average of 2.7 ppm in the Raahe-Ladoga domain Kalevian sediments (Skorospelkin, 2002).

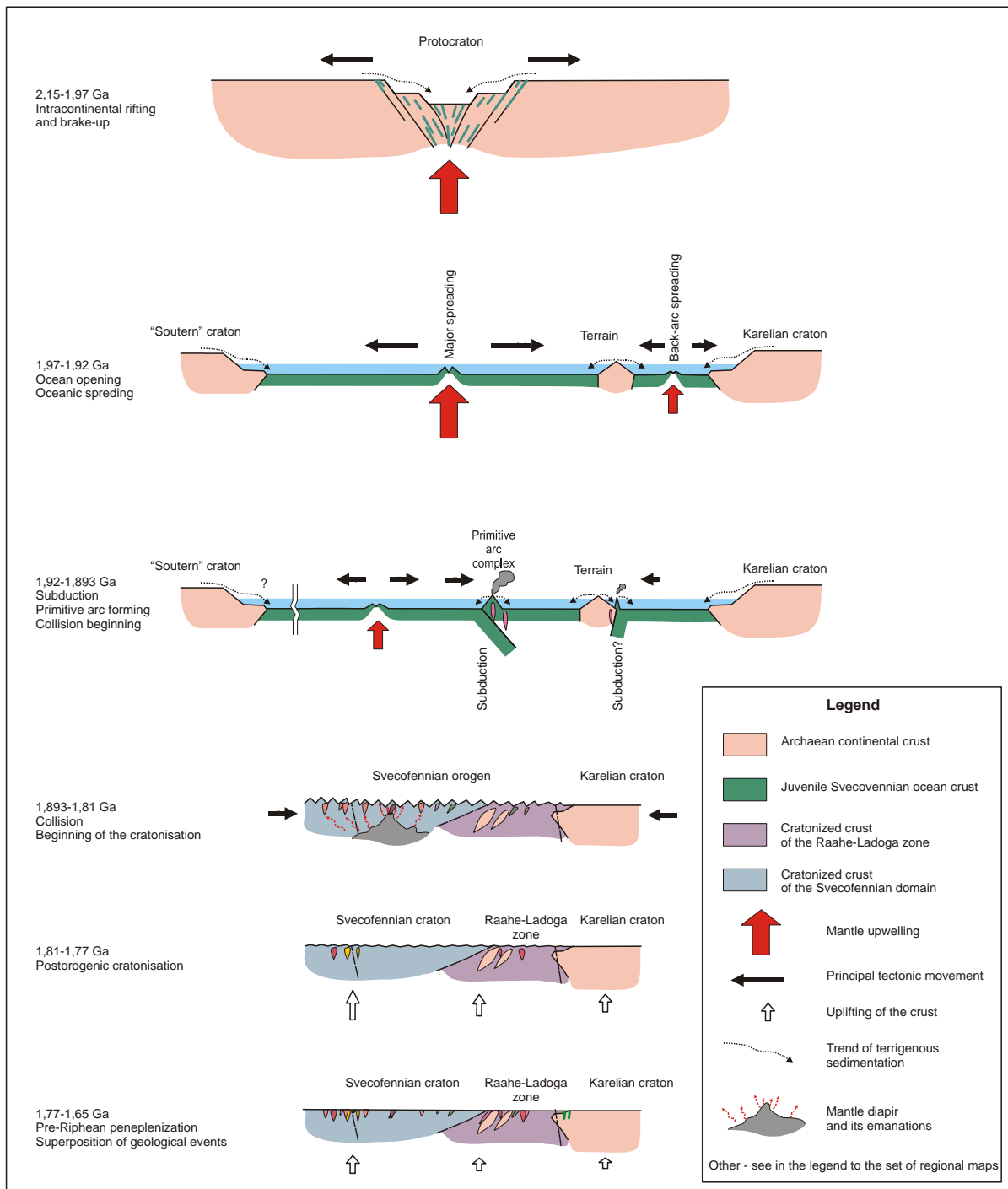


Figure 1.8. Scheme of the geodynamic evolution of the Ladoga region during the Svecofennian tectonic-magmatic event.

Closure of the ocean was not coeval throughout the entire craton margin, for example in the north-eastern part of the Raahe-Ladoga zone, where the Jormua and Outokumpu ophiolite complexes were obducted onto the Karelian craton. In the Ladoga region, such ophiolite associations are absent and, subduction prevailed instead, such that the basement of the Northern Ladoga area is composed of tectonic terrains accreted successively to craton. The early stages of prograde metamorphism are attributed to these events (fig. 1.9).

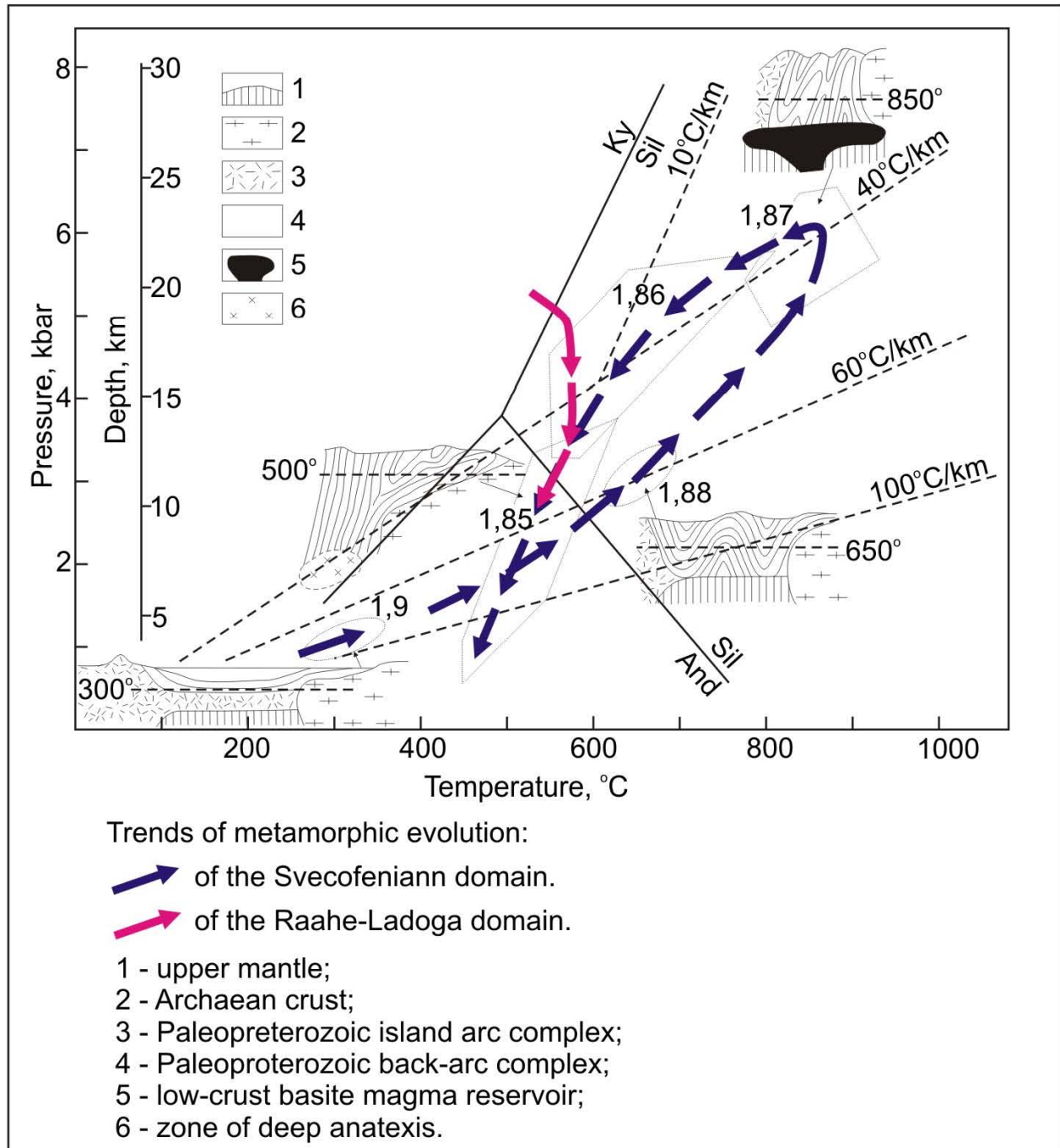


Figure 1.9. Evolution of metamorphic conditions in the Ladoga region crust during the Svecofennian orogeny (after Baltybaev et al., 2000).

During convergence, because of the reworking of former continental crustal material, magmatic composition of the magmatism shifted to the calc-alkaline series. The onset collision and the formation of mature island arcs is defined by dating the essentially andesitic-dacitic volcanics and plutonic complexes of gabbroid-tonalite-diorite and norite-enderbite composition. According to the isotopic-geochemical data, they were intruded during the interval: 1.895-1.87 Ga (Glebovitsky, 2003). As a result of high thermal gradients above the subduction zones and collisional stresses, progressive metamorphism (up to high-temperature granulite facies) occurred. Subsequently, allochthonous sheets of juvenile crust of the Svecofennian domain were overthrust upon the heterogeneous basement of the Raahe-Ladoga domain. Intensive migmatization is related to this stage of the collision and isotopic ages of migmatites are between 1869 and 1871 Ma. The collisional event culminated with the emplacement of two-feldspar I-type granites (the Lauvatsaari-Impiniemi complex) and early S-type potassic biotite granites (the Kuznechensky complex) at 1.87-1.86 Ga. These events were followed by retrograde metamorphism occurred. Thus, the duration of the Svecofennian (sometimes also called Ludicovian) ocean from its opening to the collision is estimated to have been about 110 Ma (Glebovitsky, 2003). Subsequent cratonization of the newly formed crust occurred with the intrusion of S-type granites, i.e. sodic tonalitic plutons were replaced by potassic granites. Mobilization of crustal sources for the biotite granite massifs (Tervusky, Putsaarsky, late phases of the Kuznechensky complexes) was caused by underplating during the latest phases of the Svecofennian orogeny. There was a gap in magmatic activity between 1.85 and 1.81 Ga, after which a new phase of magmatism began, with the intrusion of two-mica leucogranites of the Matkaselsky complex. Leucocratic magmas may result from adiabatic decompression following rapid uplift of deep anatectic zones (Bogachev, 1999).

The granites produced at this stage are enriched in U, Th, P and REE, some of the leucocratic varieties having 15 ppm U in average (the Matkaselsky complex). The relatively late generation of migmatites in the Northern Ladoga, produced by partial melting of newly formed continental crust, has up to 110 ppm U (Mursula dome), with sporadic extreme enrichments up to 14 000 ppm in the Puttummyaki deposit.

It is noticeable that between 1.87 and 1.86 Ga the axis of endogen activity had undergone reorientation. Before this time, the most significant Palaeoproterozoic tectonic and magmatic phenomena were related to the NW-SE structures (correlating with the Raahe-Ladoga zone trends in the study area). Afterwards, NE-SW structures, corresponding to the extension of the Baltic-Mezen belt, predominate. Potassic granite magmatism and shoshonite series rocks are

associated with this tectonic system, which can be followed from the continuation of the Late Svecofennian granite province (Migmatite belt of the Southern Finland, Bedrock Map of Finland, 1997) and also with an area of shoshonitic massifs (Eklund et al., 1998). Apart from alkali shoshonite intrusions, which only occur within the Svecofennian domain, Vepsian (1.8-1.65 Ga) terrigenous sediments were deposited in the Prionejskaya depression along the eastern continuation of the Baltic-Mezen belt and intruded by the Ropruchei gabbro-dolerite sill at 1770 ± 12 Ma (Bibikova et al., 1990). Subsidence occurred at that time, instead of the uplift characteristic of the Svecofennian craton.

A tectonically quiescent time gap occurred between 1.77 and at least 1.67 Ga throughout almost the entire Baltic Shield. The only exception, far to the west of the study area, in Sweden, within the Transscandinavian igneous belt, was the 1.71-1.68 Ga, Dala A-type granite plutonism and accompanying volcanism (Ahl et al., 1999). Just before and during the early Lower Riphean (1665-1500 Ma), a number of rapakivi intrusions were emplaced in the southern part of the Baltic Shield. In the Ladoga region, the duration of this period was about 130 Ma, from 1665 Ma (the earliest phase of the Wiborg pluton), until 1535 Ma (the latest phases of the Salmi pluton). The abundance of U and Th in these intrusions increased from early to late phases and reach 14 and 100 ppm respectively.

A regional sedimentary hiatus corresponding to the middle Lower Riphean, from 1535 until about 1460 Ma, indicates that the entire craton underwent uplift, caused, at least partly, by isostatic compensation of the low-density granitic crust. As a result, numerous granite intrusions, of Svecofennian and early Lower Riphean age, were exhumed. The magnitude of this uplift was not less than 5-10 km (corresponding to the emplacement depth of the rapakivi massifs).

During late Lower Riphean time, the Ladoga region was affected by a tectonic rejuvenation marking the beginning of a new rifting cycle. Crustal thinning occurred, and ancient NW-SE and NE-SW tectonic zones were reactivated. Renewed movements along faults internal to and bordering the Raahe-Ladoga and Baltic-Mezen tectonic belts resulted in formation of the Pasha-Ladoga sedimentary basin, which was filled with predominantly alluvial arkosic sediments. The basin was also the locus for sub-alkaline basaltic magmatism, with two specific intrusive centers being recognized: the well-preserved Valaam sill on the Valaam archipelago within Lake Ladoga, and a more deeply eroded feeder conduit represented by the Hopunvaara intrusion in the Pitkjaranta area. Intercalation of volcanic flows with terrigenous

sediments indicates an episodic pulse character to this magmatic activity. Based on the age determination of the Valaam sill, sedimentation must have begun not later than 1.46 Ga.

The diversity of lithofacies in the Pasha-Ladoga basin sequence indicates deposition in highly variable conditions. It is inferred that, following a period of general subsidence, accommodating the basal volcanogenic-sedimentary units of the Priozersk, Salmi and Pasha suites, the Pasha-Ladoga basin continued to subside along its southwestern margin, with some stabilization of its eastern parts. This can explain the presence of carbonate layers in the sequence preserved in the Priozersk depression and their absence from the Salmi and Pasha areas.

Erosion of the U-enriched basement formations (firstly late-Svecofennian and Lower Riphean granites, and then Ludicovian and Kalevian supracrustals) can also account for their relatively high abundances in the Pasha-Ladoga basin sediments. Diagenetic and mild deformational events within the newly deposited units and the underlying basement formation, with hydrothermal activity driven by anomalous geothermal gradients, with migration of brines would have all contributed to extraction of uranium from the basin sediments and from the basement, and its concentration at the geochemical and mechanical trap represented by the Riphean unconformity.

The late Lower Riphean geodynamic setting in the Ladoga area corresponded to the early stages of the formation of the triple junction rift system above the mantle upwelling, possibly centered on the southeastern part of the modern Lake Ladoga basin. The southwestern branch of the rift was along the Baltic-Mezen tectonic belt, while the southeastern branch is represented by the Pasha graben and the northern one corresponds to the dyke swarm cutting the Salmi massif. However, the crust of the region was apparently too strong to permit complete cratonic breakup, and the effects of rifting become weaker by the end of the Middle Riphean. The locus of magmatic activity moved relatively to the west, where the Dalslandian (Sveconorwegian) orogeny occurred, and the Pasha-Ladoga basin continued to develop episodically as a typical aulacogen since Upper Riphean time. The broadly concentric pattern of sedimentation in the Pasha-Ladoga basin maybe attributed to collapse and subsidence of the cooling mantle upwelling.

It is inferred from the absence of contemporaneous sediments in eastern Fennoscandia that the time interval from 900-650 Ma was a quiescent period of gradual uplift and erosion. As a result, formerly widespread Riphean sediments have been preserved only in some depressions (Pasha-Ladoga, Satakunta, Muhos, etc).

During Lower Vendian time (650-620 Ma), Laplandian/Varanger glaciation occurred throughout the area corresponding to the modern Baltic Shield (Nikishin et al, 1996). Remnants of tillite sediments have been preserved in the low lying areas, as in the Pasha-Ladoga depression.

The platform stage of development of the East-European craton commenced during Upper Vendian time (620-550 Ma) with a widespread transgression, corresponding to the opening of the Iapetus ocean to the west of the Baltic Shield (Kohonen and Rämö, 2002). The uniform thickness of the Upper Vendian sequence northward and its occurrence in the Bothnian gulf testify that these sediments have covered at least the south-eastern part of present Baltic Shield (Nikishin et al, 1996), or possibly the entire craton (Amantov and Voronov, 1993). The Upper Vendian-Lower Cambrian transgression was interrupted at the end of Lower Cambrian (ca 530 Ma) by a mild uplift event throughout the Baltica. This regression event, known as the Soligalich inversion coincides with the climax of the Timan-Pechora-Ural orogenesis to the east of the study area and to transtensional deformation accompanying the oblique opening of the Tornquist Ocean to the southwest (Nikishin et al, 1996).

The period from Middle Cambrian until Early Devonian (530-420 Ma) corresponds to the Caledonian orogenic cycle. From Middle Cambrian to Upper Silurian (530-424 Ma) a vast shallow marine basin occupied the southern part of present Baltic Shield. Biogenically mediated accumulation of uranium from sea water led to its anomalous enrichment in organic-rich rock units such as the Cambrian bituminous shale of southern Sweden, and Ordovician Dictyonema shale of Estonia and western Russia (Pakerortsy horizon). During the Upper Silurian-Lower Devonian (424-386 Ma) the craton was uplifted, as a consequence of the Caledonian orogeny when Baltica collided with the Laurentia to the northwest (Norwegian Caledonides), to form the Laurassia continent (Nikishin et al, 1996). As a result of collision-related stresses, NE-SW - trending brittle displacements of Silurian age occurred within the Baltic Shield. In response to ongoing compression, uplift continued until Middle Devonian time, resulting in the complete erosion of the Upper Ordovician-Silurian sediments in the Ladoga region. The Caledonian orogeny was the last significant tectonic event in the long process of formation of the Baltic Shield as a united continental crust domain; later reactivations have only had a minor influence on its structure. A thermal signature of the Caledonian event has been recognized in the Ladoga region by isotopic dating where, for example U-Pb age determinations of zoned zircon grains from the Svecofennian Velimyaki massif gave 1893 ± 6 Ma for the core and 507 ± 53 Ma for the rim of the crystals, while chalcopyrite from a late schistose zone in the same massif was dated

by the Pb-Pb method at about 550 Ma. U-Pb dating of zircon from the Svecofennian Kuznechnoye massif yielded ages of 1881 ± 66 and 410 ± 100 Ma (Lokhov et al., 2004). Hydrothermal redistribution of uranium ores at 400 ± 40 Ma related to the Caledonian orogeny has also been recognized in the Kola Peninsula (Anderson et al., 1990). On the north-western continuation of the Janisjarvi fault zone in Finland diamond-bearing kimberlites dated at 434-592 Ma occur (O'Brien and Peltonen, 1998).

Indications of late Middle to Upper Devonian intracratonic rifting, relating to the initiation of the Hercynian (Variscan) tectonic cycle (385-300 Ma), occur to the north and northeast of the study area. This is particularly manifest through alkaline magmatism: concentric nepheline-syenite intrusions (Hibiny and Lavozero), carbonatites (Kovdor) and kimberlite-lamproite intrusions (Archangelsk kimberlite province, Povenetz diatreme). It is noteworthy, that the fault systems controlling this magmatism usually trend NE-SW. The Ladoga region however has little evidence of Hercynian reactivation and from Middle Devonian to Carboniferous time; the area corresponded to a continental to proximal shelf environment, with a shallow sea present to the south-southeast. During the Lower Carboniferous Lower Visean epoch (350-345 Ma), renewed uplift led to exhumation, followed by a further marine incursion from the east at the beginning of the Upper Carboniferous (311-303 Ma). The climax of the Uralian orogeny coincided broadly with the Carboniferous-Permian boundary (290 Ma) in the easternmost part of the East European craton, far to the east of the study area. To the west, the youngest significant period of magmatic activity took place in Late Carboniferous to Permian time, when the aborted Oslo intracratonic rift developed. It has been proposed that anomalous (up to economic grade) abundances of uranium in Upper Vendian sandstones are mainly a result of Hercynian activation (Mikhailov et al., 1999).

Since Triassic time, stable cratonic conditions have presumably prevailed in the Baltic Shield. In contrast with the adjacent Eastern Europe platform, there has been gradual (or episodic) uplift and exhumation. It is also inferred, that continental sediments, principally derived from the Scandinavian Caledonides buried a significant part (or all) of the Baltic Shield until their removal by erosion about 250 Ma ago (Larson et al., 1999). The existence of lateritic paleoregolith dated at 140 Ma (Anderson et al., 1990) indicates that Russian Karelia was at least partly exhumed during Cretaceous.

During Mesozoic time, denudation alternated with marine transgressions; in particular, Lower Cretaceous marine sedimentation took place on the southern part of the shield (Ziegler, 1981). The fact, that Lappajärvi (Finland) meteorite impact site was buried under sedimentary

rocks at about 75 Ma provides further evidence of the recent age of the final exhumation (Kohonen and Rämö, 2002). A peneplaned environment then prevailed until the end of the Mesozoic (Amantov et al., 1989).

The Cenozoic Era is characterized by a general uplift of the Baltic Shield, with weak oscillations, probably controlled by a combination of deep-seated endogenous (mantle upwelling) and exogenous (erosion, glacial isostasy) factors.

The Ladoga region, as a marginal area between the Eastern European platform depression and the uplifted Baltic Shield, has been subjected to intermittent tectonic activity during the Cenozoic era. The northern part of the Ladoga region is rising at an average rate of 1 mm/year, locally up to 6,4 mm/year (Kakkuri, 1997), whereas the southern part is subsiding at a rate of 0.4 mm/year. The Ladoga Lake, formed during the Quaternary, is also subsiding at a rate of 0.7-3.1 mm/year (Akromovskii et al., 2000). Some of the ancient faults were reactivated and elongated graben (Vuoksa) and local horsts (Toksovo) developed. The present landscape was formed as a consequence of at least five successive glaciations during Pliocene-Holocene, followed by isostatically driven transgressions and regressions. The latest glaciation took place about 21,500 years ago. Glacial events and subsequent geodynamic responses led to surficial and subsurface remobilization of ancient U ores, with formation of secondary mineralization (Reed et al., 2007).

There is abundant evidence of seismic activity in historical times. Since the beginning of the 20th century, several earthquakes with a magnitude up to 3-4 have been registered. Most of the epicenters are located in the Valaam archipelago and northern coastline of the Northern Ladoga region (Akromovskii et al., 2000).

Analysis of uranium distribution reveals a gradual increase in its average abundance with the time (fig. 1.10): 0.5 ppm in Mesoarchaeon, 1.4 ppm in Neoarchaeon, 2.5 ppm in Palaeoproterozoic, 3.4 ppm in Mesoproterozoic, 4 ppm in Neoproterozoic, 8.6 ppm in Palaeozoic rock units. Within the Proterozoic rock units of the Ladoga region an increase in U content with time is also observed: 1.1 ppm in Sumian-Sariolian, 1.5 ppm in Jatulian, 2 ppm in Ludicovian, 4.1 ppm in Kalevian, 8.2 ppm in Vepsian (granites), 5 ppm in Riphean and 4 ppm in Vendian. Maximal dispersion of U occurs in Jatulian and Ludicovian rocks (Mikhailov et al., 1999). The most enriched ones are the Matkaselsky leucogranite complex (9.5 ppm U on average, in the Matkaselka massif – 17 ppm) and the latest phases of the Wiborg rapakivi massif (14 ppm U). High U abundances in Palaeozoic sediments are a consequence of their enrichment

in Lower Ordovician phosphorites and especially the Dictyonema shales of the Pakerortsky horizon where it reaches subeconomic grades (130 ppm). Combined data on U and Th abundances in geological formations of the Ladoga region are presented in the General Appendix 2.1.

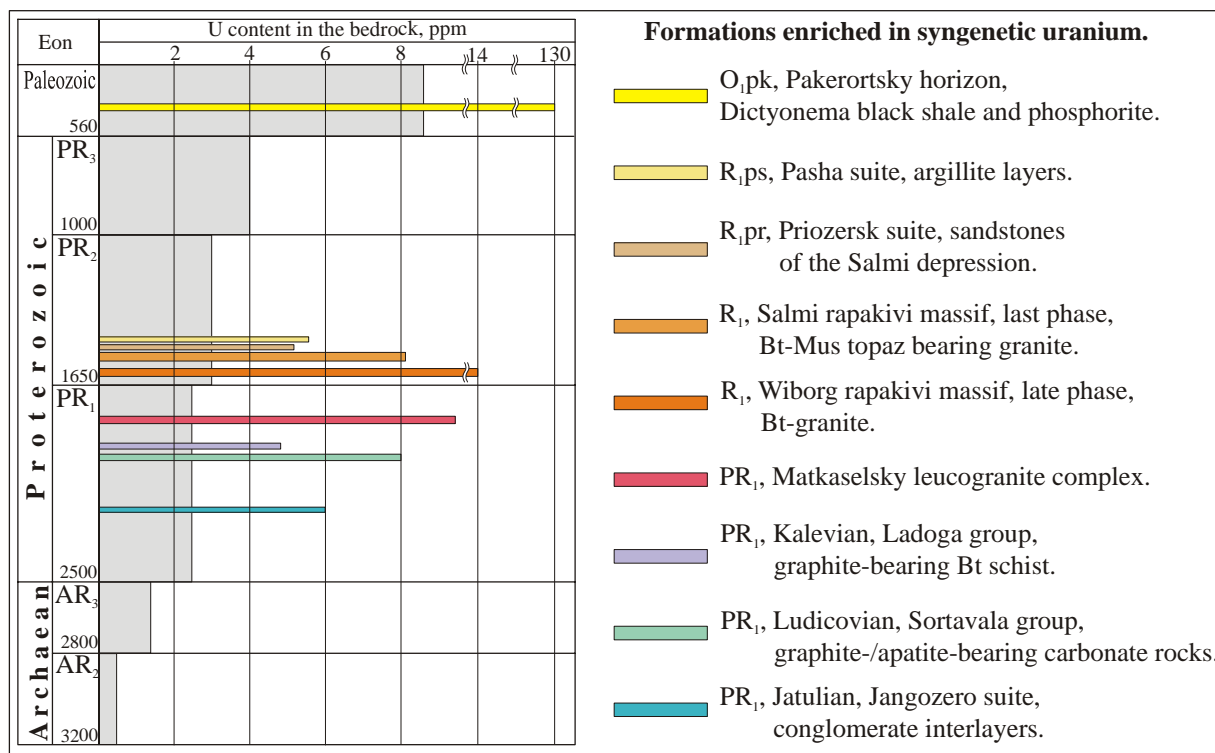


Figure 1.10. Evolution of uranium contents in the bedrocks of the Ladoga region.

**APPENDIX
TO PART 1**

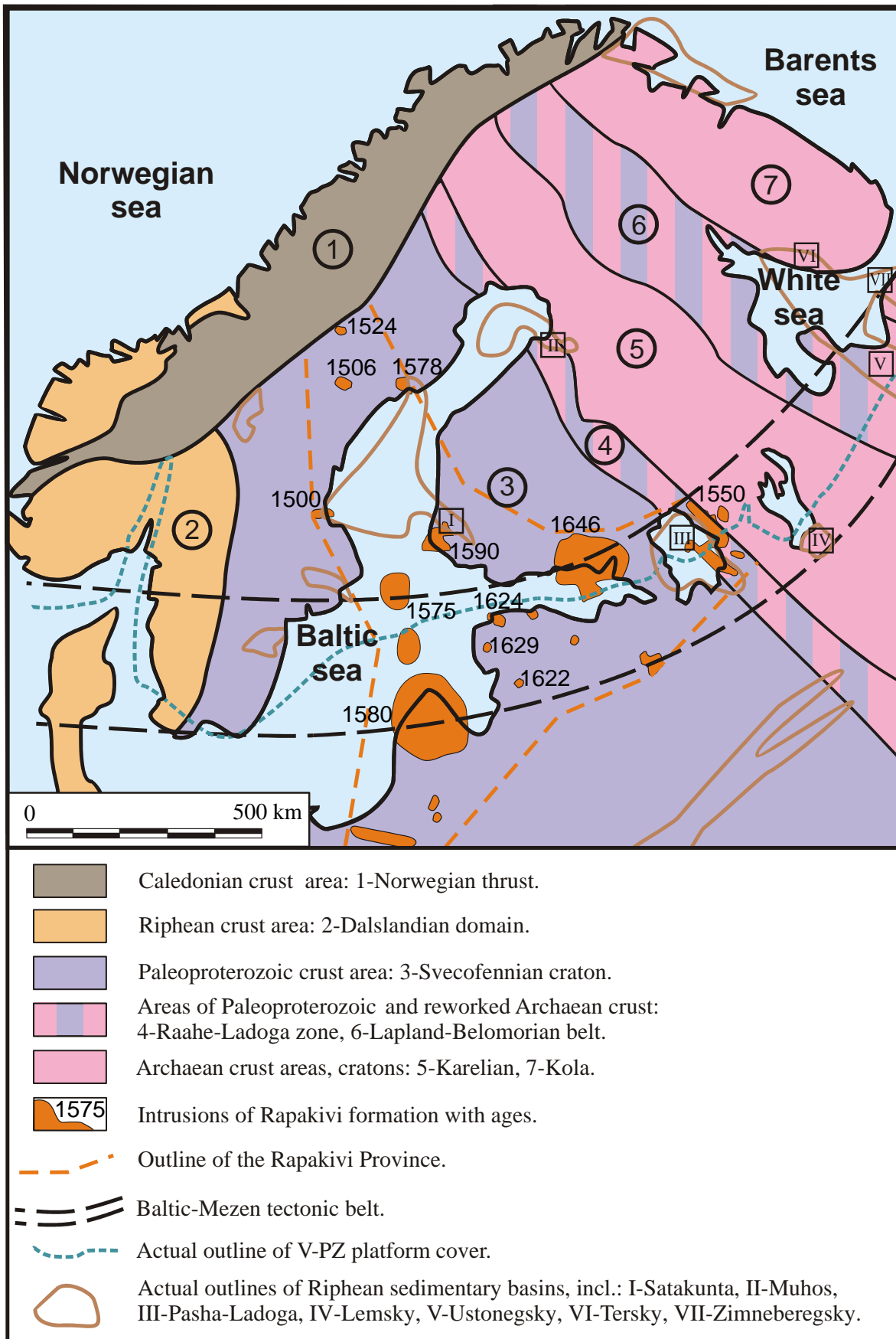


Figure 1. Generalized map of the tectonic zoning of the Baltic Shield.

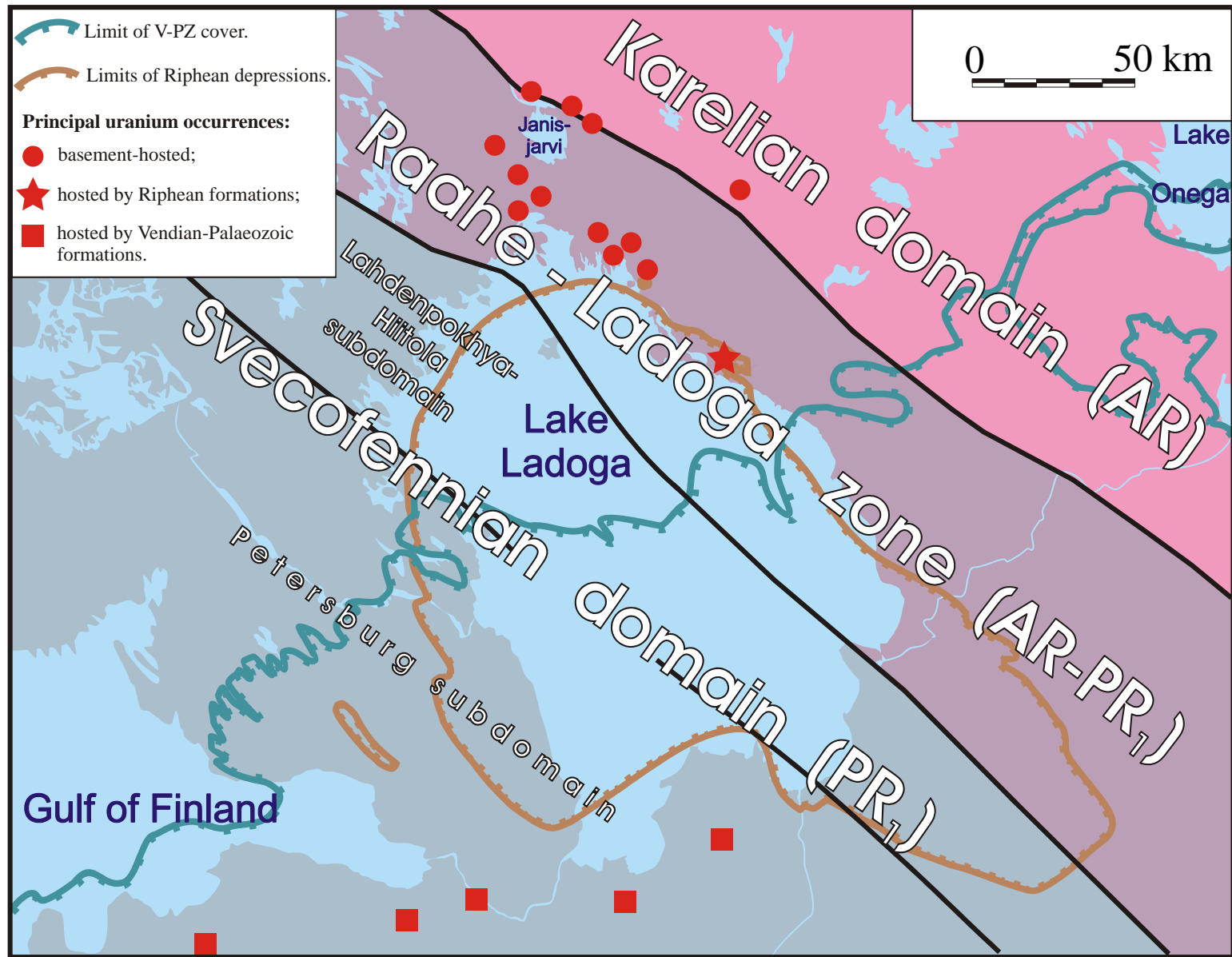


Figure 2 a. Map of the regional tectonic zoning of the Ladoga region.

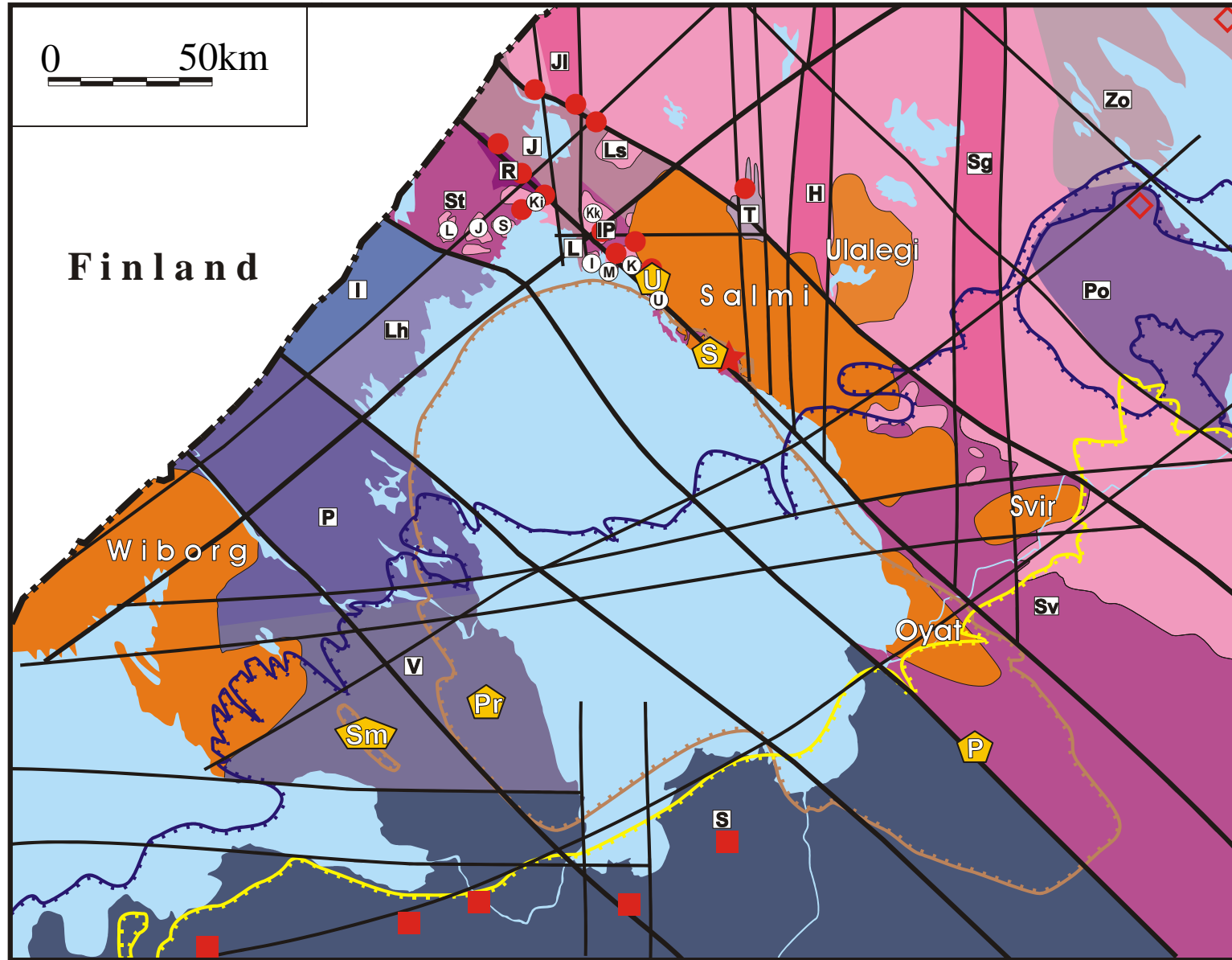


Figure 2 b. Map of the detail tectonic zoning of the Ladoga region.

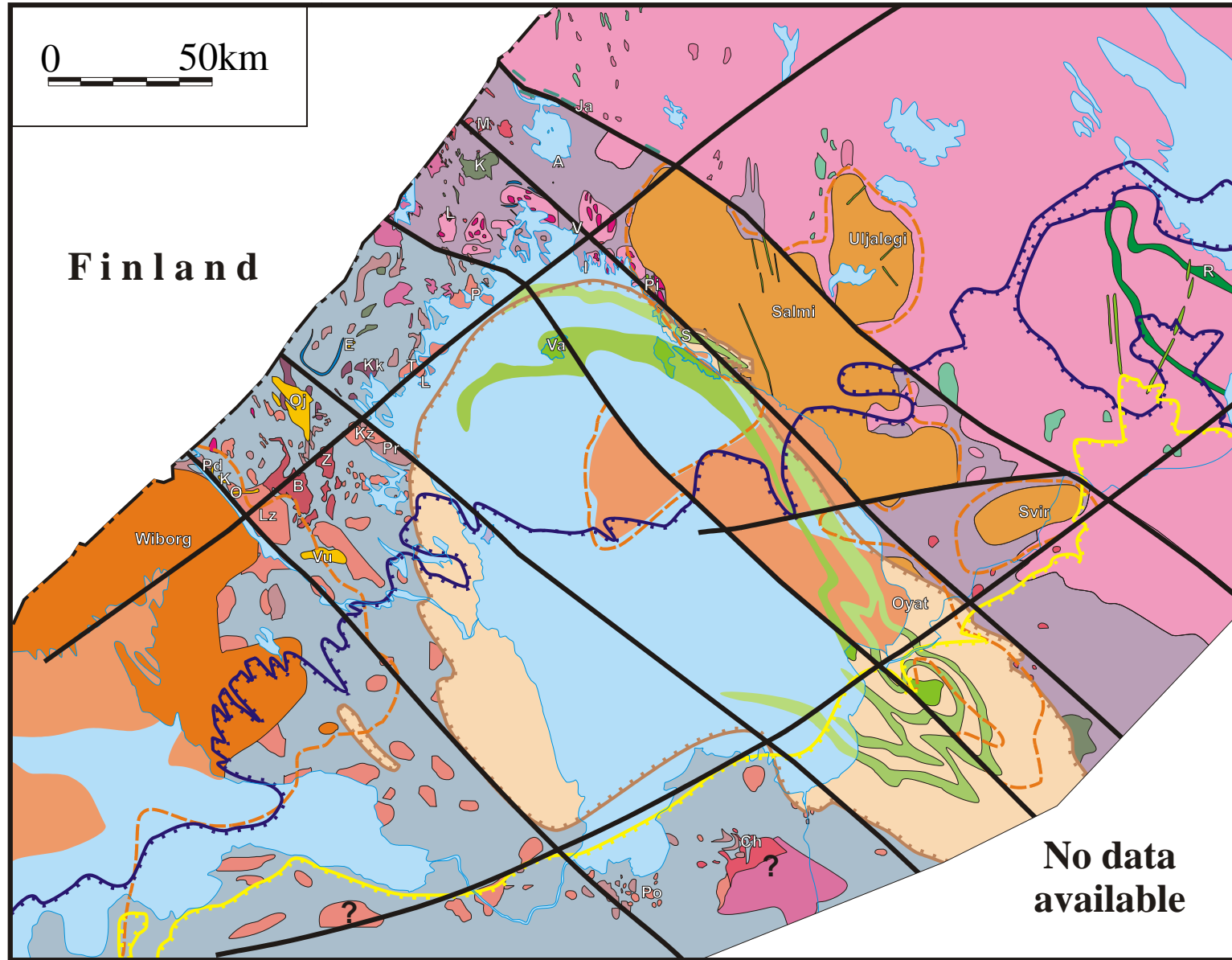


Figure 2 c. Map of the magmatic formations of the Ladoga region.

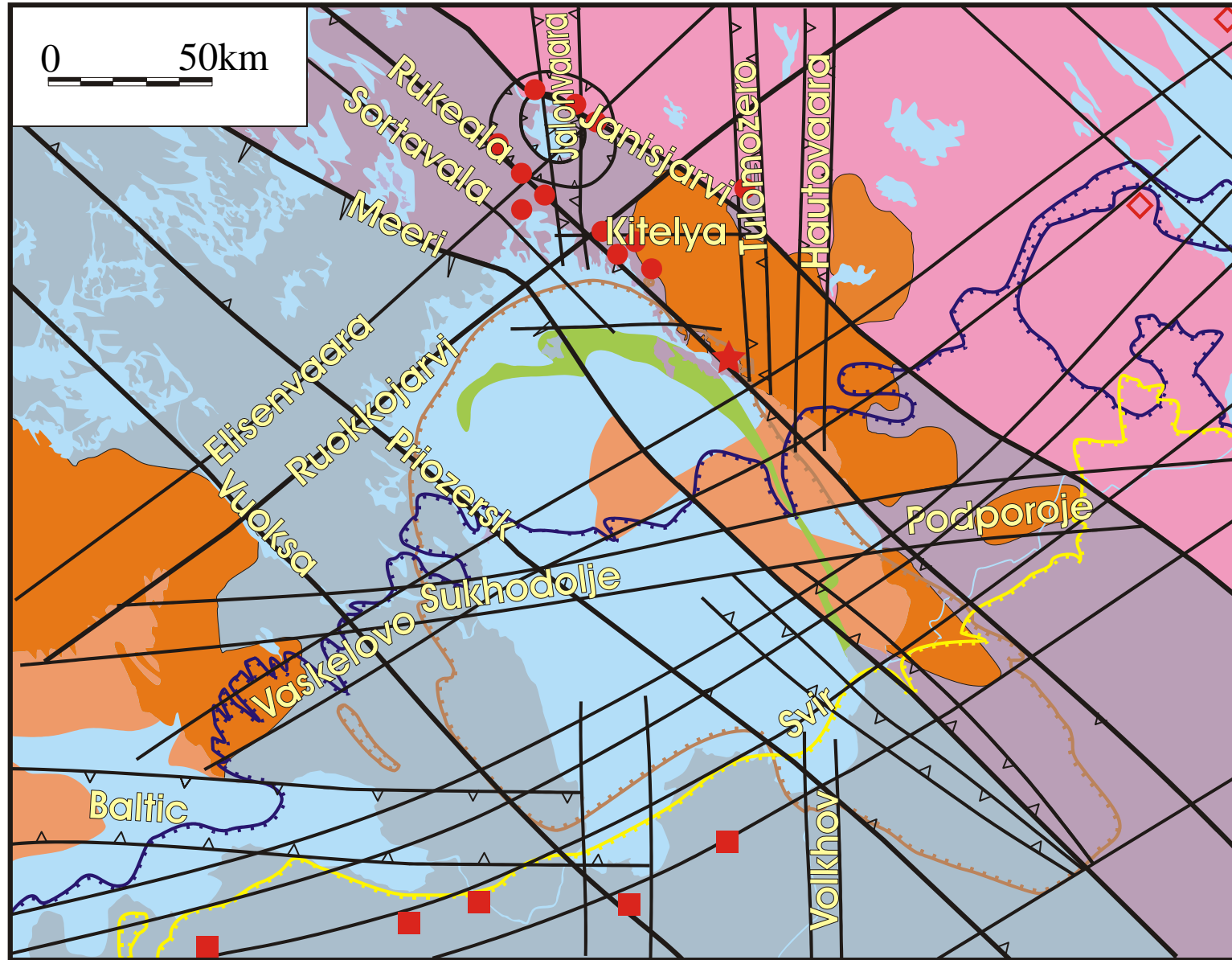


Figure 2 d. Map of the major fault zones of the Ladoga region.

Figure 2 e. Legend to the set of maps of the Ladoga region.



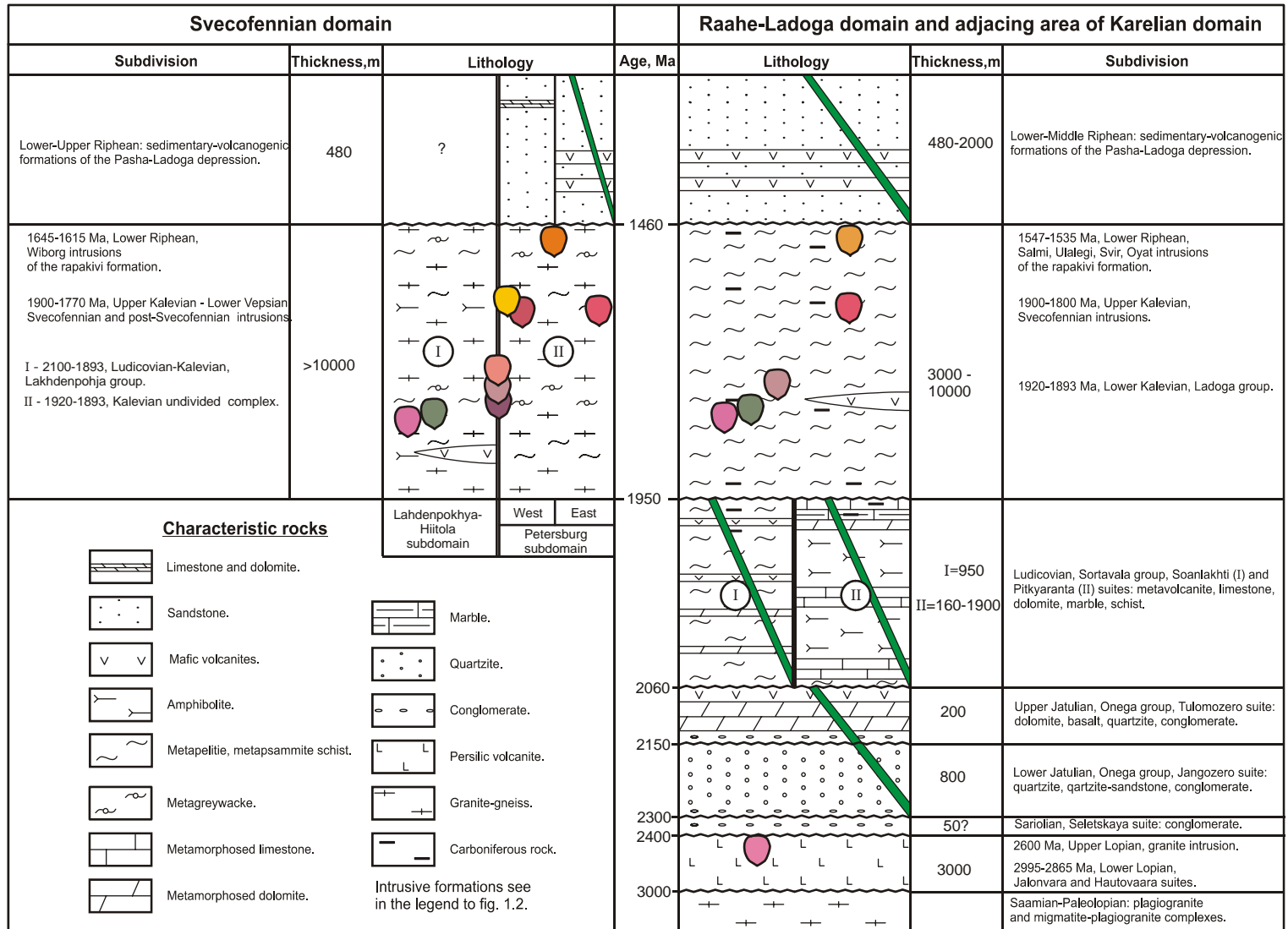


Figure 3. Column of pre-Vendian geologic formations of the Ladoga region.
NB: formations of the granite-gneiss domes of the Raahe-Ladoga domain are not shown because of uncertain reference.

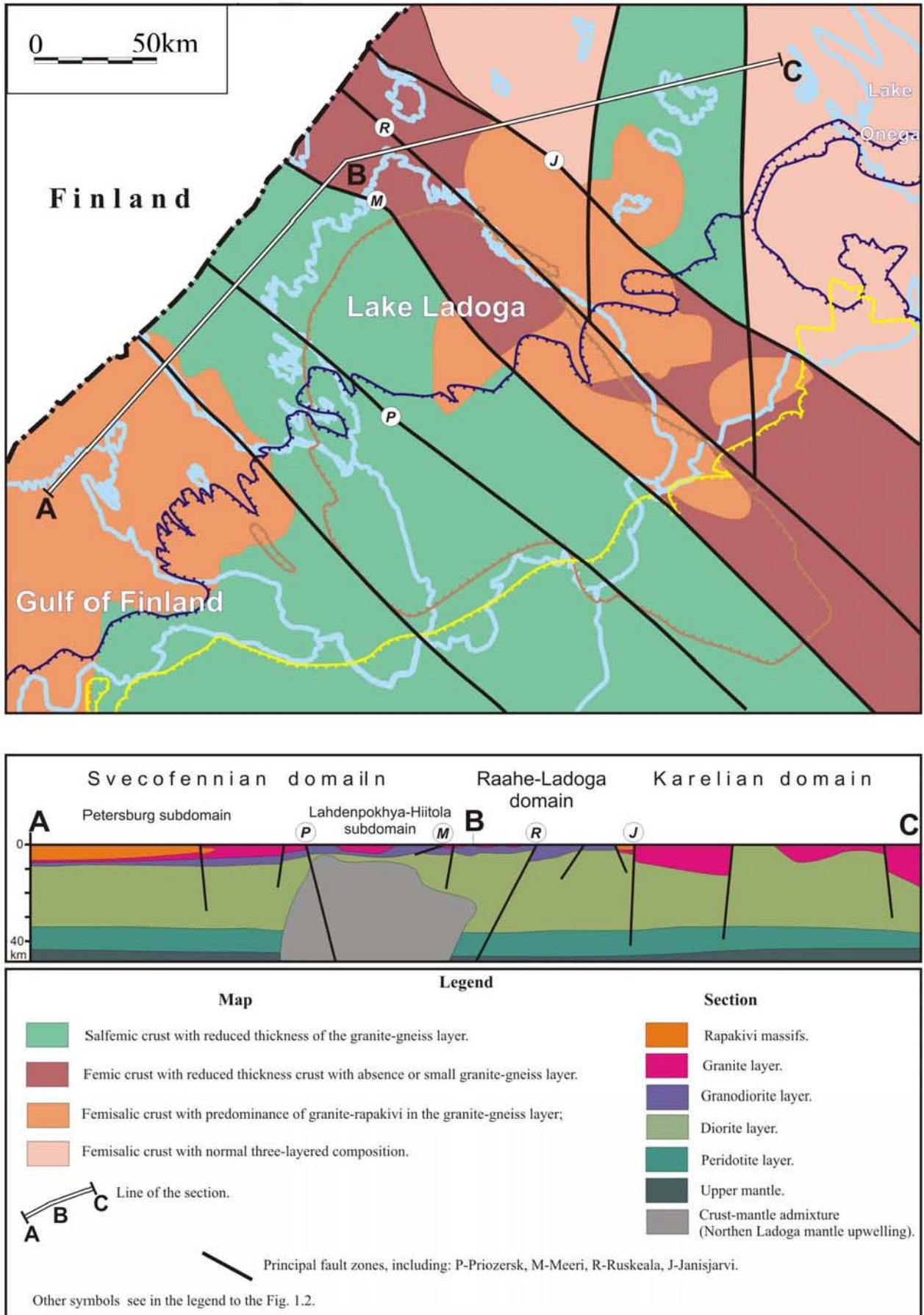


Figure 4. Map and section of the deep structure of the Ladoga region.

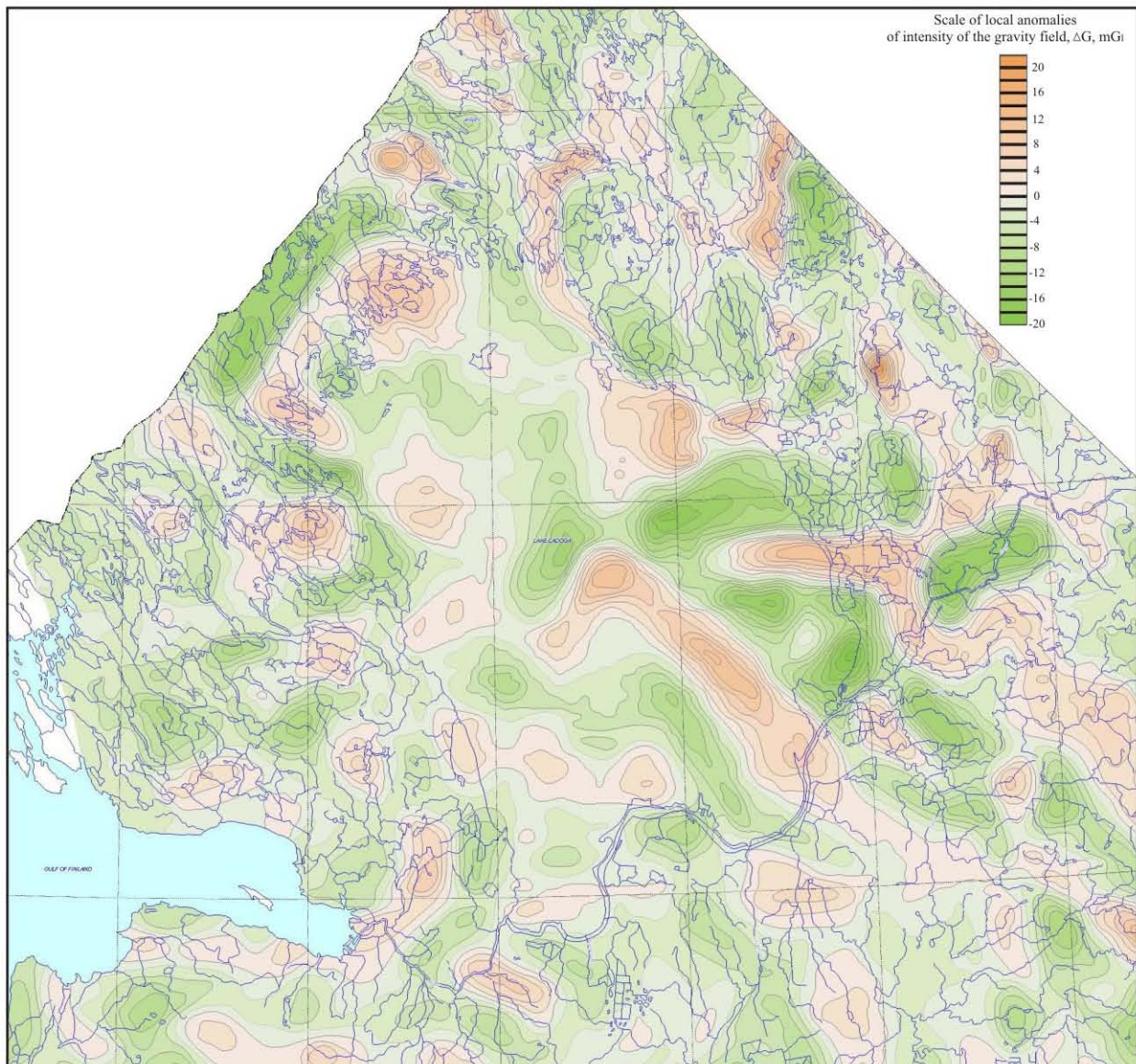


Figure 5. Map of the gravity field anomalies of the Ladoga region. Compiled by Shipota A.P. et al., edited by Apanasevich A.V., "Nevskgeologia", 2005.

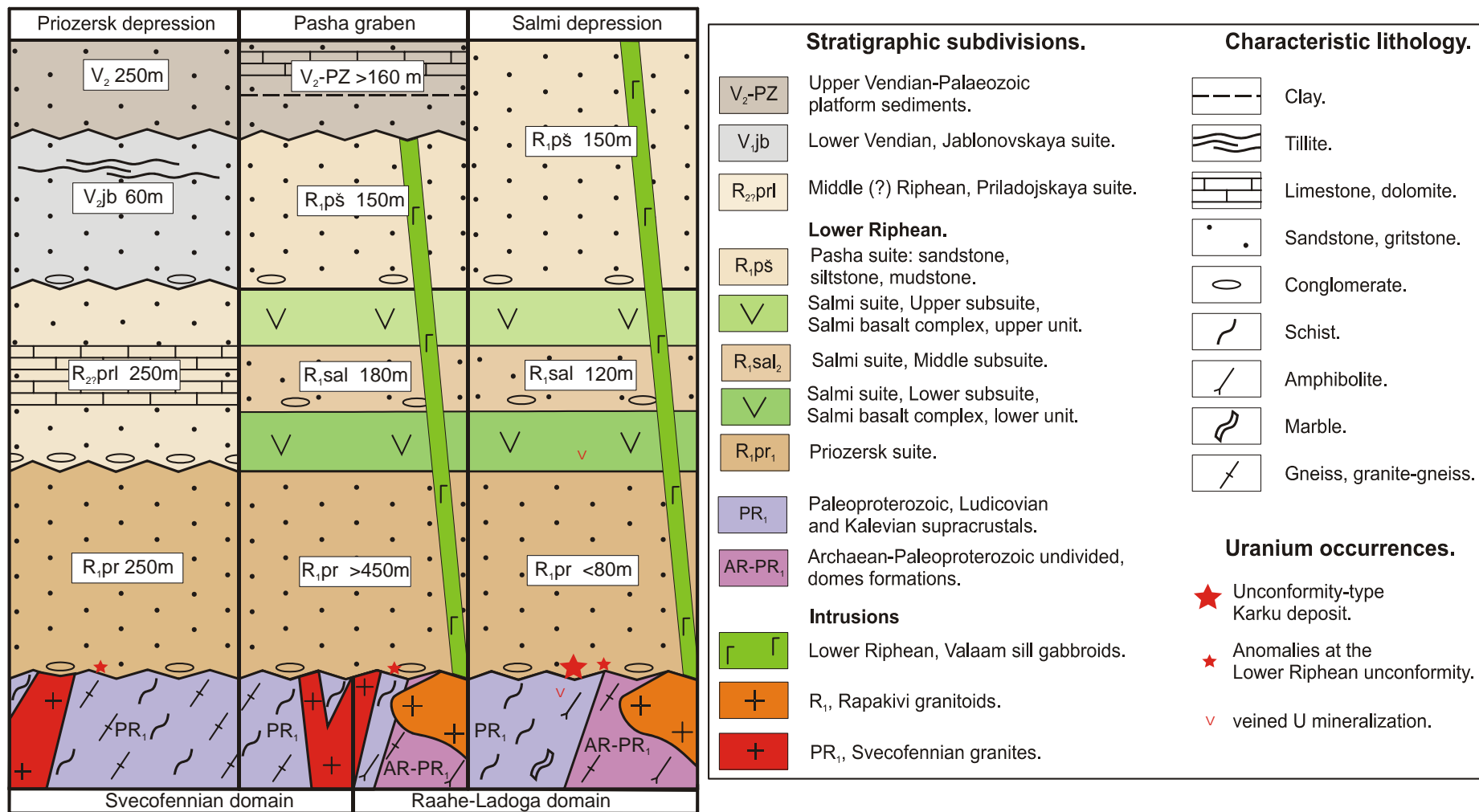


Figure 6. Geological column of the Pasha-Ladoga basin.

Table.1.1.Accessory minerals of the potassic granitoids of the Ladoga region (after Bogachev, 1999).

Massif	Rock	Minerals									
		Fluorite	Apatite	Zircon	Monazite	Garnet	Tourmaline	Orthite	Titanite	Ilmenite	Magnetite
Putsaari	Bt granite	0	xx	x	E	E	0	E	0	x	xxx
Tervus	Bt granite	E	xx	x	x	x	0	0	x	x	E
	Mus-Bt granite	x	xx	x	x	xx	0	0	E	xx	0
Kuznechensky	Bt granite	E	xx	x	x	xxx	0	0	0	x	0
Lazurny	Bt granodiorite	0	xx	x	x	xxx	0	0	0	xx	0
	Bt granite	x	xx	x	x	xx	0	0	0	xx	0
Zavetnensky	Bt granite	E	xx	x	xx	xx	E	E	0	xx	E
Borodinsky	Bt granite	E	xx	x	xx	xx	0	E	0	xx	E
Matkaselsky	Mus leucogranite	0	xx	E	E	xxx	xxx	0	E	E	x
Oja-Jarvi	Amf-Bt quartz monzonite	x	xxx	xx	0	E	0	x	xx	x	xxx
Vuoksa	Amf-Bt quartz monzonite	x	xxx	xx	0	0	0	xx	xx	x	xxx
Ostrovsky	Amf-Bt quartz monzonite	x	xx	xx	0	0	0	xx	xxx	xx	E
Prudinsky	Amf-bearing Bt granosyenite	E	xx	xx	E	E	0	xx	x	xx	E
Salmi	Amf-Bt rapakivi granite	xx	x	xx	E	0	E	xx	x	xx	x
	Bt granite	xx	x	xx	E	0	0	xx	E	x	xx

0 – mineral is absent, E – mineral occurs in single, x – rare mineral, xx – common mineral with content up to 0,n%,
xxx – widespread mineral, referred as subordinated rock-forming one.

Table 1.2. Average chemical composition of Svecofennian potassic granites of the Ladoga region (after Bogachev, 1999).

	Kz	L₁	L₂	P	T	B	Z	G	M	La	Oj	V	O	Pr	Km
SiO ₂ , %	72.90	67.06	71.49	71.57	72.50	71.08	70.51	70.25	73.86	73.46	64.40	61.86	64.19	65,94	65,02
TiO ₂ , %	0.25	1.01	0.50	0.44	0.38	0.49	0.43	0.53	0.03	0.06	1.15	0.95	1.31	0,86	1,10
Al ₂ O ₃ , %	13.42	15.51	14.36	14.53	14.56	14.59	14.44	14.35	14.27	13.98	15.03	15.51	14.50	14,06	14,00
Fe ₂ O ₃ , %	0.52	1.08	0.56	1.14	0.73	0.71	0.61	2.75	0.53	0.50	1.37	2.73	1.64	1,69	0,51
FeO, %	1.97	3.53	2.33	1.38	1.37	1.67	1.95		0.24	0.91	3.23	2.56	4.57	3,34	5,29
MnO, %	0.04	0.08	0.06	0.04	0.03	0.03	0.03	0.02	0.06	0.09	0.08	0.07	0.10	0,10	0,06
MgO, %	0.53	1.07	0.67	0.66	0.57	0.59	0.72	0.79	0.12	0.34	1.74	2.07	1.44	1,42	1,31
CaO, %	1.17	2.15	1.57	1.88	1.13	1.33	1.49	0.89	0.34	0.42	2.85	4.11	2.86	2,96	3,22
Na ₂ O, %	2.58	2.82	2.69	3.13	3.28	2.89	2.84	2.5	4.09	4.01	3.47	3.37	2.88	2,77	2,71
K ₂ O, %	5.52	4.23	4.88	4.36	4.69	5.36	5.64	6.95	4.23	4.74	4.39	5.18	4.66	5,53	5,10
P ₂ O ₅ , %	0.10	0.10	0.07	0.02	0.09	0.09	0.18	0.10	0.23	0.06	0.67	0.48	0.45	0,26	0,35
LOI, %	0.62	1.28	0.80	0.73	0.78	0.83	1.02	0.62	0.60	0.36	1.13	0.62	1.32	1,15	0,98
A/CNK	1.09	1.18	1.14	1.08	1.16	1.12	1.07	1.09	1.20	1.11	0.95	0.84	0.96	0,88	0,88
C/NK	0.105	0.21	0.145	0.18	0.097	0.115	0.125	0.070	0.027	0.033	0.25	0.33	0.25	0,26	0,29
F, ppm	600	900	600	490	880	590	640		330	210	2500	1120	2970	2300	
Li, ppm	26	23	21	13	29	17	18		60	21	20	16	21	19	
Cr, ppm	14	27	12	8	14	12	16	19	9	9	47	34	23	16	
Rb, ppm	216	133	169	92	204	224	205	259	296	307	153	146	185	217	
Sr, ppm	94	177	115	541	151	185	273	167	14	48	1250	1660	433	370	
Y, ppm	48	36	41	<10	22	16	10	18	13	19	25	48	41	26	
Zr, ppm	172	287	201	175	193	302	314	306	14	78	301	504	710	650	
Hf, ppm	5.2	5.0	4.2	3.8	4.9	8.6	8.3	7.9	12		13		28	26	
Nb, ppm	12	17	14	9	15	14	8	20	1.4	15	20	29	36	31	
Ta, ppm	0.84	0.39	0.46	0.41	0.82	0.78	0.54	0.48	3.1		1.6	1.6	1.7	1	
Ba, ppm	697	1290	722	1530	1080	1060	1350	630	205	176	1670	2690	1770	1550	
La, ppm	41	37	34	31	44	111	123	138	4.2	15	144	212	134	173	
Yb, ppm	6.3	3.7	5.5	0.35	1.27	0.94	0.88	0.49	1.1	1.8	2.1	3.0	3.55	2,65	
Th, ppm	16	20	15	6.5	17	55	47	123	1	24	20	35	25	39	
U, ppm	2.8	1.4	1.5	1.3	3.0	2.1	2.6	4.7	17	10	1.3	2.3	0.8	1,2	
Th/U	5.7	14	10	2.1	5.5	26	18	26	0.06	1.7	15	15	31	32	

Massifs: Kz-Kuznechnoye, L₁-L₂-central and marginal facies of Lazurny, P-Putsaari, T-Tervus, B-Borodino, Z-Zavetnensky, G-Gory, M-Matkaselka, La-Latvasursky, Oj-Oja-Jarvi, V-Vuoksa, O-Ostrovsky, Pr-Prudinsky, Km-Kamennogorsky.

Table 1.3. Succession of the geological events in the Ladoga region (combined from: Baltybaev et al., 1999; Bogachev, 1999; Glebovitsky, 2005; Heiskanen, 1990; Kohonen and Rämö, 2002; Akromovskii, 2000; Stepanov, 2006). Events occurred out of the Ladoga area but influenced on its structure are shown in italics.

Lower age limit, Ma	Era	Tectono-magmatic circle	Stage	Geological event	Magmatism	Metamorphism	Deformation	
3500	Saamian	<i>Forming of nucleuses of the continental crust of the Karelian domain</i>						
3200	Lopian	Lopian	Rifting and collision – forming of the greenstone belts		Mafic and felsic volcanites, granite intrusions, pegmatites	Ultrametamorphism of Saamian basement and metamorphism of the greenstone belts	N-S faults	
2500	<i>Sumian-Sariolian</i>	<i>Belomorian</i>	<i>Rifting, collision</i>	Continental sedimentation				
2300	Lower Jatulian			Littoral sedimentation, psammite				
2150	Upper Jatulian	Karelian	Intracraton rifting, beginning of the spreading	Marine sedimentation, dolomite	Mafic dykes, sills			
2100	Ludicovian	Svecofennian	Extension of the crust of the Karelian craton		Mafic dykes			NW faults
1970			Continental crust break up, Svecofennian ocean opening	Marine sedimentation, limestone, dolomite	Mafic dykes, sills, traps			
1920	Kalevian		Forming of juvenile island arcs	Turbidite series, littoral sediments	Volcanites of polymodal series			
1917			Beginning of the collision		Primitive tonalites (Jakkima complex), migmatites (leucogranites), pegmatoids	Zonal prograde metamorphism T=650-850°C, P=4.5-6.4 kbar	Isoclinal folds, foliation.	
1893				Uplifting	Gabbro-norite-diorite-monzodiorite (Kaalamo complex)		Open and isoclinal folds, foliation.	
1883			Mature island arc, continental crust growing		Enderbite (Kurkijoki complex), trondhjemite migmatites	Early retrograde metamorphism T=720-650°C, P=4.5-3.5 kbar	NW-ward thrusts, faults, NW shear zones, open and isoclinal folds, foliation.	
1880				Cratonization, uplifting.	Diorite-tonalite (Lauvatsaari complex), pegmatites, intensive migmatization; early massifs of potassic Bt-granites (Kuznechensky, Putsaarsky complexes), migmatites.			
1870			Culmination of the collision event					

Table 1.3. Succession of the geological events in the Ladoga region (continued).

Lower age limit, Ma	Era	Tectono-magmatic circle	Stage	Geological event	Magmatism	Metamorphism	Deformation
1860		Svecofennian (finalization)	Finalization of the collision	Cratonization, uplifting	Potassic Bt-granites (Tervusky complex), late migmatites.	Late retrograde T=650-400°C, P<3.5 kbar metamorphism	NE faults, NW folds. shear zones, small
1810							
1800							
1780	Vepsian			Uplifting, erosion	Potassic bi-mica granites (Matkaselka complex), gabbro-monzonite-syenite-granite, shoshonitic series (Elisenvaara, Vuoksa, Oja-Jarvi etc massifs)		NE faults
1650							
1645							
1615							
1550							
1530							
1500							
1350	Lower Riphean		<i>Local intracraton rifting. Peneplenization</i> Beginning of the crust extension		Wiborg massif of rapakivi formation and accompanying rhyolite volcanism		NE, W-E, NW faults
1100							
1000	Upper Riphean				Local continental sedimentation (Hoagland suite)		
900							
770-720							
650	Lower Vendian			Intensive uplifting and erosion	Salmi massif of rapakivi formation		
500							
1500	Dalslandian		Intracraton rifting	Intracraton basin sedimentation	Trapp basalts, gabbro-diabase intrusions		NW and NE normal faults and shifts
1350							
1100	Middle Riphean		<i>Collision</i>				
1000							
900	Upper Riphean			Uplifting and erosion	Janisjarvi impact event		
770-720							
650	Lower Vendian			Glaciation, then uplifting and erosion			
500							
0.62	Upper Vendian-Lower Cambrian	Salairian	Platform (shelf to early foredeep) sedimentation, then regression	Moderate downlifting, then uplifting and erosion	Proximal continental and marine sedimentation		NE faults

Table 1.3. Succession of the geological events in the Ladoga region (continued).

Lower age limit, Ma	Era	Tectono-magmatic circle	Stage	Geological event	Magmatism	Metamorphism	Deformation
0.53	Middle Cambrian-Upper Silurian	Caledonian	<i>Spreading-Rifting-Subduction-Collision</i> , shelf sedimentation, then regression	Moderate downlifting, then uplifting and erosion	Proximal continental and shelf sedimentation		NE faults
0.42				Moderate uplifting and erosion			
0.39	Middle-Devonian-Upper Carboniferous	Hercynian	Shelf sedimentation, then regression	Transgression-regression			NE faults
0.3	Permian-Paleogene			Uplifting and erosion			
0.02-recent	N			Multiple glaciations, upliftings and erosion.			NW, NE, W-E, local N-S normal faults

PART 2

URANIUM OCCURRENCES OF

THE LADOGA REGION

PART 2. URANIUM OCCURRENCES OF THE LADOGA REGION.

Introduction

There are three principal stratigraphic levels in the geological sequence of the Ladoga region (upward succession):

1. AR-PR₂ crystalline basement;
2. Riphean-Lower Vendian proto-platform formations;
3. Upper Vendian-Palaeozoic platform sediments.

According to their stratigraphic localization uranium occurrences of the Ladoga region can be subdivided into three groups:

- I. Basement-hosted;
- II. hosted by Riphean basinal formations;
- III. hosted by Upper Vendian-Palaeozoic sediments.

Part 2 of the thesis is devoted to the description of uranium occurrences of all these groups with consideration of the most representative examples. Basement- and Riphean-hosted occurrences have been visited and sampled during field trips of this thesis and will be described in detail. Uranium occurrences in the Vendian-Palaeozoic platform sediments do not outcrop and rock material from them is no more available. They will be briefly described on the base of published and archive data.

CHAPTER 1
BASEMENT-HOSTED
URANIUM OCCURRENCES

Chapter 1. Basement-hosted uranium occurrences.

Introduction.

All significant uranium occurrences in the crystalline formations of the basement are known in the Northern Ladoga area of the Raahe-Ladoga domain (General Appendix 1, fig. 1.1 and 5). Farther to the south-east along the Raahe-Ladoga zone the basement is concealed under the platform sediments and in spite of the similar structure of the basement, no basement-hosted uranium occurrences have been found (General Appendix 1, fig. 1.2). Basement of the Svecofennian domain is poor in respect of uranium occurrences. Only rare uranium anomalies referred to granite accessories have been discovered in outcropped part of the Western Ladoga area (General Appendix 1, fig. 1.3).

Next groups of uranium occurrences in basement rocks of the Northern Ladoga area can be distinguished in accordance to its stratigraphic-petrologic reference and structural features (in order of their location in the basement sequence):

1. granite-hosted U-Th occurrences;
2. Th-U anomalies in the Jatulian quartzites;
3. U-P in carbonate rocks of the Ludicovian Pitkjaranta suite;
4. vein-type U occurrences in different lithologies.

The most representative specimens of all of these groups have been visited and sampled during field trips of this thesis. Descriptions of these occurrences and groups in a whole are presented in the subsequent paragraphs.

Paragraph 1.1. Granite-hosted uranium occurrences.

Introduction

Granite-hosted uranium occurrences are widespread in the Ladoga region. In general they can be subdivided into two groups:

1. hosted by anatectic granites.
2. hosted by intrusive granites;

This subdivision is quite conditional. At first, it is not always possible to recognize the nature of the granite without more detailed work, especially in zones of intensive ultrametamorphism like in the Northern Ladoga granite-gneiss domes, diverse points of view on the origin of the same granites often takes place. Besides, in many occurrences radioactive mineralization occurs in the both types of rocks. Typology of uranium occurrences described below is given depending on the major type of mineralization for each occurrence.

Svecofennian anatectic granites of the Ladoga region are much more fertile with respect to uranium ore mineralization compared to intrusive ones. They host many ore-showings whereas U concentrations in the last ones are ranged as anomalies only. That is why the present research has been concentrated on the anatectic-hosted U occurrences; description of most uranium-enriched intrusive granites is given briefly.

1. U-Th-REE occurrences in anatectic granites.

Different types of anatectic granites are widespread in the Ladoga region. The oldest ones are related to the Lopian diastrophism and occur in gneisses of the Karelian domain and granite-gneiss domes of the Raahe-Ladoga zone. In the last ones, the Archaean granitization is obscured by Svecofennian orogenic processes. Svecofennian anatectic granites occur in all basement metamorphic formations, in the Raahe-Ladoga as well as in the Svecofennian domains (fig. 2.1.1.1). Increased radioactive background is quite common for these formations, but all more or less significant uranium occurrences are hosted by specific intradome anatexites attributed to the latest phases of the Svecofennian event. In other areas of the Ladoga region, in the interdome formations-hosted migmatites of the Raahe-Ladoga zone as well as in diverse migmatites of the Svecofennian domain, only very rare low-intensity anomalies occur.



Figure 2.1.1.1. Svecofennian ptigmatites in the Kalevian micaschist in the Pitkjaranta area.

In the Northern Ladoga area most of U-Th-REE occurrences in anatectic granites have been discovered in granite-gneiss domes the Impilakhti-Pitkjaranta block (General Appendix 1, fig. 1.1). A few ones (mostly of anomaly grade) occur in the Sortavala block and in the Karelian domain. The Mursula dome of the Impilakhti-Pitkjaranta blocks is the richest in uranium occurrences, but several occurrences have been discovered in the Korinoya-Pitkjaranta and Kokkaselsky domes as well.

U-Th-REE occurrences in anatectic granites have been discovered during exploration programs undertaken by “Nevskgeologia” from 1947 to 1978. Several uranium occurrences of the Impilakhti-Pitkjaranta block have been mapped and sampled during my own field work in 2005 and 2006.

Uranium-bearing anatectic granites of the Northern Ladoga area are hosted by diverse formations of the domes – granite-gneiss, amphibolites, earlier migmatites. Two types of uranium-bearing anatexites have been distinguished:

1. pegmatoids;
2. migmatites.

Both groups are quite common for zones of intensive ultrametamorphism as the granite-gneiss domes are. Pegmatoids are more typical for the internal parts of the domes although occur

on the periphery as well. Uranium-bearing migmatites occur in the dome periphery only, a few hundred meters from contact with the enveloping PR₁ formations.

The pegmatoids are middle/coarse-grained granitoid rocks, forming irregular-shaped bodies conformable to discordant with respect to the host rocks. The pegmatoid is composed mainly of K-feldspar (microcline) and quartz; Fe-biotite is a common accessory mineral. As a rule, transition between pegmatoid and host rocks is gradual although sharp borders occur as well. They have no obvious differentiation as it is in chamber pegmatites, although a mineralogical and geochemical zoning at the transition part can be revealed (see below). Typical for pegmatites eutectic graphic structures are rare in the pegmatoids.

The migmatites are rather elongated formations – up to tens meters length. They are composed of alternating leucocratic (mainly quartz and feldspars) and melanocratic (mainly biotite) layers. Uranium-bearing migmatites are related to extended linear tectonic zones occurring around the domes periphery and parallel to domes borders. The origin of these tectonic zones has been attributed to dome fracturing during its emplacement (Letnikov, 2000).

Description of the most representative specimens of the uranium occurrences in anatectic granites of the Impilakhti-Pitkjaranta block is presented below.

1.1. Uranium mineralization in the pegmatoids.

The Sjuskinsaari group of anomalies.

There are over 40 uranium anomalies hosted by pegmatoids on the eastern slope of a local synclinal structure complicating the western part of the Mursula granite-gneiss dome, in the Sjuskinsaari island (Appendix to Chapter 1, fig. 1). They present the Sjuskinsaari group of anomalies (or the Czerkovnaya ore zone). This area is composed of plagioclase-microcline gneiss-granites with amphibolite interlayers (about 25 % of the sequence). Migmatization is widespread.

Veins and lenses of quartz-microcline pegmatoids 2 to 70 m long (maximum 300 m) and 0.1-10 m thick occur among all rock varieties. Especially they are concentrated at the contacts between amphibolites and granitic-gneisses. Generally pegmatoids bodies have N-S striking, conformable to a foliation of the host rocks, but often local contacts are discordant (fig. 2.1.1.2).



Figure 2.1.1.2. Uranium-mineralized pegmatoid granite body in the Sjuskinsaari area.

Many of these pegmatoids host radioactive mineralization located in nests or related to undulating biotite schlierens (fig. 2.1.1.3). U content reaches up to 4 300 ppm and Th – 1 810 ppm. Th-U ratio usually is between 0.1 and 1, rarely up to 2 (Korotaev et al., 1978).



Figure 2.1.1.3. Biotite aggregates in uranium-mineralized pegmatoid in the Sjuskinsaari area.

Primary uranium mineralization is represented by euhedral uraninite crystals disseminated in the rock (fig. 2.1.1.4). It occurs enclosed into the feldspar crystals but is especially concentrated in biotite schlierens (fig. 2.1.1.5). Pitchblende develops after uraninite.

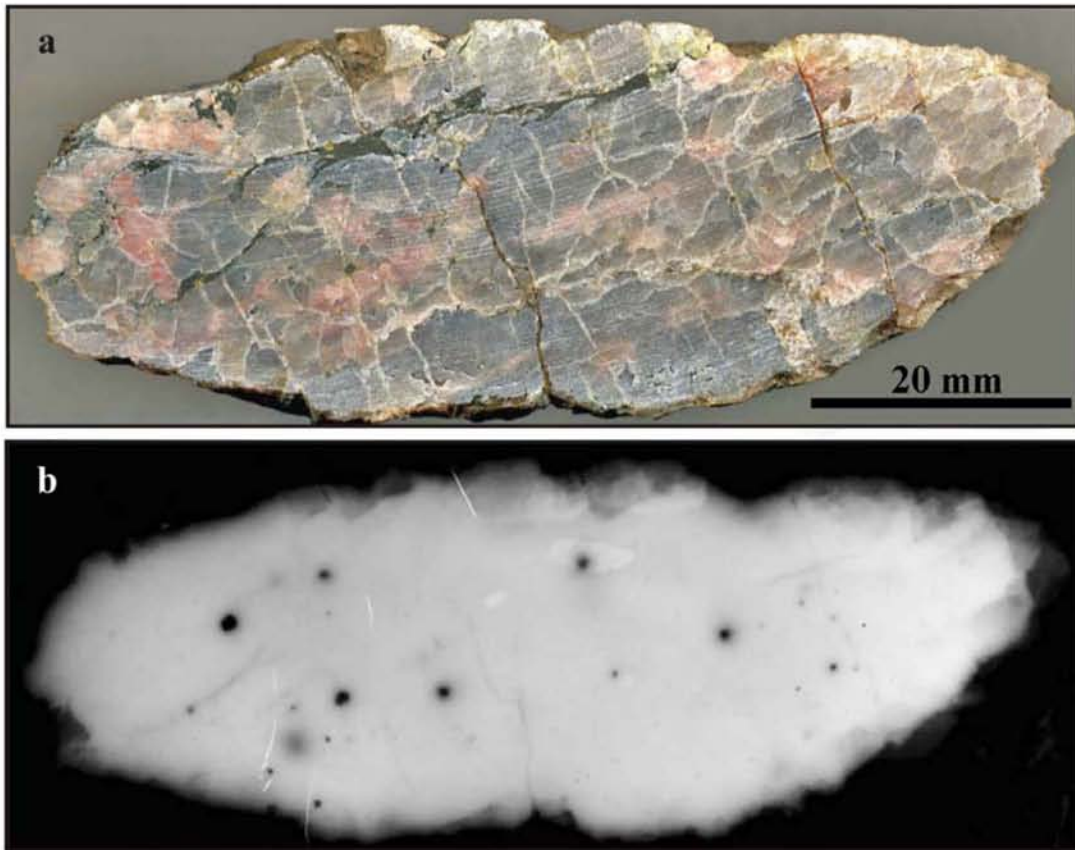


Figure 2.1.1.4. Impregnated uraninite mineralization in pegmatoid from the Sjuskinsaari area; a – sample Sju-4; b – 14 days exposition autoradiography.

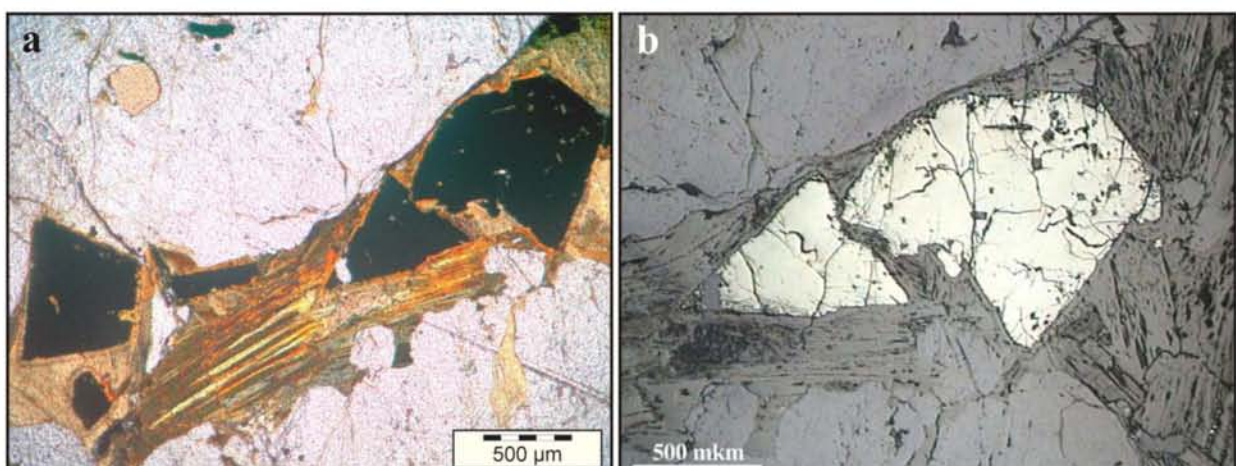


Figure 2.1.1.5. Idiomorphic uraninite crystals in biotite aggregates in the pegmatoid from the Sjuskinsaari area. Sample Sju-1, optical photos of a polished thick section: a – plain transmitted light; b – reflected light.

The uraninite from the Sjuskinsaari area is characterized by evaluated Th and REE contents that correspond to the high-temperature origin. The pitchblende developing after the uraninite generally inherits particularities of its chemical composition, but it is relatively contaminated with Si and Ca that can be referred to alterations and essentially lower Pb content. According to the last one, the age of the pitchblende can be approximately estimated as Palaeozoic. Compositions of the uranium oxides from the Sjuskinsaari area are presented in table 1 of General Appendix 2.3 and table 1 of General Appendix 2.4.

Late coffinite replaces both uranium oxides (fig. 2.1.1.6). Hexavalent uranium minerals (uranophane, kasolite, autunite) occur, especially along late fractures. Locally it can be observed in outcrops (fig. 2.1.1.7).

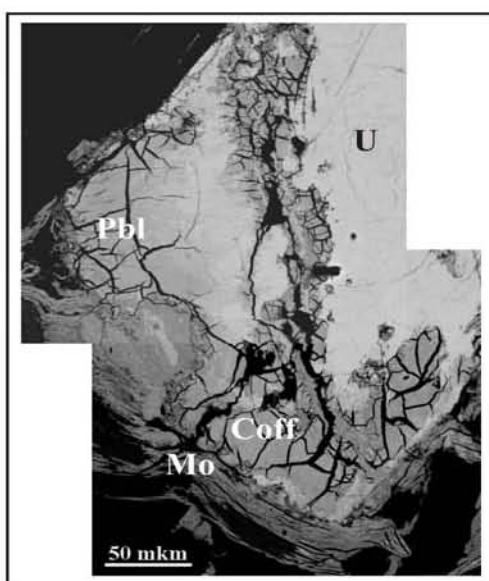


Figure 2.1.1.6. Development of pitchblende (Pbl) and coffinite (Coff) after uraninite (U). Molybdenite (Mo) occur around the uraninite. The Sjuskinsaari area, sample Sju-1, BSE photo.

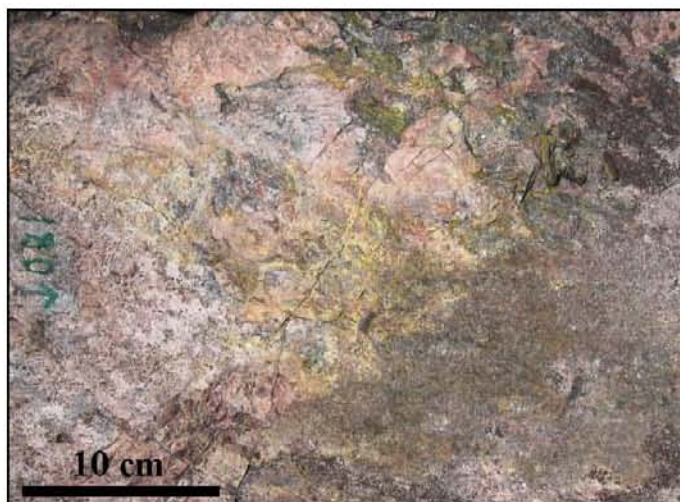


Figure 2.1.1.7. Hexavalent uranium mineralization in pegmatoids of the Sjuskinsaari area. Radioactivity 180 μ R/h.

The uranium mineralization is accompanied by high content of Mo, Cu, Ag, Y, Ga, Be, Yb.

A U-Pb isotopic age 1818 ± 27 Ma has been obtained on the uraninite from the Sjuskinsaari area (fig. 2.1.1.8). Five points of the sample Sju-1 have been analyzed. The lower intercept of the discordia 527 ± 200 Ma has a large error and possibly corresponds to formation of the coffinite alteration.

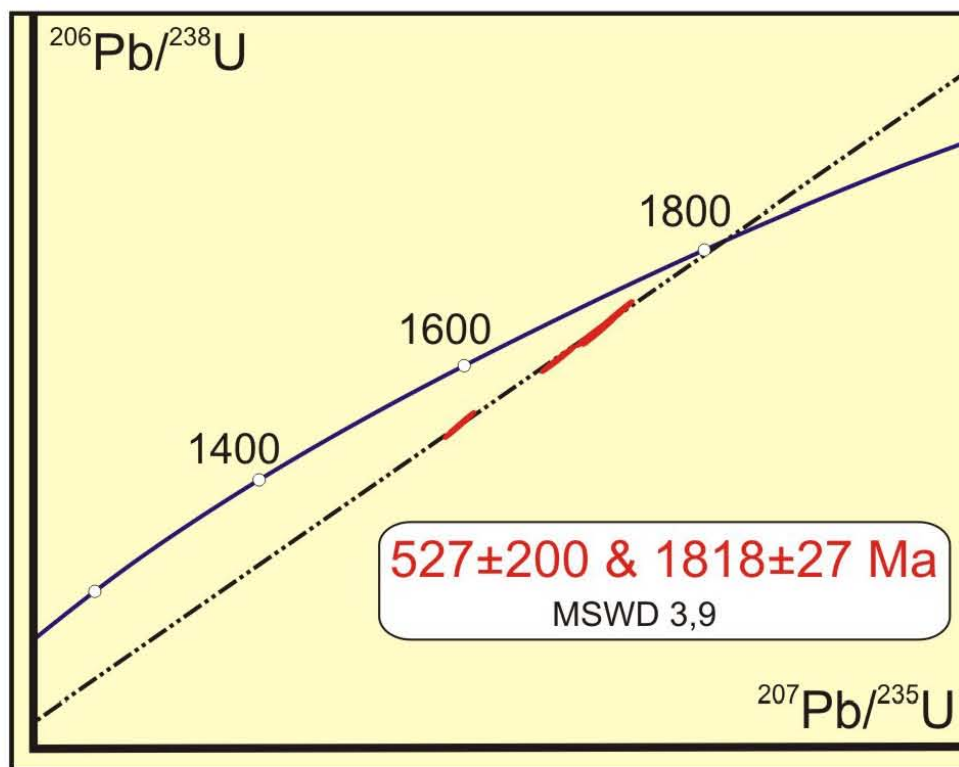


Figure 2.1.1.8. Concordia diagram for the uraninite from the Sjuskinsaari area; sample Sju-1.

REE content in the same uraninite has been analyzed by the same tools (fig. 2.1.1.9; General Appendix 2.7, table 2). REE contents are elevated and the pattern is weakly fractionated with slightly increasing from the LREE to the HREE as generally observed for magmatic uraninite (Bonhoure et al., 2007; Bonhoure, 2007). Contents of Gd and Yb have not been obtained because of technical problems occurred during the analyses.

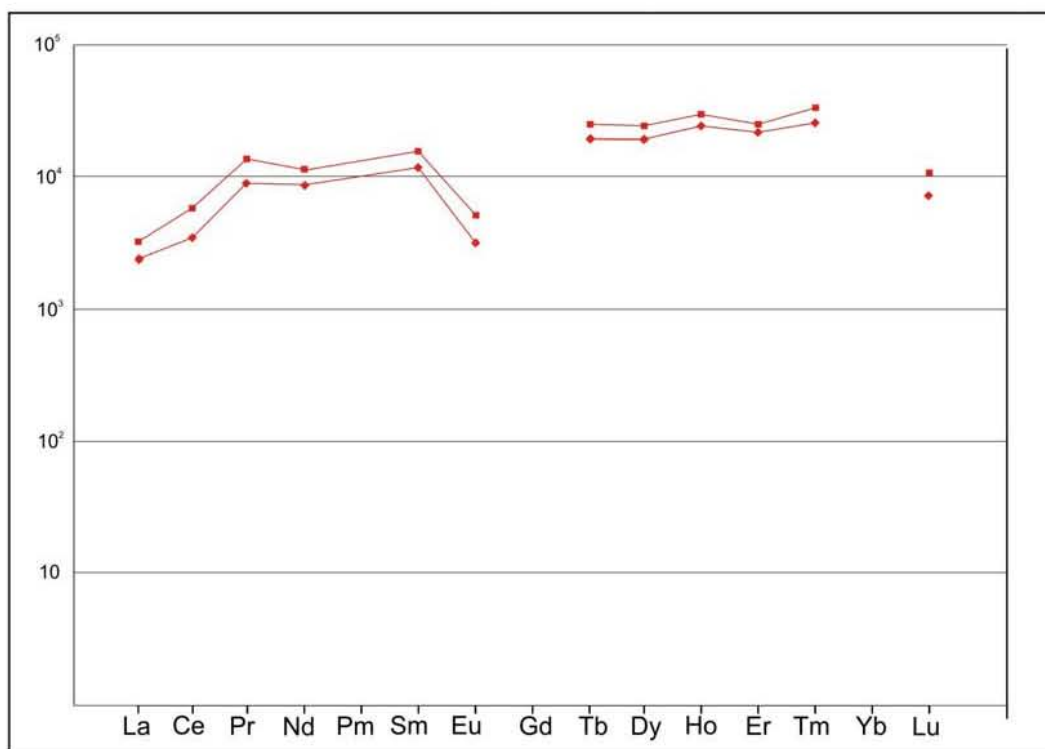


Figure 2.1.1.9. Pattern of chondrite-normalized REE contents in uraninite from the Sjuskinsaari area; sample Sju-1.

1.2. Uranium mineralization in the migmatites.

Uranium mineralization from the following ore-showings occurs in the migmatites as well as in the pegmatoids, but the migmatite-hosted ones represent the most important resources for these ore-showings.

The Mursula-Puttumyaki ore zone. The Puttumyaki and Hirsimyaki ore-showings.

The N-S striking (340-360°) Mursula-Puttumyaki zone represent a large number of uranium occurrences on the eastern slope of the Mursula dome (Appendix to Chapter 1, fig. 1). It occurs at 300 to 1000 m from the contact with PR₁ Ludicovian formations and over a length about 5.5 km. It is associated to the Ruokojarvi fault zone striking N-S 340-360°. The Mursula-Puttumyaki ore zone is located in a wide geochemical halo (sometimes called the Mursula-Puttumyaki geochemical zone) with increased uranium content (> 100 ppm) which can be followed over 8 km along the eastern slope of the Mursula dome. This U enrichment halo is associated with high Pb (30-50 ppm) and Cu (30-40 ppm) contents and in its southern part by high Mo (40-100 ppm, up to 500 ppm) contents. Spot anomalies of Zr (2 000 ppm), Y (1 000 ppm), Nb (300 ppm) also have been found. To the north of the halo, increased contents of U (2.7-4 ppm), Bi (2.5-3 ppm), Y (150 ppm) and La (200 ppm) occur over 15 km along the Ruokojarvi fault zone (Korotaev et al., 1978).

The Mursula-Puttumyaki ore zone comprises a series of U occurrences. From the north to the south there are Puttumyaki, Hirsimyaki, Mursula and Lesnoye occurrences. Puttumyaki, Hirsimyaki and Lesnoye define an alignment of mineralized zones striking about 345° . The Mursula occurrence is situated to the west of the southern part of this line (Appendix to Chapter 1, fig. 1).

The Puttumyaki and Hirsimyaki uranium ore-showings are located at the northern part of the Mursula-Puttumyaki zone. The Hirsimyaki ore-showing is located to the south and separated from the Puttumyaki occurrence by a submeridional fault corresponding to a narrow valley.

The Puttumyaki occurrence is 400 m wide and 1200 m long and the Hirsimyaki occurrence is 2000 m long and 200 m wide.

Geological environment.

The environment of the uranium occurrences is mainly composed of amphibole-biotite and granitic gneisses; in addition, migmatized biotite-plagioclase gneiss, plagioclase-hornblende, biotite and amphibole-biotite schists and amphibolites occur (Appendix to Chapter 1, fig. 2). Generally, the foliation of the supracrustals is striking $340-350^{\circ}$ with a steep dipping to the east. Quartz-microcline coarse-grained pegmatoids are widespread. Rare quartz veins occur. All formations are cut by quartz-microcline non-zonal pegmatites mostly striking NE ($20-30^{\circ}$).

Three principal groups of fractures have been measured (fig. 2.1.1.10):

- 1) NNW $340-350^{\circ}$ with a $70-90^{\circ}$ NE dipping ;
- 2) NWW $280-290^{\circ}$ with a $80-90^{\circ}$ NE dipping ;
- 3) NE-latitudinal $75-90^{\circ}$ with a $60-90^{\circ}$ NW-N dipping.

The most prominent fractures strike NNW $340-350^{\circ}$ and are conformable to the foliation. They represent a few extensive tectonic zones discovered along a distance of about 1500 m, and a width of 500 m across the strike. They are referred as the Ruokojarvi fault zone. Blastomylonites and microbreccias occur along the NNW dislocations. The tectonites are thin-parallel banded formations composed of elongated lenses of biotite, quartz and feldspar (microcline, oligoclase, locally – albite). They are enriched in accessories. Besides the uranium-bearing mineral phases there are magnetite and sulphides.

NWW- and NE-latitudinal fracture zones displace NNW-striking ones and are not mineralized as a rule.

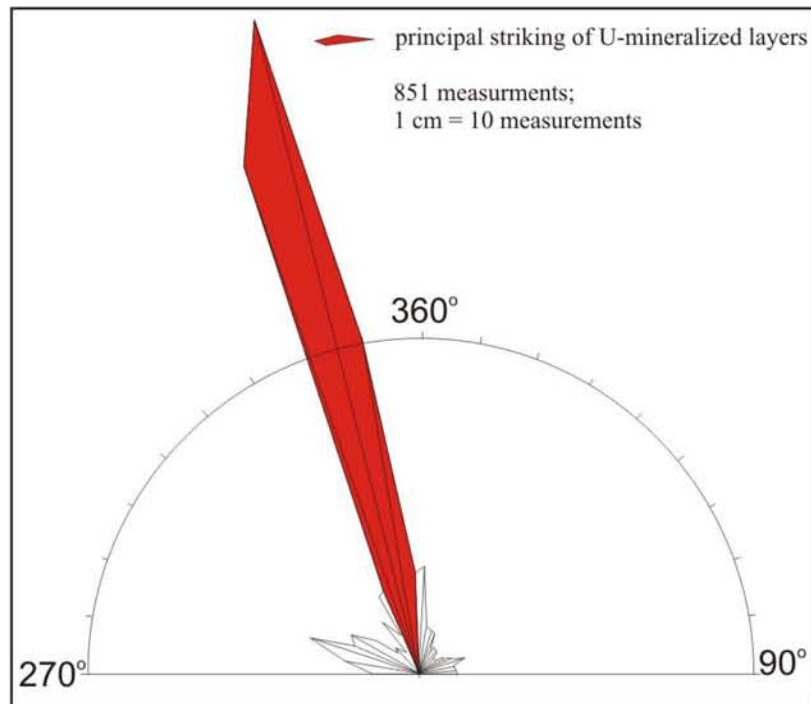


Figure 2.1.1.10. Rose-diagram of fissuring in the Puttummyaki ore-showing area (after Korotaev et al., 1978).

Ore bodies.

Uranium occurrences consist of several parallel ore zones 200-1400 m long and related to the migmatite layers (fig. 2.1.1.11). The zones are composed of many mineralized lenses 5-7 up to 15 m long with thicknesses of 0,1 to 0,4 m (fig. 2.1.1.12).



Figure 2.1.1.11. Tectonized migmatites hosting uranium mineralization in the Puttummyaki ore-showing. Part of the Outcrop 23.

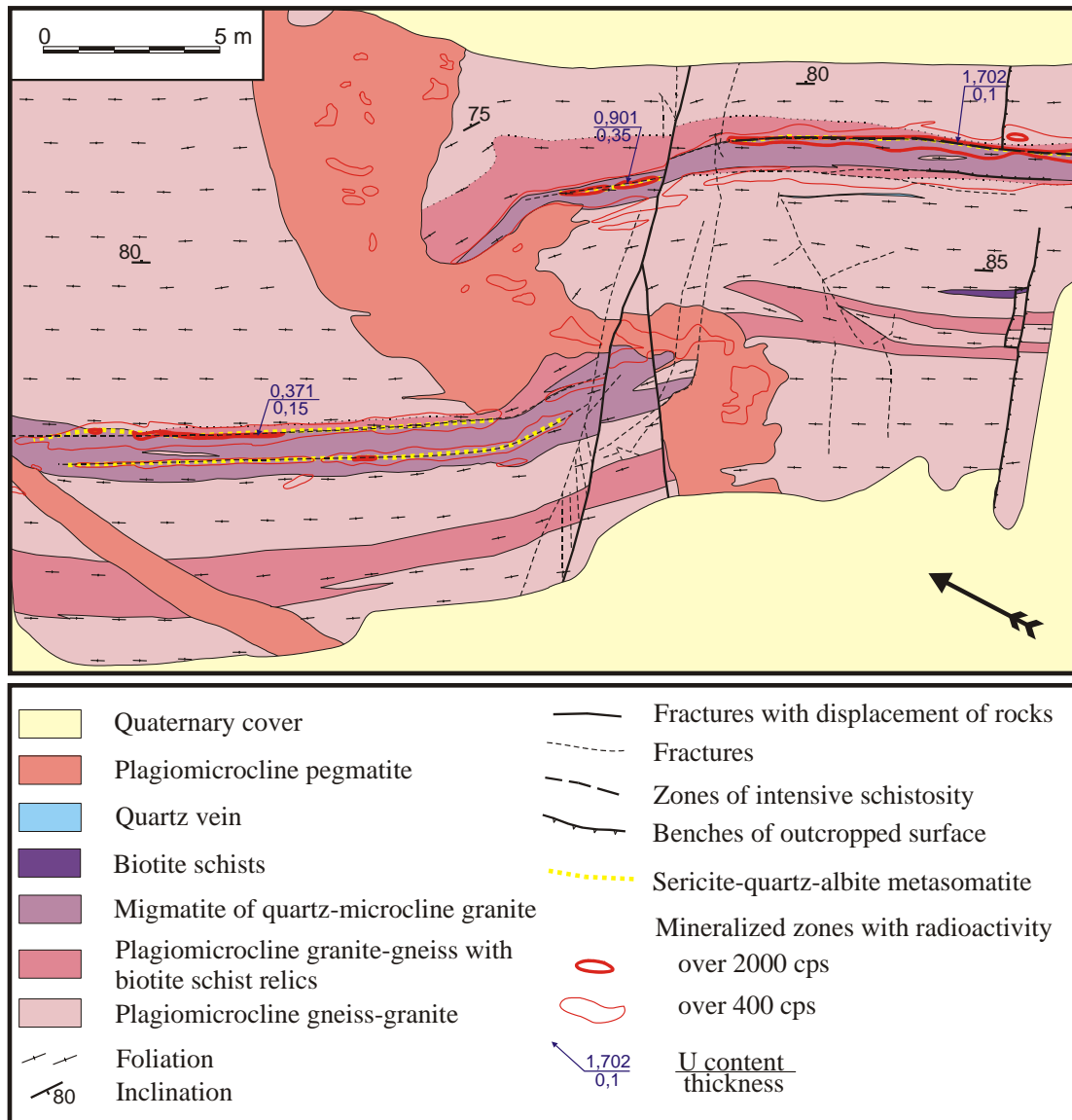


Figure 2.1.1.12. Outcrop 23 of the Puttummyaki ore-showing (after Korotaev et al., 1978).

Uranium ore mineralization is especially concentrated in sericite-quartz-albite alteration in shattering zones conformable to the migmatites. Lower-grade mineralization occurs in quartz-microcline pegmatoids. Spotty low-grade anomalies also occur in the cutting pegmatite bodies as well, but those have lower radioactive backgrounds in comparison with the migmatites.

Uranium mineralized zones have been followed by drilling down to 390 m. Average U-content is 400 ppm with a maximum of 17 800 ppm over 0.1 m. The grade decreases with depth. Average Th-content is 80 ppm and may reach, up to 260 ppm. The uranium ore is in equilibrium.

The uranium resource of these occurrences is evaluated at about 90 t for a depth of 60 m and about 500 t for a depth of 300 m (Korotaev et al., 1978).

Uranium mineralization.

According to previous studies (Grigorieva, 1977; Korotaev et al., 1978), there are two principal types of the uranium mineralization in the Mursula-Puttumyaki occurrences.

(i) The first type corresponds to disseminated, 0.01 to 0.5 mm large euhedral uraninite crystals. It occurs in quartz-microcline-rich rocks interpreted as metasomatites in microfissures of amphibole, biotite, plagioclase, quartz, titanite. Aggregates of quartz and uraninite within apatite sometimes occur (Grigorieva, 1977).

(ii) The principal uranium mineral of the Mursula-Puttumyaki occurrences is pitchblende forming 1-5 mm thick, up to 20 cm long, chained aggregates localized in tectonic zones (fig. 2.1.1.13). The mineral has irregular or rounded shapes. Small crystals (up to 0.15 mm) have a shelly structure and form clusters up to 7 mm size (fig. 2.1.1.14). Gradual replacement of uraninite by pitchblende occurs as well.

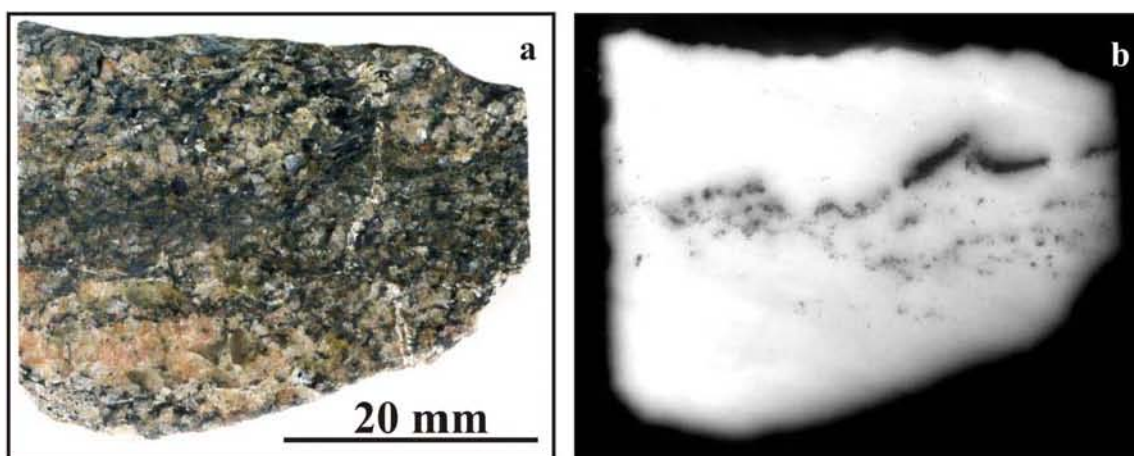


Figure 2.1.1.13. Chained pitchblende mineralization from the Hirsimyaki ore-showing; a – sample Hm-1, b – autoradiography (7 days).

Two generations of pitchblende have been distinguished in the samples taken from the Puttumyaki and Hirsimyaki occurrences. Pitchblende-1 is replaced by pitchblende-2 (fig. 2.1.1.15). Both uranium oxides also suffer of partial replacement by coffinite (fig. 2.1.1.16). Chemical compositions of these minerals are represented in tables 2 and 3 of General Appendix 2.3 and in table 2 of General Appendix 2.4. Low content of Th in the pitchblendes differs them from pegmatoid-hosted uraninite and indicates relatively low temperature regime during the deposition.

Uranium oxides are associated with quartz, biotite, apatite, sericite, albite, monazite, zircon, hematite, magnetite, sulphides of Fe, Cu, Pb, Zn (Grigorieva, 1977; Polekhovsky, 2007).

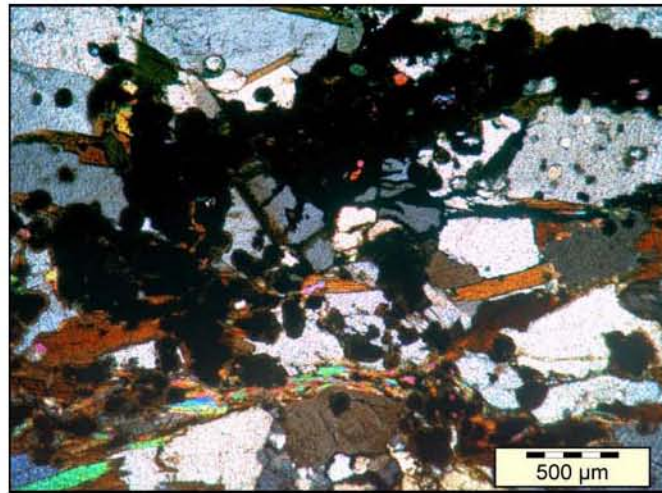


Figure 2.1.1.14. Pitchblende segregation in the quartz-feldspar “metasomatite”. The Hirsimiyaki ore-showing, sample Hm-1; optical photo of a thick section, polarized transmitted light.

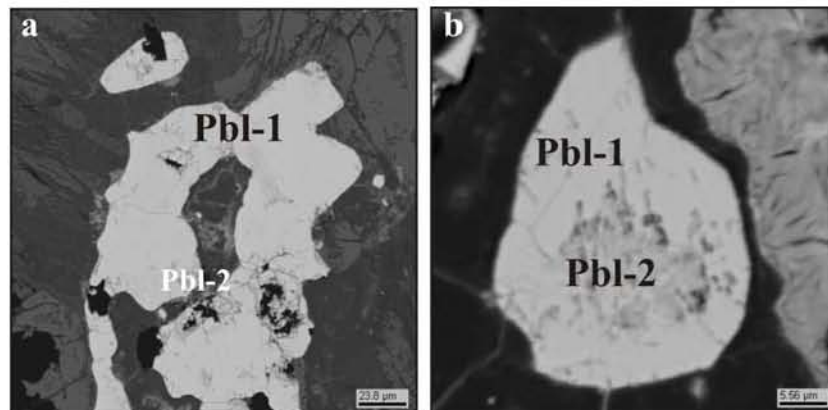


Figure 2.1.1.15. Development of pitchblende-2 (Pbl-2) after pitchblende-1 in the Puttummyki ore-showing, sample Pt-1, BSE photos: a - from the periphery and along the fractures; b - from the center of the grain.

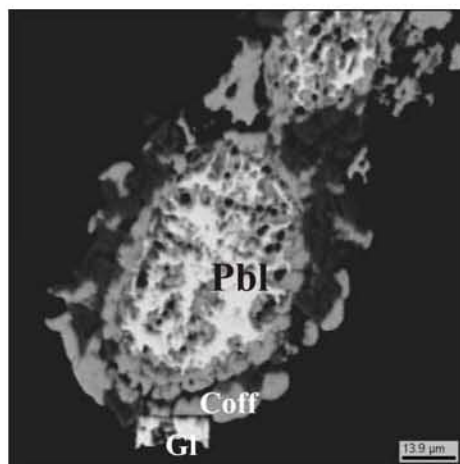


Figure 2.1.1.16. Development of coffinite (Coff) after pitchblende (Pbl). Galena crystal (Gl) occurs at the periphery. The Puttummyki ore-showing. Sample Pt-H6. BSE photo.

Hexavalent uranium minerals: uranophane, kasolite, rarely – schoepite and curite replace early tetravalent uranium oxides. They also frequently occur as late fracture fillings with quartz, calcite, K-micas and sulphides.

High contents of Th, Pb, Mo, Ag, P and REE have been revealed in the occurrences.

U-Pb isotopic dating of the pitchblende mineralization has been undertaken. Six points of the sample Pt-1 have been analyzed. The upper intercept of the Discordia with the Concordia define an age of 1789 ± 31 Ma for the pitchblende mineralization (fig. 2.1.1.17). Three points are nearly concordant and define an age of 1798 ± 65 Ma.

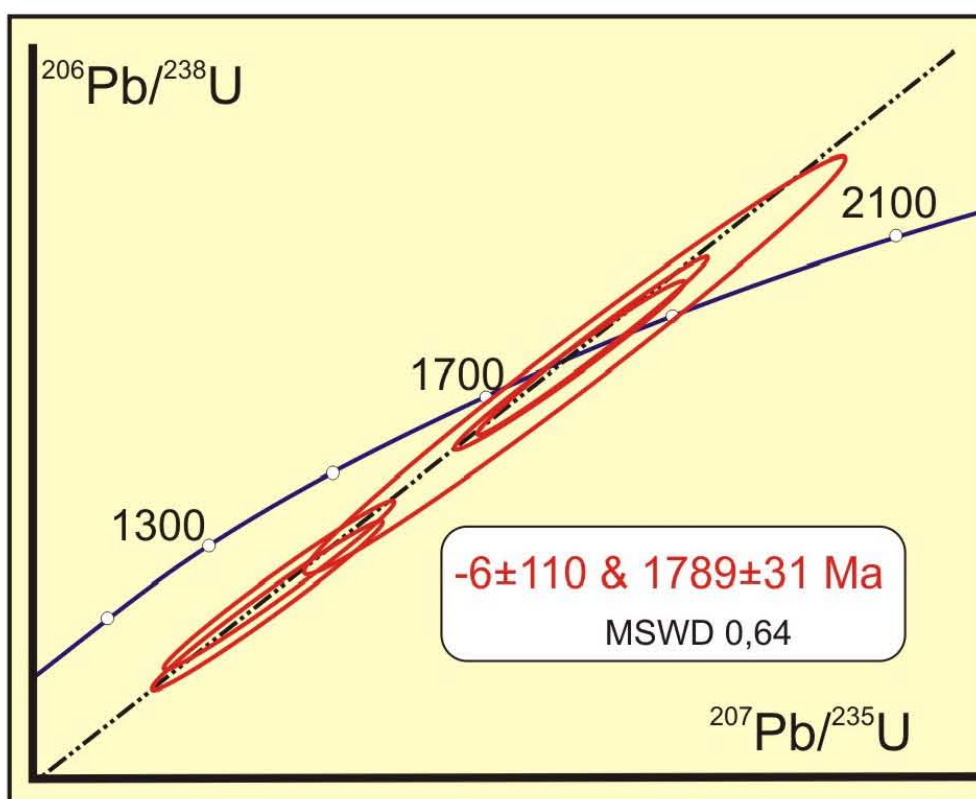


Figure 2.1.1.17. Concordia diagram for pitchblende from the Puttummyaki ore-showing, sample Pt-1.

The Korennoye ore-showing.

Geological environment.

The Korennoye uranium ore-showing is located in the southern part of the Korinoya-Pitkjaranta AR-PR₁ granitic gneiss dome, at 20-50 m from its contact with the PR₁ Ludicovian Pitkjaranta suite (Appendix to Chapter 1, fig. 3). The ore-showing area is composed of biotite-plagioclase and hornblende gneisses, granitic gneisses, amphibolites and plagioclase-microcline

migmatites. All types of rocks are microclinized. The uranium occurrence is localized in lenses of fine/medium-grained microcline granites (alaskite) occurring inside of the dome at the contact with the Pitkjaranta suite layers. According to Korotaev et al., (1978) this granite has a metasomatic origin.

Migmatized biotite-amphibole gneiss and amphibolites occur inside of the granitic lens. These rocks form bands and lenses (schlierens) of 0.1-0.7 m thick with a sublatitudinal strike and gently dipping (20-40°) to the south.

The ore-showing is related to the intersection of two tectonic zones. The oldest one striking 350° to the NNW and dipping steeply (75-80°) to the SW cuts only the dome formations, not the Pitkjaranta suite layers. This structure is responsible for local undulation of the lithological layers. There are zones of blastomylonites, schistosity, fractures and microbreccias along this tectonic zone. Host rocks alterations as biotitization, albitization, sericitization, silicification, hematitization are widespread in the zone. Intensity of these alterations increases southward inside the dome formations, but alterations do not penetrate into the Pitkjaranta suite. Only the Cu-rich geochemical halo occurs in rocks located above the tectonic zone in the Pitkjaranta suite formations, but local Cu enrichments are quite common for this suite and in this case it can be caused by lithological particularities.

Another tectonic zone is a flat sublatitudinal structure occurring along the contact between the dome formations and the Pitkjaranta suite. It is represented by small displacements parallel to the Pitkjaranta suite roof and gently dipping to the south.

Ore bodies.

The uranium ore bodies are hosted by the microcline granite lenses; the highest-grade mineralization is related to the shattering zones with sericite-albite-quartz alterations developed after the migmatization of the biotite-amphibole gneiss and amphibolites.

Uranium ore mineralization forms lenses (up to 6×10 m) and small stockworks. They dip quite gently (about 20°) to the south. The ore bodies have been recognized by drilling for 460 m along their strike and 110 m down the dip, and have a thickness up to 30.6 m.

U mineralized breccias have been discovered in one of drillholes. Fragments of migmatized rocks of the dome are cemented by quartz. Hematitization and argillization (K-micas+chlorite+montmorillonite) occur along fractures. Pitchblende has very low Pb content (Korotaev et al., 1978). It is an indication of a late, possibly Palaeozoic uranium redistribution.

There is only outcrop of the ore bodies expressed as an anomalously radioactivity zone with 50 $\mu\text{R/h}$ over 12 \times 50 m (fig. 2.1.1.18).

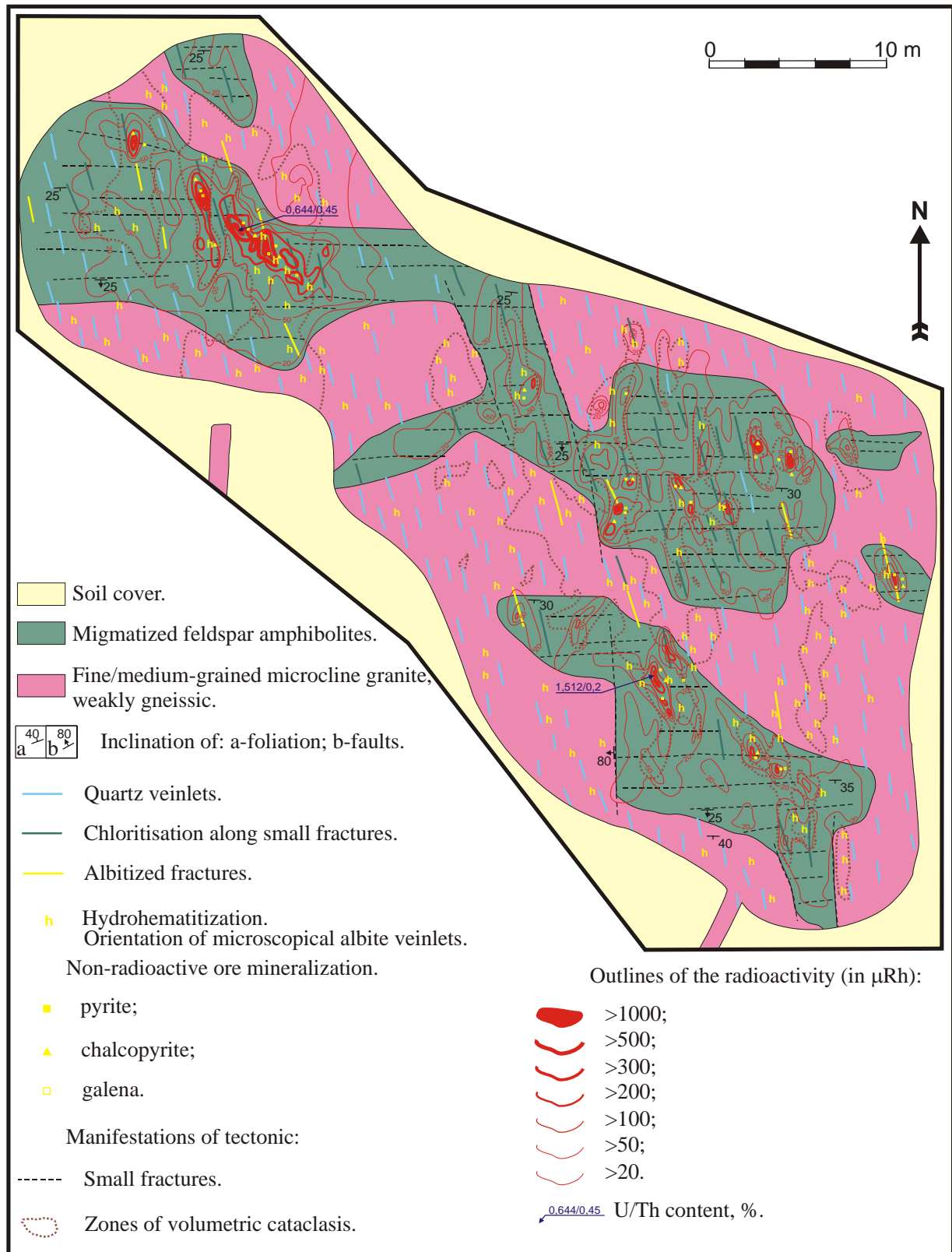


Figure 2.1.1.18. Outcrop of the Korennoye ore-showing (after Korotaev et al., 1978).

Average U content in the Korennoye ore-showing is 500 ppm, with a maximum of 15 120 ppm over a thickness of 0.2 m. The ores are at equilibrium.

The resource of the Korennoye ore-showing is evaluated at about 130 t (Korotaev et al., 1978).

Uranium mineralization.

According to previous works, uranium ores are mainly composed of uraninite and pitchblende. Coffinite, schoepite, uranophane, kasolite and curit also occur. Uranium mineralization is accompanied with hematite, pyrite, chalcopyrite, galena, rarely molybdenite. Uranium is associated with increased contents of Zr, Be, Pb and to lesser extent in Zn and P (Korotaev et al., 1978).

Uraninite occurs as a disseminated rare mineral impregnation of 0.01-0.08 mm crystals, locally up to 0.1 mm large, included in plagioclase, in the vicinity of accumulations melanocratic minerals (biotite and amphibole) and within the melanocratic minerals, mainly in amphibole.

Pitchblende is more common and distributed as nests (up to 3×6 mm) and veins. Pitchblende replaces uraninite and develops in shattering zones of with sericite-albite-quartz alterations. Very subordinated pitchblende mineralization in late fractures has been observed.

Three generations of pitchblende partly replaced by coffinite have been distinguished in samples taken from the outcrop of the ore-showing during this thesis field work (Polekhovskiy et al., 2007). Compositions of uranium-bearing mineral phases are presented in table 4 of General Appendix 2.3.

Pitchblende-1 occurs within feldspar-biotite aggregates in quartz-feldspar rock where it forms chained accumulations (fig. 2.1.1.19). Pitchblende-2, partly replaced by pitchblende-3, occurs in veinlets (fig. 2.1.1.20) controlled by latitudinal structures, dipping 20-25° southward.

In comparison with pitchblende-1, pitchblendes from the veinlet contain more U, they are enriched in Al, Fe and Mn, whereas Pb content is essentially lower. That is an evidence of late and probably low-temperature hydrothermal origin of fracture-bound pitchblende-2 and pitchblende-3.

Hexavalent yellowish uranium minerals were observed in the mineralized outcrop.

Two samples from the Korennoye ore-showing have been selected for U-Pb isotopic analyses for the determination of the ages of the uranium minerals.

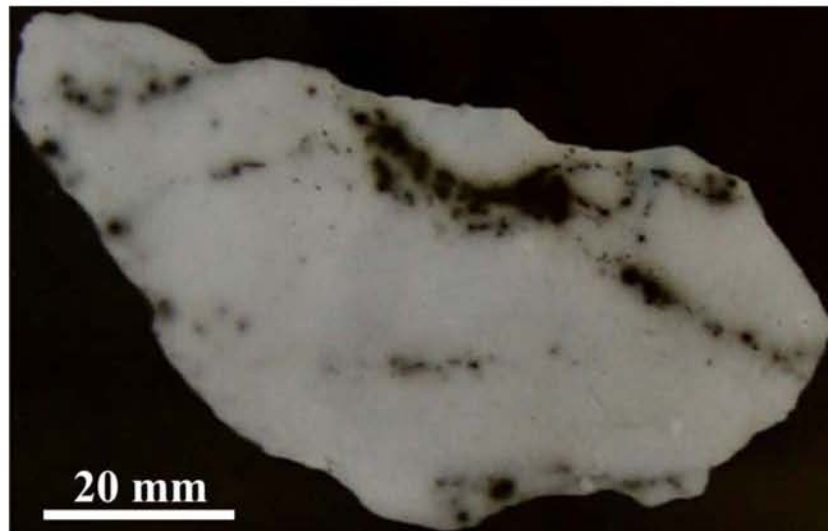


Figure 2.1.1.19. Autoradiography of chained impregnations of pitchblende in the Korennoye ore-showing. (from Korotaev et al., 1978).

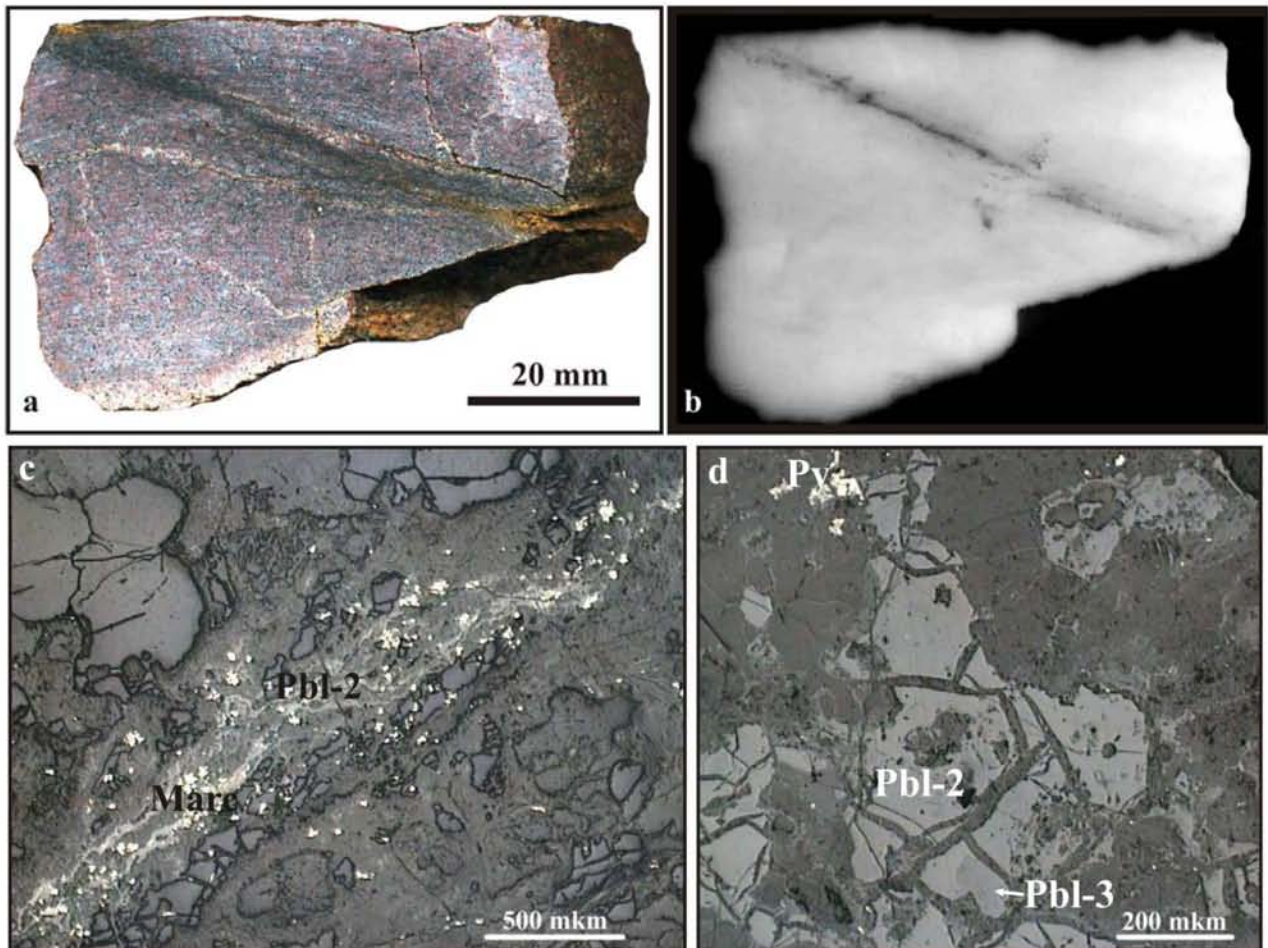


Figure 2.1.1.20. Fracture-bound pitchblende mineralization in the Korennoye ore-showing, sample Ko-1; a – sample; b – autoradiography (7 days); c and d – optical photos of thick sections, reflected light, c – veinlet of pitchblende-2 (Pbl-2) accompanied with marcasite (Marc); d – partial replacement of pitchblende-2 by pitchblende-3, pyrite (Py).

The first sample (Ko-2) corresponds to the pitchblende-1 with was taken from the mineralized migmatite, the second one (Ko-1) corresponds to the pitchblende-2 – from above mentioned veinlet. 9 points have been analyzed in the sample Ko-1, but because of strong heterogeneity only 3 in the Ko-2.

The analytical results are not precise because technical problems have occurred during the analyses, but at least two different uranium mineralization events: one of Palaeoproterozoic age and another of Palaeozoic age can be distinguished (fig. 2.1.1.21).

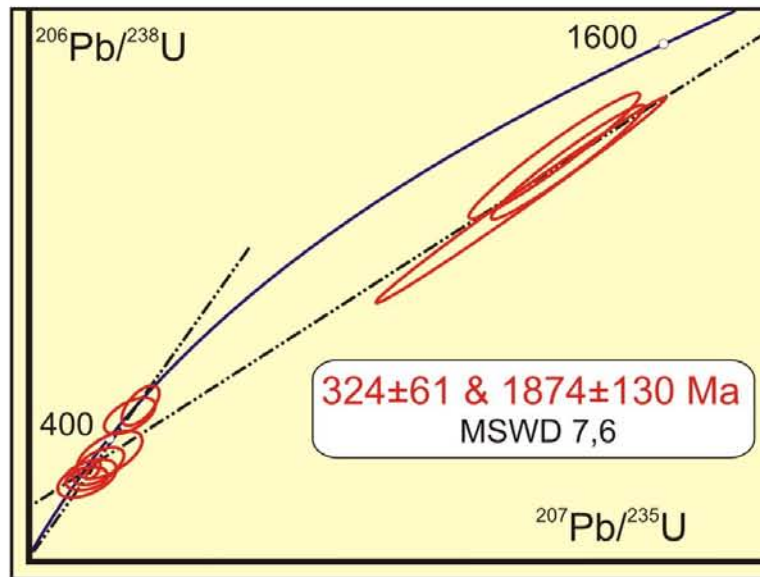


Figure 2.1.1.21. First possible interpretation of U-Pb isotopic data in a Concordia diagram for the pitchblende from the Korennoye ore-showing. Samples Ko-2 (upper group) and Ko-1 (lower group).

Because of poor accuracy of the data, several interpretations of the results can be proposed. A first interpretation suggested by Philippe Kister, propose an age of 1874±130 Ma for pitchblende 1 and 324±61 Ma for pitchblende by fitting all the points along the same Discordia. But this interpretation should be considered cautiously. If pitchblende 2, located in veins, does not result from a remobilization of pitchblende-1 but from two distinct precipitation events the two pitchblende generations should not be associated for the calculation of the Discordia. Each group of analyses has to be interpreted as an independent Discordia.

In another interpretation, the discordia has been drawn through the isotopic data obtained on pitchblende-1 and forcing the Discordia to pass through 0 using a continuous diffusion model, and an age of 1772±43 Ma has been obtained (fig. 2.1.1.22 a).

The Discordia calculated only using the isotopic data obtained on pitchblende 2 gives an upper intersect with the Concordia at 469±180 Ma and lower one at 127±180 Ma (fig. 2.1.1.22b). The low quality of these analyses does not allow to propose a more precise

interpretation. However this U-mineralization event is probably of Palaeozoic age.

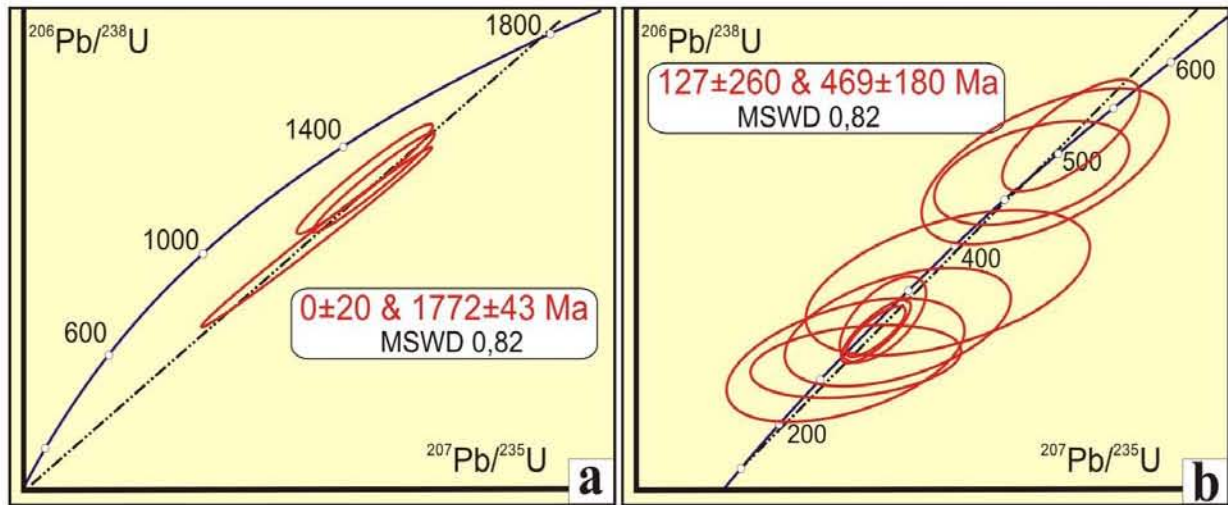


Figure 2.1.1.22. Second possible interpretation of U-Pb isotopic data in a Concordia diagram for the pitchblende from the Korennoye ore-showing

Pitchblende-2 was analyzed for its REE contents as well (General Appendix 2.7, table 2). With decreasing fractionation from the LREE to the HREE the pattern is typical for vein-type mineralization (according to Bonhoure, 2007) and similar to one of the pitchblende of a vein-type occurrences of Finland, especially the Särkijärvi occurrence (Bonhoure, 2007) (fig. 2.1.1.23). However the REE pattern of the Korennoye pitchblende is more fractionated.

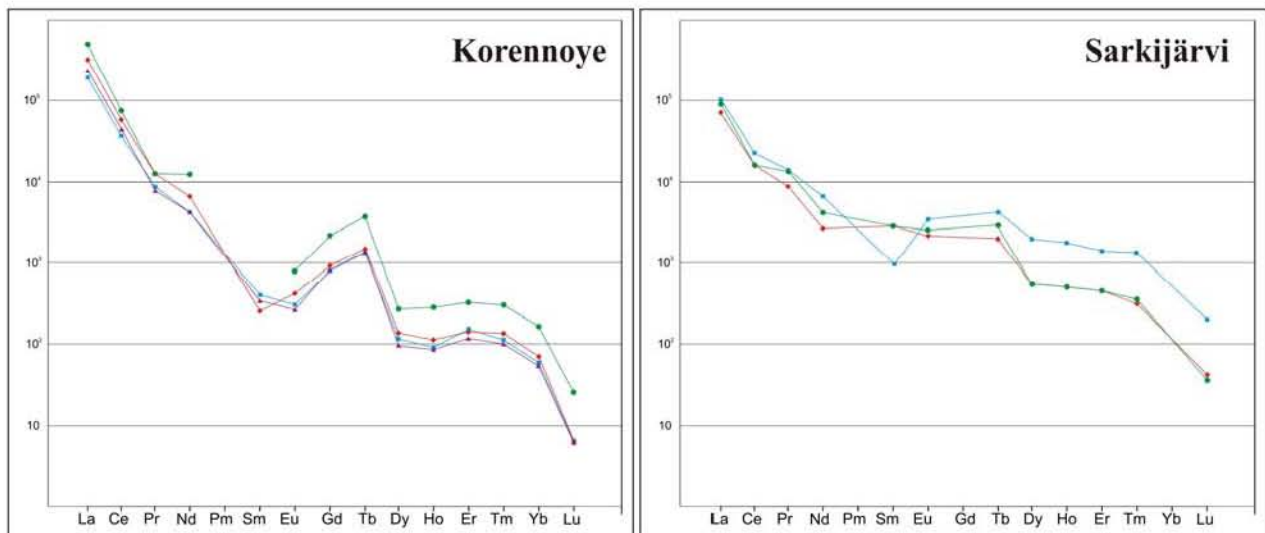


Figure 2.1.1.23. Chondrite-normalized REE patterns of uranium oxides from late vein type mineralization of the Korennoye and Särkijärvi occurrences (after Bonhoure, 2007).

1.3. Other uranium occurrences in the anatexites.

There are many other uranium occurrences hosted by the anatectic granites in the Northern Ladoga area. As a rule those located in the migmatites have larger resources, whereas pegmatoid-hosted ones are ranged just as anomalies.

The *Sumeria* uranium ore-showing is located on western flank of the Mursula dome in a similar structural position as occurrences of the Mursula-Puttumyaki zone. The mineralization is related to elongated zones of tectonized migmatites of N-S striking. During this study, U-Pb age of 1748 ± 130 Ma (MSWD 206) was yielded for pitchblende from the *Sumeria* ore-showing. The small number of analytical data does not allow a better accuracy of the results. Chemical compositions of pitchblende and coffinite from this ore-showing are presented in table 5 of General Appendix 2.3 and in table 3 of General Appendix 2.4. In general it corresponds to compositions of pitchblendes from the Mursula-Puttumyaki zone.

Besides of the above-mentioned ore-showings, the most significant of anatexite-hosted uranium occurrences is the *Vuorilampi* ore-showing, located in the southern part of the Kokkoselka dome (Appendix to Chapter 1, fig. 1). It is an ore showing of combined type – uranium mineralization occurs as in pegmatoids as in migmatites. Resource of the ore showing is estimated to about 300 t of uranium (Korotaev et al., 1978). The ore-showing had been discovered by trenches and drilling; presently just a few mineralized outcrops are available for the observation.

1.4. Generalized geological parameters characterizing the anatexite-hosted uranium mineralization of the Northern Ladoga area.

I. Petrologic control.

The uranium-bearing anatexites are represented by two varieties:

- 1) complex shaped lenses of microcline pegmatoids;
- 2) elongated linear migmatites composed of interbedding of leucocratic (mainly of quartz and feldspar) and melanocratic (mainly of biotite) layers.

In both cases uranium (uraninite) mineralization is mainly related to biotite schlierens, but occurs also in the feldspar crystals.

Locally developed sericite-albite-quartz rocks host the most concentrated uranium (pitchblende) mineralization.

II. Structural and tectonic control.

1. Principal structural feature of the anatexite-hosted uranium mineralization of the Northern Ladoga area is its distinct affinity to granite-gneiss domes. Early uraninite mineralization occurring in pegmatoids occurs in different parts of the domes, but it is more typical for their internal parts. Pitchblende-mineralized migmatites occurs only on the periphery of the domes.

2. Most of anatexite-hosted uranium occurrences are located along the Ruskeala fault zone. For rest of them an affinity with other NW and NE striking regional fault zones is characteristic.

3. The most high-grade mineralization is related to local dislocations of the domes periphery and conformable to zones of linear migmatites.

III. Ore mineralogy.

Main bulk of ores is composed of uranium oxides. Uraninite forms impregnations in microcline-quartz granite, whereas pitchblende, besides of partial replacement of the uraninite, also occurs in thin and elongated zones of sericite-albite-quartz rocks. Subordinated coffinite partly replaces the uranium oxides. Hexavalent uranium mineralization occurs.

IV. Geochemical features.

The anatexite-hosted uranium mineralization is accompanied with increased content of Th, REE, Rare metals, P, Mo, Pb, Ag, less – Zr, Be, Cu, Zn, Y, Ga.

V. Grade of the occurrences.

All discovered in the Northern Ladoga area anatexite-hosted uranium occurrences are ranged from anomalies up to few hundred tons ore-showings. Maximum identified resource is about 300 tons of uranium (the Vuorilampi ore-showing). Average uranium content is 500 ppm, maximum – up to 17 800 ppm. Total identified resource of the anatexite-hosted uranium occurrences of the Northern Ladoga area is about 1 500 tons, prognostic resource is 5 000 tons.

1.5. Remarks to the genesis of the anatexite-hosted uranium occurrences of the Northern Ladoga area.

Anatexite-hosted uranium mineralization of the Northern Ladoga has a complex origin. By Grigorieva (1977) two principal stages are suggested.

1. High-temperature “quartz-microcline metasomatism”.

Traditionally, in the Russian geological literature, the origin of above described anatexites considered as a result of high-temperature potassic metasomatism producing granitoid rock of essentially quartz-microcline composition (Sudovikov, 1964). The structural features of quartz-microcline metasomatites depend on the characteristics of the replaced rock: composition, structure, permeability, tectonization. Quartz-microcline metasomatites after migmatites compose extended plate bodies with indented pinching out along the strike (see fig. 2.1.1.12). Ones after intradome amphibolites compose complex-shaped bodies, often with S-like bends. In general metasomatite bodies have conformable striking with host rocks. Contacts of the metasomatite bodies can be as sharp (with quartz-biotite fringe) as gradual.

The quartz-microcline metasomatite are pink, mainly middle/coarse-grained rock with dark lenses or undulating layers (schlierens composed of melanocratic minerals aggregates. Microcline forms big isometric porphyroblasts and fine-grained aggregates. Banded quartz occurs.

Characteristic mineral association of the quartz-microcline metasomatites: quartz + lattice microcline + microcline-perthite + oligoclase (relics mainly) + Fe biotite ± garnet-almandine + apatite (F-apatite) + cyrtolite (metamict zircon) + magnetite + titanite + uraninite + bröggerite (uraninite with high Th content, up to 14 % ThO₂) + xenotime + monazite ± uranothorite ± molybdenite. Mineral association and theirs abundance depend on the replaced rock.

According to (Grigorieva, 1977), the quartz-microcline metasomatites have a zoned structure which depends on composition of replaced rock (Table 2.1.1.1).

Table 2.1.1.1. Quartz-microcline metasomatic alteration paragenesis for different types of host rocks (after Grigorieva, 1977).

Zones	Principal minerals	
	Granitoid	Amphibolite
Non-altered	Quartz, oligoclase ₁₆₋₂₄ , microcline-perthite, biotite, hornblende.	Oligoclase ₂₂₋₂₈ , hornblende.
External	Quartz, oligoclase ₁₂₋₂₄ , microcline-perthite, biotite, actinolite, garnet.	Oligoclase ₁₂₋₂₄ , microcline-perthite, quartz, actinolite.
Intermediate	Quartz, oligoclase ₁₂₋₂₄ , microcline-perthite, biotite, epidote, chlorite.	
Internal	Quartz, lattice microcline, Fe-biotite.	

REE-U-Th accessories form chain-like, banded and nest concentrations in the metasomatites. Monazite, xenotime and uranothorite are localized in leucocratic varieties of the rock, especially in fine-grained quartz-microcline matrix surrounding microcline porphyroblasts. Often they are related to the biotite aggregates, sometimes they occur along the cleavage inside microcline crystals.

Uraninite and bröggerite are concentrated in Fe-biotite or biotite-quartz clusters and undulate lenses. They are cubic crystals up to 0.5 mm size associated with apatite and titanite. In the biotite-quartz lenses they form clusters with the cyrtolite and molybdenite crystals. Sometimes, uraninite occurs inside of the microcline porphyroblasts as well.

Also according to Grigorieva (1977) the geochemical characteristics of the quartz-microcline metasomatites depends on composition of the replaced rock (Table 2.1.1.2).

Table 2.1.1.2. Geochemical characteristics of the quartz-microcline metasomatites developed from different protoliths (after Grigorieva, 1977).

Particularity	Granitoid	Amphibolite
Alkali	high, $K \gg Na$.	high, $K > Na$
Silica	high	relatively low.
Enrichment in rock-forming elements	low Ca, Mg, Fe	high Fe
Enrichment in accessory elements	Zr, REE, Th, U.	Zr, REE, Th, U, P, Ti, Mn.
Increased content	Mo, Ti, Ba, Mn, Nb.	Co, Cr, Nb, Cu, sometimes Mo.

The REE-U-Th mineralization is localized in the internal zone of the metasomatites. The highest abundances of U, Th and REE occur in metasomatite varieties enriched in Fe, P, Ti that would be formed after amphibolites (U content – up to 23 000 ppm, Th – up to 8 000 ppm).

Western country geologists considered formations similar to the above described quartz-microcline rocks as derived from partial melting of quartz-feldspathic metasediments or metigneous rocks. Those with syngenetic uranium mineralization are described in the Rössing deposit and in the Grenville belt of Canada (Cuney, 1980; 1981; 1982; Cuney and Barbey, 1982).

2. Low-/middle-temperature sodium sericite-quartz-albite “metasomatism”.

In the reports of VSEGEI (Grigorieva, 1977) and “Nevskgeologia” (Korotaev et al., 1978) indications of late Na-metasomatism were described for uranium occurrences in the anatexites of the domes.

Specific sericite-quartz-albite rock was discovered in linear tectonic zones along the peripheries the migmatite domes. These zones represent overprinted schistosity, blastomylonite and microbreccias. Grigorieva (1977) had studied uranium mineralization of these zones in details and considered the sericite-quartz-albite rock as a metasomatite formation after the above described quartz-microcline granitoids. Presented below description of this rock and uranium mineralization is based on her study (Grigorieva, 1977).

The alterations are represented by sericitization of the biotite, silicification of feldspars and biotite, albitization of feldspars, alkalination of hornblende, hematitization of magnetite and feldspars. The alterations are weak and local. Thickness of intensively altered halos is 0.1-0.25 m. Zoning in the alteration halos can be distinguished sometimes (Table 2.1.1.3).

Table 2.1.1.3. Sericite-quartz-albite metasomatic alterations for various host rocks (after Grigorieva, 1977).

Zones	Principal minerals	
	Granitoid	Amphibolite
Non-altered	Oligoclase ₁₈₋₂₄ , microcline-perthite, quartz, biotite ₃₀ *, hornblende.	Oligoclase ₂₀₋₂₈ , hornblende.
External	Quartz, biotite ₃₀ , chlorite, microcline-perthite, oligoclase ₁₄₋₂₀ .	Quartz, oligoclase ₁₄₋₂₂ , microcline-perthite, actinolite, chlorite, epidote.
Intermediate	Quartz, lattice microcline, microcline-perthite, oligoclase ₁₂₋₁₄ , biotite ₅₀ .	Quartz, lattice microcline, microcline-perthite, oligoclase ₁₄₋₁₈ , albite, biotite ₅₀ .
Internal	Quartz, albite, sericite.	Quartz, albite, sericite, alkali hornblende.

*in biotite_n n = $\text{Fe}^{2+}/(\text{Fe}^{2+}+\text{Mg})$.

Zones of the sericite-quartz-albite alterations are the most uranium-enriched formations of the domes. The uranium content is up to 17 800 ppm. The uranium mineralization in the sericite-quartz-albite metasomatites is represented by uraninite and pitchblende.

The uraninite probably is presumed to crystallize during the earlier quartz-microcline stage (“metasomatism”). During sericite-quartz-albite alteration it was partly or completely replaced by pitchblende.

Pitchblende is a major uranium mineral of the sericite-quartz-albite metasomatites. Besides uraninite replacements, it occurs in shattering zones. The cement of the fractured rock is composed of quartz (75-80 %), albite (5-10 %) and hematite (10-15 %). Sericite develops after biotite and feldspar. Skeletal crystals of pitchblende and their fragments form chained and banded aggregates, often with a boudin-like shape (fig. 2.1.1.24). Small spherulites (up to 2 mm size) and veinlets (up to 3 mm thick) of pitchblende are rarer.

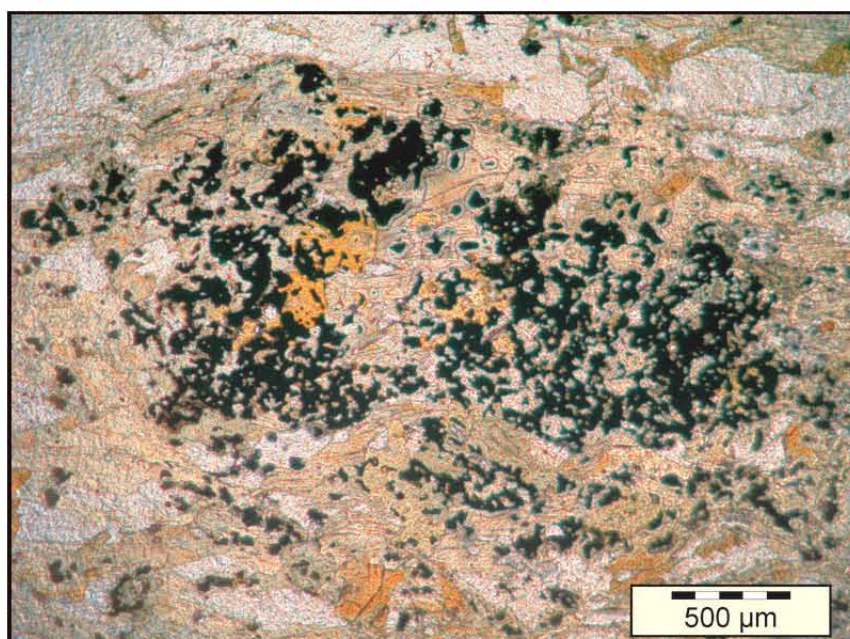


Figure 2.1.1.24. Boudin-like pitchblende aggregate in tectonized migmatites from the Sumeria ore-showing. Sample Su-1, optical photo of the polished thick section, plain transmitted light.

Veinlets and spherulites of pitchblende have a complex structure: zones of pitchblende alternate with zones composed of gangue minerals. Pb content decreases and Fe content increases from the center to the periphery of the spherulites and veinlets.

Uranium mineralization is accompanied by apatite, titanite, cyrtolite and molybdenite. The most widespread is the association of pitchblende with apatite; it is common for the mineralization hosted by migmatites and amphibolites. Titanite is associated with uranium oxides in the amphibolites. A less common association is pitchblende with cyrtolite (sometimes accompanied by molybdenite) which occurs in silicified zones with overprinted schistosity.

In the whole rocks U-enrichment is positively correlated with P, Pb and Sn, and to a lesser extent with Yb, Be, Mo. Increased contents of Ag and Bi occur as well.

From gas-fluid inclusions studies in the apatite accreted with the pitchblende in the sericite-quartz-albite metasomatite temperatures of ore-forming process has been estimated at 240-380° and carbonic-acid composition has been determined.

In the samples obtained from migmatite-hosted uranium occurrences of the Impilakhti area albitization has not been observed. Distinguished alterations referred to shattering zones along the migmatites are represented by sericitization of biotite, silicification of feldspars and hematitization of magnetite and feldspars. Uranium mineralization is represented by disseminated impregnations and boudinated chains of pitchblende.

3. Overlapped vein-type mineralization.

Indications of low-temperature uranium metallogenesis have been revealed in some of anatexite-hosted uranium ore-showings (Korennoye, Maisunmyaki, Sumukanmyaki, Raskenjarvi etc). Pitchblende and coffinite mineralization occurs in fractures cutting all rocks and early ores.

4. Age of the uranium mineralization

All available isotopic data constraining the age of uranium mineralization in anatectic granites are presented in Table 2.1.1.4. Results of Anderson (1990) and of this study have acceptable precision where as those of Gromov (1980 and 1981) are based probably on isotopic-spectral analyses and have not a good accuracy. They should be considered cautiously.

Statistically, the uraninite from the quartz-microcline metasomatites is older than the pitchblende from the sericite-quartz-albite metasomatite. Uraninite crystallization can be limited occurs at 1820-1800 Ma, an age corresponding to the emplacement of the late-orogenic Svecofennian leucogranites (in the Northern Ladoga – the Matkaselsky complex).

Reliable age constrains of pitchblendes from the anatexites of the Northern Ladoga should be limited 1800-1770 Ma that corresponds to autometamorphic alterations of the granite systems during post-orogenic processes.

Indications of late uranium redistribution have been identified during this study in a sample from the Korennoye ore-showing. Palaeozoic age about 400 Ma has been obtained for pitchblende-2 related to fractures cutting mineralized anatexites.

The late supergene mineralization develops in outcropping ore bodies, but it does not modify significantly a distribution of the mineralization.

Table 2.1.1.4. Isotopic age constrains of U mineralization hosted by anatexites in the Northern Ladoga area (SIMS – CAMECA IMS-3F ion-microprobe; TIMS – mass spectrometer; n – number of analyses; T_o – upper intercept and T_m – lower intercept of the Concordia).

Occurrence	Host rock	Mineral	Method	n	Isotopic age, T_o , T_m , Ma	Reference
Sjuskinsaari	mcl-qtz metasomatite	uraninite	U-Pb, SIMS	5	1818±27, 527±200	This study
Puttummyaki	ser-qtz-ab metasomatite	pitchblende	U-Pb, SIMS	6	1789±31, -6±110	This study
		pitchblende	U-Pb, TIMS	13	1770, ~1100	Anderson, 1990
		pitchblende	U-Pb, TIMS	7	1753±61, 243±45	Anderson, 1990
Korennoye	ser-qtz-ab metasomatite	pitchblende	U-Pb, SIMS	3	1772±43 (constrained to 0)	This study
	quartz veinlet	pitchblende	U-Pb, SIMS	9	469±180, 127±260	This study
Sumeria	ser-qtz-ab metasomatite	pitchblende	U-Pb, SIMS	4	1748±130, 104±440	This study
Mursula	mcl-qtz metasomatite	uraninite	U-Pb, TIMS	2	1800 (concordant)	Anderson, 1990
		uraninite	U-Pb, TIMS	13	1808±95, 204±83	Anderson, 1990
		uraninite	U-Pb, TIMS	5	1816±14	Anderson, 1990
		uraninite	Pb-Pb, TIMS	5	1813±26	Anderson, 1990
	ser-qtz-ab metasomatite	pitchblende	U-Pb, TIMS	5	1770-1750	Anderson, 1990
Sumukanmyaki	ser-qtz-ab metasomatite	pitchblende	U-Pb, TIMS	5	1786 (~ concordant)	Anderson, 1990
		pitchblende	Pb-Pb, TIMS	5	1760±10	Anderson, 1990
		uraninite, pitchblende, coffinite	?		1560±70	Gromov, 1980
Raskenjarvi	mcl-qtz metasomatite	uraninite, pitchblende,	?		2000±70, 1780	Gromov, 1981
Kokkoya	mcl-qtz and ser-qtz-ab metasomatites	uraninite, pitchblende	?	26	1680±50	Gromov, 1980
		uraninite, pitchblende	?	15	2000±70	Gromov, 1980
		uraninite, pitchblende	?	13	1430±130	Gromov, 1980

5. Stages of the uranium metallogenesis.

Thus, three main episodes of uranium deposition associated with anatectic granites in the granitic-gneiss domes of the Northern Ladoga area have been identified by mineralogical and isotopic studies:

- I. 1.82-1.8 Ga high-temperature “potassic metasomatism” or in another terms “partial melting”;
- II. 1.8-1.77 Ga medium- to low-temperature hydrothermal sericitization with local Na metasomatism;
- III. Palaeozoic low-temperature hydrothermal uranium redistribution.

6. Typological reference of anatexite-hosted uranium mineralization of the Northern Ladoga area.

Complex character of uranium mineralization in the anatexite-hosted occurrences of the Northern Ladoga makes difficult their typological identification. The early uraninite mineralization related to quartz-microcline pegmatoid granites can be compared with one of the Rössing deposit (Namibia). Second stage is not studied enough and in depends on opinion it could be considered as very weak manifestation of albitization principally resemble to more advanced one of the Arjeplog-Arvidsjaur area (Sweden), but in the last one sericitization is not typical, or to hydrothermal fracture-bound type, possibly similar to Beaverlodge area deposits. Third event of hydrothermal vein-type uranium redistribution has no big importance in the occurrences resource. Until more detail study, these uranium occurrences are presented as anatexite-related.

2. U-Th occurrences hosted by intrusive granites.

High abundance of U and Th is quite common for certain types of intrusive granites of the Ladoga region (General Appendix 2.2), but there is no uranium ore-showings hosted by the granite intrusions themselves, only local anomalies are known. In general, they can be subdivided into three groups:

1. Th-U anomalies in the Upper Lopian granites of the Karelian domain;
2. U-Th anomalies in the late-Svecofennian leucogranites;
3. U-Th anomalies in the latest phases of rapakivi granites.

The most U-enriched granites are latest phases of the late-Svecofennian granite intrusions forming pegmatites swarms referred as the Matkaselka, Latvasurje and especially Impilakhti-Pitkjaranta pegmatite complexes.

2.1. U-Th-REE-rare metal late-Svecofennian pegmatites of the Impilakhti-Pitkjaranta area.

Late-Svecofennian pegmatites of the Impilakhti-Pitkjaranta area are concentrated in tectonic zones of different strike. The most saturated are submeridional-striking dislocations. Most of the pegmatites occur inside granite-gneiss domes, to a lesser extend within the Ludicovian and rarely the Kalevian formations. Their length reaches up to 700 m, width up to 25 m. Their average size is 30×3 m.

There are two mineralogical subtypes of rare-metal-REE pegmatites in the Impilakhti-Pitkjaranta area (Bogachev, 1999):

- 1) pegmatites with orthite-thorite-cyrtolite mineralization;
- 2) pegmatites with monazite-viikite mineralization.

Pegmatite veins with the *orthite-thorite-cyrtolite mineralization* usually occur in the amphibolites and plagio-microcline migmatites in the amphibole-biotite schist. In general they are located in internal parts of the granite-gneiss domes.

The pegmatite bodies are not zoned, form complex-shaped veins composed of light-gray granite with variable grain size. Microbreccias structures are common. Geochemically the rock corresponds to a granite with 10 % K₂O+Na₂O and 0.6-1.3% CaO.

The rock composition is of: 40 % of plagioclase (An₁₂₋₂₂), 40% of microcline-perthite, about 20 % quartz and less than 1 % biotite. Accessories are magnetite, almandine, apatite, titanite, cyrtolite, orthite and thorite (ferrithorite prevails). Bröggerite rarely occurs.

The REE-Th-U mineralization is localized mainly in peripheral parts of the pegmatite bodies and concentrated in the shattering zones cutting fine-grained quartz-microcline or quartz-microcline-biotite granite. It occurs in intergranular settings and in cleavage fractures in biotite and feldspars.

U contents in the pegmatites with the orthite-thorite-cyrtolite mineralization is up to 3 300 ppm and Th – up to 4 300 ppm.

Monazite-viikite mineralization is hosted by pink microcline pegmatites typically occurring at the periphery of the domes and in inter-dome synclines. They typically occur as dykes. They are zoned, with from center to periphery: a quartz core, a coarse-grained microcline zone, a graphic granite and a quartz-biotite salband ($K_2O=5.7-9.4\%$, $Na_2O=3.2-4.8\%$).

The mineral composition of the pegmatite is: 50 % of microcline and microcline-perthite; 40% of plagioclase (An14-20; less than 20 % quartz and 5 to 7 % coarse-grained Fe-biotite. Major accessories are (total content about 1 %): zircon, cyrtolite, monazite, apatite, titanite, tourmaline, magnetite, molybdenite, rare Fe and Cu sulphides, epidote, muscovite, chlorite.

Accessory REE-Th-U mineralization is represented mainly by monazite, cyrtolite, xenotime, viikite (collective name of complex REE-Ta-Nb minerals with U and Th, including euxenite and samarskite). Rarely orthite, thorite and bröggerite occur. Accessories form disseminations and nest concentrations.

The distinctive feature of these pegmatites is the occurrence of widespread metasomatic alterations. Albitization after syngenetic feldspar occurs in the shattering zones. Microcline and biotite are also replaced by fine-grained quartz and sericite. Replacement of plagioclase by epidote and zoisite, biotite by chlorite occur in the shattering zones and at the contacts of the pegmatite bodies.

U content in pegmatites with the monazite-viikite mineralization reaches 13 000 ppm, Th – up to 10 000 ppm, but the anomalous areas are very local. U-mineralized zones do not exceed 30 m² for a 100 ppm U cutoff.

2.2. Other granite-hosted uranium occurrences.

Other radioactive anomalies are of very low grade and we have not studied them in details, although some of them have been visited during field trips and should be mentioned.

The most ancient granite-hosting radioactive mineralization occurs in the northernmost part of the Ladoga region and is related to the Karelian domain. They have been discovered in the Kuhilaslampi area (Appendix to Chapter 1, fig. 5) during exploration by “Nevskgeologia” from 1957 to 1976. They are always spot anomalies and only a few ones spread over tens of square meters. The anomalies are hosted by coarse- and middle-grained microcline granites. U content in these anomalies reaches up to 150 ppm and Th up to 800 ppm. Radioactive mineralization is represented by thorite and zircon (fig. 2.1.1.25). Thorite has suffered of

intensive alterations followed with Th loss. Replacing minerals have increased content of Th (General Appendix 2.3, table 3).

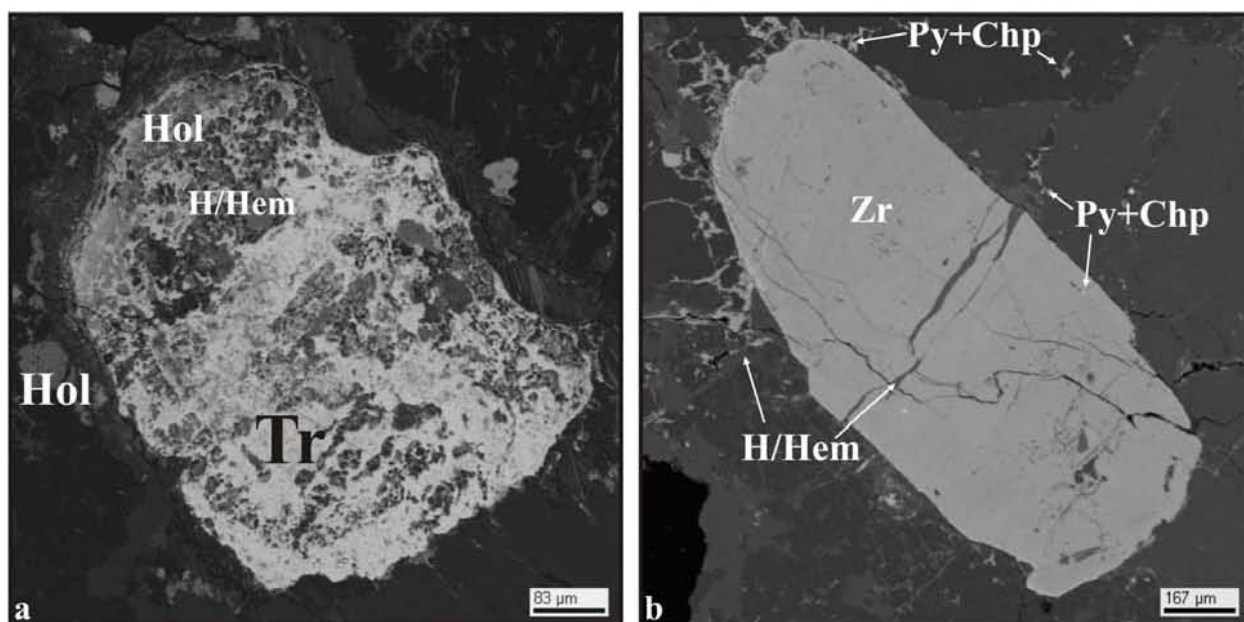


Figure 2.1.1.25. Th-bearing minerals from Archaean granites from the Kuhilaslampi area. Sample Jn-1, BSE photos: a -replacement of thorite (Tr) grain by hollandite (Hol) and hydrohematite (H/Hem); b – zircon grain (Zr), hydrohematite develops around it and in the (H/Hem), pyrite and chalcopyrite (Py+Chp) occur in fractures.

Local low-grade radioactive anomalies referred to U- and Th-bearing accessories are widespread the late Svecofennian granite massifs occur all around the Ladoga region. Most of them have been discovered in the Northern Ladoga area of the Raahe-Ladoga domain and in the Priozersk block of the Svecofennian domain. According to previous works (Ivanikov et al., 1984; Bogachev, 1999), the granites of the Western Ladoga (the Svecofennian domain) are enriched in Th, but relatively poor in U. On the contrary the granites of the Northern Ladoga (Raahe-Ladoga zone) have high U and moderate Th contents (General Appendix 2.3, table 2). The most U-enriched are those of the Matkaselka complex. Local radioactive anomalies up to 3500 cps related to muscovite aggregates in the coarse-grained granite have been observed inside the massifs (fig. 2.1.1.26). “Nevskgeologia” carried out local drilling of the Matkaselka complex intrusions during regional prospects, but all discovered uranium occurrences are of low grade and have no economic importance.

The late phases of the rapakivi granites have increased U abundance. Spotty radioactive anomalies referred to U- and Th-bearing accessories occur.

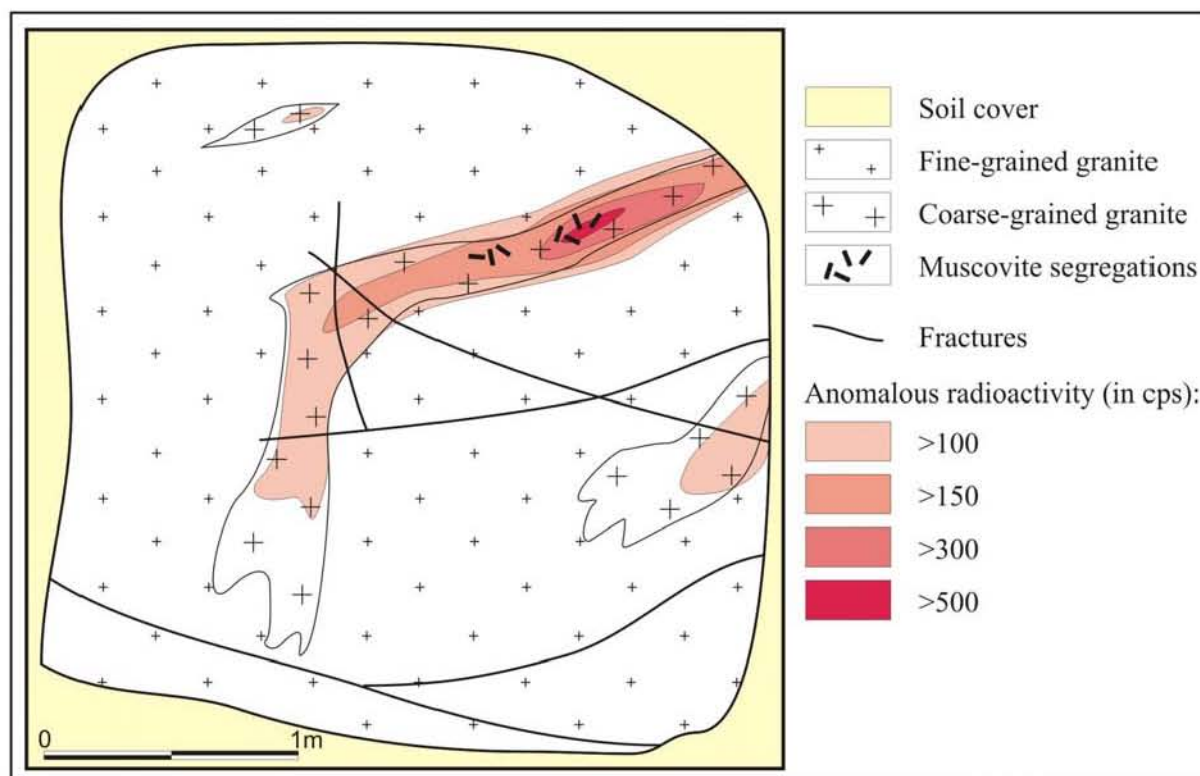


Figure 2.1.1.26. A radioactive anomaly related to muscovite segregation in coarse-grained granite in the Matkaselka massif.

Conclusion.

Diverse granite-hosted radioactive mineralization occurs in the Ladoga region. The most fertile are anatectic quartz-feldspar granites of the granite-gneiss domes referred to latest stages of the Svecofennian event, but even they host uranium occurrences ranged just up to ore-showing grade.

Uranium mineralization in the intrusive granites of the Ladoga region is of low grade. Uranium occurs mostly as substituted in the structure of the refractory accessory minerals, its content is low and the size of the mineralized zones is small.

Thus, granite-hosted uranium occurrences of the Ladoga region have no economic importance and, taking in account their quite detail prospect studying carried out in the past, it is difficult to expect here undiscovered large uranium deposit of this type. But it is necessary to note, that indications of latest hydrothermal uranium redistribution revealed in some of the granite-hosted uranium ore-showings in the Ladoga region allow considering these concentrations as a probable source of uranium for late occurrences.

Paragraph 1.2. Th-U anomalies in the Jatulian quartzites.

Introduction.

In the Ladoga region the Jatulian formations occur only along boundary between Karelian and Raahe-Ladoga domains (General Appendix 1, fig. 1.1). They are located in the Tulomozero and on north-eastern slope of the Janisjarvi syncline where they unconformably overlays the weathered Archaean granite-gneiss basement of the Karelian domain (Appendix to Chapter 1, fig. 6). Numerous Th-U occurrences hosted by the Jatulian sediments had been found in the Janisjarvi syncline.

Exploration works in the area of north-eastern slope of the Janisjarvi syncline were carried out in 1946, 1957-1960, 1974-1975. Diverse uranium and thorium anomalies have been found. They can be subdivided into three types:

- 1) Th and U anomalies related to the accessory minerals (zircon, allanite and thorite) in the Upper Lopian granitoids. These anomalies are briefly considered in the Paragraph 1.1.
- 2) Fracture-bound U and Th anomalies in different geological environment. Some of these occurrences will be described in the paragraph 1.4 concerning the vein-type mineralization.
- 3) Th-U anomalies in the Jatulian quartzites. This Paragraph is devoted to these occurrences.

1. Geological structure of the Kuhilaslampi area.

In the Russian territory Th-U anomalies in the Jatulian quartzites have been discovered in the area from Vyartselya village on the Russian-Finnish frontier to the south-east over a distance of about 20 km along the northern shore of the Maloye Janisjarvi Lake. The central part of this area (named Kuhilaslampi area) has been studied in the present work (Appendix to Chapter 1, fig. 5).

The lower stratigraphic layer of the area is composed of Archaean formations of the Karelian domain. Most Archaean rocks are Saamian-Lower Lopian tonalite granite-gneiss, oligoclase gneiss-granites and migmatites. In the Kuhilaslampi area plagiogranite gneiss prevails in the Archaean sequence. Generally they are characterized by low uranium and thorium contents: 0.5 and 4.3 ppm respectively in average.

Upper Lopian formations occur to the east from Kuhilaslampi area, within the Ilomasi-Jalonvara granite-greenstone belt. In the Janisjarvi fault zone they are cut by the Jalonvara granitoid intrusion. Quartz diorites of the Jalonvara intrusion have increased uranium content (up to 6.1 ppm).

Palaeoproterozoic formations unconformably overlay Archaean basement of the Karelian domain. In the Kuhilaslampi area they occur in the closure of local fold complication of the Janisjarvi syncline. Palaeoproterozoic formations dip 25-50° to the center of the fold, whereas along the northern limb of the Janisjarvi syncline the dip is 15-40° to SW.

There is a thick layer of Sariolian quartz conglomerates at the base of the Palaeoproterozoic sequence of the Janisjarvi depression. They occur very locally and have been discovered to the east from the Kuhilaslampi area.

In the Kuhilaslampi area the Palaeoproterozoic sequence starts with Jatulian sediments unconformably overlaying Archaean formations. Karelian basement regolith in this area is about 2-4 m thick (Polikarpov et al., 1976). It is composed of white or light-greenish-gray rock. The rock is brecciated. Isometric fragments (up to 3×4 cm size) of fine-grained carbonate with relics of carbonated granite-gneiss are cemented by a carbonate-hydromica material.

The proper Jatulian succession in the Kuhilaslampi area is represented by terrigene, littoral, shallow-marine sediments of the Jangozero and Tulomozero suites. The basal horizon of the Lower subdivision of the Jatulian Jangozero suite is composed of light-gray coarse-grained quartzite; upward they are replaced by middle-grained quartzite (fig. 2.1.2.1 a). The rock composition is: quartz grains cemented with sericite and minor chlorite, biotite and carbonate. Light-gray rocks are overlain by dark-gray analogs.

Cross-bedding of littoral type is often observed in the quartzitic-sandstone of the Jangozero suite (fig. 2.1.2.2 b). Lenses of weakly ferruginous coarse-grained quartzitic-sandstones, gritstones and minor conglomerates occur at the contact of the cross-bedded series. Concentrations of accessories occur at the base of the conglomerate layers: zircon, rutile, leucoxene, apatite, hematite, pyrite (with jarosite pseudomorphs) and monazite. Usually the accessories are well-rounded and are detrital, unlike pyrite which is considered as authigenic (Kondakov et al., 1963).

According to drilling data, the quartzitic-sandstones are locally overlaid with a thick layer of quartz-sericite schist. The upper horizon of the Jangozero suite of the Kuhilaslampi area consists of pink-gray massive arkoses. The total thickness of the suite is about 200 m.

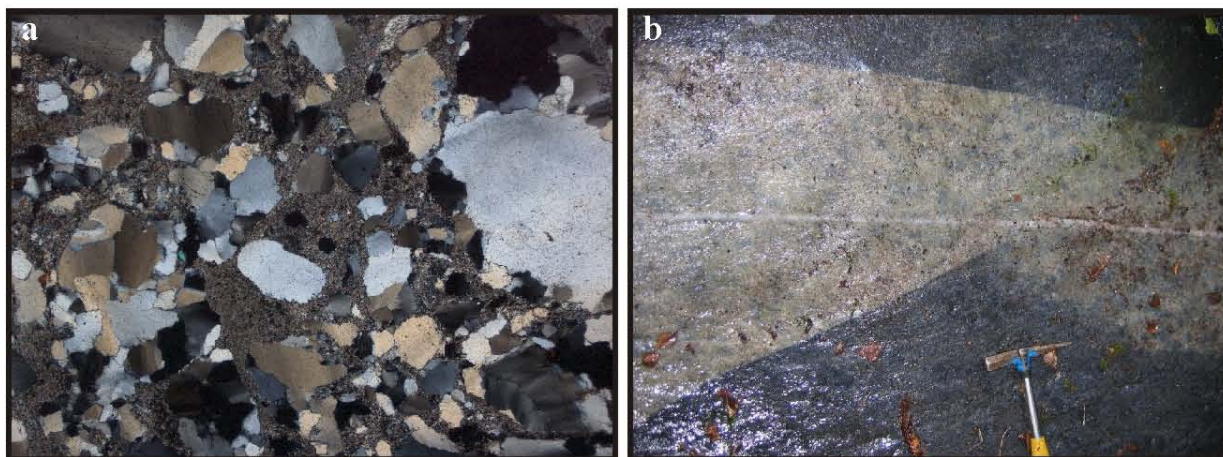


Figure 2.1.2.1. Jatulian quartzite from the Kuhilaslampi area: a – thin section of sample Jn-3, optical photo, polarized transmitted light; b – quartzites cross-bedding, photo of outcrop.

The Jangozero suite is conformably overlaid by dolomites and phyllites of the Tulomozero suite of the Upper Jatulian to the south and south-east of the Kuhilaslampi area.

The Jatulian layers dip under the Ludicovian carbonate and metabasite rocks (the Soanlakhti suite of the Sortavala group) to the south. Usually the contact between the Jatulian and the Ludicovian is not obvious although sometimes indications of erosion can be distinguished (Bogdanov et al., 2000). Lithologically, the Ludicovian sequence differs from the Jatulian one by an increased proportion of mafic volcanites and graphite abundance in the carbonate lithologies.

AR and PR₁ formations of this area are cut by mafic dykes swarms mainly striking NW-SE. They are mostly of Jatulian age – 2150±60 Ma (Bogdanov et al., 2000), but presumably there are older (Sumian and Sariolian), or younger (Ludicovian, Kalevian, Riphean) intrusions.

This area is referred to the Janisjarvi fault zone and is composed of numerous structures striking NW-SE. There is local rotation of the faults striking in the Kuhilaslampi area: they strike 290-300° compared to the usual 330° striking for the Janisjarvi fault zone. Sub-meridional faults are widespread in the central and eastern parts of the area. They continue from the Karelian domain and correspond to the striking of the Ilomasi-Jalonvara granite-greenstone belt. To the SE, the area of the Jatulian formations is limited by NE-striking faults referred to the Leppyasurja horst of the Karelian domain basement.

Manifestations of diverse and multiphase epigenetic processes are widespread along the fault zones. Mineral paragenesis of hydrothermal alteration zones corresponding to low and medium depths predominate: propylites, beresites, secondary quartzites, hydrothermal

argillizites, tourmaline-chlorite alterations. Deep skarns and serpentines occur rarely (Polikarpov et al., 1976).

2. Th-U mineralization in the Jatulian quartzites.

Over 40 radioactive anomalies related to the Jatulian Jangozero suite quartzites have been found in the Kuhilaslampi area. They occur as in light as in dark-gray varieties of the quartzites. As a rule the anomalies are localized in small interlayers of conglomerates in the basal parts of cross-bedded series (fig. 2.1.2.2). The mineralized layers with radioactivity over 100 cps are 0.5-70 cm thick and up to 150 m long. Average Th content is 500 ppm, up to 7 000 ppm over 0.2 m; U contents are up to 50 ppm (one sample with 120 ppm of U, without Th) (Kondakov et al., 1963). Total U resource of the Jatulian conglomerates of the Kuhilaslampi area is evaluated to a few tons and these occurrences are below of economic grade.

The major radioactive mineral is Th-enriched monazite; zircon and Th-bearing rutile occur as well (fig. 2.1.2.3). Thorite is also present according to the previous works (Kondakov et al., 1963) (fig. 2.1.2.4). It occurs in the Jatulian conglomerates hosting gabbro-diabase dykes. Th enrichment has been also discovered in rutile and iron hydroxides (Table 2.1.2.1).

Table 2.1.2.1. Chemical compositions of Th and U bearing minerals from the Jatulian quartzites of the Kuhilaslampi area.

No	Code	SiO ₂	TiO ₂	Al ₂ O ₃	Fe ₂ O ₃	MgO	CaO	UO ₂	ThO ₂	Nb ₂ O ₅	ZrO ₂	HfO ₂	Ce ₂ O ₃	La ₂ O ₃	V ₂ O ₅	P ₂ O ₅	Sum
MONAZITE																	
1	Jn-3-1-1	1.2			37.0		4.6	0.3	21.4				4.1	0.3		15.2	84.1
2	4	0.7			11.8		5.7	0.8	20.7				13.9	2.2		25.5	81.3
3	6	6.7			21.8		6.5	0.1	21.6				7.3	0.8		19.3	84.1
4	9	5.2		1.3	25.2	0.5	1.7		43.3				0.8	0.2		4.7	82.9
ZIRCON																	
5	Jn-3-1-2	33.7									65.5	2.4					101.6
6	3	13.5			2.0			0.8	24.9		38.9	2.4					82.5
RUTILE / altered RUTILE																	
7	Jn-3-1-7	1.8	91.0		1.6					2.1					1.2		97.7
8	8	14.0	33.6	0.4	29.9	0.1	0.4		14.9	0.1					0.4		90.8
IRON HYDROXIDE																	
9	Jn-3-1-5	4.1			70.9				0.1				0.1				75.2

The origin of these anomalies is considered as syngenetic. Primary sedimentary accumulation in the conglomerates was the principal mechanism. Some diagenetic redistribution occurred after deposition. The epigenetic alterations of the radioactive mineralization are only indicated by weak increasing of radioactivity along the fractures (fig. 2.1.2.5), but the radioactive mineral phase has not been identified.

As this area is located in a mobile zone (the Janisjarvi fault zone) with evidences of multiple activations and of vein-type uranium mineralization (see Paragraph 1.4. Vein-type uranium mineralization), it is possible that U may have been leached from the quartzites by hydrothermal fluids during these activations.

The syngenetic origin of the Th-U mineralization in the Lower Jatulian quartzites of the Kuhilaslampi area allow to estimate the age of these occurrences between 2.3 and 2.15 Ga.

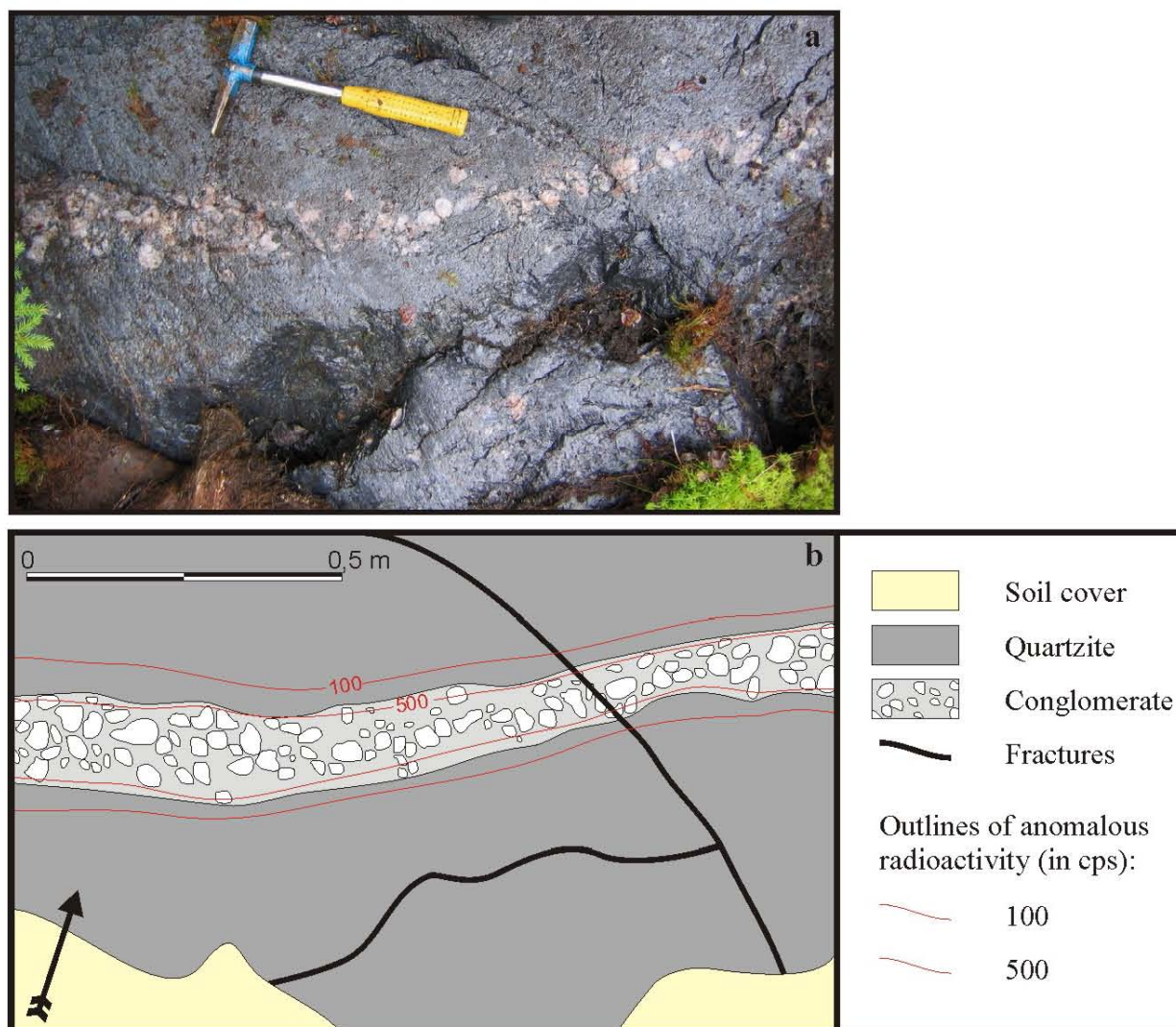


Figure 2.1.2.2. Jatulian quartzite with radioactive conglomerate from the Kuhilaslampi area.

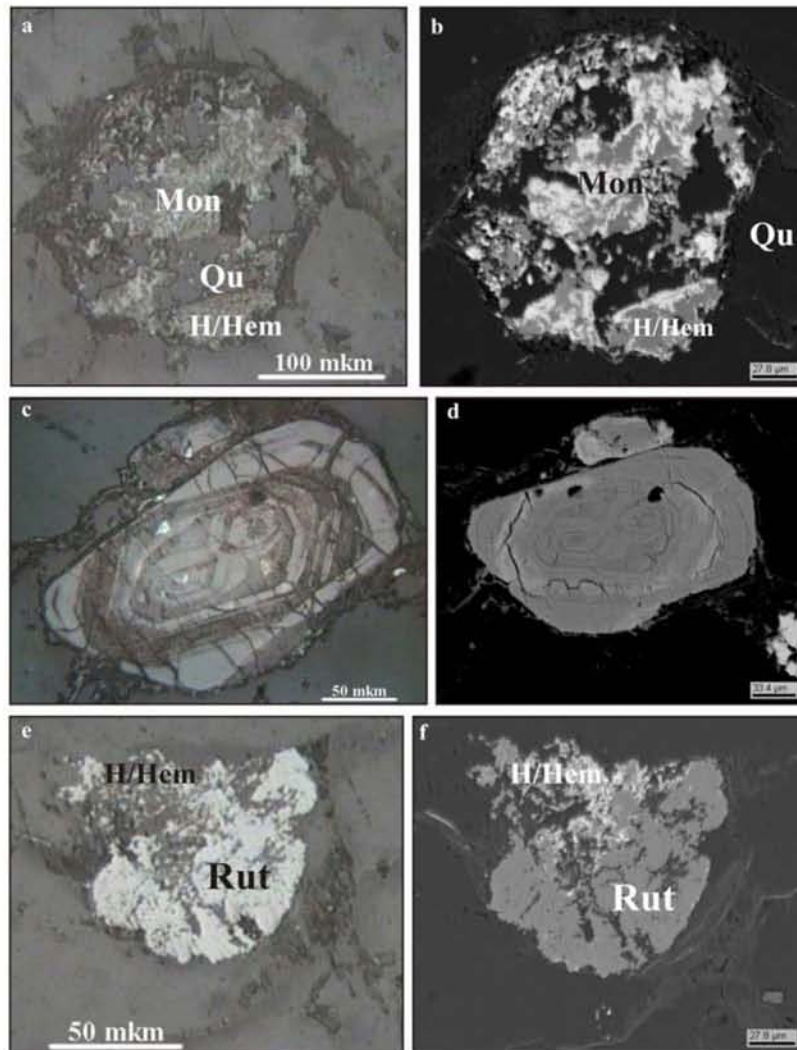


Figure 2.1.2.3. Th-bearing mineral phases from the Jatulian quartzites, sample Jn-3, left column – optical photos, reflected light, right column – BSE photo: a, b – monazite crystal (Mon) partly replaced by iron hydroxides (H/Hem) and quartz (Qu); c, d – zircon; e, f – rutile replaced by the Fe hydroxides.

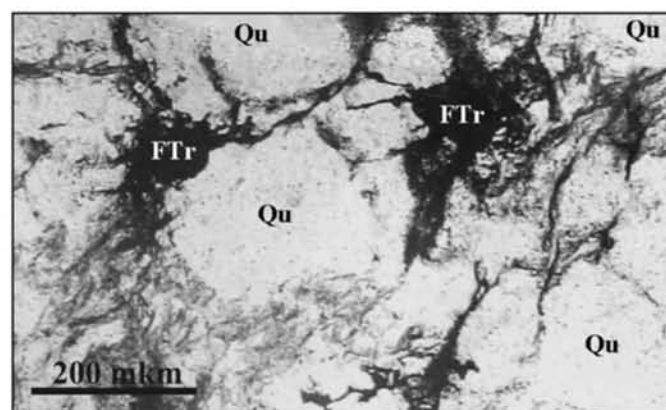


Figure 2.1.2.4. Ferrithorite (FTr) segregations in the quartzite; fractures around the ferrithorite are composed of hydrothorite. Transmitted plain light (from Kondakov et al., 1963).

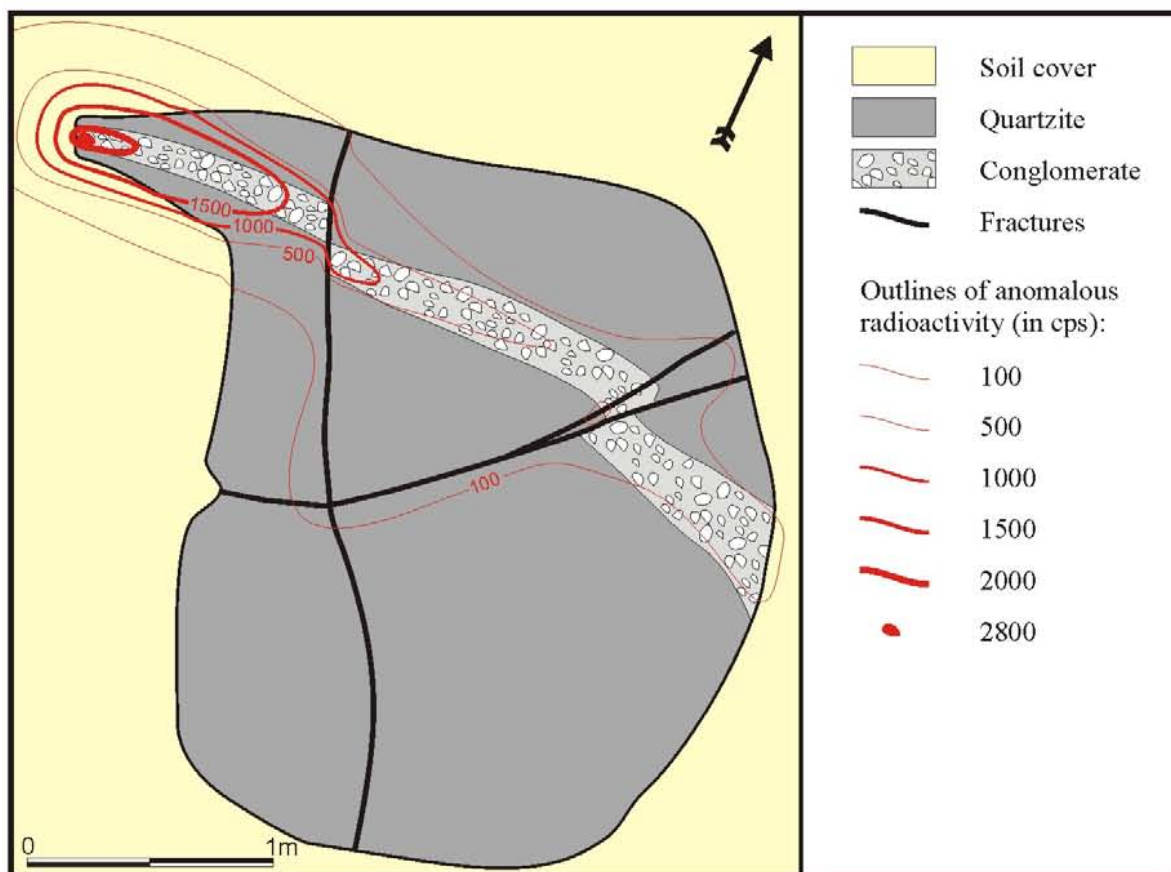


Figure 2.1.2.5. Radioactive anomaly in the Jatulian quartzite from the Kuhilaslampi area.

There are also many Th anomalies in the Jatulian conglomerates in Finland (Koli province) and they seem to be similar to the Janisjarvi area ones.

Several small U deposits hosted by the Jatulian quartzites have been discovered in Finland (Martinmonttu, Hermanninmonttu, Ruunaniemi, Ipatti etc). Thorium mineralization is absent or subordinated there. Uranium mineralization is represented mainly by pitchblende and uranophane related to the conglomerate layers. Origin of those deposits considered as synsedimentary-diagenetic, but vein-type uranium mineralization occurs as well. Sometimes it makes the principal contribution to the deposits resource (the Paukkajanvaara deposit).

Conclusion.

Th-U mineralization in the quartz conglomerates of the Maloye Janisjarvi area is referred to syn-sedimentary quartz-pebble conglomerate type. Very low uranium content and small size of mineralized layers make these occurrences not interesting for economic targets.

Paragraph 1.3. U-P occurrences in the Ludicovian carbonate rocks.

Introduction.

Uranium occurrences hosted by Ludicovian formations of the Northern Ladoga area are subdivided into two groups:

1. U-P occurrences in marbles and carbonate schists (metamorphosed phosphorites);
2. vein-type U-polymetallic occurrences.

The last ones occur not only in the Ludicovian formation and will be described in the Paragraph 1.4 Vein-type uranium occurrences. The Paragraph 1.3 deals with the U-P occurrences of the first group.

1. U-P occurrences of the Northern Ladoga area.

Most of U-P occurrences are located along the Ruskeala anticline (General Appendix 1, fig. 1.1). The Ruttu ore-showing was discovered in the south-striking apophysis of the anticline. The Pappinmyaki ore-showing occurs on the Kalamsaari island in the Sortavala area. The Impilakhti group of U-P occurrences was found in the Impilakhti area on the south-eastern continuation of the Ruskeala fault zone. Few low-grade anomalies presumably of the same type were discovered in the Ludicovian carbonate enveloping granite-gneiss domes in the Latvasurje area.

All U-P occurrences of the Northern Ladoga area are hosted by carbonate rocks of the upper carbonate horizon of the Pitkjaranta suite. The most significant specimen of this type is the Mramornaya Gora ore-showing.

1.1. The Mramornaya Gora ore-showing.

The ore-showing was discovered by “Nevskgeologia” during the 1951-1953 and 1978-1980 geological surveys. A large amount of exploration work was undertaken at that time (especially during the fifties): trenching, drilling, prospecting shafts and pits. The main ore-showing was visited and sampled during field work performed during this thesis.

Geological environment.

The Mramornaya Gora ore-showing area is located at the north-eastern slope of the central part of the Ruskeala anticline (fig. 2.1.3.1 and 2.1.3.2).

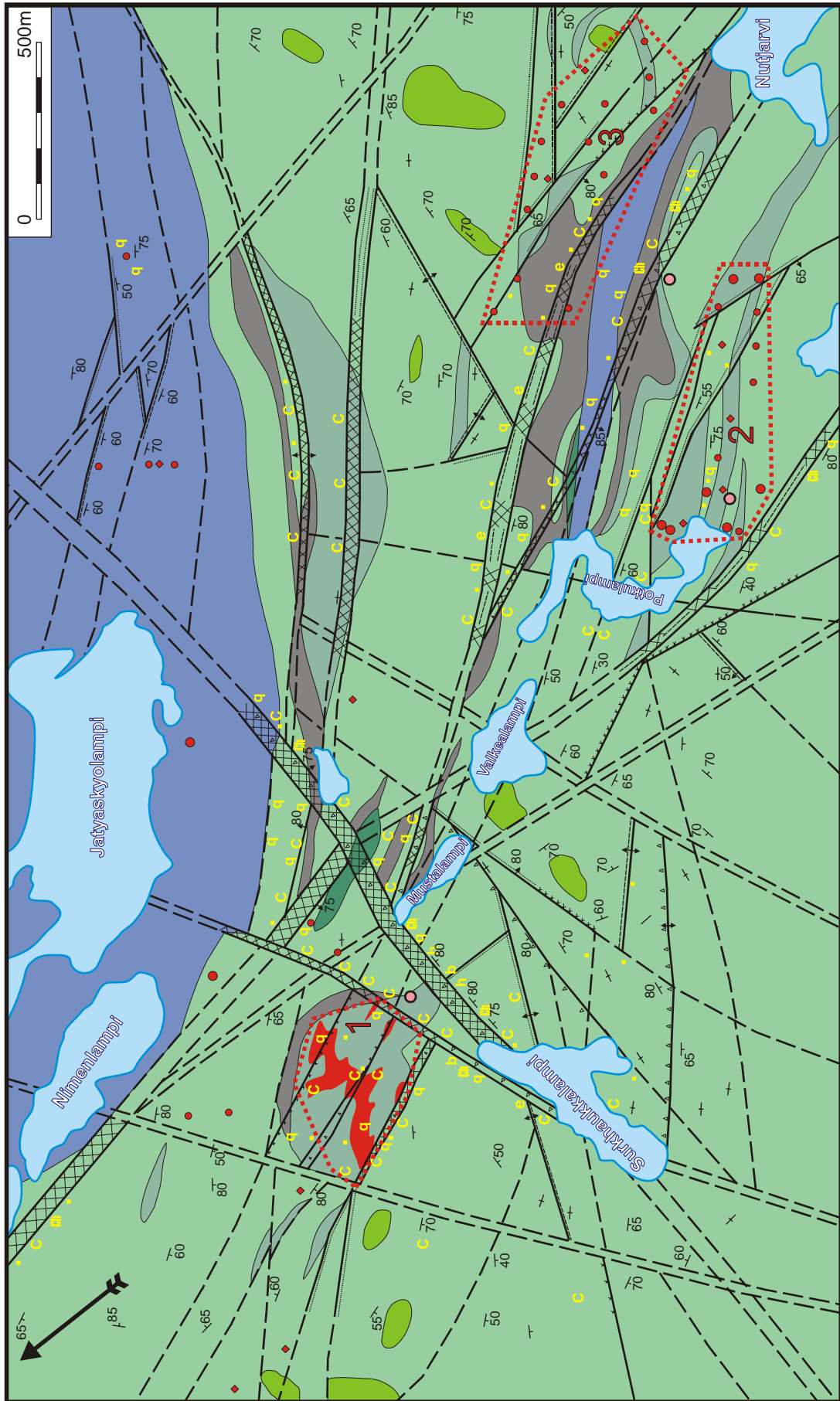


Figure 2.1.3.1. Geological map of the Miramornaya Gora ore-showing area (after Gromov et al., 1981).

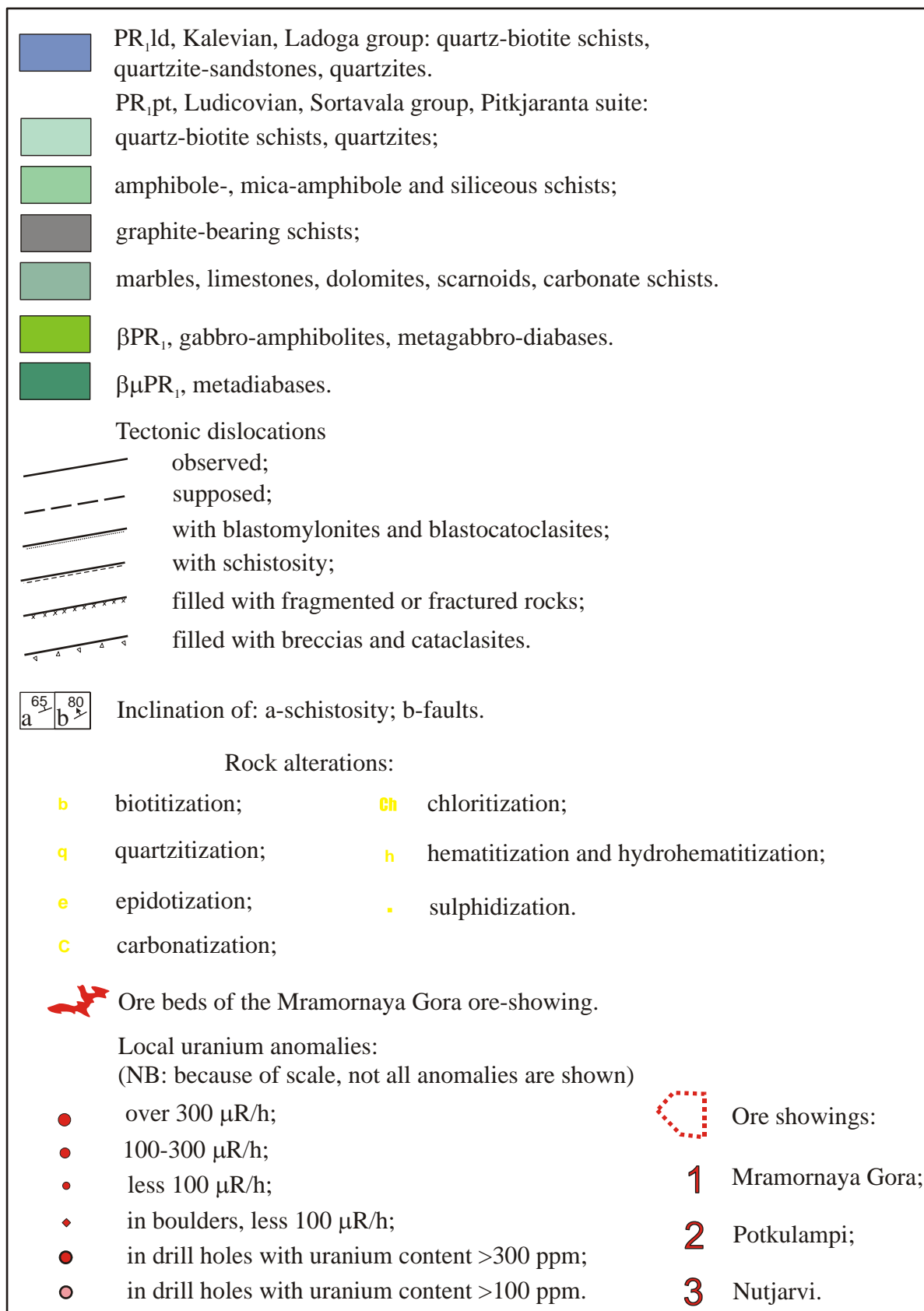


Figure 2.1.3.1 (continued). Legend to geological map of the Mramornaya Gora ore-showing area.

The ore-showing is hosted by lenses of calc-silicate metamorphic rocks of the upper carbonate horizon of the Pitkjaranta suite (fig 2.1.3.2 and 2.1.3.3). The main lens of 800×380 m size, NW striking (320°, SW dipping 70-80°), is composed of (in order of importance) dolomite, calcite-dolomite and calcitic marbles, mica-amphibole and amphibole schists. It is broken into smaller tectonic lenses deformed with disharmonic folds. It is enveloped by the Pitkjaranta suite hornblende schists.

There are small (0.1-0.7 m thick) dykes of metabasites, granodiorite-porphyries and pegmatites, quartz and quartz-calcite veins.

All rocks except pegmatite and late quartz veins are complexly deformed. The most intensive deformations are observed at the contact between the carbonate lens and the hornblende schists, whereas the central part of the lens is relatively weakly fractured. Quartz veins are of several generations. Early ones are deformed and boudinated; the latest generation forms a complex system of small veinlets cutting all metamorphic formations. Rare pegmatites occur as small size dykes without significant deformations. They are related to the late Svecofennian granites and can be correlated with the pegmatites of the Matkaselsky complex.

Analysis of the spatial relationships, deformations and alterations of the rocks composing the Mramornaya Gora area reveals the following succession of formation:

1. Schists

- hornblende;
- actinolite-tremolite and cummingtonite;
- mica-amphibole;
- carbonate;
- silicification;

2. Marbles

- calcite;
- calcite dolomitized;
- calcite-dolomite;
- dolomite;

3. Skarnoids

- amphibole;
- pyroxene-amphibole;
- amphibole-pyroxene;
- pyroxene;

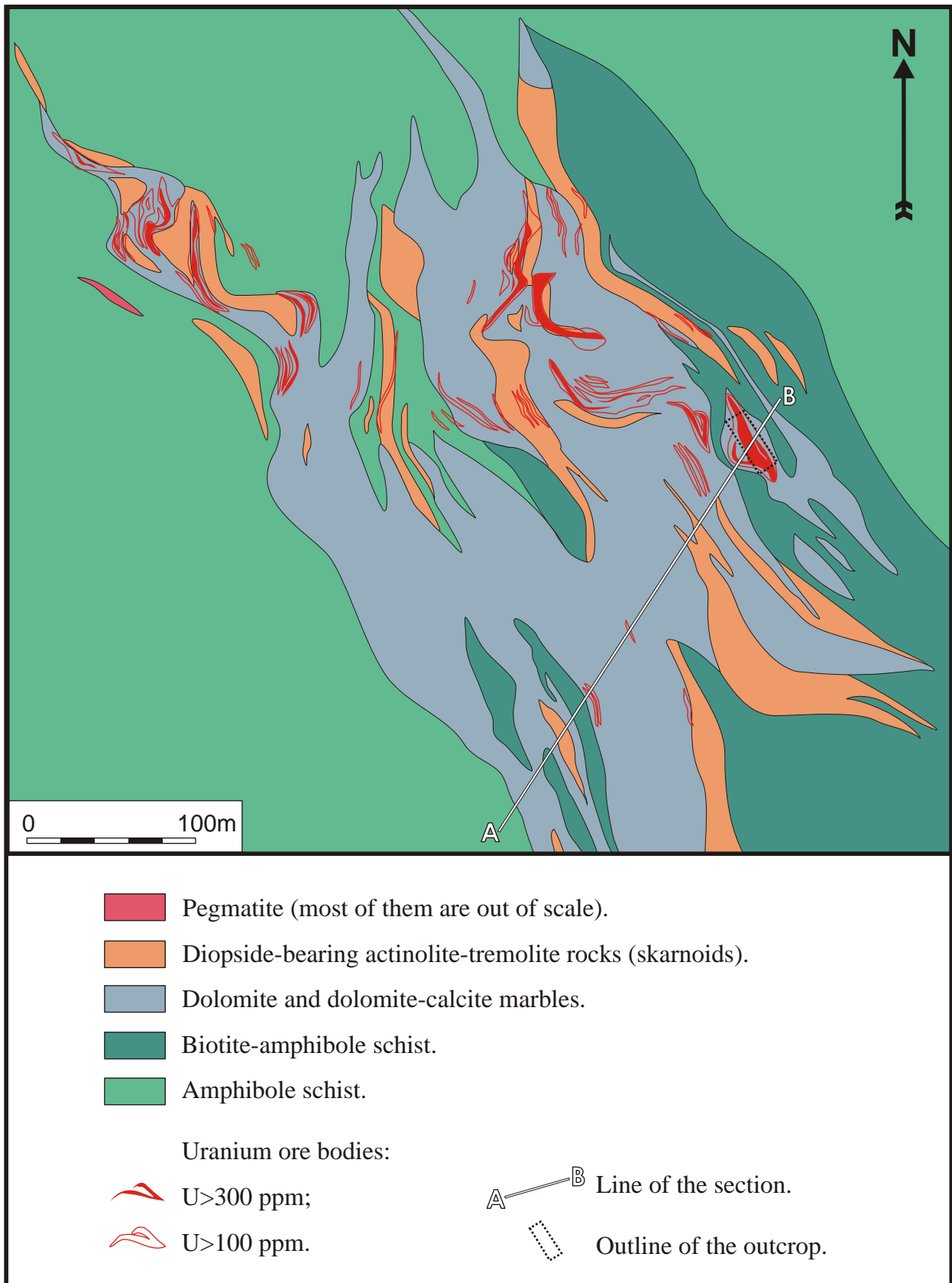


Figure 2.1.3.2. Geological map of the Mramornaya Gora ore-showing (compiled from Nemtsov et al., 1954, Kitsul, 1963, Gromov et al., 1981).

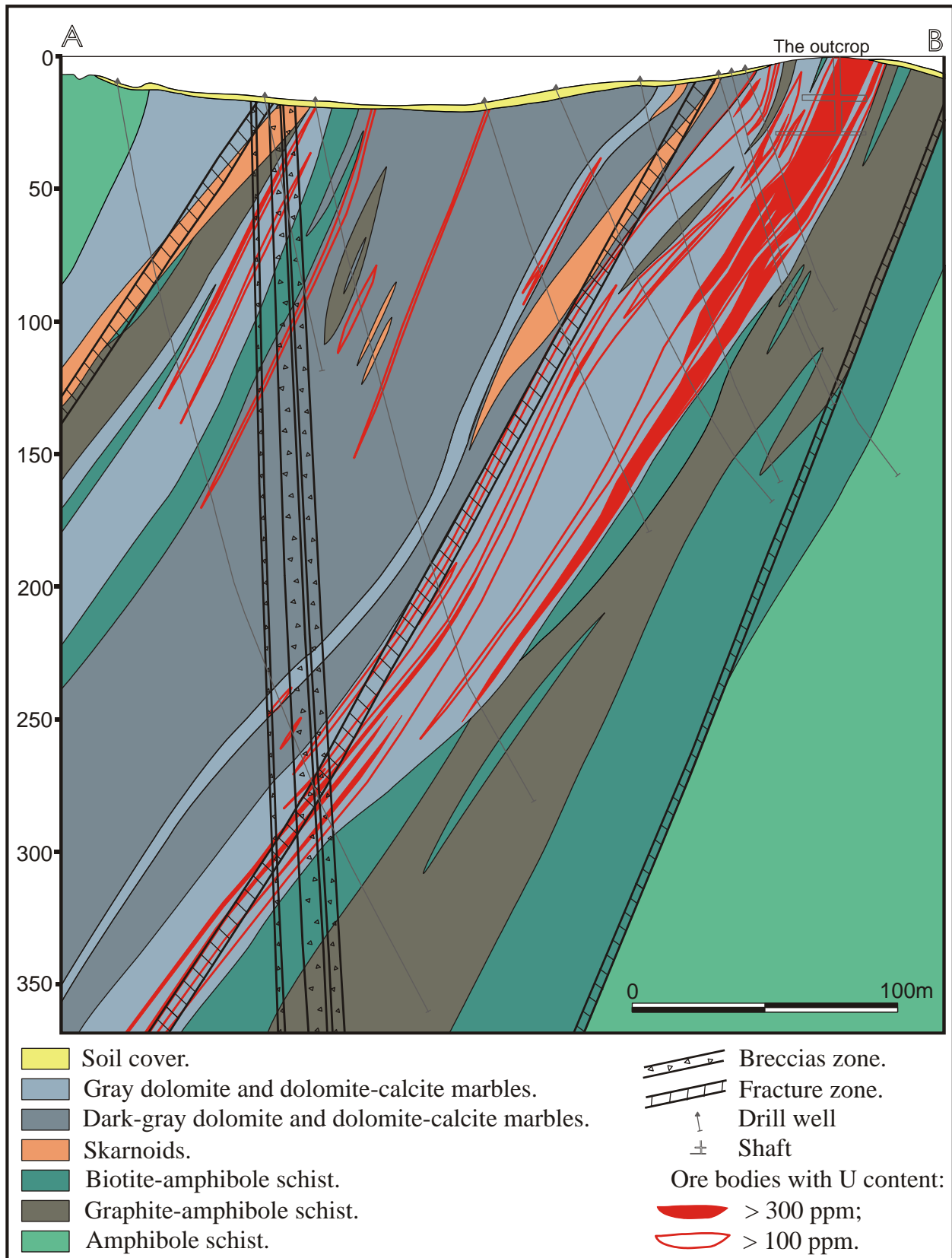


Figure 2.1.3.3. Geological section of the Mramornaya Gora ore-showing (after Gromov et al., 1981).

4. Dyke and vein complex

- metadiabase;
- granodiorite-porphyry;
- quartz and quartz-carbonate veins;
- pegmatite.

The tectonic structure of the Mramornaya Gora results mostly from intense ductile deformations forming numerous disharmonic folds and lenses of different lithologies. The brittle displacements, although quite common, have less importance and amplitudes of those displacements are small. Most of them are normal or reversed faults striking NW, in accordance with the general strike of the host rocks and related to the Ruskeala tectonic zone. Usually those are represented by small-thickness (2-30 cm) dislocated zones conformable with the bedding, filled with hydrothermal calcite, quartz and granodiorite-porphyry hosting sulphide mineralization (pyrite, pyrrhotite, more rarely sphalerite and arsenopyrite). Prospecting shafts and drill holes have discovered more significant fault zones controlling metadiabase dykes and pegmatite veins, quartz-carbonate breccias zones with sulphide, palygorskite and uranium mineralization. Neotectonic corresponds to cliffs up to few meters height.

The most uranium-enriched structure is the most deformed eastern part of the carbonate lens. The rocks are intensively folded and boudinated at the folds limbs. Uranium mineralization is hosted by marbles, actinolite-carbonate schists, pyroxene- and pyroxene-tremolite and tremolite skarnoids. The brecciated gray dolomitic marbles enriched in apatite and sometimes in graphite are the most mineralized rocks are. Uranium mineralization is especially concentrated in intensively deformed areas, particularly in curved parts of small folds. Silicification, chloritization, carbonatization and sulphidization occur in uranium mineralized zones.

Uranium mineralized rocks have been observed in several artificial outcrops and trenches. The most representative outcrops are located nearby the closed entrance to a prospecting shaft. The outcrops were refreshed and mapped during field work made for this thesis (fig. 2.1.3.4).

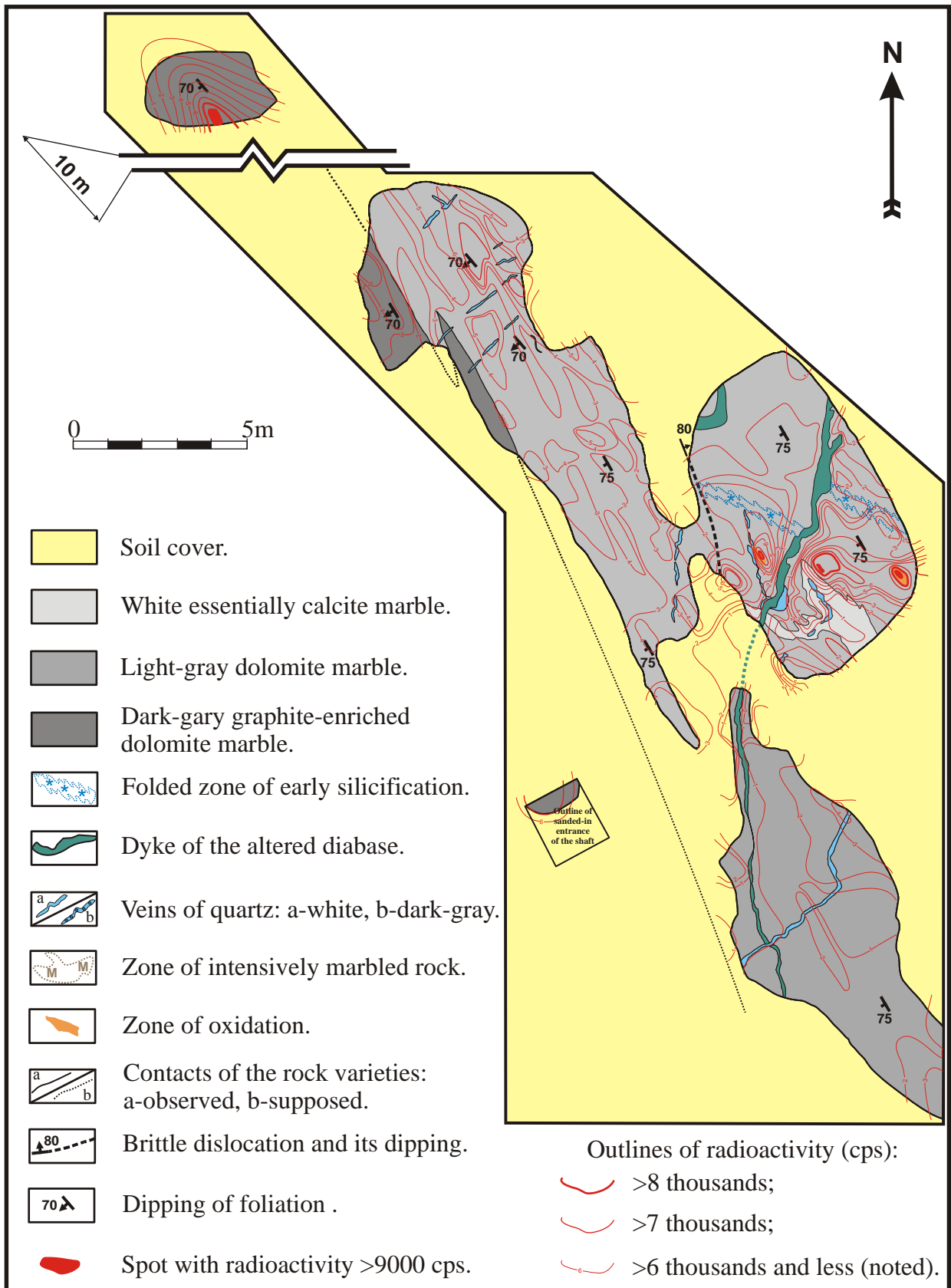


Figure 2.1.3.4. The outcrop of the Mramornaya Gora ore-showing (compiled by Polekhovskiy Y., Shurilov A., Vinogradov L.).

The outcrop is mostly composed of marbles with predominance of dolomitic varieties (fig. 2.1.3.5). Skarnification occurs as linear segregations of actinolite-tremolite, diopside, wollastonite and garnet. Dark-gray dolomitic marbles are relatively enriched in graphite, whereas in light grey ones its content is low. Almost white marbles are essentially calcitic and are subordinated. Dolomitic marbles are enriched in apatite occurring as small drop-like crystals. Several generations of sulphides, arsenides and Ti minerals (titanite and rutile) are common.



Figure 2.1.3.5. Microstructure of the Ludicovian dolomite marble hosting the Mramornaya Gora ore-showing; thin section of sample MG-1, optical photo, polarized transmitted light.

The carbonate rocks are strongly deformed and boudinated into specific spindle-shaped bodies composed of dolomite and enveloped by calcite (fig. 2.1.3.6). The spindles dip 75-80° SE and SW (170-230°). On outcrops they look like rectangular blocks or lenses of dolomite up to 30 cm size, but along the dip these lenses are up to a few meters long. According to old data obtained from 30 m-deep prospect shaft and drill holes, these structures continue at depth at least over tens meters (Nemtsov S.N. et al, 1954).

There are series of metadiabase dykes in the area. They are 5-70 cm thick, generally NE striking with steep dipping to NW. They are folded and sometimes fractured into separated blocks. Schistosity striking NW 310-330° was observed in the metadiabases. It is oblique on the dykes, but corresponds to the regional strike of the host rock foliation.



Figure 2.1.3.6. Uranium ore-hosting brecciated dolomitic marble cemented by calcitic marble in the Mramornaya Gora ore-showing.

Several types of silicification of the metamorphic rocks occur. The earliest one is represented by zones impregnated by small quartz lenses (up to 1 mm thick) and individual grains (fig. 2.1.3.7).

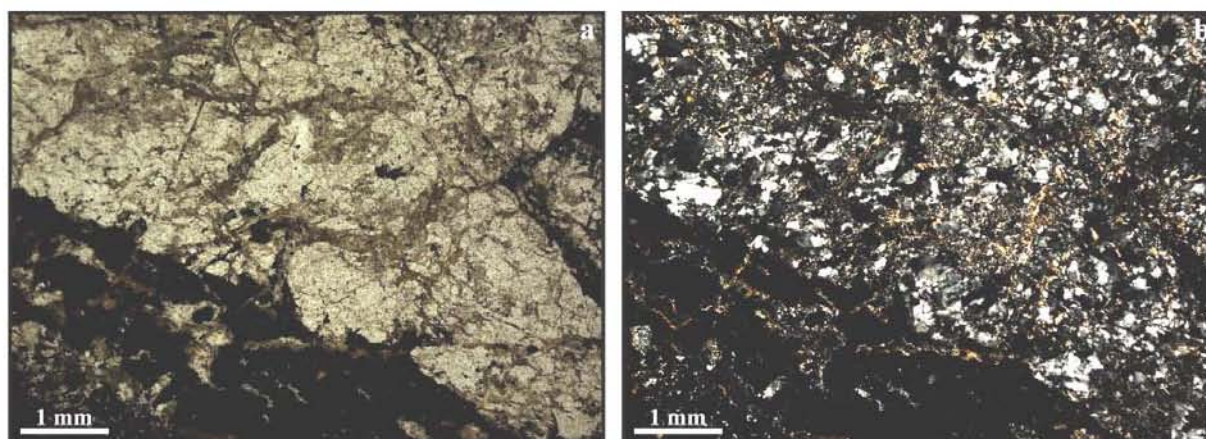


Figure 2.1.3.7. Early silicification of uranium ore hosting marbles in the Mramornaya Gora ore-showing; pitchblende and sulphide mineralization occur in lower left corners of the images. Sample MG-5, thin section optical photos: a – plain transmitted light; b – polarized transmitted light.

These zones are strongly deformed conformably with hosting marbles. Silicification is accompanied with development of sericite, phlogopite, titanite and sulphides. The next generation of silicification corresponds to complex shaped, often boudinated quartz veins (0.5-

10 cm thick) of general NE strike (fig. 2.1.3.8). Small quartz and quartz-carbonate veins cutting all formations are rarer. They often contain late sulphide mineralization (fig. 2.1.3.9).

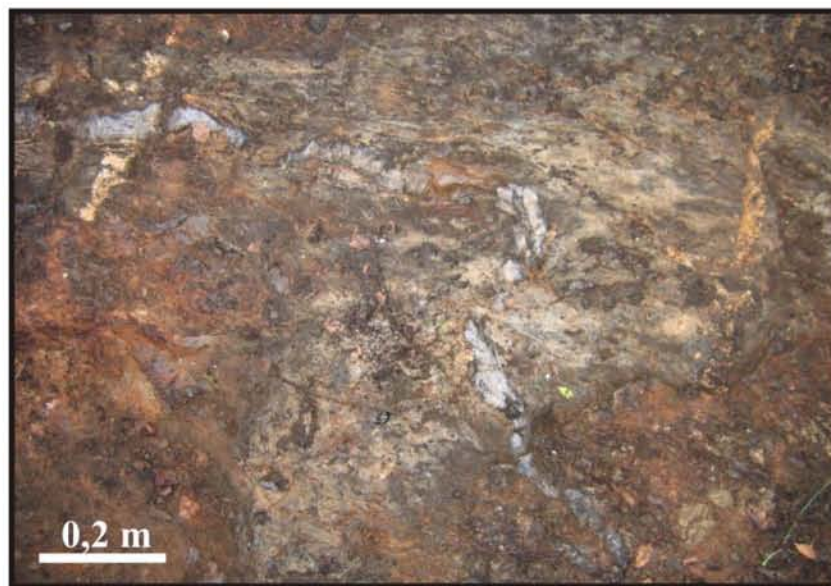


Figure 2.1.3.8. Folded quartz vein in the marble hosting the Mramornaya Gora ore-showing.

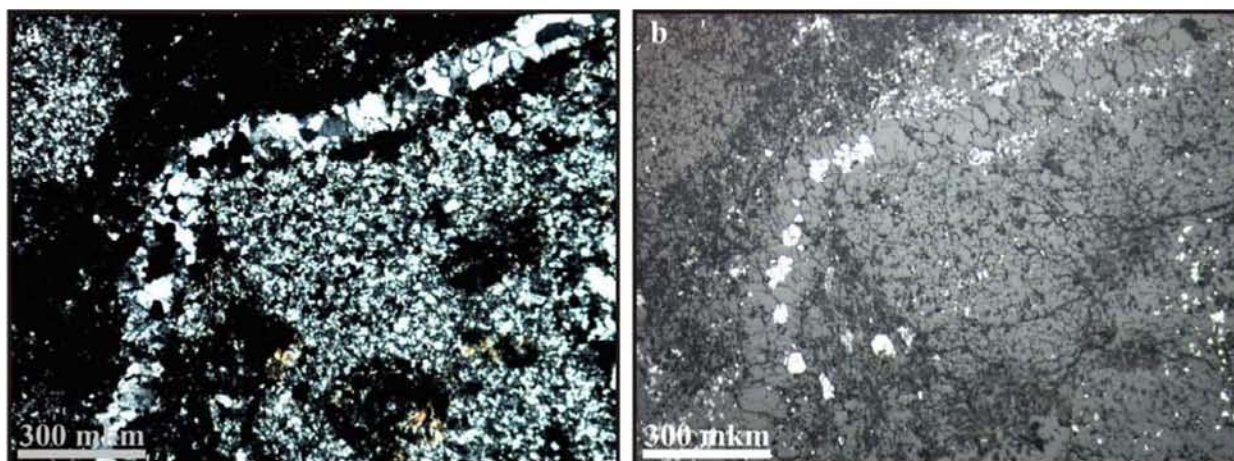


Figure 2.1.3.9. Late quartz-sulphide veinlet cutting silicified marble of the Mramornaya Gora ore-showing. Sample MG-5, thick section optical photos: a – polarized transmitted light, b – reflected light.

On the outcrop, uranium mineralization was observed in different carbonate rock types. The most uranium-enriched rocks are the dolomitic marbles, calcitic ones being less radioactive. The highest grade uranium mineralization is localized in oxidized spots corresponding to sulphide enrichment (fig. 2.1.3.10). Veins of mafic rocks and zones of silicification are poor in uranium.



Figure 2.1.3.10. High-radioactive spot (over 1300 $\mu\text{R/h}$) in brecciated marbles associated with local enrichment in oxidized sulphides; the Mramornaya Gora ore-showing.

Ore bodies.

The Mramornaya Gora ore showing comprises 40 ore bodies with cut-off 100 ppm U. They are conformable with hosting carbonates. Ore bodies are lens-like shaped, 38-250 m long, average thickness is 4 m (up to 7.8 m). They are followed by drilling down to -295 m. The largest ore bodies are localized in vicinity of the carbonate layer roof. U ores are of low-grade layered and highest grade breccias types (fig 2.1.3.11). First ones are more widespread.

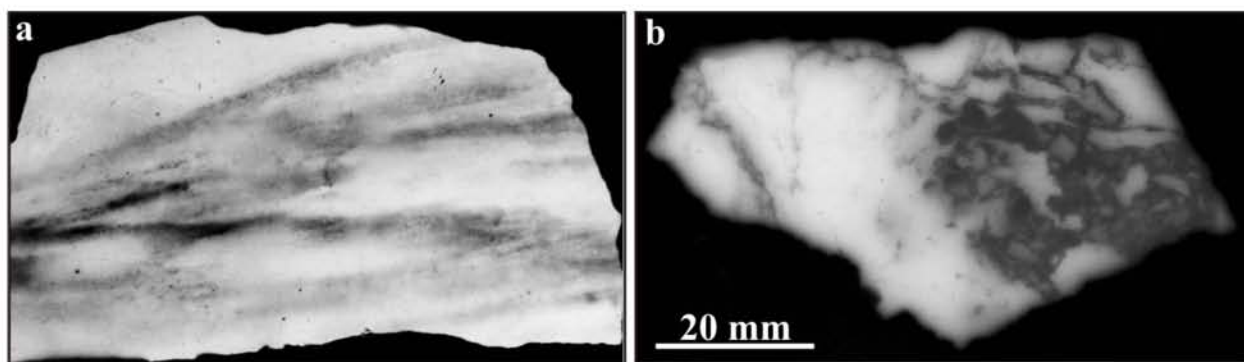


Figure 2.1.3.11. Different texture types of uranium ore of the Mramornaya Gora ore-showing: a - low-grade layered type (from Andersson, 1990); b – high-grade breccias type.

U ores are associated with high P content concentrated in apatite. Apatite content in the ore-hosting marbles is 1520 ppm in average (up to 130 000 ppm). P content is 14 000-55 000

ppm. U associated apatite has high F content (0.59-0.62 wt %), Zr, Pb, Cu, Yt, Ba, Be, Yb, U (up to 0.1 wt %) (Grigorieva, 1977).

Also brecciated ore-hosting dolomites have increased contents of Fe up to 80 000 ppm, Ba – up to 20 000 ppm, Sr – up to 3000 ppm, Ni – 1000 ppm, Zn – 500 ppm, V – 200 ppm, Mo – 200 ppm, (Gromov et al., 1981; Rybakov and Golubev, 1999).

U ores of the Mramornaya Gora ore-showing are characterized by significant radioactive disequilibrium – from 82 to 139 %, with a tendency of Ra enrichment upward to the surface (Gromov et al., 1981).

U resource of the Mramornaya Gora ore-showing is evaluated to about 136 tons with a cut-off 500 ppm and about 400 t with cut-off of 100 ppm.

Uranium mineralization.

Uranium mineralization of the Mramornaya Gora ore-showing is complex. Previous works show that the earliest uranium mineralization is represented by thin impregnations and chained aggregates of uraninite, less by U-bearing apatite (Nemtsov S.N. et al, 1954; Grigorieva, 1977). Idiomorphic uraninite is associated with graphite, sulphides and apatite (fig. 2.1.3.12).

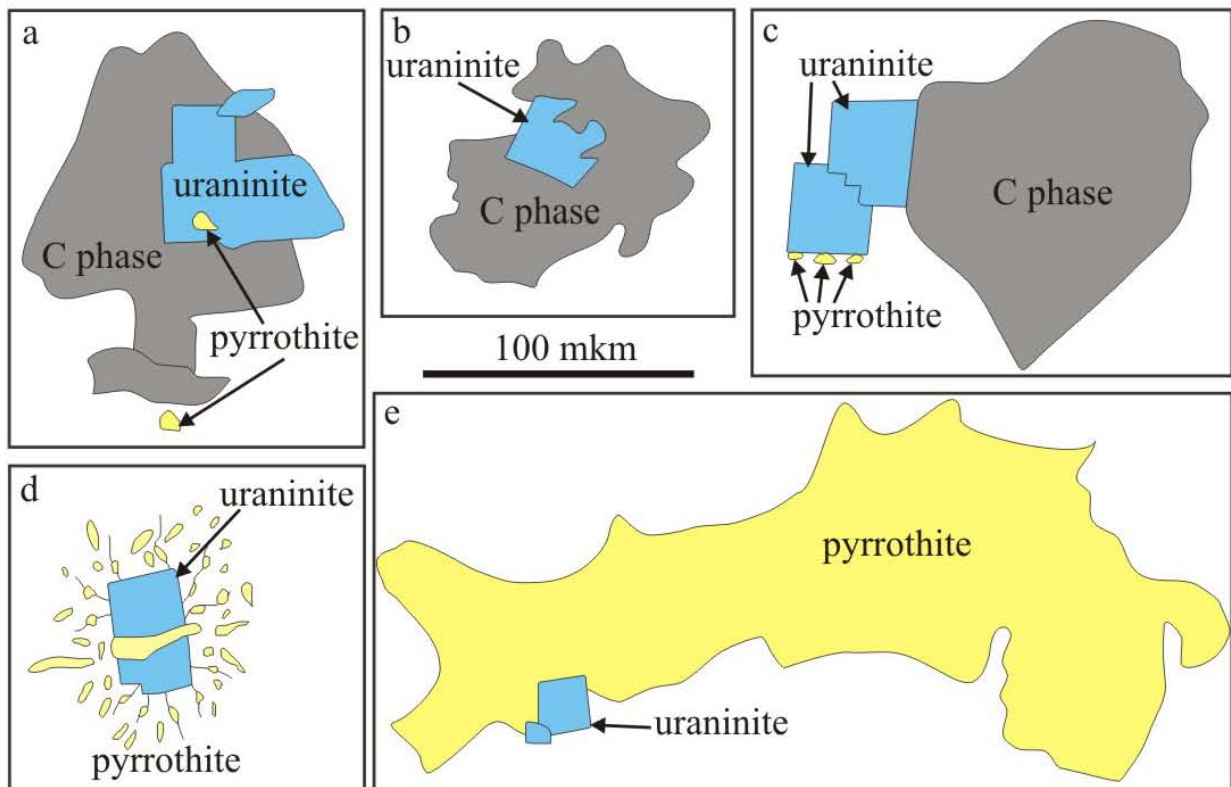


Figure 2.1.3.12. Uraninite mineralization associated with carbonaceous phase (C phase) and different generations of pyrrhotite in the Mramornaya Gora ore-showing (compiled after Nemtsov et al., 1954).

The uraninite mineralization is disseminated and in the samples taken during field work for this thesis it has not been recognized. Only pitchblende was identified in the brecciated marble samples. Autoradiographies of these samples have revealed two types of U distribution in these rocks (fig. 2.1.3.13).

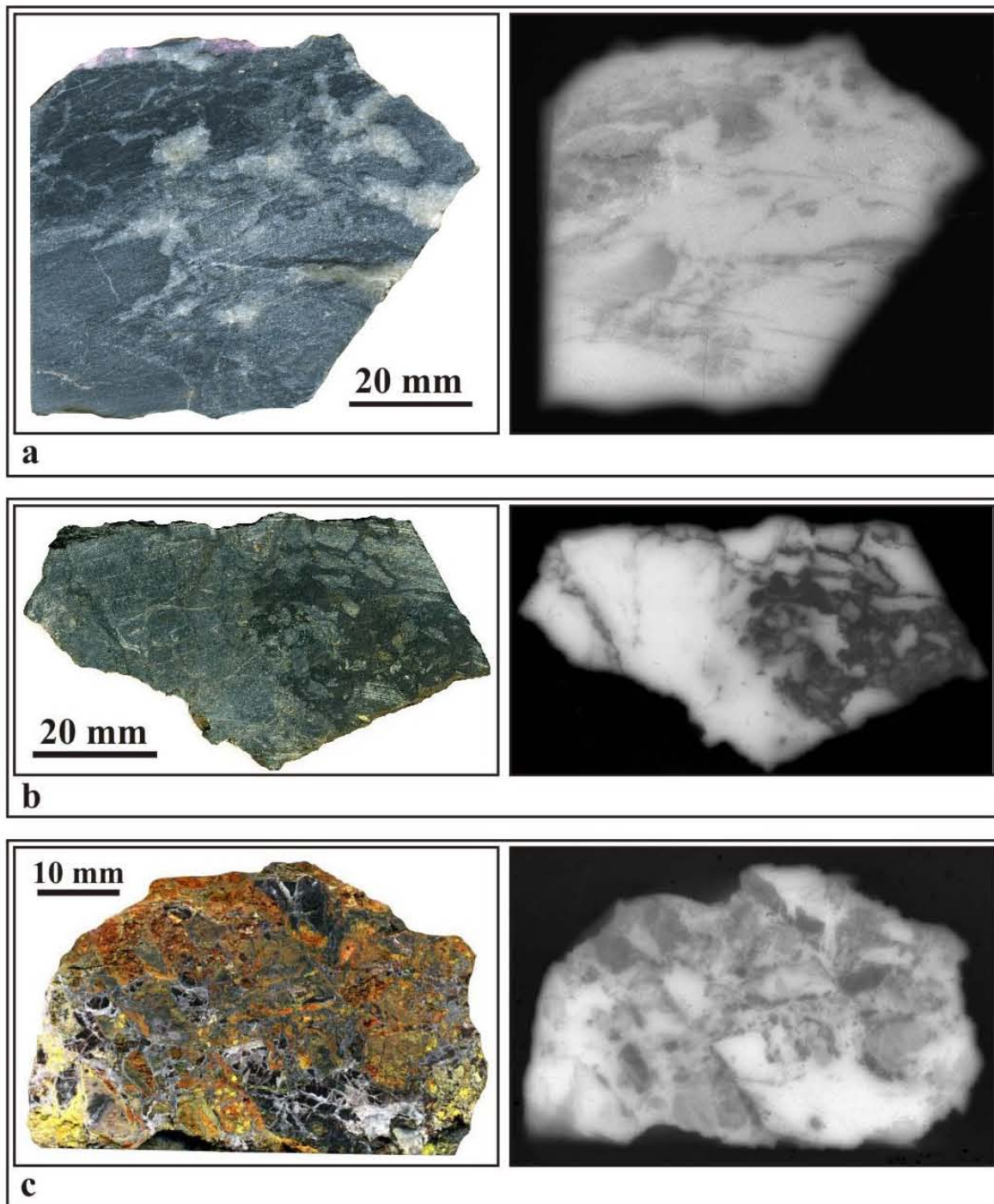


Figure 2.1.3.13. Diverse distribution of uranium mineralization in the brecciated marbles of the Mramornaya Gora ore-showing, samples (left column) and corresponding autoradiographies (right column): a – sample MG-7, uranium concentrated in the dolomite fragments (autoradiography – 14 days); b (sample MG-6) and c (sample MG-10) – uranium concentrated in a cement of the breccias (autoradiographies – 3 days).

In the first one (fig. 2.1.3.13a) the low-grade radioactive mineralization occurs in dolomite fragments and is absent in the calcite cement; it is represented by disseminated pitchblende-1 associated with apatite, amorphous carbonaceous phase and sulphides (fig. 2.1.3.14 and 2.1.3.15). This pitchblende may develop after earlier uraninite. It is characterized by high Pb content (General Appendix 2.3, table 8).

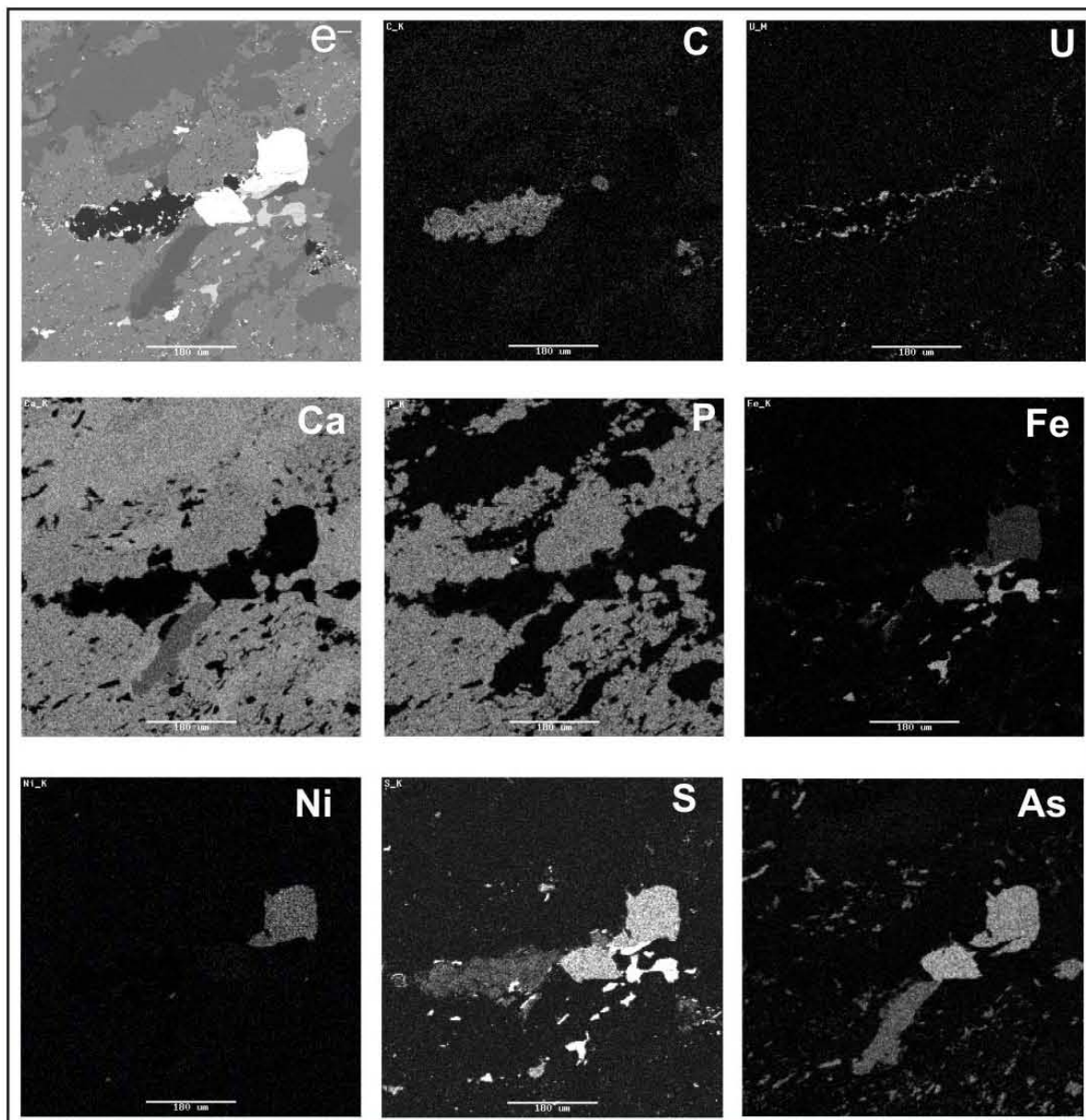


Figure 2.1.3.14. Characteristic spectrum photos of the Mramornaya Gora ore-showing early uranium mineralization associated with apatite, carbonaceous phase, sulphides and arsenides; sample MG-1, scale – 100 µm.

In the second type the cement is more enriched in U than the fragments (fig 2.1.3.13b), when they are irregular and angular (fig. 2.1.3.16) and related rather to brittle deformations than to a regional metamorphic event.

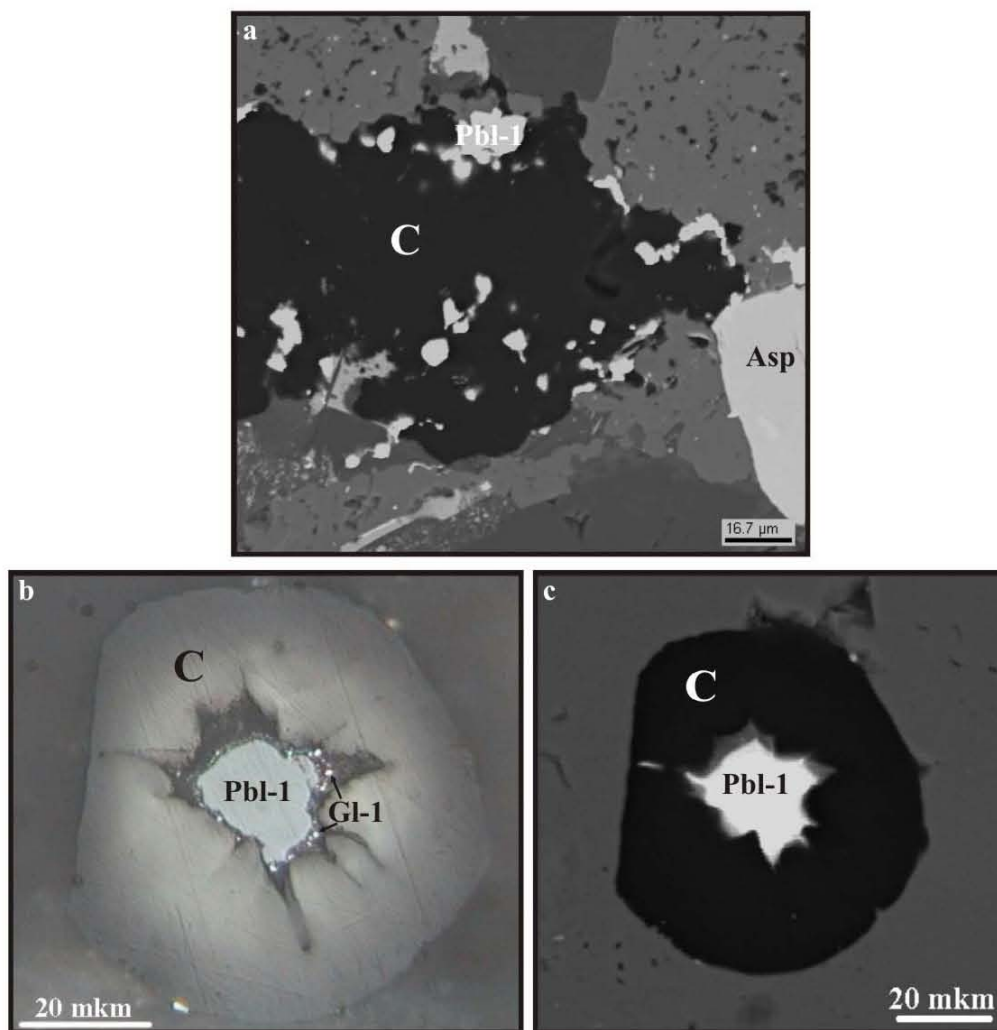


Figure 2.1.3.15. Early pitchblende (Pbl-1) from the Mramornaya Gora ore-showing associated with carbonaceous phase (C), sample MG-1: a – pitchblende develops on the periphery and inside of amorphous carbonaceous phase; arsenopyrite (Asp) occurs (BSE photo); b and c – pitchblende enveloped by colloform carbonaceous phase; early galena (Gl-1) develops on the periphery of the pitchblende (b – optical photo, reflected light; c – BSE photo).

Uranium mineralization of this type is composed of several varieties of pitchblende:

1. disseminated impregnation of pitchblende spherulites with cores replaced by coffinite (fig. 2.1.3.17a) (up to 40 % of the preparation);
2. aggregates of pitchblende spherulites rich in gangue inclusions (fig. 2.1.3.17b);
3. pitchblende spherulites overgrowths on gangue fragments (fig. 2.1.3.17c);
4. aggregates of pitchblende spherulites developing after rutile (fig. 2.1.3.17d);
5. pitchblende spherulites veinlets cutting earlier non-radioactive ore (fig. 2.1.3.17e);
6. veinlets of chained aggregates of large (up to 200 μm) massive pitchblende spherulites cutting pitchblende mineralization rich in gangue inclusions (fig. 2.1.3.17f).

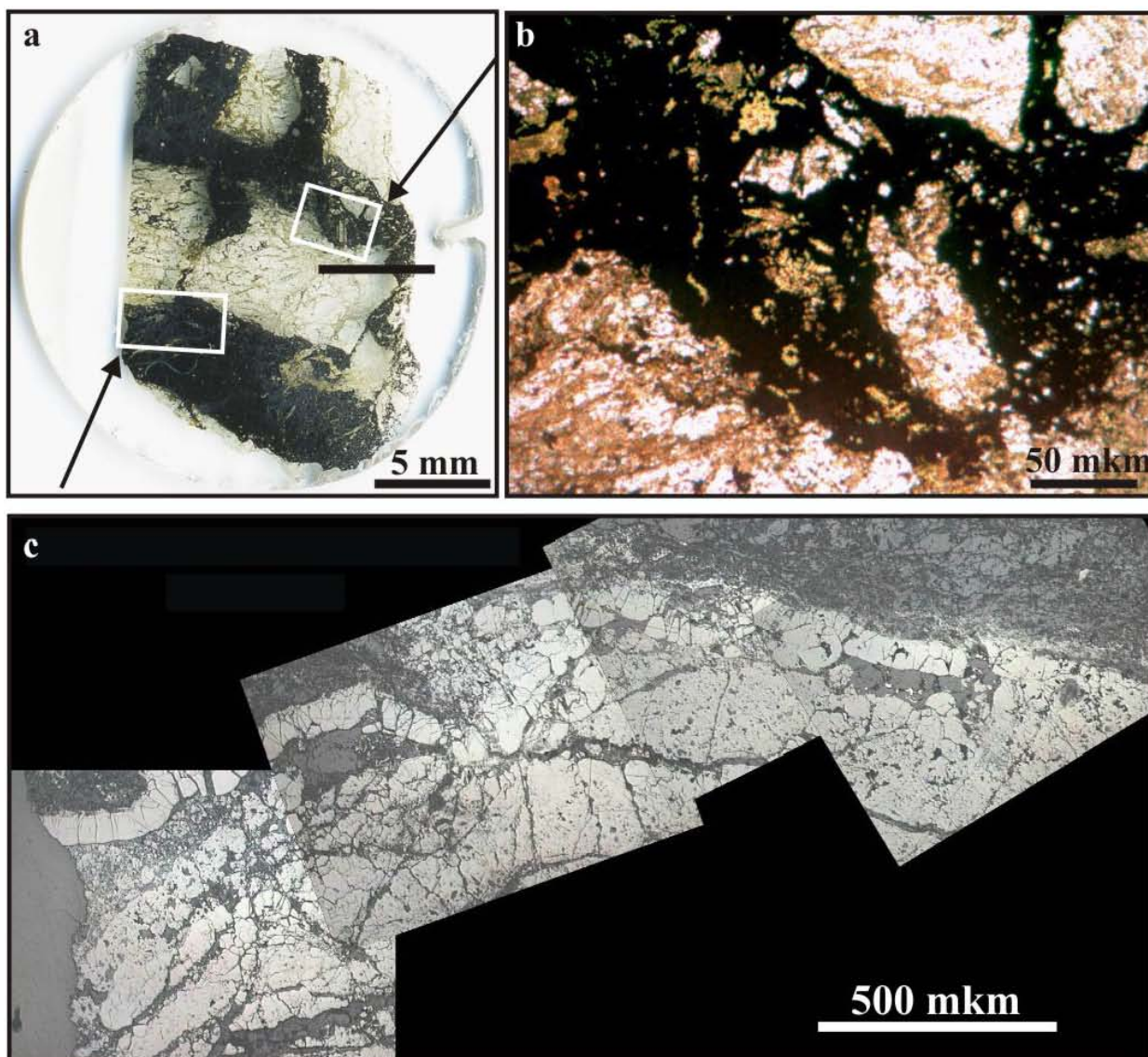


Figure 2.1.3.16. Uranium-bearing cement of late breccias from the Mramornaya Gora ore-showing; sample MG-6: a – macro photo of the thick section, fields of b and c images are outlined; b – optical photo, transmitted plain light; c – combination of optical photos, reflected light.

All of above-listed pitchblende types except the last one are characterized by strongly heterogeneous structure (fig. 2.1.3.18). Many of them have more complex composition compared to chained pitchblende of the 6th variety (General Appendix 2.3, table 8, General Appendix 2.4, table 4 and table 5). Nevertheless, most of them have relatively low Pb contents, corresponding to rather young ages. Only in some grains Pb content is high. It can be explained by strong reworking of the tectonized zones with replacement of older pitchblende generations by younger ones. This process was not studied enough to separate surely these generations, that is why all these phases have been combined under the name “pitchblende-2”.

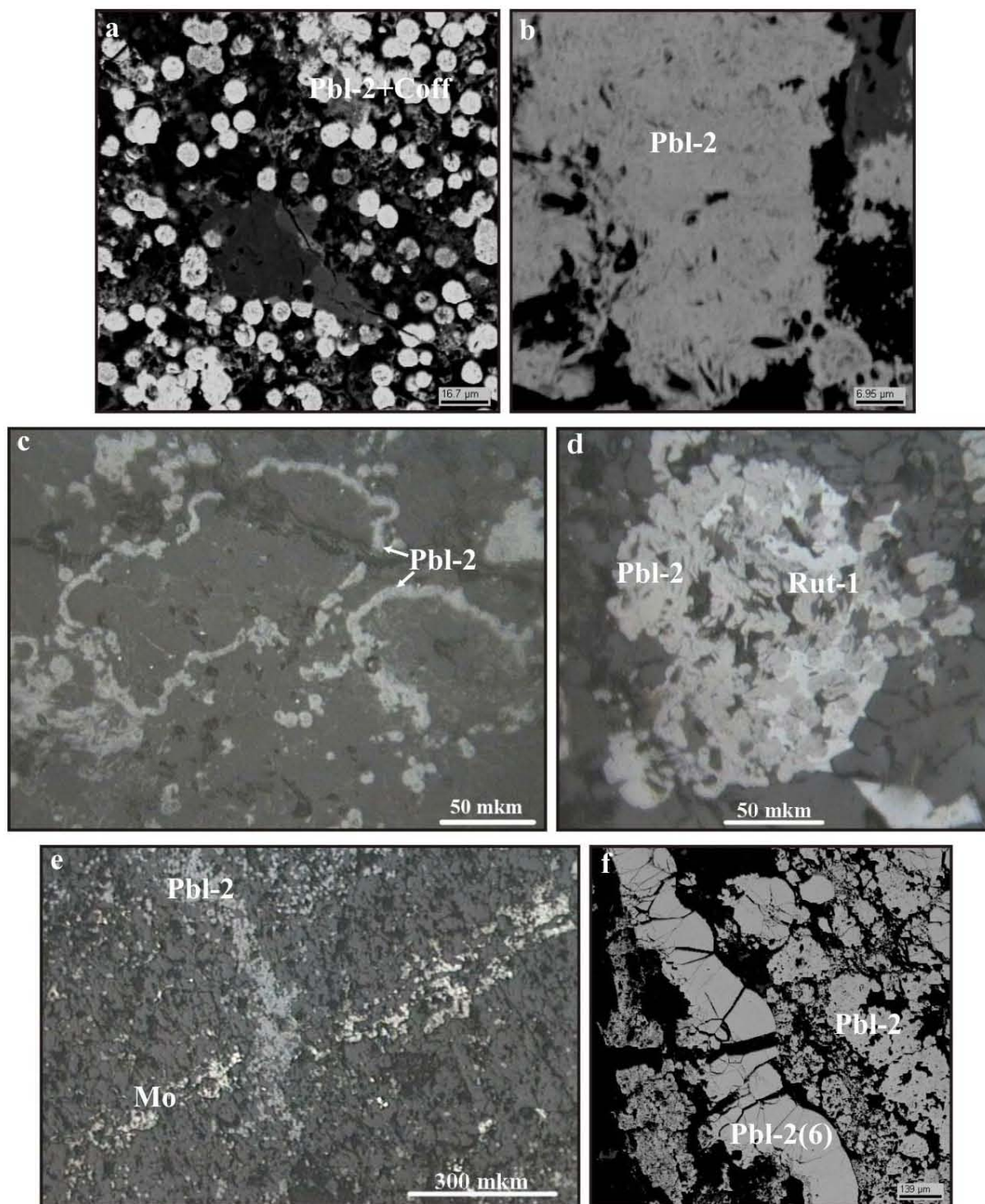


Figure 2.1.3.17. Different types of late pitchblende (Pbl-2) from the Mramornaya Gora ore showing: a – disseminated pitchblende (sample MG-5, BSE photo); b – aggregate of pitchblende spherulites with gangue inclusions (sample MG-5, BSE photo); c – pitchblende spherulites overgrowing gangue fragments of quartz-chlorite-mica aggregate (sample MG-5, optical photo, reflected light); d – aggregates of pitchblende spherulites developing after early rutile (sample MG-5, optical photo, reflected light); e – veinlet composed of pitchblende spherulites cutting early non-radioactive ore mineralization (sample MG-5, optical photo, reflected light); f – veinlets of chained aggregates of late pitchblende (Pbl-2(6)) cutting mineralization of pitchblende saturated with gangue inclusions (sample MG-6, BSE photo).

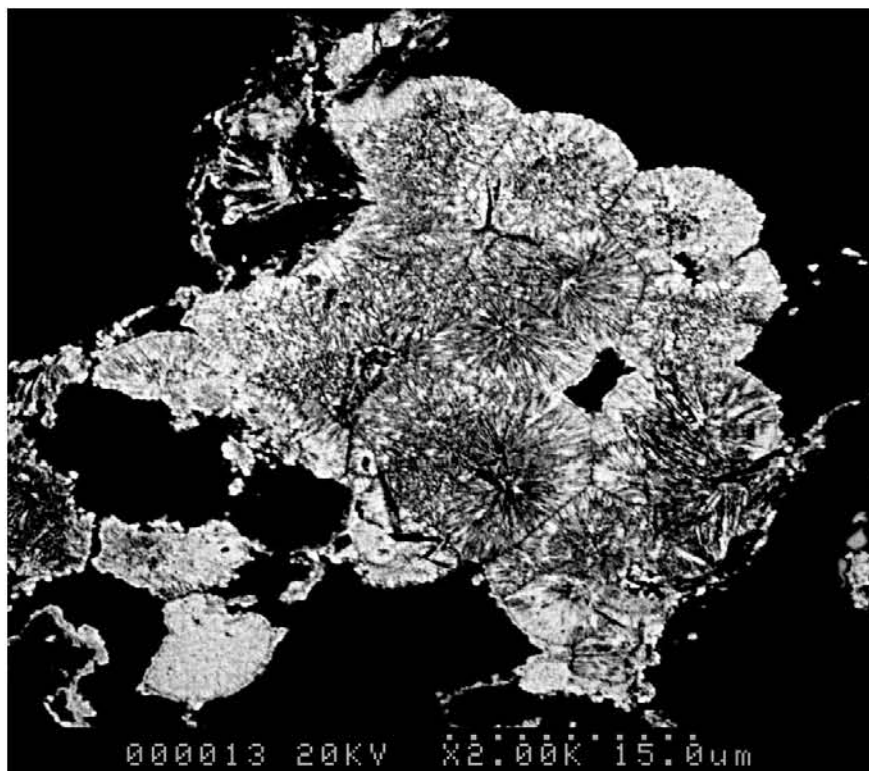


Figure 2.1.3.18. Heterogeneous structure of the pitchblende-2 spherulites from the Mramornaya Gora ore-showing. Sample MG-1, BSE photo.

Ore mineral paragenesis in the samples from the Mramornaya Gora ore-showing is presented in the Table 2.1.3.1.

Because of small size and heterogeneous structure most of the pitchblendes in the Mramornaya Gora ore-showing, isotopic researches are very difficult. Previous works obtained a Svecofennian age about 1850 Ma was obtained (see Table 2.1.3.2. at the end of the Paragraph). For U-thuicolite from the similar Nuottajärvi deposit in Finland an isotopic U-Pb age of 1897 ± 7 Ma was obtained (Vaasjoki et al., 1980). During this study only successful age determination was for more “fresh” variety 6 of pitchblende-2. A U-Pb isotopic age of 397 ± 19 Ma was yielded (fig. 2.1.3.19).

For the same points in the pitchblende an analysis of REE content was undertaken (fig. 2.1.3.20 and table 3 of General Appendix 2.7). REE contents are relatively low and the chondrite-normalized pattern is weakly fractionated with some LREE gap from Ce to Nd (contents of Pm, Gd and Yb have not been obtained because of technical problems occurred during the analyses). The pattern is differentiated from ones obtained for all well studied examples of uranium oxides from different uranium deposits (Bonhoure, 2007).

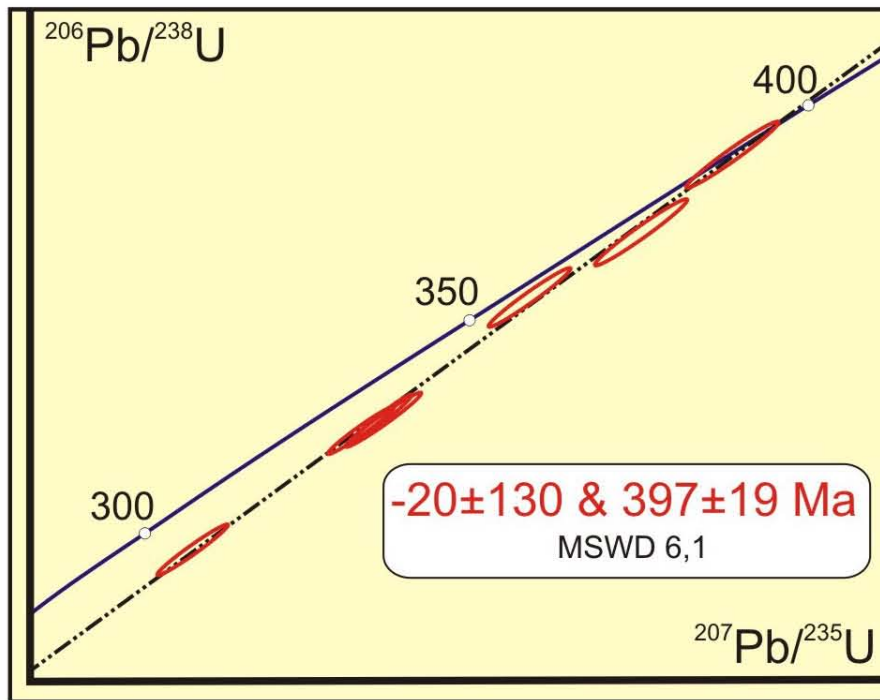


Figure 2.1.3.19. Concordia diagram for late pitchblende from the Mramornaya Gora ore-showing; sample MG-6.



Figure 2.1.3.20. Pattern of chondrite-normalized REE contents in uraninite from the Sjuskinsaari area; sample MG-6.

Table 2.1.3.1. Ore mineral paragenesis of the Mramornaya Gora ore-showing
(Polekhovsky et al., 2007).

No	Minerals	Paragenesis						
		Of rock	Sulphide-arsenide	Sulphide	U-1 (early)	U-2 (late)	Low-temperature	Hypergene
1	Rutile-1	+						
2	Titanite	+						
3	Arsenopyrite		+					
4	Pyrite-1		+					
5	Gersdorffite		+					
6	Pyrrhotite-1			+				
7	Pentlandite			+				
8	Sphalerite			+				
9	Chalcopyrite			+				
10	Molybdenite			+				
11	Carbonaceous phase				+			
12	Mo phase				+			
13	Pitchblende-1				+			
14	Galena-1				+			
15	Pyrrhotite-2				+			
16	Pyrite-2				+			
17	Ti-U phase					+		
18	Pitchblende-2					+		
19	Galena-2					+		
20	Galena-3					+		
21	Pyrite-3						+	
22	Marcasite						+	
23	Rutile-2						+	
24	Coffinite						+	
25	Hydrohematite							+
26	Leucoxene							+
27	Uranophane							+
28	Curite							+
29	Demesmaeckerite							+

Besides of uranium oxides, uranium mineralization of the Mramornaya Gora ore-showing is also represented as much subordinated coffinite and Ti-U phase. Coffinite develops after pitchblende (fig. 2.1.3.21), also in late calcite veinlets (fig. 2.1.3.22). The Ti-U phase occurs in areas where rutile is replaced by pitchblende-2 (fig. 2.1.3.23). Development of rutile-2 after pitchblende-2 was observed (fig. 2.1.3.24).

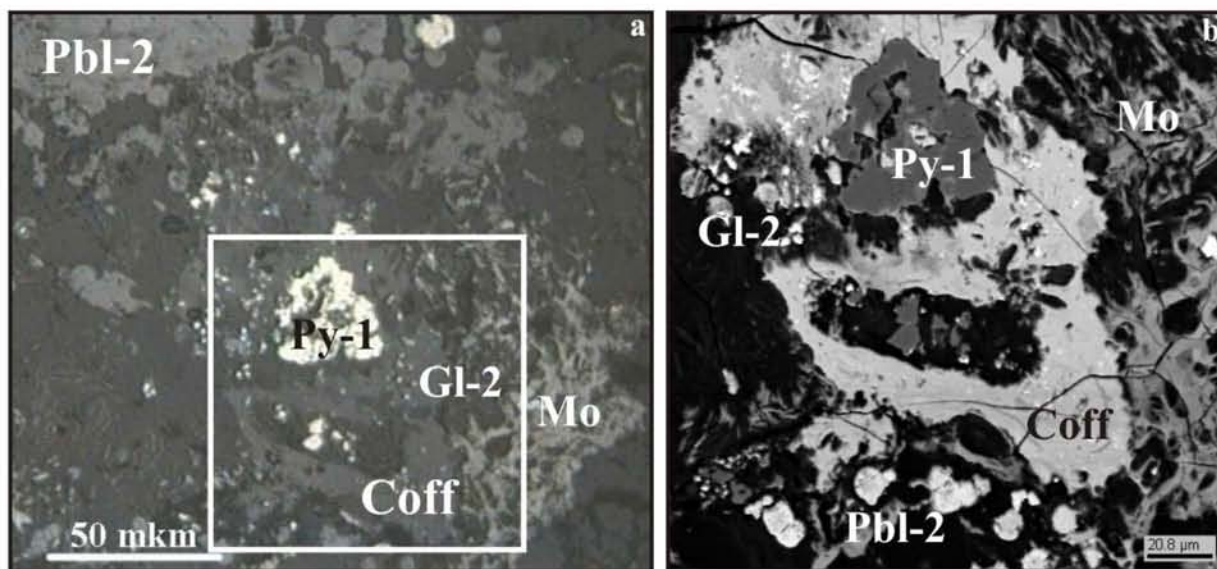


Figure 2.1.3.21. Coffinite (Coff) replacing pitchblende-2 (Pbl-2); pyrite (Py-1), galena (Gl-2); Mo-phase (Mo) occur, sample MG-5; a – optical photo, reflected light, image b area is outlined; b – BSE photo.

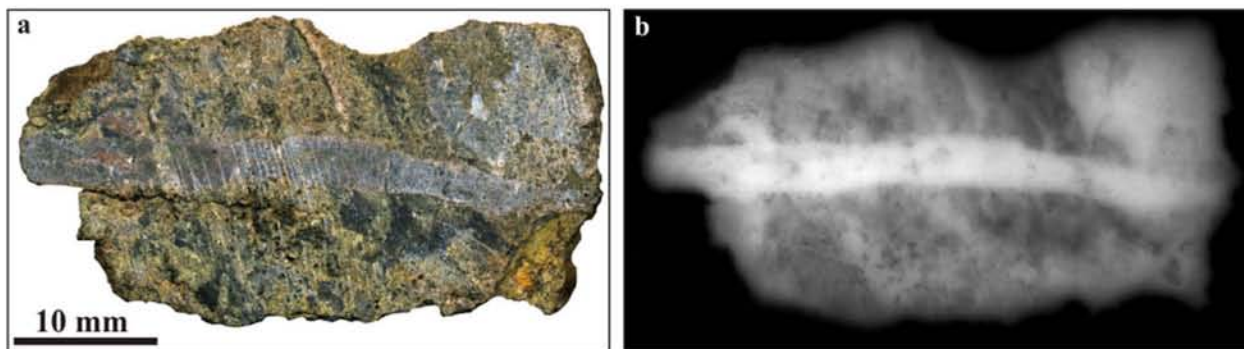


Figure 2.1.3.22. Late calcite veinlet with coffinite mineralization cutting early pitchblende ores in the Mramornaya Gora ore-showing; sample MG-29.

Hexavalent U minerals: uranophane $\text{Ca}(\text{UO}_2)_2(\text{SiO}_3\text{OH})_2 \times 5\text{H}_2\text{O}$, curite $\text{Pb}_3(\text{UO}_2)_8\text{O}_8(\text{OH})_6 \times 3\text{H}_2\text{O}$ and demesmaekerite $\text{Pb}_2\text{Cu}_5(\text{SeO}_3)_6(\text{UO}_2)_2(\text{OH})_6 \times 2(\text{H}_2\text{O})$ were recognized by X-ray diffraction (Polekhovsky et al., 2007).

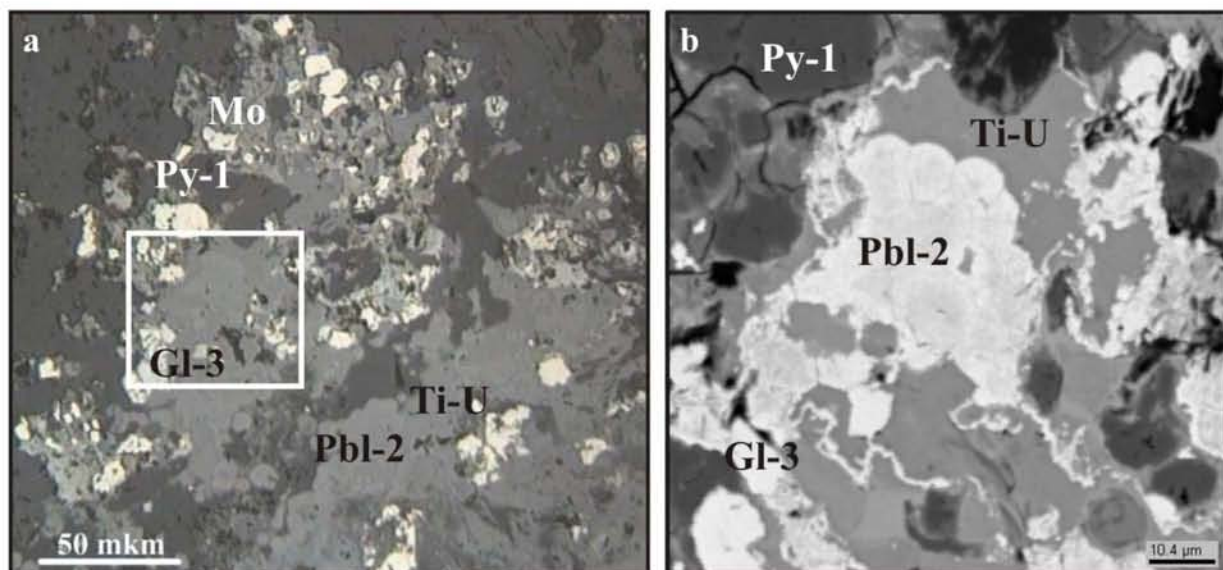


Figure 2.1.3.23. Development of pitchblende-2 (Pbl-2) after rutile-1 with forming of intermediate cryptocrystalline Ti-U phase (Ti-U); early pyrite-1 (Py-1), Mo phase (Mo) and galena (Gl-3) occurs; sample MG-5, a – optical photo, reflected light, image b area is outlined; b – BSE photo.

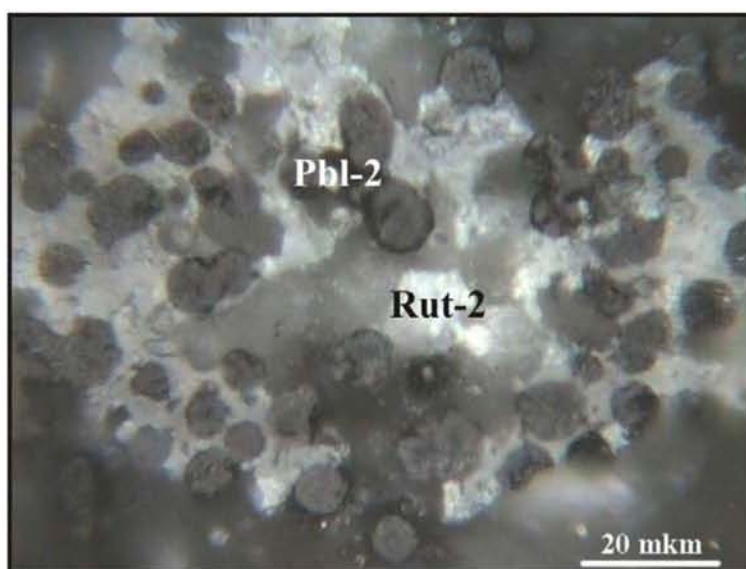


Figure 2.1.3.24. Development of late rutile (Rut-2) after pitchblende-2 (Pbl-2); sample MG-5, optical photo, reflected light.

1.2. The Ruskeala group of uranium ore-showings.

The Ruskeala area is located at the NW closure of the Ruskeala anticline (fig. 2.1.3.25). The basement is composed of Ludicovian Pitkjaranta suite marbles, skarnoids, carbonate tremolite-actinolite and mica-amphibole schists. They are enveloped by Kalevian Ladoga group mica schist and quartzites. All rocks are cut by small dykes of metadiabases and granodiorites. Quartz and quartz-carbonate veins are also widespread.

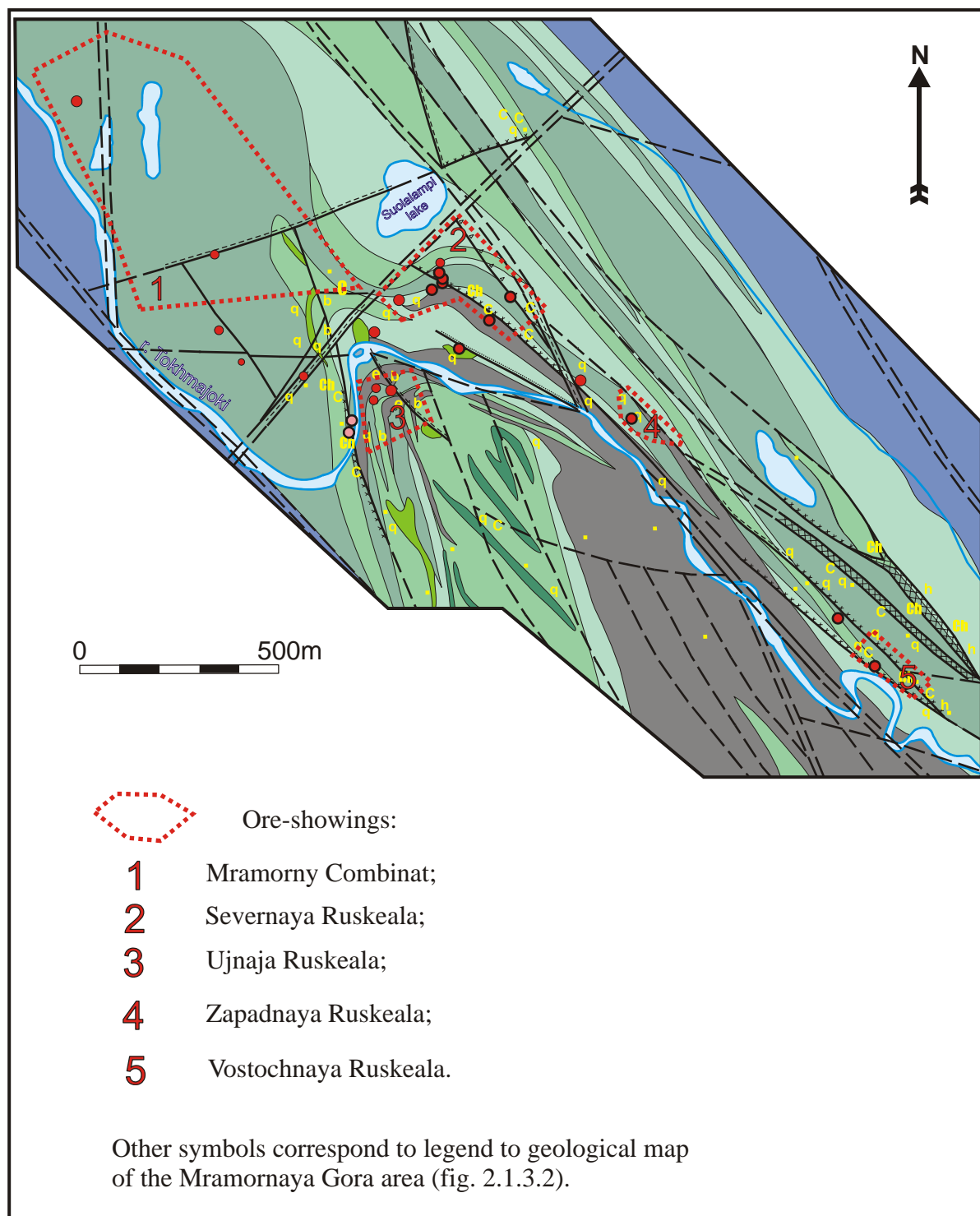


Figure 2.1.3.25. Geological map of the Ruskeala area (after Gromov et al., 1981).

The metamorphic formations mainly strike NW 310-320°, dip 70-85° SW. In the area of the anticline closure, undulations striking 270-280° and dipping 50-70° were observed. Second-order folds are widespread in the limbs of the anticline.

The specific feature of the geological structure of the Ruskeala area is an increased

thickness of the upper carbonate layer of the Pitkjaranta suite in the curvature of the anticline. Here this layer is composed of interbedded marbles, carbonate and mica-amphibole schists. Its thickness is up to 1.5 km; total thickness of pure marble layers is up to 600 m. Several marble quarries are in exploitation since the XIXth century in the Ruskeala area (fig. 2.1.3.26).



Figure 2.1.3.26. Folded marbles in a quarry of the Ruskeala area.

Several U ore-showings compose the Ruskeala ore district: Mramorny Kombinat, Ujnaya Ruskeala, Severnaya Ruskeala, Vostochnaya Ruskeala and Zapadnaya Ruskeala. They were discovered by “Nevskgeologia” during exploration work of the fifties and 1977-1981. Very locally outcropping zones in the Ujnaya Ruskeala and Severnaya Ruskeala ore-showings were visited and sampled during the field work for this thesis.

Uranium mineralization is richer in fine-grained gray marbles and carbonate-tremolite schists of the upper carbonate horizon of the Pitkjaranta suite. Skarnoids are relatively depleted in U. Layered distribution of U mineralization prevails. Mineralized layers are conformably folded with the host rocks (fig. 2.1.3.27a). Like at Mramornaya Gora, two types of U mineralization distribution occur in brecciated marbles: an early mineralization concentrated in dolomitic fragments and absent in calcite cement; whereas in late tectonites the cement contains uranium (fig. 2.1.3.27 b and c).

Over 50 U ore beds with size up to 170×80×25 m are known in the Ruskeala area. They are composed of complex shape lenses up to 5×4×3.5 m conformable to the host rocks. Average U content is 570 ppm over 1.2 m, up to 1350 ppm. Th content is up to 20 ppm.

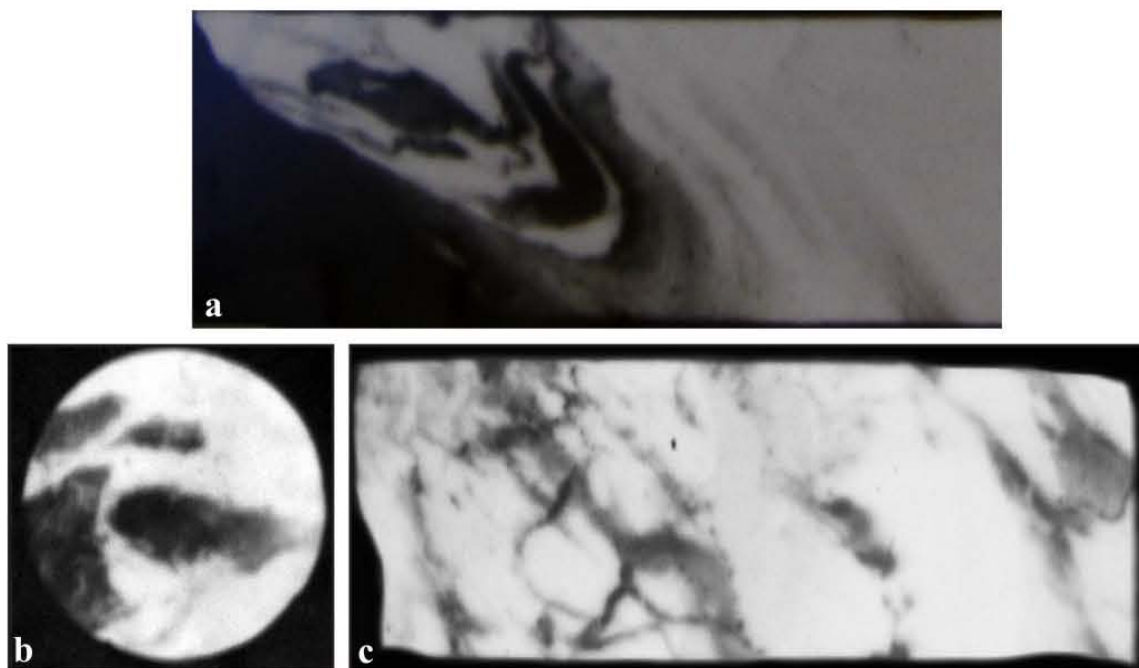


Figure 2.1.3.27. Autoradiographies of drill core samples with U mineralized rocks from the Severnaya Ruskeala U ore-showing (5 days exposition, from Gromov et al., 1981): a – U mineralization conformably folded with host carbonate rock; b – brecciated carbonate rock with U mineralization concentrated in the fragments; c – brecciated carbonate rock with U mineralization concentrated in the cement.

Total uranium resource of the Ruskeala ore-showings is about 600 tons with a 300 ppm cut-off. Radioactive equilibrium in the ore-showings varies from 85 to 201 % with radium enrichment at the surface (Gromov et al., 1981).

U mineralized rocks are enriched in P (up to 70 000 ppm), Pb (100-4 000 ppm), Mo (300 ppm), Ba (15 000-30 000 ppm), Be (10 ppm), La (100 ppm), Ni (700-1500 ppm), Ti (10 000 ppm), Fe (150 000 ppm).

Previous researchers observed rounded uraninite (possibly they meant pitchblende) and U-bearing apatite as a principal U mineral phases of the Ruskeala ore-showings. The U mineralization is associated with apatite, pyrite, pyrrhotite, sphalerite, chalcopyrite, molybdenite, ilmenite and graphite (Nemtsov et al., 1954; Gromov et al., 1981).

In samples obtained during a field trip U mineralization occurs as pitchblende. The most common association is pitchblende with titanite and rutile, less with graphite and sulphides.

Indications of late hydrothermal U redistribution have been discovered in the Ruskeala ore-showings by previous exploration (Nemtsov et al., 1954; Gromov et al., 1981). Few

anomalies with U content up to 360 ppm occur in fractures in pink-colored marbles in the Mramorny Kombinat ore-showing. U-Pb ages of pitchblende from these fractures are 1221 ± 64 Ma (Anderson, 1990). Mineralized veinlets cutting all formations including early U mineralization occur in the Severnaya Ruskeala ore-showing as well (Gromov et al. 1981). Unfortunately, this mineralization is no more available from the surface.

1.3. The Impilakhti group of uranium ore-showings.

U-P mineralization in the Impilakhti area on the south-eastern continuation of the Ruskeala fault zone was discovered by “Nevskgeologia” in the beginning of fifties. One prospecting shaft, 10 drillholes and few trenches have been realized.

The Impilakhti group of U ore-showings is composed of Centralno-Impilakhtinskoye and Vostochno-Impilakhtinskoye showings localized in the carbonate formations of the Pitkjaranta suite enveloping the Impilakhti granite-gneiss dome (Appendix to Chapter 1, fig.1). The first one is located on northern slope of the dome, whereas the second one on its eastern slope.

The ore-showings are hosted by tremolite-pyroxene carbonate schist and pyroxene skarnoid of the upper carbonate horizon of the Pitkjaranta suite. Here, the thickness of the horizon is 10-15 m. In the Centralno-Impilakhtinskoye showing its strike is sublatitudinal (80-90°), in the Vostochno-Impilakhtinskoye showing its strike is submeridional (345-355°).

U mineralization is concentrated in 5-10 m long and 0.1-1.1 m thick lenses conformable to the host rocks (fig. 2.1.3.28 and 2.1.3.29).

In the Centralno-Impilakhtinskoye ore-showing two parallel mineralized zones can be followed over 175 m and to depth of 95 m (fig 2.1.3.30). One zone 0.25-1.1 m thick is located in the upper part of the carbonate horizon, another one 0.3-0.4 m thick occur in median part. U-bearing layers are displaced of 3 m by a sinistral fault striking N-S. Some radioactive anomalies up to 1500 $\mu\text{R/h}$, hosted by granite-gneiss of the Impilakhti dome, are related to fracture zone on the southern continuation of the fault (Grigorieva, 1977).

The Vostochno-Impilakhtinskoye ore-showing comprises three separated mineralized zone. They have a cumulated extension of 417.5 m and were followed down to 115 m. U mineralization is very low-grade, average U content is 250 ppm, maximum 740 ppm. The mineralized rocks are also enriched in Fe – up to 100 000 ppm



Figure 2.1.3.28. Outcropped U-mineralized tremolite-pyroxene-carbonate rocks in the Centralno-Impilakhtinskoye ore-showing.

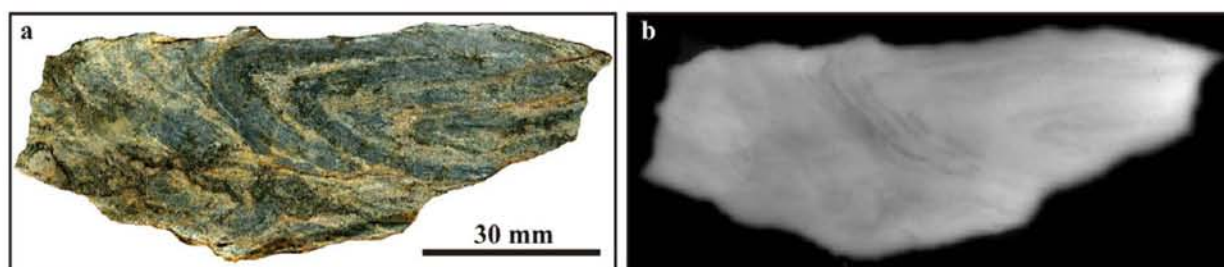


Figure 2.1.3.29. Tremolite-pyroxene-carbonate rocks from the Centralno-Impilakhtinskoye ore-showing and its autoradiography (20 days exposition). Concordant folding of U mineralized layers can be observed. Sample VI-3.

According to previous studies uranium ores are formed by small crystals (up to 0.02 mm) of uraninite always associated with apatite (Sukhanova, 1952). Uraninite is included in crystals of pyroxene and apatite, rarely plagioclase, exceptionally in phlogopite, carbonate and ore minerals. It occurs in fractures or between the minerals.

In the samples obtained during field work for this thesis pitchblende was recognized, but not uraninite. It forms separated spherulites, aggregates are associated with a carbonaceous phase, titanite, rutile and sulphides (fig. 2.1.3.31). Chemical composition of pitchblende from the Centralno-Impilakhtinskoye showing is presented in the General Appendix 2.3, table 9.

Development of coffinite after pitchblende occurs locally.

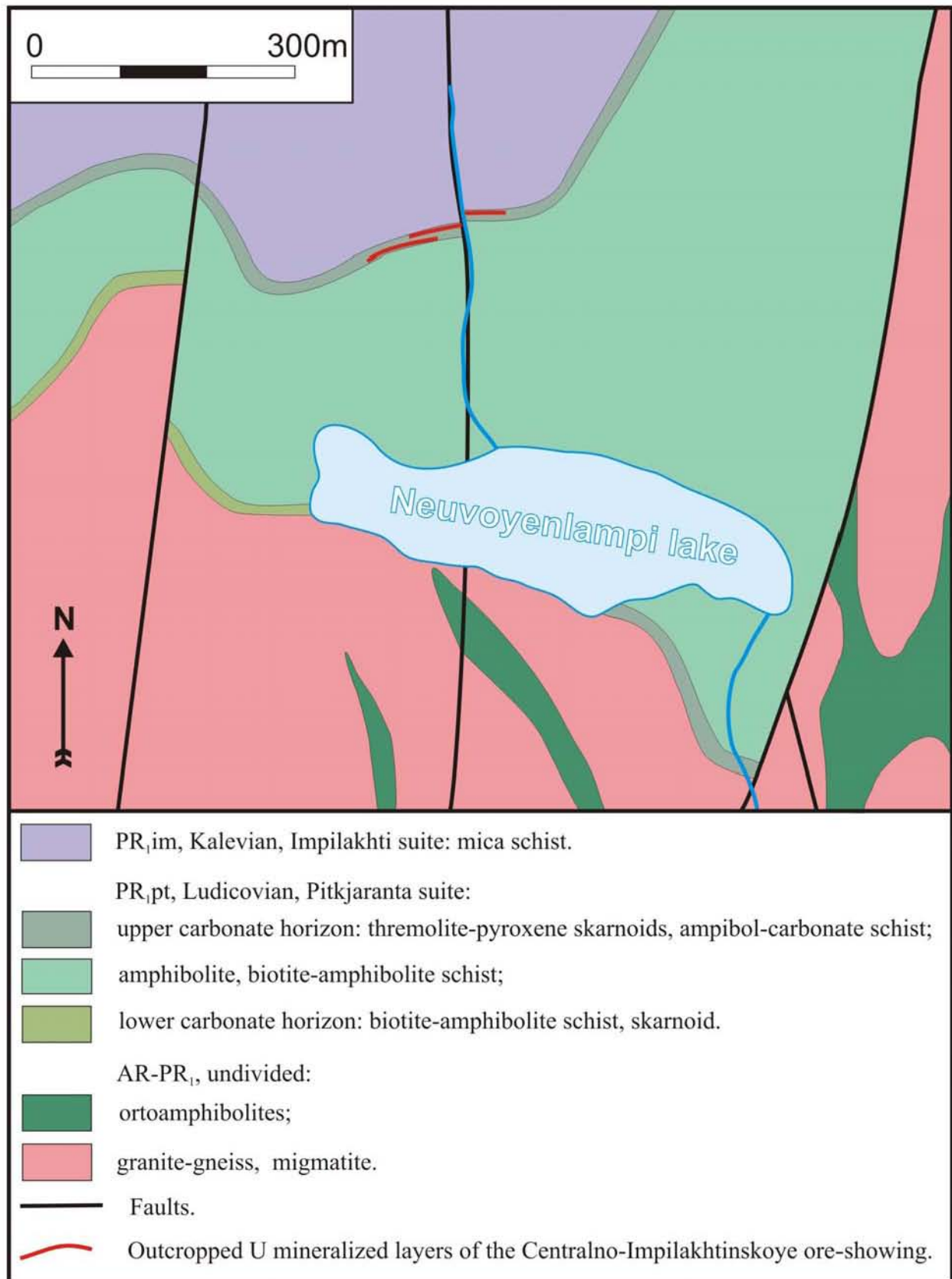


Figure 2.1.3.30. Geological map of the Centralno-Impilakhtinskoye ore-showing area (after Korotaev et al., 1978).

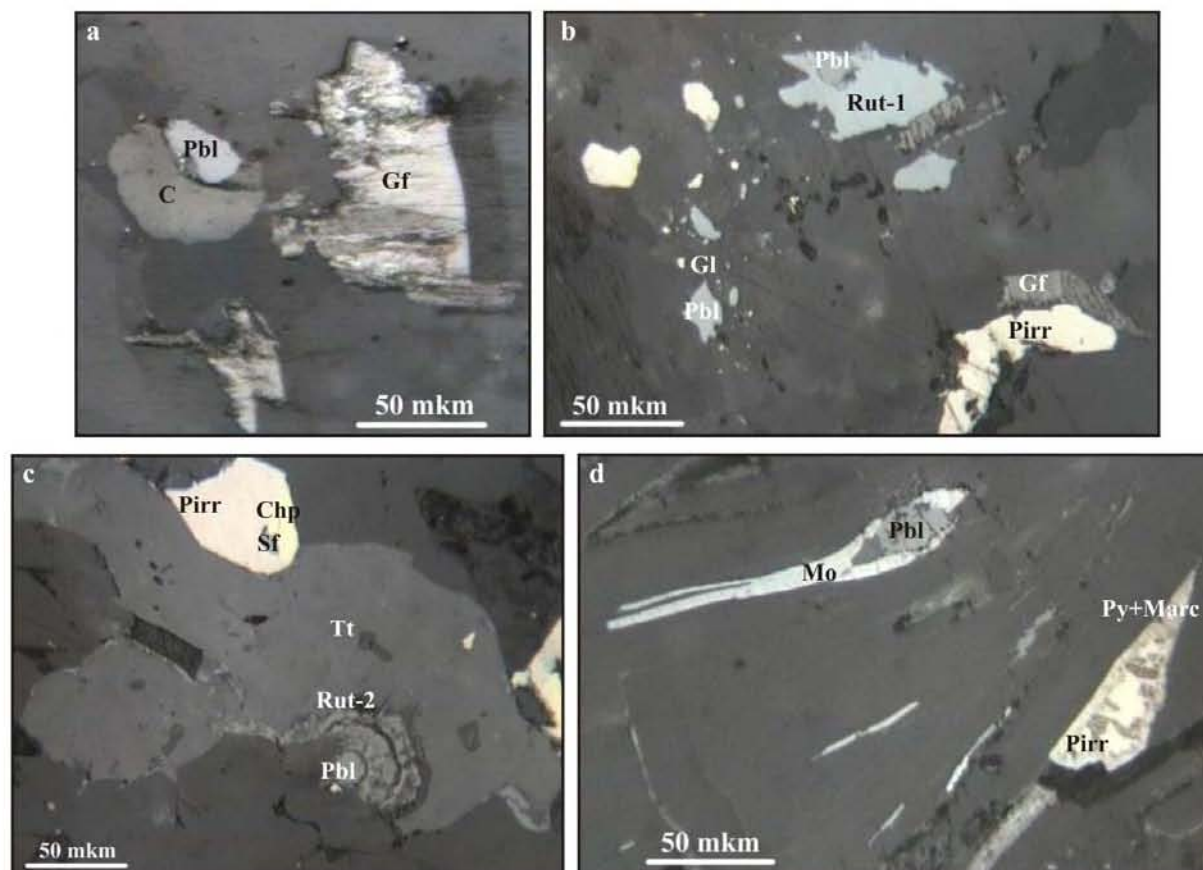


Figure 2.1.3.31. Pitchblende (Pbl) mineralization from the Vostochno-Impilakhtinskoye ore-showing, optical photos, reflected light: a – sample VI-1, pitchblende associated with carbonaceous phase (C), deformed graphite (Gf) occurs; b – sample VI-1, development of pitchblende after early rutile (Rut-1) and independently, galena (Gl) and pyrrhotite (Pirr) occur; c – sample VI-3, development of late rutile (Rut-2) after titanite (Tt) in association with pitchblende spherulite, aggregate of pyrrhotite (Pirr), chalcopyrite (Chp) and sphalerite (Sf) occur; d – sample VI-3, molybdenite (Mo) enveloping pitchblende, partial replacement of pyrrhotite (Pirr) by aggregate of pyrite and marcasite (Py+Marc).

2. Generalized characteristic features of the U-P occurrences.

U-P occurrences of the Northern Ladoga area can be characterized by following distinctive features.

1. Petrologic control.

1. There is an exact stratigraphic control of the U-P occurrences – all of them are localized in upper carbonate horizon of the Ludicovian Pitkjaranta suite.

2. There is exact lithological control of the U-P occurrences – all occurrences are hosted by carbonate rocks (dolomitic marbles and carbonate schists).

II. Structural and tectonic control.

1. Most of the U-P occurrences were discovered in the Ruskeala anticline related to the Ruskeala fault zone.
2. The most significant occurrences are localized in upper parts of swells of carbonate rocks interlayers.
3. As a rule, the U ore bodies have a lens shape conformable to the host rocks; subordinated high-grade vein type mineralization occurs locally in late breccias zones.

III. Ore mineralogy.

1. Uranium mineralization is represented mostly by U oxides with predominance of pitchblende; coffinite and Ti-U mineral phase are subordinated.
2. Uranium mineralization is associated with apatite, carbonaceous matter and sulphides. Positive correlation of U with P, Pb, Mo, Zn was recognized.
3. Uranium ore mineralization is characterized by significant differentiation of radioactive equilibrium with uranium depletion upward to the surface.
4. Most isotopic results constrains the age of the mineralization between 1.9 and 1.8 Ga (table 2.1.3.2).

Earliest attempts of age determinations (Gromov et al., 1981) used an uncertain method and are not reliable. They give only very approximate age limits of the U-producing event. More precise constrains of Anderson (1990) reveals two generations of the U mineralization. First one was obtained for most widespread low-grade uraninite-pitchblende mineralization. It has an age about 1860 Ma that corresponds to culmination of the Svecofennian metamorphism. Vein type pitchblende from the Mramorny Kombinat ore-showing is correlated with the Riphean tectonic reactivation at the origin of the Pasha-Ladoga sedimentary basin and the unconformity-related Karku deposit (see Chapter 2). During this study, a Palaeozoic age of 397 ± 19 Ma was obtained for pitchblende mineralization in tectonic breccias zones in the Mramornaya Gora ore-showing.

IV. Grade of the occurrences.

All occurrences are of low grade – size of mineralized zones is small, resource is less 200 tons, average uranium content is low (about 400 ppm). It is notable that low grade is peculiar for such type deposits in the Baltic Shield. So, same type deposits known in Finland are small as well: Vihannti deposit 700 tons of uranium with 300 ppm average content and Nuottijarvi 1000 tons of uranium with 400 ppm average content.

Table 2.1.3.2. Isotopic age constrains of U mineralization hosted by Ludicovian carbonate rocks of the Northern Ladoga area.

Occurrence	Mineral	Method	n	Isotopic age, T _o , T _m , Ma	Reference
Mramornaya Gora	uraninite, pitchblende	U-Pb, TIMS	6	1856±180, 100±100	Anderson, 1990
		U-Pb, TIMS	1	1850	Gromov et al, 1981
		Pb-Pb	199	1830±70	-/-
		-/-	79	1960±50	-/-
		-/-	63	1720±30	-/-
	pitchblende	U-Pb, TIMS	10	1432±201, ~320	-/-
	pitchblende	U-Pb, SIMS	8	397±19, -21±140	This study
Mramorny Kombinat	pitchblende	U-Pb, TIMS	7	1221±64, 366±41	Anderson, 1990
Severnaya Ruskeala	uraninite	U-Pb, TIMS	5	1860±20	Anderson, 1990
	-/-	-/-	3	1780±20	-/-
	-/-	Pb-Pb	3	1640±30	Gromov et al, 1981
Ujnaya Ruskeala	uraninite	Pb-Pb	3	1900±10	Gromov et al, 1981
	-/-	-/-	3	1780±20	-/-
Pitkyajarvi	uraninite	Pb-Pb	159	1790±100	Gromov et al, 1981
	-/-	-/-	44	1830±50	-/-
	-/-	-/-	43	1580±70	-/-
	-/-	-/-	22	1680±50	-/-
	-/-	-/-	20	2040±50	-/-
	-/-	-/-	19	1970±70	-/-
(Anomaly 73)	uraninite	Pb-Pb	?	1800±30	Gromov et al, 1981
Savipuro	uraninite	Pb-Pb	4	1900±10	Gromov et al, 1981

U-P deposits in metamorphosed FZ phosphorites with resource up to few tens of kilotons of U are known in the Kazakhstan (Kushnerenko et al., 1985). Some of them were mined in the past (the Zaozernoye deposit).

Total identified resource of U-P occurrences of the Northern Ladoga area is about 1100 tons U, prognostic resource is about 4000 tons U.

3. Remarks to origin of the U-P occurrences.

The origin of U mineralization in the U-P occurrences of the Northern Ladoga area is complex. A model based on previous works (Nemtsov et al., 1954; Grigorieva, 1977; Rehtijärvi et al., 1979; Vaasjoki et al., 1980; Äikäs O., 1980; Gromov et al., 1981) and our observations is proposed below.

The U ore hosting upper carbonate horizon is composed of interbedded carbonate, marly, sandy-clayey and sandy sediments metamorphosed during the Svecofennian orogeny into marbles, schists and quartzites. This lithological association corresponds to sublittoral environment with unstable position of the coastline.

The properly carbonate sequence is composed of dolomitic and calcitic marbles interbedded with subordinated transitional formations. Initially dolomite and limestone were produced by chemical precipitation of Ca and Mg from sea water and diagenesis of the carbonate silt.

Calcitic marble prevails in the lower part of the sequence. Graphite content in this rock is low. Dolomite and graphite contents increase upward in the sequence.

Predominance of dolomite in the upper part of the sequence can be explained by increasing sea water salinity during progressive chemical weathering and mass transfer in conditions favorable to migration of Ca and Mg.

A characteristic feature of the upper carbonate horizon is a higher P content concentrated in apatite. Origin of the P enrichment is considered as chemogenic sedimentary, syngenetic to the carbonate rocks. Maximum average P content in light dolomitic marbles is 2-4 wt %.

Uranium is spatially associated with apatite, graphite and dolomite. Prevalence of the chemical weathering in the feeding areas was favorable for the derivation of U, P and Mg. High CO₂ content in the Precambrian atmosphere caused acidification (Ph<7) of the waters contributing to the migration of these elements.

Phosphates and carbon matter are good sorbents of uranium from aqueous solutions, especially phosphates (Altgauzen, 1956). According to Neruchev (1982), the jelly-like consistence of the sea bottom during the sedimentation of the dolomites favored U precipitation.

Diagenetic redistribution of U and P occurred during the formation of the dolomites. Uranium at this stage mainly occurred in apatite, less – in carbonaceous matter.

Thus it is supposed that the primary U accumulation in the phosphate-bearing carbonate rocks occurred during the sedimentation (U-bearing phosphorite). Other evidences are:

- 1) U mineralization is strictly related to the upper carbonate horizon of the Ludicovian Pitkjaranta suite;
- 2) high U background is quite common for the Pitkjaranta suite carbonate formations (General Appendix 2.1), U-enriched rocks can be followed over tens of kilometers;
- 3) U mineralization is especially related to apatite-bearing dolomite marbles;

- 4) early uranium ore mineralization is conformable with the host rocks;
- 5) U is associated with characteristic complex sedimentary-metamorphogenic minerals such as dolomite, apatite and graphite (initially carbonaceous matter).

Svecofennian regional metamorphism transforms phosphate-carbon carbonate sediments into apatite-graphite-bearing marbles. U was extracted from the apatite and formed its own mineral phase; in early high-temperature stages it forms thinly disseminated uraninite. During following retrograde metamorphic events pitchblende mineralization was formed. As a result of the metamorphism, the banding of the U-bearing layers became more contrasted. Skarnification of the carbonate rocks led to a redistribution and impoverishment of the early U ore.

Ductile deformations related to the Svecofennian orogeny caused complex folding of ore-hosting layers. The uranium mineralization was especially concentrated in the keystones of the folds. As a result of tectonic movements of this stage early breccias were formed. Dolomite fragments more enriched in uranium are enveloped in more plastic calcite.

Latest brittle deformations led to local redistribution of U along fracturing zones.

Thus, U-P occurrences of the Northern Ladoga are presumed as metamorphosed uranium-bearing phosphorites with principal uranium enrichment during the metamorphism and according to Dahlkamp (1993) can be referred to the synmetamorphic type. Subordinated vein-type mineralization occurs locally as a result of low temperature hydrothermal remobilization of the uranium.

Conclusion.

Numerous U-P phosphorus occurrences of the Northern Ladoga area have been discovered during exploration from the fifties to the seventies. Processing of the Mramornaya Gora ores have shown the possibility of an effective uranium extraction by sodium leaching (Il'in, 1984). Nevertheless, all of these attempts have led to negative evaluation, because of the small resources and the low uranium contents. Moreover, a low grade is typical for such type of deposits in general. Consequently, this type of occurrences cannot be considered presently of economic interest. However, widespread indications of hydrothermal alterations and especially occurrences of telescoping vein type uranium mineralization, allow to consider the areas where the U-P ore-showings occur as prospective for vein-type uranium deposits.

Paragraph 1.4. Vein-type uranium occurrences.

Introduction.

All known vein-type uranium occurrences of the Ladoga region are located in the Northern Ladoga area.

There are three varieties of vein type uranium mineralization in the Northern Ladoga area (General Appendix 1, fig. 1.1):

1. uranium as a principal ore mineralization in quartz-carbonate veins;
2. subordinated uranium mineralization telescoping complex ore occurrences;
3. late fracture-bound uranium mineralization in other type of uranium occurrences.

This paragraph is mostly devoted to proper vein type uranium occurrences (type 1). Uranium mineralization telescoping complex ore occurrences (type 2) is briefly described. Fracture-bound uranium mineralization in other type of uranium occurrences will be just mentioned; it is considered in other paragraphs corresponding to the leading type of the mineralization. In addition, a few occurrences of vein-type Th mineralization are described in this paragraph.

1. Uranium as a principal ore mineralization in quartz-carbonate veins.

Uranium mineralization hosted by fracture zones in a quartz-carbonate gangue has been discovered in different parts of the Northern Ladoga. The most representative uranium occurrence, where uranium is a major product, is the Varalakhti ore showing.

1.1. The Varalakhti uranium ore-showing.

The ore showing was found by “Nevskgeologia” in 1952, additional occurrences were worked in the seventies by the same enterprise. The ore-showing was recognized by an adit, 3 drillholes down to 50 m and trenching. The Varalakhti ore showing was sampled during this work.

Geological environment.

The Varalakhti U ore showing is located at the southern limb of a sublatitudinal syncline between the Sortavala and Kirjavalakhti AR-PR₁ granite-gneiss domes. The depression is filled with Pitkjaranta suite amphibole schists. Generally, in the syncline they have a latitudinal strike and dip 20-50° to the south, but its undulation caused by a local prominence of the Kirjavalakhti dome in the immediate area of the Varalakhti ore-showing. Here, the layers are striking 5-20° NE

and dipping 30-60° to the NW (40-45° in average). The amphibole schists are cut by dykes of metadiabases and granodiorite-porphyry referred to the Svecofennian orogeny. Quartz lenses conformable to the schists are widespread. They contain xenoliths of the host rocks.

The U ore-showing is located in vicinity of the intersection of the N-S 355° striking Varalakhti and W-E 275° striking Kirjavalakhti fault zones. The first one is traced by granodiorite-porphyry dykes, zones of blastomylonites, schistosity and breccias. The second one is marked by numerous fractures. On the eastern continuation of the Kirjavalakhti fault zone, 2 km from the Varalakhti ore-showing, the Kirjavalakhti fracture-hosted anomaly occurs (General Appendix 1, fig. 1.1 and 5).

Three systems of local tectonic displacements are distinguished in the ore-showing area:

- 1) NE 5-20° breccias zones, with steep dipping, generally conformable to the host rocks, filled by host rock fragments, quartz, carbonate, sometimes ore minerals;
- 2) NE 70-80° mylonite zones, dipping steeply, several meters long, up to 2 m thick; sometimes accompanied with a dense network of thick quartz-carbonate veinlets;
- 3) sublatitudinal 270-290° fractures, with diverse dipping, cutting all rocks, sometimes filled with carbonate or clayey material; blastomylonites zones with about the same strike occur farther to the north among the granite-gneiss of southern periphery of the Kirjavalakhti dome.

The Varalakhti ore-showing is related to a second order fracture of NE strike accompanying the Varalakhti fault. U mineralization is localized in a complex breccias zone hosted by amphibole schists of the Pitkjaranta suite (fig. 2.1.4.1 and 2.1.4.2). The zone is conformable to the host rock foliation and strikes 10-20° NE with a 50-80° NW-dip. At the surface it can be followed over 40 m along the strike, with a thickness up to 8 m.

The breccia zone is composed of fragments of quartz, carbonate rocks and amphibole schists cemented by quartz, calcite and ankerite (fig. 2.1.4.3), locally by pitchblende and sulphides (fig. 2.1.4.4). Biotitization, chloritization, microclinization, local scapolitization of the rocks are observed. Newly-formed pyroxene, epidote and zoisite rarely occur.

The breccias zone is complex and was formed in several stages:

- I. fracturing and silicification of the amphibole schists;
- II. succession of breccia and cataclastic events with a cementing of the fragments by quartz, calcite, ankerite, several generations of sulphides, pitchblende and native bismuth;
- III. latest ramified small veinlets of pink calcite with sulphide mineralization.

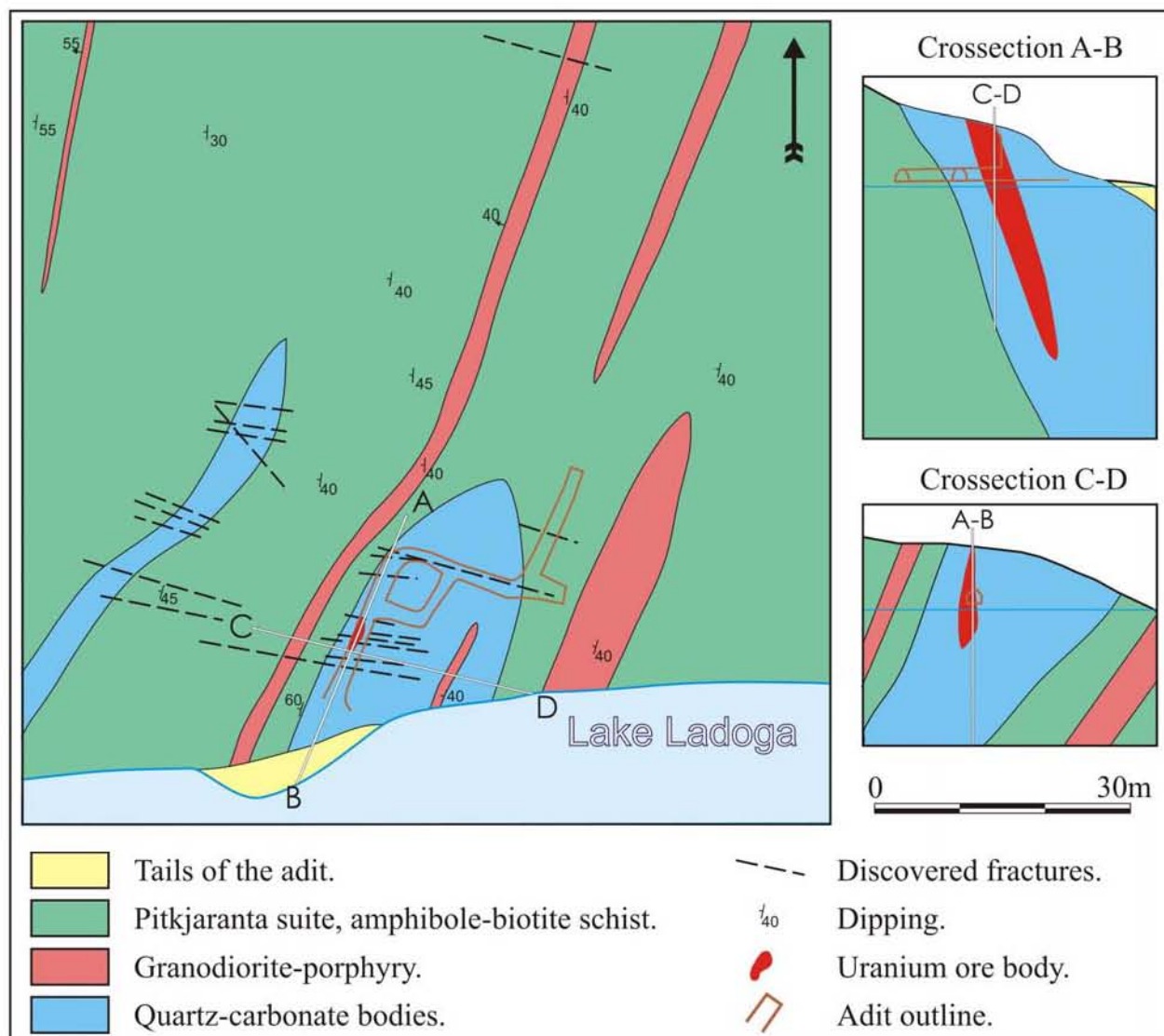


Figure 2.1.4.1. Geological map and sections of the Varalakhti ore-showing area (after Nemtsov S.N. et al, 1954).

Quartz-carbonate breccias zones in this area are very abundant. Generally they have not suffered from late tectonics, except in the U-mineralized zone of the Varalakhti ore-showing where late cataclasis has occurred. Quartz of the early breccias was deformed and fractured (fig. 2.1.4.5), and ankerite-pitchblende-sulphide mineralization were deposited as a late cement of the breccia.

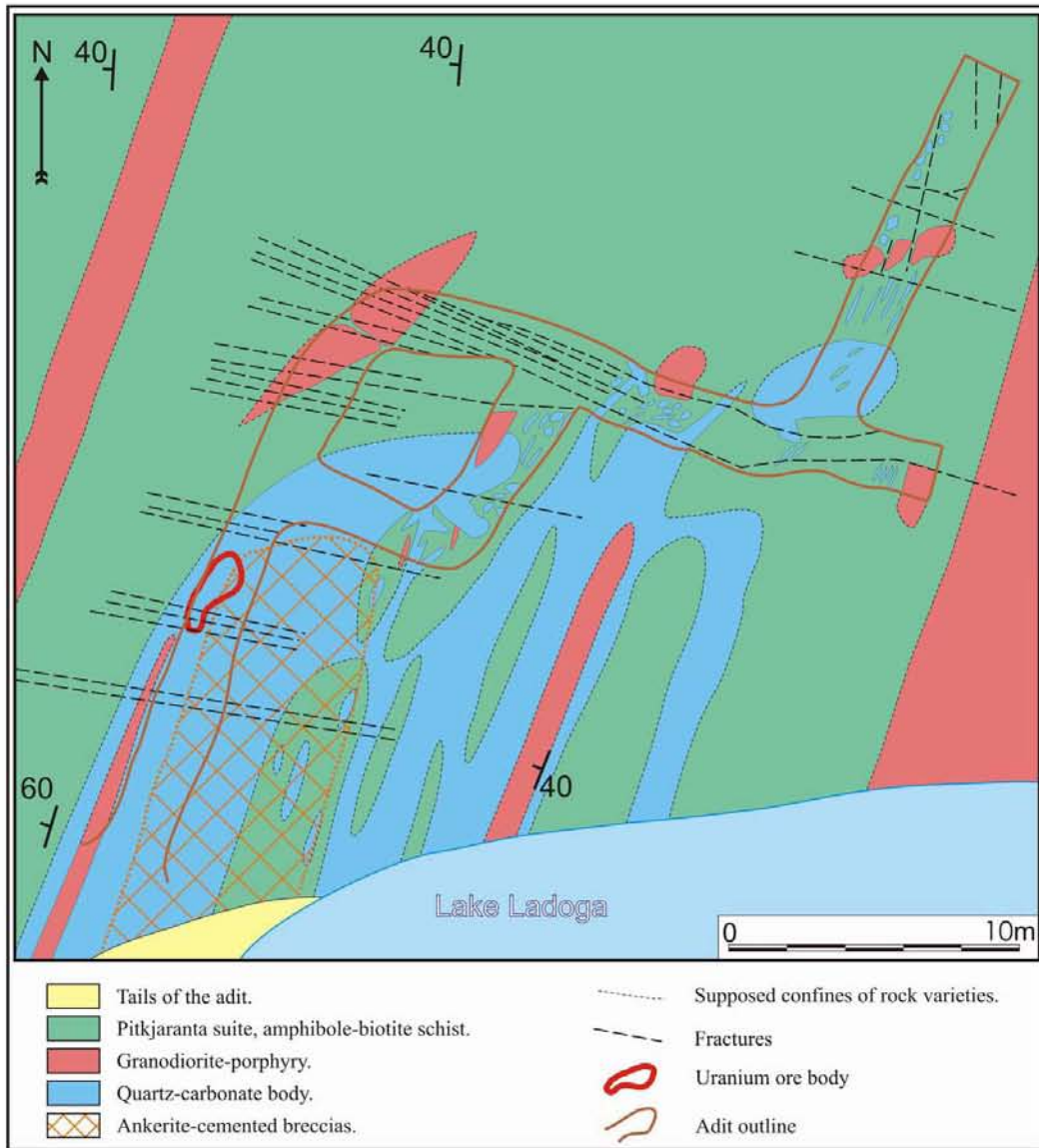


Figure 2.1.4.3. Quartz breccias cemented by calcite and ankerite from the Varalakhti ore-showing.

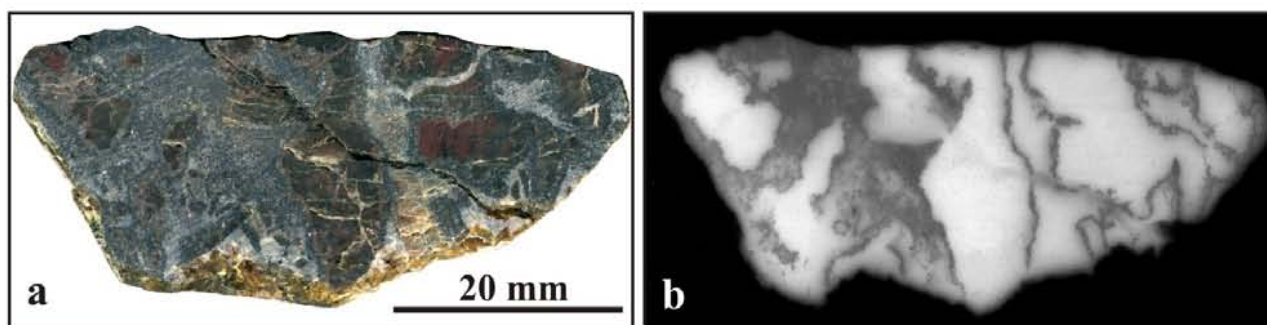


Figure 2.1.4.4. U mineralized breccias from the Varalakhti ore-showing; a – sample Va-6; b – autoradiography (3 days).

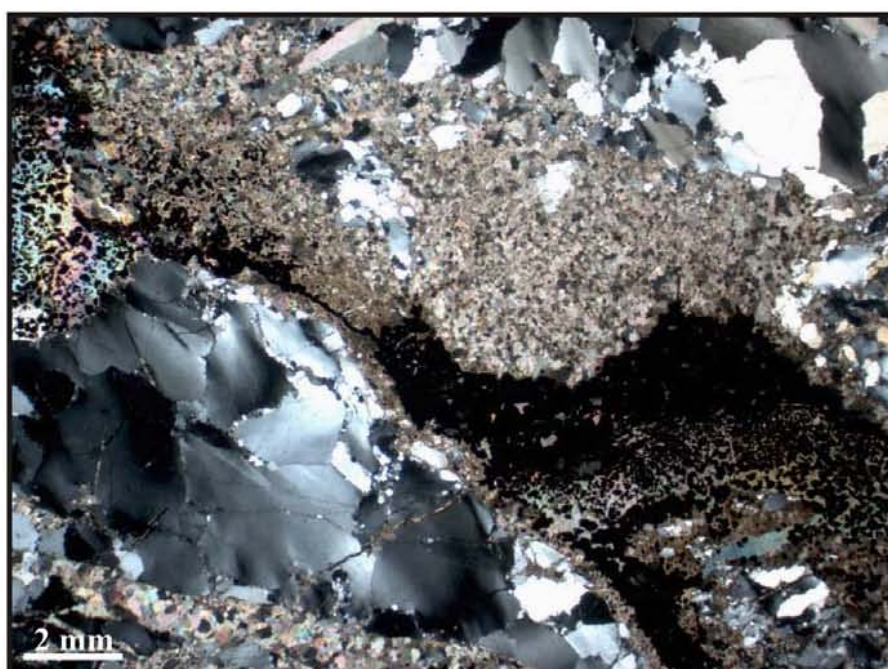


Figure 2.1.4.5. Quartz deformations in the U mineralized breccias of the Varalakhti ore-showing. Sample Va-1, optical photo, polarized transmitted light.

Ore-body.

Uranium mineralization is concentrated in the hanging wall of the breccia lens, in the tectonic zone between quartz-ankerite breccias and quartz cataclasite (fig. 2.1.4.6). The ore body is columnar, steeply dipping to the NW and conformable with the breccia zone. It is composed of U-mineralized lenses up to 8 cm thick and up to 10 m long. The total length of the ore body is presumed to be 30 m along the dip. The size of the ore body in section is up to 1.2×4.5 m with an extension conformable to the host rock. Average U content is 5 000 ppm with a maximum of 16 600 ppm. Resource of the ore-showing is about several tons U (Nemtsov et al., 1954).

U is associated with Cu (0.01-6 %), Pb (0.1-10 %), Ni (0.01-0.03 %), Zn (0.03-0.3 %). Anomalous contents of Bi, Ag, Co, Zr, Y and As occur.



Figure 2.1.4.6. U mineralized zone (oxidized rock inside of the dotted line) inside of the adit.

Uranium mineralization.

Uranium mineralization of the ore showing is represented by pitchblende and coffinite.

Pitchblende occurs in the carbonate cement of the breccias as isolated rounded spherulites and botryoidal aggregates developing along fracture, overgrowing gangue and ore minerals (fig. 2.1.4.7). During the latest fracturing, pitchblende spherulites were fractured and the fragments were cemented by a new generation of calcite and sulphides (fig. 2.1.4.8).

According to electron microprobe analyses, pitchblende composition is characterized by following features (General Appendix 2.3, table 10; General Appendix 2.4, table 6):

- UO_2 and PbO contents vary between 74-77 % and 16-18 wt%, respectively;
- SiO_2 content is quite rather low (<1.8 wt%) indicating a weak alteration;
- Al_2O_3 detected in some analyses might be attributed to the presence of clay minerals;
- CaO contents are quite high 3-4 wt%, probably related to the presence of carbonates;
- Th content is below the detection limit.

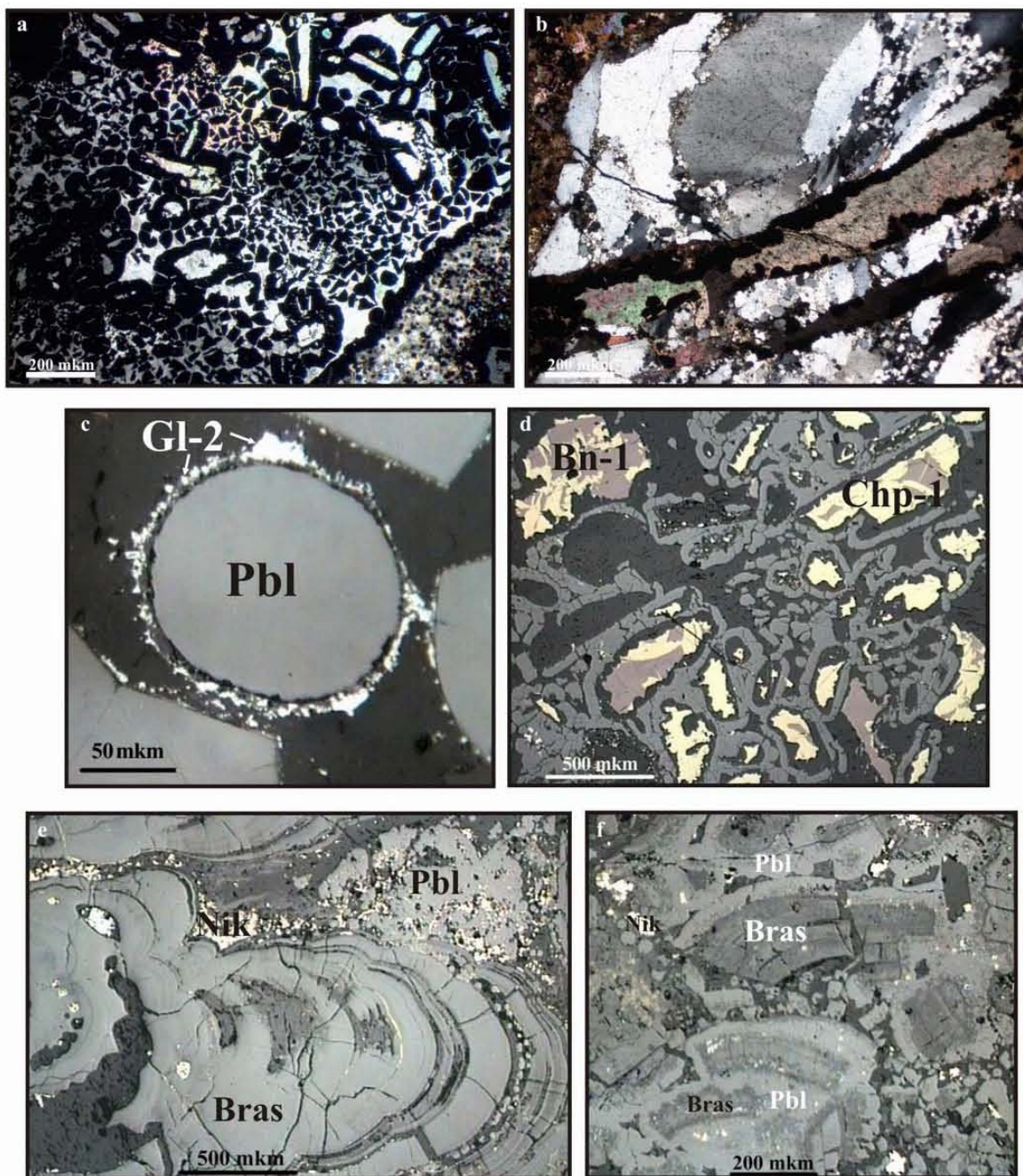


Figure 2.1.4.7. Pitchblende (Pbl) mineralization of the Varalakhti ore-showing, optical photos. Sample Va-1: a – pitchblende impregnations in the calcite cement, overgrowths of the fracture confines, sulphides and gangue minerals (polarized transmitted light); b – pitchblende development along the fracture confines (polarized transmitted light); c – single pitchblende spherulite with galena (Gl-2) framing (reflected light); d – pitchblende aggregates overgrowing chalcopyrite (Chp-1) and bornite (Bn-1) aggregates (reflected light); e – pitchblende overgrowing and penetrating inside of brassevelite (Bras) (reflected light); f – pitchblende overgrowing of brassevelite (Bras) fragments, late nickeline (Nik) occurs (reflected light).

Coffinite develops after pitchblende and occurs in late veinlets (fig. 2.1.4.9). Analyses of coffinite indicate an admixture of PbO (up to 19.2 wt %), Y₂O₃ (up to 4.7 wt %), Fe₂O₃ (up to 6.0 wt %), CuO (up to 1.7 wt %), CaO (up to 5.1 wt %) and MgO (up to 3.3 wt %).

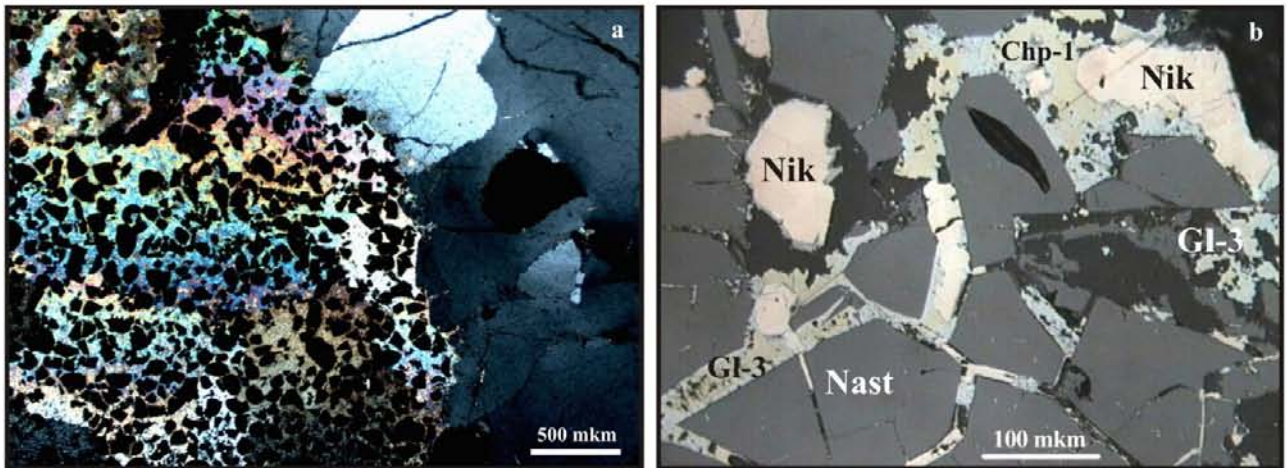


Figure 2.1.4.8. Pitchblende (Pbl) fragments cemented by late gangue (quartz and calcite mainly) and sulphide minerals. Sample Va-1, optical photos: a – predominating calcite cement, polarized transmitted light; b – chalcopyrite (Chp-1) and nickeline (Nik) cementing pitchblende fragments are replaced by galena (Gl-3), reflected light.

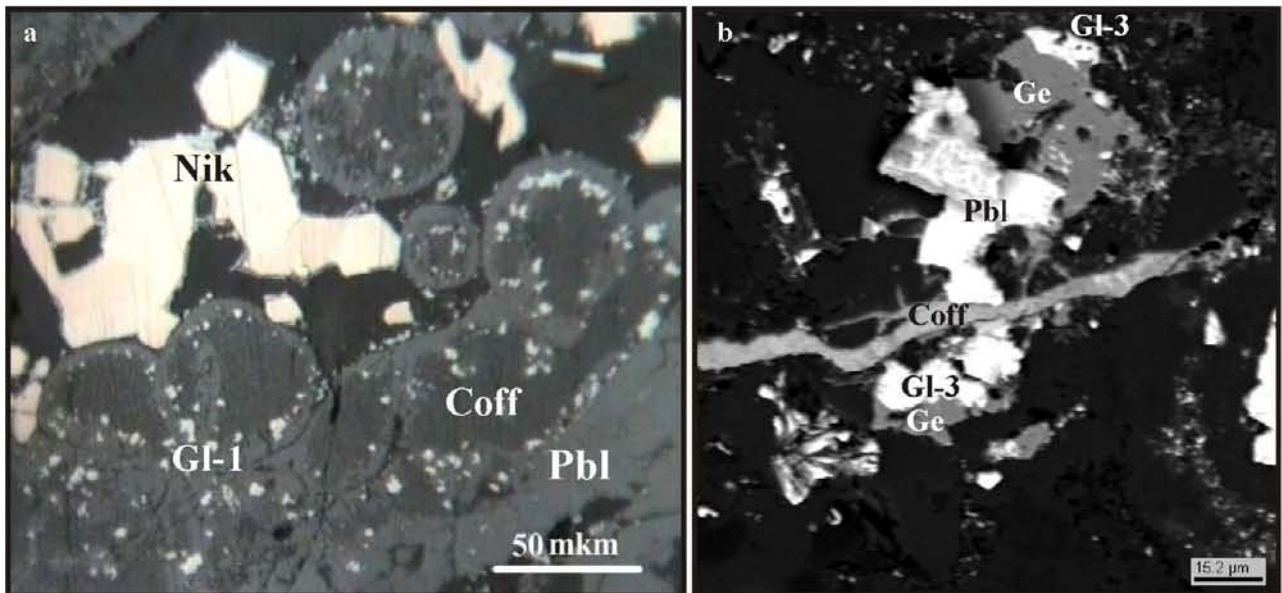


Figure 2.1.4.9. Two types of coffinite mineralization. Sample Va-1: a – development after pitchblende (Pbl), late nickeline (Nik) occurs, optical photo, reflected light; b – the latest coffinite (Coff) veinlet cutting (Pbl) and galena (Gal-3), the last one is partly replaced by geerite (Ge), BSE photo.

Uranium mineralization is accompanied with diverse non-radioactive ore mineralization. Ore parageneses revealed in the samples from the Varalakhti ore-showing are presented in the table 2.1.4.1.

Table 2.1.4.1. Ore parageneses of the Varalakhti ore-showing (after Polekhovsky et al., 2007).

No	Minerals	Paragenesis							
		Pre U-ore	U-ore	Galena-2	Arsenide	Galena – noble metal	Cu sulphide	Low-temperature	Hypergene
1	Rutile	+							
2	Bracewellite	+							
3	Chalcopyrite-1	+							
4	Chalcopyrite-2						+		
5	Bornite-1	+							
6	Bornite-2						+		
7	Co-pentlandite	+							
8	Pitchblende		+						
9	Galena-1		+						
10	Galena-2			+					
11	Galena-3					+			
12	Nickeline				+				
13	Safflorite				+				
14	Electrum					+			
15	Native Bi					+			
16	Altaite					+			
17	Coffinite							+	
18	Native Cu							+	
19	Geerite							+	
20	Covellite							+	
21	Iron Hydroxides								+

In a Concordia diagram the U-Pb isotopic data of pitchblende (5 points) are discordant. The upper intercept defines an age of 1538 ± 180 Ma and the lower intercept an age of 243 ± 430 Ma. The large uncertainty of the upper intercept age results from the clustering of the analytical data (fig. 2.1.4.10a). If the Discordia is constrained through 0 the upper intercept age is 1460 ± 26 Ma (fig. 2.1.4.10b). Previous age determinations obtained close results: 1588-1420 Ma (Anderson, 1990, see the table 2.1.4.8 in the end of the Paragraph 1.4).

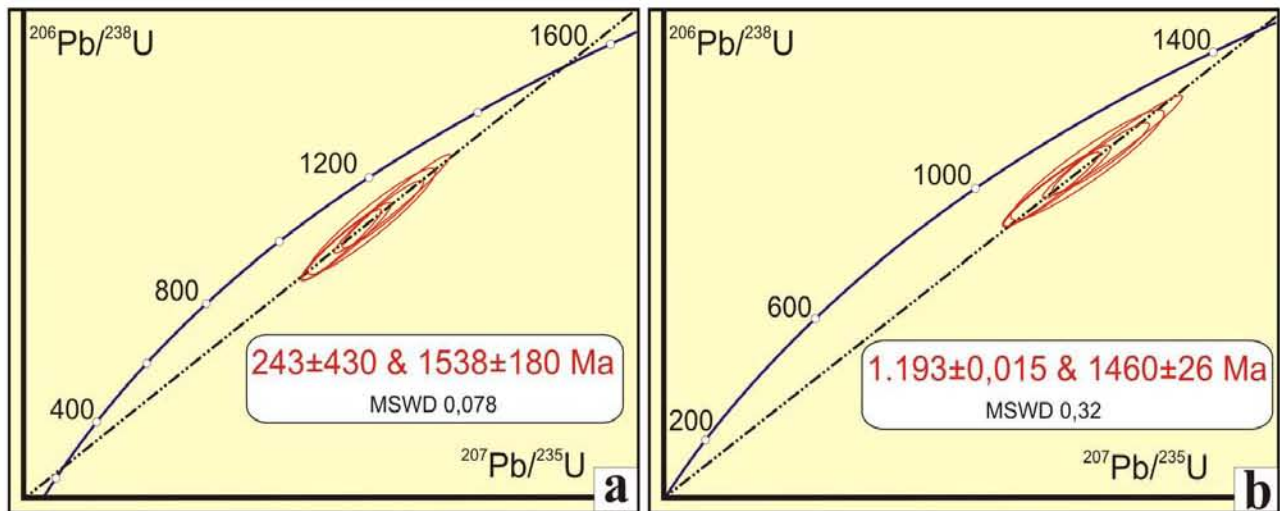


Figure 2.1.4.10. Concordia diagrams with two possible interpretation of isotopic U-Pb ratio for pitchblende from the Varalakhti ore-showing; sample Va-1.

1.2. Vein-type uranium mineralization of the Latvasurje area.

Several uranium occurrences of hydrothermal origin were discovered during exploration by “Nevskgeologia” in the seventies and eighties in the Latvasurje area in western part of the Sortavala tectonic block.

This area is located in an interdome depression between the Latvasurje and the Jokiranta granite-gneiss uplifts (Appendix to Chapter 1, fig. 6).

The domes are composed of AR-PR₁ plagioclase-microcline gneiss-granites, migmatites and subordinated concordant amphibolite bodies. Ludicovian formations of the Sortavala group surrounding the domes are represented by rocks metamorphosed in high grade amphibole facies: amphibole and biotite-amphibole schists, dolomitic and calcitic marbles, skarnoids. The Ladoga group consists of quartz-biotite and quartz-feldspar-biotite gneiss. Palaeoproterozoic formations are migmatized and intensively folded with a general N-S strike of the folds. The foliation of all crystalline formations strikes N-S in general, with a variable dip because of numerous folds.

There are many indications of magmatic activity in the Latvasurje area. The intrusive bodies generally are generally elongated N-S. Small granodiorite dyke intrusions of the synorogenic Lauvatsaari-Impiniemi complex are widespread. They represent the oldest orogenic formation of the area as indicated by their important deformation and migmatization.

The late Svecofennian Latvasursky granite complex is composed of small intrusions, stocks and veins of leucocratic pegmatoid and aplitic granites. There are two types of intrusions:

- stock-like intrusions (from 20×30 m to 3×3 km large) of even-grained leucocratic plagioclase-microcline and microcline granites often enclosing fragments of hosting metamorphic rocks

- N-S-extended lens- or vein-like bodies (up to 150×1000 m large) of even- and coarse-grained plagioclase and microcline-plagioclase granites. Crosscutting relations between the different granites were observed (fig. 2.1.4.11). The granites of the Latvasursky complex have increased U content (9 ppm in average).



Figure 2.1.4.11. Two generations of veins of late Svecofennian leucogranites cutting Ladoga group mica schists in the Latvasurje area.

The youngest rocks of the area are gabbro and gabbro-diabase dykes (up to 25×150 m large) striking N-S, cutting all formations. The age of these dykes is not known; they may be Riphean, because there are Riphean mafic dykes 10 km to the east, along Ladoga lake coast.

There are many N-S, NE-SW and NW-SE faults in the area. The most widespread are N-S and referred to the Latvasurje fault zone. Then, among the NE-SW ones, the Elisenvaara fault is the largest. Carbonatization, chloritization and sulphidization occur along faults of different strike.

Subeconomic fluorine-scheelite mineralization is hosted by magnesium skarns after carbonate rocks of the Pitkjaranta suite.

There are three types of U occurrences in the area. The most widespread are granite-hosted concentrations of U- and Th-bearing accessories. All of them are local and low-grade. Content of U is up to 270 ppm, Th up to 100 ppm (Gromov et al., 1981).

Few local anomalies with radioactivity up to 500 cps are hosted by the Ludicovian carbonate rocks. Presumably they are of the same type as ones of the Ruskeala anticline (see Paragraph 1.3 U-P mineralization in the Ludicovian carbonate rocks).

More interesting are several hydrothermal U occurrences related to fracture zones. The most significant is the Karinmyaki ore-showing. It was visited and sampled during this work.

The Karinmyaki ore-showing.

The ore showing is related to the intersection of two fault systems: a submeridional one (second-order fracture accompanying the Elisenvaara fault of striking NE) and a 290° NW striking one. It is hosted by the Ludicovian Pitkjaranta suite biotite-amphibole schist and the Kalevian Ladoga group migmatized biotite gneiss (sometimes graphite-bearing) (fig. 2.1.4.12.).

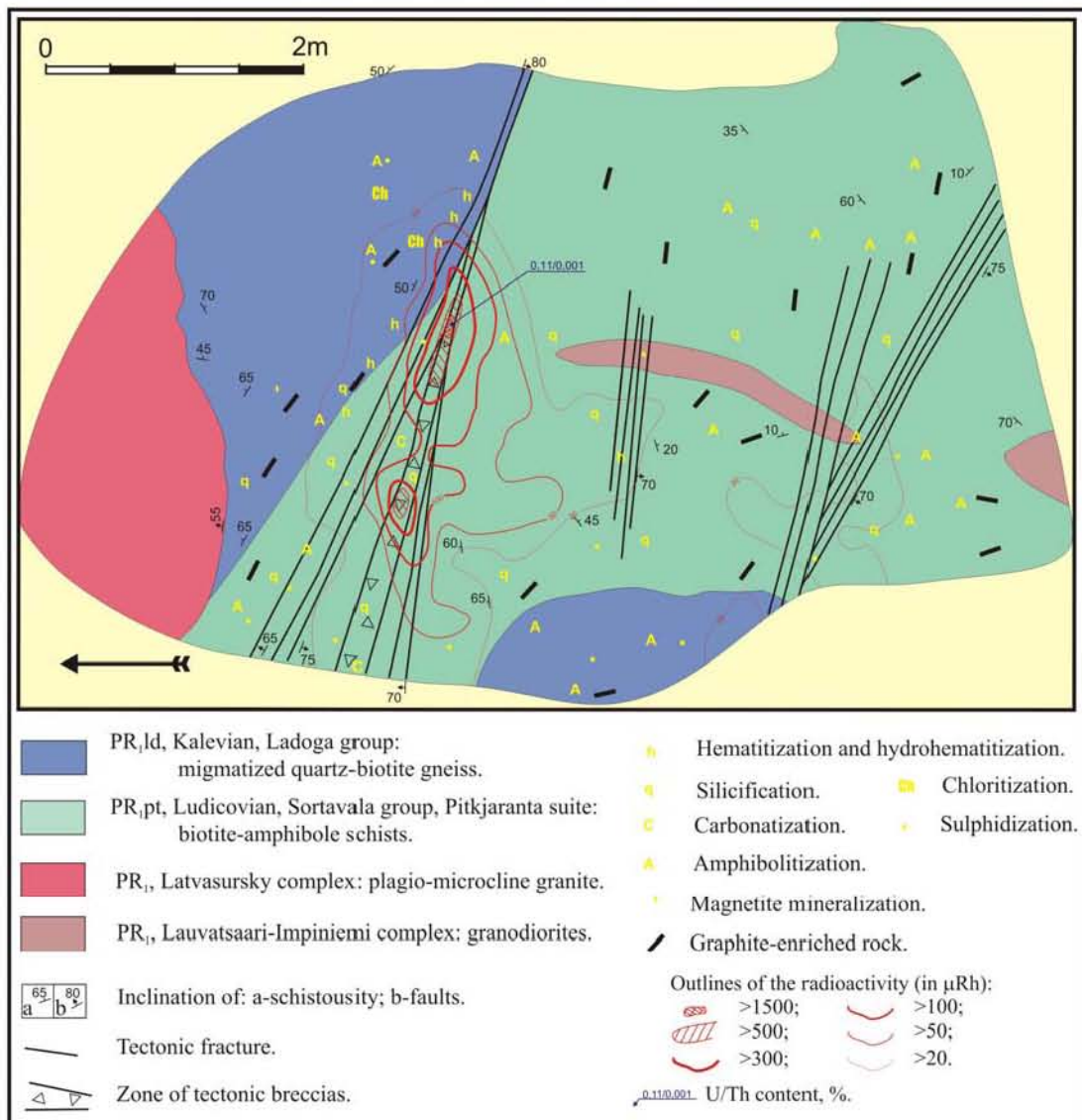


Figure 2.1.4.12. Outcrop of the Karinmyaki ore-showing (after Gromov et al., 1981).

Intrusion of coarse-grained plagioclase-microcline granite of the Latvasurje complex occurs to the north. Usual for the Latvasurje area the submeridional strike of the gneiss foliation is disturbed, especially at the contact with the granites where plication of the gneiss is widespread.

Uranium mineralization is localized in a 280-300° NW striking fracture zone steeply (75-85°) dipping to the SW. The thickness of the zone is about 10 m. It is composed of individual zones of intensive fissuring and brecciation 0.3-1 m thick and 0.5-12 m long. Intensive biotitization, amphibolization, silicification, carbonatization, graphitization, sulphidization (pyrite, galena, molybdenite) and local epidotization, chloritization and hydromicanization occur along the fractures. U-mineralized rocks are intensively carbonatized, silicified and sulphidized.

7 ore bodies with U content over 100 ppm were discovered in the ore showing. They have lens and nest shape and are 0.3×0.3 up to 3×1 m large. U content is 210 ppm in average, with a maximum of 3200 ppm; Th content is less than 10 ppm (Gromov et al., 1981).

U mineralization in the ore-showing is accompanied by very high contents of Pb (up to 1100 ppm), Zn (up to 700 ppm), Mo (up to 300) and high contents of P, Sr, La, Sn, Ag, Cu and V.

The radioactive mineralization of the Karinmyaki ore-showing form spot impregnations, nest aggregates or disseminated in the cement (fig. 2.1.4.13).

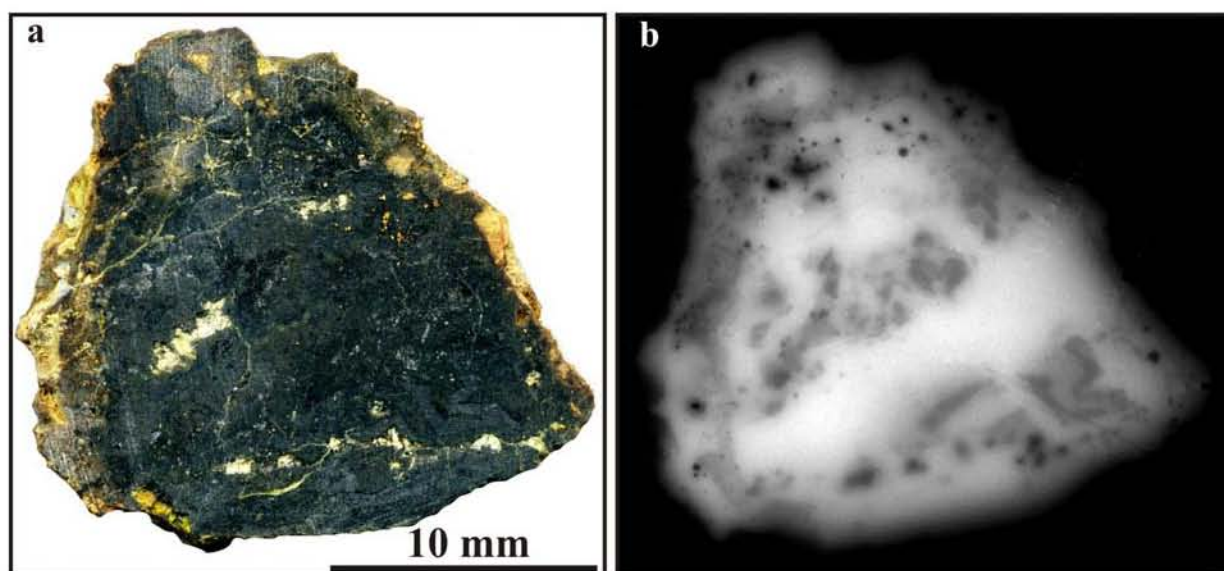


Figure 2.1.4.13. U-mineralized breccias from the Karinmyaki ore-showing; a – sample Ka-1; b – autoradiography (8 days). Impregnated uraninite mineralization and cementing pitchblende mineralization can be recognized.

According to previous researches, uranium mineralization of the ore-showing is composed of uraninite, pitchblende and hexavalent U minerals (uranophane, kasolite, becquerellite and ianthinite) (Gromov et al., 1981). In the samples obtained during the present field work, uraninite, pitchblende, hydropitchblende and kasolite have been identified (Polekhovsky et al., 2007).

Uraninite is preserved as relics of idiomorphic grains forming disseminated impregnations. It is mainly replaced by pitchblende and other late U minerals (fig. 2.1.4.14).

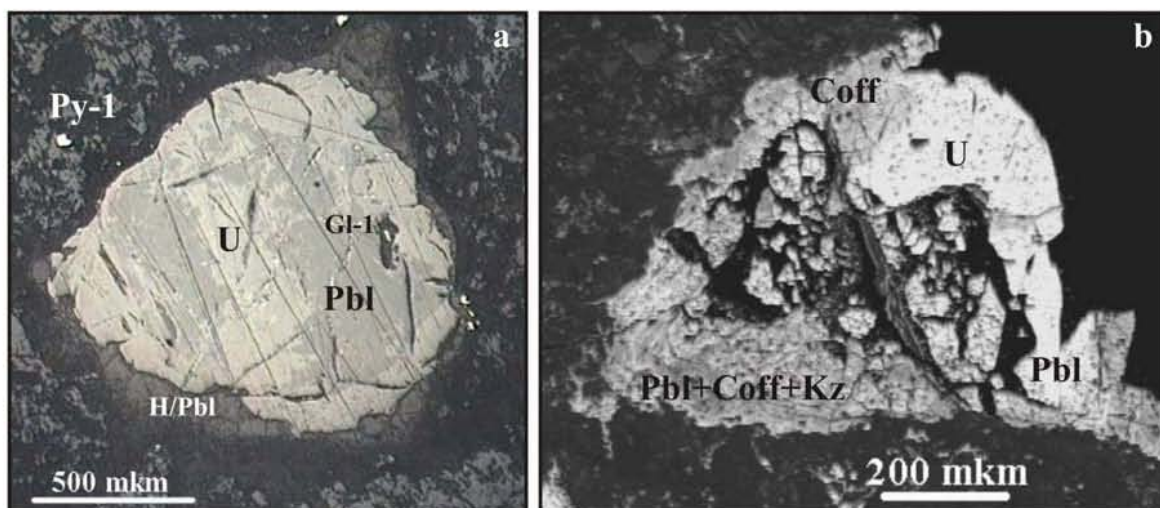


Figure 2.1.4.14. Karinmyaki ore-showing uraninite crystals (U) partly replaced by pitchblende (Pbl), coffinite (Coff), kasolite (Kz) and hydropitchblende (H/Pbl); a – sample Ka-1, optical photo, reflected light; b – sample La-1, BSE photo.

Pitchblende development after uraninite was associated with thin galena crystals. Coffinite was locally observed. It develops at the edges and in fissures of the uranium oxides. Supergene hydropitchblende and kasolite replace earlier U minerals. Kasolite also develops after sphalerite and in veinlets cutting rock-forming minerals (fig. 2.1.4.15).

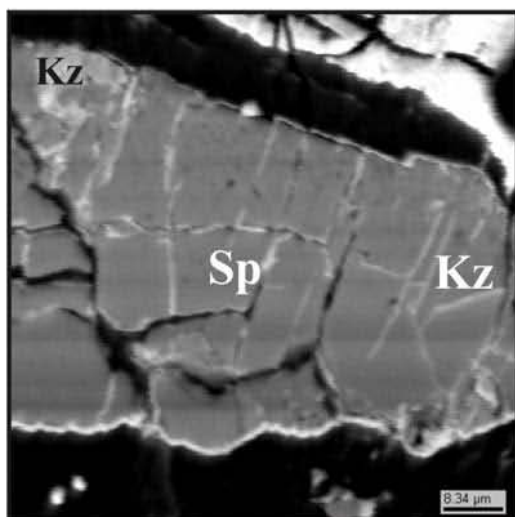


Figure 2.1.4.15. Karinmyaki ore-showing; development of kasolite (Kz) in fractures in sphalerite; sample Ka-1, BSE photo.

Composition of U minerals from the Karinmyaki ore-showing is given in the table 11 of General Appendix 2.3 (Th has not been analyzed). There is trend of decreasing of U content from early mineral phases to the latest ones:

- 80.1-83.0 wt % of UO_2 in uraninite;
- 77.2-79.9 wt % of UO_2 in pitchblende;
- 49.2-69.2 wt % of UO_2 in coffinite;
- 66.1 wt % of UO_2 in hydropitchblende;
- 45.9-59.0 wt % of UO_2 in kasolite.

Presence of significant amount of SiO_2 in the uranium oxides composition is an evidence of strong alterations of these minerals.

The paragenetic mineral succession is presented in Table 2.1.4.2.

Table 2.1.4.2. Ore paragenesis of the Karinmyaki ore-showing (after Polekhovsky et al., 2007).

No	Minerals	Paragenesis				
		Early epigenetic	U-ore	Polysulphide	Low-temperature	Supergene
1	Titanite	+				
2	Rutile	+				
3	Graphite	+				
4	Pyrite-1	+				
5	Uraninite		+			
6	Pitchblende		+			
7	Galena-1		+			
8	Galena-2			+		
9	Sphalerite			+		
10	Chalcopyrite			+		
11	Coffinite				+	
12	Marcasite				+	
13	Pyrite-2				+	
14	Covellite				+	
15	Hydropitchblende				+	
16	Kasolite					+
17	Iron Hydroxides					+

Gromov (1981) had obtained a Pb-Pb age for the U mineralization for the Karinmyaki ore-showing Pb-Pb at 1640 ± 20 Ma. This age is based on isotopic-spectral analyses may not be reliable. Such an age correspond to a quiescent time in the considered area with no significant tectonic activation, but the Wiborg rapakivi granites were emplaced about 150 km to the south.

1.3. Vein-type uranium and thorium mineralization of the Kuhilaslampi area.

There are many indications of hydrothermal alterations and diverse mineralization along the Janisjarvi fault zone caused by repeated tectonic activity. The most significant was the Svecofennian event when the Karelian craton was faulted along this zone and when the Raahe-Ladoga new crust was accreted to the Archaean craton. Late reactivations (the most important was the Riphean one) have had less influence on the tectonic structure and metallogeny of the area.

These occurrences were discovered by exploration works of “Nevskgeologia” in the fifties and beginning of the seventies. Few occurrences of vein type U and Th mineralization were visited and sampled during the present work in the Kuhilaslampi area, located in the Janisjarvi fault zone (Appendix to Chapter 1, fig. 4 and 5).

Anomalies hosted by Archaean formations.

Apart from the Th-U anomalies referred to syngenetic accessories concentrations in the Upper Archaean granitoids mentioned in the Paragraph 1.1, there are few indications of hydrothermal redistribution of radioactive elements in the Karelian domain formations. Kondakov et al. (1963), in the Kuhilaslampi area reported U contents in fracture zones within a AR₂₋₃ tonalitic gneiss up to 710 ppm (15 000 ppm in one sample) and Th contents up to 2 500 ppm. The main U mineral is uraninite. There are also uranophane, curite and minor nenadkevite. Other ore minerals are titanite, pyrite, ilmenite, hematite and magnetite. The size of the mineralized zones is up to 20×0.5 m. Anomalies are located along NW faults.

Point 1 is the most prominent radioactive anomaly in the Kuhilaslampi area discovered during the present work (Appendix to Chapter 1, fig. 5). It is hosted by Middle-Upper Archaean granite-gneiss with indications of migmatization possibly related to the Svecofennian orogeny. A radioactivity of 6500 cps is related to a fracture striking 280° and cutting pink microcline-plagioclase granite-gneiss. The fracture is filled with oxidized red-brown clayey material. As sampled radioactive materials are very altered and friable, it was not possible to identify the radioactive mineral phase.

The Razlomnaya uranium anomaly in a carbonate schist lens.

The anomaly is localized in the vicinity of the Kuhilasvaara dextral fault striking 300°, one of faults of the Janisjarvi tectonic zone. This is also a contact zone between the Karelian and the Raahe-Ladoga domains. Palaeoproterozoic Jatulian Jangozero suite metaterrigenous formations unconformably overlay the Archaean Saamian-Lopian tonalitic gneisses. The Jatulian formations are folded here (Appendix to Chapter 1, fig. 5). Fold structure is shifted to the SE with downthrow of its south-western limb. In the relief this downthrow forms cliff 25 m high.

There are gabbro-dabase dykes swarms inside a zone 300-500 m wide along the fault. Archaean granite-gneisses in this zone are strongly fractured and partly altered.

The U anomaly is located in a basal horizon of the Jatulian quartzitic sandstone, over a distance of 4 m to the SE of a gabbro-dabase dyke striking NW (fig. 2.1.4.16). The gabbro-dabase is medium-grained, dark gray, with mica-enriched zone at its contact with hosting quartzitic sandstone. In the vicinity of the dyke, the quartzitic sandstone is dark-green, fine-grained, with contact metamorphism. The quartzitic sandstone is becoming lighter outward from the contact. It is enriched in pyrite in 2-3.5 m a thick zone (with 5-8 mm cubes). All the rocks are chloritized, carbonatized, enriched in magnetite, pyrite and chalcopyrite along the tectonic zone.

Maximum radioactivity is up to 1400 cps localized in the cataclasite rock. The size of the anomalous area is 1.1×3.2 m. U content is up to 770 ppm over 10 cm. U mineralization associated with magnetite is represented by pitchblende replaced by coffinite and rutile (fig. 2.1.4.18). The paragenetic succession in the Razlomnaya anomaly is presented in table 2.1.4.3.

Table 2.1.4.3. Ore paragenesis of the Razlomnaya anomaly (after Polekhovsky et al., 2007).

No	Minerals	Paragenesis			
		Host rock magnetite	Pitchblende sulphides	Low temperature	Supergene
1	Magnetite	+			
2	Pitchblende		+		
3	Pyrite		+		
4	Chalcopyrite		+		
5	Galena		+		
6	Coffinite			+	
7	Hematite			+	
8	Rutile			+	
9	Iron Hydroxides				+

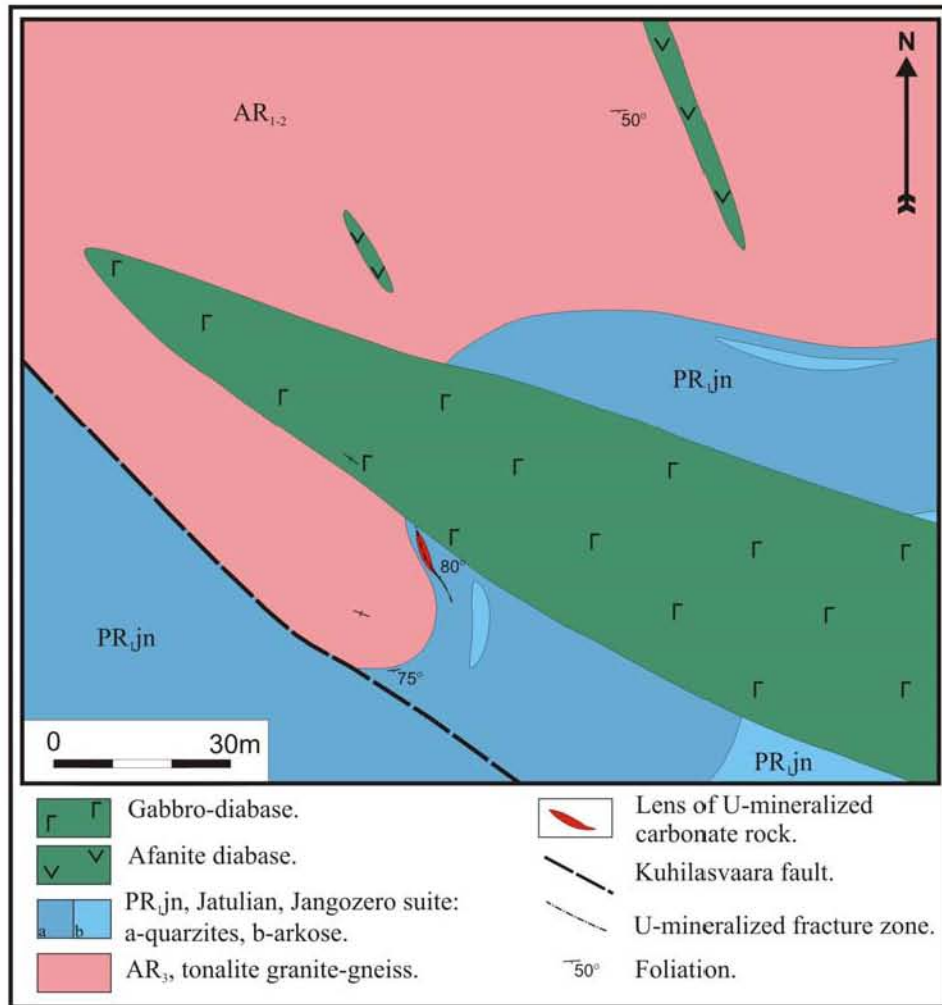


Figure 2.1.4.16. Geological map of the Razlomnaya anomaly area (after Kondakov et al., 1963).



Figure 2.1.4.17. Fracture-bound U mineralization of the Razlomnaya anomaly; the mineralization is located in the fracture in central part of the image.

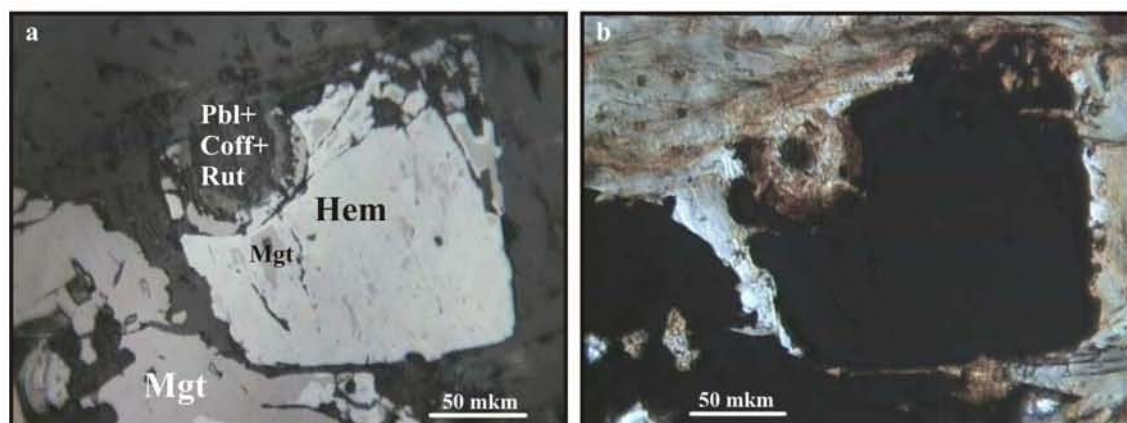


Figure 2.1.4.18. The Razlomnaya anomaly; relic of a pitchblende spherulite replaced by coffinite (Coff) and rutile (Rut) associated with magnetite (Mgt) replaced by hematite. Sample Jn-4, optical photos: a – reflected light; b – plain transmitted light.

There are few other anomalies in the vicinity of the Kuhilasvaara fault farther to NW of the Razlomnaya anomaly. They are also located in the vicinity of the gabbro-diabase dykes, but hosted by Archaean gneisses. Host rocks are altered with chloritization and carbonatization. All these anomalies are low-grade and they are interesting as evidences of hydrothermal U redistribution.

The Dyke thorium anomaly hosted by the gabbro-diabase dyke.

In addition to hydrothermal uranium anomalies, a specific vein type Th anomaly hosted by a gabbro-diabase dyke should be mentioned. The dyke is striking 320° NW-SE. It forms a ridge-like uplift of 40×200 m, up to 15 m height. Enclosing Th-bearing Jatulian Jangozero suite quartzites are metamorphosed to solid dark-green rock consisting of quartz, chlorite and iron oxides in vicinity of the dyke. The periphery of the gabbro-diabase dyke is fine-grained and strongly altered. The rock has a granoblastic structure and consists of 50-60 % amphibole replacing pyroxene, plagioclase (partly albitized), albite, biotite, chlorite, sericite, quartz. Accessories are magnetite, apatite and titanite. In its central part the dyke becomes coarser with a gabbro structure and is less altered (with pyroxene relics).

Anomalous radioactivity was discovered in the vicinity of the northern and southern salbands in the western part of the dyke outcrop. Fractures with different strikes cut the dyke in the mineralized area. Three major directions can be distinguished: NE, NW and N-S. Quartz veinlets occur in small fractures striking N-S in the northern salband of the dyke. The radioactive mineralization is localized in fractures striking 35-50° NE and dipping 60-65° NW. It can be followed along the fractures over 3-5 m. The gabbro-diabase is altered in the fractured zone. There

is partial recrystallization of the rock with appearance of granoblastic and lepidoblastic structures, replacement of pyroxene and plagioclase by amphibole, biotite, chlorite, albite, quartz and carbonate. The orientation of the mineralized fracture coincides with a ferrithorite-bearing conglomerate layer adjacent to the dyke. A maximal radioactivity of 370 $\mu\text{R/h}$ was observed in one of the fractures in the southern part of the dyke (fig. 2.1.4.19).

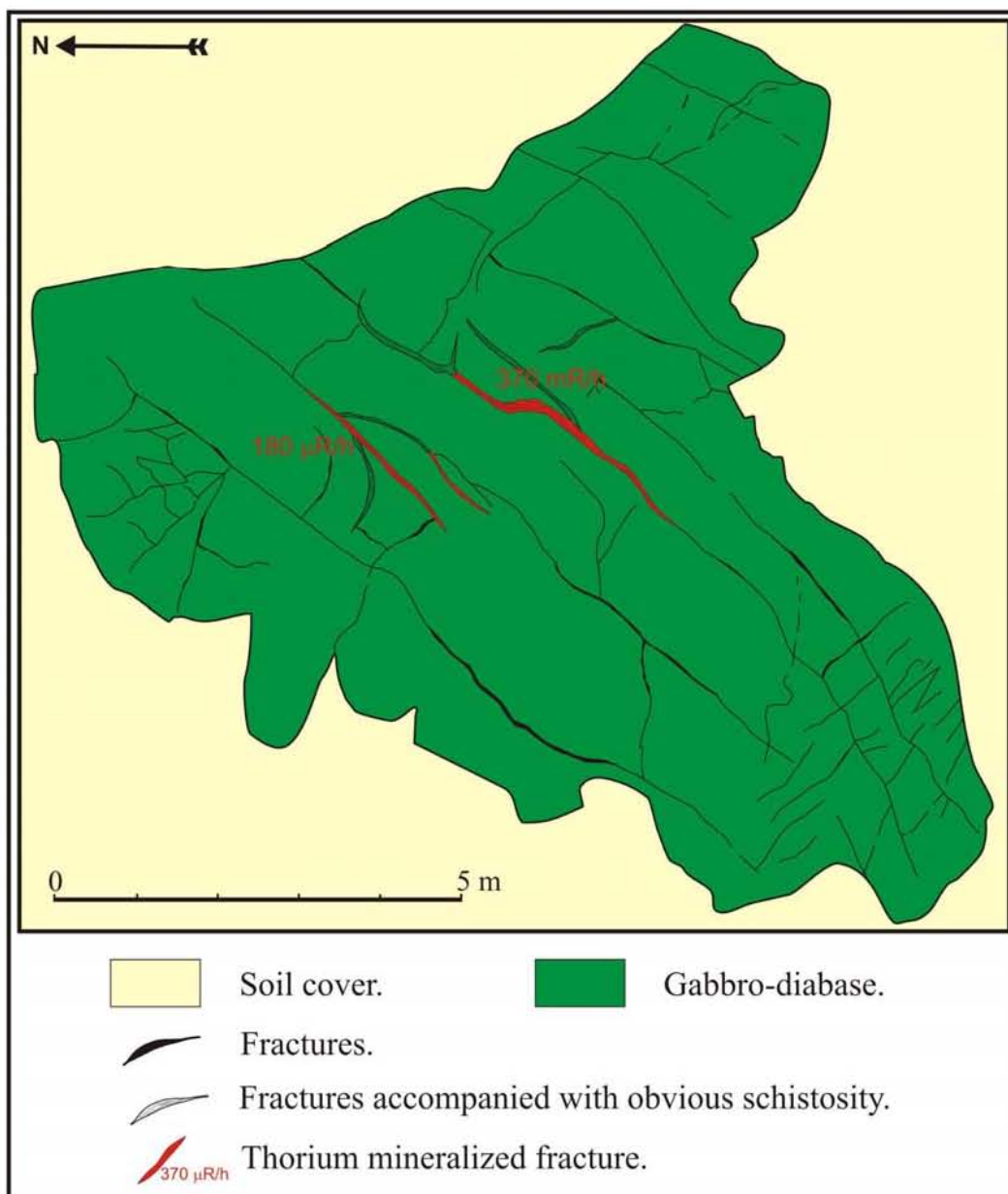


Figure 2.1.4.19. Geological map of the Dyke anomaly southern flank (after Kondakov et al., 1963).

The mineralized fractures are filled with quartz, biotite, chlorite and thorite. Primary minerals of the parent rock are totally replaced. The fracture has zonal structure, with from periphery to center:

- 1) a silicified gabbro-diabase, 1-2 cm thick;
- 2) a biotite-quartz rock with augen structure formed by rounded aggregates of quartz surrounded by sub-parallel biotite laths, 1 cm thick;
- 3) a biotite zone composed of corroded mica laths, partially replaced by chlorite, very rare quartz, 1 cm thick;
- 4) a chlorite zone with small laths of chlorite and radial aggregates, quartz and biotite are subordinated, 0.5-0.7 cm thick;
- 5) a central zone with a complex shape (fig. 2.1.4.20) composed of thorite with subordinated quartz, biotite and rare chlorite, 0.4 cm thick.

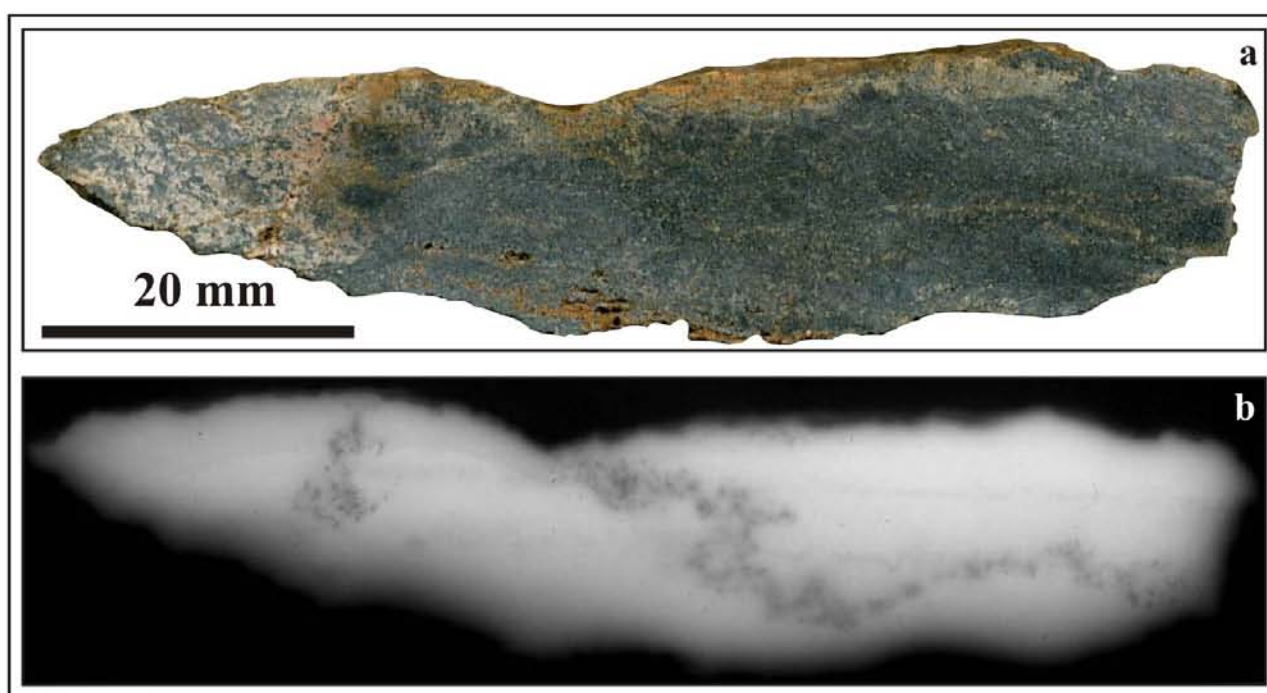


Figure 2.1.4.20. Altered gabbro-diabase from the Dyke anomaly; a – sample Jn-8; b – 30 days radiography

Paragenetic succession in the Dyke anomaly is presented in table 2.1.4.4.

Thorite crystals are of 0.2-0.7 mm size. They are often strongly altered and replaced by sulphides and latest iron hydroxides. (fig. 2.1.4.21). The chemical composition of the thorite from the Dyke anomaly is presented in Table 2.1.4.5. It is characterized by high Th contents and low U content.

Table 2.1.4.4. Ore paragenesis of the Dyke anomaly (after Polekhovsky et al., 2007).

No	Minerals	Oxide-silicate	Paragenesis		
			Sulphides	Low temperature	Supergene
1	Ilmenite	+			
2	Thorite	+			
3	Pyrite		+		
4	Chalcopyrite		+		
5	Galena		+		
6	Rutile			+	
7	Leucoxene				+
8	Anglesite				+
9	Iron Hydroxides				+

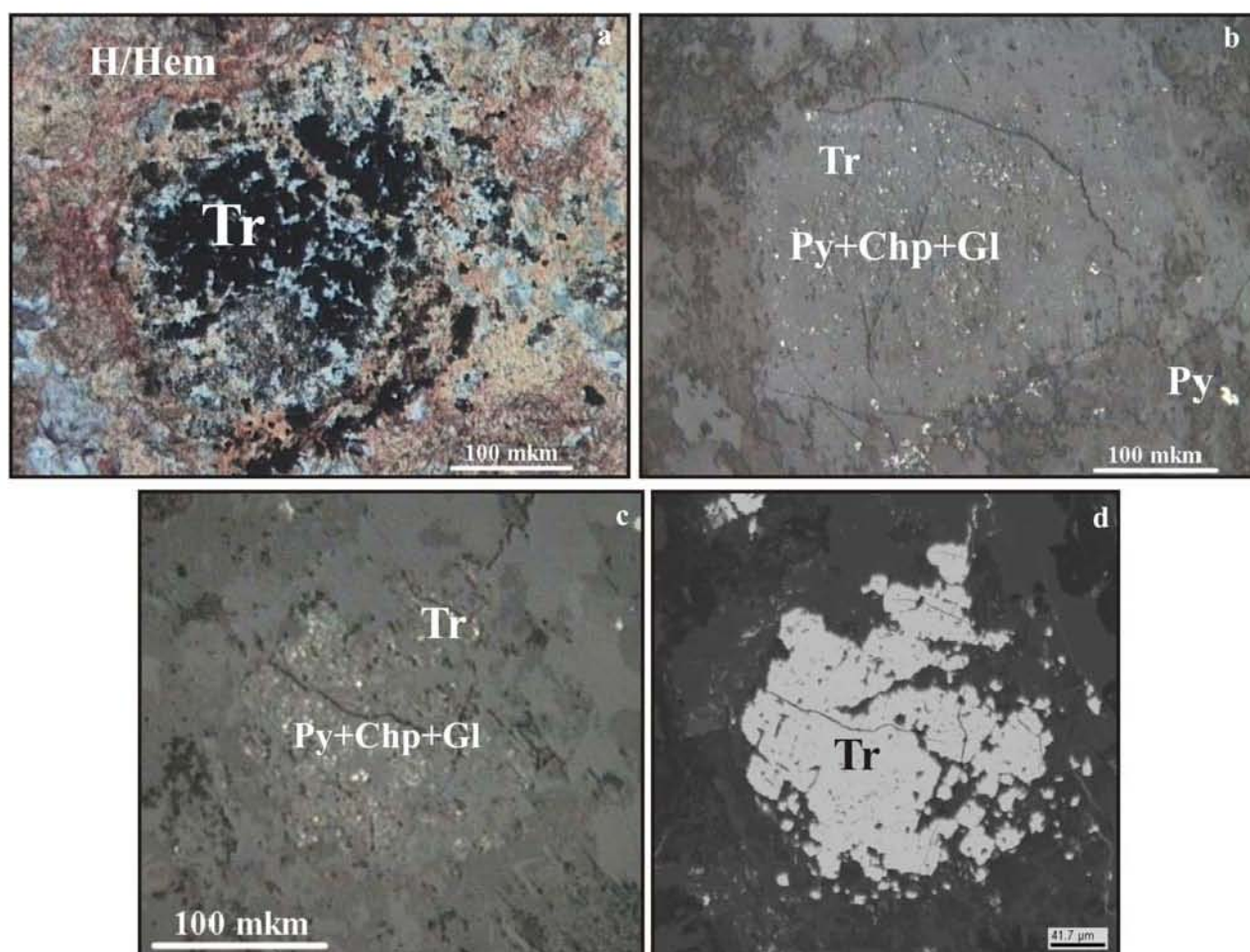


Figure 2.1.4.21. Thorite (Tr) mineralization from the Dyke anomaly; development of pyrite (Py), chalcopyrite (Chp), galena (Gl) and iron hydroxides (H/Hem) takes place, sample Jn-8: a – optical photo, polarized transmitted light; b and c – optical photos, reflected light; d – BSE photo.

Table 2.1.4.5. Chemical composition of vein-type thorite mineralization in the Dyke anomaly. Sample Jn-8. Analyzed with ABT-55 Akashi electron microprobe (Polekhovsky et al., 2007).

No	SiO ₂	UO ₂	ThO ₂	Sum
1	23,5		76,5	100,0
2	25,4	1,0	73,5	99,9
3	22,7	2,1	75,2	100,0
4	23,7	0,7	75,6	100,0

2. Uranium mineralization in the complex-ore occurrences.

There are several examples of late uranium mineralization telescoping complex-ore deposits and occurrences.

2.1. The Jalonvara complex ore deposit.

There is the Jalonvara small deposit of complex ores at the border between the Karelian domain and the Raahe-Ladoga zone (Appendix to Chapter 1, fig. 4). Uranium mineralization was discovered in 1949 and explorations (shaft and drilling) were carried out in 1950-52 and 1973-75. The deposit was visited during the present work. Mineralized rocks are not outcropping and are available in the shaft tailings only.

The Jalonvara deposit is related to the NW-striking Kuhilasvaara fault related to the Janisjarvi tectonic system. The deposit is hosted by quartz-chlorite-sericite schist (sometimes graphite-bearing), andesite-basalt and dacite metavolcanite of the Middle Lopian Jalonvara suite. These formations are underlain and cut by the Upper Lopian Jalonvara granitoid intrusion in the deposit area. The Jalonvara suite rocks are propylitized, beresitized (sericite-pyrite), silicified and argillized. Complex ore is composed of pyrite, pyrrhotite, chalcopyrite, sphalerite and magnetite. Associated uranium mineralization occurs in late fractures striking NW and in a lesser amount to the NE, and is related to the contacts of the sulphide ores with silicified zones and quartz-sericite schists. The fractures are filled with crushed host rocks, calcite, melnikovite, chalcopyrite, subordinated galena and U minerals. The length of the mineralized parts in the fractures is 5-9 m and 0.05 - 0.2 m thick. Ore nests and columns up to 1 m thick occur in the intersection of NW- and NE fractures. The total extension of the U-mineralized zone is 40 m along the strike and 50 m along the dip. Average U content is 3 700 ppm over 0.5 m, with a maximum of 34 280 ppm over

0.2 m. On base of available data (Guptor and Ufa, 1953; Polikarpov et al., 1976) it can be very approximately ranged about 10 tons.

Polikarpov et al. (1976) and Grigorieva (1977) showed that the U mineralization occur as pitchblende associated with antraxolite, coffinite and U-bearing leucoxene. Because of strong supergene alteration, no primary uranium mineralization has been found in the tailings, but heterogeneous admixtures only (fig. 2.1.4.22). Electron microprobe data suggest two types of admixtures (Table 2.1.4.6). The first one may correspond to hydrocoffinite aggregate predominating over Fe-hydroxides. The second mineral phase develops at the edges and in microcracks of pyrite grains. Their size of 3-5 μm , does not allow getting a precise chemical composition.

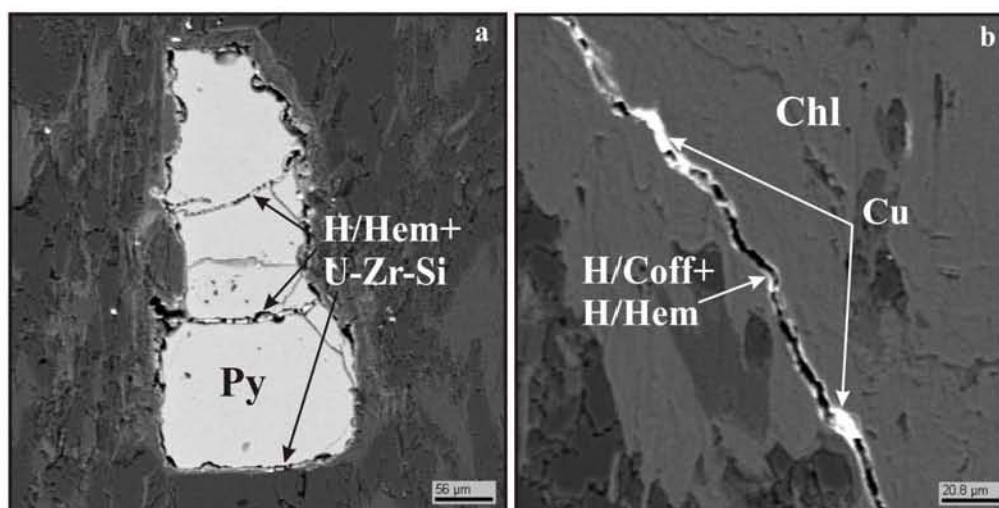


Figure 2.1.4.22. Secondary uranium mineralization from the Jalonvara deposit, BSE photos: a – sample JI-1, uranium-zirconium-silicate mineral phase (U-Zr-Si) associated with hydrohematite (H/Hem) in the veinlets and periphery of the pyrite (Py) grain; b – sample JI-2, hydrocoffinite+iron hydroxides (H/Coff+ H/Hem) and Cu mineralization in the veinlet cutting intensively chloritized (Chl) rock.

Table 2.1.4.6. The Jalonvara complex ore deposit. Vein-type uranium mineralization.

Analyzed with ABT-55 Akashi electron microprobe (Polekhovsky et al., 2007).

No	Sample	SiO ₂	TiO ₂	Al ₂ O ₃	Fe ₂ O ₃	MnO	MgO	UO ₂	PbO	ZrO ₂	SO ₃	Sum
ADMIXTURE No 1												
1	JI-2	17,7		10,4	19,0	0,4	5,9	28,5	2,8			84,7
2	JI-2	9,0	0,3	4,1	11,6	0,2	1,7	36,0	2,5			65,4
3	JI-2	7,9		3,7	11,1	0,2	2,2	45,0	4,0			74,1
ADMIXTURE No 2												
4	JI-1	11,8		3,0	23,9		0,3	22,7	0,9	13,3	8,0	83,9
5	JI-1	10,6		3,2	29,4		0,4	18,0	0,4	11,4	9,0	82,4
6	JI-1	7,2		4,9	35,5		0,5	11,4	0,7	6,2	7,7	74,1

Age of the complex ore is ranged 2200-1850 Ma (dating of galena). For uranium mineralization different ages were obtained: 1800, 1600-1400 and 600 Ma. The accuracy of these data is not satisfactory.

2.2. The Prolonvara complex ore-showing.

The Prolonvara ore-showing is located 5 km to the NW of the Jalonvara deposit along the Janisjarvi fault zone and is related to breccias and cataclasites. U mineralization at Prolonvara was discovered and studied by the same exploration project as for the Jalonvara deposit. The showing is hosted by Jatulian quartzitic sandstones, phyllite schists of the Jangozero suite, dolomites and arkoses of the Tulomozero suite. A Mn mineralization (manganite, pyrolusite, psilomelane) is associated with barite on the walls of cavities filled with drusy quartz and in lenticular concretions 15-40 cm large. Native Cu, hematite and pyrite occur in the cement of the arkoses. The schists host lenses with fine hematite impregnation. Age of the complex ore is about 1840 Ma.

U mineralization occurs in fractures in the quartzitic sandstones, phyllite schists, rarely – dolomites. Morphology of the mineralized zones has not been recognized surely. It seems to form a system of 25 m long ore lenses along a local N-S fracture. U content is 100-400 ppm over 0.25-2.5 m thickness (in the drilling), up to 2600 ppm over 0.4 m. U resource is small. U mineralization is composed of pitchblende, coffinite, hypopitchblende, sooty pitchblende and other minerals (Polikarpov et al., 1976).

2.3. The Faddein-Kelya complex ore deposit.

The Faddein-Kelya deposit of complex ores (Au, Cu, Pb, Zn) is telescoped by U mineralization in the Tulomozero depression at the edge of the Karelian domain (General Appendix 1, fig. 1 and 5). It was discovered and mined in XIXth, beginning of XXth centuries. In the fifties U mineralization in the deposit was studied by “Nevskgeologia”. The deposit was recognized with a small pit and a few drill holes. Now the U mineralization is no more available at the surface.

The Faddein-Kelya deposit is located in 5 km to NW from the Salmi granite in the vicinity of the Janisjarvi fault zone. The mineralization is controlled by the intersection of N-S and W-E fractured zones cutting Jatulian and Saamian-Lopian formations. Pitchblende was discovered in small veinlets in an E-W fracture zone. U content is 400 ppm in average, up to 40 000 ppm (Lobanov and Bryzgalova, 1956). Discovered occurrences of U mineralization are very local, but the ore-showing have not been studied sufficiently (Skorospelkin, 2002).

2.4. Uranium ore-showings of the Pitkjaranta-Kitelya ore district.

There are series of complex-ore deposits in the Pitkjaranta district – Pitkjaranta, Kitelya, Hopunvaara (Sn, Zn, Cu, Fe, Be, fluorite) partly mined in the past (Appendix to Chapter 1, fig. 1). The area is composed of AR-PR₁ granite-gneiss domes enveloped by amphibolites and carbonate rocks of the Ludicovian Pitkjaranta suite. Interdome formations are composed of the Kalevian Impilakhti suite micaschists (sometimes graphite-bearing). Late Svecofennian pegmatites of the Pitkjaranta granite complex are widespread. Aplite and pegmatites correspond to the latest phases of the Salmi rapakivi granite intrusion. The complex-ore deposits are localized in exo-contact zone of the Salmi massif. All rocks of the area have suffered of alterations related to the emplacement of the granite: greisenisation, albitization, chloritization and silicification.

Complex ores are hosted by carbonates and skarns of the Pitkjaranta suite. Molybdenite from these deposits was dated at 1750-1820 Ma (Re-Os analysis, Sterm et al., 1996), but ore-hosting skarn and greisen give Lower Riphean ages (1546±28 and 1492±25 Ma from Sm-Nd analyses, Larin et al., 1991). So, the origin of these deposits is presumed to be a multiphase process referred to two events: the Svecofennian orogenic granites and Lower Riphean Salmi massif emplacement.

U mineralization is considered as being the latest one, because it is related to fractures cutting all formations and complex ores. It occurs as small (1-5 m long, 0.25-1.5 m thick) lenses and nests in deformed granite-gneiss and feldspar amphibolites of the domes, also in thin (0.05-3 mm thick) cleavage fractures in aplite pegmatites of the Salmi intrusion. U mineralization is accompanied by chloritization, silicification, fluoritization and sericitization of the host rocks.

Average U content in the dome formations is 110-580 ppm, maximum 2 900 ppm over 0.95 m. In the fractures cutting aplitic granites referred to the Salmi massif, U content is 380-1150 ppm over 1-3 mm, Th content is 270 ppm. U mineralization with contents up to 25 000 ppm was found in skarns from the tailings of old shafts (Korotaev et al., 1978).

High content of radon in the ground water has been detected.

Bryzgalova et al. (1956) described several U mineral phases differing for different host rocks: uraninite, pitchblende, uranophane occur in the granite-gneiss; sooty pitchblende and U-bearing fluorite are typical Salmi massif granite veins.

In the radioactive samples of the altered Pitkjaranta suite carbonate rocks obtained during the present work from the Bekk shaft of the Hopunvaara ore-showing tailings, U mineralization has not been detected, but disseminated and chained ferrithorite concentrations (fig. 2.1.4.23 and 2.1.4.24). The ferrithorite composition (Table 2.1.4.7) is rich in Y and P.

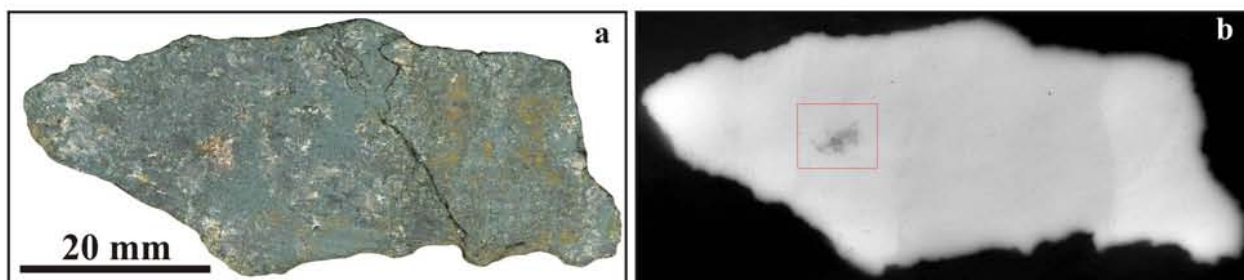


Figure 2.1.4.23. Low-grade ferrithorite mineralization from the Hopunvaara complex-ore deposit: a – sample BV-1 of altered chlorite-carbonate rock; b – 30-days radiography, spot of increased radioactivity is red outlined.

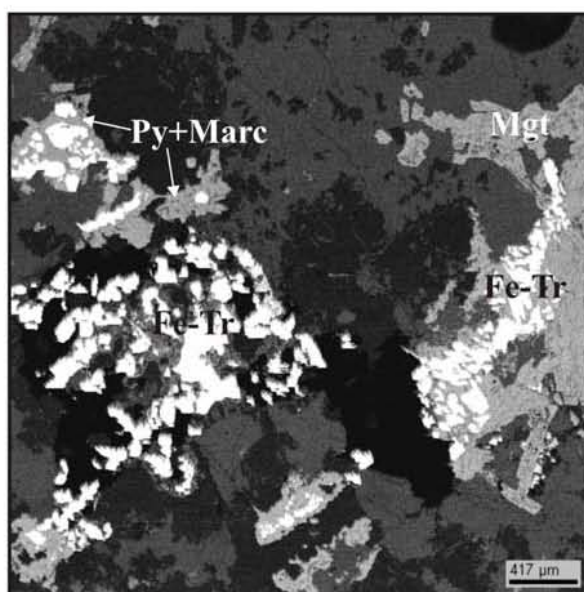


Figure 2.1.4.24. Ferrithorite (Fe-Tr) impregnations associated with pyrite (Py), marcasite (Marc) and magnetite (Mgt) from the Hopunvaara deposit, sample BV-1, BSE photo.

Table 2.1.4.7. The Hopunvaara complex ore deposit. Ferrithorite from veins. Sample BV-1. Analyzed with ABT-55 Akashi electron microprobe (Polekhovsky et al., 2007).

No	SiO ₂	Fe ₂ O ₃	ThO ₂	Y ₂ O ₃	P ₂ O ₅	Sum
1	13,3	14,9	44,9	5,6	2,0	81,3
2	15,1	8,7	50,8	6,9	2,2	84,7

3. Late vein-type uranium mineralization in other type of uranium occurrences.

Subordinated overprinted vein type uranium mineralization has been observed in other types of Palaeoproterozoic U occurrences: in granite-hosted ones (the Korennoye and the Raskenjarvi ore-showings) and in the Ludicovian carbonate rocks (the Mramornaya Gora and the Mramorny Kombinat ore-showings). These examples are described in dedicated paragraphs. Specific fracture-bound U mineralization in sericite-quartz-albite alteration zones (Puttummyaki, Hirsimyaki, Korennoye ore-showings) hosted in tectonized intradome migmatites can be

presumed to be of hydrothermal origin, but for some of them to vein-type occurrences. Additional study is however needed. In this thesis such kind mineralization is considered in Chapter 1, Paragraph 1.1 “Granite-hosted uranium occurrences”. The Riphean basalts of the Salmi depression also host late uranium mineralization related to fracture zones (the Karku deposit area, the Kotalakhti ore-showing). It will be described in Chapter 2.

4. Generalized geological characteristics of vein-type uranium mineralization of the Northern Ladoga area.

In spite of their diversity, vein-type uranium mineralization of the Northern Ladoga area, share several characteristic geological parameters.

1. Tectonic control.

All U vein type (and Th) occurrences of the area are related to long-living brittle tectonic structural zones. The mineralization usually occurs not in major fault zones but in second-order associated structures. The striking of the structures controlling 20 U occurrences (including late vein type mineralization in the complex-ore deposits and in other types of U occurrences is presented in figure 2.1.4.25.

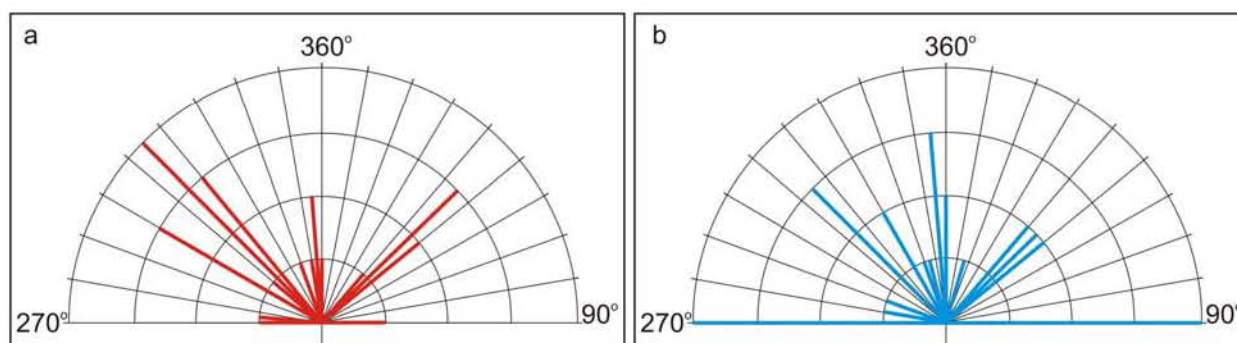


Figure 2.1.4.25. Diagrams of striking of ore controlling brittle tectonic dislocations of vein-type uranium occurrences of the Northern Ladoga area: a – regional faults; b – local dislocations.

The predominance of NW-striking regional fault zones (Janisjarvi and Ruskeala) as U-controlling tectonic structures is demonstrated in figure 2.1.4.25a. Notable that the Kotalakhti vein type U showing in the Riphean basalts is located in the NW-striking Ruskeala fault zone as well.

Local U-controlling tectonic structures have more diverse orientation (fig. 2.1.4.25b), but most of them are dominantly NW. Specific kinds of structures are the fracture zones occurring at the peripheries of the granite-gneiss domes. These structures result from the emplacement of partly melted dome material into plastic crystalline formations of the frame (Letnikov et al., 2000). U

enrichment of these zones was described by Skorospelkin (1974), Grigorieva (1977) and Korotaev et al. (1978). Fracture-bound U mineralization in quartz-feldspar pegmatoids are related to these zones (see Paragraph 1.1 of Chapter 1, the Puttummyaki, Hirsimyaki and Korennoye ore-showings).

It is important to notice, that ancient fault zones usually correspond to depressions in the present topography; therefore they are often concealed under Quaternary sediment cover.

II. Petrologic control.

Vein type mineralization often has an affinity with U-enriched bedrocks, although it is not systematic. Most of the discovered vein type U occurrences of the Northern Ladoga area are hosted by Ludicovian formations (Fig. 2.1.4.26). The main one, the Varalakhti ore-showing, is hosted by breccias zone within the Pitkjaranta suite amphibolites.

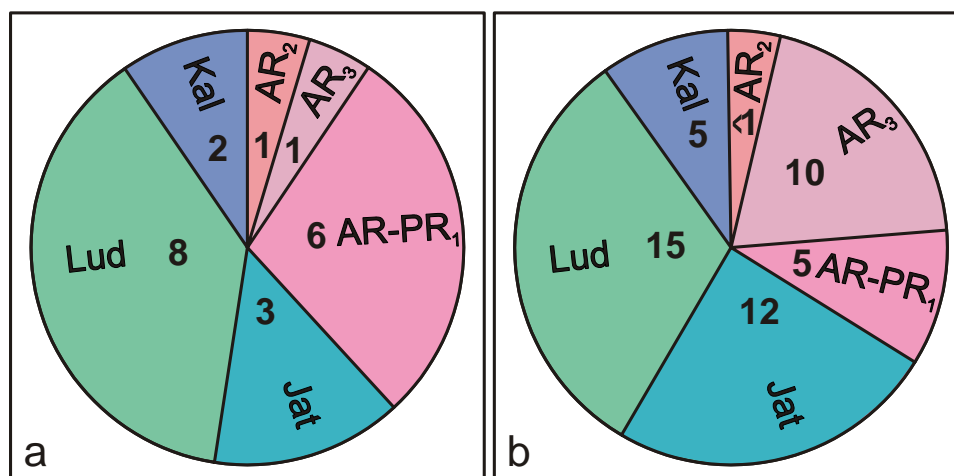


Figure 2.1.4.26. Distribution of different type uranium occurrences of 20 vein-type uranium occurrences of the Northern Ladoga area according to the host rocks: AR₂ – granite-gneiss of the Karelian domain; AR₃ – quartz-chlorite-sericite schists and quartzites of Jalonvara suite; AR-PR₁ – granitoids of the domes; Jat – Jatulian sediments; Lud – Ludicovian formations; Kal – Kalevian mica schists. NB: Karinmyaki ore-showing is hosted as Ludicovian as Kalevian formations and is referred to both sectors; a – number of occurrences; b – approximate total resources.

Many occurrences show affinity with granites of different ages: Upper Lopian (Jalonvara), Svecofennian (Karinmyaki, Korennoye) and Lower Riphean (Kitelya, Pitkjaranta, Hopunvaara). Some of them are hosted by granitoids (intragranitic subtype – Korennoye), some are hosted by enclosing metamorphic formations (perigranitic subtype – Karinmyaki, Jalonvara); many occur in both kinds of rocks (Kitelya, Pitkjaranta, Hopunvaara).

A smaller number of U occurrences are hosted by Jatulian formations of the Janisjarvi fault zone and the Tulomozero depression, but some of them are relatively big as the Faddein-Kelya and Prolonvara ones, explaining why the total resources of these units is significant.

Kalevian sediments are the least representative with respect to discovered U occurrences (not only vein type ones), but it is noteworthy that they commonly outcrop badly because of their low resistance to erosion.

III. Ore mineralogy.

Vein type uranium occurrences are mostly composed of pitchblende, less of coffinite and are referred to low-middle temperature metallogenesis. Rare rudimental uraninite was identified in the Karinmyaki ore-showing. Carbon-associated pitchblende mineralization (pitchblende-antraxolite) was described in the Jalonvara complex-ore deposit (Grigorieva, 1977). Exhumation of the mineralized rocks led to the development of hexavalent supergene U mineralization.

All available isotopic age constrains on the vein type uranium mineralization, including the overprinted granite-hosted ones and U-Pb occurrences are summarized in Table 2.1.4.8. Age determinations were undertaken since the seventies, but only the results of Anderson (1990) and those of the present study are reliable.

Table 2.1.4.8. Isotopic age constrains of vein-type U mineralization of the Northern Ladoga area.

Occurrence	Host rock	Mineral	Method	n	Age, T _o , T _m , Ma	Reference
Varalakhti	Quartz-carbonate breccias in amphibole schist of the Pitkjaranta suite (Ludicovian)	pitchblende	U-Pb, SIMS	5	1538±180, 243±430 or 1460±26 (constrained to 0)	This study
		pitchblende	U-Pb, TIMS	6	1588±946, ~890 or 1510±20, ~100 and 1420±20, ~ 0	Anderson, 1990
Karinmyaki	amphibole schist of the Pitkjaranta suite (Ludicovian) and biotite gneiss of the Ladoga group (Kalevian)	pitchblende	Pb-Pb	?	1640±20	Gromov et al., 1981
Jalonvara	Fracturated quartz-sericite-chlorite schist of the Jalonvara suite (Lopian)	pitchblende-antraxolite	?	?	1800±50	Grigorieva, 1977
			?	4	1600-1400	
		coffinite and hydropitchblende	?	?	600±50	
Korennoye	Quartz veinlet in anatectic granite of the granite-gneiss dome	pitchblende	U-Pb, SIMS	9	469±180, 127±260	This study
Mramornaya Gora	Fracturated marble of the Pitkjaranta suite (Ludicovian)	pitchblende	U-Pb	8	396±21, -21±140	This study
Mramorny Kombinat	Fracturated marble of the Pitkjaranta suite (Ludicovian)	pitchblende	U-Pb, TIMS	7	1221±64, 366±41	Anderson, 1990

According to these data, Lower-Middle Riphean (ca 1600-1200 Ma) and Palaeozoic (ca 500-350 Ma) ore-producing events can be distinguished. The first event can be correlated with the

early stages of the Riphean (Dalslandian) activation, the second one with the Caledonian orogeny or early phases of Hercynian orogeny.

IV. Grade of the occurrences.

Vein-type ore mineralization is characterized by quite high U contents: 1000 ppm in average. Maximum content is 34 800 ppm U. However, the resources of the discovered occurrences are low and correspond to several t U maximum. Total resources of the vein type occurrences of the Northern Ladoga have not been evaluated precisely, but approximately it can be estimated to 50 tons.

Conclusion.

The quite high U contents and the diversity of vein type uranium occurrences of the Northern Ladoga area make them one of the most attractive prospecting targets. From 1948 to 1981 limited exploration of vein type uranium mineralization was undertaken by “Nevskgeologia” in the Northern Ladoga area, but no economic deposit has been found so far.

Discovery of vein type deposits is difficult because they are related to tectonic zones that are often strongly eroded and concealed under thick Quaternary cover. In addition the basement is covered by Riphean and V-PZ platform sediments in the southern part of the Ladoga region. That is why some of the vein-type uranium occurrences of the Ladoga region may be still undiscovered. Promising zones for vein-type uranium mineralization will be given in Part 3.

Conclusion to Chapter 1.

Generalized characteristics of the basement hosted U occurrences.

Diversity of uranium metallogenesis has been discovered in the Northern Ladoga area by over 50-years of prospects carried out by “Nevskgeologia”.

Uranium occurrences of the region previously have been combined into four groups in accordance to their structural features and stratigraphic-petrologic reference:

1. granite-hosted U-Th occurrences;
2. Th-U anomalies in the Jatulian quartzites;
3. U-P in carbonate rocks of the Ludicovian Pitkjaranta suite;
4. vein-type (fracture-bound) U occurrences in different lithologies.

Generalized characteristic of these occurrences is presented in followings items.

1. Petrologic reference.

The basement-hosted uranium occurrences of the Northern Ladoga can be subdivided into eight groups in accordance to its stratigraphic and petrologic reference:

1. hosted by Middle Archaean gneiss-granite;
2. hosted by Upper Archaean (Lopian) granitoids;
3. hosted by Jatulian quartzites and carbonate schists;
4. hosted by late Svecofennian anatectic granites of the domes;
5. hosted by late Svecofennian intrusive granites;
6. hosted by Ludicovian carbonate rocks;
7. hosted by Kalevian mica schists;
8. hosted by Lower Riphean rapakivi granites.

Following diagram introduces approximate distribution of resources of the Northern Ladoga uranium occurrences in depends with hosting lithologies (Fig. 2.1.5.1). Approximate character of this estimation is caused by not precise evaluation most of the occurrences.

As it is demonstrated at the diagram, most of the uranium occurrences are hosted by granitoid formations of the granite-gneiss domes, especially tectonized migmatites of the dome periphery and pegmatoids.

Ludicovian formations host numerous U-P occurrences and significantly contribute into total uranium resource of the Northern Ladoga area as well.

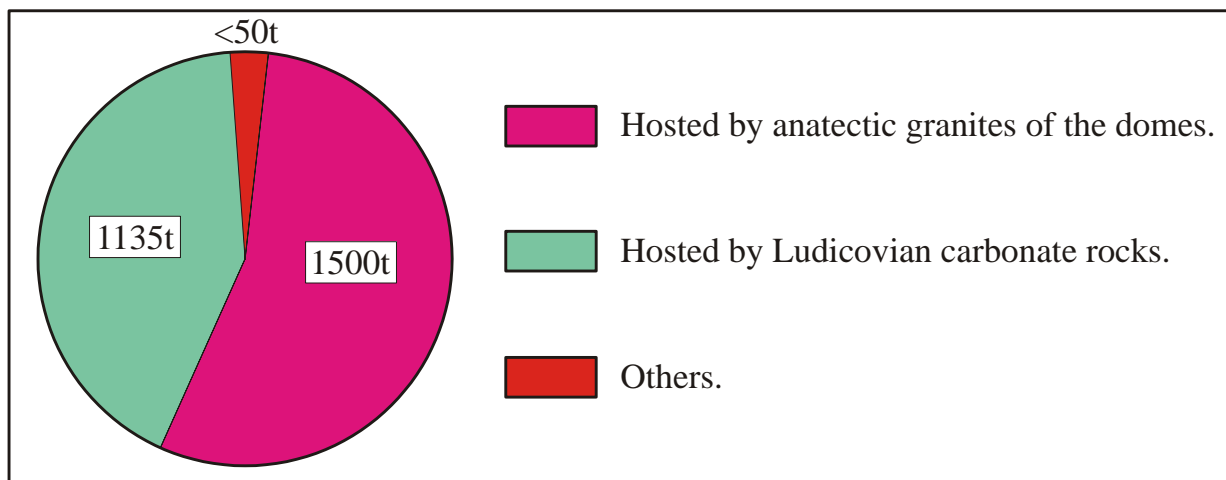


Figure 2.1.5.1. Distribution of basement-hosted uranium ore resources of the Northern Ladoga area according to the host rocks.

Other formations host much subordinated uranium resource composed mainly of fracture-bound (veined) mineralization. Resource of the Jatulian sediments also includes very minor part of conglomerate-hosted Th-U concentrations.

II. Tectonic control.

The most uranium enriched tectonic structure of the Northern Ladoga area is the Ruskeala fault zone of NW striking. Most of U-P occurrences hosted by the Ludicovian carbonate rocks, many granite-hosted U occurrences and some of veined occurrences are related to this zone. The occurrences are of different types and ages. Direct genetic link between dislocations of the Ruskeala zone and uranium mineralization not always can be distinguished, but undoubted spatial coincidence is an evidence of their affinity.

The Janisjarvi fault zone (of NW striking as well) is less saturated in discovered uranium occurrences, but many previous researchers notified significant contamination of bedrocks of this zone by foreign uranium (Polikarpov et al., 1976; Grigorieva, 1977 etc). Another important feature is that veined uranium mineralization is the most common for this zone; pebble-conglomerates are much subordinated. It is an evidence of significant and possibly multiply hydrothermal redistribution of uranium in the Janisjarvi fault zone.

Local dislocations of peripheral parts of the granite-gneiss domes often controls uranium occurrences in metasomatic granites. The most saturated in such kind uranium occurrences is the Mursula dome cut by the Ruskeala fault zone.

NE-striking faults are the most favorable for localization of veined uranium occurrences of other tectonic dislocations of the Ladoga region.

III. Age.

There are no evidences of uranium ore deposition during Archaean and early Palaeoproterozoic in the Ladoga region. Although there are uranium occurrences hosted by Archaean basement in the Karelian domain, their origin is presumed to be referred to the Svecofennian event.

Uranium mineralization with the most ancient proven age has been discovered in the Jatulian quartz conglomerates. Low-grade uranium concentrations occur in refractory accessories and presumed to be of synsedimentary genesis. If it so, age of Th-U anomalies of the Kuhilaslampi area is ranged in 2.3-2.1 Ga.

Main bulk of resource of basement-hosted uranium occurrences of the Northern Ladoga area had been formed during period 2.0-1.79 Ga referring to the Svecofennian tectonic event. U-P mineralization of occurrences hosted by the Ludicovian phosphatic carbonate rocks in general was formed during those deposition (about 2.0-1.9 Ga) and following metamorphism (not later than 1.85 Ga). U-Th-REE granite-hosted mineralization has been formed during late stages of the Svecofennian orogeny and post orogenic processes in 1.82-1.77 Ga.

The basement-hosted veined uranium mineralization was partly formed during the Lower-Middle Riphean tectonic activation in period 1.6-1.2 Ga.

Late indications of uranium redistribution and deposition are related to Caledonian and Hercynian activations and ranged in 0.5-0.35 Ga. It is presented by synsedimentary and hydrogenous mineralization in the V-PZ platform cover and hydrothermal fracture-bound mineralization in basement formations and Riphean volcanites of the Northern Ladoga.

IV. Typology.

Most of considered basement-hosted uranium occurrences can be classified accordingly to the IAEA classification of U deposits (Dahlkamp, 1993), only those in anatectic granites have uncertain typological reference because of their complex genesis. In the present study they are related to anatexite-hosted occurrences. Thus, there are five types of uranium occurrences in the Northern Ladoga area:

1. Th-U anomalies in quartz-pebble conglomerates;
2. anatexite-hosted occurrences;

3. anomalies in intrusive granites;
4. Synmetamorphic U-P occurrences (metamorphosed phosphorite);
5. Vein-type occurrences.

V. Grade and total resource of the occurrences.

Total resources of different type basement-hosted uranium occurrences of the Northern Ladoga area are presented in the Figure 2.1.5.2.

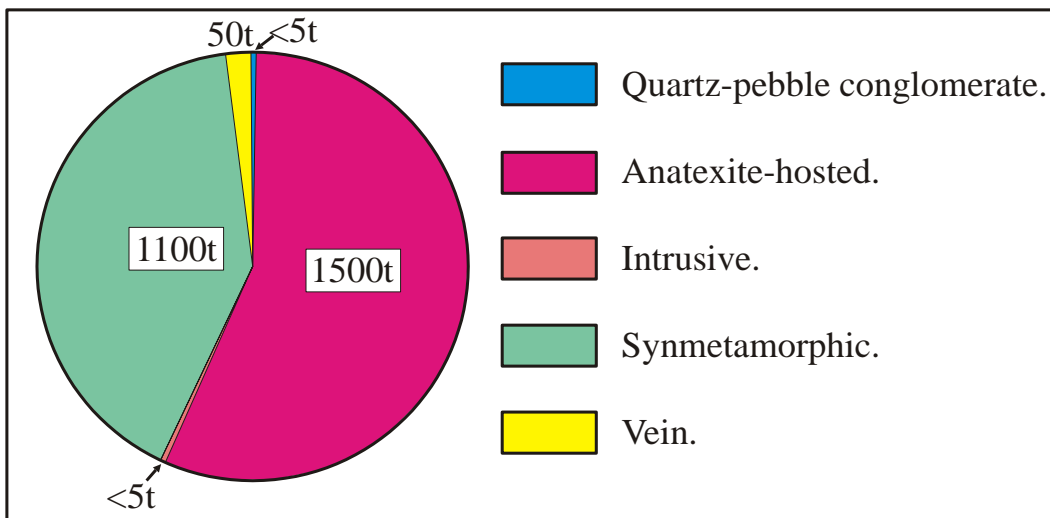


Figure 2.1.5.2. Typological distribution of the basement-hosted uranium ore resources of the Northern Ladoga area.

Most of the basement-hosted uranium resource in the Northern Ladoga of the occurrences are related to anatectic granites of the granite-gneiss domes and especially concentrated in zones of tectonized migmatites. Average uranium abundance in these occurrences is 500 ppm, in mineralized zones of sodium alterations – up to 17 800 ppm. Resource of an occurrence reaches few hundreds tons, total resource of this type is the biggest for basement hosted occurrences of the Northern Ladoga – about 1 500 tons.

U-P occurrences in the Ludicovian formations of synsedimentary-metamorphogenic origin also significantly contribute into total uranium resource of the Northern Ladoga area. Resource of single occurrence is less 200 tons and uranium content is just 400 ppm in average, but local enrichment up to few percent have been revealed in late breccias zones.

Veined uranium mineralization is widespread in the Northern Ladoga area, but usually uranium is a by-product of non-radioactive complex ores, or late uranium-bearing veins are related to previous uranium occurrences of other types. Independent uranium occurrences of

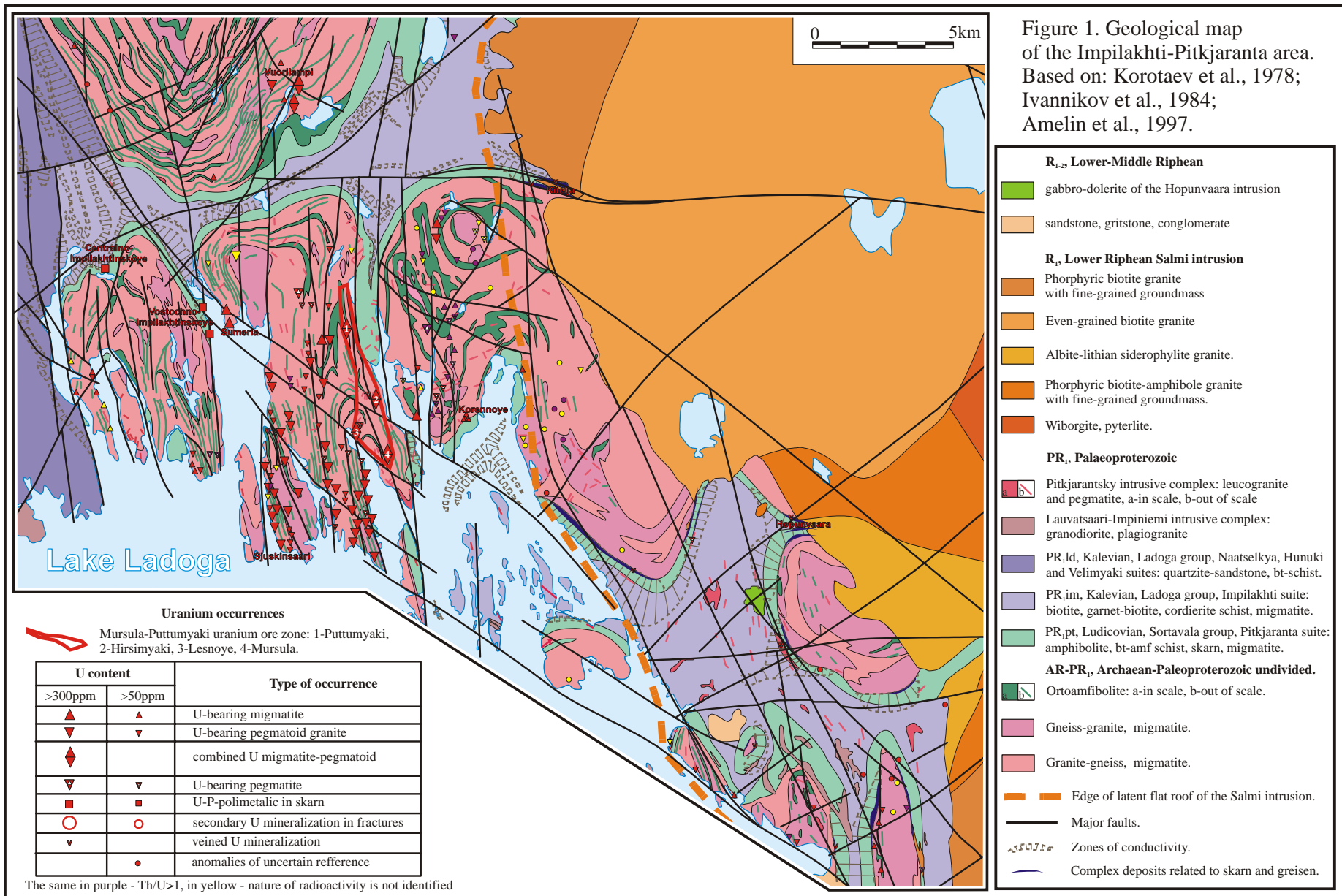
vein-type are rare. Despite of quite common high uranium content (1000 ppm in average, maximum – up to 34800 ppm), resource of single vein-type uranium occurrence and total resource of the type is low in the Ladoga region. Peculiarity of the vein-type mineralization, especially its reference to fault zone usually eroded and concealed under Quaternary, leave some chance for undiscovered vein-type deposits in the Ladoga region.

All intrusive-type uranium occurrences of the Northern Ladoga area are ranged as anomalies only and have no significant importance as they are.

The Th-U bearing Jatulian quartz conglomerates occur only in pericratonic depressions along the Janisjarvi fault zone. They are enriched in Th-bearing accessories, U content is very low and total resource of this type is unimportant.

Thus, of all considered basement-hosted uranium occurrences, only the vein-type mineralization has some economic potential in the Ladoga region. Fracture-bound uranium discovered in the Riphean formations of the Salmi depression (see Chapter 2) is an additional positive indication.

**APPENDIX
TO CHAPTER 1**



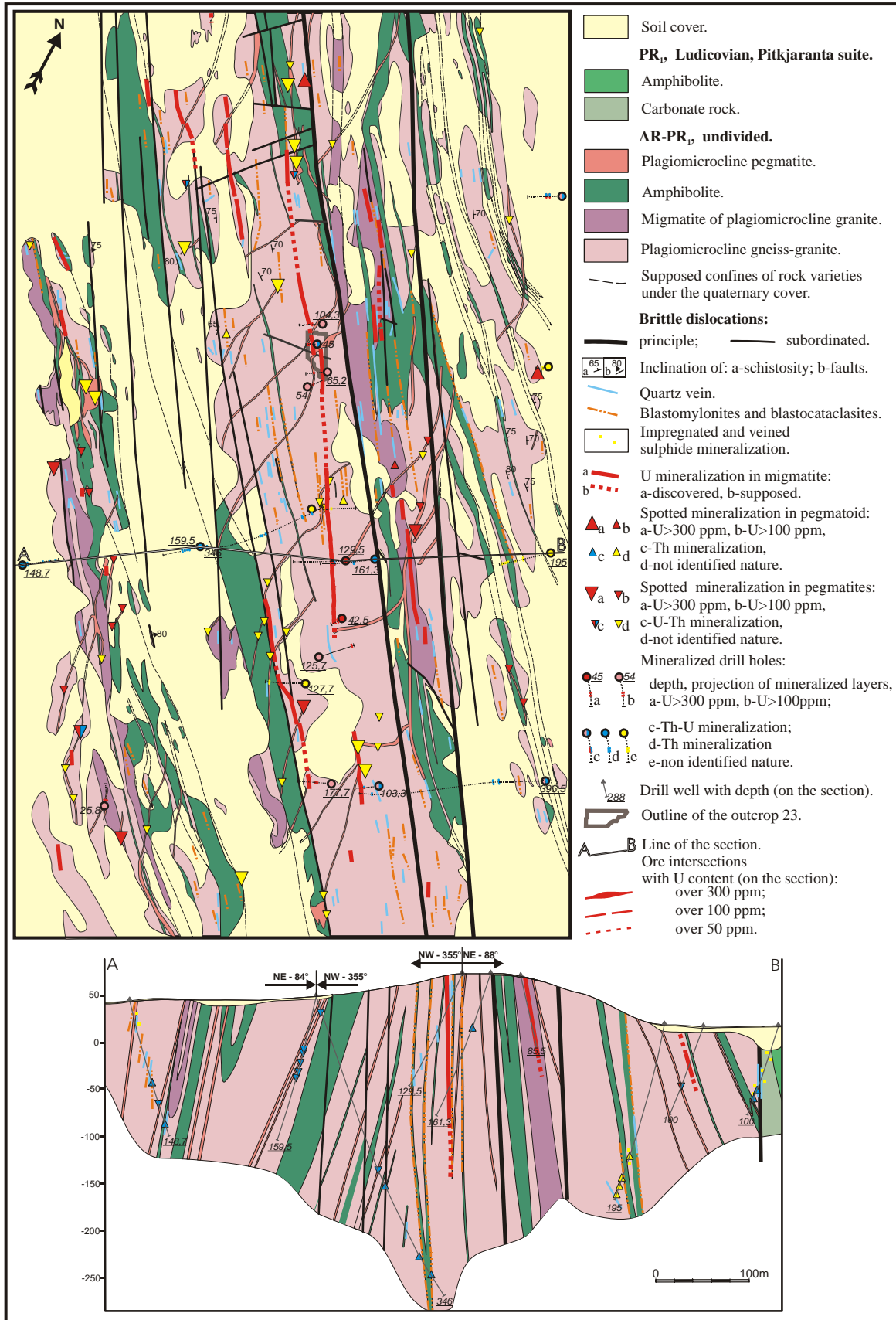


Figure 2. Geological map and section of the Puttummyaki ore-showing (part).

Based on Korotaev et al., 1978.

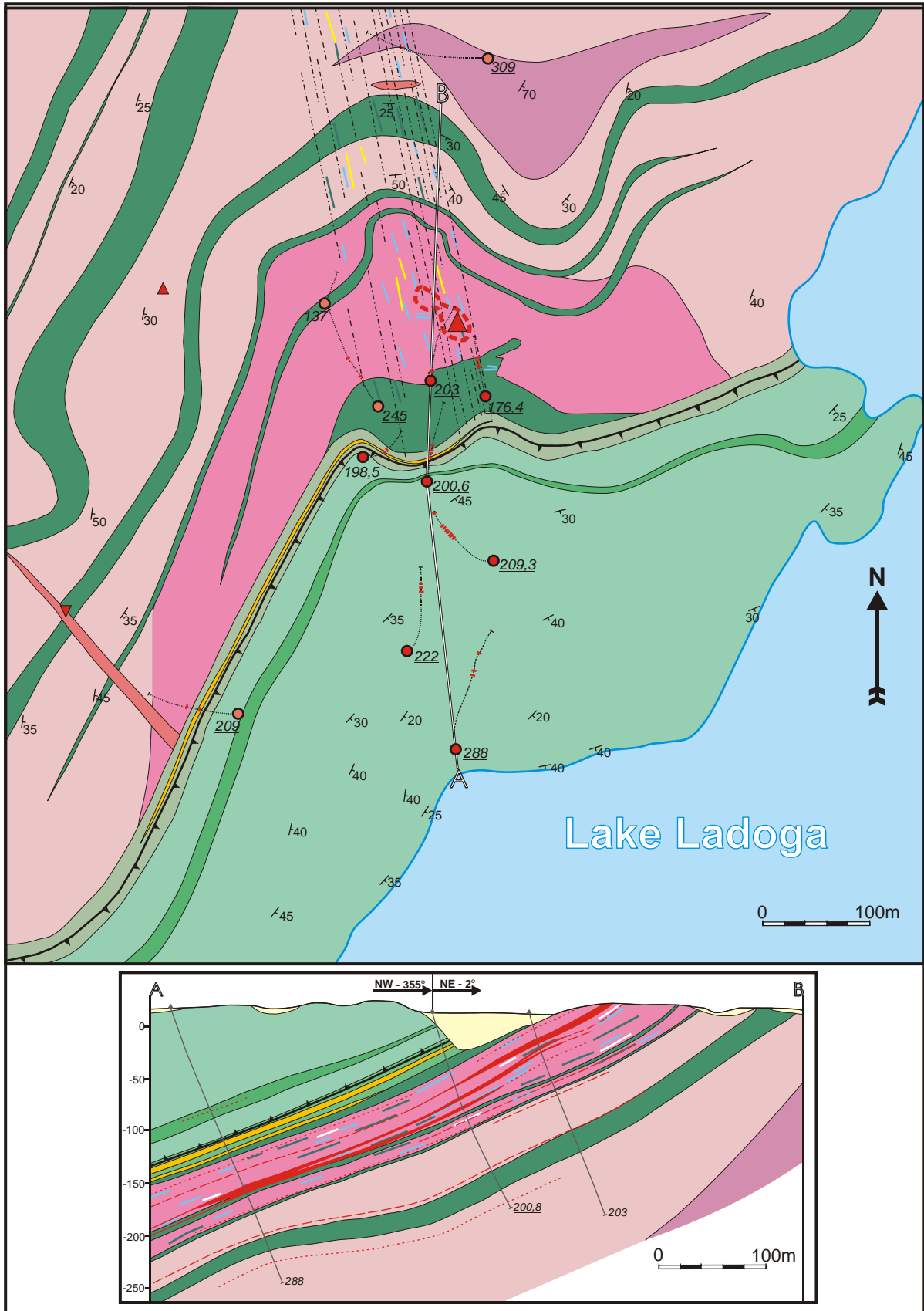


Figure 3. Geological map and section of the Korennoye ore-showing.

Based on Korotaev et al., 1978.

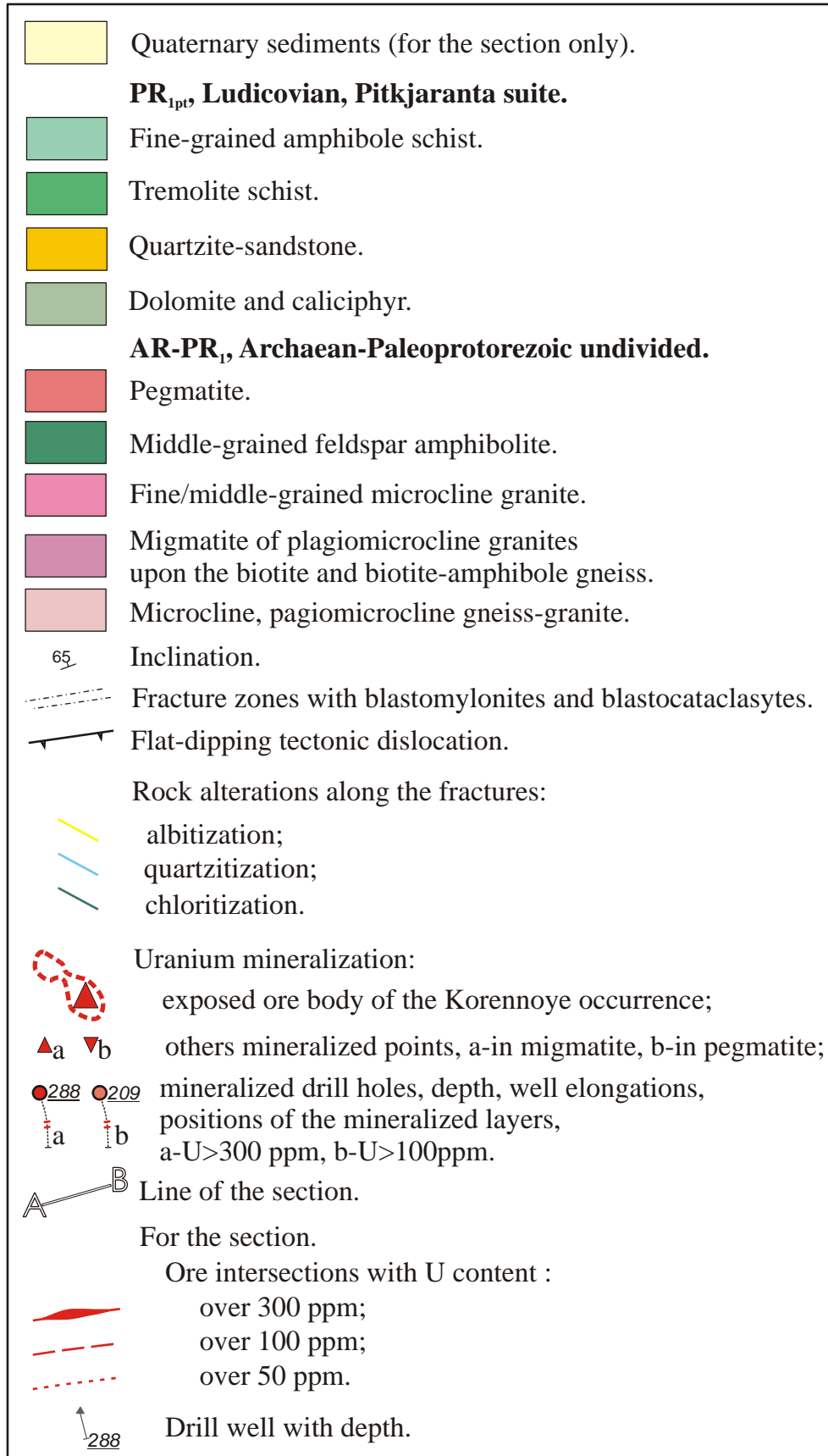
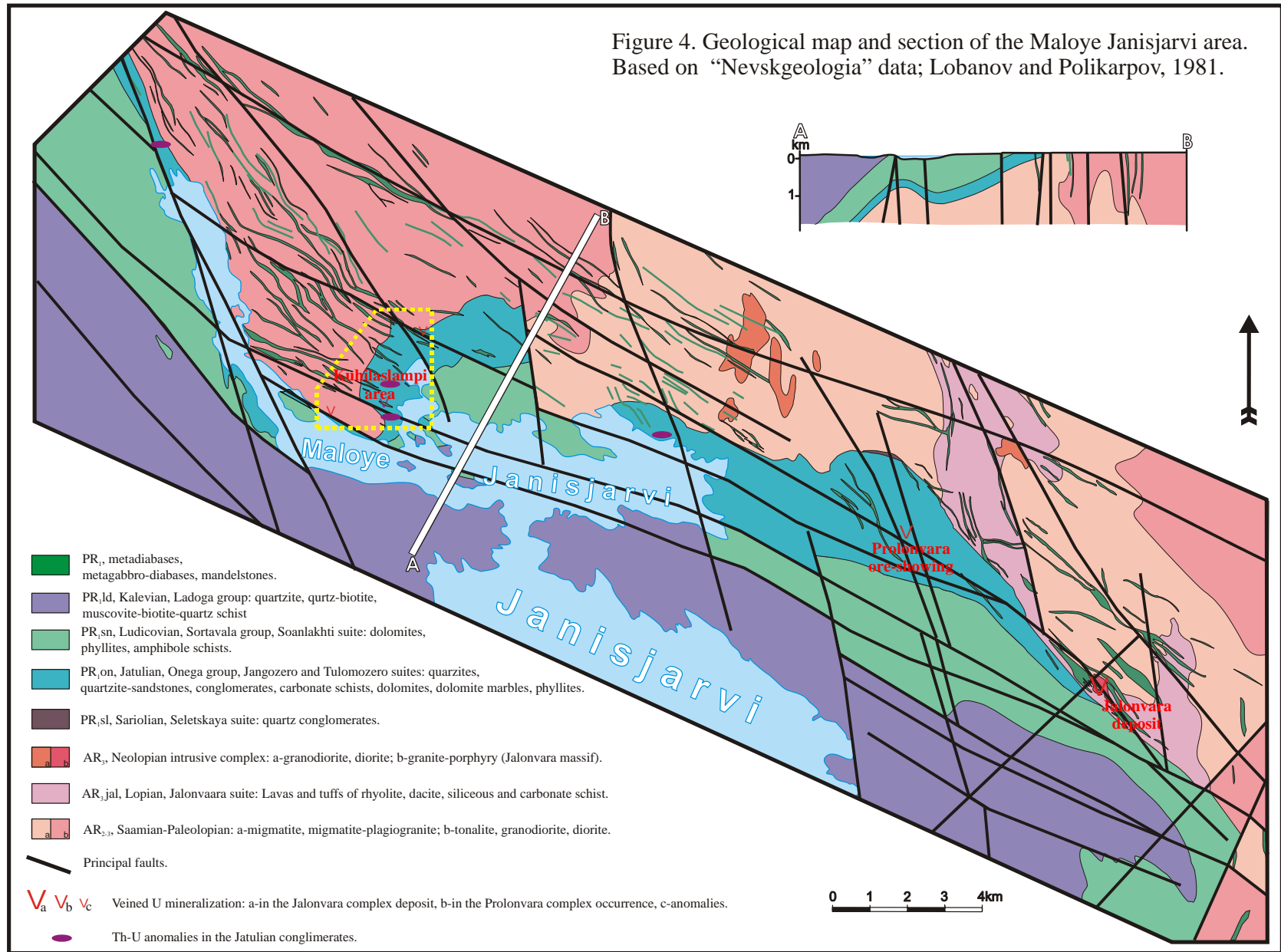


Figure 3 (continued). Legend to geological map and section of the Korennoye ore-showing.

Based on Korotaev et al., 1978.



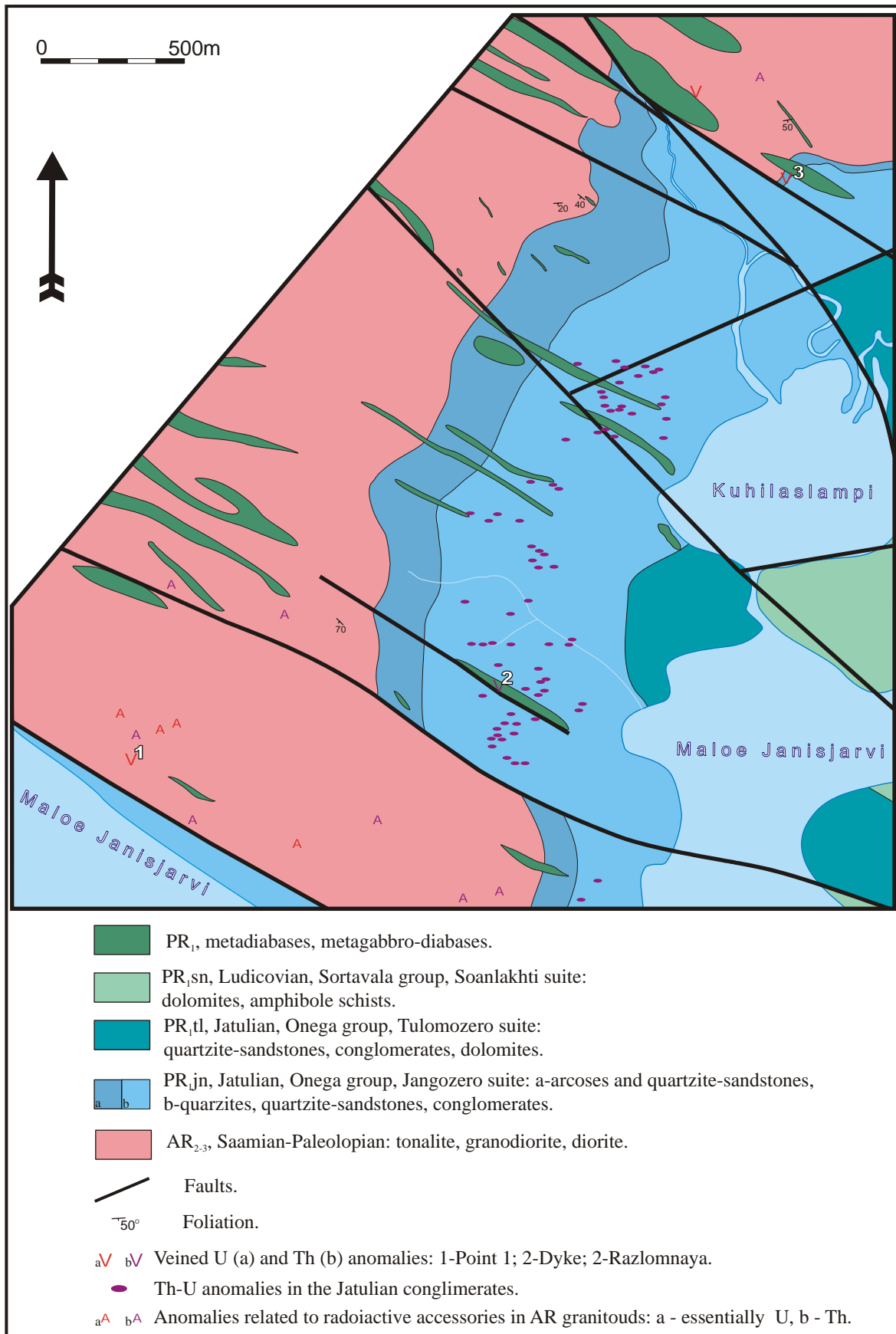


Figure 6. Geological map of the Kuhilaslampi area.

Compiled from Kondakov et al., 1963 and Polikarpov et al., 1976.

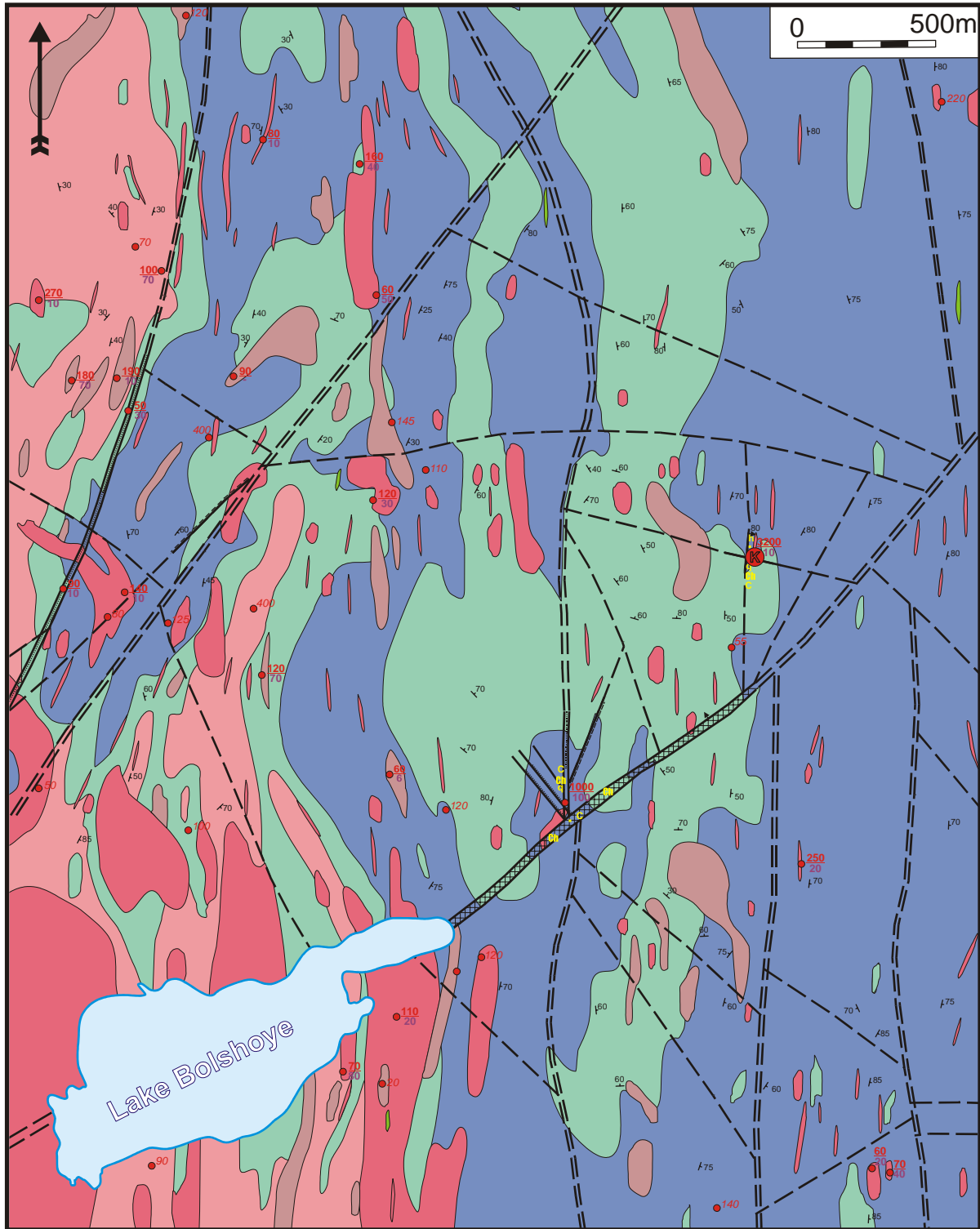


Figure 6. Geological map of the Latvasurje area (fragment).

Based on Gromov et al., 1981.

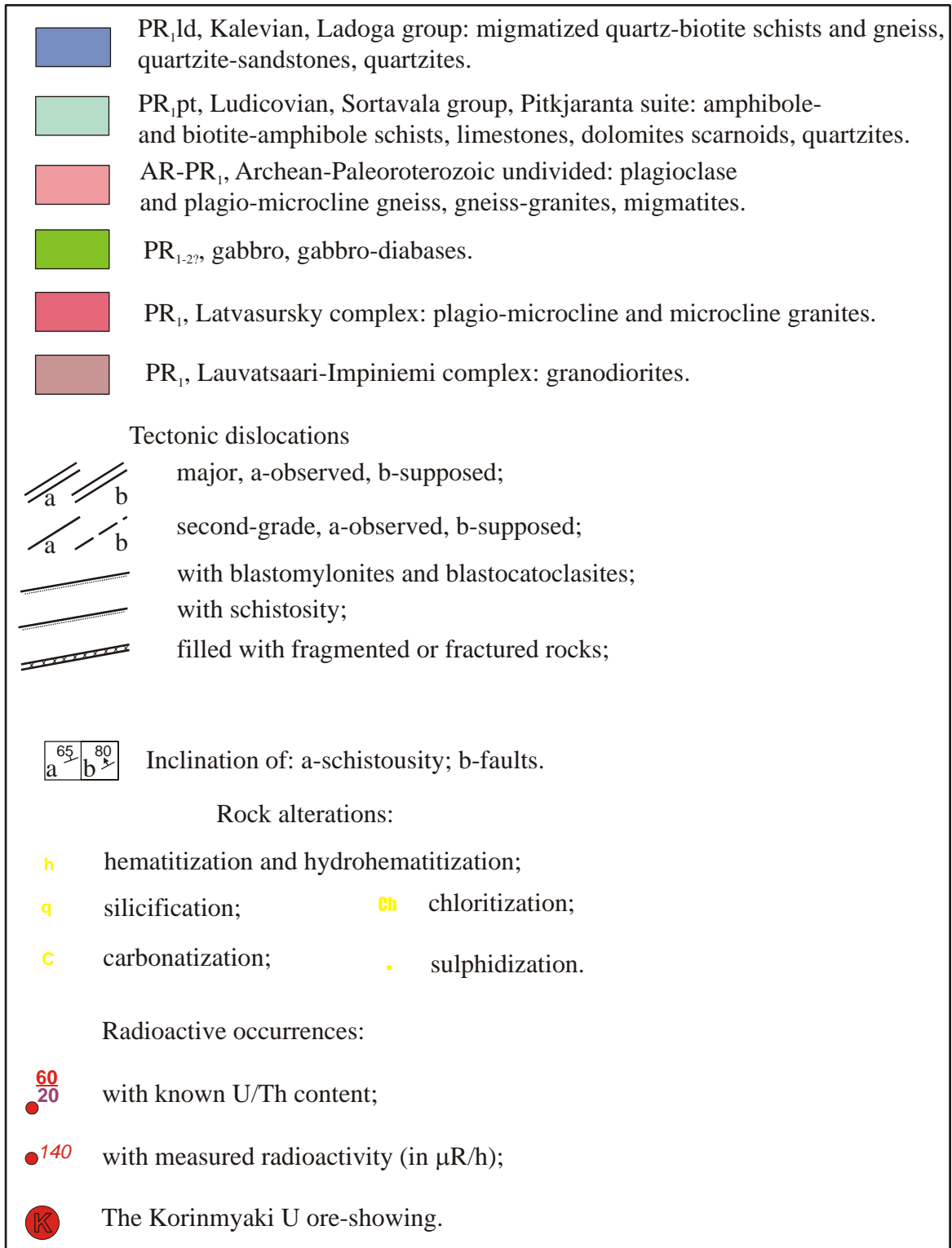


Figure 6 (continued). Legend to geological map of the Latvasurje area.

CHAPTER 2
URANIUM OCCURRENCES
HOSTED BY RIPHEAN
FORMATIONS

Chapter 2. Uranium occurrences hosted by the Riphean formations.

Introduction.

The Riphean volcanogenic-sedimentary complex of the Pasha-Ladoga basin unconformably overlies AR-PR₁ basement of the Raahe-Ladoga and the Svecofennian domains. Most of the Pasha-Ladoga basin is concealed under the Ladoga Lake. Three terrestrial occurrences of the Pasha-Ladoga basin formations represent under the glacial sediments overburden occur in the western, south-eastern and north-eastern shoulders of the basin: the Priozersk, Pasha and Salmi depressions correspondingly.

Because of its similarity to the Athabasca basin, since beginning of 1980th the Pasha-Ladoga basin has been considered as a potential area for the discovery of unconformity type uranium deposits. Exploration programs for this target have started at 1984. The Karku deposit has been discovered in 1989 and exploration programs in the Salmi depression have been carried out until 2007 with an interruption in the 1990th because of technical problems. Since 1999 exploration programs started as well in the Priozersk and Pasha depressions, but drilling in those areas has been limited.

Until now, all discovered uranium occurrences hosted by the Riphean formations (including the Karku deposit) are located in the Salmi depression. Only few low-grade (up to 100 ppm of U) local anomalies at the unconformity are known in the Svir-Oyat area in the north-eastern slope of the Pasha graben and the Jablonovka area in the northern part of the Priozersk depression (General Appendix 1, fig. 2.1 and 3.1).

1. The Salmi depression.

1.1. Geological environment.

Local sub-basin called the Salmi depression occurs on the north-eastern shoulder of the Pasha-Ladoga basin, in the continuation of the Ruskeala fault zone (General Appendix 1, fig. 1.1). The bottom of the depression gently dips (4° in average) to the WSW with local complications determined by the paleorelief of the basement surface and late tectonic structures. The size of the depression is about 300 km² (Appendix to Chapter 2, fig. 1).

Many brittle tectonic structures occur in the Salmi depression area.

NW striking faults correspond to the Ruskeala tectonic zone. They seem to dip steeply (70-80°) to the NE. Many of them only affect basement formations, but some cut the Riphean sequence as well. The Salmi depression is first controlled by NW structures.

N-S and E-W faults produce local uplifts of the depression. The Karku deposit is located within one of the most prominent uplift called the Central Block.

N-E faults are rare and have a weak influence on the structure of the depression. No significant displacement along these faults has been observed.

The basement below the Salmi depression is composed of AR-PR₁ granitic-gneiss domes surrounded by the carbonate and amphibole schists of the Ludicovian Pitkjaranta suite and metapelites of the Kalevian Impilakhti suite intruded by the Lower Riphean Salmi granitic massif.

On land occurrence of the Riphean volcanogenic-sedimentary complex in the Salmi depression extends for 40 km along the Lake Ladoga coast line and for 10-12 km to the NE from it. Here its thickness is up to 360 m. The succession is subdivided into three suites: Priozersk (Priozerskaya), Salmi (Salminskaya) and Pasha (Pashskaya). Significant variation of thickness of the suites (especially the basal Priozersk suite) and of the whole Riphean succession and the diversity of erosion level of the basement regolith indicate the importance of the basement paleorelief before and during sedimentation. If late tectonic displacements are excluded, the basement surface below the Riphean sediments was a very hilly landscape. Many elongated depressions represent former paleo-valleys. Location and configuration of these valleys are determined by former tectonic structures of the basement: and variations of resistance of the various basement lithologies to erosion.

The petrology of the Salmi area is described in the thesis of Lobaev (2005). Therefore only the main rocks varieties will be briefly presented below.

1.2. Bedrock petrology.

Basement rocks.

The lowest structural level of the basement is represented by the AR-PR₁ formations forming the core of the domes. Generally these formations are more leucocratic compared to overlying PR₁ ones. Strongly folded tonalite gneisses and pink plagioclase-microcline granitic-gneisses are the most common rock varieties. Migmatization is widespread. Late lenses and dykes of coarse/medium-grained quartz-oligoclase-microcline pegmatoids occur. The transition between pegmatoids and hosting gneisses is gradual, sharp contacts are common for the granite injections only (fig. 2.2.1).

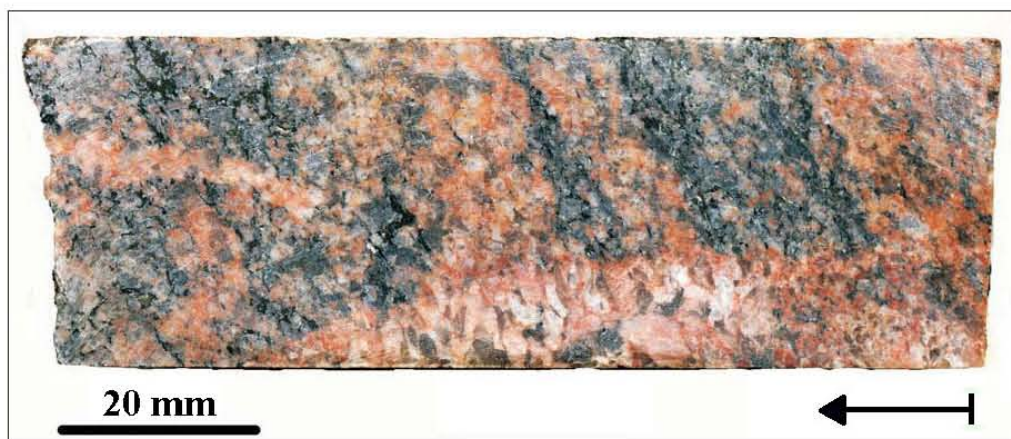


Figure 2.2.1. Biotite granite-gneiss cut by the granophyre vein from the Salmi depression, DDH 1044, 110 m.

In the Salmi depression area, the Palaeoproterozoic Pitkjaranta suite (150-200 m thick), which surrounds the granitic-gneiss domes, is mostly composed of amphibole-bearing rocks: amphibole-biotite schist and subordinated amphibolite, carbonate rocks are subordinated.

The base of the suite, mainly consists of fine/medium grained pyroxene-amphibole and quartz-feldspar-amphibole gneiss, granite-gneiss occur. Migmatization is widespread.

Its middle part is composed of alternating layers of amphibolites, hornblende and hornblende-biotite gneisses and schists and marbles. Migmatites and pegmatites occur. Carbonate rocks are often skarnified.

The upper horizon of the suite is composed of biotite-hornblende schist, sometimes graphite-bearing (1-2 % graphite).

The Pitkjaranta suite is overlapped by the 400 m thick Impilakhti suite. Because of their strong metamorphism (in the upper amphibolite facies), the contact between them is uncertain and is only recognized by the lithological difference. The Impilakhti suite is more homogeneous. Meta-terrigenous flyshoid formations prevail: biotite, garnet -biotite, quartz-biotite, in the upper part also garnet -cordierite-biotite gneiss and schist. Rare interlayers of amphibole-bearing rocks occur. Migmatization of the Kalevian rocks is the weakest for the supracrustal formations of the area, however granites dykes sometimes occur. Local microclinization takes place in the lower horizons (Skorospelkin, 2002). Accessory sulphides (pyrite and pyrrhotite) and graphite are quite common. Graphite content is 1-2 %, but schist lenses of with up to 5 % occur (fig. 2.2.2). They more typically occur in the lower part of the suite. Apart from the stratified distribution, there are indications of graphite and sulphide enrichments in fractures; sulphide-graphite-enriched shattering zones and veinlets are also widespread (fig. 2.2.3, 2.2.4).



Figure 2.2.2. Graphite/sulphide- bearing biotite schist of the Impilakhti suite from the Karku deposit, DDH 627, 146.8 m.



Figure 2.2.3. Blastocataclasite of graphite-bearing biotite schist of the Impilakhti suite from the Salmi depression, DDH 890, 79.2 m.



Figure 2.2.4. Newly formed graphite (G) and pyrite (Py) in tectonized biotite schist of the Impilakhti suite from the Karku deposit area, a – DDH 711, 89.5m; b – DDH 890, 79.2m.

Over 50 % of the Salmi depression basement is composed of even-grained and ovoid granites of the Salmi complex (fig. 2.2.5). According to geophysical data they underlay the AR-PR₁ metamorphic complex. The roof of the intrusion gently dips to the WSW.



Figure 2.2.5. Rapakivi granite of the Salmi massif from the Salmi depression, DDH 1045, 69 m.

There is a wide zone of metasomatic alterations around the Salmi massif. The metamorphic rocks are cut by pegmatitic granites related to the Salmi intrusion. Quartz-sericite-muscovite greisen formed after the granite-gneiss and the Salmi massif granites occur. Epidote-amphibole-pyroxene skarns of the Pitkjaranta carbonates are widespread in areas with abundant leucogranite veins to the SE of the Salmi depression. To the NW of the depression, the Salmi massif granites are intensively microclinized and albitized. Sometimes albitization is accompanied with fluorite.

Regolith.

The intensity of the alteration of the upper part of the basement formations at contact with the Riphean sediments is variable (fig. 2.2.6). Leucocratic coarse-grained rocks are less resistant to weathering than melanocratic ones. The alteration of the upper part of the basement has a thickness of 5 to 20 m, but may reach up to 70 m and more along the faults. The alteration of the upper part of the basement is attributed to paleoweathering but probably also results partly from late hydrothermal alterations, occurring especially along the faults.

The alteration of the upper part of the basement is zoned with a physical and a chemical zone. The upper zone is composed of alluvium-diluvium breccias and quartz-mica shale. Intensive kaolinitization and chloritization, also sporadic ferruginization occur. Usually the thickness of the physical weathering zone is less than 1 m, and up to a few meters in the tectonized zones.

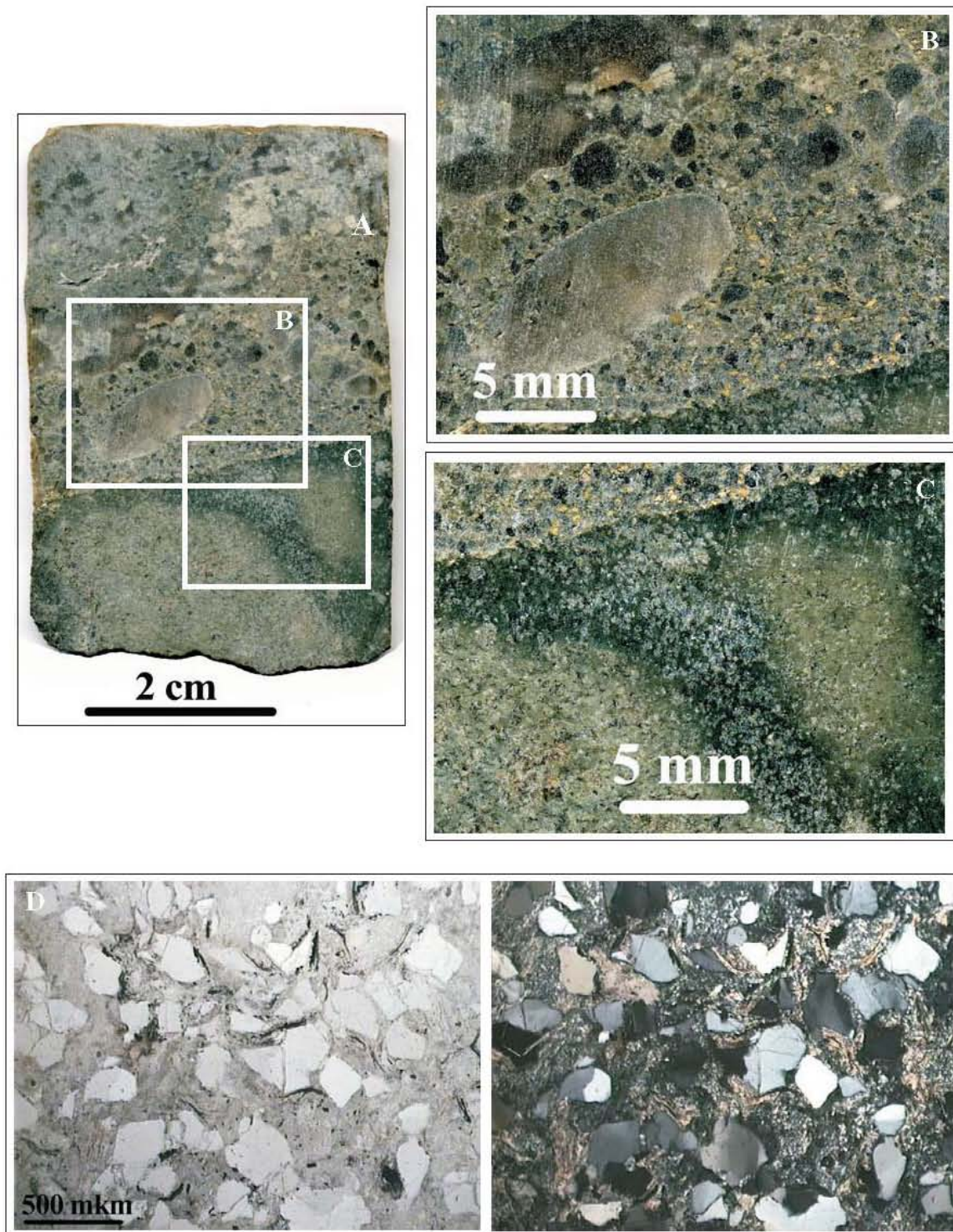


Figure 2.2.6. Contact of the Priozersk suite gritstone and physical weathering crust of the basement from the Karku deposit, DDH 665, 122.6 m; a – sample; b – gritstone at the contact; c – weathering crust rock; d – thin section of the weathering crust rock; optical photos, plain (left) and polarized (right) transmitted light.

The underlying chemical weathering zone is characterized by changing of mineral composition of the underlying rock with preservation of its structure. There is gradual decrease of the intensity of rock alteration with depth. Metamorphogenic minerals are replaced by

hydromicas, chlorite, sericite and kaolinite in the upper part of the zone. Intensively altered rocks have friable clayey constitution and a greenish-gray color. Hydration of biotite is followed by Fe hydroxides development and forms rusty-brownish spots. The alteration is not complete, relics of primary metamorphic rock are widespread. In the lowest levels alteration is sporadic and represented by development of hydromicas after plagioclase and along small fractures, chloritization of biotite. The lower limit of the chemical weathering zone is uncertain but its approximate thickness 5 to 20 m, down to 70 m along the faults. As it was noted before, the alterations could be produced partly by late hydrothermal processes.

A complete section of the regolith is represented in the succession of pictures of the drill core of DDH 627 from the Karku deposit (fig. 2.2.7-10).

The sample in the figure 2.2.7 is a rock from the contact zone between the Priozersk suite sediments and the physically weathered basement. The rock has a shale structure composed of fragments of basement formations. This rock represents a new-formed sedimentary rock, derived from the underlying basement and deposited *in situ*.

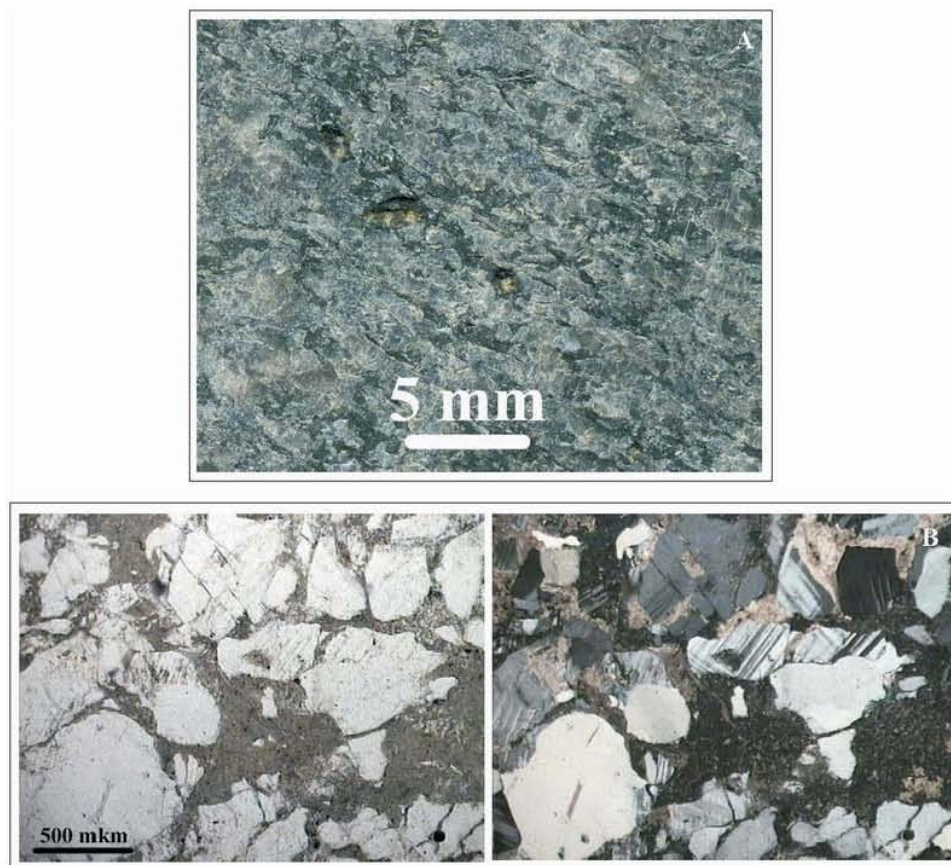


Figure 2.2.7. Shale from the physical zone of the regolith of the basement from the Karku deposit, DDH 627, 133.75 m (70 cm from the contact with the sandstone); a – sample; b – thin section, optical photos, plain (left) and polarized (right) transmitted light.

The contact of the physical zone with the proper basement rock (migmatized gneiss) is presented in the figure 2.2.8.

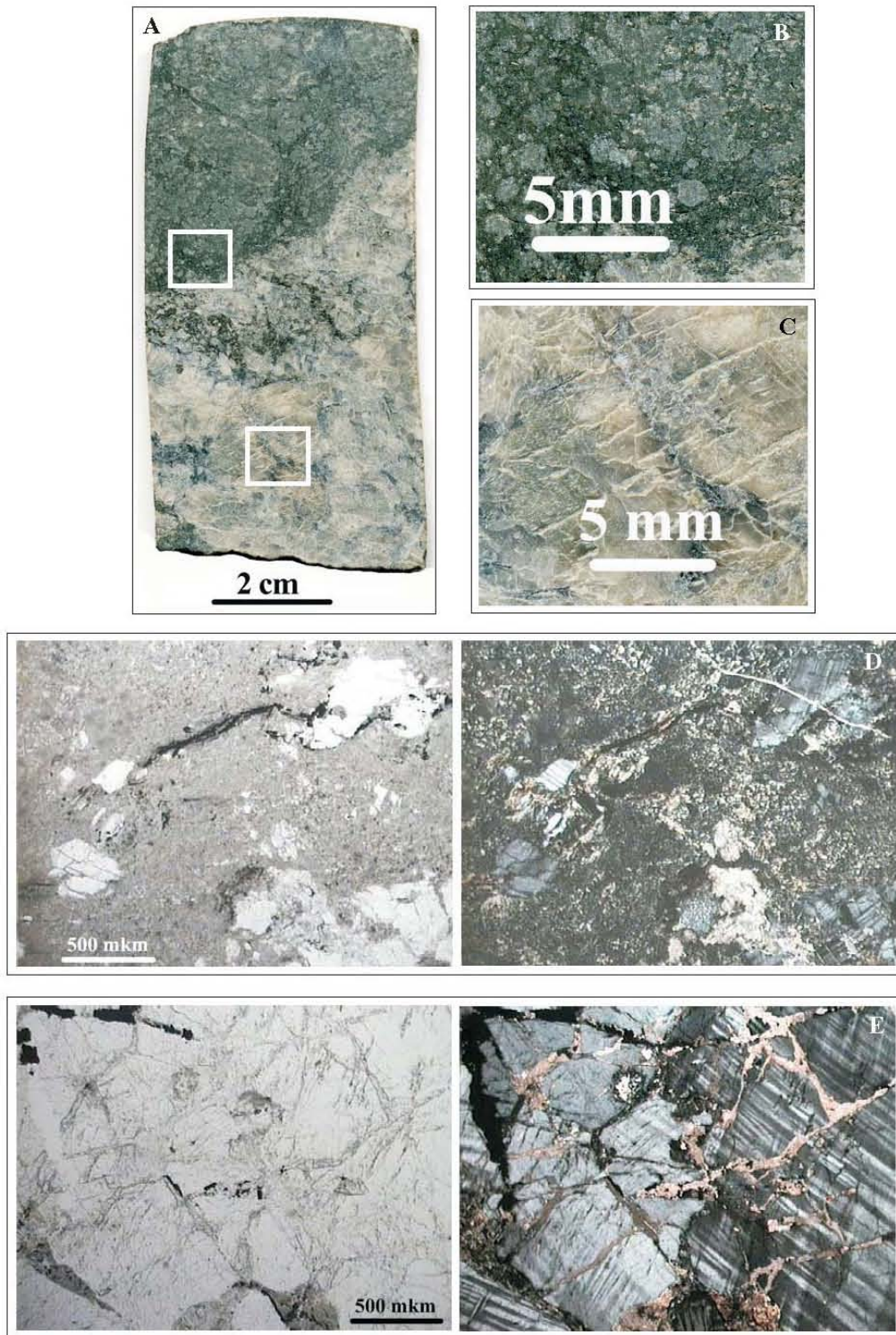


Figure 2.2.8. Contact of the physical altered shale with the chemically altered quartz-microcline gneiss of the Impilakhti suite from the Karku deposit, DDH 627, 134.05 m; a – sample; b – enlarged fragment of the shale; c – enlarged fragment of the gneiss; d – thin section of the shale, plain (left) and polarized (right) light; e – thin section of the gneiss, plain (left) and polarized (right) light.

The sample of altered biotite schist is presented in the figure 2.2.9. In the sample the alterations are not obvious because the quartz grains and graphite laths are preserved and the rock preserves original schist structure, but in the thin sections replacement of biotite and feldspar by hydromicas aggregates can be observed.

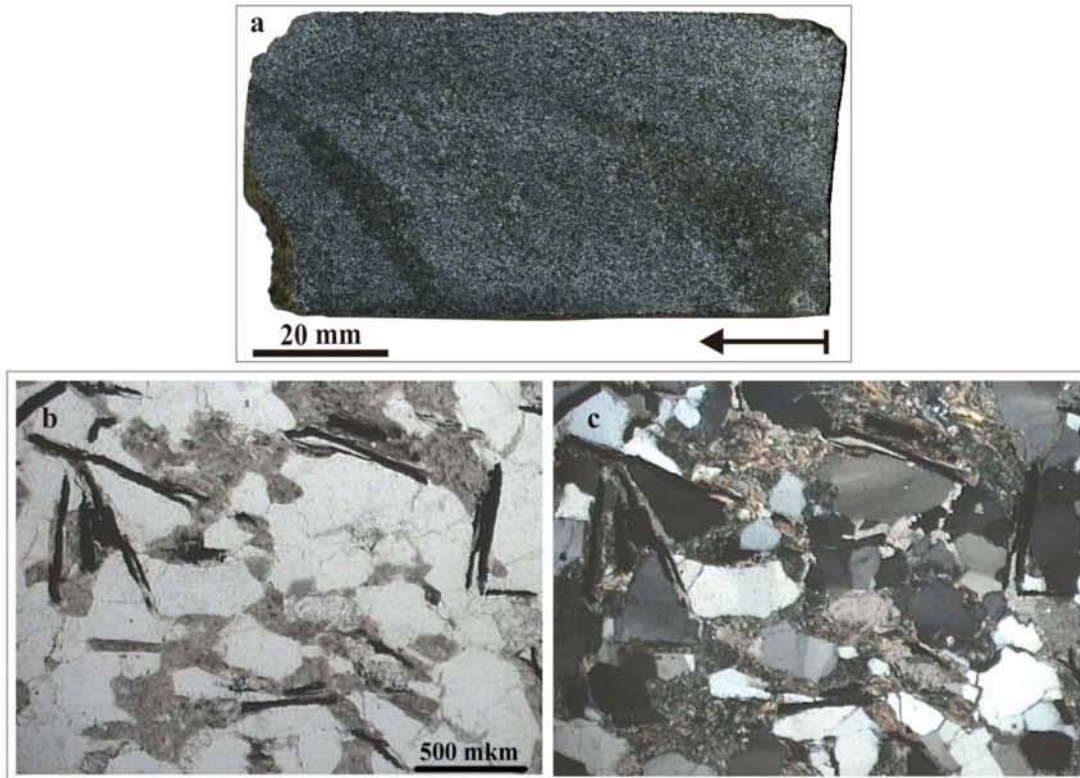


Figure 2.2.9. Altered graphite-bearing biotite schist of the Impilakhti suite from the zone of the chemical alterations from the Karku deposit, DDH 627, 134.5 m; a – sample; b and c – thin section, optical photos, transmitted light, b – plain light, c – polarized light.

Thin section from the non-altered graphite-bearing gneiss is presented in the figure 2.2.10).



Figure 2.2.10. Non-altered graphite-bearing biotite gneiss from the face of the bore well from the Karku deposit, DDH 627, 166 m; a – sample; b – thin section, optical photos, plain (left) and polarized (right) transmitted light.

It is important to notice, that a zoning of reddish to greenish regolith alterations typical for the Athabasca Basin has not been discovered in the Karku area. Described by Lobaev (2005) reddish and greenish regolith-like alterations only occur in the area where the Riphean sediments pinch out and rather refer to supergene alteration.

Riphean rocks.

The *Priozersk* suite is the lower unit of the Riphean sequence. In the Salmi depression it has thickness from 5 to 80 m. It is composed of clastic sediments of quartz-feldspar composition. Pink- or beige-colored coarse-grained sandstones prevail (fig. 2.2.11a); gritstones (fig. 2.2.11b) are subordinated. Coarse polymictic conglomerates with well- and coarse-rounded pebbles locally occur at the base of the suite (fig. 2.2.11c). Pebbles are mainly of quartz, but fragments of the basement rocks (gneiss, granite and amphibolite) occur as well. Rare mudstone pebbles exist (fig. 2.2.12). Lenses of dark-gray siltstone and mudstone rarely occur; as a rule they are related to shoulders of the paleovalleys.



Figure 2.2.11. The Priozersk suite quartz-feldspar sandstone (a), gritstone (b) and conglomerate (c) from the Karku deposit, DDH 612, a – 98.5 m, b – 100.5 m; c – south of the Salmi depression, DDH 1043, 96.8 m.

Clastic material composes 70-80 % of the rock. The main clastic minerals are quartz (65-95 %, 80 % in average) and feldspar (up to 20 %) (fig. 2.2.13). The most common accessories are: amphibole, micas (biotite, muscovite), garnet, zircon, tourmaline, apatite, ore minerals (ilmenite, rutile, titanite, pyrite, pyrrhotite, chalcopyrite, sphalerite, magnetite, brannerite, ferrithorite), sporadically – epidote and monazite. They have siltstone size and are dispersed in the cement or compose thin interlayers of heavy minerals (fig. 2.2.14).



Figure 2.2.12. The Priozersk suite polymictic conglomerate with soft pebbles (mud rolls) from the Karku deposit, DDH 690, 129.5 m.

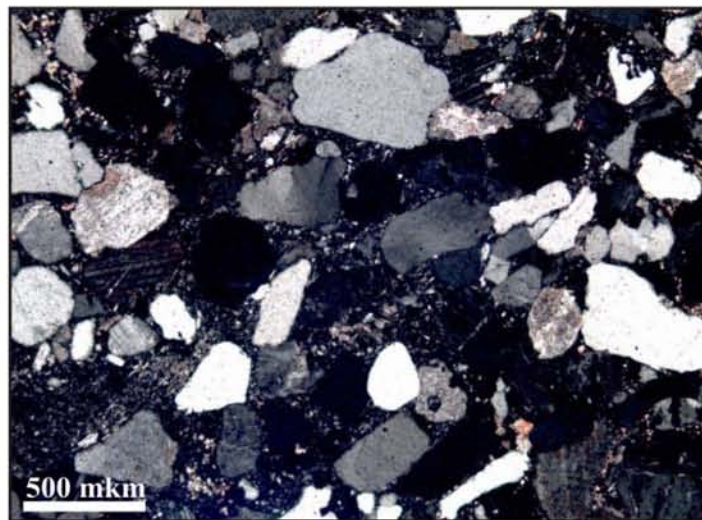


Figure 2.2.13. The Priozersk suite sandstone from the Salmi depression, DDH 1021, 62 m; quartz and feldspar clasts are cemented with kaolinite and hydromicas; optical photo of a thin section, polarized transmitted light.

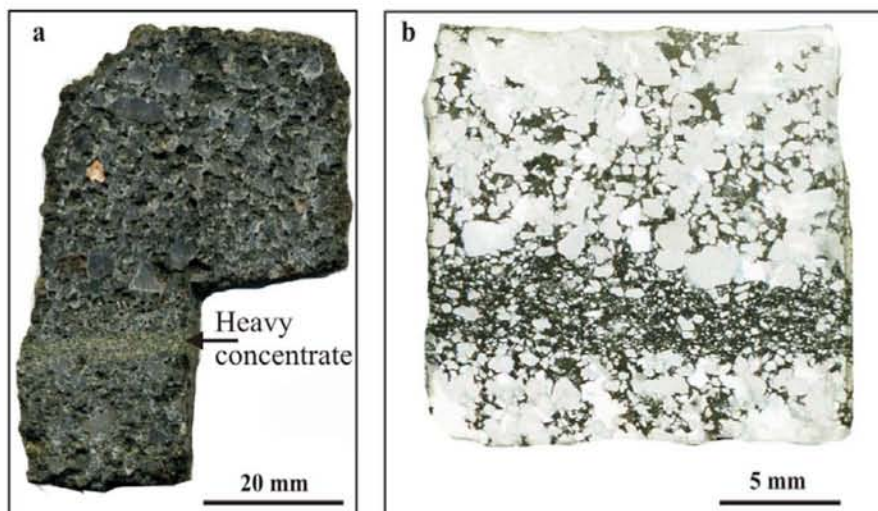


Figure 2.2.14. Heavy mineral concentration in the leached sandstone of the Priozersk suite from the Karku deposit, DDH 627, 127.2 m.

The cement of the sediments is composed of hydromica-kaolinite with subordinated chlorite, Fe-chlorite and calcite. Where local chlorite enrichment occurs the rock becomes gray. Calcite and chlorite enrichments in the sandstone cement occur near the contact with overlying effusives. A small layer of dark-gray tuffaceous-sandstone is localized at the contact.

Diagenetic alterations are represented by the replacement of the detrital particles of the cement by kaolinite and to a lesser extent by sericite, chlorite, carbonate and hematite. Mikhailov (2001) and Velichkin (2005) mention also diagenetic overgrowths over detrital quartz, but our observations do not allow to consider these overgrowths as a typical process in the sediments. Clear quartz overgrowths occur in vicinity of the U-ore bodies and we consider them as belonging to the ore-forming epigenesis (Kushnerenko et al., 2004).

The middle part of the Riphean sequence of the *Salmi* suite has a complex composition. Lower and upper effusive subsuites are separated by a sedimentary layer. Total thickness of the suite in the Salmi depression is up to 250 m.

The lower and the upper subsuites are composed of mafic volcanites with 2 to 5 more or less regular rhythms in each of them. A complete rhythm is composed of basal thin to thick layer of gray vesicular basalt (with small chlorite amygdalae), basalt porphyry (main part of the rhythm), vesicular basalt (with chlorite and carbonate amygdalae), volcanogenic breccias and tuffs at the roof (fig. 2.2.15). There is a thin (up to 1 m) layer of strongly altered brecciated dark-gray effusive ash at the bottoms of each effusive subsuite.

The thickness of the lower effusive subsuite is 130 m. There is a unique outcrop of the Riphean formations in the Salmi depression represented by the lower subsuite basalts in the rapids of the Tulema river. Distinctive feature of this subsuite is the existence of widespread agate inclusions in the upper vesicular basalt layer of the middle rhythm. Agate fills amygdalae or veins with several morphologic types (Polekhovskiy et al., 2002) (fig. 2.2.16).

Petrographic characteristics of the lower subsuite effusives, in particular the occurrence of relatively well-crystallized lavas, indicate an accumulation of this layer during a rather brief period. Rapid deposition of a thick basalt succession provides the necessary conditions for slow cooling of the internal parts of the rhythms and their crystallization as a doleritic rock. For the basalts of the lower subsuite a Sm-Nd age of 1499 ± 68 Ma was obtained (Bogdanov et al., 2003).

According to Spiridonov (2001), agate filling of the amygdalae in the basalts is an indication of its burial at a depth about 2.5 km.

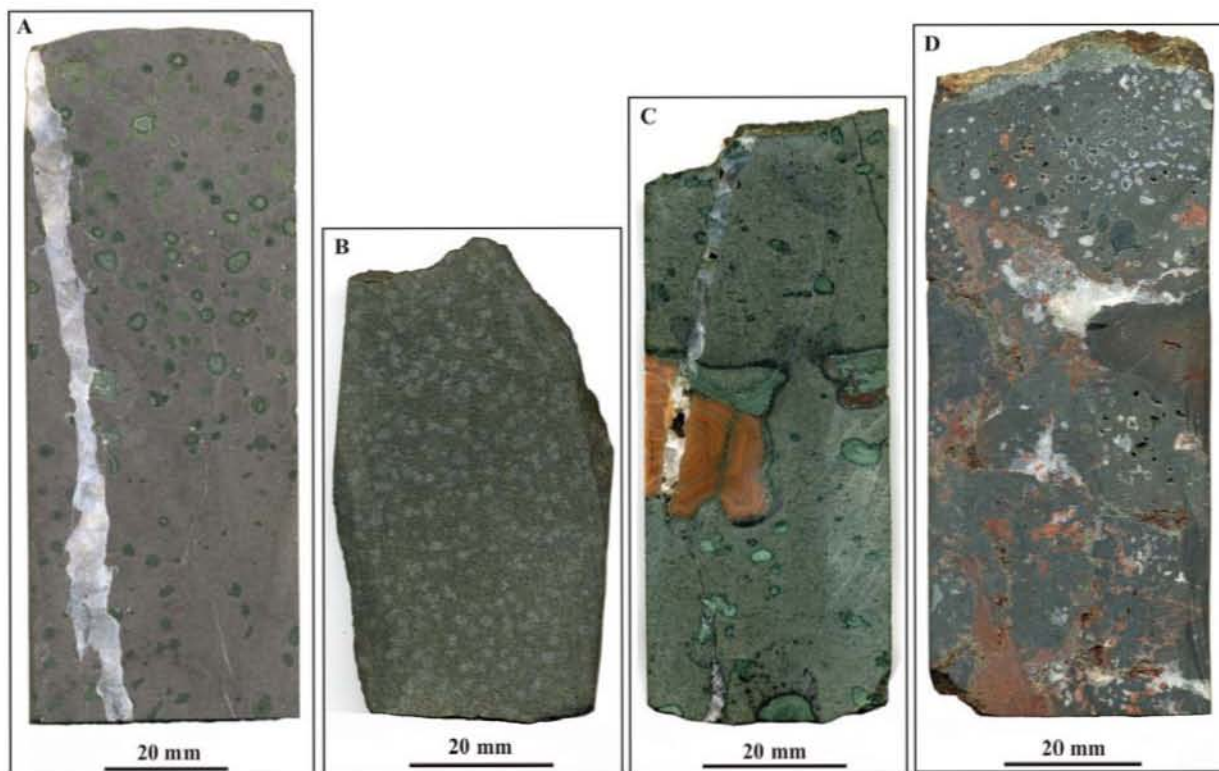


Figure 2.2.15. The Priozersk suite mafic effusives of the lower subsuite from the Salmi depression; a – vesicular basalt with chlorite amygdalae cut by calcite veinlet (DDH 627, 71.1 m); b – porphyrites (DDH 627, 91 m); c – vesicular basalt with chlorite-calcite and agate amygdalae cut by calcite veinlet (DDH 1043, 54.8 m); d - volcanogenic breccias and tuff (DDH 627, 63.8 m)

Sedimentary interlayer of the Salmi suite overlaps eroded lower effusive subsuite. The thickness of the interlayer is up to 35 m. It is composed of Quartz-feldspar or polymictic coarse-grained beige and pink sandstones mainly, subordinated gritstones and conglomerates (fig. 2.2.17). Cement consists of kaolinite and hydromicas with hematitized and chloritized spots and interlayers. Fe-chlorite is developed in the cement of the rock at its upper contact with the effusives. An occurrence of pebbles of the basalts, including agates (fig. 2.2.18) refers to the quite long period of erosion between the formation of the Salmi suite lower subsuite basalts and deposition of the sedimentary interlayer.

The upper effusive subsuite (up to 90 m thick) conformably overlay the sandstone subsuite. The vesicular basalt is thicker than in the lower subsuite and tuffs are less abundant.

Hydrothermal alterations of the effusives are more intensive in the fault zones. Secondary minerals are chlorite, carbonate, quartz, Fe-hydroxides, and minor albite, biotite and epidote. The two last minerals have been observed in the porphyries.

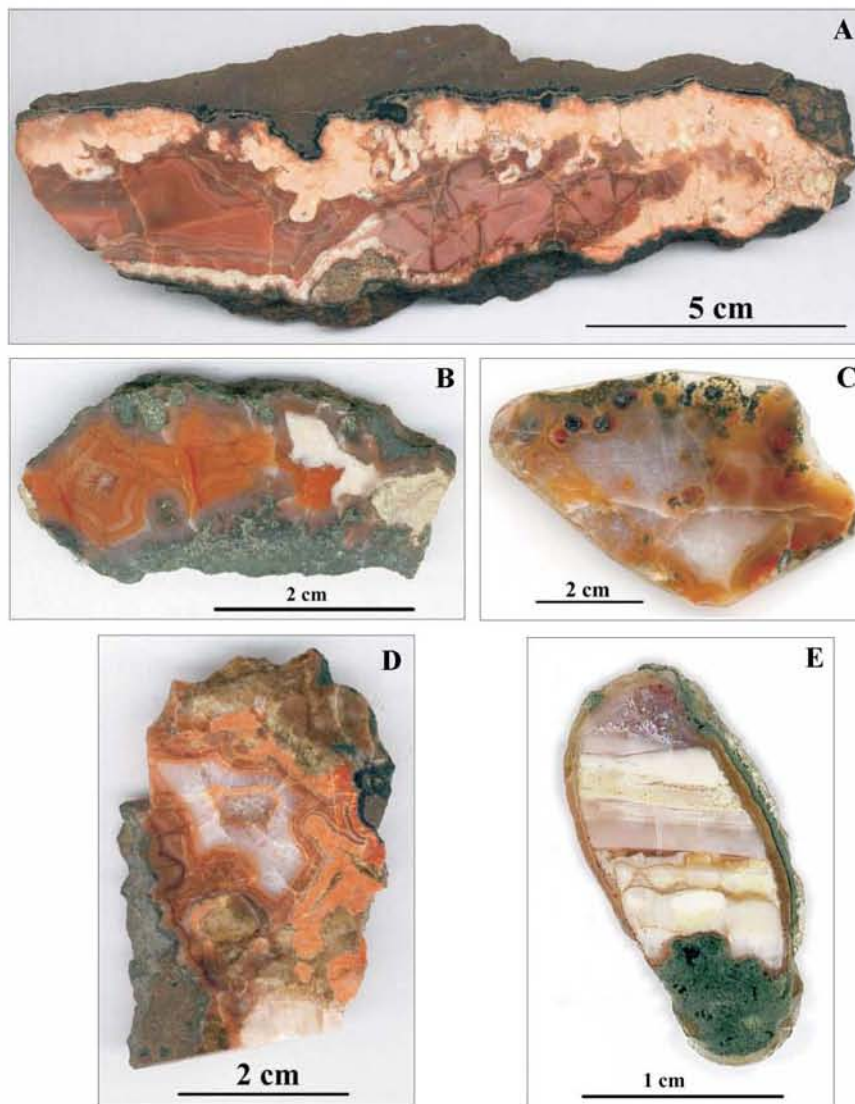


Figure 2.2.16. Different types of agates from the Salmi suite basalts (sampled at the Tulema river rapids): a – vein agate (sard) surrounded by the calcite; b – zonal-concentric bastion agate; c – spheroidal and vaguely zonal agate; d – patter agate of the mixed type; e – onyx.



Figure 2.2.17. The Salmi suite polymictic conglomerate from the Karku deposit, DDH817, 63m.

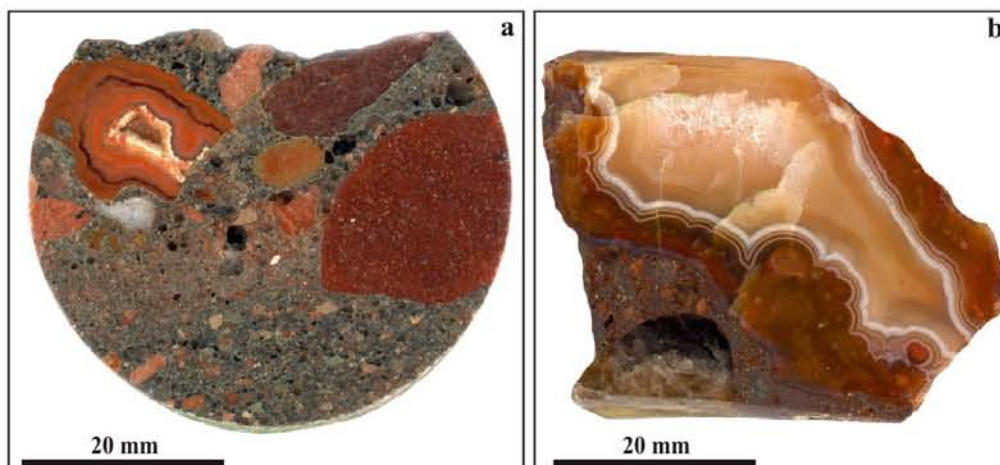


Figure 2.2.18. Conglomerates with agate fragments from the basal horizon of the Salmi suite sedimentary interlayer from the Karku deposit, DDH 817, 63 m.

The upper part of the Riphean sequence is called the *Pasha* sedimentary suite. In the Salmi depression it has thickness up to 290 m and is composed of interlayered polymictic sandstones, siltstones and mudstones with predominance of the fine-grained varieties. The clasts are cemented by hydromicas with minority of kaolinite. A layer of conglomerates with well-rounded pebbles occurs in the base of the suite. Apart of fragments of the basement and underlying effusives, unique pebbles of red quartzites, similar to Vepsian Shoksha suite quartzite (age 1.8-1.77 Ga) of the Onega depression have been discovered in the Pasha subsuite. This observation and the discovery of numerous fragments of red-colored quartzite-sandstones refer to wider development of the Vepsian formations in comparison with the present situation.

To the west, the formations of the Salmi depression are cut by gabbroic Valaam sill. In the Salmi area they outcrop at the Lunkulansaari and Mantsinsaari islands.

1.3. Metallogenic characteristic of the bedrocks.

Geological units of the Salmi depression are enriched in U, Mo, Pb and Zn. Granite-gneisses of the domes and amphibolites of the Pitkjaranta suite are enriched in Pb (20 ppm) and Zn (200 ppm) (Skorospelkin, 2002). Biotite gneiss and schist of the Impilakhti suite are weakly enriched in Mo (3.6 ppm), Pb (28 ppm) and Zn (180 ppm). The graphite-bearing varieties of the Impilakhti suite are enriched in U (5.8 ppm) and Mo (5.6 ppm). Granites of the Salmi intrusion in the Salmi area have 4.1-5 ppm U in average, 18-20 ppm Th and 3.3-3.5 ppm Mo. Numerous spotty radioactive anomalies related to local U and Th-bearing accessories clusters are common in the Salmi granites around the study area. The regolith is depleted in U, Mo, Pb and Zn

compared with the original rocks, but slightly enriched in Ti and Nb. Increased U contents occur in the sedimentary rocks: 4.8 to 6.5 ppm U in the Priozersk suite sandstone and gritstone, 3.9 ppm in the Salmi suite sandstone, 4.6 to 5.6 ppm in the siltstone of the Pasha suite. They also have increased Mo contents (2-3.9 ppm) and the Pasha suite is also enriched in Pb (up to 30 ppm) and Zn (up to 170 ppm) (Skorospelkin, 2002).

In addition, the Riphean sediments have increased contents of Th, Nb, W, B, Ag As and basement rocks – of Ag, As, Bi, Cr, W, Y, Li, B. For Dolgushina and Kushnerenko (2004) the above-clarke association U-Mo-Y-Li-Bi-B occurring in the basement rocks is an indication of their greisenisation presumably in relation with the Salmi granite intrusions.

Two occurrences of complex-ore similar to the ones of the Pitkjaranta ore district exist in the Salmi depression. The Salmi Fe-Zn-Pb ore-showing occurs in the altered Ludicovian formation at the contact with the Salmi intrusion, at the eastern edge of the Central Block. The Karkunlampi polymetallic ore-showing is related to the south-western slope of the Vipuoiskii granitic-gneiss dome in the eastern part of the Central Block (Appendix to Chapter 2, fig. 2).

There are a few uranium occurrences hosted by the Riphean sediments in the Salmi depression: the Karku deposit and the Matala and the Kotalakhti ore-showings.

2. The Karku uranium deposit.

2.1. Geological environment.

The Karku deposit area is localized in the Central Block – a local tectonic uplift of the basement and Riphean formations (Appendix to Chapter 2, fig. 2). The Block resulted from an orthogonal fault system and has an almost square shape covering 40 km². The total amplitude of the vertical displacement of the basement roof is up to 200 m. Formerly this block was considered as a horst-like uplift and was called Central Horst. According to new obtained data it is in fact an allochthonous block of the basement and Riphean formations overthrust to the north through series of E-W striking thrusts (Petrov, 2006).

The basement consists of AR-PR₁ granitic-gneiss domes mantled with PR₁ amphibole-biotite schist, amphibolites, skarns of the Pitkjaranta suite and biotite schists of the Impilakhti suite. All rocks are migmatized and injected by plagioclase-microcline and microcline granites and pegmatites. There is a low-density gravimetric anomaly below the Block that probably indicates the presence of the Salmi granites. According to these data, the upper contact of the massif dips from 600 to the east to 2000 meters to the west of the Central Block (Skorospelkin,

2002). Such a structure may result from the overthrusting of the supracrustals and Riphean sediments upon the roof of the massif.

The surface of the basement in the Central Block is complex, with local hills and valley-like depressions (Appendix to Chapter 2, fig. 3). The hills correspond to granitic-gneisses of the domes due to their more resistance to the erosion, and the depressions to interdome synclines composed of the Palaeoproterozoic schists. The basement roof tends to dip to the west. In the Karku deposit area its depth reaches 77 to 190 m.

The Riphean sequence is reduced on the Central Block because of late erosion resulted from the uplift of the Block. Local variations of thickness of whole Riphean sequence and its components are determined by the paleorelief (it increases in the depressions and decrease above the dome uplifts) and by late tectonic displacements (Appendix to Chapter 2, fig. 4). In the central part of Central Block Riphean volcanogenic-sedimentary formations are eroded and the basement is covered with Quaternary sediments only.

The Riphean sequence in the Central Block consists of the Priozersk suite (8 m thick above the basement surface hills and up to 40 m thick in the depression) and the lower volcanogenic subsuite of the Salmi suite. Lower horizons of the sedimentary layer of the Salmi suite occur in the easternmost edge of the Central Block only.

All the Central Block is covered by 25-140 m thick Quaternary moraine sediments.

Tectonic displacements of different striking and age are numerous. Orthogonal structures limit the Central Block and influenced also its internal structure. There are ancient Palaeoproterozoic faults cutting the whole sequence among the NW faults. A unique NW-striking upthrow of the Riphean sequence over 17 m has been revealed at the westernmost flank of Ore body 1 of the Karku deposit (DDH 653). Priozersk suite sandstone presents cataclasis along NW faults. NE faults do not disturb the Riphean sequence although some of them presumably have been reactivated during the post-sedimentary period.

2.2. Characteristics of the deposit.

The Karku deposit comprises 3 separated ore bodies located in the south-eastern part of the Central Block. All of them are related to the unconformity between the Priozersk suite sediments and the basement.

Ore body 1 is the largest one. In the NW-SE direction it occurs along 1.5 km, in the NE-SW direction presumably along 2 km. Last estimation is not precise because of low density of the drill net. Sometimes the eastern flank of Ore body 1 is considered as the distinct Bolotnoye

ore-showing. Thickness of the ore lens with 300 ppm cut-off is up to 20.5 m, 8.2 m in average. Thickness at a 1 000 ppm cut-off is up to 5.6 m. Average U content is 840 ppm, up to 34 600 ppm over 0.5 m. Estimated resources of the ore body is about 6 600 t of U (Petrov, 2007).

Ore body 1 is localized in a valley-like depression of the basement surface corresponding to biotite schist of the interdome Impilakhti suite. The general extension of the ore body coincides with a NE fault zone. The highest-grade ore concentrations of Ore body 1 occur at the intersection of NE and NW faults where graphite-rich biotite schists of the Impilakhti suite are.

Uranium ore is hosted by the Priozersk suite sediments, rarely the ore occurs in the very upper part of the regolith. Rare low-grade U mineralization (up to 470 ppm) has been discovered in fracture zones in the basalts of the Salmi suite (DDH 609 and 641).

Anomalous Th contents (over 300 ppm, up to 1840 ppm) have been discovered in the sandstones at the unconformity in several drillholes (DDH 605, 607, 609, 642). In DDH 608 they are located in the upper part of the Priozersk suite, in DDH 646 in the weathered basement rock. Only in the DDH 605 high Th content (930 ppm) accompanies the uranium ore.

Ore body 2 is the smallest one. The size of the ore body is not certain because of the low density of drilling. The known size is 250×150 m (for a 300 ppm cut-off). Ore body thickness for a 300 ppm cut-off is up to 6.5 m, 1.2 m in average. Its thickness for a 1 000 ppm cut-off is up to 3.2 m, and its size: 90×140 m. Average U content is 1040 ppm for a resource of about 400 t U (Petrov, 2007).

Ore body 2 is located on the south-western slope of the Vipuoiskii granitic-gneiss dome and located at the intersection of NW and N-S faults. It is located within the Karkunlampi polymetallic ore-showing outline. A distinctive feature of the ore body is its location mostly above Pitkjaranta suite formations.

Ore body 3 is the best studied and the drill net is the densest in the Karku area. Ore body size with a 300 ppm cut-off is 220×620 m, and 50×430 m at a 1 000 ppm cut-off. The ore body thickness increases southwards up to 7 m. Average U content is 1 800 ppm, with a maximum of 166,200 ppm over 0.25 m. The resource of the ore body is about 1 300 t U (Skorospelkin, 2002).

The ore body is localized mainly where graphite-bearing biotite schist of the Impilakhti suite exist; only the eastern flank of the ore body partly occurs above the graphite-bearing amphibole-biotite schist of the Pitkjaranta suite. It has a wedge shape with two lenses corresponding to NW and N-S faults (fig. 2.2.19, Appendix to Chapter 2, fig. 5).

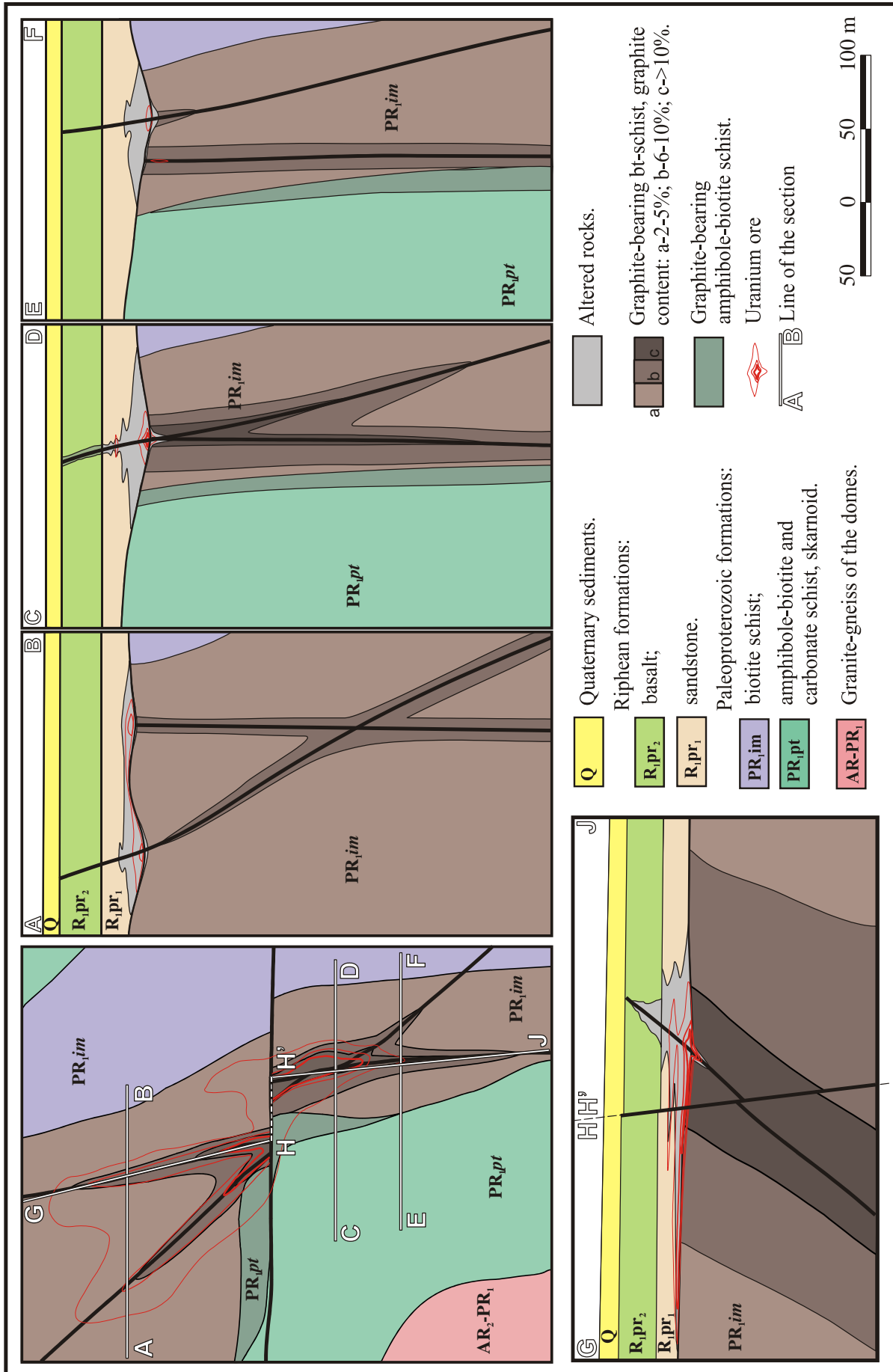


Figure 2.2.19. Geological map and sections of Karku deposit Ore body 3.

Basement rocks are graphitized along these faults (fig. 2.2.20). Cataclastic zones have been recognized in the sandstone along the NW fault (fig. 2.2.21).



Figure 2.2.20. Development of graphite (G-2) in tectonized biotite schist of the Impilakhti suite; two generations of epigenetic pitchblende (Pbl 1+2) occur; the Karku deposit, DDH 665, 136.3 m. Polished section, optical photo, reflected light.

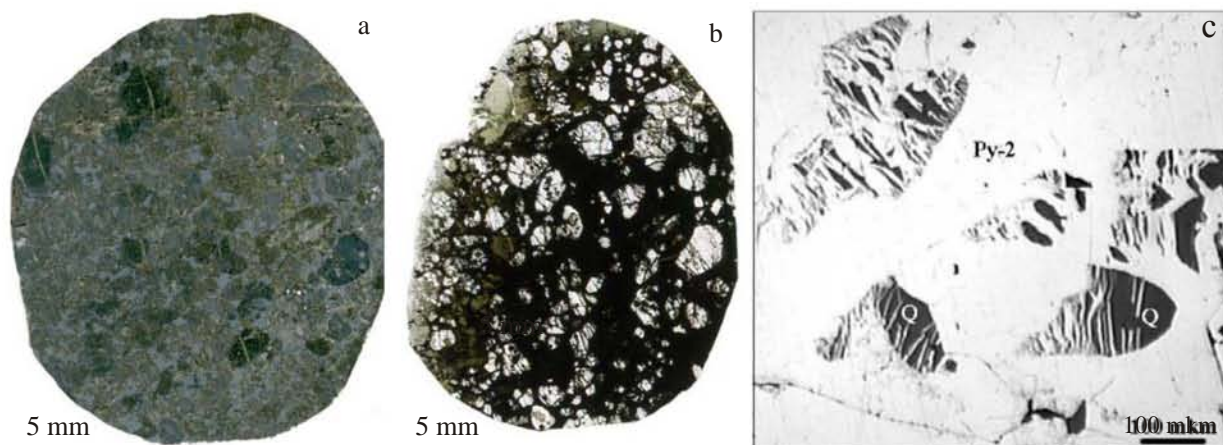


Figure 2.2.21. Cataclasis of the ore-hosting sulphide-chlorite-carbonate Priozersk suite rock; the Karku deposit, optical photos: a –polished section, reflected light, DDH 625; b – thin section of the same sample, plain transparent light; c –development of epigenetic pyrite (Py-2) in the cement and fractures in detritus quartz (Q), DDH 680, reflected light.

The highest-grade ores are localized at the intersection of this zone with graphitized schists (6-10 % graphite) of the Impilakhti suite. The high-grade ore is enveloped by a wide halo of low-grade mineralization located in a valley-like depression of the basement surface (Appendix to Chapter 2, fig. 6) with corresponding increase of the sandstone layer thickness (Appendix to Chapter 2, fig. 7). This indicates that the depression was pre-existing sediment deposition.

There is a sinistral strike-slip fault in the central part of Ore body 3. It displaces the Ore body over 40 meters. Vertical displacement is small – about 3 m, with the southern block being downlifted. Apart from the mechanical displacement, no indications of the fault influence on the uranium distribution have been observed. Consequently it is a late fault.

The main part of the ores, including the high-grade mineralization, is hosted by the Priozersk suite and spatially related to the unconformity. Lenses of low-grade ores occur in the upper and middle part of the suite. In the southern part of the ore body, uranium mineralization penetrates into the regolith down to 4 m below the unconformity. Unique low-grade ore intersection has been discovered at a distance of 50 m to the south of Ore body 3, in a breccias zone at a depth of 9.8-10.8 m below the unconformity (DDH 674, 146.1 m; fig. 2.2.22).

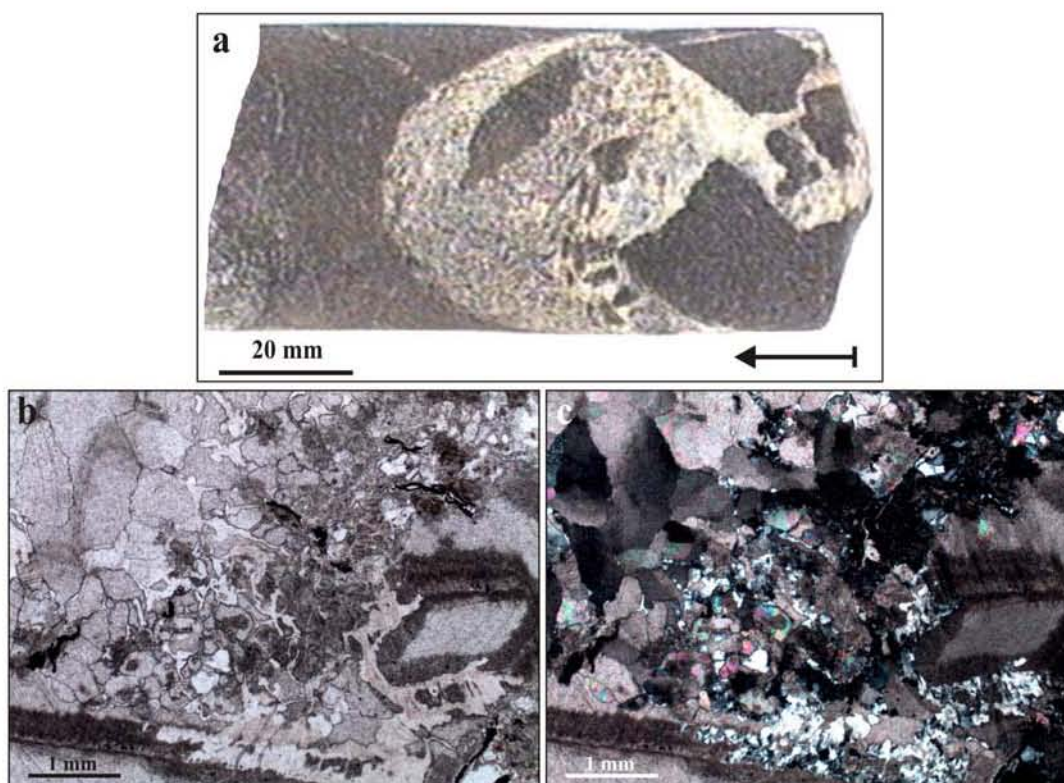


Figure 2.2.22. Brecciated graphite-bearing biotite schist of the Impilakhti suite from the Karku deposit area, DDH 674, 146.1 m; a – sample; b and c – thin section, optical photos, transmitted light, b – plain light, c – polarized light.

Fragments of the graphite-biotite schists of the Impilakhti suite are cemented by calcite with increased U content (up to 635 ppm). Unfortunately, because of low density of the drill grid this zone has not been studied as it would be worth to do. Close to the northern flank of Ore body 3, increased U content has been discovered in a fracture zone in the basalts of the lower subsuite of the Salmi suite (DDH 851, 102 m; fig. 2.2.23)

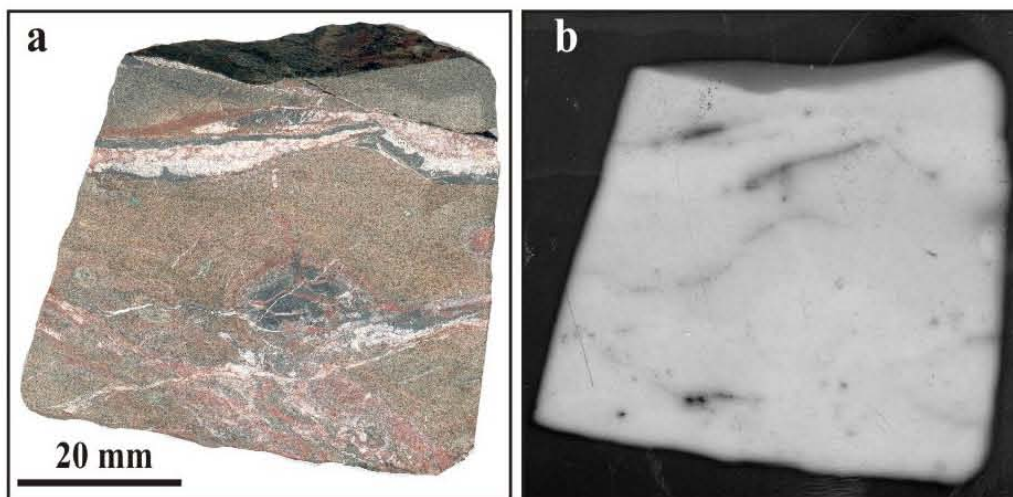


Figure 2.2.23. Brecciated basalt of the Salmi suite lower subsuite from the Karku deposit area, DDH 851, 102 m; a – sample; b – autoradiography.

Identified resource of the Karku deposit is about 8 300 t of uranium. The resource of the high-grade ores with U content over 3 000 ppm is about 1 300 t (Skorospelkin, 2002; Petrov, 2007). Prognostic resource of the Karku deposit is estimated in 11 000 t, of the Central Block – 22 000 t (Vladimir Kushnerenko personal comment).

2.3. Host rocks alterations.

High-grade U mineralization in the Karku deposit is surrounded by a wide halo of host rocks alterations. The halo has a zoned structure. Limits of the zones are not sharp, metasomatic variations gradually replace one another.

In Ore body 1 these alterations have been discovered locally and their structural features are not well studied. In Ore body 2 the ore-associated alterations are weak, and mostly represented by dickitization and hematitization, less by chloritization.

Ore body 3 is the best studied and zoning in the halo is the best defined (Appendix to Chapter 2, fig. 8). That is why the following description of the alterations is mostly documented from Ore body 3 drill cores.

The following succession of alteration zones from external to internal zones of the Karku deposit ore bodies can be proposed (fig. 2.2.24, 2.2.25):

- 1) weak altered bleached sediments;
- 2) chloritized rock;
- 3) leached porous sandstones;
- 4) chlorite-carbonate alteration – external zone of carbonatization;
- 5) sulphide-carbonate alteration hosting high-grade ore.

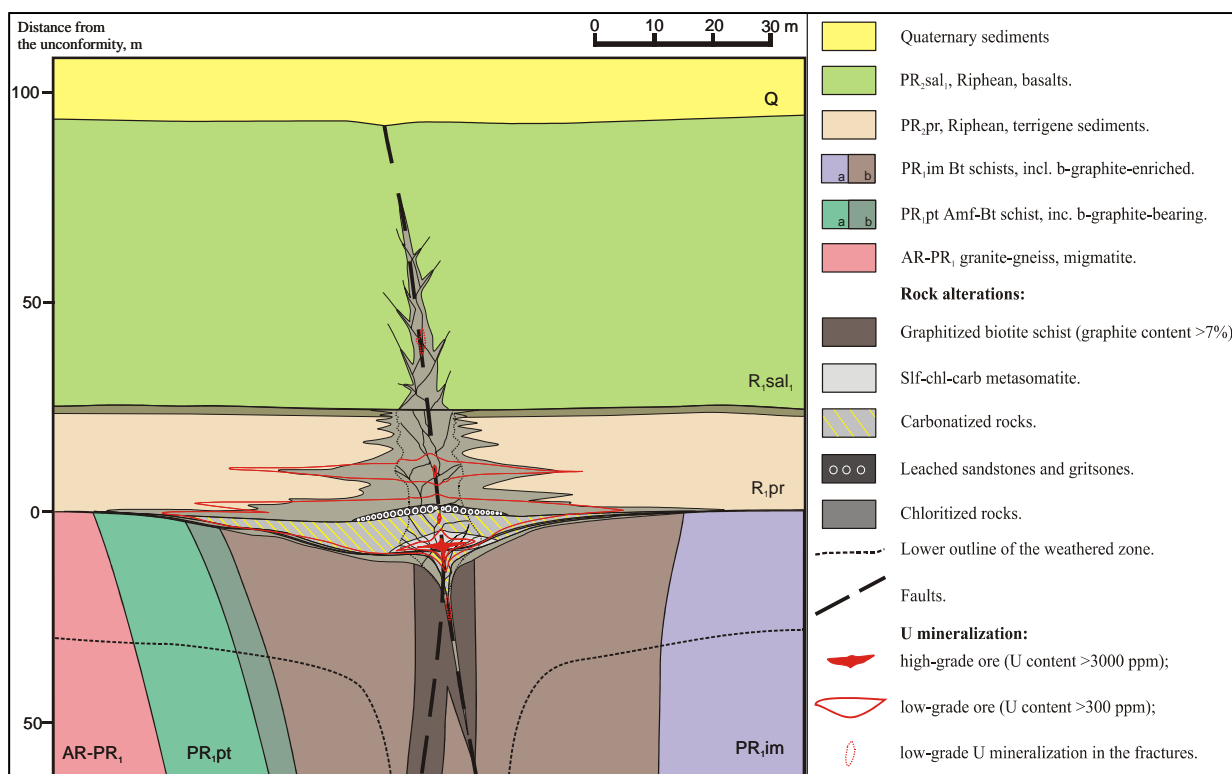


Figure 2.2.24. Generalized geological section of the Karku deposit ore body.

1) *Weakly altered and bleached sediments.*

The external zone of the ore-hosting alteration extends over hundreds meters from the ore bodies and has very gradual contacts with the non-altered sediments. It is characterized by replacement of the clayey cement and partially the clasts by dickite and dissolution of Fe oxides and hydroxides leading to bleaching of the pink and beige background sandstone (fig. 2.2.25 a).

Significant overgrowths on the quartz clasts occur in the sediments of this zone. Often the contact between these two quartz generations is marked with brownish clinocllore and Fe hydroxides aggregates.

2) *Chloritized rocks.*

The external zone of the halo of the strong ore-hosting alteration is composed of dark-grey chloritized rocks (fig. 2.2.25 b). The zone has lens shape with complicated “pine-tree” edges. The indented shape of the flanks of this zone results from the heterogeneity of the sediments – coarse-grained varieties are more permeable than fine-grained ones.

The alteration zone has the largest extension along the unconformity. In Ore body 3 its size is over 400×1000 m. The zone has an increased thickness above the ore bodies. Chloritization reaches the effusive layer along the faults and penetrate into it for a distance over

50 m from the bottom of the layer. Chloritization is developed down to 8 m below the unconformity below the high-grade ores (Roman, 2004).

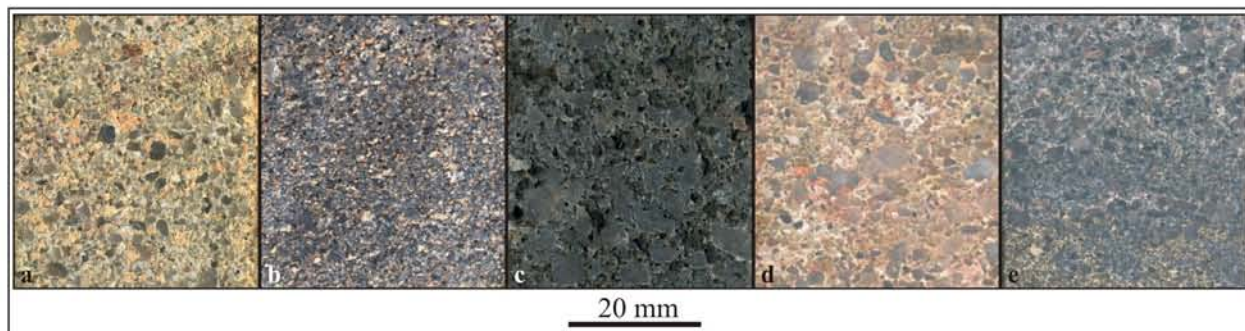


Figure 2.2.25. Samples of ore-hosting altered sandstones from the Karku deposit: a – bleached sandstone, DDH 627, 117 m; b – chloritized sandstone, DDH 627, 124 m; c – leached sandstone, DDH 627, 127.2 m; d – carbonatized sandstone, DDH 671, 123.8; e – sulfide-carbonate metasomatite DDH 671, 123.8.

The composition of the clastic material in this zone slightly differs from the regional sandstones of the Priozersk suite. Proportion of quartz is 85 % in average, overgrowing of detrital grains is widespread (fig. 2.2.26). Feldspar is corroded, partly replaced by dickite, sericite and late kaolinite.

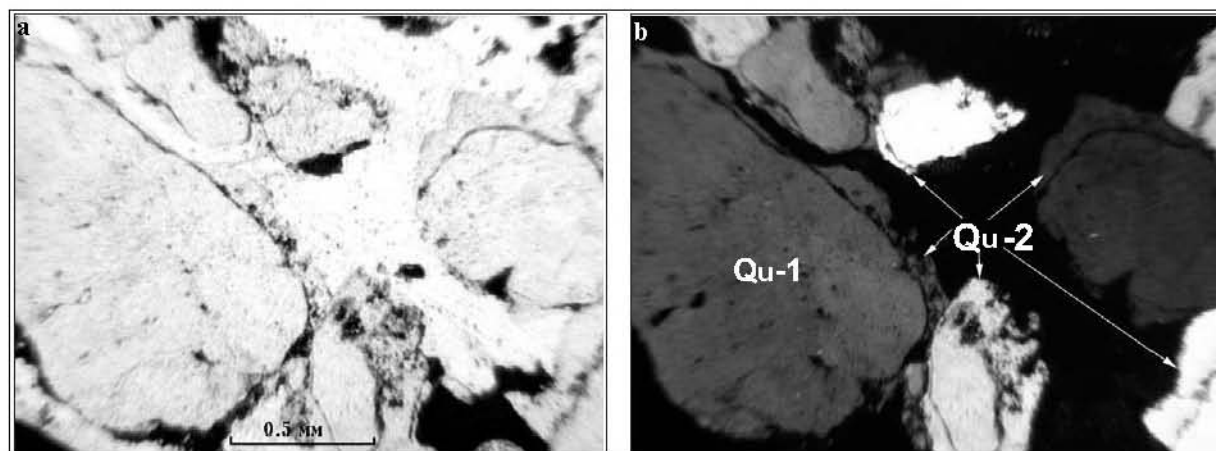


Figure 2.2.26. Overgrowth of epigenetic quartz (Qu-2) on detrital quartz (Qu-1). The Karku deposit, DDH 627, 125.5. Thin section optical photo: a – plain transmitted light, b – polarized transmitted light.

The cement mainly consists of dark-gray chlorite with $FeO/MgO=5.4-7.5$ with subordinated amounts of leucoxene, Fe-hydroxides, dickite and calcite. The hydroxides and dickite contents decrease and calcite content slightly increase toward the halo center.

It is necessary to differentiate ore-associated chloritization and the one occurring in the sandstones at the contact with the overlapping effusive layer. Chlorite from the basalt/ sandstone contact has more Fe and its growth was promoted by the lavas. Besides chlorite, calcite is

abundant in the cement and has a similar origin. The thickness of the alteration in the contact zone is up to 2-3 m with a rather constant extension and has no relation with U mineralization.

3) Leached porous sandstone (euhedral quartz zone).

There is a thin lens (1-2 m thick) of dark-gray (sometimes almost black) porous sandstone above the high-grade ores bodies (fig. 2.2.25 c). It has a cap-like upwards curved shape. Local decrease of the thickness of the lens of porous sandstones occurs where the ore-controlling NW-striking fault crosscut it.

Clastic material is generally of gray to dark-gray quartz (smoky) and, in minor amount of pink to pink-grey K-feldspar (< 6 %). A specific feature of this zone is the presence of quartz overgrowths but also of euhedral crystals, forming tiny druse-like aggregates in the pores.

Dark color of the rock is caused by almost total chloritization of the cement. Calcite content is low, but increases from the top to the bottom of the layer toward the center of the alteration halo.

4) Chlorite-carbonate alteration.

Zone of the chlorite-carbonate alteration is identified with an increase of calcite content. In Ore body 3 this zone is followed over a few hundreds meters along the ore-controlling NW-faults and is tens of meters wide. It is localized along the unconformity. The zone has lens-like profile with a maximum thickness of 22 m above the high-grade U ore body. It occurs mostly in the sandstone layer, but upper part of the regolith (usually less than 1.5 m below the unconformity) with calcite as well and can be considered as part of this zone. In addition, such kind of alteration extends into the ore-controlling faults of the basement down to 12 m from the unconformity.

The color of the carbonatized sandstone varies from dark-gray to light-gray depending on the chlorite-calcite ratio in the cement. Sometimes it has a red color because of Fe-hydroxides (fig. 2.2.25 d). The clastic material is more corroded than in the external zones. Quartz overgrowths are partly resorbed. Carbonatization increases toward the ore bodies, the rock becomes denser and lighter.

5) Sulphide-carbonate alteration.

Specific quartz sandstone cemented with sulphides and carbonates (in Russian literature it is called “sulphide-carbonate metasomatite”) composes the central part of the altered rocks

halo. It is localized at the unconformity and host the high grade U mineralization. The thickness of the sulphide-carbonate zone is up to 5 m. In Ore body 3 this zone extends along the NW fault for distance up to 180 m with a width up to 30 m. Sulphide-carbonate metasomatites are localized mostly in the sandstone layer, although the same kind of alteration occurs locally in the uppermost part (usually < 0.4 m) of the regolith below the high grade mineralization.

This zone is characterized by a very intensive carbonatization. Whole rock CaO contents exceed 15 %. Carbonates replace all minerals of the cement and forms large (up to 20 mm) poikiloblasts including clastic material (fig. 2.2.27). The color of the rock varies from light to dark-gray, depends on the relative calcite, chlorite and pitchblende contents (Appendix to Chapter 2, fig. 9). High-grade U-ore samples are dark grey, since pitchblende composes up to 25 % of the rock. The rock becomes yellowish where sulphides are abundant in the cement (fig. 2.2.25 e). Hematite gives a pink hue to the rock.

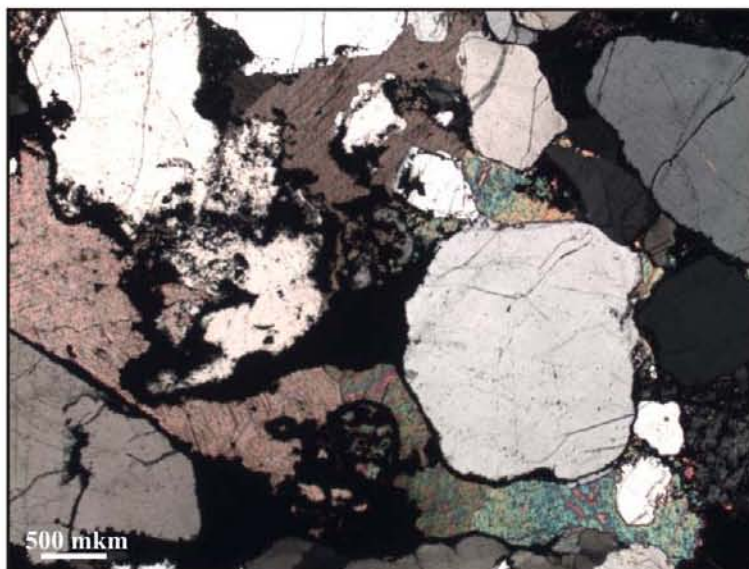


Figure 2.2.27. Poikilitic calcite cement in a sulphide-carbonate altered rock of the Priozersk suite sandstone. The Karku deposit, DDH 671, 124.5 m. Thin section optical photo, polarized transmitted light.

Intensive carbonatization and ore deposition make the rock very dense and resistant. Good calcite cleavage can often be observed on the break of such rock. In this rock the clastic material is corroded. The amount of feldspar is much lower than in the non altered sandstones and in the center of this zone they disappear. Quartz also suffered corrosion and partial replacement by calcite. Smoky quartz is associated with the high-grade U mineralization. Also detrital accessory minerals such as zircon, apatite and garnet are partly corroded.

Chlorite is subordinate and its importance in the cement decrease to the center of the

carbonate-rich zone. Chlorite FeO/MgO ratio varies from 0.24 up to 10. Its Mg content increases towards the central part of the alteration halo where high-grade ores occur. Such tendency is typical for the unconformity-type deposits, but in comparison with ore-accompanying chlorites from the Shea-Creek deposit, those from the Karku have essentially lower Al content (fig. 2.2.28)

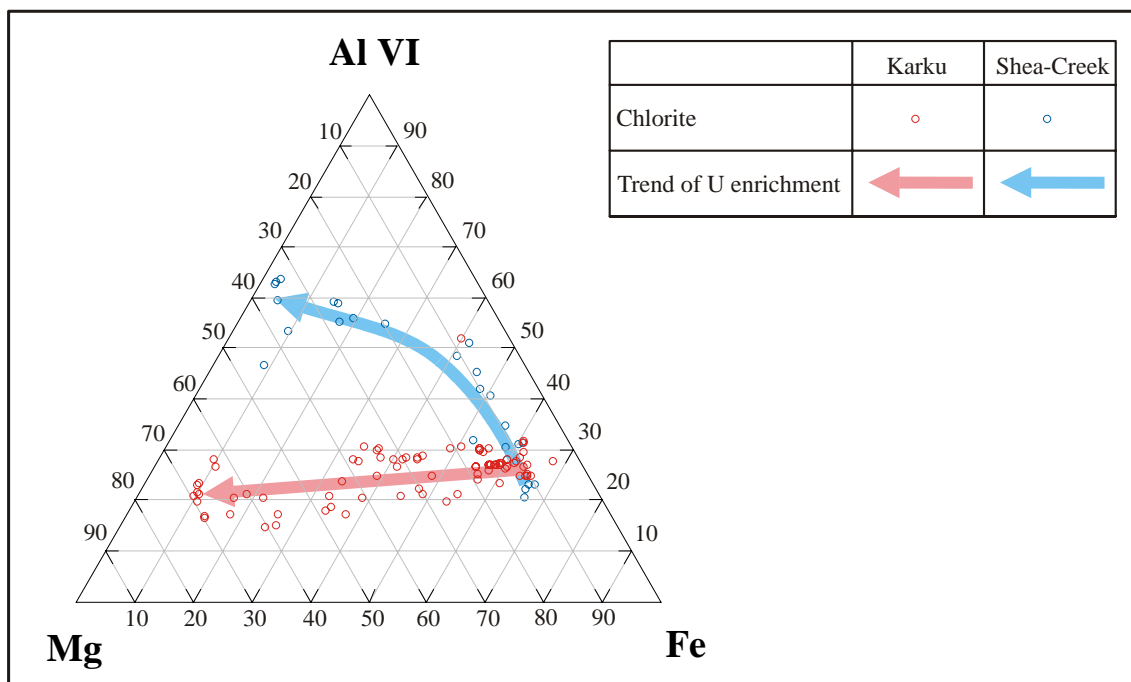


Figure 2.2.28. Composition of chlorites from the Karku and Shea-Creek deposits in Al^{VI} -Mg-Fe ternary diagram; arrows correspond to general trend from background to U-mineralized rock. Chlorite compositions from the Karku after Polekhovskiy et al., 2005 (2), those from the Shea-Creek after Lobaev (2005).

In the diagram MgO/FeO of chlorites versus whole rock U, two types of chlorites can be recognized in the sulphide-carbonate zone according to their MgO/FeO ratio but both are enriched in Mg compared to weaker mineralized rocks (fig. 2.2.29). However, this interpretation is based on X-ray analyses and the valence of iron state is not distinguished.

There is also small amount of other epigenetic minerals, such as apatite, fluorite, Al-lizardite, ilmenite, rutile and sulphides (pyrite, marcasite, pyrrhotite, pentlandite, chalcopyrite, bornite, sphalerite, molybdenite) and a Mo mineral. Bitumen locally occurs in association with the Mo phase and pitchblende (fig. 2.2.30). The amount of sulphides increases toward to the central part of the halo. They often form the main part of the sandstone cement close to high-grade ore. Chemical compositions of altered Priozersk suite sandstones from the Karku deposit are presented in the table 2.2.1.

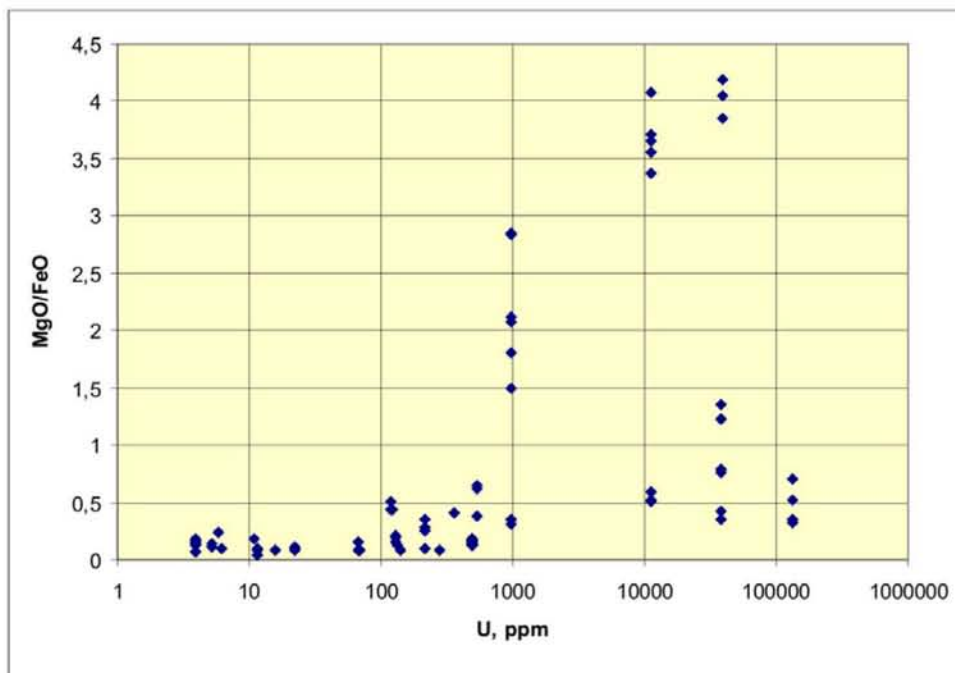


Figure 2.2.29. MgO/FeO diagram of the chlorites versus whole rock U in the Karku deposit (compiled after data of Polekhovskiy et al., 2005 (2)).

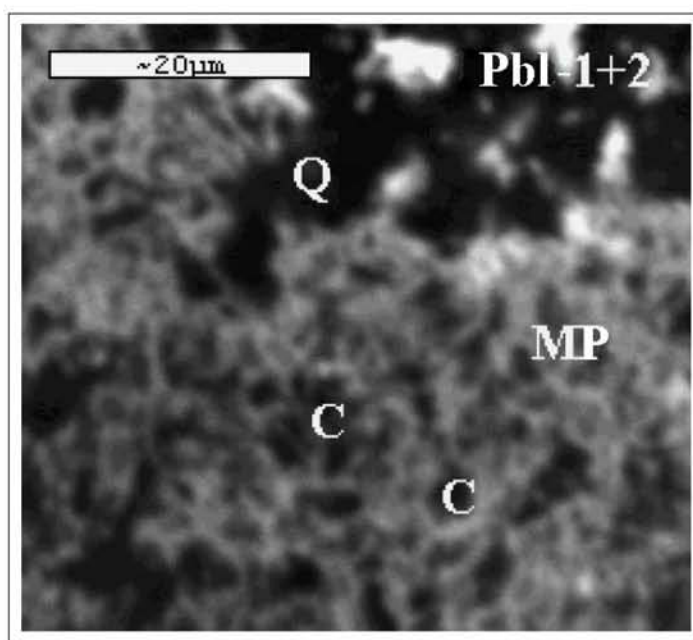


Figure 2.2.30. Bitumen aggregates (C) associated with Mo phase (MP) in sulphide-carbonate metasomatite; quartz (Q) fragments are cemented by pitchblende of two early generations (Pbl-1+2). The Karku deposit, DDH 671, 124.75; BSE photo.

A qualitative diagram of the mineral and element behavior in the different zones of the halo is presented in the (fig. 2.2.31).

Table 2.2.1. Chemical composition of the Priozersk rocks (Polekhovsky et al., 2005 (2)).

Oxides	Low-altered bleached sandstone DDH 671, -113 m	Leached dark gray sandstone DDH 671, -119.5 m	Sulphide-carbonate metasomatite DDH 671, -130.7 m
SiO ₂	89.1	83.6	62.7
Al ₂ O ₃	5.7	4.5	3.4
TiO ₂	0.081	0.081	0.062
FeO	0.62	6.28	3.47
Fe ₂ O ₃	0.21	2.13	0.15
MnO	<0.005	0.051	0.32
MgO	0.25	0.61	0.47
CaO	0.068	0.068	15.9
Na ₂ O	0.11	0.81	0.063
2.2.2O	3.0	0.8	1.3
P ₂ O ₅	<0.05	<0.05	0.11
loss	0.78	1.89	12.8
Sum	99.92	100.09	100.75

SiO₂ and Al₂O₃ depletion towards the center of the alteration halo is caused by quartz and feldspar dissolution. Mg content in the rock increases with increasing of chloritization of the rock and Mg content in the chlorites; the central part of the halo is relatively depleted in Mg because of the low chlorite content of the sulphide-carbonate alteration zone. Dickite content is maximal in the external zone of the alteration; towards the center it is replaced by the chlorite and calcite. A characteristic feature of the Karku deposit zoning is a drastic carbonatization and sulphidization of the high-grade ore-hosting central zones. Local drop of calcite and sulphide contents in the very center of the halo is caused by predominance of the uranium oxides in the cement of the rock.

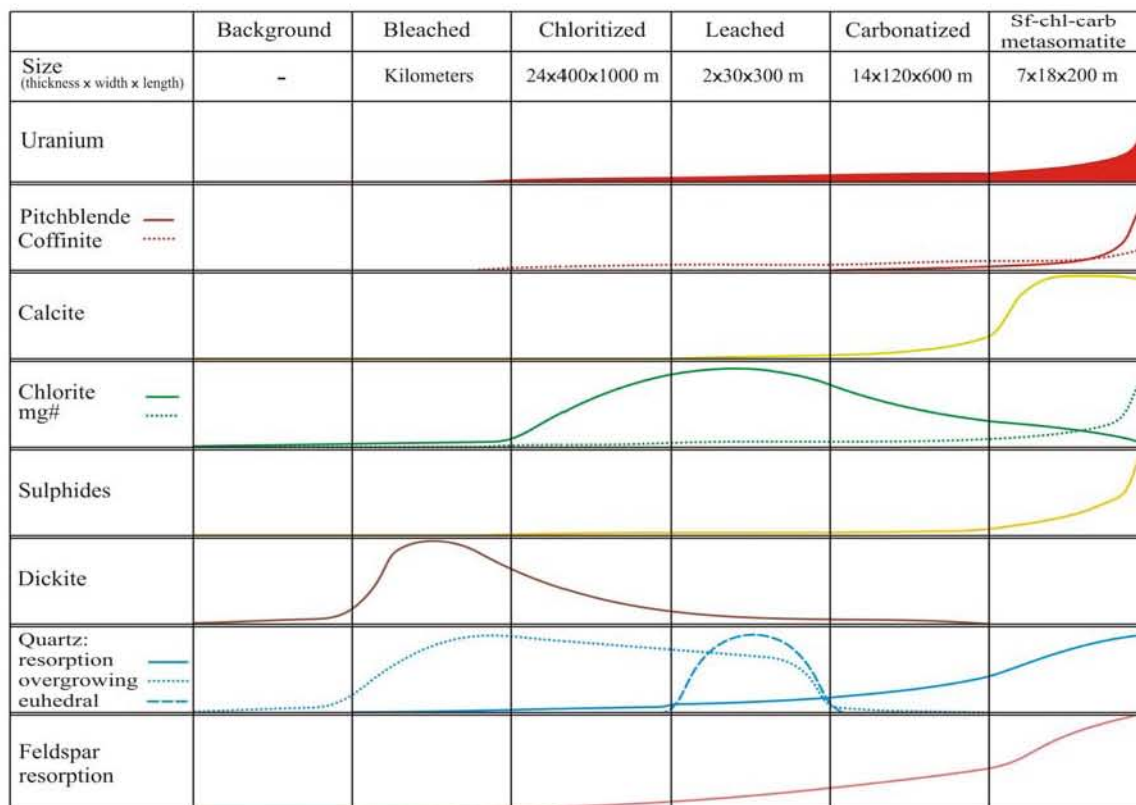


Figure 2.2.31. The mineral and element behavior in the different zones of the Karku deposit alteration halo.

3. Other uranium occurrences in the Riphean formations of the Salmi depression.

There are few uranium occurrences besides the Karku deposit in the Salmi depression. The most significant are the Matala and the Kotalakhti ore-showings.

The Matala ore-showing is located in the Central Block, 1 km west from Ore body 3 on the other flank of the Ilyarantskii granitic-gneiss dome (Appendix to Chapter 2, fig. 2). The uranium mineralization is hosted by the Priozersk suite sandstone and occurs above graphite-enriched biotite schist of the Impilakhti suite as in the Karku deposit. U mineralization occurs at the unconformity and as a halo in the middle part of the sandstone layer. U content is up to 1800 ppm over a thickness of 1.75 m. Increased contents of Pb, Zn, As and Ag accompany it. Ore hosting sandstone is cut by latest fractures filled with hexavalent U minerals.

The Kotalakhti ore-showing is located in the north-western part of the Salmi depression (fig. 2.2.32). Even-grained biotite granites of the Salmi massif occur below the Riphean sediments in that area. The ore-showing is hosted by a fracture zone in basalts of the Salmi lower subsuite. Pitchblende and coffinite occur within quartz-hematite-carbonate veinlets. Deeper along the drilling uranium mineralization has not been observed in the sandstones, but

increased content of Th occurs right above the unconformity.

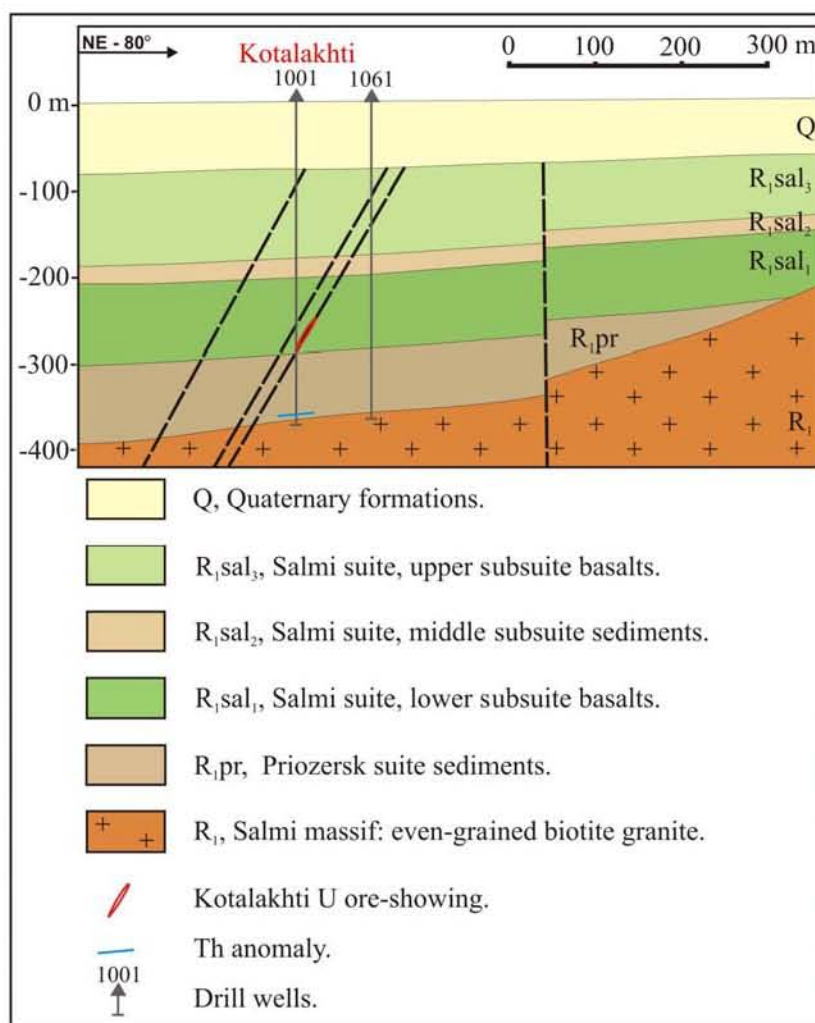


Figure 2.2.32. Geological section of the Kotalakhti ore-showing (compiled after Petrov, 2006).

U contents are up to 890 ppm over 0.4 m in the ore-showing. Two generations of pitchblende and late coffinite are accompanied by increased contents of Pb, Mo and As.

Most of the uranium anomalies in the Salmi depression have been discovered in the best studied Central Block and most of them are hosted by the Priozersk suite sandstones. Several uranium anomalies are located at the northern part of the Central Block and related to thrust structures (Surjamyaki showing). Duplicated sections have been discovered there. Uranium mineralization occurs at different levels of the Riphean sequence: in the sandstones and in the basalts and are related to fracture zones. U contents reach up to 350 ppm. Few U anomalies are hosted by basement rocks. Unfortunately this occurrence was poorly studied because of technical problems and its real resource remains to be evaluated.

Other radioactive anomalies of the Salmi depression occur at different levels of the

sequence, but most of them are localized close to the unconformity. As a rule the mineralization is related to tectonic structures and sometimes it penetrates along them in to the basement and in the upper levels of the Riphean sequence. So few U anomalies accompanied by high content of Ag, Zn, and Pb have been discovered in the Pasha suite sediments.

Several radioactive anomalies have been discovered in the Priozersk suite sandstones overlying the Salmi granites but they are mainly Th rich. Also spots with increased Th contents are quite common for the Priozersk suite and especially for its basal horizons.

Total prognosticate resource of the Salmi depression is estimated in 41 000 tons (Vladimir Kushnerenko personal comment).

4. Characteristics of the radioactive mineralization.

The following of mineralogical and petrographic descriptions of the U mineralized rocks is based on the observation of drill core samples from the Karku deposit (mainly DDH 612, 621, 625, 627, 656, 671, 674, 680, 687, 749, 770, 817, 843, 844, 851). In addition, some other sites have been studied: DDH 872 and 890 in the Central Block area, DDH 913 and 929 for Matala and DDH 1001 for Kotalakhti ore-showings, south of the Salmi depression (DDH 1043).

4.1. Textural types of the radioactive mineralization

Six types of textures for the radioactive mineralization have been distinguished in the Karku area as a result of the drill core autoradiographic observations (Polekhovsky et al., 2005 and 2007 (2)): 1) layered, 2) impregnated, 3) striated, 4) nested, 5) massive, 6) vein.

Layered type (fig. 2.2.33 a): occurs in the sandstones and gritstones. It has the lowest radioactivity. Existence of layered-type concentrations is caused by local syn-sedimentary heavy radioactive minerals concentrations (U and Th-bearing accessories). They have been discovered in the Karku deposit area and at the distance from the epigenetic mineralization.

Impregnated type of uranium mineralization (fig. 2.2.33 b) is formed by local concentrations of epigenetic radioactive minerals (pitchblende and coffinite mainly) and was discovered in the Karku deposit and other occurrences. This type is more radioactive than the layered mineralization (40-90 $\mu\text{R/h}$, rarely – up to 150 $\mu\text{R/h}$ in the drill core samples).

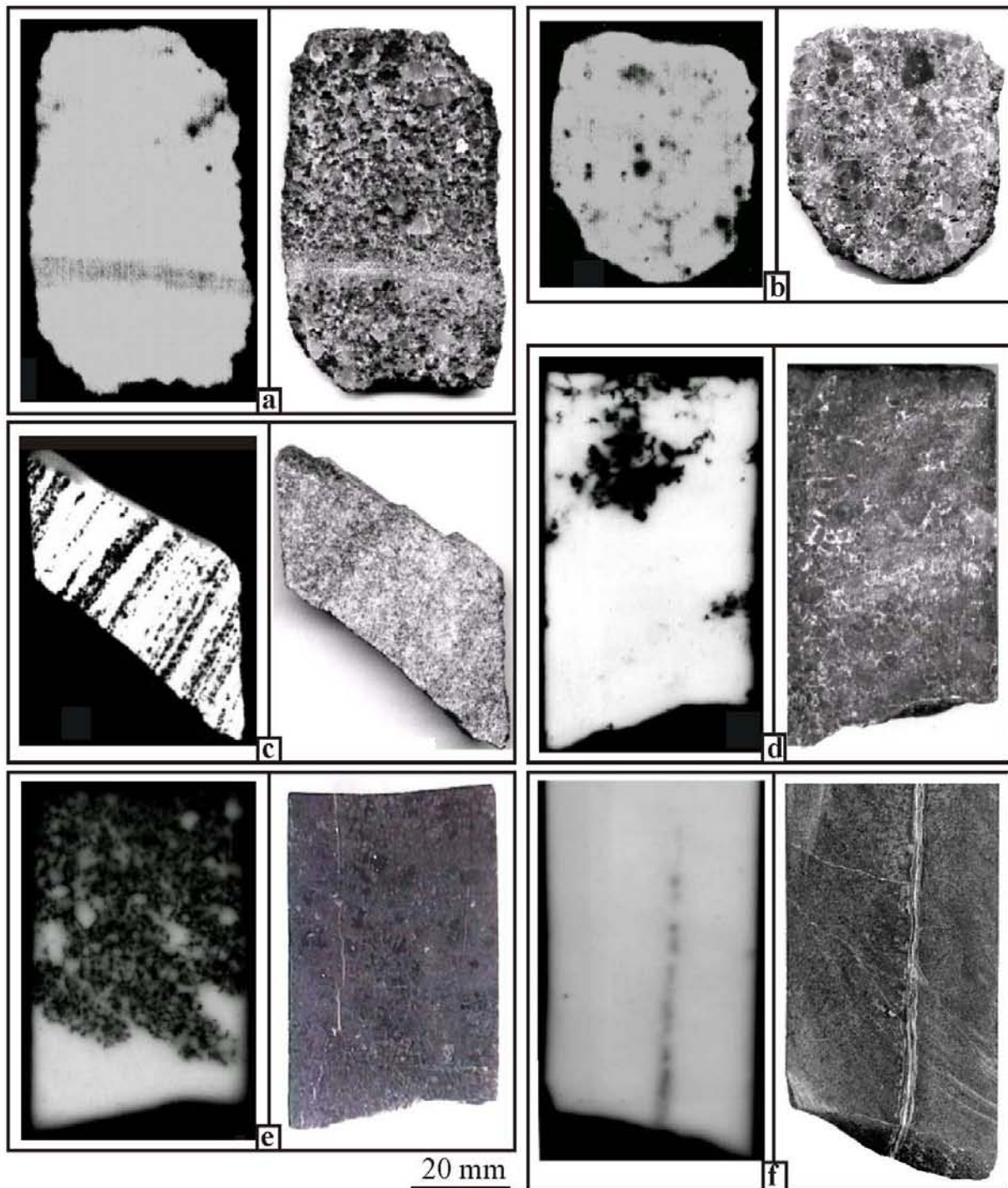


Figure 2.2.33. Autoradiographies and corresponding samples of different textural types of the radioactive mineralization (a-e – from the Karku deposit, Ore body 3, f – the Kotalakhti ore-showing): a – layered type in the leached quartz-feldspar gritstone, DDH 627, 127.2m (16 days exposition autoradiography); b – impregnated type in the bleached quartz-feldspar gritstone, DDH 627, 127.4 m (16 days exposition autoradiography); c – striated type in the graphite-biotite schist, DDH 627, 137.2 m (16 days exposition autoradiography); d – nested type in the sulphide-carbonate cemented quartz sandstone DDH 621, 122.5 m, (72 hours exposition autoradiography); e – massive type in the pitchblende-sulphide-carbonate cemented quartz sandstone, DDH 625, 131.3m: a – (20 hours exposition autoradiography); f – vein mineralization in the basalts of the Kotalakhti ore-showing, DDH 1001, 238.2m, (16 days exposition autoradiography).

Striated type of U mineralization (fig. 2.2.33 c) was observed in graphite-bearing biotite schists of the Impilakhti suite at the very bottom of Ore body 3. This type mineralization is composed of epigenetic uranium minerals: pitchblende and coffinite. Radioactivity of the samples is up to 250 $\mu\text{R/h}$.

The high-grade uranium ore is composed of the *nested* (fig. 2.2.33 d) and *massive* (fig. 2.2.33 e) *types* of the mineralization. They are typical for the sulphide-carbonate alteration zone of the Karku deposit. These types of the mineralization are composed of pitchblende with subordinated coffinite. Samples of nested and massive ore have radioactivity of 400-800 $\mu\text{R/h}$, sometimes exceeding 3000 $\mu\text{R/h}$.

Late redistribution of the uranium ores produced the *vein type* mineralization. The veinlets cut all the rocks of the Karku area, but only a few U mineralized ones have been discovered. Three drill holes with pitchblende-coffinite mineralization in fractures occur in the Salmi suite basalts from the Karku deposit area (Ore body 1, DDH 609 and 641; DDH 851 at the northern flank of the Ore body 3). The Kotalakhti ore-showing (DDH 1001, fig. 2.2.33 f) located in 18 km to the north-west from the Karku is an occurrence of uranium mineralization in the fractured Salmi suite basalts. Vein-related mineralization forms low-grade concentrations with radioactivity up to 200 $\mu\text{R/h}$.

4.2. Radioactive mineralogy.

Diverse radioactive minerals have been recognized in different parts of the Salmi area, but principal ones are pitchblende and coffinite composing absolutely dominating part of resources of the Karku deposit and uranium ore-showings.

Uranium oxides

Uranium oxides discovered in the Salmi depression are represented by several generations of pitchblende. Early generations form separated nodules (2-30 μm large) and aggregates. They compose main part of the cement of the high-grade mineralized sandstones of the Karku deposit (fig. 2.2.34). Also they occur as loop-shaped aggregates in the Priozersk suite sediments of the altered halo or in an intergranular space in the Impilakhti suite graphite-biotite schist (fig. 2.2.35). Chemical compositions of the uranium oxides are presented in the General Appendix 2.5 and 2.6.

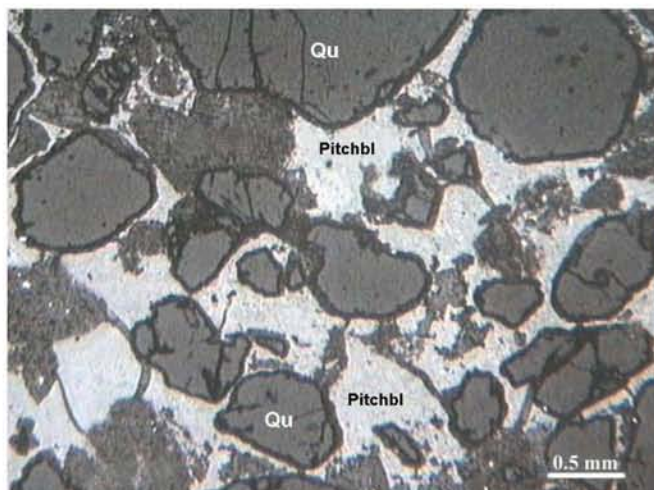


Figure 2.2.34. Pitchblende (Pitchbl) as a cement of the high-grade mineralized sandstone in the Karku deposit, central part of Ore body 3, DDH 627, 131.75 m; optical photo of a polished section, reflected light.

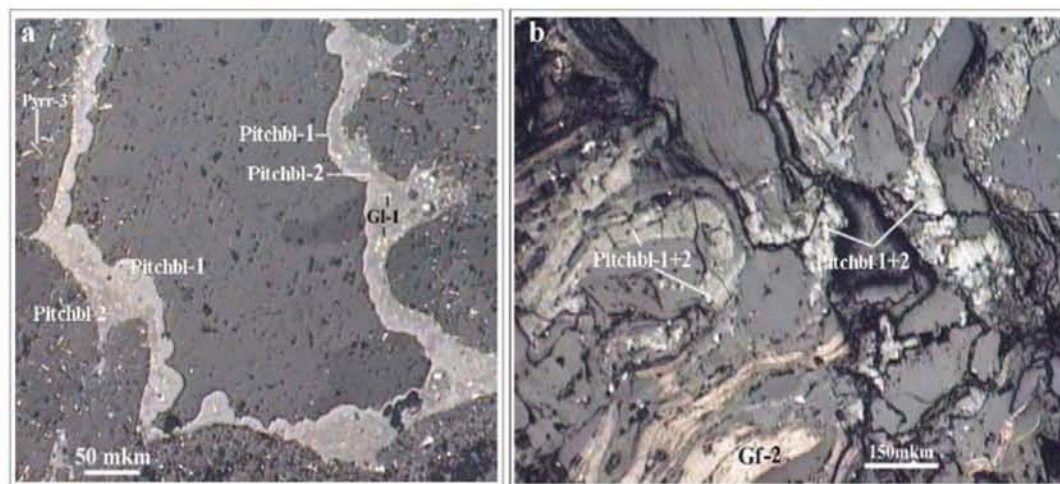


Figure 2.2.35. Intergranular aggregates of two pitchblende generations (Pitchbl-1 & 2); the Karku deposit, central part of Ore body 3, optical photos of polished sections, reflected light: a – altered quartz sandstone with the carbonate cement, DDH 627, 131.8 m; b – altered graphite-bearing schist, DDH 656, 136.3m.

Pitchblende-1 ($\text{UO}_{2,3}$) is a light-gray mineral a little bit more reflective than sphalerite. It occurs in the sandstone cement and in weathered basement rocks where it replaces as pre- and early-epigenetic minerals. Contents of UO_2 is 68.2-86.4 wt%, PbO – 1.5-16.5 wt%, SiO_2 – 1.6-16.5 wt%, although the highest SiO_2 content may result from the simultaneous analysis of quartz micro inclusions. In pitchblende-1 high TiO_2 (up to 1.9 wt%), MnO (up to 1.8 wt%), Al_2O_3 (up to 1.1 wt%), FeO (up to 2.2 wt%), CaO (up to 5.4 wt%) and ThO_2 (up to 5.4 wt%) have been also measured. Pitchblende-1 has collomorph shelly structure, especially revealed when replaced by pitchblende-2 or coffinite (fig. 2.2.36 a). There are radial and concentric shrinkage fractures in the massive pitchblende filled with galena-2 (fig. 2.2.36 b) or pyrrhotite (fig. 2.2.36 c).

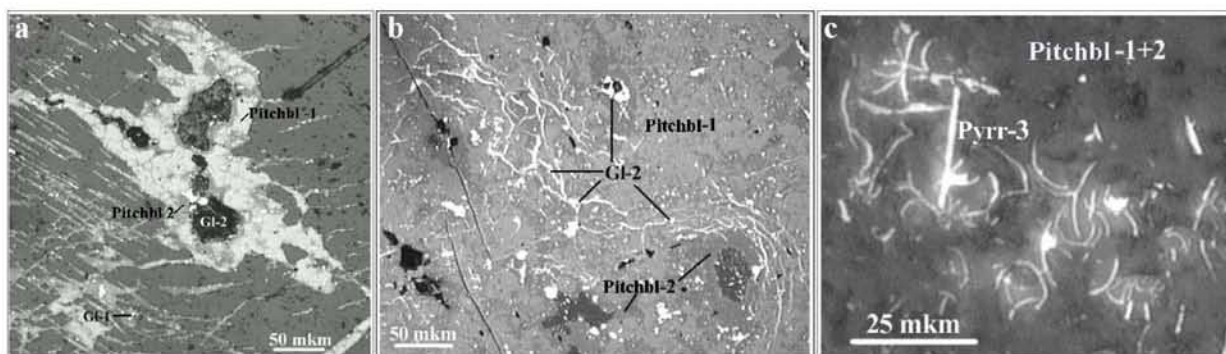


Figure 2.2.36. Mineralogical particularities of the pitchblendes from the high-grade ores of the Karku deposit (central part of Ore body 3, DDH 680, 125 m), optical photo of polished sections, reflected light: a – colloform-conchoidal structure of the pitchblende (Pitchbl-1 & 2), small grains of galena (Gl-1 & 2) occur; b – development of galena (Gl-2) in the desiccation fissures of the pitchblende (Pitchbl-1 & 2); c – stick- and curve-like aggregates of pyrrhotite (Pyrr-3) in pitchblende (Pitchbl 1+2).

Intensive carbonatization precedes pitchblende deposition. Calcite overgrowths replace quartz grains (fig. 2.2.37 a), and enclose brannerite (fig. 2.2.37 b), zircon, garnet and secondary pyrite (fig. 2.2.37 c).

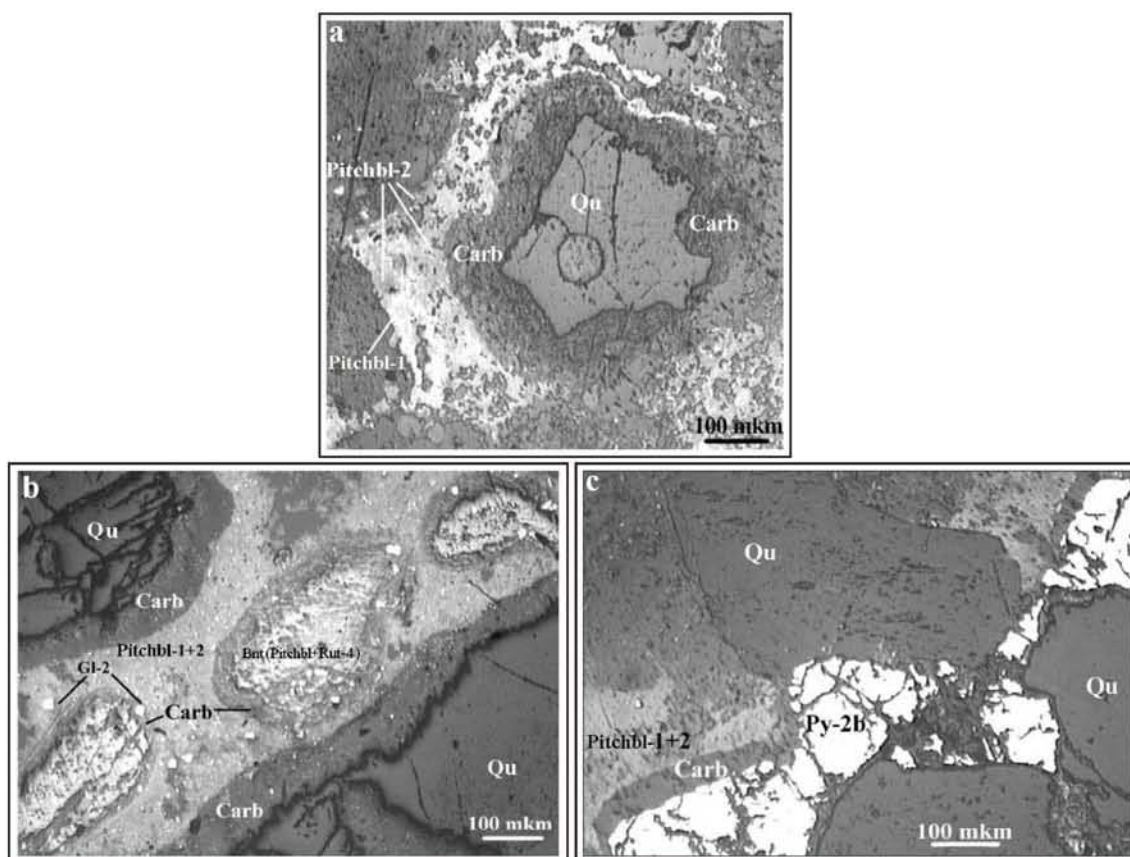


Figure 2.2.37. Carbonate overgrowths and replacement of different mineral phases; the Karku deposit, central part of Ore body 3, DDH 680; optical photos of polished sections, reflected light: a – of quartz (Qu), 125.2 m; b – of brannerite (Bnt), 125.4 m; c – of pyrite (Py-2b), 125.7 m.

Pitchblende content increases toward the central part of the ore body. At the periphery of the high-grade ore bodies pitchblende replaces carbonate of the cement and pyrrhotite impregnations are widespread in the carbonate-chlorite borders (fig. 2.2.38 a). When pitchblende content increases in the intergranular space, sulphides disappear from the borders. Thus, the highest-grade mineralization is mainly composed of clastic quartz relics cemented by pitchblende, carbonate and galena mainly associated with pitchblende-2 (fig. 2.2.38 b).

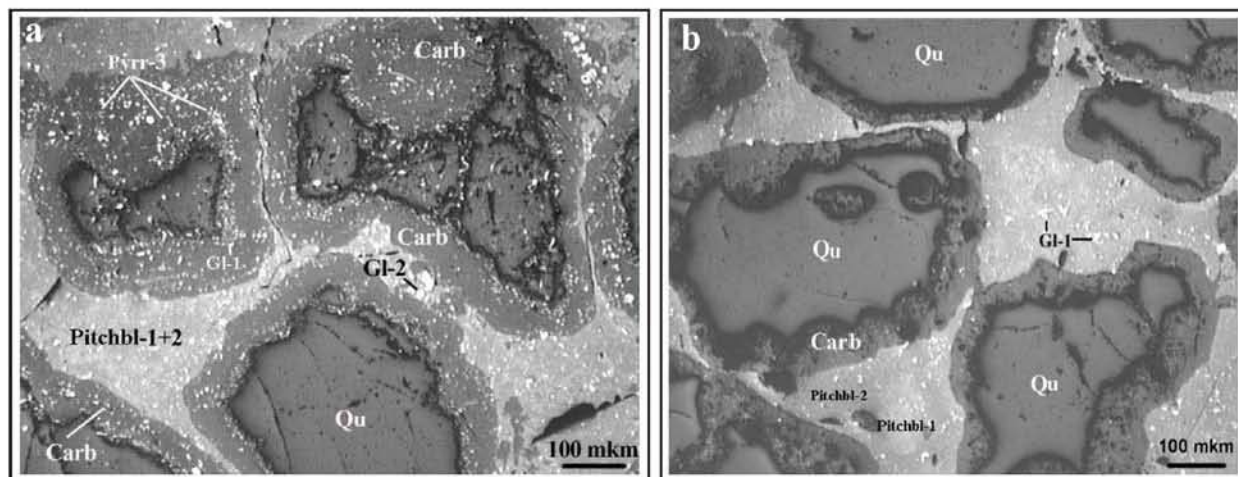


Figure 2.2.38. High-grade pitchblende mineralization of the Karku deposit, central part of Ore body 3, DDH 680, optical photo of the polished sections, reflected light: a – thin impregnation of pyrrhotite (Pyrr-3) in carbonate rims of corroded quartz (Qu); pitchblende (Pitchbl 1+2) includes small grains of galena (Gl-1); 125.3m; b –pitchblende (Pitchbl-1&2) cements quartz fragments enveloped by carbonate; galena (Gl-1) impregnations occur in pitchblende; 125.4 m.

Pitchblende-2 is a darker-gray mineral. It partly replaces pitchblende-1 and forms of irregular cloud-like aggregates. Pitchblende-2 is usually accompanied by disseminated fine-grained radiogenic galena (fig. 2.2.39). UO_2 contents are lower in pitchblende-2 (63.8-82.9 wt%). PbO content varies from 0.7 to 13.0 wt% (high contents may be due to contamination by galena-1). SiO_2 content varies from 4.3 to 12.8 wt%. Content of Y_2O_3 is up to 3.9 wt%, BaO – up to 1.3 wt% and SrO – up to 1.0 wt% (Polekhovsky et al., 2005).

The following ore minerals are associated with pitchblende-1 and 2 in variable proportions: galena-1 and 2, Cd-sphalerite, greenockite, howlite, Mo phase, Cu-arsenides, Fe, Ni, Co arsenides and sulphoarsenides. Pitchblende-1 and 2 are partly replaced by coffinite and hydropitchblende.



Figure 2.2.39. Pitchblende (Pitchbl-1 & 2) cement of the altered quartz sandstone; galena (Gl-1) impregnations occur in the pitchblende; the Karku deposit, central part of Ore body 3, DDH 680, 125.4m; optical photo of a polished section, reflected light.

Pitchblende-3&4. Late U mineralization occurs in the quartz-chlorite-carbonate veinlets cutting the lower volcanogenic layer (fig. 2.2.40). Mineral paragenesis of pitchblende-3 is similar to one of the unconformity-related high-grade mineralization. Pitchblende-3 is associated with galena, pyrite, marcasite and chalcopyrite (fig. 2.2.40 b). UO_2 content of pitchblende is 72.9-89.8 wt%, PbO – 0.7-8.1 wt%, SiO_2 – 3.7-6.4 wt%. Pitchblende-3 is replaced by pitchblende-4 and coffinite. UO_2 content of pitchblende-4 is up to 86.6 wt%, PbO – up to 3.7 wt%, SiO_2 – up to 6.4 wt% (Polekhovsky et al., 2005). Low PbO indicates rather young age of the mineralization. High SiO_2 is an evidence of late alterations of the mineral phases.

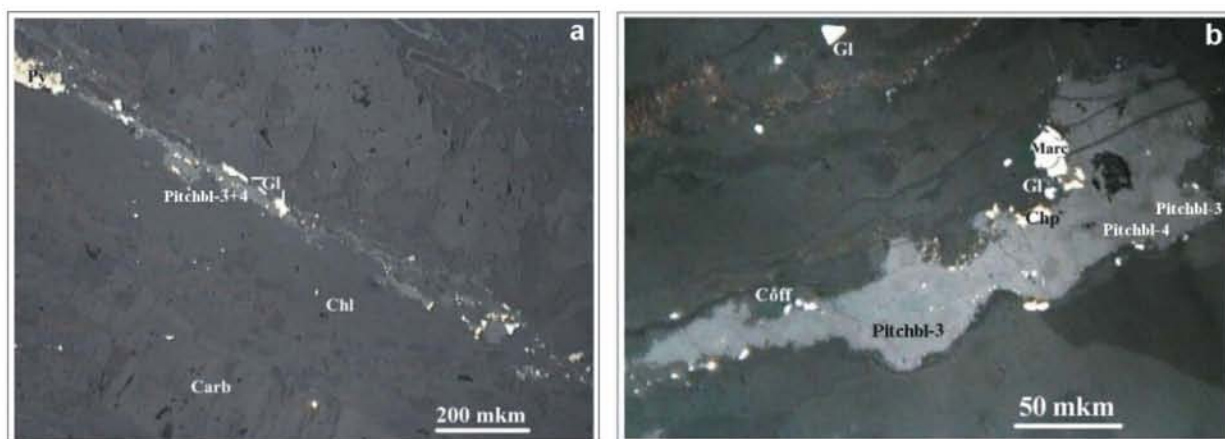


Figure 2.2.40. Vein-type U mineralization in the Salmi suite basalts; the Kotalakhti ore-showing, DDH 1001, 238.2m; optical photos of a polished section, reflected light; a – two generations of pitchblende (Pitchbl 3+4) in the quartz-chlorite(Chl)-carbonate(Carb) veinlet; b – enlargement of the same veinlet introduces consecutive replacement of pitchblende-3 (Pitchbl-3) by pitchblende-4 (Pitchbl-4) and both – by coffinite (Coff); galena (Gl), chalcopyrite (Chp) and marcasite (Marc) occur on the pitchblende aggregate periphery.

Uranium silicates

Coffinite $U[SiO_4]$ is the most widespread uranium mineral in the Karku deposit area. It occurs in the Priozersk suite sandstones, in graphite-bearing schists and in fracture zones in the basalts. In high-grade ores it is subordinated and replaces pitchblende (fig. 2.2.41 a). It is a major uranium mineral of the ore bodies periphery where it partly composes the sandstone cement.

Coffinite is a dark mineral with low reflectivity close to that of non-ore matrix. Sometimes it can be found finely disseminated in sulphides inherited from replaced pitchblende; there is disseminated rutile when coffinite replaces brannerite and ilmenite (fig. 2.2.41 b).

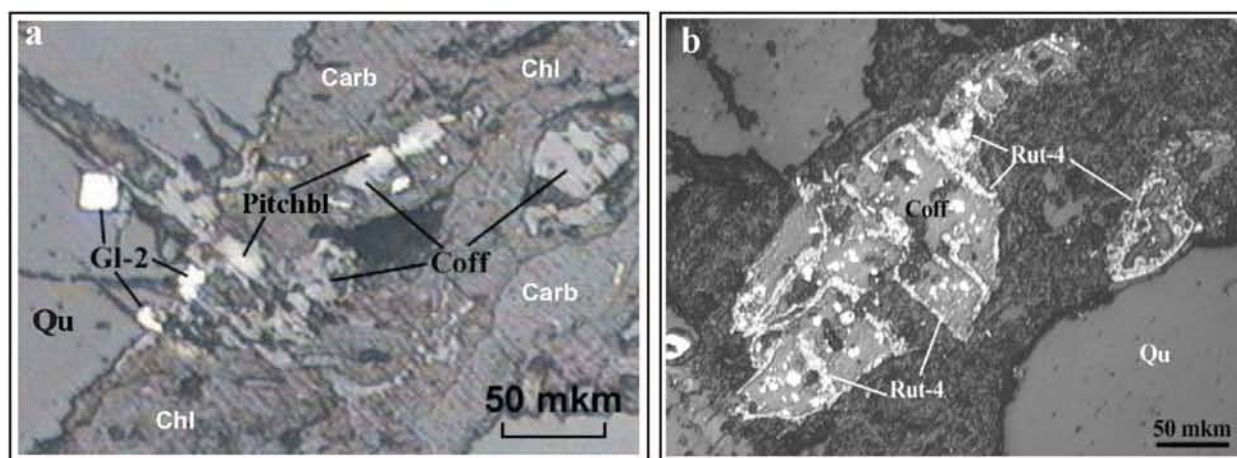


Figure 2.2.41. Coffinite (Coff) mineralization in the altered sulphide-carbonate Priozersk suite sandstone; the Karku deposit, central part of Ore body 3; optical photos of polished sections: a –coffinite develops after pitchblende, DDH 627, 135.3m; b – pseudomorphs of coffinite after the ilmenite; development of late rutile (Rut-4) occurs; DDH 680, 126.7m.

Coffinite forms xenomorphic replacement of pitchblende or can be observed isolated. The last case is common for ore body periphery where coffinite is associated with carbonate, sulphides and Fe-hydroxides composing the cement of the altered sandstone (fig. 2.2.42, 2.2.43). Coffinite nodules occur in fractures and at the rim of pyrite-2 (fig. 2.2.44a) and chalcopyrite (fig. 2.2.44b) grains. Coffinite pseudomorphs develop inside the zircon grains (fig. 2.2.45).

Sometimes coffinite fills thin veinlets in the sandstones (fig. 2.2.46), basement rocks and effusives. These veinlets can be monomineralic or with hydropitchblende and carbonate.

As it is a hydrated mineral, trace element content varies largely in the coffinite composition. The following composition variations have been measured: UO_2 – 27.8 to 67.9 wt%; SiO_2 – 5.8 to 28.6 wt%; P_2O_5 up to 7.9 wt%; Y_2O_3 up to 8.9 wt%; V_2O_5 up to 2.1 wt%, Ce_2O_3 up to 3.0 wt%. Chemical composition of the coffinite from the basement-hosted breccias zone at southern flank of the Ore body 3 (DDH 674) is presented in General Appendix 2.6.

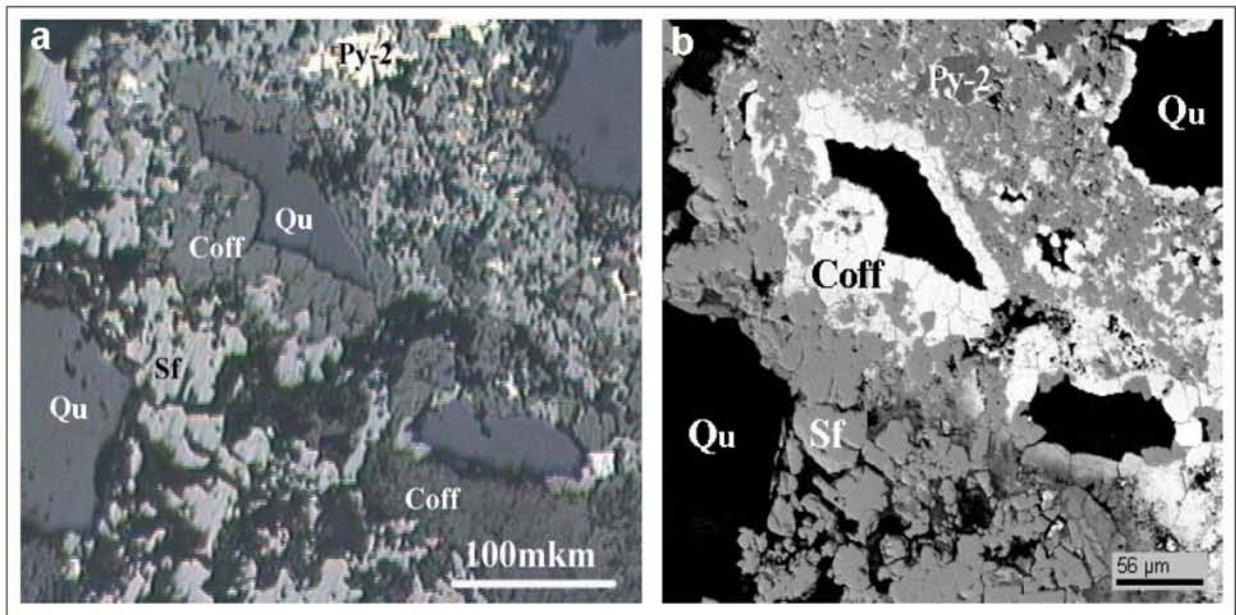


Figure 2.2.42. Coffinite (Coff) replaces quartz (Qu); sphalerite (Sf) and pyrite (Py-2) develop in the intergranular space of the Priozersk suite sandstone; the Karku deposit, Ore body 2 periphery, DDH 817, 171.0 m; a – optical photo of a polished section, reflected light; b – BSE-photo.

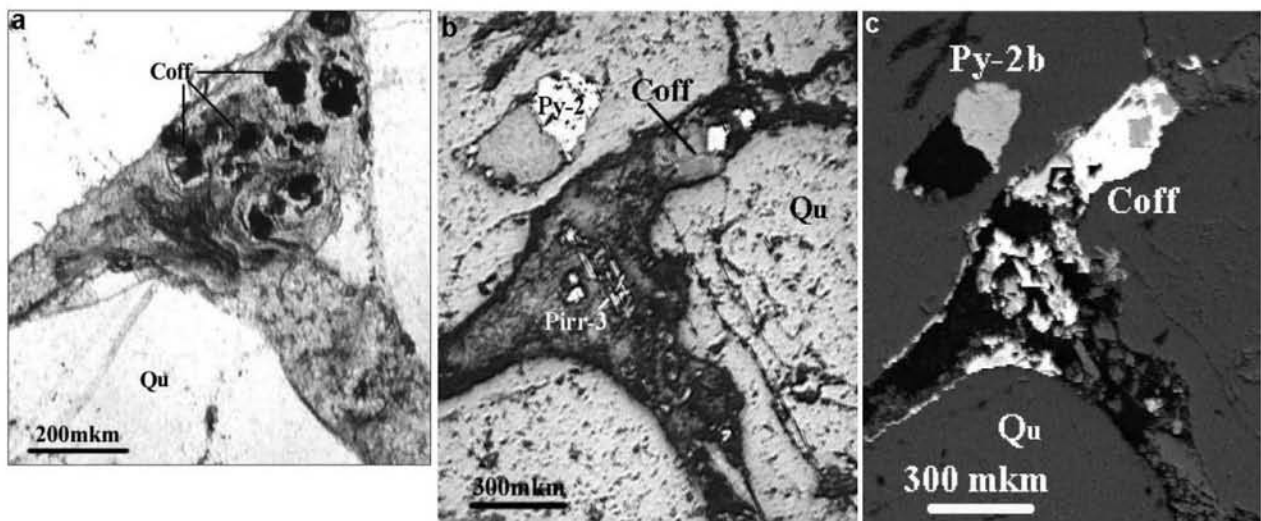


Figure 2.2.43. Coffinite-carbonate cement of the quartz-feldspar sandstone; the Karku deposit, Ore body 3 periphery, DDH 656, 129.6 m, thick section: a – optical photo, plain transmitted light; b – optical photo, reflected light; c – BSE-photo.

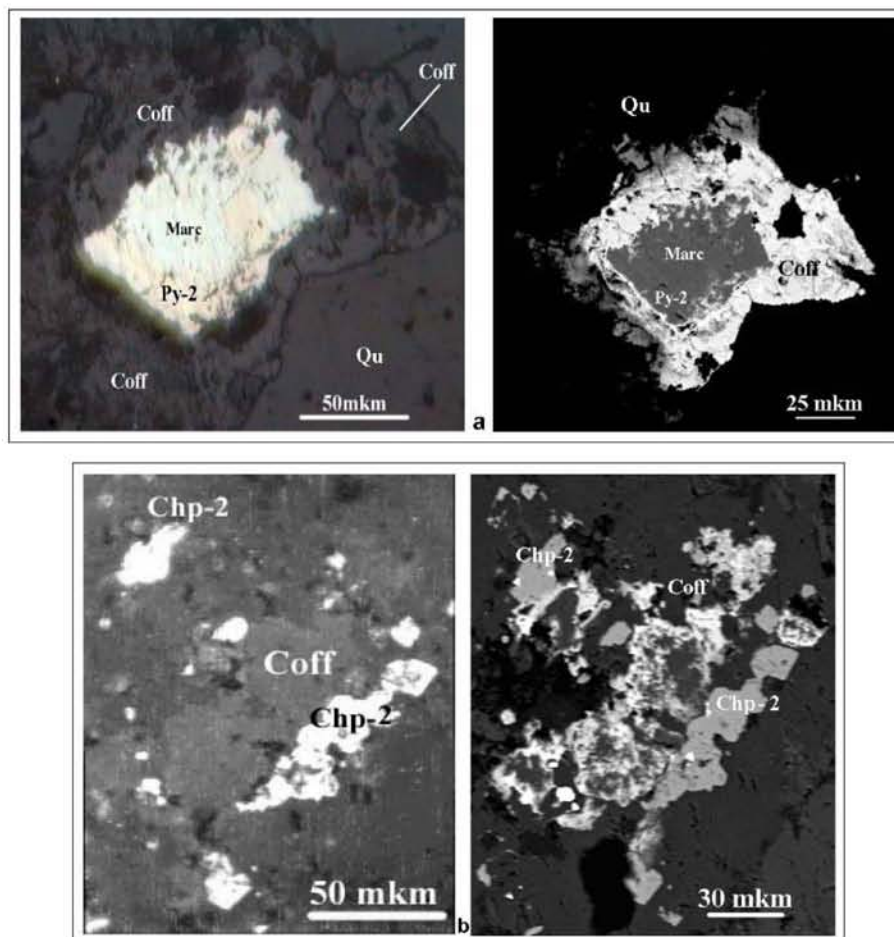


Figure 2.2.44. Diverse types of coffinite (Coff) development, the Karku deposit, optical photos in reflected light in the left column, BSE-photos in the right one: a – coffinite in fractures and on periphery of pyrite (Py-2), the Priozersk suite sandstone, Ore body 2, DDH 817, 171 m; b – coffinite replaces chalcopyrite (Chp-2) in brecciated schist of the Impilakhti suite at the southern flank of Ore body 3, DDH 674, 143.1 m).

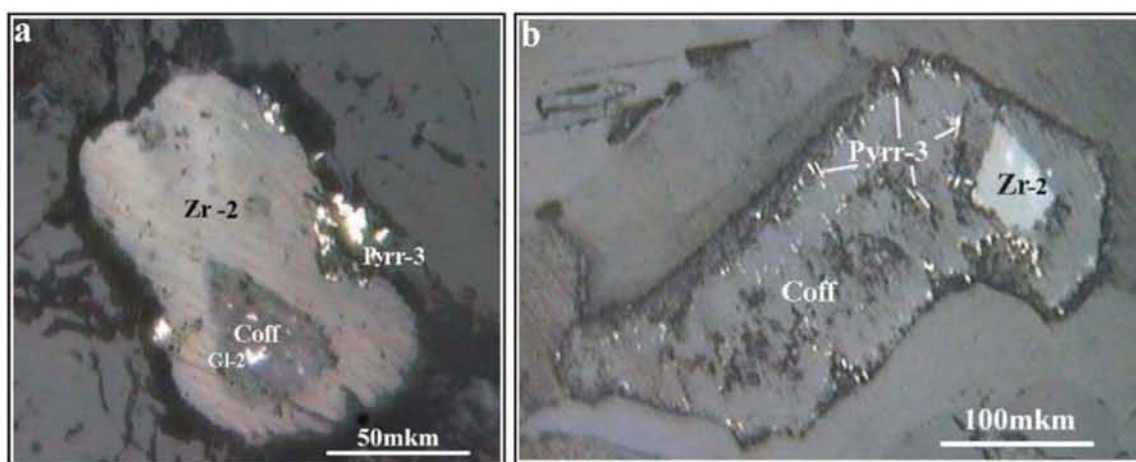


Figure 2.2.45. Coffinite (Coff) replacement of zircon (Zr-2); optical photos of polished sections, reflected light: a – partial replacement with development of the coffinite on periphery and in center of the zircon grain; galena (Gl-2) and pyrrhotite (Pyrr-3) porphyroblasts occur as well; the Karku deposit, the Ore body 1, DDH 844, 185 m; b – almost total replacement of the zircon grain, central part of the Central Block, DDH 890, 79.2 m.

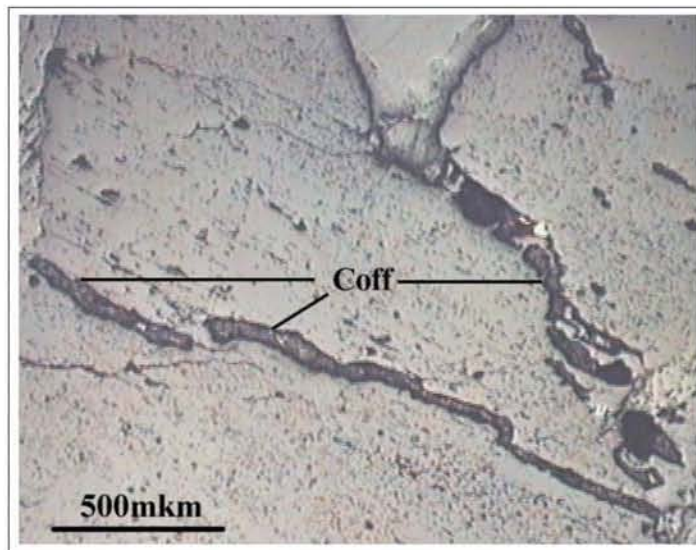


Figure 2.2.46. Coffinite (Coff) veinlets in the quartz-feldspar sandstone; the Karku deposit, northern flank Ore body 3, DDH 890, 79.2 m, optical photo of a polished section, reflected light.

Apart of above-described coffinite varieties, there is a rare mineral coffinite-like phase with Y_2O_3 content up to 16.9 wt% and Nd up to 0.7 wt%. It is characterized by UO_2 content up to 45.9 wt%. Usually it has a collomorph structure (fig. 2.2.47a). Sometimes this mineral is idiomorphic (fig. 2.2.47b), probably in relation with the replacement of a former mineral.

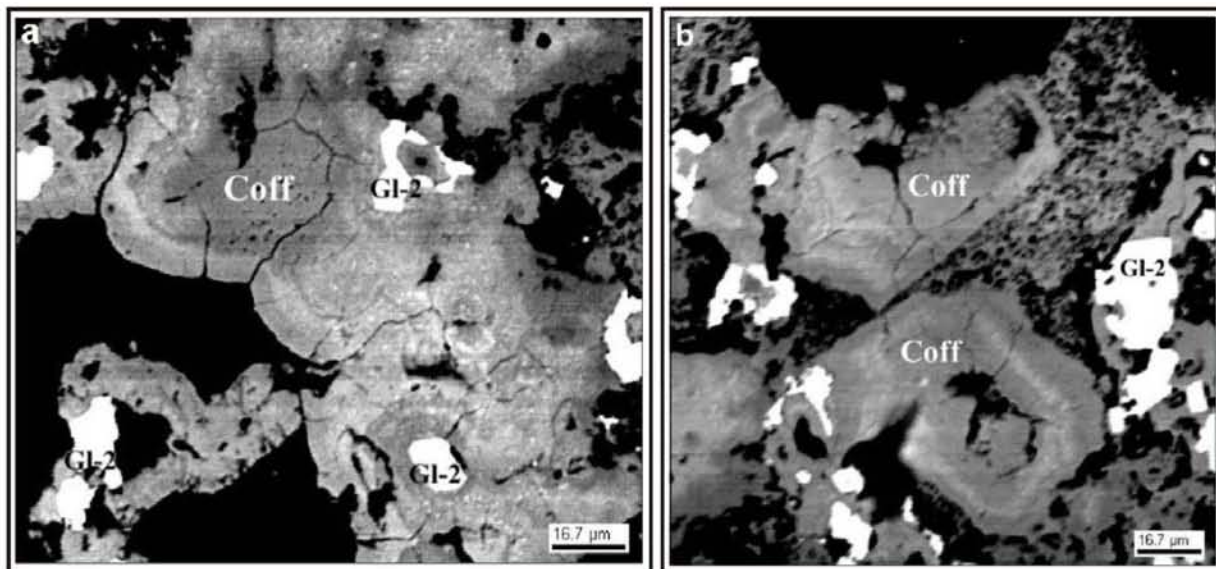


Figure 2.2.47. Coffinite-like phase (Coff) in cement of the Priozersk suite sandstone, northern part of the Central Block, DDH 872, 113.3m, BSE-photos: a – colloform aggregates; b-pseudo-idiomorphic aggregates.

Uranium vanadates.

Carnotite ($K_2[UO]_2[VO_4]3H_2O$) has been discovered in the tectonized sandstones of the Matala ore-showing only. It occurs in the sandstone cement as aggregates in the intergranular space and as thin veinlets (fig. 2.2.48). Aggregates of carnotite are small (1-5 μm) with different oriented plates (fig. 2.2.49). In the Matala ore-showing the mineral has almost stoichiometric composition, with small (<1.2 wt%) contents of Si, Ti, Al, Fe, Mg, Ca, Cr and Ba. There are V-celadonite, hollandite and hydrohematite associated with carnotite in the tectonized sandstone (fig. 2.2.50).

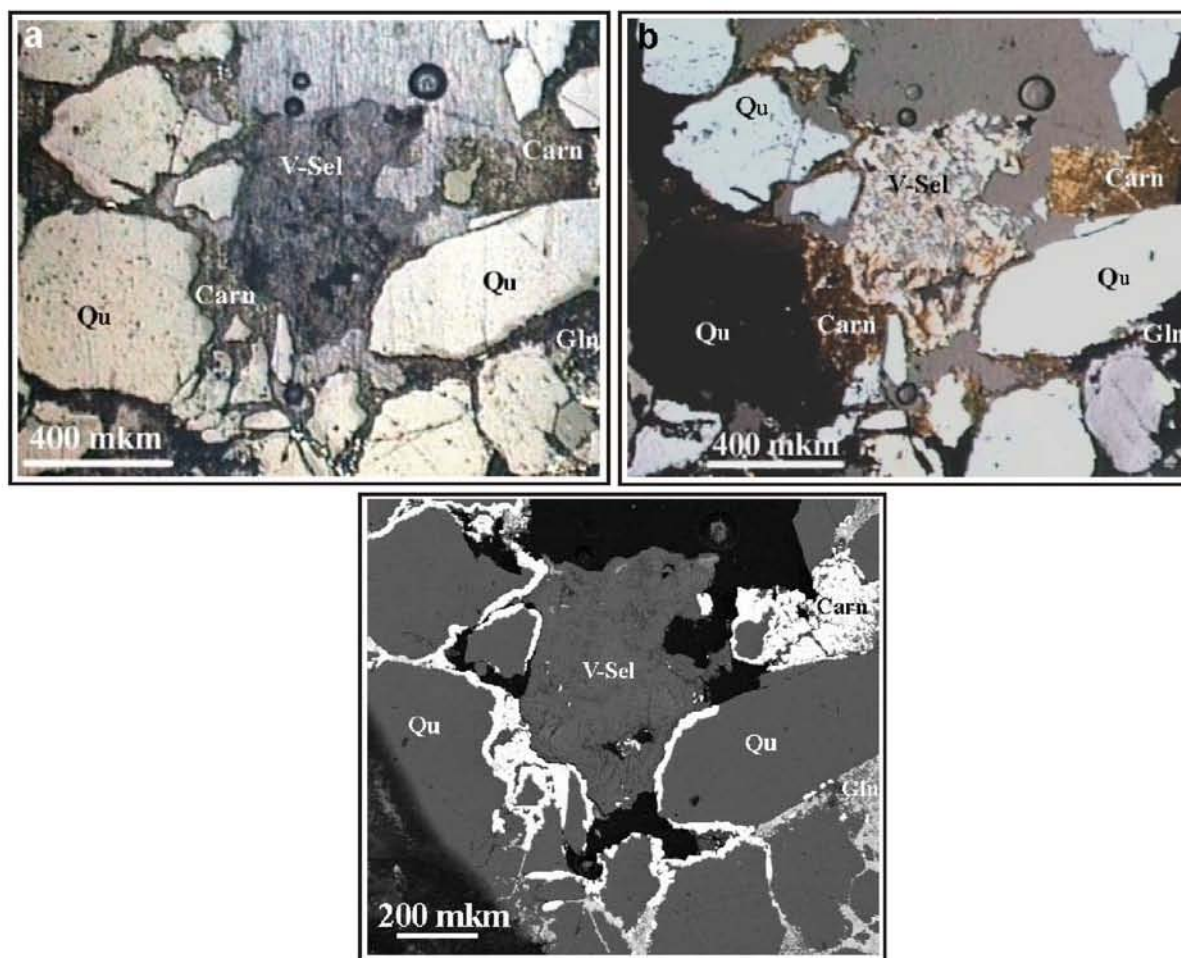


Figure 2.2.48. Carnotite (Carn) and V-bearing celadonite (V-Sel) in the Priozersk suite sandstone cement and in the fractures of quartz grains; the Matala ore-showing, DDH 929, 203.1m, thick section; a – optical photo, reflected light; b – optical photo, polarized transmitted light; c – BSE-photo.

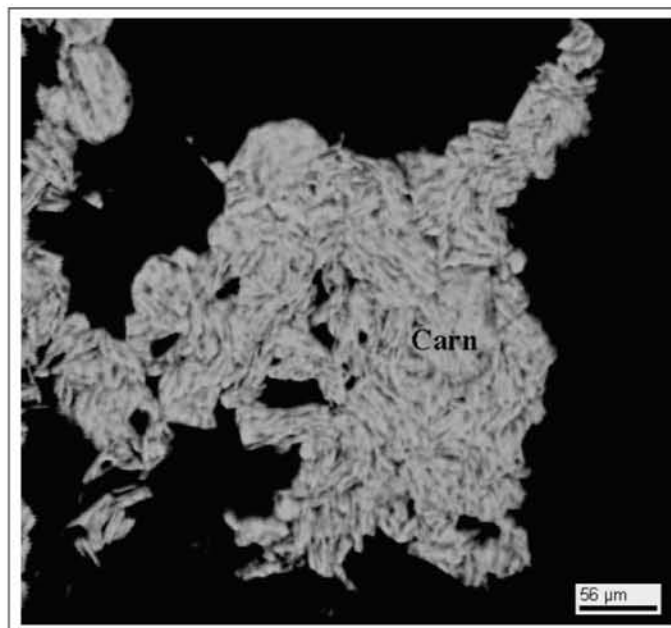


Figure 2.2.49. Microstructure of carnotite; the Matala ore-showing, DDH 929, 203.1m; BSE-photo.

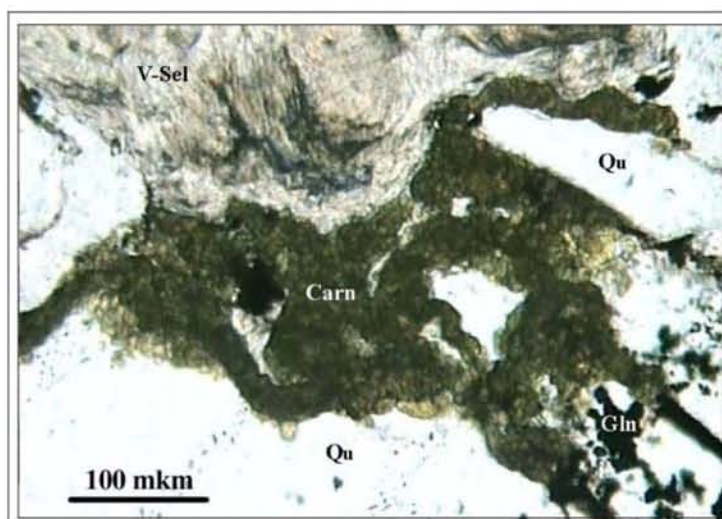


Figure 2.2.50. Carnotite, V-bearing celadonite and hollandite in the cement of the Priozersk suite sandstone; the Matala ore-showing, DDH 929, 203.1 m; optical photo of a thick section, plain transmitted light.

Uranium hydroxides.

Hydropitchblende ($\text{UO}_{2.3n}\cdot\text{H}_2\text{O}$) has been identified by optical microscopy studies (Polekhovsky et al., 2005). It forms thin hair-like veinlets in association with hydromicas and graphite in tectonized basement rocks (the Karku deposit, Ore body 3, DDH 627, 137.2 m). Sometimes it contains low amounts of fine-grained galena-1 inherited after hydropitchblende replacement of pitchblende.

Uranium titanite.

Brannerite ($[U.Ca.Ce][Ti.Fe]_2O_6$) relics form rounded grains separated or concentrated in thin layers in the sandstones. In the ore bodies the grains are totally replaced by pitchblende 1 and 2 (fig. 2.2.51a), at the margins by pitchblende-2 and coffinite, everywhere by finely crystallized rutile-4 (fig. 2.2.51b). As brannerite is strongly altered its composition varies largely: UO_2 : 25.5 - 60.5 wt%. TiO_2 : 13.1 - 58.1 wt%, SiO_2 up to 15.1 wt%, Nd_2O_3 up to 4.0 wt%, ThO_2 up to 3.1 wt%.

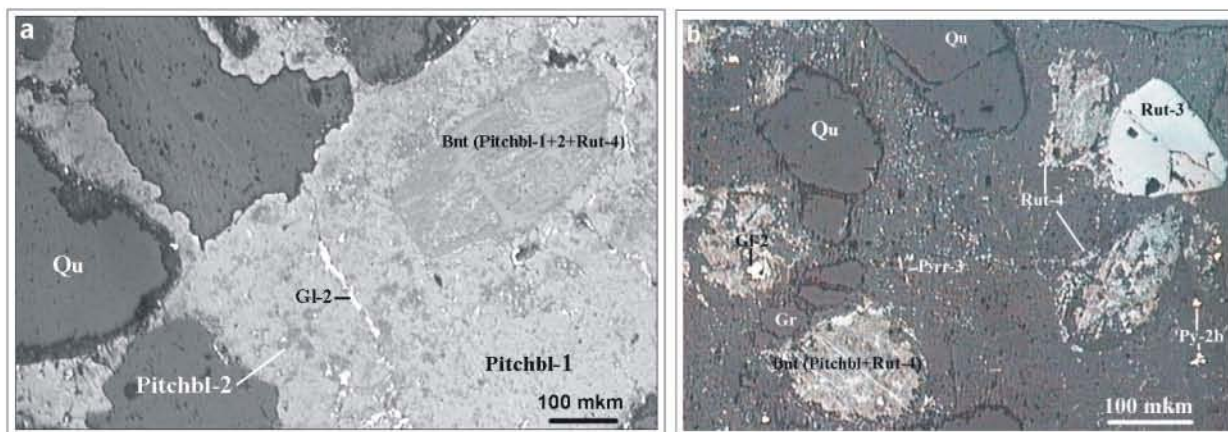


Figure 2.2.51. Replacement of brannerite fragments (Bnt) by pitchblende (Pitchbl) and late rutile (Rut-4) in altered quartz sandstone of the Priozersk suite; the Karku deposit, Ore body 3, optical photos of thick sections, reflected light: a – DDH 680, 125.0 m; b – DDH 627, 131.65 m; other mineral phases: veinlet and impregnations of late galena (Gl-2); rutile-3 (Rut-3), pyrite-2 (Py-2), geerite (Gr).

Thorium mineralization.

Increased Th contents have been discovered in many drillholes in the Salmi area. Besides numerous spot anomalies related to the Th-bearing accessory minerals common in the granites of the Salmi massif and sometimes in the migmatized supracrustals, there are numerous anomalies in the Priozersk suite sediments attributed to syn-sedimentary heavy minerals concentrations. Their identification is difficult. The only identified mineral, ferrithorite in one of the heavy mineral concentrations (Polekhovsky et al., 2007) (fig. 2.2.52).

Th redistribution was discovered in the Karku deposit area. In general Th is depleted around the ore bodies, but local Th enrichment may also occur (Appendix to Chapter 2, fig. 10). Th content in these sites is up to 1840 ppm, but no Th-bearing mineral phase has been identified. Th anomalies occur at the periphery of the alteration halos, whereas the inner parts with the high-grade U mineralization are not so enriched or even depleted in Th. character of Th distribution allows to presume its epigenetic nature.

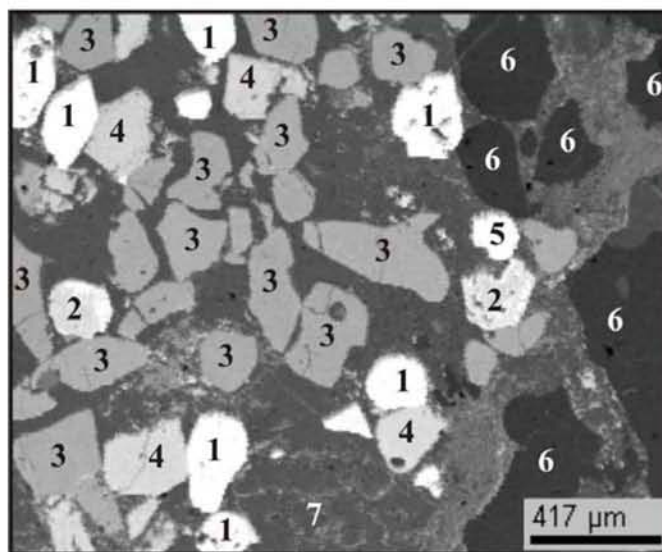


Figure 2.2.52. Heavy mineral concentration in the Priozersk suite sandstone of the Salmi depression, DDH 838, 264.4 m, BSE-photo: 1 – ferrithorite, 2 – zircon, 3 – ilmenite, 4 – hematite, 5 – marcasite, 6 – quartz, 7 – feldspar.

Radium mineralization.

Radioactivity independent of uranium was found in the small (0.5-0.7 mm) zoned veinlets in one of the drill holes of the Matala U occurrence (DDH 929, 200.1 m) (fig. 2.2.53).

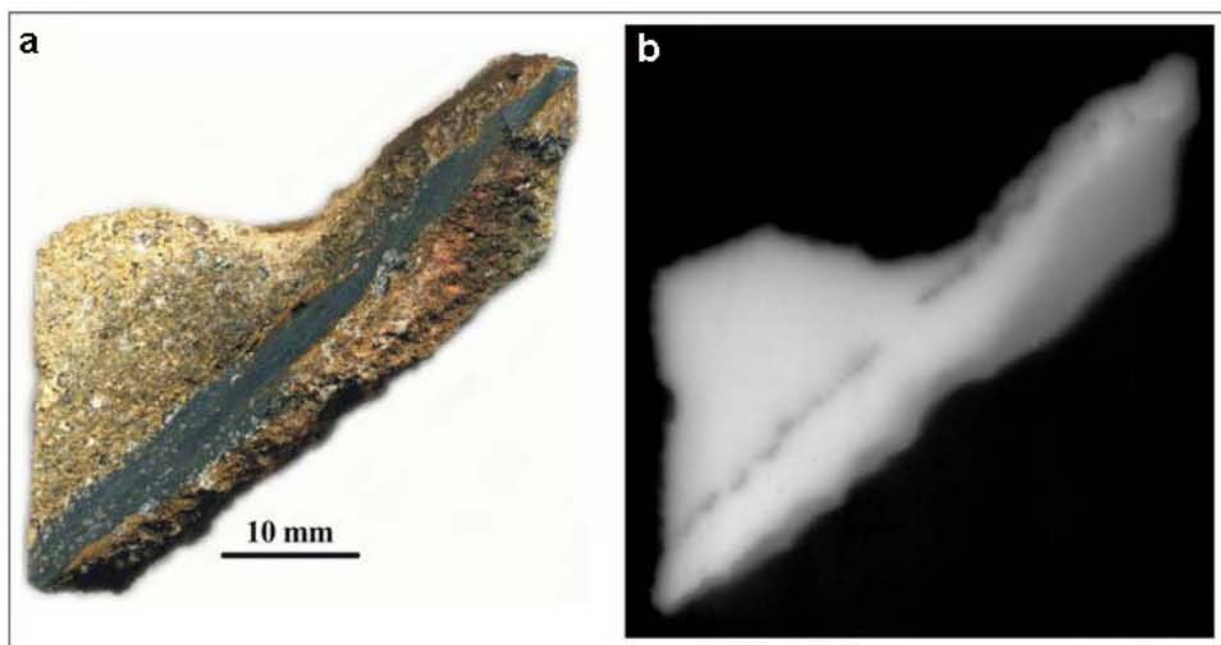


Figure 2.2.53. Romanechite veinlet cutting the Priozersk suite quartz-feldspar sandstone; the Matala ore-showing, DDH 929, 200.1 m: a – sample; b –autoradiography (14-days exposition). Radioactivity is concentrated in upper part of the veinlet.

Its central part is massive whereas its periphery is brecciated. Zoned and collomorph Fe-hydroxides (goethite and hydrogoethite) occur at the border between the massive and the brecciated zones. The salbands of the veinlets are composed of radial-axial romanechite ($\text{BaMn}_9\text{O}_{16}[\text{OH}]_4$) and coronadite $(\text{Pb}, \text{Ba})\text{Mn}_8\text{O}_{16}$ replacing quartz fragments. Radioactivity is concentrated in salbands of the veinlet.

Measurements with an “Ortec” gamma-spectrometer (Ge detector, 24-hour exposition, operator A. Alekseev, RIAN) show no traces of ^{238}U and other radioactive isotopes (^{235}U , ^{234}U , ^{234}Th etc) up to ^{226}Ra in the obtained spectra (fig. 2.2.54), but lines of ^{226}Ra and its radioactive decay products: ^{214}Pb and ^{214}Bi do occur. It is an indication of a recent (less 1600 a) redistribution of uranium radioactive decay products in the host veinlet. Radioactivity of the sample is 150 Bk. It corresponds to 0.001 ppm of radium. Ra mineral phase has been found neither by roentgen-phase nor by microprobe analysis. Ra occurs as an isomorphic replacement of Ba and Pb in romanechite and coronadite crystalline structures.

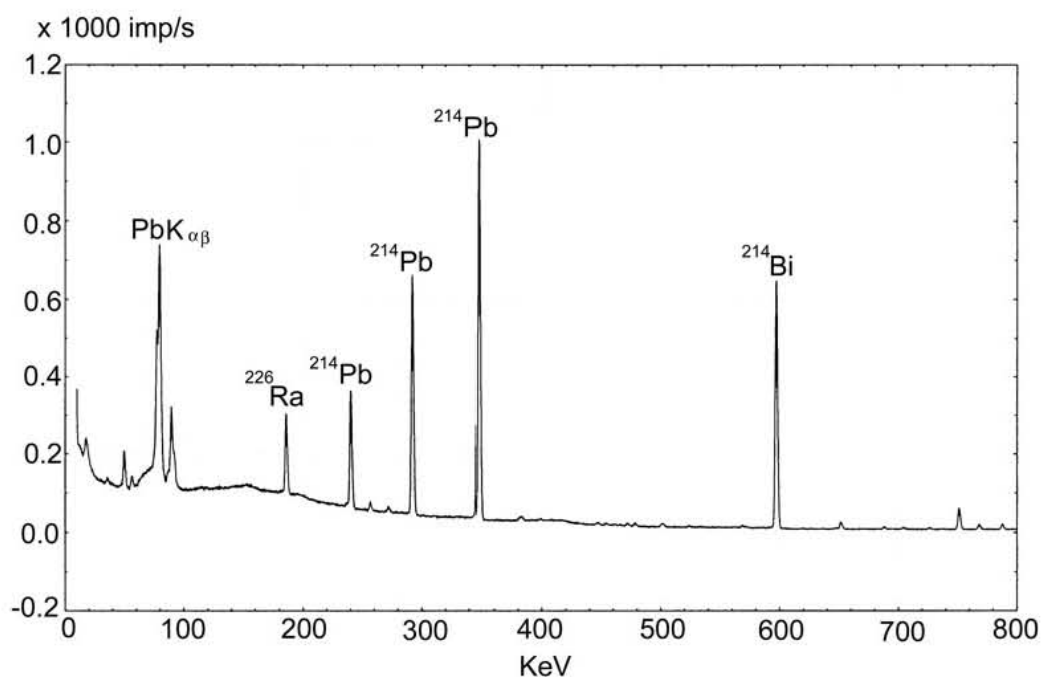


Figure 2.2.54. Spectra of radioactive isotopes of the sample 929 from the Matala ore-showing, DDH 929, 200.1 m (Polekhovsky et al., 2005).

4.3. Isotopic study of the uranium mineralization of the Salmi depression occurrences.

Isotopic age determinations.

Isotopic age determinations of the Karku uranium mineralization have been realized by many researchers since beginning of the 1990th. Available isotopic age constrains are presented in table 2.2.2. As it is known from the research performed on the uranium mineralization of the world-known unconformity-related deposits. Interpretation of the isotopic analysis of the

pitchblende is very difficult because of strong alteration and heterogeneity of the U-minerals. It explains the wide variation of ages obtained for these deposits and also for Karku.

Table 2.2.2. Isotopic ages determined on Riphean-hosted uranium mineralization (SIMS – CAMECA IMS-3F ion-microprobe; TIMS – mass spectrometer; n – number of analyses; T_o – upper intercept and T_m – lower intercept of the Concordia).

Occurrence, host rock	Mineral	Method	n	Isotopic age (for the U-Pb method – T_o , T_m), Ma	Reference
Karku deposit, sandstone	pitchblende-1	U-Pb, IMS	5	1405±76, 412±11	Shurilov et al., 2005
	pitchblende-1	Pb-Pb, LA-ICPMS	3	1371±46	Sergeev et al., 2001
	pitchblende-1	Pb-Pb, TIMS	?	1690-1550	Miguta et al., 2002
	pitchblende-2	Pb-Pb, LA-ICPMS	3	1131±32	Sergeev et al., 2001
	pitchblende-2	Pb-Pb, TIMS	?	1260-1210	Miguta et al., 2002
	pitchblende ?	Pb-Pb: wall rock roentgen-spectral analyses; pitchblende mass-spectrometric analyses	450	1450	Polikarpov, 1993
			4	1000-900 and 350 - redistribution	
		coffinite	Pb-Pb, LA-ICPMS	17	1370-790
	coffinite	Pb-Pb, TIMS	?	1225-1100	Miguta et al., 2002
Kotalakhti ore-showing, basalt	pitchblende-3	U-Pb, IMS	3	412±73 or cca 474	Shurilov et al., 2005

We analyzed two types of pitchblendes: one from the Karku deposit (DDH 625, 131.1 m) and another one from the vein mineralization in the Salmi suite basalts from the Kotalakhti ore-showing (DDH 1001, 238.2 m).

The 5 analytical points of pitchblende from the Karku deposit are strongly discordant, defining an upper intercept at 1496±340 Ma and a lower intercept at 525±310 Ma (fig 2.2.55 a). The large inaccuracy of the data results from the clustered and very discordant location of the points on the Concordia diagram. This reflects the very strong heterogeneity of the U phase and high degree of remobilization, as recognized by petrography and electronic microprobe (see General Appendix 2.6).

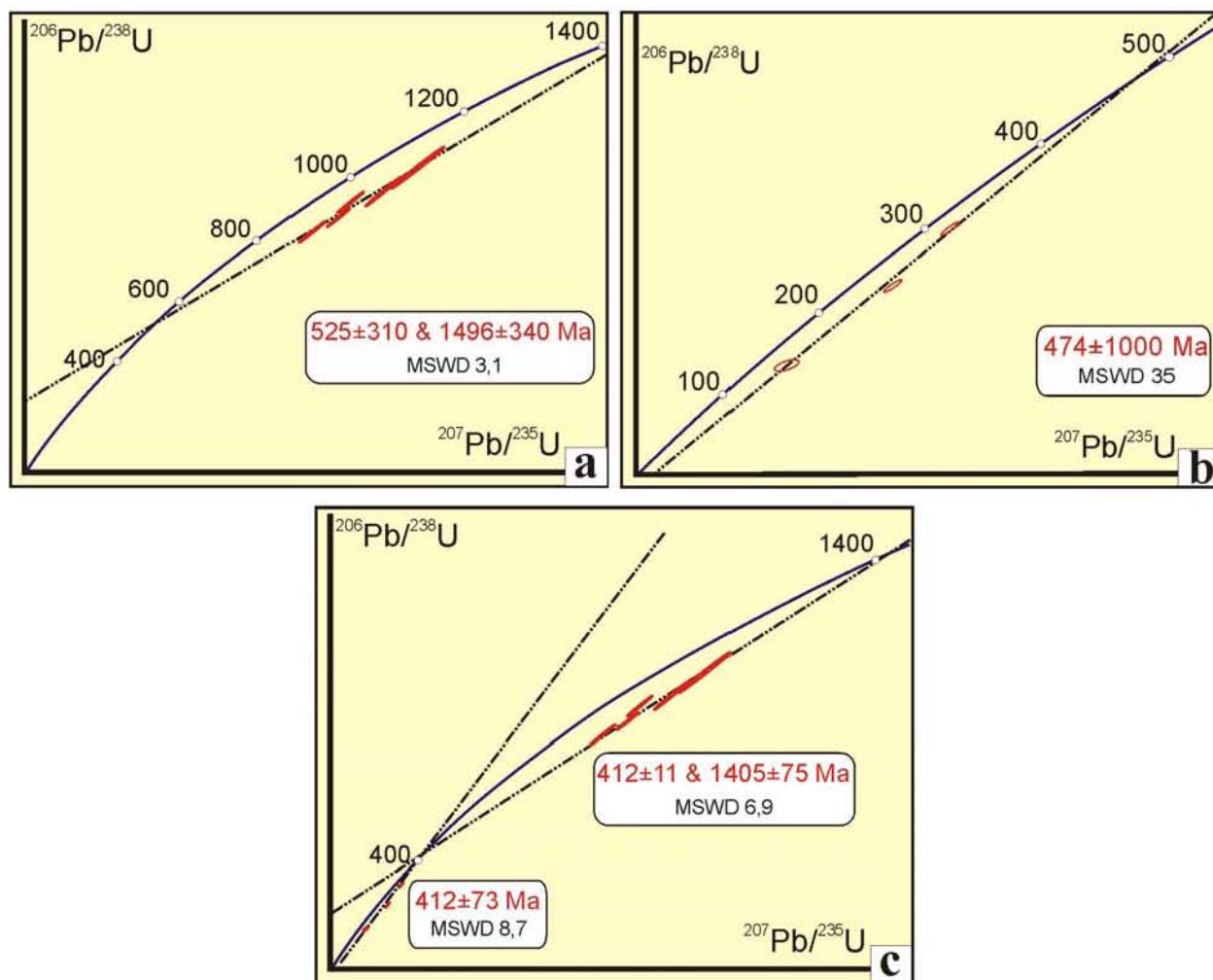


Figure 2.2.55. Different interpretations of U-Pb isotopic data in Concordia diagrams for the pitchblende from the Karku deposit; b – for pitchblende-3 from the quartz-chlorite-calcite veinlet from the Kotalakhti ore-showing; c – combined diagram for both samples.

The result approximately corresponds previous isotopic constrains giving Lower-Middle Riphean ages. Taking in account significant inaccuracy of results, it can be correlated with Lower-Middle Riphean ages obtained for some occurrences of basement-hosted vein-type uranium mineralization (the Varalakhti and the Mramorny Kombinat ore-showings, see Paragraph 1.4 of Chapter 1). These ages are correlated with early stages of the Lower-Middle Riphean activation (the Dalslandian tectonic event), responsible for forming of the Pasha-Ladoga basin and other occurrences of intracraton sedimentation in the Baltic shield (of the Muhos and Satakunta basins etc) locally accompanied with the mafic volcanism.

Only 3 analyses have been performed on the pitchblende vein from Kotalakhti due to the very small sized of the U minerals. On a Concordia diagram they displayed discordant points defining an upper intercept at 412 ± 730 Ma and lower intercept at -294 ± 2900 Ma (fig 2.2.55 b).

The poor accuracy of the data is due to the strong heterogeneity of the analyzed material. Nevertheless a parallelism with some ages obtained for basement-hosted vein-type uranium mineralization of the Northern Ladoga area (the Korennoye and the Mramornaya Gora ore-showings see Paragraphs 1.1, 1.3 and 1.4 of Chapter 1) can be recognized. This age can be correlated with a culmination of the Caledonian activation in the Baltic shield.

Although the isotopic U-Pb data of the two analyzed samples provide poorly constrained Discordia ages, there seems to be two major events:

- A first one occurring in Lower Riphean time as indicated by the upper intercept age of the first sample. Such an age might be attributed to primary ore deposition.
- A second age in Paleozoic time as indicated by the lower intercept age of the second sample and the upper intercept age of the first sample. Such an age might be attributed to a remobilization event of the primary U ore, possibly associated with a partial redeposition of U as pitchblende vein.

To more accurately define the age of U mineralization and remobilization, a possible model would be to constrain the lower intercept age of the first sample, by the upper intercept age of the second sample (fig 2.2.55 c). In this case, the modeled age of primary U deposition would be 1405 Ma with a better accuracy ± 76 Ma.

Of others isotopic constrains, the Pb-Pb age determinations realized with LA MC-ICP-MS NEPTUNE in the Center of Isotopic Researches of VSEGEI, St.-Petersburg, Russia (Sergeev et al., 2001) is the most credible. The age of pitchblende-1 obtained by this research is 1371 ± 46 Ma, that well corresponds to results yielded during this study. Pitchblende-2 was dated as well and has an age of 1131 ± 32 Ma that can be approximately correlated with a finalization of the Dalslandian orogeny.

1690-1550 Ma Pb-Pb age of pitchblende-1 obtained with thermal ionization mass spectrometry (TIMS, Miguta et al., 2002) apparently is incorrect, because the Salmi rapakivi massif underlying the ore-host sediments had been emplaced not early than 1.55 Ga.

Pb-Pb wall rock roentgen-spectral and mass-spectrometric analyses can give just very approximate idea on age of the uranium mineralization.

Isotopic age determinations of coffinite are always very difficult because of its mineralogical peculiarities (easy led loss for example) and all results presented in the table 2.2.2

should be considered very cautiously.

REE distribution in the uranium oxides.

For the first time research of REE content in the uranium oxides from the Salmi are (the Karku deposit and the Kotalakhti ore-showing) was undertaken. The same fields in the preparations as for the above described age analyses were used.

The chondrite normalized REE patterns of pitchblende from the high-grade ore of the Karku deposit is weakly bell-shaped centered on Sm and Eu, with a significant enrichment in the lightest REE (fig. 2.2.56). The absolute REE content is low.

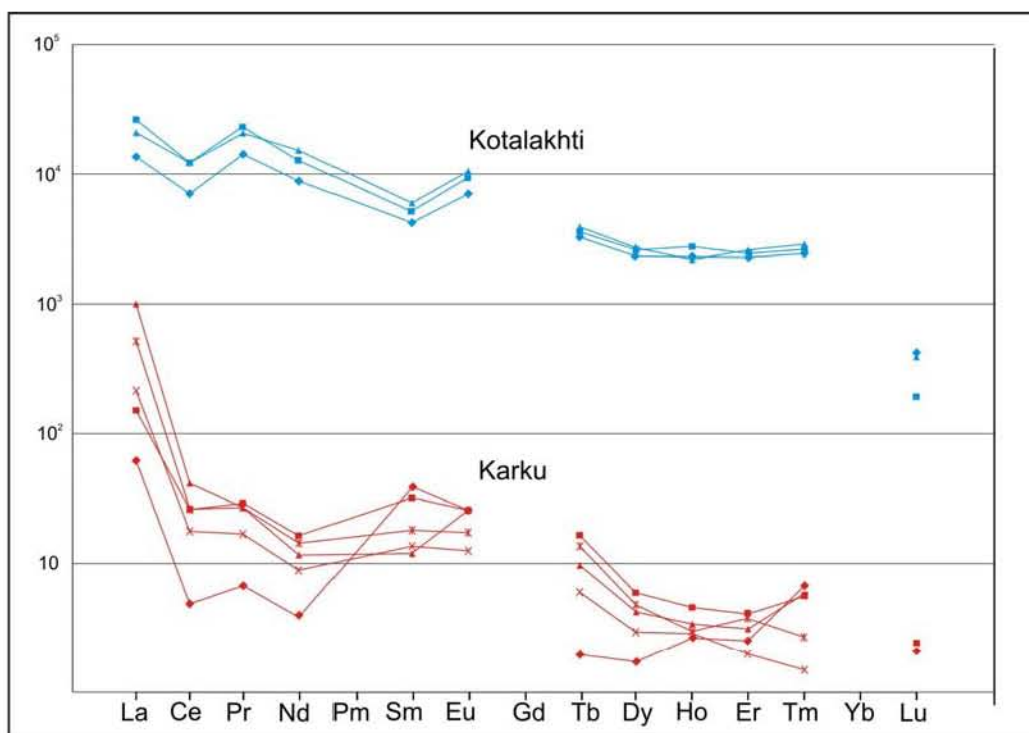


Figure 2.2.56. Chondrite-normalized REE patterns of pitchblendes from the Kotalakhti ore-showing (sample 1001-7b, in blue) and the Karku deposit (sample 625-1, in red).

The REE patterns of pitchblende from the unconformity-related uranium ore of Karku are atypical for the unconformity-type deposits. U oxide REE patterns in last ones have bell shape centred on Tb and Dy (fig. 2.2.57) and REE contents are higher. No other reference spectra found in literature display similar shape. As seen with the U-Pb isotopic data and from petrographic observations, the analysed U oxides in Karku experienced strong alteration (probably during the Palaeozoic). It is possible the REE composition might have been remobilised during these later events (especially the light REE).

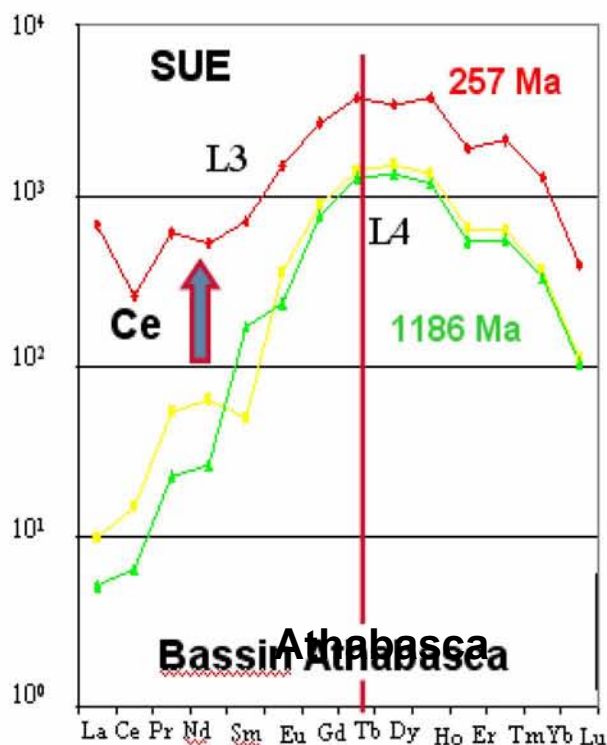


Figure 2.2.57. Chondrite-normalized REE patterns of two generations of uraninites from the Sue deposit (Athabasca Basin) (Bonhoure et al., 2005).

The chondrite normalized REE patterns of pitchblende from the Kotalakhti ore-showing, are relatively flat shaped; slightly decreasing from light REE to heavy REE. No specific Eu anomaly may be highlighted. The absolute amount of REE is relatively high.

Although the absolute REE contents are variable, the similarities in the shape of the REE patterns from Kotalakhti, with those from the vein-type Särkijärvi and Alho occurrences in Finland are consistent with the interpretation that these occurrences may be of similar origin (fig. 2.2.58) (Bonhoure, 2007). This interpretation is further supported by the similar U-Pb isotopic ages obtained for these localities (Palaeozoic).

It is also remarkable that the REE patterns of vein type mineralization from the Kotalakhti occurrence differs from that of the Karku deposit especially by its much higher REE contents. Since there is no early uranium mineralization at the unconformity beneath the Kotalakhti occurrence, it can be interpreted as a difference in the origin of the mineralization. The Kotalakhti U mineralization has probably no genetic links with the Riphean unconformity-type uranium mineralization and refers to another (Palaeozoic) uranium-producing event.

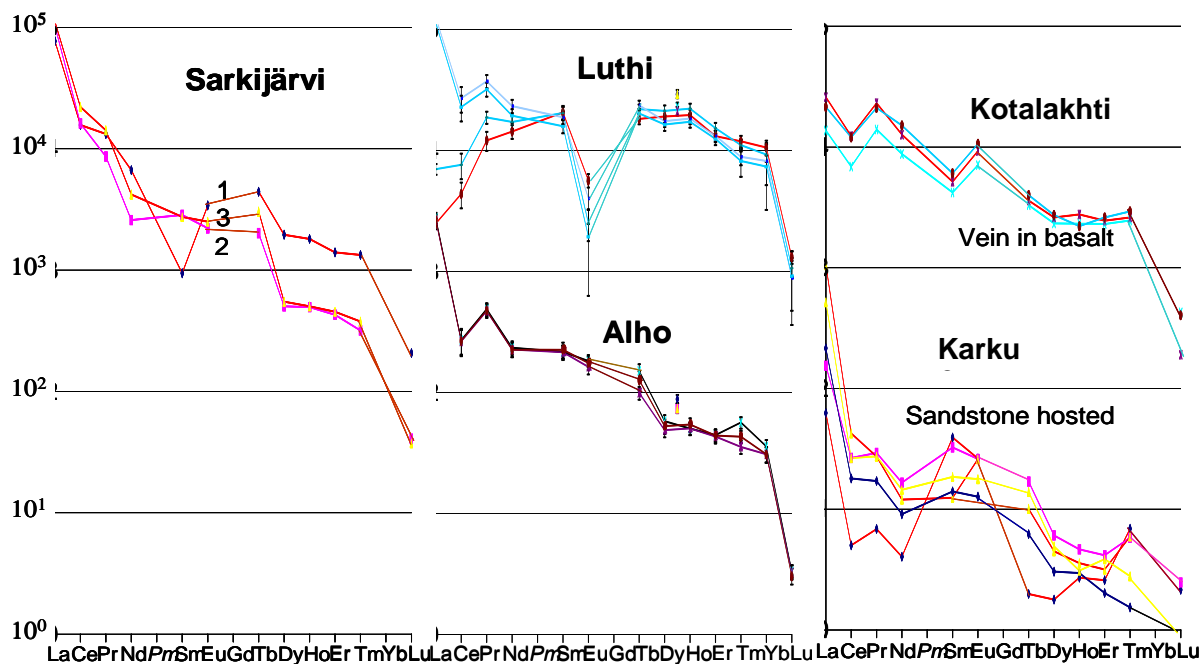


Figure 2.2.58. Chondrite-normalized REE patterns of uranium oxides from the Kotalakhti ore-showing and the Karku deposit in comparison with those of the Särkijärvi, Luthi and Alho vein-type occurrences of Finland (Bonhoure, 2007).

Valency of uranium in the Karku deposit ores.

The valence of uranium in the high-grade U mineralization from DDH 671 (124,5 m) and DDH 627 (131,75 m) have been determined (crystal-diffraction roentgen-spectrometer measurements, Polekhovsky et al., 2005): U^{4+} prevails and content of the most mobile U (VI) is quite low (less than 25 % of total U amount, table 2.2.3).

Table 2.2.3. U (IV), U (V) and U (VI) contents in pitchblendes of the Karku deposit (Polekhovsky et al., 2005).

Sample U valence	671/15-5	627p/5
U(IV)	57.80 %	64.80 %
U(V)	21.85 %	10.75 %
U(VI)	20.35 %	24.45 %

4.4. Succession of uranium metallogenesis in the Karku deposit area.

As shown in the previous chapter, Svecofennian U mineralization is widespread in the basement rocks of the Raahe-Ladoga domain. The Salmi depression being related to this domain, the same kind U deposit is expected to occur under the Riphean sediments, although no significant occurrences in the basement have been discovered here, only rare anomalies of uncertain type. Local radioactive anomalies related to U-Th accessories occur in Salmi granites.

Erosion of the basement U-bearing rocks led to the U enrichment of the Riphean sediments. The earliest radioactive anomalies in the Priozersk suite correspond to thin heavy mineral layers with U- and Th-bearing minerals such as monazite, zircon and ferrithorite. The U-Th bearing accessories are disseminated in the cement of the sandstones. They represent a possible U source, because they have been partly altered during the diagenesis. Sometimes epigenetic ore (pitchblende, coffinite, rutile and sulphides) can be observed in fractures and edges of altered zircon. Lobaev (2005) had shown a U and Th enrichment of zircon during its alteration – from 0.04 wt% U and 0.06 wt% Th in unaltered grain up to 1.5 wt% and 2.0 wt% respectively in altered one.

The paragenetic mineral succession of the Karku deposit area is presented in figure 2.2.59.

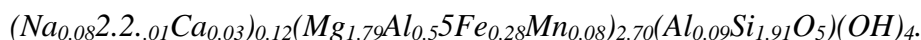
Replacement of the sandstone cement and clasts by dickite took place during *the first stage* of the epigenetic process. It can be observed in the external part of the alteration halo hosting the Karku ore bodies. Dissolution of hematite in the sandstone cement led to the bleaching of the initially pink-colored rock. Quartz and especially feldspar clasts have been corroded. Silica dissolved from the internal part of the halo has been transported to the periphery, where detrital quartz grains were overgrown with epigenetic quartz. Resorption of the sandstone components in the central part of the halo led to the decompaction of the rock. Compared to the huge, frequently total, quartz dissolution occurring in the classical unconformity-related deposits, in the Karku this process was relatively weak. Feldspar clasts disappeared in central parts of the alteration halo, whereas quartz (although partially corroded) remains anywhere.

Further alteration is represented by intensive carbonatization of the sandstone and of the upper part of the regolith. There is wide development of Fe-chlorite ($\text{FeO/MgO} = 5.4\div 7.5$) and local sulphidization, new formation of apatite, rutile and ilmenite.

Stages Minerals	I			II	III	IV
	1	2	3			
Quartz	██████				██████	
Dickite	██████					
Chlorites	████ ██████████				██████	
Calcite	████	████████████████		██████	██████	
Fe-sulphides		████████████████				
Cu-Fe sulphides		██████				
Zn-sulphides		████████████████				
Molybdenite		██████				
Apatite		████████████████				
Ilmenite & rutile		██████		██████		
Fe-oxides				██████	██████	
Cd-sulphides			████████████			
Sulphoarsenides & arsenides Fe, Ni, Co			████████████			
Mo phase			████████████			
Fluorite			████████████			
Al-lizardite			████████████			
Bitumen			████████████			
Galena			████████████	██████	██████	
Pitchblende			████████████	██████	██████	
Coffinite				██████	██████	
Hydropitchblende					██████	██████
Carnotite						██████
Fe hydroxides	████			██████		██████
Hydrochlorite & hydromicas				██████		██████
Cu-sulphides						██████
Copper						██████
Mn-oxides						██████
Kaolinite						██████

Figure 2.2.59. Succession of the epigenetic mineral paragenesises of the Karku deposit, Matala and Kotalakhti ore-showings (based on Polekhovsky, 2007).

The next phase of this stage corresponds to the introduction of the earliest generation of uranium mineralization – pitchblende-1 dated at 1405 ± 76 Ma. It occurs in paragenesis with two types of Fe-Mg aluminosilicates. The first one is a chlorite with relatively high Al content and wide variation of the Fe-Mg ratio (from 0.3 to 10). There is a trend of Mg enrichment of the chlorites toward the central part of the halo, where high-grade ores occur. The second group of aluminosilicates has a low Al content and $Fe/Mg = 0.5 \div 0.7$ and corresponds to Al-lizardite:



It forms accretions with calcite and pyrrhotite.

There are also a non-identified Mo phase of non-identified mineralogical reference, galena, Cd-sphalerite, Co-Ni arsenides, sporadically fluorite and apatite in this paragenesis. Bitumen has been observed as well.

During *the second stage* pitchblende-1 was replaced by pitchblende-2, coffinite, hematite and hydromicas which led to an impoverishment of the ore. Pb-Pb age of pitchblende-2 is 1131 ± 32 Ma. Low-grade coffinite mineralization at the periphery of the ore body is often associated with sulphides and hematitization. Increased uranium content in the oxidized sandstones corresponds to U adsorption by Fe oxides (Roman, 2004).

The third stage corresponds to a hydrothermal mineralization in veinlets cutting the whole sequence, including the ores. Several generations of the veinlets have been distinguished. Most of them dip steeply ($70-90^\circ$). In a unique outcrop of the Riphean cover formations (basalts of the Priozersk suite at the Tulema river rift) NW ($290-310^\circ$) veinlets predominate.

Rarely veinlets in the basalts contain late U mineralization. Pitchblende-3 from the mineralized veinlets in the basalts of the Kotalakhti occurrence was dated at 412 ± 73 Ma. It is partially replaced by pitchblende-4 and coffinite.

Apart from the uranium minerals, late chlorite, calcite, quartz, chalcedony, barite, fluorite, galena, chalcopryrite, pyrite, marcasite, hematite, coronadite, hollandite and romanechite occur in the veinlets related to this stage.

The fourth stage refers to supergene alterations. They are represented by limonitization and kaolinitization developed especially along late fractures. Clayey formations occur in sites of where very intensive alterations are present. Sometimes they are accompanied with a radioactive

mineralization optically identified as a hydropitchblende. Locally the early uranium oxides are replaced by carnotite. Native copper, replacement of Cu-arsenides by geerite and chalcocite are locally observed. Fe hydroxides occur along the fractures, grain confines and partially form cement of the sandstone. High intensity hypergene alterations have been observed in the drill core from tectonized zones in the Matala occurrence and to the east from the Karku deposit, where Riphean basalts and sediments pitch out and meteoric water directly achieve the unconformity.

It is necessary to notice that only the first and probably the second stages can be considered as real events, while the others represent a succession of several events referring to multiply tectonic reactivation of the region during and after deposition of the Riphean cover.

4.5. Particularities of the epigenetic uranium mineralization in the Salmi depression.

Summarizing the preceding information allow to propose the following specific characteristics for the epigenetic uranium mineralization discovered in the Salmi depression.

1. Uranium mineralization has a rather simple composition. Main part of the ores and all high-grade mineralization are composed of two generations of pitchblende and coffinite. As the grade of the mineralization decreases. The importance of the U-silicates increases. At the periphery of the ore bodies coffinite is a major U-mineral and occurs without direct association with the uranium oxides. Low-grade coffinite mineralization predominates in Ore body 1 and especially Ore body 2. Ore body 3 is composed of pitchblende (dominating in the center) and coffinite (dominating on the flanks).

2. The polychrone character of U-forming process has been confirmed by isotopic dating. High-grade U mineralization hosted by the sandstones and the regolith is composed of pitchblende-1 and pitchblende-2 dated at 1405 ± 76 and 1131 ± 32 Ma, respectively, and early coffinite. Vein mineralization in the fractured basalts of the lower subsuite of the Salmi suite has a Palaeozoic age – 412 ± 73 Ma. The latest U mineralization (carnotite and hydropitchblende) occurs in the fractured sandstones and basement rocks altered by supergene processes.

3. Secondary (supergene) U mineralization is quite rare because of a good preservation of the early one by a thick basalt layer and the dense sulphide-carbonate alteration envelop around the high-grade ore.

A list of uranium minerals from the Salmi depression and their associated rock is presented in table 2.2.4.

Table 2.2.4. Location of epigenetic uranium mineral phases in the different rock types (**in bold**) and types of the uranium mineralization (*in italic*).

Mineral	Effusive	Sandstone		Weathered basement rock		Basement rocks	
	<i>vein</i>	<i>impregnated</i>	<i>vein</i>	<i>impregnated</i>	<i>vein</i>	<i>impregnated</i>	<i>vein</i>
Pitchblende-1		+		+		+	
Pitchblende-2		+		+		+	
Pitchblende-3&4	+						
Coffinite	+	+	+	+	+	+	+
Carnotite		+					
Hydropitchblende							+

5. Factors controlling uranium mineralization in the Salmi depression.

There are several geological factors controlling uranium occurrences in the Salmi depression.

I. Petrologic control.

1) *Priozersk suite sandstone*. Main bulk of the ore is localized in the lower layers of the Priozersk suite sediments. Sometimes low-grade uranium mineralization occurs in middle and upper levels of the suite.

2) *Regolith*. A much subordinated part of the deposit resource is hosted by the upper part of the regolith. As a rule, in this case, the mineralization continues from the sandstone to the altered rock, but few ore intersections have been discovered only beneath the unconformity. Non-regolithized basement rocks host no uranium ores, rare anomalies only.

3) *Graphite and sulphide enriched schists*. High-grade ores of the Karku deposit are

localized above graphite and sulphide-rich zones of the Impilakhti suite biotite schists (graphite > 10 % and more). Generally, low-grade mineralization from graphite-bearing schist areas (with graphite > 2 %), but at the periphery of the ore bodies may also occur out of those areas.

4) *The alteration halo.* Ore bodies of the Karku deposit are enveloped by wide halos of sulphide-chlorite-carbonate alterations of the host rocks. Toward the central part of the halos, where high-grade ore occurs, carbonatization of the rock increases.

II. Structural control.

1) *Riphean unconformity.* The Karku deposit ore bodies are related to the unconformity between the Riphean Priozersk suite sediments and metamorphic Palaeoproterozoic basement formations. The main part of the ores is localized above the unconformity, subordinated amount occurs below. The ore bodies are located in valley-like depression of the unconformity surface with a corresponding increase of the sandstone layer thickness (Appendix to Chapter 2, fig. 3 and 4). High grade ores are located in the vicinity of the paleovalley axis but not necessarily its deepest part. Low-grade ore may occur above the uplifts, but mainly extends along the paleovalleys.

2) *Interdome depressions.* The uranium ore bodies are located in the depressions between the domes of the crystalline basement, mainly in the margin of them. The depressions consist of PR₁ schists and gneisses of the Impilakhti suite, and to a lesser extend of the Pitkjaranta suite; the domes are composed of AR-PR₁ granite-gneiss and migmatites.

3) *Tectonic displacements.* There is an apparent relation between the U mineralization and the tectonic displacements. The crystalline basement is intensively faulted. Some faults cut but rarely displace Riphean formations. Influence of all these structures to the U distribution is diverse.

i) Graphite and sulphide enrichment occurs along the faults of Palaeoproterozoic age. This enrichment has been recognized in NW and N-S structures. Graphite content reaches 10 % and more in tectonized Impilakhti suite schists, against 1-2 % outside such zones. High-grade U mineralization is related to graphite and sulphide enriched zones of the basement rocks.

ii) A sulphide-chlorite-carbonate alteration halo striking NW has been mapped in Ore body 3. It corresponds to a zone of cataclasis in the Priozersk sandstone. The highest grade ores of Ore body 3 are related to the intersection of NW-striking cataclased zones of the Riphean

sediments and N-S tectonic zone enriched with graphite in the basement rocks.

It is proposed that the high-grade uranium concentrations of Ore body 1 are related to the intersection of NW and NE-striking faults (Appendix to Chapter 2, fig. 2). Ore body 2 is located at the intersection of NW-striking tectonic zone and local N-S striking faults.

iii) Several uranium occurrences have been discovered in tectonic zones at some distance from the unconformity: few ones occur in fractured zones in the basalts of the lower subsuite of the Salmi suite and in the graphite-biotite schist of the Impilakhti suite.

Rare Ra mineralization has been discovered in fractures cutting the Matala ore-showing.

III. Geochemical control.

Several geochemical features of the Karku deposit host rocks differentiate them from the background rocks of the Salmi area.

1) There is high uranium content in some of the rock types in the Karku deposit area (table 2.2.5). The fraction of mobile uranium in the sediments is about 40 %.

Table 2.2.5. Average U abundance in rocks of the Karku deposit area (Skorospelkin, 2002).

Rock type	Average U content, ppm	
	Karku deposit area	Background
Basalts of the Salmi suite lower subsuite	>5	2
Priozersk suite sediments	6.5-7.4	3.6
Upper part of the weathering crust	2.6	No data
Impilakhti suite Bt schist	4.0	2.6
Impilakhti suite graphite-bearing Bt schist	5.8	4.8

2) In mineralized rocks U is positively correlated with Pb, Zn, Mo, Mn, also Ag, Cd, Tl, less with Cu and As, negatively with Th, Nb, Sn (fig. 2.2.60). The association U-Pb-As is common for the Riphean sediments and the basement rocks in the Karku deposit. U-ore hosting sandstone is enriched in Mo, Ag, Pb, Zn, often in As and Mn. Depletion of the sandstones in Th, Sn, Nb, Zr and Ti has been revealed in the Karku deposit area. A 1200×400 m halo of lower (< 12 ppm) Th content has been evidenced around of Ore body 3. U-Th ratio in the mineralized sandstone is 2.5-10 contrasting with background of 0.5 (Dolgushina and Kushnerenko, 2004).

3) Around the Th depleted domain in the mineralized area, local zones of epigenetic Th enrichment occur close to the uranium ore-bodies.

4) An increase in disseminated U and associated elements occurs in the vicinity of the

ore bodies: up to 200 % for U, 110 % Ag, 82 % Pb, 80 %, Zn, 80 % Mo (Dolgushina, 2005).

5) Uranium content in the basalts of the Salmi suite lower subsuite increased up to 5 ppm above the U ore bodies of the Karku deposit, whereas the background values for these rocks is 2 ppm in the Salmi depression (Dolgushina, 2005).

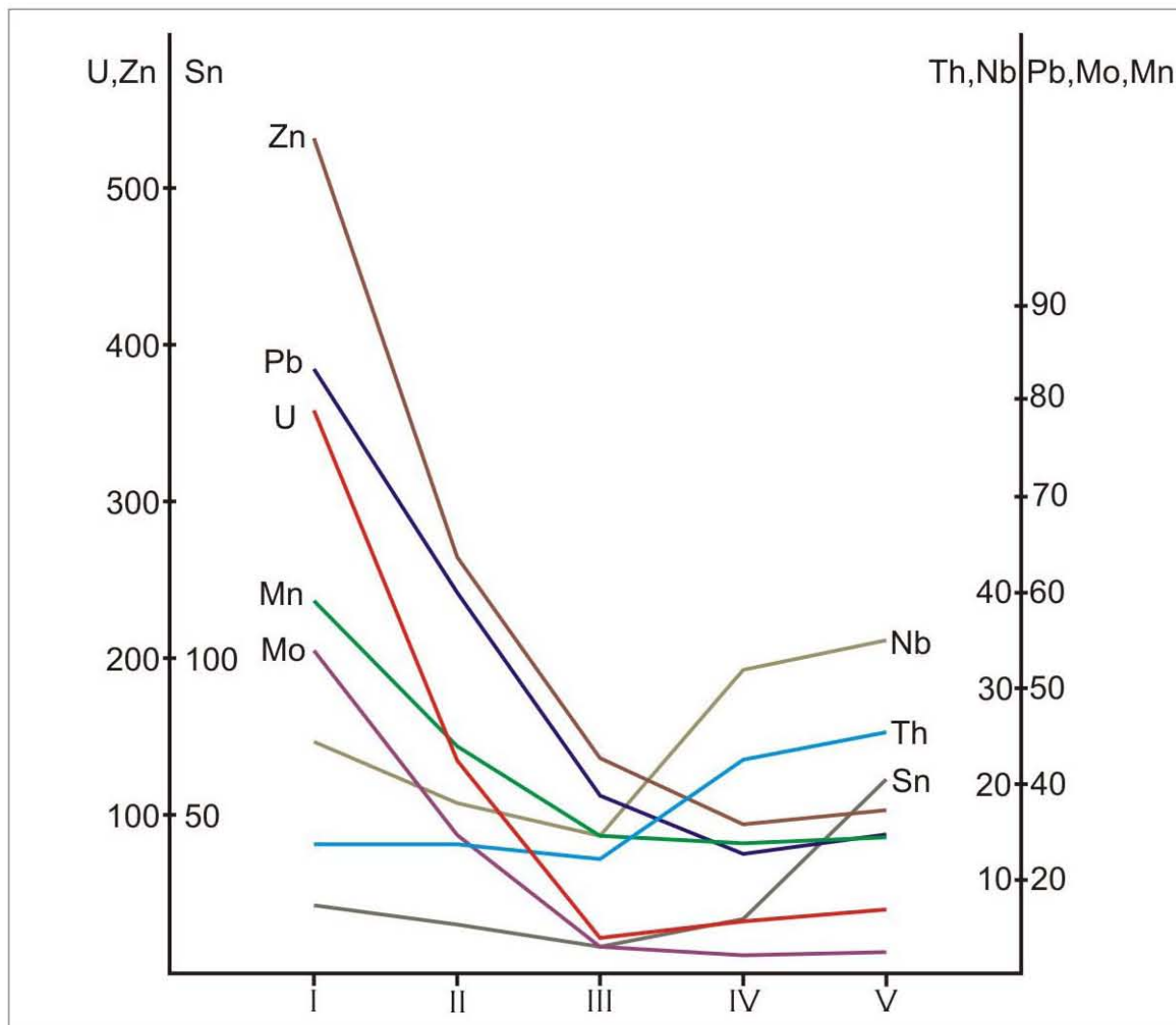


Figure 2.2.60. Diagram of the geochemical zoning in the Karku deposit area (based on Dolgushina and Kushnerenko, 2004). Zones: I-sulphide-carbonate metasomatite, II-carbonatized sandstone, III-chloritized sandstone, IV-bleached sandstone, V-background sandstone.

6) There is a local increase of radioelement abundance in the Quaternary sediments above the ore bodies. Discovery of the Karku deposit had happened as a result of verification of radon anomalies in the soil cover (Polikarpov, 1993). Nevertheless, efficiency of surface geochemical methods is reduced in the Karku area, because the ore-hosting sandstones are covered with low permeable thick basalt layer and significant watering of the upper bedrocks layers and the glacial cover (the Karku deposit area is rather swampy).

6. Typology of the Karku deposit.

Unconformity type uranium deposits have been subdivided into two subtypes: “sandstone-hosted” and “basement-hosted” (fig. 2.2.61).

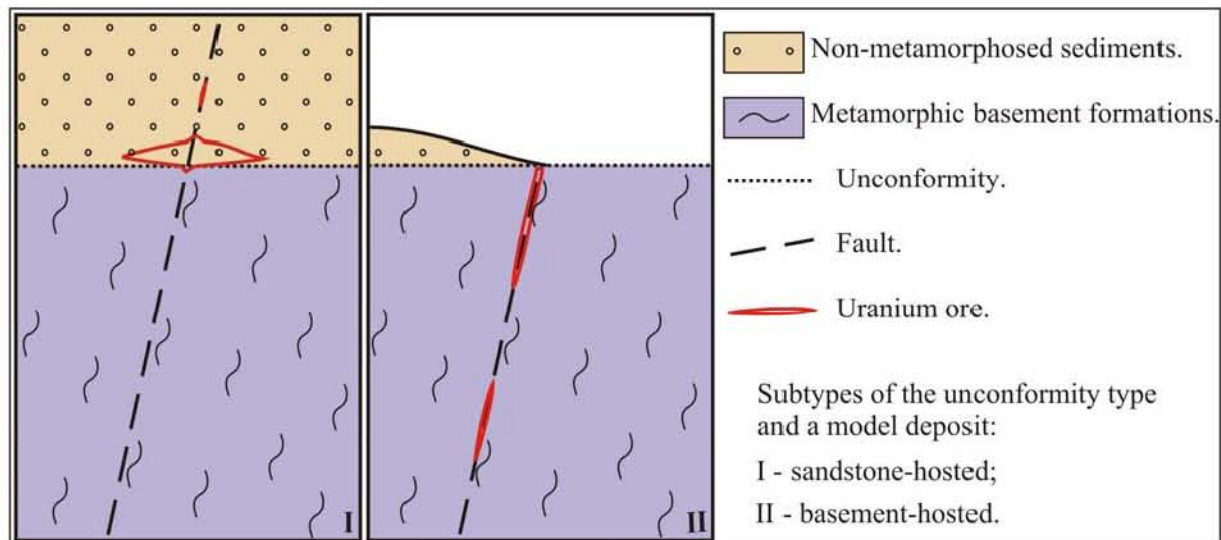


Figure 2.2.61. Sandstone-hosted and basement-hosted subtypes of unconformity-type deposits.

Basement-hosted unconformity type deposits (Subunconformity-Epimetamorphic type after Dahlkamp, 1993) are typical for the Pine Creek geosyncline (Australia) whereas sandstone-hosted ones occur in the Athabasca basin (Canada) only. However, there are many basement-hosted unconformity type deposits in the Athabasca basin as well, including the newly discovered Millennium deposit (Roy et al., 2005). Many deposits in the Athabasca basin refer to a transitional subtype with the mineralization above as well as deep below the unconformity.

Structural setting of the Karku deposit allows to link it to the sandstone-hosted subtype unconformity-related deposits. It has many similarities with a classical example of sandstone-hosted Athabasca basin uranium deposits – the Cigar Lake deposit (fig. 2.2.62). Nevertheless, many distinctive features have been recorded by the detailed study of the Karku deposit.

6.1. Comments on the origin of the Karku deposit and unconformity-type deposits of the Athabasca basin.

The genesis of the unconformity-related deposits is still not perfect understood. The epigenetic character of such high-grade U concentrations first time was proposed by Hoeve J. and Silbadd T. (1978).

Former uranium concentrations in the basement (Palaeoproterozoic U occurrences and

U-enriched basement bedrocks) and basinal sediments are considered as probable U sources.

Uranium from the uranium minerals from the uranium occurrences in the basement is quite mobile, but they cannot be the only source for the large unconformity-type deposits because of the small size of these occurrences.

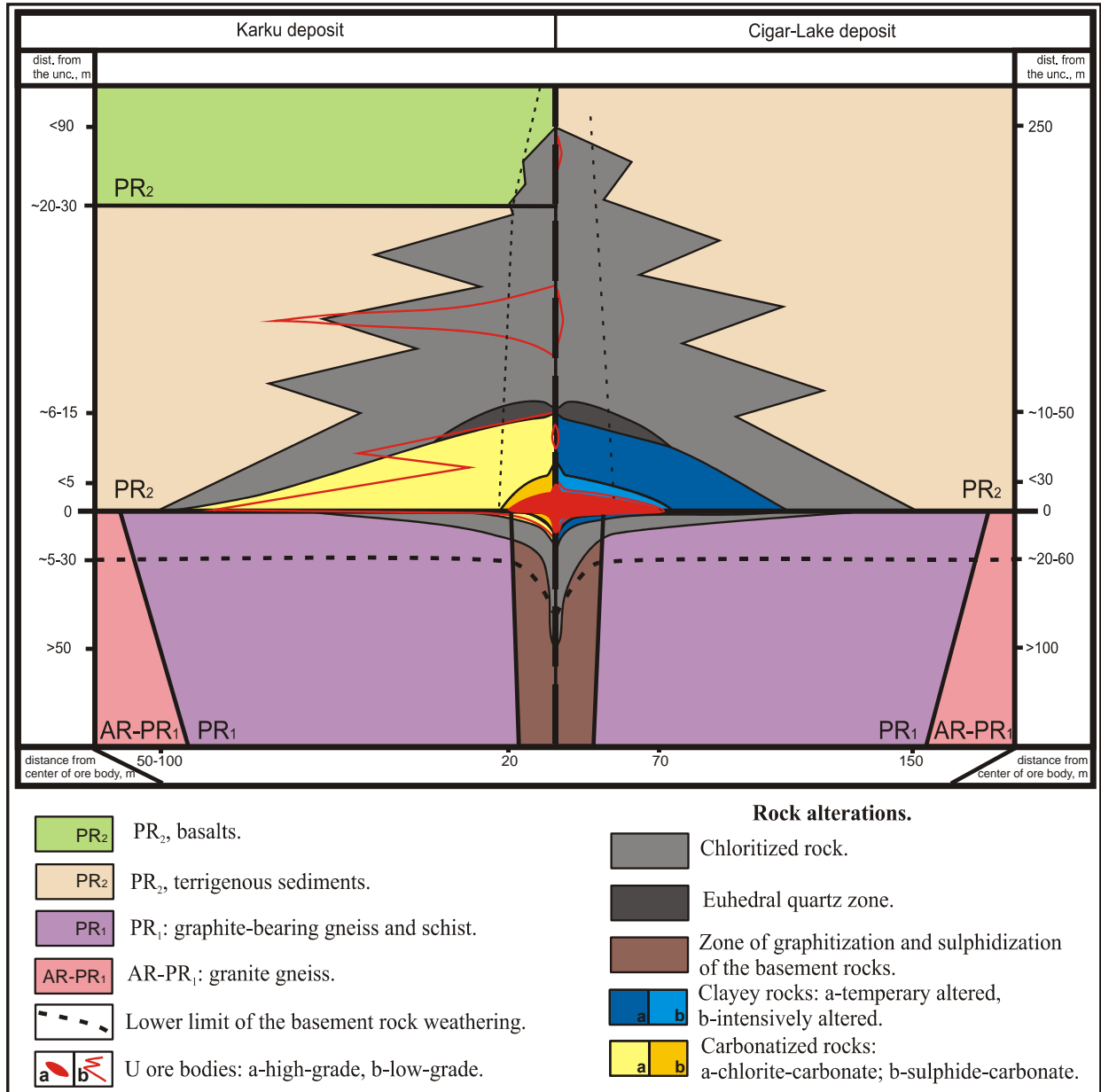


Figure 2.2.62. Comparative geological sections of the Karku and Cigar-Lake deposits (structure of the Cigar Lake deposit is based on Bruneton, 1987 and 1993).

The total uranium resource in the basement bedrocks is high, but their contribution as a uranium source is limited by high density of the magmatic and metamorphic rocks. Uranium could be mobilized rather locally, mainly along the faults. Rock alterations (for example greisenisation of granites) increases ability of the basement formation to contribute uranium into

the mobile brines (Mikhailov et al., 1999). Indirect evidence that extraction of U took place at the Karku during the ore-producing process is the occurrence of fluorite in association with pitchblende-1 and late veinlets. It may represent an indicator of biotite chloritization in basement rocks that leads to the extraction of F and U from the mica (Gortsevsky, 1993).

The permeable basinal sediments presumed as an important contributor to the unconformity-related uranium occurrences by many authors. Extraction of uranium from the refractory accessories was possible because of the extreme reactivity of the oxidized, highly saline, Ca-Na brines (Cuney, 2005). They were generated at the base of thick sedimentary basins and have been circulating for a long period in the basin and upper part of the basement (“free convection” model, Raffensperger and Garven, 1995). The application of the “free convection” model to the Karku environment is difficult because of the quite small space for such cells in a less 40 m sedimentary cover below the basalts and the relatively thin regolith (in comparison with more than 1 kilometer of silicoclastic sediments and regolith in the Athabasca).

Regolith alteration zones characteristic of the Athabasca basin (upper oxidized red zone and lower reduced greenish one) have not been clearly evidenced in the Karku area. If this alteration results from the circulation of oxidized basinal brines (Cuney, 2005) its absence at Karku is an indication of the weak intensity of this process and/or of a lower reactivity of the brines.

Uranium deposition occurred in the space created by open fractures accompanying new (or renewed) faults and massive quartz dissolution in the sandstone by aggressive acidic brines preceding the uranium-bearing fluids (Cuney, 2005). As a result, the most high-grade ore concentrations have been formed at the geochemical barrier represented by the unconformity between the basin sediments and basement supracrustals. The importance of the redox front between U-transporting oxidizing basinal brines and reducing emanations above the layers of graphite/sulphide-enriched supracrustals exposed at the unconformity is accepted by many authors. An intense graphite resorption has been observed above the ore bodies in the Athabasca basin (Fouques et al., 1986), however, a credible model of influence of the graphite conductors on uranium deposition at the unconformity still has not been elaborated. Graphite depletion beneath the Karku deposit has not been well identified, but micro-inclusions of the epigenetic bitumen have been found in the ore-hosting alteration zone (Polekhovsky et al., 2005 (2)).

According to studies of fluid inclusions in the sediments, the fluid composition changed from Na-rich basinal brines of the diagenetic stage to Ca-rich aqueous fluids during the uranium-ore event in the Athabasca and Kombolgie basins (Derome et al., 2003, 2005).

Uranium precipitation at the unconformity of the Athabasca basin occurred at $T=140-160^{\circ}\text{C}$ and $P=600-700$ bar (Derome et al., 2005).

Some modeling of the ore-producing process in the Karku deposit have been undertaken (Mikhailov, 2001; Bylinskaya, 2004; Polekhovsky et al., 2005 (2), Velichkin et al., 2005). It is presumed that major uranium deposition event in the Karku occurred at $T=90-170^{\circ}\text{C}$, $P=200-300$ bar and variable oxidizing-reducing regime (Bylinskaya, 2004). According to studying of fluid inclusions in the quartz overgrowths, the uranium-bearing brines had chloride-Na-Ca-Mg composition (Velichkin et al., 2005).

Increased Na contents in leached sandstone at the border of the carbonate alteration and in external chloritized sandstones can be interpreted as an indication of occurrence here a zone of contact between Na-rich basinal brines a Ca-rich uranium-bearing fluids ascending from the basement and responsible for the intensive carbonatization and high-grade U mineralization in the central part of the halo.

Atypical for unconformity-type deposits, a wide halo of low grade coffinite mineralization occurs in the Karku deposit. Late spindle-like coffinite aggregates have been observed on the surface of the sulphides and bitumen. Such kind of aggregates is quite common for sandstone hosted uranium deposits and their presence indicates an infiltration process (Miguta et al., 2002). This fact and the paleovalley-related location of the low-grade uranium halo can be considered as an evidence of its origin as a result of hydrogenous redistribution of early high-grade ores.

Late mineralization in veinlets occurs in the vicinity of unconformity-related ores (periphery of the Karku deposit) and at some distance (Kotalakhti ore-showing). If in the first case a genetic link between the two types of the mineralization can be supposed, the second case is obscure. Moreover, difference of REE patterns for the Karku pitchblende and the Kotalakhti occurrence possibly indicates the derivation of uranium from independent sources. Because of absence of link between the Kotalakhti vein-type uranium ore-showing and the unconformity related uranium mineralization, it seems more correct to classify this ore-showing as a vein-type occurrence.

Indications of a meteoritic water influence in the remobilization of the primary uranium mineralization are widespread in the Karku area (Matala occurrence at the NE flank of Ore body 1). This process is especially intense in Ore body 1. The north-easternmost flank of it (the Bolotnoye ore-showing) is in vicinity of an area where the Riphean sequence pinches out and where meteoric waters reach the productive horizon directly. High-grade ore concentrations are

very rare in Ore body 1, but a wide halo of low-grade and sub-economic mineralization occurs with overlapping oxidation stretches over few kilometers.

Thus, four different processes have played a role in the genesis of the uranium mineralization in the Karku deposit:

- 1) early hydrothermal-diagenetic of unconformity-type;
- 2) hydrogenous;
- 3) late hydrothermal of vein-type;
- 4) supergene.

6.2. Generalized comparison of the Karku deposit with unconformity-related deposits of the Athabasca basin.

Similarities between the Karku and Cigar-Lake and other unconformity-related deposits of the Eastern Athabasca are the followings:

1. Relation of the U ore bodies with the regional unconformity between AR-PR₁ basement and non-metamorphosed clastic formations of a vast sedimentary basin.
2. Location of the deposits in a mobile tectonic zone with heterogeneous AR-PR₁ basement (the Wollaston belt and the Raahe-Ladoga zone).
3. Ore bodies are located in vicinity of granitic-gneiss domes.
4. Uranium mineralization is related to fault zones cutting hosting sediments.
5. Main part of ores is related to graphitized and sulphidized zones of the basement.
6. Uranium mineralization is hosted mainly by the sediments above the unconformity. And to a lesser extend by weathered basement rocks.
7. Subordinated U mineralization occurs at some distance from the unconformity in the tectonic zones – as above as below.
8. Ore bodies are surrounded by a chlorite alteration halo in the host rocks.
9. Uranium ore mineralization is composed mainly of pitchblende and coffinite.
10. Uranium mineralization is polychronous, but high-grade ore has been formed during the 1450-1100 Ma interval.
11. Sulphides, sulphoarsenides and arsenides accompany the uranium mineralization.
12. Uranium is associated with increased content of Mo, Pb, Zn, Cu, Fe and As.

Main differences between the Karku and unconformity-type occurrences of the Athabasca basin are following.

1. Sedimentation of the Priozersk suite sandstones started at about 1470 Ma only, whereas in Athabasca it occurred between 1700-1650 Ma (Cumming et al., 1987).

2. Feldspar-quartz sandstones of the Priozersk suite are less mature in comparison with the highly quartzose ones of the Athabasca Group.

3. Thickness of the Priozersk suite is less than 40 m and of the whole Riphean sequence is up to 160 m in the Karku deposit area whereas the thickness of the Athabasca Group sediments in the areas of the unconformity-type deposits is up to more than 700 m. Weak development of diagenetic overgrowth on detrital quartz and presence of kaolinite in non-altered sandstones cement in the Karku area, instead of dickite in the Athabasca indicates a less thick sequence of Riphean sediments in the Salmi depression at the time of the diagenesis.

4. Thick basalt layers are present in the Riphean sequence of the Salmi depression, but are absent in the Athabasca basin.

5. Mesoproterozoic granites of rapakivi types occurring in the basement of the Salmi depression are unknown in the Athabasca Province.

6. Graphite- and sulphide-bearing rocks are widespread in the Northern Ladoga, but the epigenetic graphite and sulphide enrichment of the basement rocks is less in the Karku deposit area; elongated zones of sulphide-graphite mylonites (augen gneisses) like in the Athabasca basin deposits are not typical in the Karku area.

7. Ore bodies of the Karku deposit are localized in the valley-like depressions of the basement roof. This is not so common for the Athabasca basin deposits although exists sometimes (at the Key Lake deposit for example); the Cigar Lake deposit ore body is situated above a local bump of the basement corresponding to a zone of augen gneisses.

8. Regolith alterations are weak in the Karku deposit area; the regolith thickness is much smaller in Karku than in the Athabasca.

9. Host rock alterations of the Karku deposit are less intense and have different composition compared to the ones associated with the Athabasca basin deposits:

- there are no complete dissolution of detrital quartz in the Karku deposit area;
- diagenetic kaolinite in the cement of non-altered sandstones in the Karku deposit area is replaced by dickite around the ore-enveloping alteration halo. whereas diagenetic dickite is replaced by illite in the external alteration zones of Athabasca basin ores;

- the altered zone hosting high-grade ore in the Karku deposit has a sulphide-chlorite-carbonate composition with abundant calcite contrasts with clayey alteration mainly composed of Mg-Al chlorite and dravite in the Athabasca basin deposit host rocks.

10. Breccias bodies frequently associated with U mineralization in the Athabasca basin (Lorilleux et al., 2003) have not been discovered in the Karku area; only a relatively weak cataclasis of the ore-hosting sandstones occurs in the Karku deposit.

11. High-grade ores of the Karku deposit are surrounded by a wide halo of low-grade mineralization forming the main part of the deposit resource, whereas U mineralization in the Athabasca basin consists mainly of high-grade ores.

12. Positive correlation between the U and Ag characterizes Karku ores is uncommon feature for the Athabasca basin deposits. On contrary, high contents of Au and Pt may occur with U ores from Athabasca and have not been discovered in Karku.

13. Epigenetic Th enrichment of the sandstone and basement rocks in the vicinity of the U ore bodies in the Karku deposit has not been observed in other unconformity-related deposits.

14. Chondrite-normalized REE-content patterns of uranium oxides from most unconformity-type deposits have a bell shape; the ones from the Karku deposit uranium oxides is similar to that of vein type deposits; also REE contents in the pitchblende from the Karku deposit high-grade ores are much lower than in the ones from the Athabasca basin deposits.

Conclusion.

The discovery of the Karku deposit happened in the 1989, but unfortunately the area of the deposit and even more the Salmi depression have still not been covered with a sufficiently dense drilling net. Therefore, a more detailed estimation of the resource of the Pasha Ladoga basin remains to be done, but already obtained information allows to draw some conclusions.

The similarities between the Karku deposit with the Cigar Lake and other unconformity-type deposits also testifies some similarities in the ore-producing processes and allows to refer it to the same type. At the same time numerous differences need to be taken into account when estimation of the prospects of the Karku area and whole Pasha-Ladoga area for the occurrence of large economic uranium occurrences.

The relatively small thickness of the host sedimentary unit at Karku and its coverage with a thick low-permeable volcanite layer constitutes a much smaller volume of rocks which can be included into the circulation of uranium-leaching fluids.

The much lower alteration intensity of ore-hosting rocks in the Karku deposit is a further

evidence of the lower aggressivity of ore-producing fluids. The essentially calcitic composition of the ore-hosting alteration zone testifies a higher pH for the brines during Karku deposit formation. The Fe-rich nature of the chlorite attests the lesser oxidizing conditions prevailing in the Karku deposit. It may result from the reducing capacity of the mafic effusives overlapping the ore-hosting sandstones and relatively high content of detrital sulphides in the Priozersk suite sediments of the Salmi depression.

Faults crosscutting the ore-hosting sandstone in the Karku deposit area produced no strong brecciation, hence their effectiveness for producing trap space for the U mineralization was less than in the Athabasca basin.

Zones of epigenetic graphitization and sulphidization in the basement rocks of the Salmi depression are not so contrasted and extensive as they are in the Athabasca basin. It decreases their role as a probable reducing barrier in the ore-forming process.

There is no economic uranium mineralization hosted by the basement rocks as it is in many of unconformity-type deposits. Unique deep occurrence of a fracture-bound uranium mineralization below the unconformity is of low grade and has not been studied enough.

Wide halo of low-grade, sometimes apparently late U mineralization demonstrates the importance of late U redistribution, possibly decreasing the grade of the mineralization.

Presently, evaluated resources of the Karku deposit allow to consider it as a small-middle grade deposit. There are high-grade uranium concentrations in the deposit, but unlike Athabasca unconformity-type deposits, in Karku they form only subordinated part of the resource. The main resource consists in low-grade disseminated mineralization. This feature and the coverage of the ores by a thick overburden (including thick basalt layer) increase the costs of exploitation.

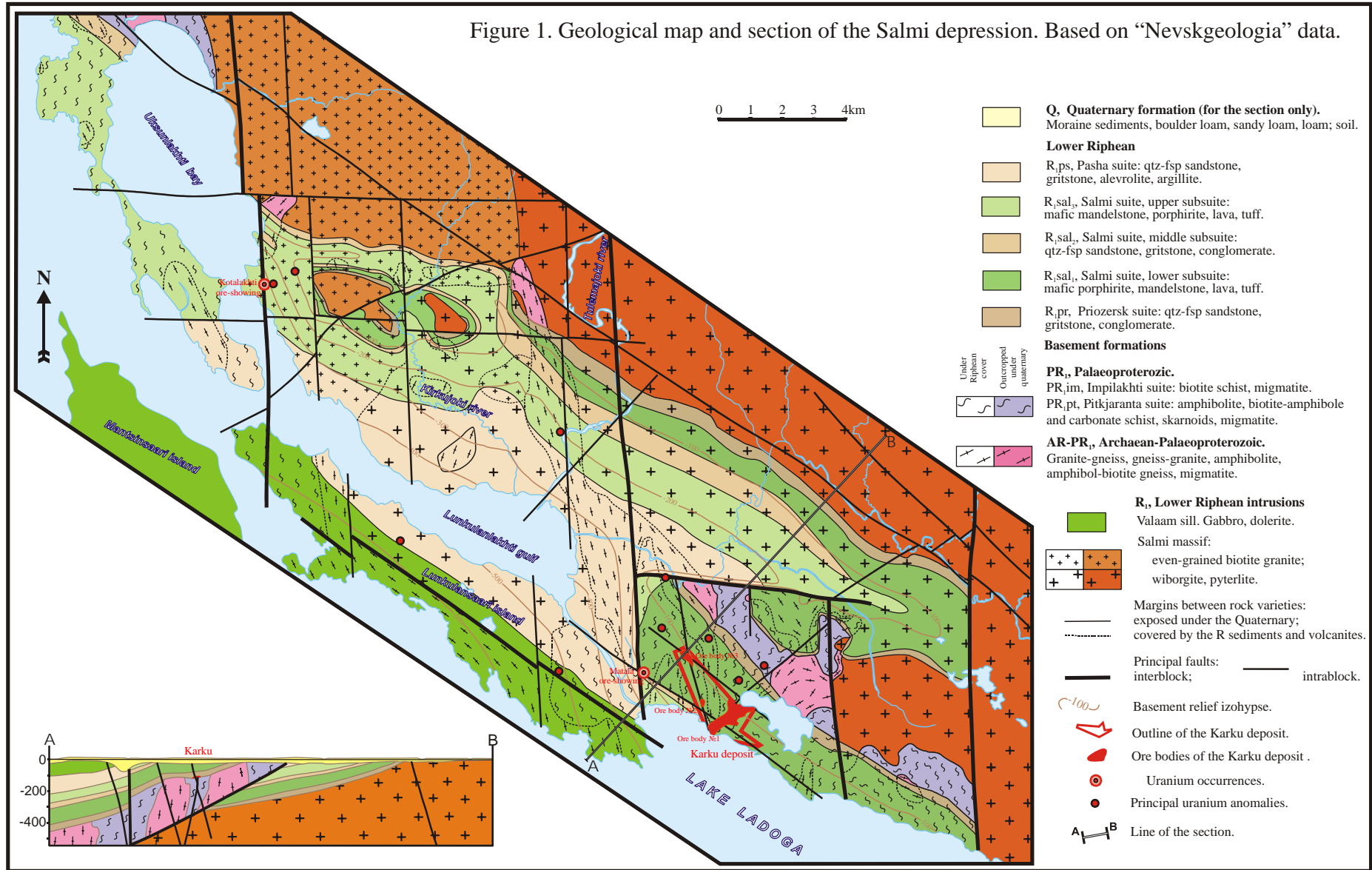
Other uranium occurrences in the Salmi depression have no economic importance although some of them have not been evaluated sufficiently and could have larger resources (the Matala and Kivis ore-showings).

Most of the Salmi depression basement is composed of Salmi granites; therefore areas favorable for the unconformity-related U deposition underlain with graphite-enriched metasediments are quite limited.

Most of above listed features decrease the attractiveness of the Karku deposit and the Salmi area. In other parts of the Ladoga region the geological environment differs and it is taken into account while the final estimation of the regional U potential in Part III of this thesis.

**APPENDIX
TO CHAPTER 2**

Figure 1. Geological map and section of the Salmi depression. Based on "Nevskgeologia" data.



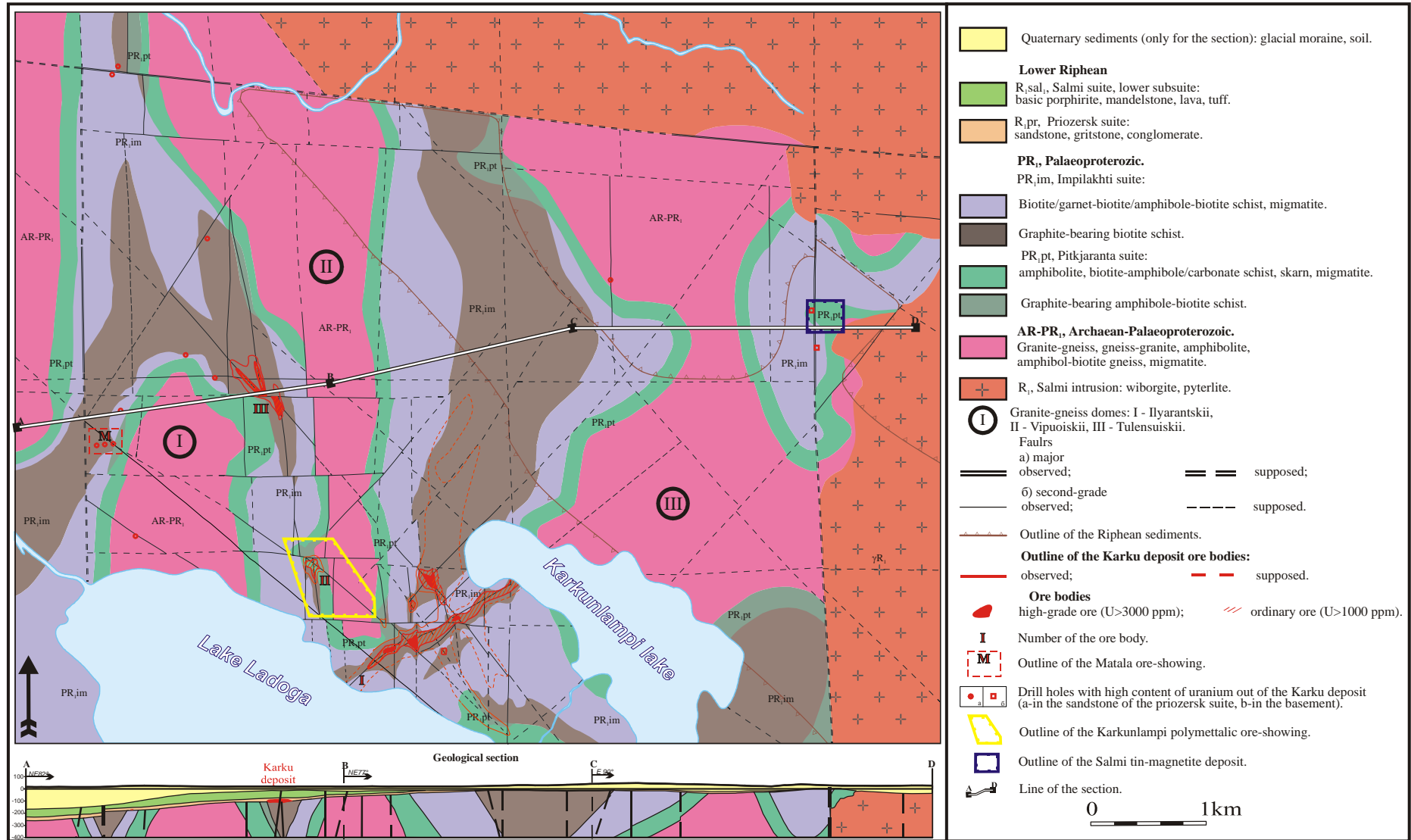


Figure 2. Geological map and section of the Central Block area. Based on “Nevskgeologia” and ZAO “NOVAYA LEKHTA” archive data.

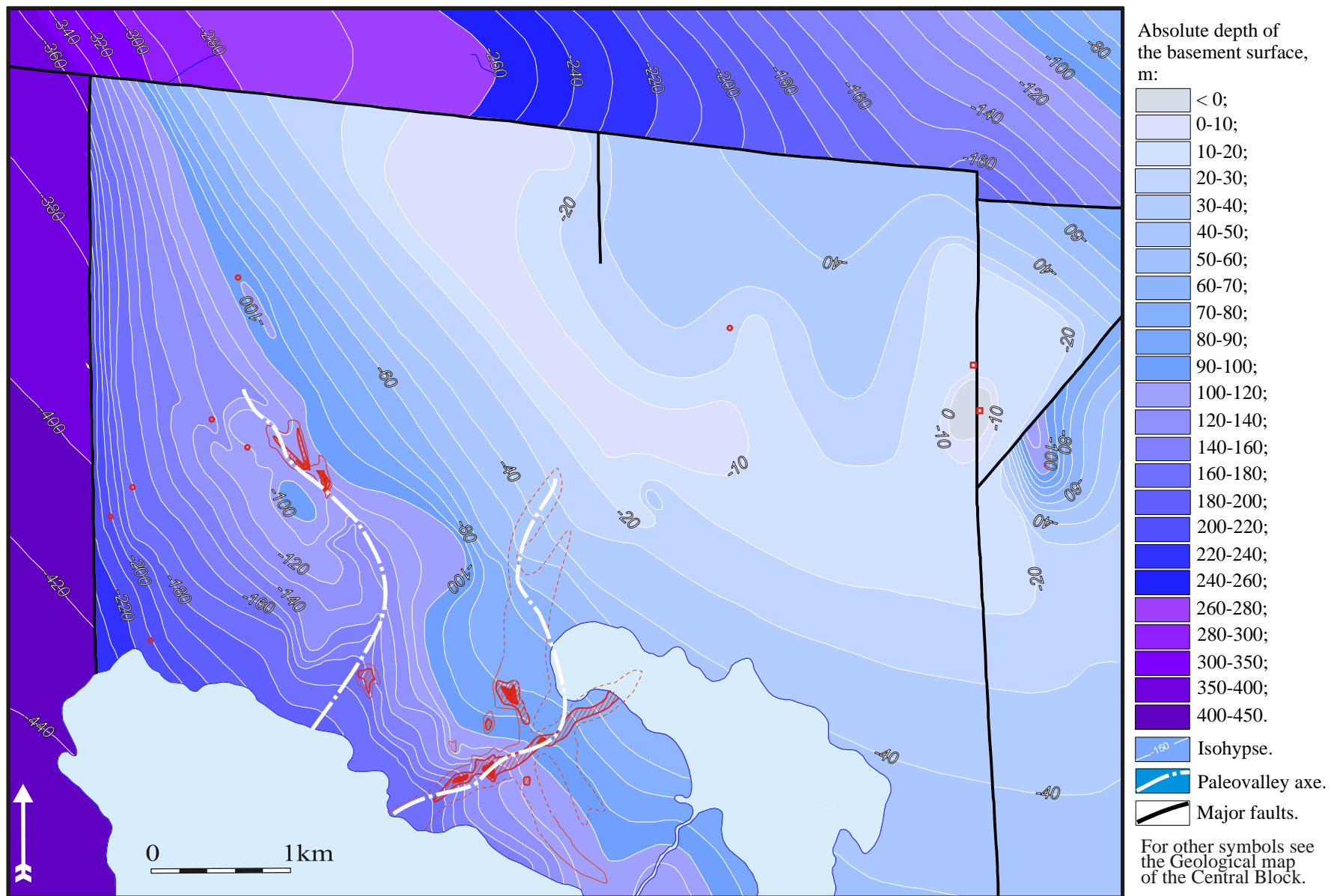


Figure 3. Map of the basement surface in the Central Block area. Based on ZAO “NOVAYA LEKHTA” archive data.

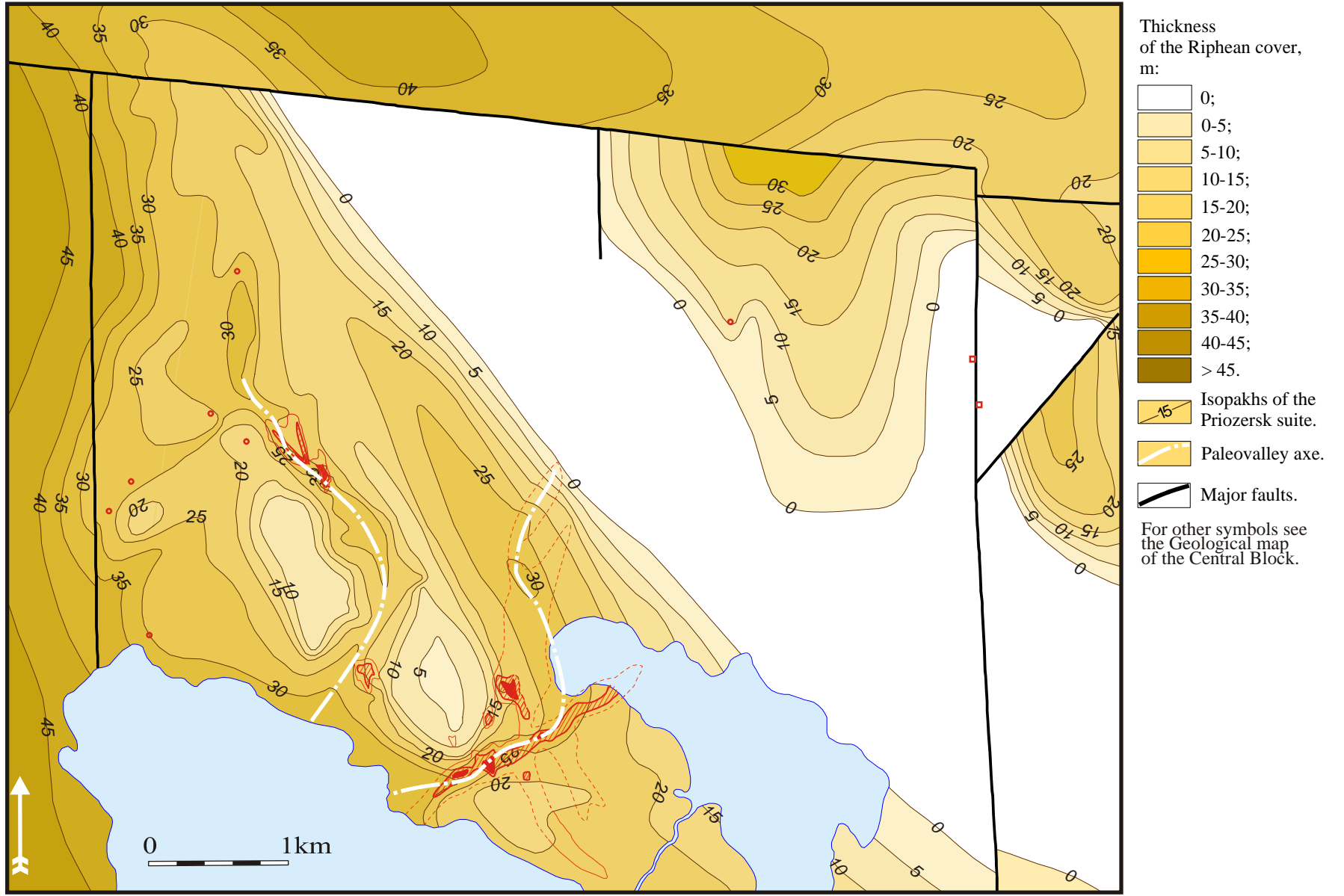


Figure 4. Map of thickness of the Priozersk suite in the Central Block area. Based of ZAO "NOVAYA LEKHTA" archive data.

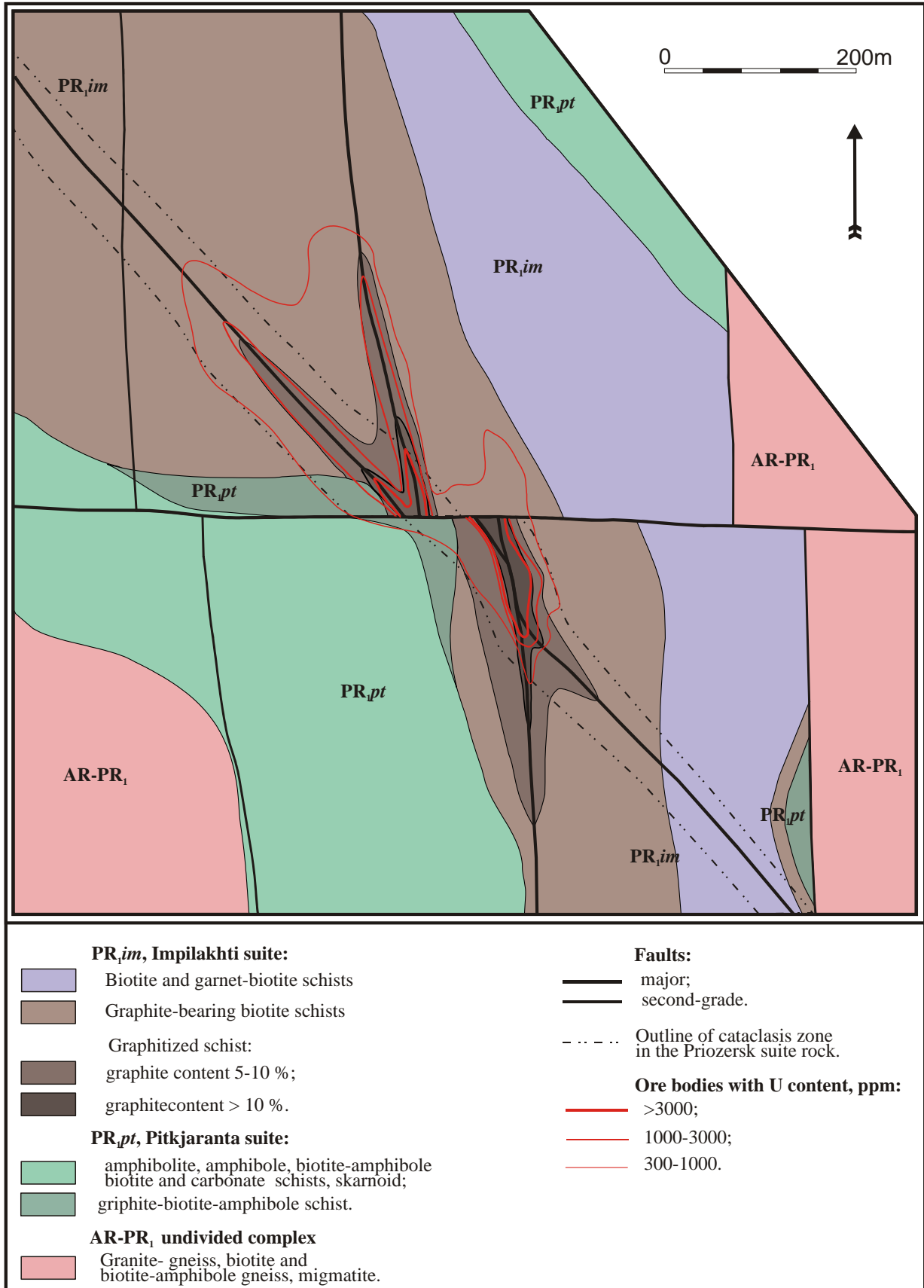


Figure 5. Geological map of the Karku deposit Ore body 3 area. Based on “Nevskgeologia” data.

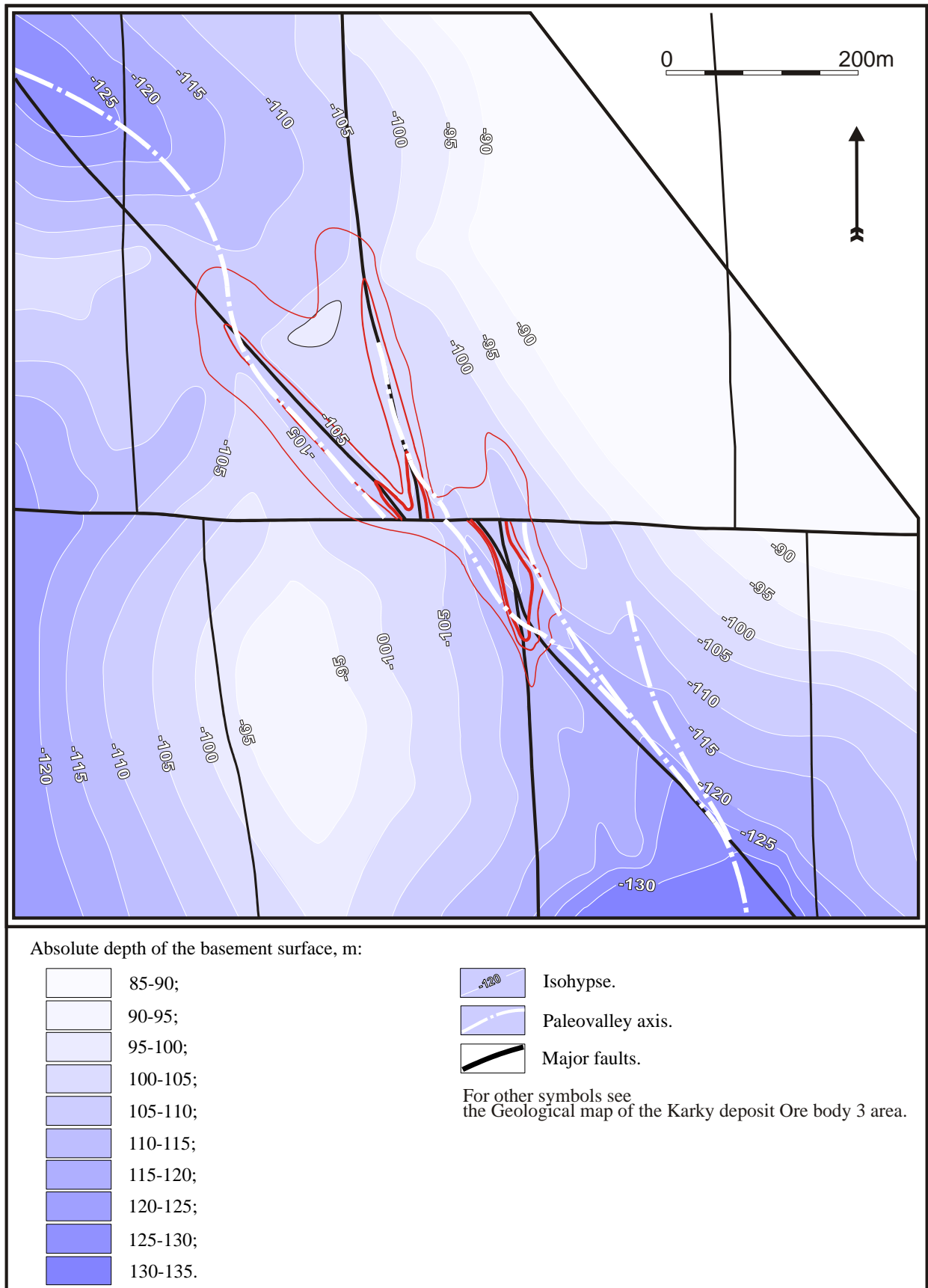


Figure 6. Map of the basement surface in the Karku deposit Ore body 3 area. Based on “Nevskgeologia” data.

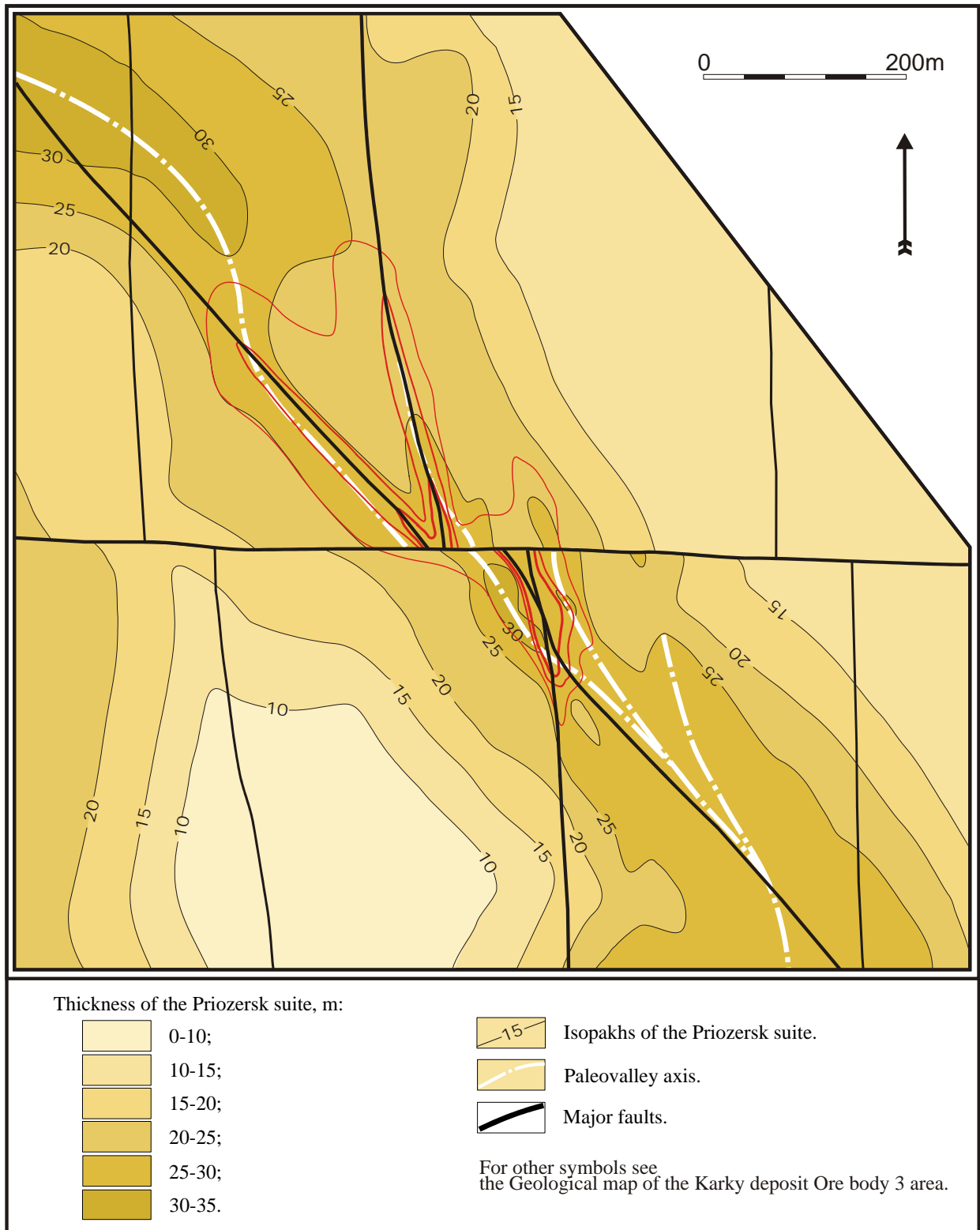


Figure 7. Map of thickness of the Priozersk suite in the Karku deposit Ore body 3 area. Based on “Nevskgeologia” data.

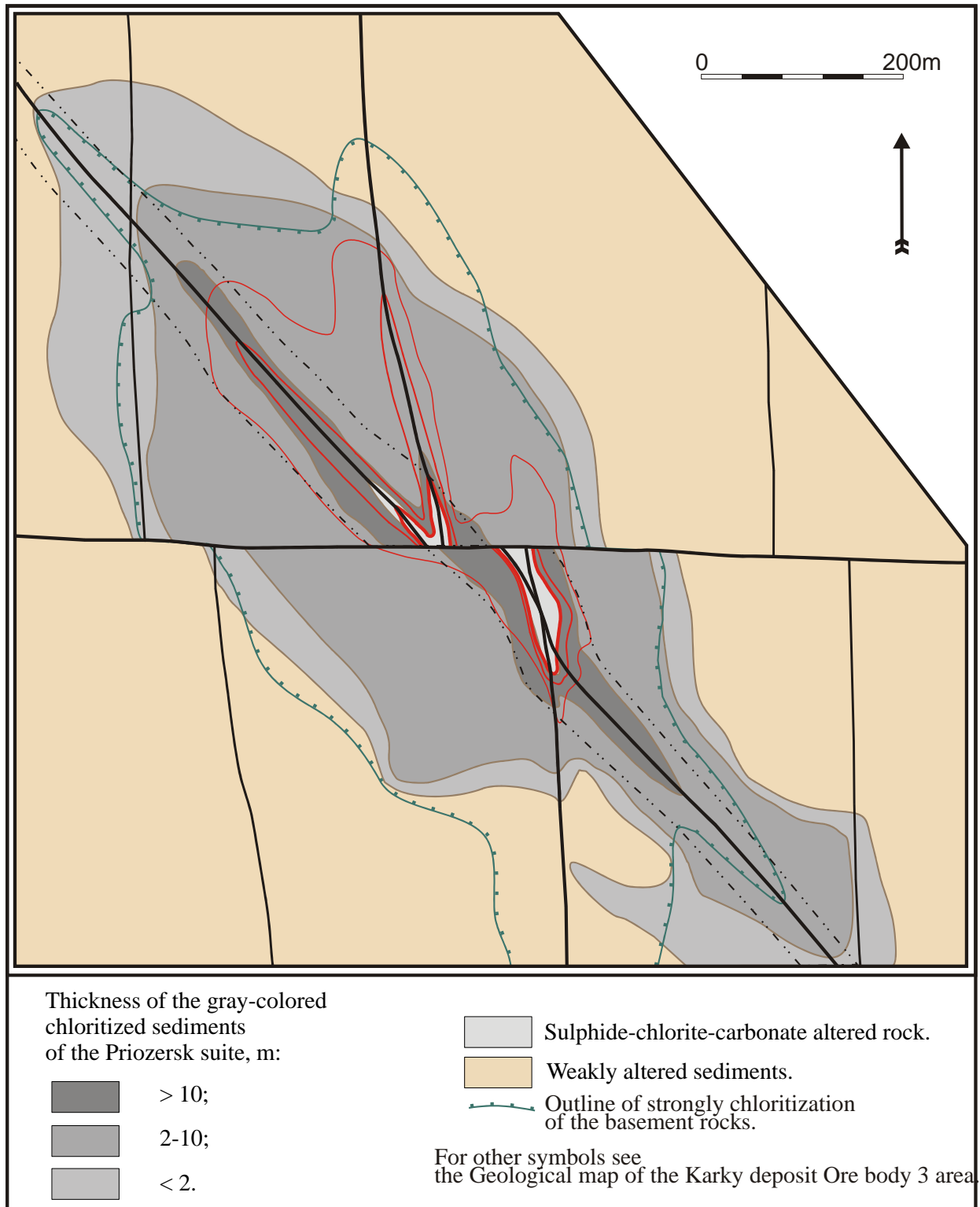


Figure 8. Map of metasomatic alterations in the Karku deposit Ore body 3 area. Based on "Nevskgeologia" data.

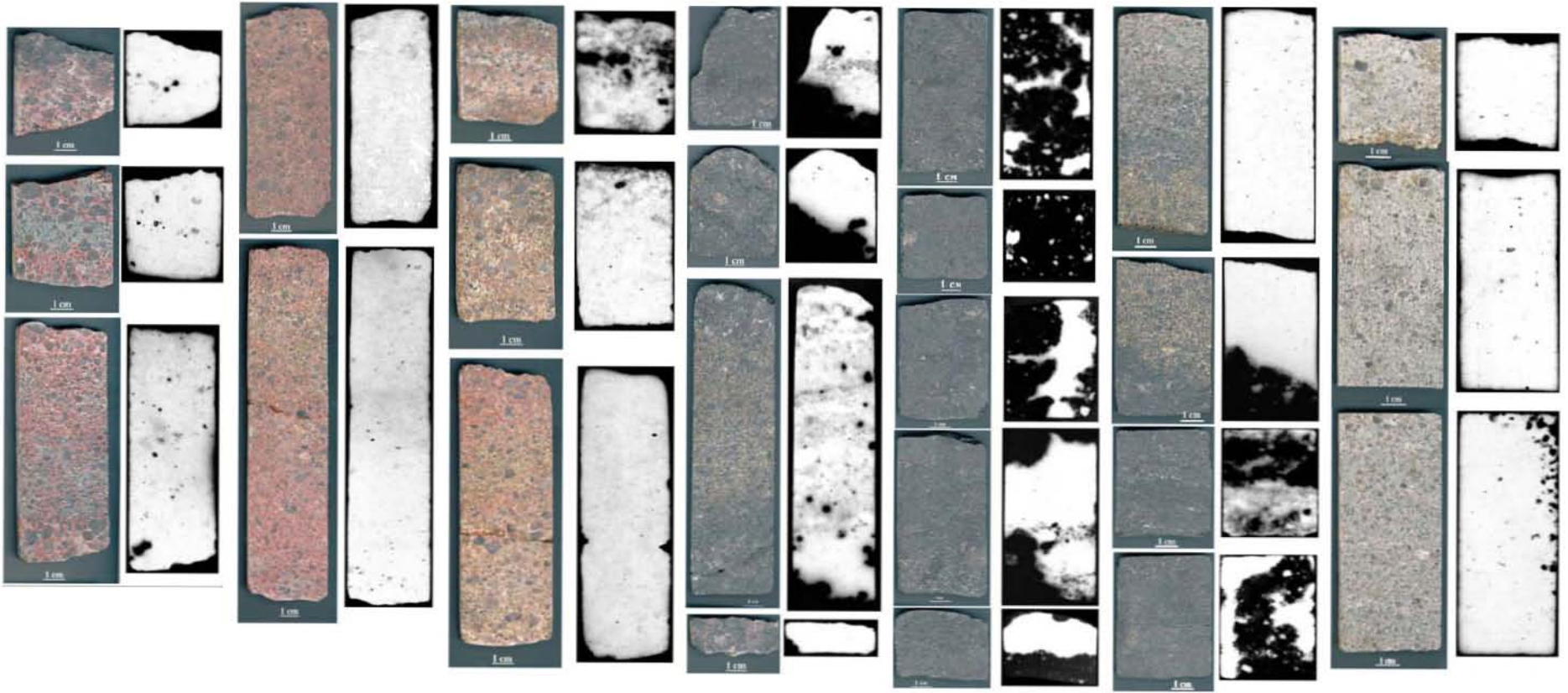


Figure 9. Drill core samples of U ore-hosting sulphide-chlorite-carbonate metasomatites after the Priozersk suite sandstone and corresponding autoradiographies. The Karku deposit, DDH 671, 123.25-125.1 m.

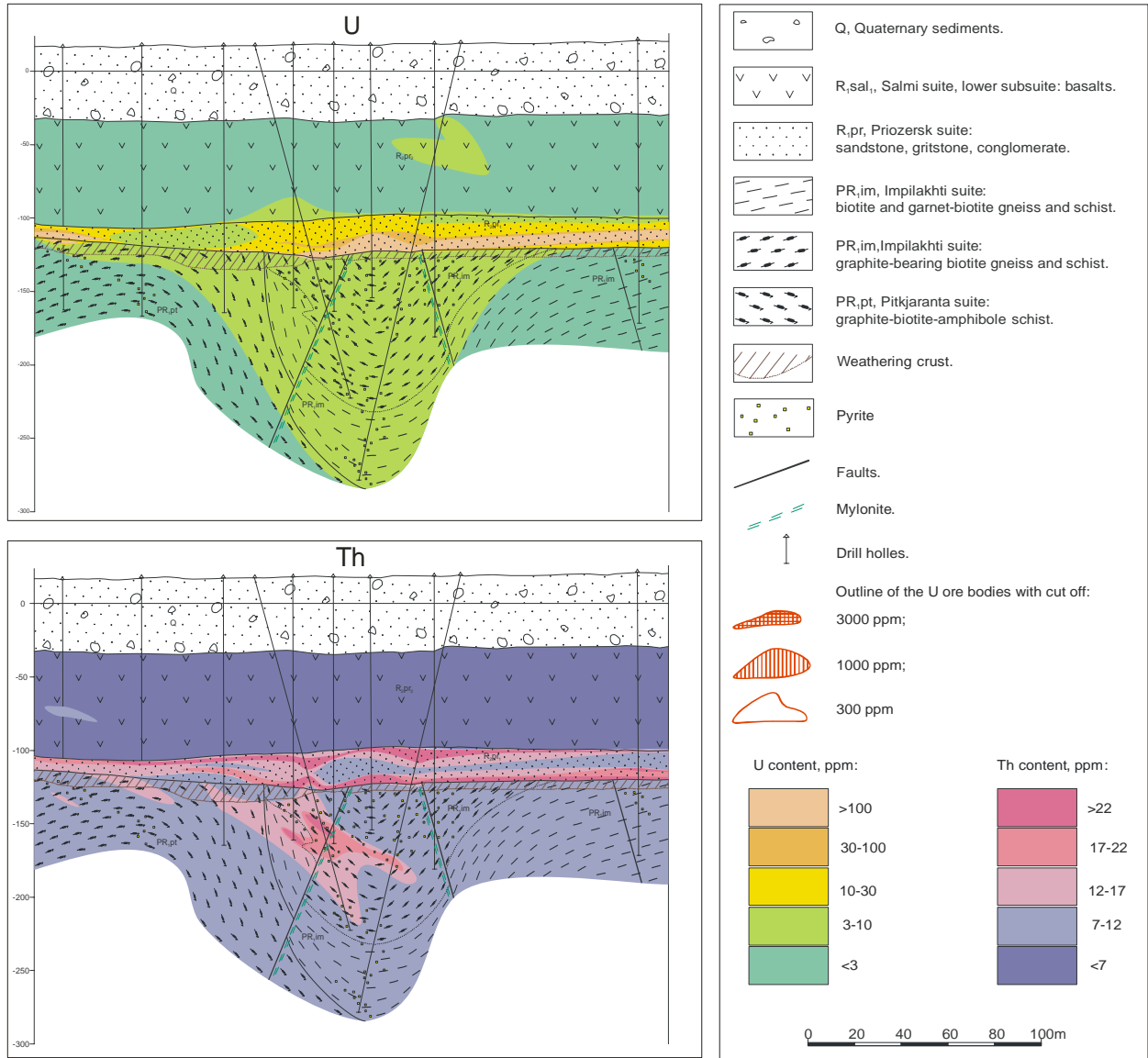


Figure 10. Sections with U (upper) and Th (lower) contents in the Karku deposit Ore body 1 Based on “Nevskgeologia” and ZAO “NOVAYA LEKHTA” data (Kushnerenko V.K. and Dolgushina I.S.)

CHAPTER 3
URANIUM OCCURRENCES
HOSTED
BY VENDIAN-PALEOZOIC
PLATFORM SEDIMENTS

Chapter 3. Uranium occurrences hosted by Vendian-Palaeozoic platform sediments.

Introduction

The Upper Vendian-Palaeozoic sedimentary cover of the East European platform occurs in the southern half of the Ladoga region. It unconformably overlays with an unconformity AR-PR₂ basement of the Karelian, Raahe-Ladoga and Svecofennian domains and Riphean-Lower Vendian formations of the Pasha-Ladoga basin. Numerous uranium occurrences hosted by Upper Vendian sandstones and Ordovician shales have been discovered in this region (fig. 2.3.1). Uranium occurrences in sandstones and siltstones of Middle-Upper Devonian occur to the south from the study area.

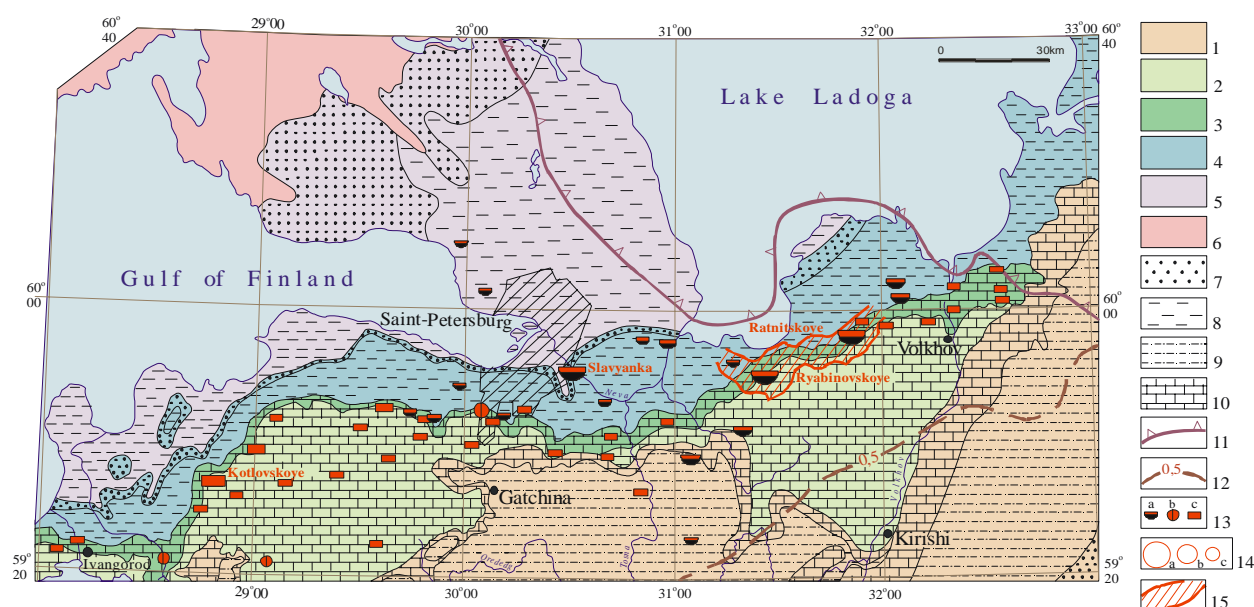


Figure 2.3.1. Geological map of the Nevsko-Volkhovskiy uranium ore district (after Fuks, 2007).

1-5 - Stratigraphic subdivisions: 1 - D₂₋₃, 2- O₂₋₃, 3- O₁, 4- Є, 5- V₂, 6- PR₁₋₂; 7-10 - lithology: 7 - sand, sandstone, aleurolite, 8 - clay confining layer, 9 - sand-clay and carbonate-clay sediments, 10 - limestone, dolomite, marl; 11 - outline of the Pasha-Ladoga Riphean basin; 12 - 0,5 km isohypse of the basement roof; 14 - uranium occurrences: a - sulphide-uranium in V₂ basal sandstones, b - rare-metal-uranium in O₁ phosphorite, c - vanadium-molybdenum-uranium in O₁ Dictyonema shales; 15 - grade of an occurrence: a-deposit, b-ore-showing, c-anomalies; 16 - outline of sulphide-uranium mineralization in V₂ basal sandstones with cut-off 100 ppm.

The uranium occurrences in the platform cover have been discovered and studied during exploration works in 1945-1947, 1957-1963, 1975, 1983-1985. There was experimental exploitation of Sillamyae uranium deposit (Estonia) hosted by Lower Ordovician shales during brief period in 1950th.

There are no outcrops with the uranium mineralization of these types and drill samples are no more available. I will only present a brief description based on archive reports of

“Nevskgeologia” and VSEGEI (Kondakov et al., 1963; Onjushko, 1979; Sharikov and Potapov, 1986; Fuks, 2007) to give a complete image of uranium metallogenesis in the Ladoga region.

3.1. Uranium occurrences in the Upper Vendian sandstones.

The Nevsko-Volkhovsky ore district comprises Slavyanskoye, Ryabinovskoye and Ratnitskoye uranium deposits, numerous ore-showings and anomalies hosted by basal sandstones of Upper Vendian (620-540 Ma). The ore district extends from the Gulf of Finland to the Southern Ladoga for distance about 150 km with a 50-80 km width and partly coincides with the eastern part of Pribaltic uranium ore district composed of occurrences in Lower Ordovician formations. The Nevsko-Volkhovsky ore district occurs along the Baltic-Mezen tectonic belt. Basement of the district area is represented by the weathered Kalevian gneiss and schist metamorphosed to amphibolite grade (sometimes graphite-bearing) and late-Svecofennian Polyansky and Chaplinsky granite complexes.

Laterites on the basement formations have thicknesses from 5 to 30 m. Linear weathering occurs along basement faults. Localities with uranium enrichment occur along these zones.

The lower layer of the Upper Vendian sequence is the Redkinsky horizon (V_{2rd}) (another name is the Gdovsky horizon). It is composed of 3 layers:

- 1) variegated and gray Fsp-Qtz gritstone-sandstone and small-pebble conglomerate, cemented by the sand-clay material, sometime containing organic matter (0.5-3.0 m thick);
- 2) gray Fsp-Qtz coarse-grained sandstone interbedding with fine-grained sandstone, mudstone and clay; rocks are enriched in organic matter and sulphides (0.5-1.5 m thick);
- 3) green-gray shaley clay (2-8 m thick).

The Redkinsky horizon sediments inherit of the trace element pattern of the weathered basement in many respects. Increased uranium content is common for the basal layers of the Redkinsky horizon and the most uranium-enriched sediments overlay the uranium-specialized magmatic complexes (Chaplino and Polyany late-Svecofennian leucogranites); above the Riphean sediments the radiogeochemical background is lower and uranium anomalies are absent. Only in the eastern slope of the Pasha graben rare uranium anomalies in the Vendian sandstone have been discovered above the uranium anomalies at the Riphean unconformity (Skorospelkin, 2002).

All uranium occurrences of the Nevsko-Volkhovskiy ore district are localized in the basal layers of Redkinsky horizon; sometimes uranium mineralization penetrates in the basement weathering crust. Uranium occurrences are located in depressions of the crystalline basement surface limited by tectonic zones. Ore bodies are tabular and conformable to the host rocks. There are several mineralized levels. Most of the ores are related to the upper part of the first gritstone-sandstone and second interbedding layers. Maximal ore concentrations occur in the gray-colored sandstone close to its contact with red-colored rocks.

The Slavyanskoye deposit is located in the lower reach of the Neva river, in SE part of the Saint-Petersburg (fig. 2.3.2. and 2.3.3). The deposit is located on a shoulder of a paleovalley. The mineralized zone has irregular shape with a size about 30 sq. km (cut off 200 ppm). The ore bodies are discovered at 241-278 m depth. The thickness of ore bodies is 0.75-3.85 m. Average uranium content is 210 ppm over 1.88 m, maximum is 1760 ppm.

Host rocks are mainly coarse- and fine-grained, cross and diagonal bedded, poorly sorted sandstones, also the lower part of overlaying shaley clays and underlying laterites after the basement rocks. Sandstones are polymictic and oligomictic. Clasts are cemented with silica-chlorite-sericite, rarely silica-carbonate matter. Sulphides form thin impregnation of idiomorphic crystals and xenomorphic grains. They replace sericite and chlorite of the cement, also fill conformable and cutting fractures. Pyrite prevails; sphalerite, chalcopyrite, pyrrhotite, chalcocite and covellite. Uranium mineralization is associated with a tabular oxidation of the host rock.

Uranium minerals are pitchblende, sooty pitchblende, micaceous uranium minerals (uranilphosphates, uranilvanadates etc) and ocher. Pitchblende envelops quartz grains, forms accretions with the sulphides and together with them replace primary minerals of the cement; also it occurs in fractures in association with carbonates. Sooty pitchblende develops as pellicles and thin coatings on clay cleavages, fills fractures, forms accumulations in the carbonate-clayey cement, together with pyrite occurs as pseudomorphs after vegetal remains. Micaceous uranium minerals and ocher accompany pitchblende and sooty pitchblende. Also uranium partly occurs as thin-dispersion and associated with the organic matter.

Uranium mineralization is accompanied with high contents of Pb (300-600 ppm), Cr (100-1000 ppm), Ag (70 ppm), Zn (60 ppm), Cu (up to 50 ppm), Y (20 ppm) and Ga (up to 300 ppm).

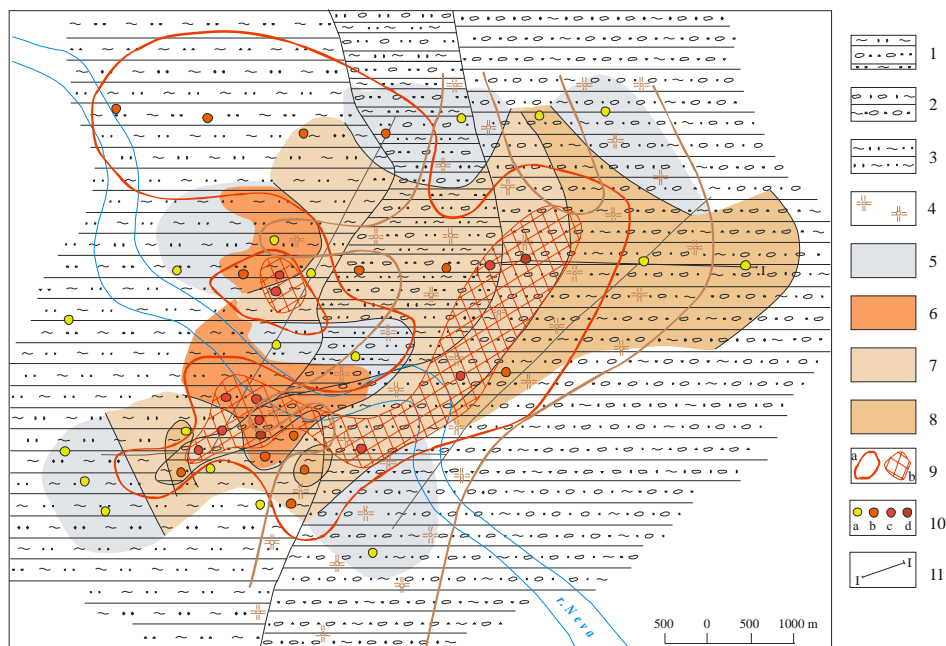


Figure 2.3.2. Geological map of the Slavyanskoye deposit (after Fuks, 2007).

1-4 - Lithological varieties of rocks: 1 - anisomeric sandstone with gritstone and pebbles, weakly cemented by clayey matter, in upper part - transition to sandstone, cemented by clayey matter, 2 - anisomeric sandstone with gritstone and pebbles, weakly cemented by clayey and carbonate-clayey matter, 3 - fine-grained sandstone, cemented by clayey matter, 4 - microcline granite; 5-8 - Geochemical varieties of rocks: 5 - gray-colored, reduced, 6 - speckled, 7 - weakly oxidized, 8 - intensively oxidized; 9 - uranium content outlines: a - < 300 ppm; b - > 300 ppm; 10 - uranium content in drill holes: a - < 200 ppm; b - 200-300 ppm, c - 300-500 ppm, d - > 500 ppm; 11 - line of the section.

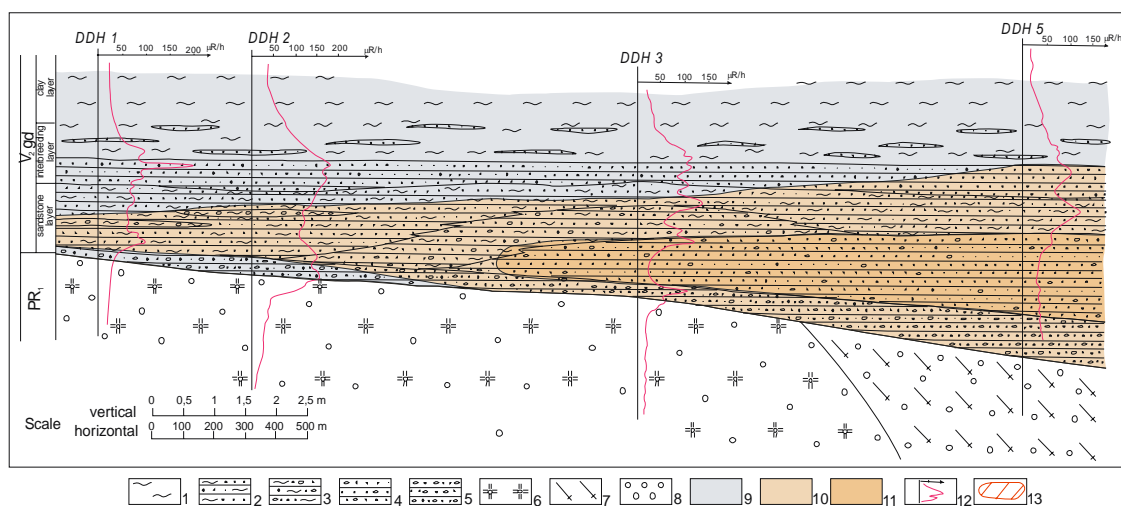


Figure 2.3.3. Geological section of the Slavyanskoye deposit (after Fuks, 2007).

1-8 - Lithological varieties of rocks: 1 - clay, clayey aleurolite, 2 - fine-grained sandstone, cemented by clayey matter, 3 - anisomeric sandstone with gritstone and pebbles, cemented by clayey matter, 4 - anisomeric sandstone with admixture of gritstone and pebbles, weakly cemented by clayey and carbonate-clayey matter, 5 - coarse-grained sandstone, weakly cemented by clayey and carbonate-clayey matter, 6 - microcline granite, 7 - migmatite, 8 - laterite; 9-13 - Geochemical varieties of rocks: 9 - gray-colored, reduced, 10 - weakly oxidized, 11 - intensively oxidized; 12 - drill holes with gamma logging diagram; 13 - ore zone.

Age determinations of uranium mineralization gives diverse ages – from 500 to 90 Ma; most frequent ages are ranging between 270-300 Ma. All analyses are old (before 1980th) and obtained by uncertain methods. That is why they give just common idea about age of the mineralization.

Ryabinovskoye deposit is located in the Southern Ladoga area, in the Polyany village area. Size of the deposit is 12×5 km with an average thickness of 1.4 m (for a 100 ppm cut-off). Ore bodies occur at a depth of 380-400 m. There are two ore bodies 3×1.5 and 5×1.5 km 0.1-5.8 m thickness with average uranium content 300 ppm for 2 m thickness. In the Polyany ore bed maximum uranium content is 800 ppm for 5.6 m, including 1900 ppm for 1 m thickness. This ore bed is cut by late brittle dislocation and doubled section of the mineralized formations has been discovered. Pitchblende, coffinite and sooty pitchblende mineralization is localized in the interbedding and sandstone layers, also in the regolith. There are uranium mineralized fragments at the unconformity between Vendian and Palaeoproterozoic formations. They occur as rounded grains in a base of the sandstone layer and as non-rounded fragments in the regolith. They consist of quartz of quartz-hematite breccias with pitchblende and coffinite. This represents an indication of the occurrence of uranium ore mineralization in the basement.

Epigenetic uranium minerals are associated with pyrite and galena, more rarely with sphalerite.

Several periods of uranium forming process have been distinguished by isotopic methods: 600-500, 400-380, 230-175, 50-5 Ma, but it is considered that the main part of the ores was formed about 380 Ma. Isotopic constrains were done in 1980th by uncertain methods and should be considered very carefully.

Generalized characteristics of uranium in occurrences in the Upper Vendian sediments of the Southern Ladoga area.

Uranium occurrences in the Upper Vendian sediments of the Southern Ladoga area are characterized by the following distinctive features:

- 1) exact lithological control – they are localized in the Upper Vendian basal sandstones, as a rule grey-colored, and to a lesser extend in the regolith;
- 2) the occurrences are localized in valley-like depression of the crystalline basement surface;

- 3) relation of the uranium occurrences to long-living tectonic dislocations (first the NE-striking Baltic-Mezen belt) has been distinguished;
- 4) the highest grade uranium mineralization is related to reducing front between carboniferous/sulphide-bearing and oxidized sediments;
- 5) the ore bodies have a tabular shape and are localized in the well permeable formations (mainly coarse-grain sandstones) between more dense basement gneiss and overlying clays;
- 6) occurrences are located above the uranium-enriched basement rocks (dominantly late-Svecofennian granites at first);
- 7) uranium mineralization is composed of pitchblende, coffinite, sooty pitchblende and hexavalent minerals;
- 8) uranium concentrations are accompanied by increased contents of Cu, Zn, Pb, Ag and Y;
- 9) uranium mineralization is of Palaeozoic age mainly, main ore-producing event refers to the Hercynian orogeny (cca 380 Ma).
- 10) identified uranium resource of the deposits is about 35 000 tons, prognostic resource is over 50 000 tons (Mikhailov et al., 1999).

It is presumed that uranium occurrences in the Upper Vendian sediments have been formed mostly as a result of leaching of uranium from the basement rocks by deep fluids that had been migrating along reactivated ancient faults (mainly NE striking) during the Hercynian event. Uranium had been transported by weakly alkaline, mildly reducing to oxidizing groundwater until its precipitation by concentrated reductants (plant remnants and sulphides). Uranium mineral paragenesis corresponds to low-temperature conditions.

According to their geological characteristics, uranium occurrences in the Vendian sandstones are referred to the tabular subtype of sandstone type uranium deposits.

In spite of the quite large resources (several tens thousands tons) these deposits were estimated as uneconomic because of low uranium content and not sufficient permeability of the ore-hosting horizon, that makes impossible using of in situ leaching (ISL). The permeability increases to the west in the Slavyanovskoye deposit, but this area corresponds to Saint-Petersburg city and its suburbs, that is why the exploitation is impossible there. Open pit exploitation is very expensive because of big overburden thickness (over 300 m).

3.2. Uranium occurrences in the Lower Ordovician formations.

The Pribaltic uranium district comprises a series of uranium occurrences hosted by the Lower Ordovician sediments. It is followed from the Pakerortsy cap area (Estonia) to the east until the Southern Ladoga.

This area corresponds to the Ordovician shallow marine basin (sometimes called Pribaltic basin). Geotectonic structure of the area is complicated with systems of sub-latitudinal- and meridional-striking structural zones. The sub-latitudinal-striking zone is localized above latent basement faults. It comprises Lower Ordovician bar-like uplift with abundance of *Obolus* shale detritus at the limbs and adjoining from the north littoral-lagoon depression filled with carbon-enriched Graptolite clays and southern Middle Ordovician depression with sapropel sediments. Phosphorites occur in the axial part of the latitudinal-striking zone, and carbon-bearing formations – at its periphery. Meridional-striking zone is presented by an uplift, where graptolite clays are absent. It is limited by a fault system.

Mineralized rocks are confined to the Pakerortsy horizon (O_{1pk}) of the Tremadoc stage comprising *Obolus* phosphorite-bearing sandstones and *Dictyonema* shales, overlain by glauconitic clays and sandstones. The thickness of the horizon varies from 2.5 to 16 m.

There are two types of uranium mineralization in the Ordovician rocks of the area: P-U mineralization in phosphorite and phosphate-bearing rocks and V-Mo-U mineralization in carbon-bearing black shales and clays.

3.2.1. P-U anomalies in the Lower Ordovician *Obolus* sandstones.

The phosphorus-bearing layer mainly consists of fine/middle-grained quartz sand and sandstones with abundant of *Obolus* shells detritus. Interlayers and lenses of small-pebble conglomerates occur at the base of the layer. The layer is of 2-10 m thickness. It is considered that P- and U-enriched rocks deposition took place in a humid shallow sea basin, and mainly intensively – in its littoral part.

Sandstones are gray, dark-gray to black. There is a secondary oxidation of the sandstones in areas where the overlying *Dictyonema* shales are eroded and the rock takes a brown-yellow color. P₂O₅ content in the sandstones and conglomerates varies from 3 to 20 %. P-bearing minerals are F-apatite and francolite.

Uranium content varies from 7 to 60 ppm, locally – up to 100 ppm. There are small concretions of phosphorites enriched in uranium up to 500 ppm. Two main form of uranium

enrichment take place: a) sorbed in lamellar silicates, b) own uranium minerals: uranium oxides UO_2 , rarely coffinite and micaceous uranium minerals.

Increased concentrations of Sr (0.003-0.26 %), F (0.3-3.3 %), Y (Y_2O_3 – 0.026-0.028 %), REE (REE_2O_3 – 0.025-0.048 %) occur.

Uranium mineralization in the Lower Ordovician phosphorites is identified as of the “phosphorite type” in the IAEA classification.

3.2.2. V-Mo-Pd-U occurrences in the Lower Ordovician Dictyonema black shales.

Dictyonema bituminous shales overlay the Obolus sandstones. This formation occurs along the 500 km latitudinal belt with a width from 15 km in its eastern part to 80 km in the western one. It is followed along the southern coast of the Gulf of Finland from the Pakerortsy cape of Estonia to river Syas in the Southern Ladoga. The northern limit of this layer is its exposition on the coastal glint of the Gulf of Finland; to the south and east it declines.

The Dictyonema-bearing layer can be subdivided into 3 parts (from the bottom to the top):

- 1) interbedding of the Dictyonema shale with the Obolus sandstones, 0.05-3.7 m thick;
- 2) Dictyonema clayey shale with small aleurolite interlayers, up to 1 m thick;
- 3) almost monotonous Dictyonema clayey shale (argillite), up to 2.5 m thick.

The total thickness of the layer is 7.2 m.

The shales are dark-brown, sometimes black. Organic matter makes 15-20 % of the rock. There are abundant concretions of pyrite, marcasite, Ca-phosphate and antraxolite. Small segregations of sphalerite and galena, rarely molybdenite occur.

Dictyonema shales are enriched in uranium along whole area where they occur. Average uranium content in the interbedding layer is 70-150 ppm; proper Dictyonema shale layers contain 160 ppm of uranium in average, maximum – 750 ppm. The lower part of the Dictyonema-bearing layer is more enriched in uranium; argillite contents more uranium than aleurolite.

Uranium is mostly sorbed by organic matter, phosphate oolites and Al-Si compounds. Only 5 % are referred to own uranium mineral phases (pitchblende and sooty pitchblende).

Besides of U, the shales are enriched in V, Mo, Ni, Ag, Pd and Cu. They also have increased contents of Zn, Pb, REE, Se, Re, Bi and Sn.

Uranium mineralization in the Lower Ordovician Dictyonema shales is referred to the “black shale” type in the IAEA classification.

Uranium content in the black shales of the Kotlovskoye and Krasnoselskoye deposits varies from 180 to 400 ppm in average. Maximum concentration occurs in monotonous argillites (up to 1970 ppm). Other elements abundances (ppm): Mo – 200-490, V – 900-1100, Ni – 100-180, S – 38 200-53 400,

Total prognostic uranium resource of occurrences hosted by the Ordovician black shales is estimated in 616.5 kt (Mikhailov et al., 2006).

V-Mo-Pd-U occurrences in the Dictyonema black shales have been mined in Estonia during brief period in 1950th. At present time they considered as uneconomic for uranium because of the low grade of the ore, technological and environmental constraints. Nevertheless, proposals on exploitation of these occurrences as complex deposits appear from time to time.

3.2.3. Origin and typology of U occurrences in the Lower Ordovician sediments.

Uranium mineralization in the Lower Ordovician formations considered of syn-sedimentary origin. Exhumation and erosion of basement formations of the Baltic Shield as a response Caledonian tectonic event about 490-480 Ma with possible contribution of uraniferous endogen brines led to enrichment of waters of the Lower Ordovician sea in uranium. Primary deposition of ore elements is referred to sedimentation and early diagenetic stages. The most productive localities were straits and lagoon with swampy shores, where favorable conditions occurred due to presence of such strong sorbents as organic matter and phosphorus. The diagenesis contributed to forming of most high-grade uranium mineralization. Hence, age of ore mineralization is ranged in 490-480 Ma. Indications of late epigenetic uranium redistribution as overgrowing of pyrite concretions by sooty pitchblende and pitchblende mineralization dated at 70 Ma (Mikhailov et al., 2006).

Conclusion.

All platform-hosted uranium occurrences of the Southern Ladoga area presently are considered as of uneconomic grade, but they have different potential. In order of decreasing of its possible future economic importance they can be ranged as follows:

- I. Uranium occurrences in the V₂ sandstones (Sandstone-type);
- II. V-Mo-Pd-U occurrences in the O₁ Dictyonema shales (Black shale type);
- III. P-U anomalies in the O₁ Obolus sandstones (Phosphorite type).

Uranium deposits in the V₂ sandstones discovered in the Southern Ladoga area in the past have been evaluated as uneconomic, but increased uranium demands make them more attractive. In addition, other territories of southern part of the Ladoga region have not been studied in detail and some of them seem to be quite promising. They will be introduced in the Part 3.

Although for now V-Mo-Pd-U occurrences in the Dictyonema black shales considered as uneconomic in respect of uranium but have some potential as complex deposits (Mikhailov et al., 2006).

P-U anomalies in the O₁ Obolus sandstones are ranged only as anomalies and have no economic importance.

Conclusion to Part 2.**Generalized characteristic of uranium metallogeny of the Ladoga region.**

The Ladoga region is characterized by a significant diversity of U metallogeny. Uranium occurrences of different types have been discovered in all stratigraphic levels of the geological sequence: in the AR-PR₁ basement, in the proto-platform Riphean formations, in the V-PZ platform cover. General characteristics of U metallogeny of the Ladoga region are presented in following paragraphs and in Table 2.1.

I. Typology of the Ladoga region uranium occurrences.

Accordingly to the IAEA classification uranium occurrences of the Ladoga region can be divided into following types introduced in order of importance in the world production.

Table 2.2. Typology of the Ladoga region uranium occurrences in the IAEA classification.

No	Type	Principal occurrences of the Ladoga region	World-known analogs
1	Unconformity	Karku	Cigar-Lake (Canada)
2	Sandstone	Slavyanskoye, Ryabinovskoye, Ratnitskoye	Monument Valley (USA)
3	Vein	Varalakhti, Jalonvara, Faddein-Kelya	Beaverlodge area (Canada)
4	Qtz-pebble conglomerate	Kuhilaslampi area	Martinmonttu, Ruunaniemi etc (Finland)
5	Intrusive	Impilakhti-Pitkjaranta area	Charlebois area (Canada)
6	Phosphorite	Anomalies in the Southern block	Florida area (USA)
7	Anatexite-hosted*	Vuorilampi, Korrennoye, Mursula-Puttumyaki	Rössing (Namibia)
8	Synmetamorphic	Mramornaya Gora	Vihannti (Finland)
9	Black shale	Kotlovskoye, Krasnoselskoye	Ranstad (Sweden)

* anatexite-hosted uranium occurrences are not enough studied for distinct identification (see Part 2, Chapter 1, Paragraph 1).

Different types U occurrences of the Ladoga region have been studied with different intensity. Unconformity-type is the best studied (especially the Karku deposit). Explorations of the Vendian-hosted sandstone-type deposits of Southern Ladoga and some of the basement-hosted ore-showings of the Northern Ladoga area (the Korennoye and Mramornaya Gora ore-showings for example) have not been very detailed but sufficient for approximate evaluations. Resource of others can be estimated just approximately.

Table 2.1. Principal types of uranium occurrences of the Ladoga region (anomalies are not included).

Characteristic	U-Th-REE in anatexite granites	U-P in Ludicovian carbonate rocks	Vein-type	Hosted by Riphean sediments	Hosted by Upper Vendian sandstone	Hosted by Ordovician Dictyonema shale
Type	“Anatexite-hosted”	Synmetamorphic	Vein-type	Unconformity-related	Sandstone, tabular subtype	Black shales
Regional location	Northern Ladoga area (at first Impilakhti-Pitkjaranta block)	Northern Ladoga area	Northern Ladoga area	Northern Ladoga area, Riphean Salmi depression	Southern Ladoga area	South-Western Ladoga area, Pribaltic region
Structural control	Granite-gneiss domes	Mostly in the Ruskeala anticline	Large fault zones, at first of NW and NE striking.	Riphean-Palaeoproterozoic unconformity	Basal horizons of the Lower Vendian, above Late Svecofennian leucogranites	Pribaltic Ordovician marine basin
Tectonic control	Local faults of the domes surrounding	At first – Ruskeala fault zone	Accompanying dislocations of big faults	NW faults (Ruskeala fault system), other local faults	Slight correlation with NE faults	Orthogonal faults
Petrologic control	Anatectic granites (qtz-fsp rocks) of the domes	Upper carbonate horizon of the Ludicovian Pitkjaranta suite	Some reference to U-enriched formations	Lower Riphean Priozerk suite fsp-qtz sandstones	Upper Vendian sandstones	Lower Ordovician Dictyonema black shale
Principal uranium minerals	Pitchblende, uraninite	Pitchblende, uraninite	Pitchblende, coffinite	Pitchblende, coffinite	pitchblende, sooty pitchblende	U in organic, phosphate and Al-Si matter, pitchblende,
Age of U mineralization, Ma	1820-1770	cca 1850	1600-1200, 500-350	1400-1100	< 380	cca 450
U content in ores, ppm (av/max)	500/17800	400/3000 (up to 25000 in late breccias)	1000/34800	1000/166200	400/1900	300/1300
Max. grade of an occurrence, t	300	136	n<10	8334	20 000	~30 000
Total identified/prognostic resources of the type	~1500/~5000	~1100/~4000	~50/~400	8500/41000	35 000/50 000	?/over 100 000
Perspective of economic deposit	negative	negative	low	medium	medium	negative

Rough comparison of total resources of the different types of U occurrences of the Ladoga region is presented in following diagrams (figure 2.1).

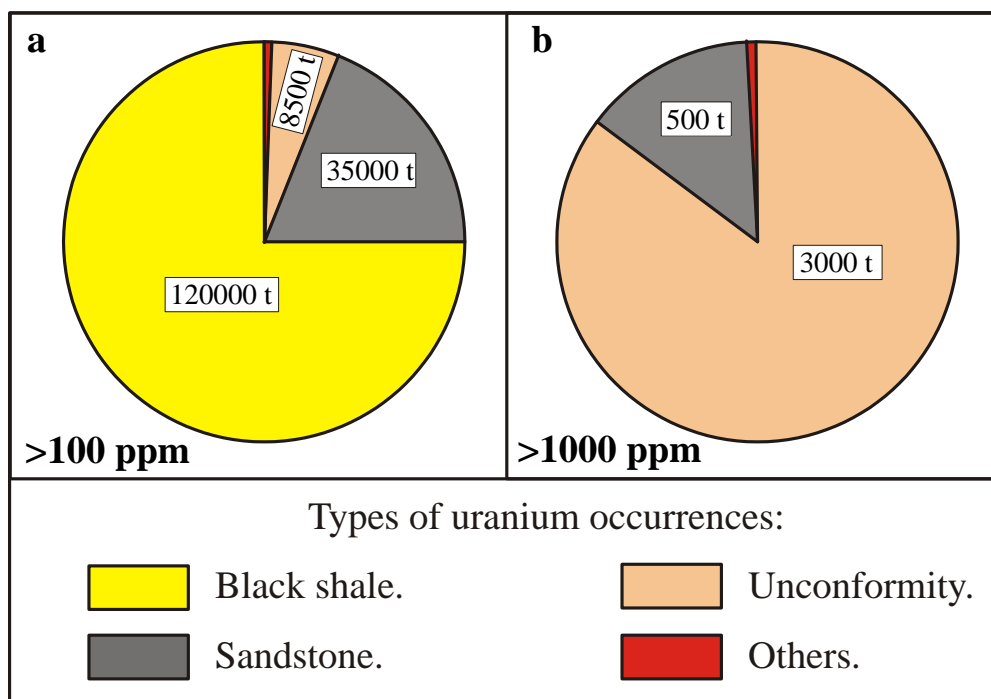


Figure 2.1. Typological distribution of uranium ore resources of the Ladoga region.

The Ordovician black shales have the largest total identified U resource (including all occurrences of the Russian part of the Ordovician basin), but the mineralization is very low-grade. Vendian-hosted sandstone-type deposits are mostly composed of low-grade mineralization as well. On a contrary, high-grade mineralization is quite common in the unconformity-type Karku deposit. As a result, the unconformity type composes overwhelmingly predominate for the resources over 1000 ppm of U, the sandstone-type is subordinated. The resources of other occurrences are small. In over 1000 ppm grade it is mostly of the vein-type and anatexite-hosted occurrences.

II. Regional structural-tectonic distribution.

1. Regional structural distribution.

There is well differentiation in the regional structural distribution of U occurrences in the Ladoga region:

- Most of basement-hosted U occurrences are located in the Northern Ladoga part of the Raahe-Ladoga domain. Few ones occur in adjacent areas of the Karelian domain.

– All significant U occurrences related to the Mesoproterozoic unconformity including the Karku deposit, ore-showings of the Salmi depression and anomalies of north-eastern slope of the Pasha graben are related to the Raahe-Ladoga domain as well.

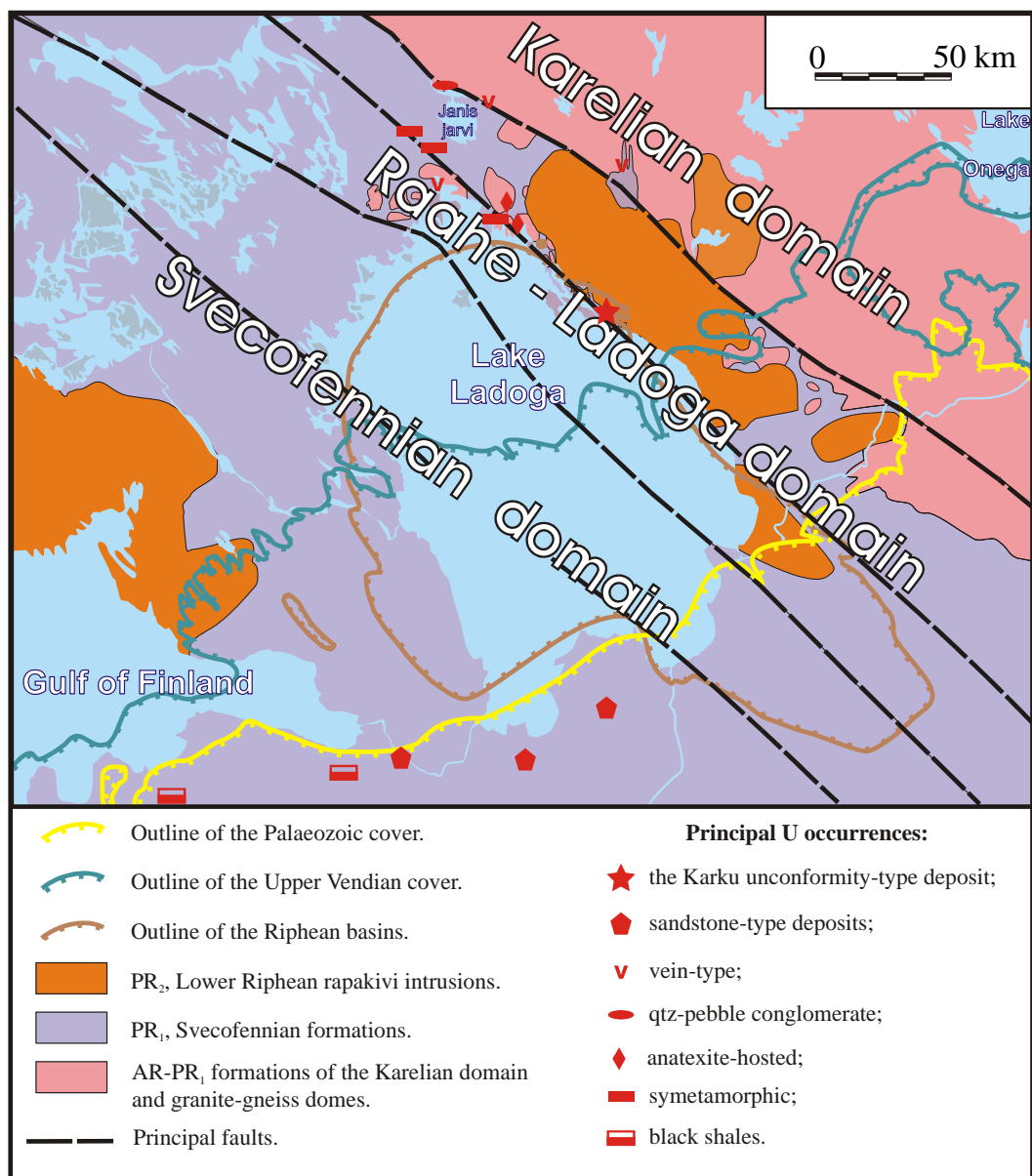


Figure 2.2. Distribution of different type uranium occurrences in the Ladoga region.

– The sandstone-type U occurrences are especially concentrated in the Southern block of the Svecofennian domain.

– Uraniferous Ordovician black shales and phosphorites are related to Early Palaeozoic basin of marine sedimentation located in southern part of the Ladoga region and farther to west along the south coast of the Baltic sea.

3. Regional tectonic reference.

The Ladoga region is located at the intersection of the Raahe-Ladoga and Baltic-Mezen tectonic belts. That is why the diagonal tectonic system is a principal one for the considering area and many of U occurrences show an affinity to brittle dislocations. The orthogonal tectonic system much less influences on tectonic structure and distribution of U in the region. Notable that westward the Baltic-Mezen tectonic belt turns from NE to sub-latitudinal striking.

Different-striking faults have not the same importance for the different type occurrences.

– NW-striking tectonic zones referred to the Raahe-Ladoga belt control the localization most of the basement-hosted U occurrences in the Northern Ladoga area. The Ruskeala fault zone is the most important in respect of U enrichment. Besides of basement-hosted U occurrences, it controls the location of Riphean-hosted ones including the Karku deposit.

– NE-striking tectonic zones host many of the basement-hosted U occurrences. They are especially important for the vein-type mineralization. Some affinity of the Karku deposit with the NE-striking faults is presumed. In the southern part of the study region all faults are concealed under the thick V-PZ cover and their role is not always clear. Presumably, the sandstone-type U occurrences are partly related to these faults.

– N-S-striking fault zones are followed from the Karelian domain and control location of a few U occurrences at its periphery. In the Raahe-Ladoga and Svecofennian domains their regional striking is not always clear and their importance for U distribution is tentative. Some of Northern Ladoga occurrences are related to local meridional-submeridional faults, but these structures are rather corresponding to local tectonic events (as a granite-gneiss domes formation for example) than to regional movements.

– E-W-striking faults as regional structures have no significant importance for U metallogenesis in the Northern Ladoga area. Only a few vein-type U occurrences related to local faults of W-E strike. Sub-latitudinal-striking faults influence the structure of the Ordovician sedimentary basin hosting U occurrences in black shales and phosphorites. Possibly these faults are related to the Baltic-Mezen tectonic belt.

III. Distribution of uranium occurrences in generalized geological sequence of the Ladoga region.

Most of U occurrences of the Ladoga region are characterized by reference to specific stratigraphic-lithological subdivisions (fig. 2.3); only the vein-type mineralization occurs in different horizons of the Precambrian sequence.

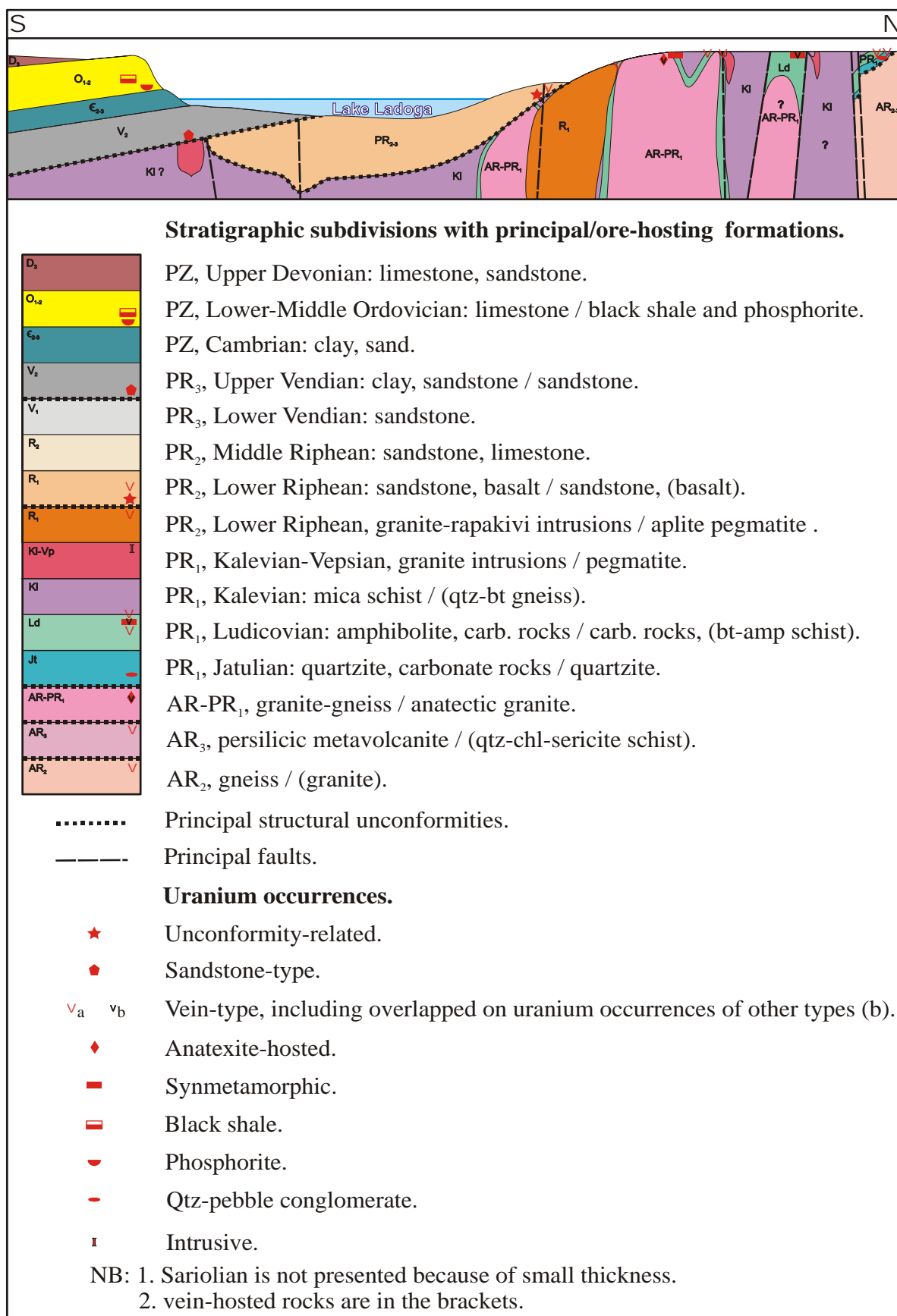


Figure 2.3. Schematic geological section and lithological column of the Ladoga region with position of the uranium occurrences.

IV. Evolution of uranium metallogenesis in the Ladoga region.

Previous and new age determinations of the Ladoga region U mineralization are compiled in the figure 2.4.

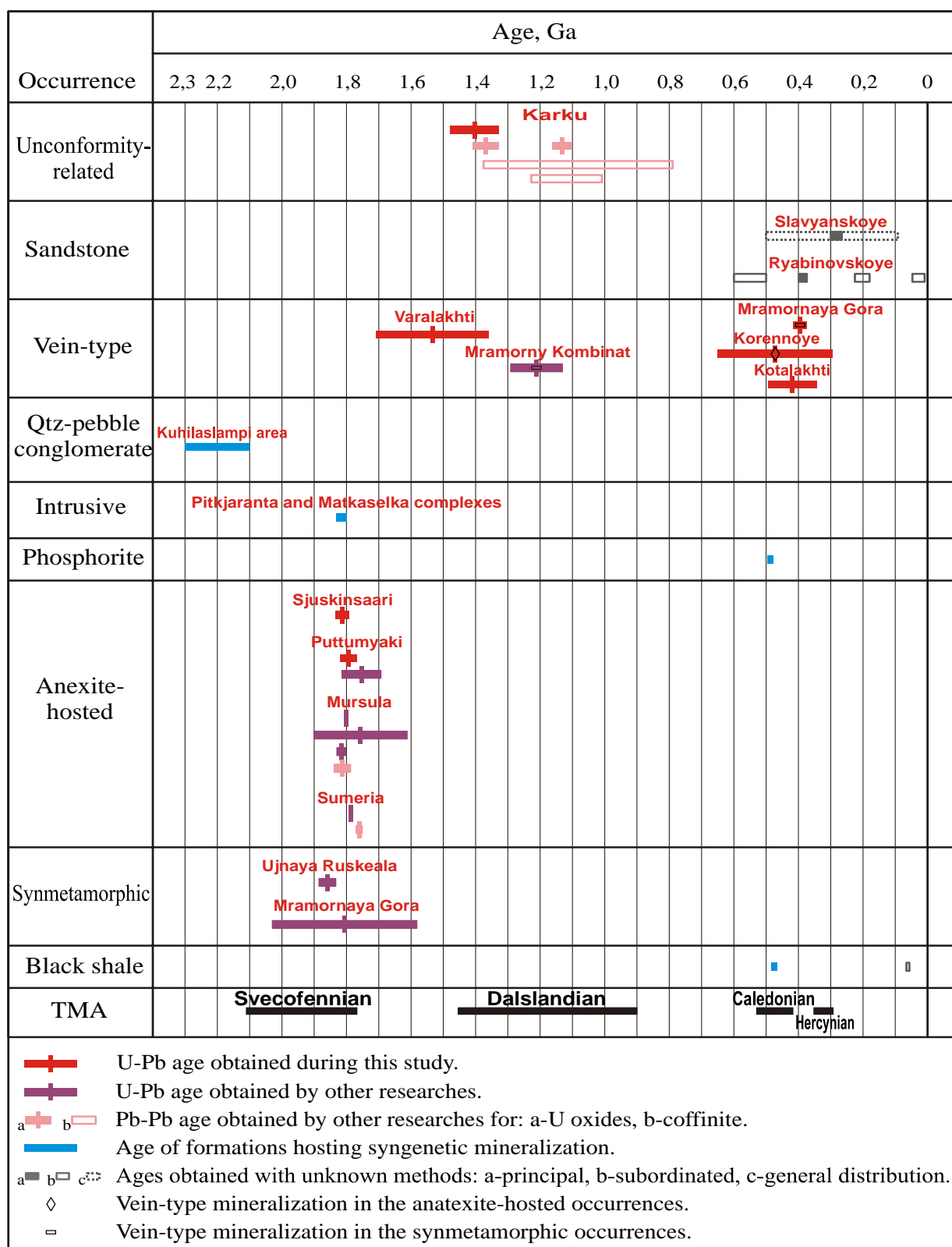


Figure 2.4. Ages of uranium mineralization discovered in the Ladoga region.

According to these data, three principal stages of U metallogensis can be distinguished in the Ladoga region.

I. Late Palaeoproterozoic (1.97-1.77 Ga):

- granite-hosted occurrences of anatexite-hosted and intrusive types;
- synmetamorphic occurrences in the Ludicovian carbonate rocks.

II. Lower-Middle Riphean (1.6-1.2 Ga):

- vein-type occurrences;
- unconformity-type occurrences and the Karku deposit;

III. Ordovician-Devonian (0.45-0.38 Ga):

- occurrences in the black shale;
- sandstone-type deposits and occurrences.

These stages in general correlate with the Svecofennian, Dalslandian (Sveconorwegian) and Caledonian-Hercynian activations. The last one probably can be subdivided into Caledonian and Hercynian stages in addition, but definitive conclusion is required for more accurate age constrains.

The Svecofennian event is characterized by a predominance of endogenic types of U enrichment in the Ladoga region. The most productive was the orogenic stage when intensive granitization and migmatization occurred. Synsedimentary U accumulation was subordinated that time, but redistribution some of these U concentrations (Ludicovian phosphorites) during regional metamorphism also significantly contribute to the basement-hosted U resource.

Lower-Middle Riphean Dalslandian activation corresponded to aborted intracratonic riftingogenesis in the Ladoga region. It was forestalled with anorogenic rapakivi intrusions which increased the U potential of the region. As a result, many hydrothermal U concentrations as vein-type mineralization and unconformity-related occurrences have been produced. Remarkable is the fact that two principal events of unconformity-related deposition are preceded by vein-type mineralization, although this assertion is still not sufficiently substantiated by available data.

Phanerozoic corresponds to a succession of transgressions and uplifts in the region. The most important tectonic activations were Caledonian and Hercynian. The Caledonian accretion finalized the structure of the Baltic Shield in general. During the Hercynian event numerous manifestations of intracratonic alkali magmatism occurred in different part of the Shield. These events produced diverse fracture-bound mineralization including vein-type U. Indications of

Palaeozoic hydrothermal U redistribution are widespread in the Ladoga region, where they often accompany early mineralization. But the principal U deposition occurred in the platform sediments preserved in southern part of the region. Ordovician black shales and phosphorite corresponds to synsedimentary U deposition deriving of U from exhumed areas of the Baltic Shield with precipitation in shallow marine environments. Sandstone-type mineralization was formed by leaching of U from basement formations (the late-Svecofennian leucogranites dominantly) and its deposition in the carbonaceous Upper Vendian sandstone. Thus, the leading ore-producing process of this epoch can be classified as exogenous.

Hence, each of these above-listed stages is characterized a specific U-producing process:

- Palaeoproterozoic (Svecofennian) stage – predominance of endogen U metallogenesis.
- Lower-Middle Riphean stage – hydrothermal U mineralization.
- Palaeozoic stage: most of U resources were produced by deriving of U from U-enriched bedrocks and have exogenous nature; hydrothermal redistribution contributes subordinately.

The U concentrations were affected suffered by supergene processes between these main stages. It led to an impoverishment of the ores and to formation of low-grade secondary mineralization.

A gradual increase of average U content through time in the geological formations of the Ladoga region has been demonstrated in the Part 1 of this thesis (see figure 1.16).

The resource of U occurrences of each type increases with time as well from low-grade Jatulian Th-U-bearing conglomerates anomalies to deposits hosted by Ordovician black shales with total resource over 100 thousands tons (fig. 2.5). But the ore grade evolution is different. U content in the ores increases and reaches its maximum in Riphean (up to 16.6 % of U in the in the unconformity-type Karku deposit). All occurrences of Palaeozoic age are characterized by low U content and it decreases theirs economic importance despite the large resources.

V. Grade and perspectives of the uranium occurrences.

As it was shown in the Conclusion to the Chapter 1, all discovered basement-hosted U occurrences are of uneconomic grade. Possibility of discovering of new economic deposits is also estimated negatively for most of these types:

- U-producing processes in granites are relatively weak in Northern Ladoga anatexite-hosted U occurrences;
- Precambrian synmetamorphic U-P mineralization has uneconomic grade as a type;
- U mineralization in the Jatulian conglomerates and Svecofennian intrusive granites is local and ranged as anomalies.

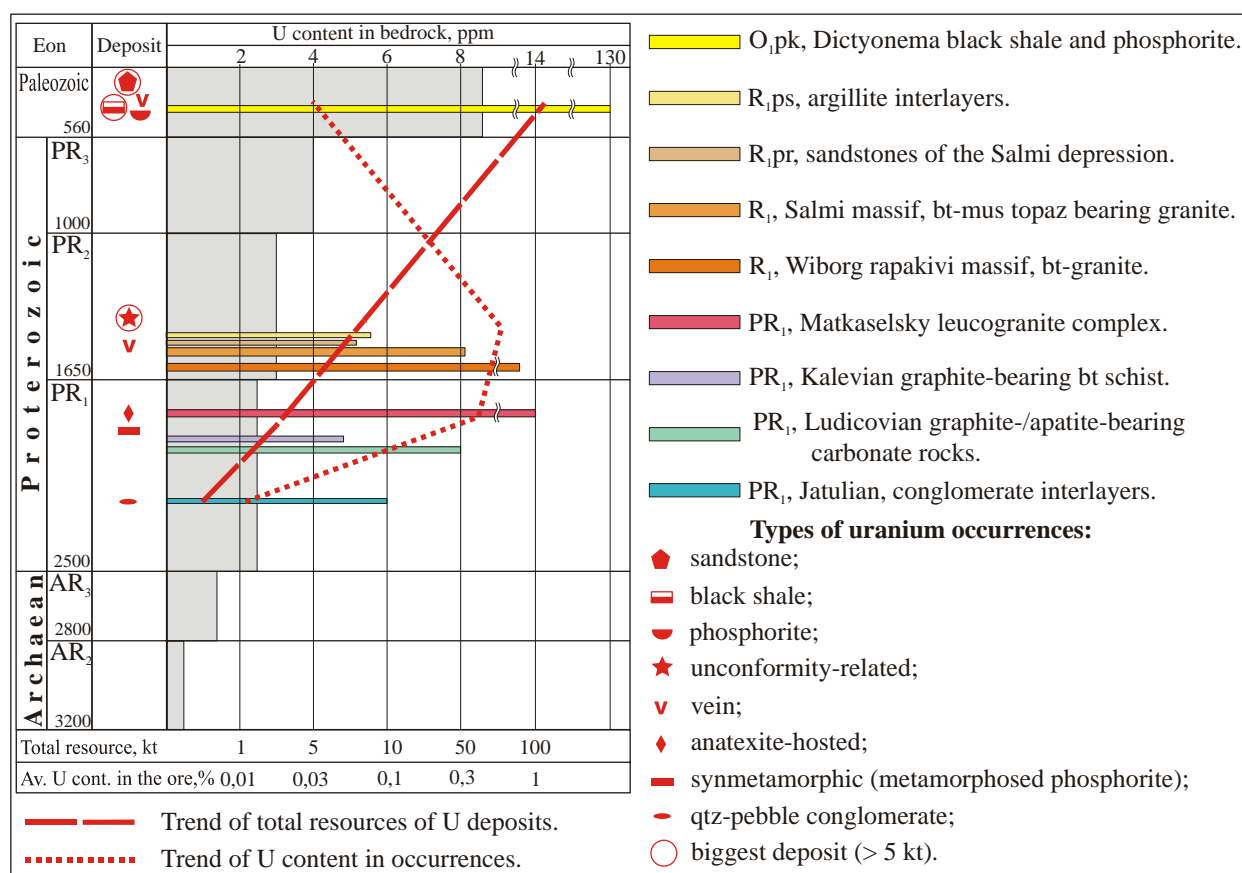


Figure 2.5. Evolution of uranium enrichment in the Ladoga region.

Among all basement-hosted U occurrences only the vein-type possibly has some economic potential. Evidences of hydrothermal U redistribution are widespread in the Northern Ladoga area and occur not only in the basement, but also in the Riphean formations of the Salmi depression. Abundance of U-enriched formations, numerous tectonic reactivations, diversity and prevalence of this type occurrences in the Ladoga region allow to hope for undiscovered deposits, although such possibility is not very high because of the many U exploration programs already carried out in the Ladoga region.

Unconformity-related mineralization is considered as the most interesting prospective target. This conclusion is based on some similarities between the Pasha-Ladoga and the Athabasca basins. The discovery of the Karku unconformity-type deposit made this opinion better grounded.

Detailed studies of the Karku deposit revealed significant differences with the world-known unconformity-type U deposits explaining relatively low grade of the first one. It and failure of all others prospects in different parts of the Pasha-Ladoga basin decrease the prospect for discovery of unconformity type U deposits in the Ladoga region. Nevertheless, for final conclusion additional researches should be undertaken. Also a subunconformity type U occurrence (basement-hosted unconformity-type deposits) could be expected below and in vicinity of the Pasha-Ladoga basin, but presently no indications for such kind mineralization have been found.

Sandstone-type is represented by three small-medium grade deposits and numerous ore-showings located in the Southern Ladoga area. Low U contents, environmental problems (vicinity of the St Petersburg agglomeration and Lake Ladoga) and technologic difficulties (low permeability of the ore-hosting sandstone and big depth) make them uneconomic at the moment, but definitive evaluation of this type requires additional exploration.

Ordovician phosphorites of the south-western part of the region are ranged as low-grade anomalies only.

Black shales hosted low-grade mineralization presently considered below the economic conditions. Because of this and environmental difficulties in addition, perspectives of Ladoga region Ordovician Dictyonema shales is estimated as negative.

There are no indications of other types of U deposits in the Ladoga region.

Thus, according to their decreasing economic importance, U occurrences of the Ladoga region can be ranged in the following order:

1. Unconformity-type;
2. Sandstone-type;
3. Vein-type;

-
4. Black shales;
 5. Anatexite-hosted;
 6. Synmetamorphic;
-

7. Intrusive;
8. Phosphorite;
9. Quartz-pebble conglomerate.

The three first types have potential economic importance; unconformity-type and sandstone-type are represented by known deposits, whereas the discovered vein-type occurrences are ranged as ore-showings or anomalies only.

Types 4 to 6 include uneconomic deposits (black shales) and ore-showings considered as not corresponding to actual economic conditions and having no perspectives in the Ladoga region.

The last three types are represented by low-grade anomalies without economic importance and perspectives.

Areas of the Ladoga region suggested as promising for the discovery of economic-grade deposits are indicated in the Part 3 of this thesis.

PART 3

URANIUM PROSPECTS OF THE

LADOGA REGION

PART 3. URANIUM PROSPECTS OF THE LADOGA REGION.

Introduction.

Inference of Part 2 is that only three types of uranium occurrences have some potential economic interest in the Ladoga region:

- I. Unconformity-type;
- II. Sandstone-type;
- III. Vein-type.

Part 3 introduces an attempt to indicate the areas which are the most promising for occurrences of these types.

For more efficiency ore-exploration projects should be forestalled and accompanied by distinguishing three principal factors:

1. possible source of ore element;
2. indication of the presence of an agent responsible for its extraction and transport;
3. possible trap for ore deposition.

Although the factors are often different for uranium deposits of different types, some parallelism can be found.

1. Uranium source.

Uranium-bearing bedrocks including previous syngenetic-epigenetic ore occurrences represent potential sources for uranium deposits. The major role of granites (especially potassic leucogranites) is suggested and abundance of granites in a region is very positive factor.

1.1. Uraniferous granites.

According to deep gravimetric data, the lithosphere of the Ladoga region is generally characterized by a quite high density indicating a small thickness of the granite layer. This feature is negative for uranium abundance.

Granites of the Ladoga region are represented by the Svecofennian intrusive and anatectic granites, and Lower Riphean rapakivi anorogenic intrusions. This differentiates the Raahe-Ladoga from the Svecofennian domains.

Late Svecofennian leucogranites are non uniformly distributed in the Raahe-Ladoga domain. The higher abundance occurs in the Impilakhti-Pitkjaranta block (the Pitkjaranta complex and anatexites of the domes), the north-eastern envelop of the Ruskeala anticline (Matkaselka complex and Pirtipohja pegmatite swarm) and the Latvasurje area (Latvasurje complex and anatexites of the domes). All these granites are U-enriched; U content in anatexites of the domes in the Impilakhti-Pitkjaranta block reaches economic grade (> 500 ppm) and occur in relatively mobile form: U oxides and silicates.

In the Svecofennian domain PR₁ granites (especially the Priozersk block) are more abundant, but of the Western Ladoga ones (the Kuznechensky, Borodinsky, Tervusky and Putsaarsky complexes) are relatively poor in U (2.1 ppm in average). U-enriched granite massifs are supposed to occur in the Southern block of the Svecofennian domain (Chaplinsky and Polyansky complexes), but their geochemical characteristics are not well known. A correlation between late Svecofennian granites of the Ladoga region and the uraniferous granites of the Southern Finland Migmatite Belt is very important for uranium potential prediction.

Rapakivi intrusions occur in both domains. There is no significant uranium occurrences related to the rapakivi granites in the Ladoga region but low-grade anomalies represented by refractory radioactive accessories and role of these rocks as a uranium source is not well identified. Two features indicate their importance as a source:

- there are several vein type uranium occurrences surrounding the most U enriched northern part of the Salmi rapakivi massif;
- Riphean sandstones of the Salmi depression partly underlain by the Salmi granites are the most enriched formation of the Pasha-Ladoga basin.

1.2. Other potential uranium-source lithologies.

Lower Ordovician Dictyonema shale is the most enriched in syngenetic U concentration from all other geological formations of the Ladoga region (130 ppm U in average). Although uranium in this rock occur mostly in mobile status, its transport is difficult due to strong reducing environment in the black shales. Also importance of the shale as a possible uranium source for other deposits is essentially limited by its late deposition – most of geodynamic processes in the Ladoga region had been terminated to the Phanerozoic. Although some indications of late epigenetic uranium redistribution have been discovered in the shales

(Mikhailov et al., 2006), there are no proves that this process was sufficient for formation of economic ores.

Uranium background in other rocks is much lower. The most prominent of them are the Ludicovian graphite-/apatite-bearing carbonate rocks (8 ppm of uranium in average). Uranium in this rock mainly occurs as proper U mineral phases (uraninite at first) or is included into apatite. It could be remobilized by hydrothermal fluids.

The Kalevian graphite- and sulphide-bearing micaschist have increased uranium contents and the proportion of mobile uranium is high – up to 50 % (Mikhailov et al., 1999).

Some of Riphean sediments of the Pasha-Ladoga basin have increased uranium content: with up to 5.6 ppm in the Pasha suite argillites. The Priozersk suite sandstones and gritstones in the Salmi depression are the uranium enriched as well –with 5.2 ppm on average.

Grade of metamorphism of the basement formations has to be considered for general estimation of uranium potential of different parts of the Ladoga region, because increasing of the metamorphism leads to depletion in uranium.

As described in the Regional geological review (Part 1), metamorphism varies from greenschist to upper amphibolite facies in the Raahe-Ladoga domain. This is favorable for uranium enrichment and presence of numerous uranium occurrences along this zone is an additional confirmation of it.

The Svecofennian domain formations are more metamorphosed in comparison with the Raahe-Ladoga one. The highest grade of the metamorphism (granulite facies) occurs in the Lahdenpokhya-Hiitola block. It is the less favorable area with respect to uranium mineralization; a unique low grade anomaly has been discovered at its border with the Priozersk block.

Metamorphic grade decreases southward and corresponds to medium-high amphibolite facies in the Southern block. There are many uranium occurrences in the platform cover of that area.

1.3. Uranium occurrences.

As described above, uranium ore occurrences have been discovered in different parts of the Ladoga region at different stratigraphic levels. Basement-hosted mineralization of the Northern Ladoga part of the Raahe-Ladoga domain has mostly a Palaeoproterozoic age and uranium from these occurrences could be remobilized by later reactivations or by exhumation and erosion. After the Svecofennian event when they had been formed, the Riphean event is the

most significant one when the unconformity-related mineralization of the Salmi depression was produced. Despite prominent uranium resource of platform cover occurrences, they can not be considered as a uranium source, because no significant uranium redistribution can be expected in quiescent environment as it was in the Ladoga region after the Caledonian and Hercynian events.

2. Extraction and transport.

Processes of uranium mobilization are indicated by specific alterations of source rocks or/and formations hosting transport channels. Type of alteration depends on the type of mineralization and will be considered in the corresponding paragraphs. In the most common cases extraction and transport of uranium occur in oxidizing environments.

Greisenisation is considered as an alteration favorable for uranium leaching from granites (Mikhailov et al., 1999). It is widespread in the Ladoga region. This process is especially intense in the Southern Ladoga Svecofennian leucogranites underlying Upper Vendian sediments that host sandstone-type occurrences. Also a remarkable greisenisation occurs under Riphean sandstones in the southern part of the Salmi depression. Greisens may have existed in presently eroded part of granites.

Fault zones are very important channels for uranium-bearing fluids and hydrothermal alterations along the faults are positive indications. Many and diverse alterations (oxidation, chloritization, albitization) have been discovered in the Northern Ladoga area of the Raahe-Ladoga zone, whereas they are not common for the outcropping part of the Svecofennian domain in the Western Ladoga; the Southern Ladoga area is concealed under Quaternary and not studied in this respect. Numerous manifestations of hydrothermal uranium redistribution related to faults occur also in the Northern Ladoga area. The most prominent in this respect are the Ruskeala and Janisjarvi fault zones. A unique and tentative indication of uranium redistribution along a fault was described in the Polyany area of the Ryabinovskoye sandstone-type deposit hosted by the Upper Vendian sediments.

Besides, retrograde metamorphism occurring along the fault zones may lead to uranium enrichment. Such zones are described in the outcropping part of the Svecofennian domain, but increased uranium content has not been observed.

3. Trap.

Generally, precipitation of uranium is caused by its reduction from the mobile hexavalent state to the stable tetravalent state. It may be also caused by drastic changing of pH or/and P-T conditions. They can be related to specific alterations of ore-hosting rocks and differ for the different types of U mineralization.

The most common uranium reductants are carbonaceous matter (in different state – plant debris, bitumen, graphite, gases etc) and sulphides. Carbon- and sulphide-enriched formations are very widespread in the Raahe-Ladoga basement (Ludicovian carbonate rocks, Kalevian mica schists). Graphite-bearing gneisses have been discovered by drilling in the Southern block of the Svecofennian domain. In the Vyborg, Priozersk and Isojarvi blocks of the Svecofennian domain neither significant graphite nor sulphide enrichments are known. A unique graphite ore-showing occurs in the northern part of the Lahdenpokhya block, in the vicinity of its border with the Raahe-Ladoga zone.

Drastic changes of P-T conditions may be produced by penetration of uranium-bearing fluids from massive to porous environment (from metamorphic basement to sandstone for example) or by tectonic opening of a fracture space often accompanied by brecciation of the host rocks.

Permeable rocks overlaying massive basement formations in the Ladoga region are represented by the Riphean and Vendian clastic sediments. They will be considered below in corresponding items.

Breccias zones and open fractures (sometimes with uranium mineralization) are widespread in the basement of the Northern Ladoga area. In the basement of the Svecofennian domain and in the platform cover they are not common.

Conclusion:

The Raahe-Ladoga domain has the most significant potential for the discovery of uranium ore mineralization in the Ladoga region. The Southern block of the Svecofennian domain is also promising. Western and north-western parts of the Svecofennian domain are not prospective.

1. Unconformity type.

1.1. Unconformity-type exploration criteria applied to the Ladoga region.

The Pasha-Ladoga depression is the largest preserved basin of Mesoproterozoic sedimentation in the Baltic Shield. It is considered as an analog of the Athabasca basin, hosting numerous large unconformity-type uranium deposits (fig. 3.1). The surrounding zone where the depth of erosion from the Riphean unconformity is presumed to be less than 200 m can be proposed as areas for possible occurrence of basement-hosted subunconformity-type deposits (General Appendix, fig. 1.2, 2.2, 3.2).

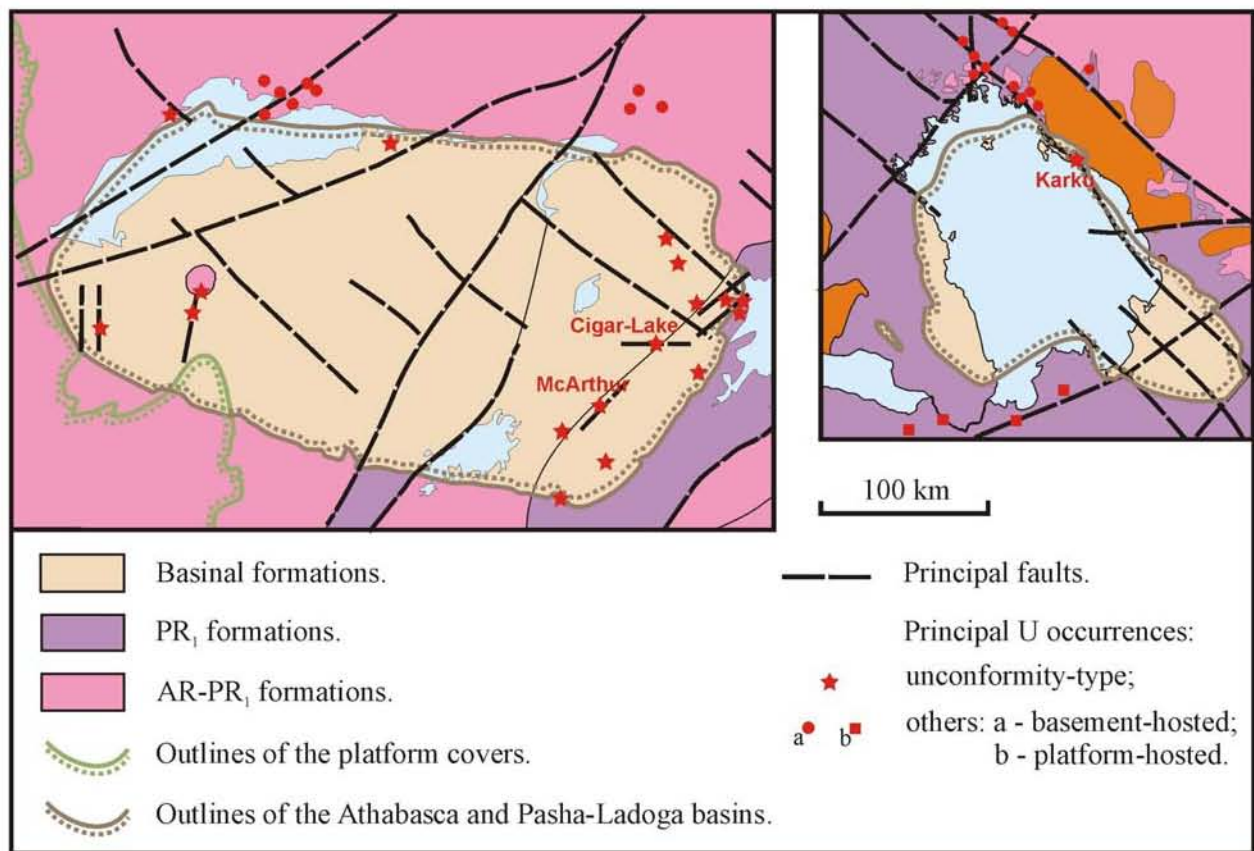


Figure 3.1. Geological maps of the Athabasca and Ladoga regions at the same scale.

A set of exploration criteria has been proposed for the unconformity-type deposits (Dahlkamp, 1993; McMillan, 1998; Cuney, 2005; Jefferson et al., 2007). Below they are considered with reference to peculiarities of the Ladoga region.

1. *Unconformity between metamorphosed AR-PR₁ basement and non-metamorphosed oxidized U-depleted quartz-dominated terrigenous strata of an intracratonic basin of late PR₁ – early PR₂ age.*

The Pasha-Ladoga basin is featured as a Mesoproterozoic intracratonic depression filled with non-metamorphosed formations and unconformably overlaying Neoarchaean-Palaeoproterozoic crystalline basement and in minor PR₂ (Lower Riphean) rapakivi-granite complexes. Unfortunately, now a major part of the basin is under the waters of the Lake Ladoga, but three onshore occurrences of Riphean sediments exist (Salmi, Priozersk and Pasha). In addition, there are two other Riphean basins (Simagino and Uljya-Risti) indicating wider extension of area where the post-Riphean erosion was not very deep.

The basinal sequence comprises siliciclastic terrigenous sediments and sub-alkaline mafic effusive interbeds (basalts).

Compared with the Athabasca basin sandstones, those of the Pasha-Ladoga basin are less oxidized and have immature essentially feldspar composition. Age of the sedimentation in the Pasha-Ladoga basin is not more than 1.47 Ga, where as one for the Athabasca group is ranged in 1.7-1.65 Ga (Cumming et al., 1987). Also above mentioned lithological features of the Pasha-Ladoga basin are considered as an indication of low reactivity of basinal brines, hence lower leaching of U from refractory accessories.

Presence of basalts in the Pasha-Ladoga sequence is considered as a negative factor, because they limit the volume of permeable sediments available for the “free convection” and leaching of uranium. Also the mafic composition of the volcanites decreases the oxidation potential of the basinal brine – a principal transport agent of uranium in classical unconformity-related deposits (Michel Cuney, personal comment). It is notable that that the basalts are absent in the Priozersk depression (Western Ladoga) and it can be considered as a positive feature from this point of view.

2. Basement is composed of Archaean continental crust formations reworked during the Svecofennian orogeny and Palaeoproterozoic syncline formations; Palaeoproterozoic mobile belts comprising the Archaean-Palaeoproterozoic domes enveloped with Palaeoproterozoic formations are the most favorable.

Generally the basement of the Pasha-Ladoga basin consists of two domains of different structure.

The Raahe-Ladoga domain has heterogenic AR-PR₁ composition. AR-PR₁ granite-gneiss domes are enveloped by PR₁ Svecofennian formations. In this respect the Raahe-Ladoga domain is similar to the Wollastone belt hosting or underlying the largest unconformity-related deposits in the Athabasca basin.

It is necessary to emphasize that the presence of the Archaean continental lithosphere under the Palaeoproterozoic crystalline formations as it is supposed in the Wollastone domain is presumed in the Raahe-Ladoga domain as well. Indications of contaminations of located in the Raahe-Ladoga domain Svecofennian potassic leucogranites, Lower Riphean Salmi rapakivi-granites and the Lower-Middle Riphean Vallaam dolerite by Archaean material have been identified by isotopic methods (Rämö, 1991 and 2001; Amantov et al., 1996; Laura Lauri, personal comment).

Juvenile crust in the Svecofennian domain was formed during PR₁ Svecofennian orogeny. Archaean isotopic age for the rocks of the domain has been obtained neither in the Ladoga region nor in Finland.

As it was noticed before, a reduced thickness of the granite layer in the crust sequence as in the Raahe-Ladoga as Svecofennian domains has been revealed by deep geophysics. It is a negative feature, especially in comparison with the intensively granitized cratonic crust of the Athabasca area.

3. Regional metamorphism of basement rocks up to amphibolite grade, locally – up to granulite grade facies; areas of low prograde (up to intermediate amphibolite facies) or retrograde metamorphism are favorable.

The Raahe-Ladoga domain is characterized by zoning metamorphic of the basement. Metamorphism grade increases from greenschist facies at the border with the Karelian domain to upper amphibolite subfacies at its contact with the Svecofennian domain.

Regional metamorphism of the Svecofennian domain is high and corresponds to granulite facies at its northern part (Lahdenpokhya-Hiitola subdomain and northern part of the Priozersk block of the Petersburg subdomain) and upper amphibolite subfacies at its southern part. The precise metamorphic grade of the basement of the southernmost part of the region has not been characterized because of its coverage with thick platform sequence.

4. Abundance of U-enriched granite intrusions and migmatites.

As mentioned above, leucogranites of the Western Ladoga part of the Svecofennian domain have low uranium content. Uranium-enriched Palaeoproterozoic granites occur in the Raahe-Ladoga zone and the Southern block of the Svecofennian domain.

Uranium-enriched phases of the rapakivi granite massifs are located in the northern part of the Salmi massif (eastern part of the Northern Ladoga area) and in western part of the Wiborg massif.

5. Uranium-enriched metamorphic basement formations are favorable.

The most uranium-enriched metamorphic basement rocks are Ludicovian phosphorous graphite-bearing carbonate rocks and the Kalevian graphite-bearing micaschists. They occur along the Raahe-Ladoga zone and have not been characterized in the Svecofennian domain where contemporary metaterrigenous formations are poor in uranium.

6. Fault zones associated with metasomatic alterations; indications of uranium redistribution along the faults are favorable.

Diverse metasomatic alterations (including albitization and hydrothermal uranium mineralization) associated with brittle dislocations are widespread in the Northern Ladoga part of the Raahe-Ladoga domain, but they are uncommon in the outcropping parts of the Svecofennian domain. The southern part of the Ladoga region is concealed under the V-PZ cover and the fault zone are not available for observation.

7. Uranium occurrences referred to previous epochs.

Other types of uranium occurrences prior to the Riphean unconformity-related uranium minerogenesis are known in the Northern Ladoga part of the Raahe-Ladoga domain only. They are numerous and diverse, but all are of small grade and less rich than ones of the Athabasca basin area where intrusive- and vein-type deposits occur.

8. Graphite-sulphide enriched metasediments (“conductors” or “reducers”).

Graphite-sulphide enriched formations are present in the Paleoproterozoic sequence of the Raahe-Ladoga domain.

In the Svecofennian domain graphite-enriched basement rocks are discovered in the Southern block only. The graphite content is always low (less than 1 %). Zones of conductivity distinguished by geophysics (General Appendix, fig. 3.2) are not associated with graphite enrichment.

Graphite-sulphide enriched formations are widespread in the Paleoproterozoic sequence of the Raahe-Ladoga domain. However it is noted that the zones of graphite enrichment in the

basement of the Athabasca are more intensive and contrast with surrounding graphite depleted metamorphic bedrocks (Claude Caillat personal comment). In application of the “free convection” model, dispersed graphite reductants in the basement could be even a negative factor impeding circulation of uranium-bearing oxidized brines (Michel Cuney personal comment).

9. Pervasive pre-ore alterations of basinal sediments and upper part of the basement.

The Pasha-Ladoga basin sediments in general are less oxidized in comparison with the Athabasca basin ones. Diagenetic silicification is lower. Diagenetic clayey alterations are widespread, but represented by dominantly by kaolinite, whereas its higher crystallinity polymorph dickite typical for the Athabasca basin in the Pasha-Ladoga is referred to pre-ore alteration.

The regolith alterations (“red” oxidized upper and “greenish” reduced lower zones in upper part of the basement) are not common for the Pasha-Ladoga basin. A unique regolith-like profile was discovered by one recent drill hole in the north-eastern flank of the Pasha graben (the Svir block, Svir-Oyat area).

Regional disturbance of Th-U ratio in the basinal sandstone with tendency of uranium depletion ($\text{Th/U} > 4$) is considered as an indirect indication of convection of uranium leaching brines (Michel Cuney personal comment). The Pasha-Ladoga basin sandstones are characterized by lower Th-U ratio in comparison with those of the Athabasca and Kombolgie groups. The low maturity of the sandstones and low alteration of accessory monazite and zircon in the Pasha-Ladoga and other Riphean (Jotnian) basins of the Baltic Shield had been shown in research of Lobaev (2005) and Ibrahim (2007) is considered as an evidence of a lower reactivity of the uranium-leaching brines, i.e. a lower effectiveness of the ore-producing process.

10. Intensive alteration of uranium ore-hosting basinal sediments and basement rocks associated with the principal ore-producing event and indicated by the development of a Mg-Al clay mineral association (illite and sudoite at first), then by turmalinization (dravite), sulphidization and silicification.

As shown in the Chapter 2, uranium ore mineralization of the sole unconformity-related Karku deposit in the Pasha-Ladoga basin is associated with alterations represented by calcite, sulphides, chlorite and silicification. Intensity of the alterations is relatively moderate. The chlorite is mostly a Fe-rich one; Mg chlorite is much subordinated and occurs only in the high-

grade mineralized ore zones. B enrichment has been evidenced neither by mineralogical nor geochemical methods.

In other parts of the Pasha-Ladoga basin such kinds of alterations have not been discovered. Local and weak disturbance of the synsedimentary geochemical association of U with petrogenic (Si, Al, Ca, Ti, Mn) and trace (Th, Nb, Zr, Sn) elements has been revealed at the north-eastern flank of the Pasha graben (the Svir block, Svir-Oyat area).

Table. 3.1. Applications of unconformity-type deposits exploration criteria to the different part of the Ladoga region.

Criteria	Northern Ladoga	South-Eastern Ladoga		Western Ladoga
		Svir block	Southern block	
1. Unconformity	++	++	++	+++
2. Orogenic belt with AR-PR ₁ basement	+++	+++	-	-
3. Metamorphism grade	+++	+++	++	-/+
4. U-bearing granitization	++	++	+++	+
5. U-enriched metamorphic basement	+++	+++?	+?	-
6. Graphite-sulphide basement rocks	+++	+++	++	-
7. Previous U occurrences	+++	-	-	-
8. Fault zones with alterations	+++	-	-	-
9. Pre-ore alterations	++	++	-	-
10. U-associated alterations	+++	+	-	-
Discovered unconformity-related U mineralization	+++	+	-	-/+
Grade of studying of the unconformity	Locally detail; generally – rare profiles	Rare profiles	Not studied	Few drillholes
Total rating	++	+	+?	-

Thus, general estimation of the Ladoga region prospects for unconformity-type deposits is not very optimistic. The Pasha-Ladoga basin is inferior to the Athabasca basin in many respects. Nevertheless prospects of the Pasha-Ladoga basin for unconformity-type deposits have not been finally defined, it demands additional explorations. The most promising areas are considered below.

1.2. Prospects.

1.2.1. The Raahe-Ladoga zone.

The area related to the Raahe-Ladoga zone is suggested as the most preferable. Three promising areas are proposed (General Appendix, fig. 1.2).

1) The Pitkjaranta area.

It is characterized by specific for the Northern Ladoga structure of the basement with ultrametamorphic granite-gneiss domes enveloped by PR₁ formations metamorphosed in medium facies of amphibolite grade. Abundance of graphite-bearing crystalline rocks and uranium-enriched late-Svecofennian pegmatites are positive features. In addition, the PR₁ basement is intruded by the Salmi rapakivi massif. Uranium-enriched late phases of the intrusion occur in the depth from several hundred meters to 2 kilometers in the Pitkjaranta area. Few veined uranium occurrences are located in vicinity of the area (the Pitkjaranta and Hopunvaara ore-showings).

Negative factors are:

- very locally preserved Riphean sediments (small Ulja-Risti depression);
- location in the vicinity of the Ladoga lake where environmental constraints are very important;
- the Pitkjaranta city suburbs are located in the northern part of the area, the population density is quite high and that limit possibilities for the exploration.

General estimation of the area is moderately positive. Unconformity-type mineralization is possible (especially basement-hosted), but the resource of the area is limited by environmental constrains and large-tonnage deposits are not expected. As exploration methods, profile drilling forestalled and accompanied by surface geophysics are suggested.

2) The Salmi area.

The area is related to the Salmi depression and includes the Karku deposit described in the Chapter 2. Despite representing of the best studied area with the unconformity in comparison with other parts of the Ladoga region, the U resource prospect of this territory is not definitively assessed. As a special target, basement-hosted unconformity-type mineralization can be proposed. It has not been well studied and few discovered occurrences deserve special attention (northern edge of the Central Block, southern part of the Ore body 3).

In general, resource prospects of the area seem not very optimistic to the moment. Negative factors revealed when comparing of the Karku deposit with classical unconformity-type deposits decrease the attractiveness of this territory and large-tonnage deposits are not expected. In additional, favorable and unstudied areas available for further exploration are quite limited here.

In the Karku area an increase of the density of the drilling pattern should be undertaken for more precise evaluation of the deposit. Deeper drilling for discovering sub-unconformity deposits should be undertaken locally. Fault zones at the southern limit of the Central Block would need more detail studies as well. In other parts of the Salmi depression preliminary surface geophysics and profile drilling should be carried out.

3) The Svir-Oyat area.

The Svir-Oyat area (or Shotkusa) geological structure has significant resemblance with the Salmi depression. The area is also located on the continuation of the uraniumiferous Ruskeala zone. The basement belongs to the Raahe-Ladoga zone and contains granite-gneiss domes mantled by the Ludicovian-Kalevian formations Graphite-bearing schists and late-Svecofennian leucogranites with increased uranium content occur. Large Rapakivi intrusions have been discovered to the north and the large Oyat rapakivi-granite pluton is presumed to exist to the south. A difference with the Salmi depression is that the rapakivi granites do not underlay the basement and Riphean sequence in the Svir-Oyat area. Also the Riphean sediments are covered with quite thick (few hundred meters) V-PZ sequence in this area and it can provide a better preservation of possible ore deposits. On other hand it makes exploration more difficult in the area, because the abilities of geophysics are reduced and drilling is deeper and more expensive.

Presently the Svir-Oyat area is considered as the most promising for economic-grade unconformity-type mineralization in the Ladoga region. The potential of the territory is limited because of the steep dipping of the unconformity surface.

As this area was preliminary studied and the position of the unconformity and basement conductors have been well localized, detail drilling can start in the most interesting zones. Preliminary and accompanying surface geophysics should be undertaken as well.

1.2.2. The Svecofennian domain.

As it was demonstrated before, the Svecofennian domain is considered as less interesting with respect to the occurrence of Precambrian uranium mineralization in general, but a definitive conclusion cannot be given because of lower level of studying of the Precambrian sequence in the territory. It differs for different areas. So, the Riphean unconformity has been reached only by a few drillholes in northern part of the Priozersk depression. That is why a proposition of prospective areas is quite speculative here. A general review of occurrences of the Riphean sediments referred in the Svecofennian domain to evaluate the areas the most interesting for uranium mineralization is presented below (see also General Appendix, fig. 2.1 and 3.1).

1) The Priozersk depression.

Despite of its large size and relatively shallow depth, the Priozersk depression is traditionally considered as the least prospective area for unconformity-related deposits (Skorospelkin 2002). It is caused by above described peculiarities of the basement as its high metamorphism grade, the lack of graphite, low uranium abundance in the bedrocks, absence of significant uranium occurrences etc.

The Riphean sequence of the Priozersk depression is devoid of effusive interlayers, and if we accept the oxidized brine convection as a principal ore-producing process, it can be considered as a positive factor.

Uranium content in the basal sandstones (the Priozersk suite) is lower than in other parts of the Pasha-Ladoga basin and it can be considered either as negative (lack of uranium source), or as positive (indication of uranium leaching) factor. The geochemistry of these rocks has not been studied sufficiently to adopt one or another opinion.

There are two territories, proposed by “Nevskgeologia” as the most prospective for the discovery of unconformity-type deposit.

– *The Otradnensko-Vaskelovskaya area*, because of the presence of conductive zones in the basement detected by geophysics. But no graphite-rich structures have been discovered in this zone at the moment. Just a few drillholes have crossed the unconformity in this area. No ore-accompanying alterations (chloritization, carbonatization etc) have been discovered. Only very low-grade anomaly (less 100 ppm of uranium) has been found.

– *The Irinovskaya area* is suggested due to a surface radioactive anomaly revealed by the airborne survey. The nature of the anomaly had not been determined, but its possible relation to the unconformity seems to be too tentative, because the Riphean sediments are concealed

under about 100 m thick Upper Vendian cover and over 10 meters of the Quaternary in addition. I think that this anomaly can be referred to an anthropogenic pollution because it is located in a harbor area. The Riphean sediment sequence and even the outline of their occurrence have not been studied in this area.

An additional negative factor of the Priozersk depression is the presence of numerous military objects in this area that makes exploration in this area very difficult.

Because the Priozersk depression is badly studied, the prospecting works should start with airborne survey for the general localization of the most promising areas. Subsequent surface geophysics and drilling in smaller areas has to define the particularities of the Riphean and the basement sequence there. Mineralogical, petrologic and geochemical study should be undertaken simultaneously.

2) The Simagino depression.

As mentioned above, this depression was weakly studied. Its exact extension is unknown. Few drillholes reach the pre-Vendian sediments supposed to belong the Hoagland suite of the Lower Riphean. The unconformity was never intersected. The basement is supposed to be similar to that of the southern part of the Priozersk depression and composed of Kalevian gneisses metamorphosed in upper amphibolite facies and late-Svecofennian granites. The depression result from NW striking normal faulting. Prospects of this depression cannot be estimated because of the lack of information. Any exploration work there should be preceded by reconnaissance exploration including surface geophysics and drilling to precise the limits of the depression, the petrologic and geochemical characteristic of the Riphean and basement.

3) South-western part of the Pasha graben.

This area is supposed to belong to the Southern part of the Svecofennian domain, but some authors refer it to the Raahe-Ladoga zone (Skorospelkin, 2002). It is still not defined because the basement and the Riphean Pasha graben is totally covered by the Vendian-Paleozoic (V-PZ) sediments in that area. The basement and upper part of the Riphean sequence in the Southern Ladoga have been recognized by numerous drill holes during exploration of the Vendian-hosted sandstone-type uranium deposits. Zones of graphite-enrichment in Paleoproterozoic metapelites have been discovered. There are numerous U-enriched late-Svecofennian leucogranites (Polyansky and Chaplinsky complexes) possibly similar to some of

the Southern Finland Migmatite Belt. NE-striking faults referred to the Baltic-Mezen belt occur. The Pasha graben is limited by NW-striking faults.

The western part of the graben represents an area for the possible occurrence of unconformity-related U deposits (*the Novoladogskaya area*). Unfortunately, the Riphean unconformity has not been reached here and there are no data on the composition of the basal sediments. Geophysical data indicate a steep dipping of the unconformity surface. Prospects of this area are uncertain because of the lack of information. The relatively low grade of metamorphism in the basement, the multiplicity of fault zones, the presence of graphite-bearing rocks and uranium-rich granites are estimated as positive factors and this area may represent one of the most promising ones in the Svecofennian domain.

Possible exploration problems in this area are mainly connected with the depth of the unconformity (> 300 m). Clayey and water aquifer Upper Vendian layers reduce geophysics efficiency. For this reason drilling is the top priority exploration tool in this area.

2. Sandstone-type.

2.1. Sandstone-type exploration criteria applied to the Ladoga region.

Sandstone-type (tabular subtype) uranium deposits were discovered only in the Upper Vendian Redkinsky horizon sandstones – the basal layer of the platform cover.

The subsequent discussion introduces generalized exploration guides for the tabular subtype sandstone-type uranium occurrences (De Vivo et al., 1988 and Dahlkamp, 1993) applied to different part of the Ladoga region.

1. Intracratonic or pericratonic basins of terrigenous or shallow marine sedimentation; they are filled with immature permeable feldspatic or arkosic, more rarely quartzose and cherty sandstone, pebble conglomerates and siltstone; interbeds of impermeable mudstone horizons is common. Fluvial arkosic sandstones with limited thickness (<10 m) interbedded with less permeable rocks deposited in an intracratonic environment are the most favorable.

Upper Vendian sediments lay at the base of the Eastern Europe platform. Uranium ore-hosting basal sandstone, gritstone and conglomerate have quartz-feldspar composition. The thickness of the permeable basal sandstone horizon is up to 4.5 m and it is limited by dense basement formations and overlaying clays.

2. Adjacent or/and ore-hosting formations with increased uranium content can serve as an uranium source; presence of felsic volcanites in the ore-hosting sequence is favorable.

Uraniferous late-Svecofennian leucogranites underlay Upper Vendian sediments. Rapakivi granite massifs partly underlay the sediments as well and outcrop laterally. Upper Vendian sediments have derived from the granitic basement of the Baltic Shield.

All Vendian-hosted uranium deposits of the Southern Ladoga area are related to uraniumiferous late-Svecofennian leucogranites of the Polyansky and Chaplinsky complexes. In other sites only ore-showings and anomalies occur and no uranium occurrences have been discovered above the Riphean formation of the Pasha graben (relatively poor in uranium).

Although the Lower Ordovician black shales and phosphorite are enriched in mobile uranium, they occur above the Vendian sediments and the possibility of downward percolation of uranium from these rocks is limited by several clayey horizons in the Cambrian and Upper Vendian sequence.

3. Alterations of host and adjacent formations indicating the uranium leaching.

A bedded oxidation is widespread in the Redkino horizon sandstones and indicates an oxidized environment favorable for uranium leaching and transport.

Intensive greisenisation of the leucogranites has been discovered in the Southern Ladoga area. According to Mikhailov et al. (1999) it could contribute to uranium mobilization.

4. Abundance of uranium precipitants/reductants (particularly carbonaceous material and/or sulphides) in the ore-hosting sediments.

Concentration of reductants as plant remnants and sulphides are widespread in the Redkino horizon sediments and uranium mineralization is definitely referred to them.

2.2. Prospects.

Large amount of exploration works have been carried out by “Nevskgeologia” in the Southern Ladoga region for the discovery of Vendian-hosted uranium mineralization. Three small-medium deposits had been discovered to the end of eighties. At that time they were estimated as uneconomic because of the insufficient ore-hosting sandstones permeability and environmental problems, making in-situ leaching impossible. Open pit exploitation would be very expensive because the Ryabinovskoye and Ratnitskoye deposits occur at depths exceeding 300 m. The depth of the Slavyanovskoye deposit ore beds is less, but it presently occurs in the

vicinity of Saint-Petersburg city. However, it is suggested that the deposits of Ryabinovskoye and Ratnitskoye should be now reevaluated because of increased prices for uranium and new technologies.

Among other areas of the Ladoga region, where sandstone-type uranium deposits could be expected, the most prospective is the Svir block to the north-east of the Pasha graben (General Appendix, fig. 3.1). The basement of this area is related to the Raahe-Ladoga zone and late-Svecofennian U-enriched leucogranites are widespread. The Upper Vendian sandstones above them are considered as the most promising. The Salmi massif occurs farther to the north, but it is represented by early phases with low uranium content there. The Svir granite has not been studied.

The Redkinsky horizon occurs at a depth of less 300 m in significant part of the area. In spite of the low density of drilling, several anomalies have been discovered there.

Denser drillings should be undertaken for recognizing prospective areas there.

3. Vein-type.

3.1. Vein-type exploration criteria applied to the Ladoga region.

The high mobility of uranium causes the diversity and multiplicity of vein type uranium mineralization, but in most cases they represent small occurrences. There are several general exploration criteria of areas favorable for economic-grade vein-type uranium deposits (Ruzicka, 1990; Dahlkamp, 1993; Lefebure, 1996; McMillan, 1996)

1. Orogenic belts with intensively cratonized continental crust are preferable.

The Ladoga region basement is composed of the PR₁ Svecofennian accretion orogen, AR Karelian craton and transitional heterogeneous AR-PR₁ Raahe-Ladoga zone. The region was intensively tectonized during the Svecofennian and Riphean events. The Upper Vendian-Phanerozoic time is a relatively quiescent period corresponding to a platform environment. The most significant tectonic movements are referred to the Caledonian and Hercynian events, but even they produced no displacements comparable with the Precambrian ones.

As described above, the earth crust of the region is cratonized to a moderate degree, the thickness of the “granite” layer is small and it decreases its uranium potential.

2. *Presence of uraniferous formations such as highly differentiated peraluminous leucogranite complexes, sediments or metasediments metamorphosed up to amphibolite facies are favorable.*

The uraniferous low-medium metamorphosed basement formations and granites are widespread along the Raahe-Ladoga zone and in the Southern block. The first ones host numerous and diverse uranium occurrences (including veined ones) in addition. The Riphean-hosted unconformity-type and vein-type uranium occurrences are in the north-eastern part of the Pasha-Ladoga basin (the Raahe-Ladoga zone as well). The platform formations of the southern part of studied region are enriched in uranium up to economic grade, a few deposits and numerous ore-showing have been discovered there.

3. *Sometimes an affinity with mafic, aplite or lamprophyre dykes exist.*

Numerous mafic dykes of PR₁ age are swarming along the pericratonic Janisjarvi fault zone and some of them are associated with Th and U mineralization. In the Sortavala block of the Raahe-Ladoga domain and in the Lahdenpokhya block of the Svecofennian domain mafic and lamprophyre dykes of presumably Low Riphean age occur. A few Low-Middle Riphean mafic dykes cut the Salmi rapakivi intrusion.

4. *Brittle dislocation environment; zones of repeatedly activated fault are the most favorable. Uranium mineralization is preferentially emplaced in subsidiary decompression dislocations forming breccias zones and fracture systems with stockwork or horsetail pattern.*

Several regional-size fault systems and numerous second-grade displacements have been observed in the Ladoga region. Many of them indicate repeated activations during different tectonic events. A few events of fracture-bound uranium deposition have been discovered by isotopic constrains. The principal ones are Mesoproterozoic (Lower-Middle Riphean) and Palaeozoic (Ordovician-Devonian) periods.

The most saturated in diverse uranium occurrences are the Ruskeala and Janisjarvi NW-striking fault zones. The last one is especially related to vein-type uranium occurrences. Several veined uranium occurrences are also related to NE-striking faults. Usually the uranium mineralization is related to subsidiary decompression dislocations of different striking.

5. *Hydrothermal ore-associated alterations depend to some degree on host rock composition; the most common are carbonatization, chloritization, argillitization, silicification,*

hematitization, K-feldspartization. Quartz-carbonate gangue is the most common for ore-hosting fracture zones.

Diverse hydrothermal alterations are widespread in the Northern Ladoga area and especially in the Ruskeala and Janisjarvi fault zones. The most significant vein type U occurrences are accompanied with carbonatization and silicification. Chloritization, hematitization, fluoritization, sericitization and argillitization occur as well.

In the Svecofennian domain fracture-bound hydrothermal alterations are not so common; the most typical is chloritization. No indications of hydrothermal uranium redistribution have been discovered in outcropping parts of this domain.

The southern part of the region is concealed by platform sediments and the possible presence of hydrothermal alterations is obscure. Rare indications of late U redistribution have been discovered by drilling in the basement and Upper Vendian formations of the Svir and Southern blocks.

3.2. Prospects.

Prospects for vein-type uranium deposits are difficult because of very limited extension of ore-accompanying alterations and reference of fault zones hosting the mineralization often significantly eroded and concealed under late sediments. Outcropping bedrocks of the northern part of the Ladoga region (especially the Northern Ladoga area) is the best studied in all respects, including the uranium occurrences and the most probable sites of veined uranium mineralization can be well localized.

The Ruskeala and Janisjarvi fault zones are considered as the most promising for vein type U mineralization. NE-striking faults are proposed as promising zones and especially when intersecting others faults. Areas where carbonaceous and uranium-enriched Ludicovian and Kalevian basement rocks are intruded with late-Svecofennian and Lower Riphean leucogranites are the most interesting (General Appendix, fig. 1.2). Deeper drilling in the proposed areas is suggested as a principal prospecting method.

The promising areas in the covered southern region cannot be defined precisely, but general criteria are the same: the areas rich in uraniferous formations and cut by NW- and NE-striking fault zones are considered as the most promising (General Appendix, fig. 2.2 and 3.2). For more efficiency, exploration in those areas should be preceded by reconnaissance drilling and geophysics.

Conclusion.

The Ladoga region is much less prospective than the Athabasca region for the discovery of unconformity-type uranium mineralization and its prospects for large deposits of this type should be estimated quite cautiously. Nevertheless several interesting areas are suggested. The most promising are related to the Raahe-Ladoga zone and the Svir-Oyat area.

Sandstone-type deposits discovered in the Ladoga region had been estimated as of uneconomic grade in the past, but in present uranium market conditions they deserve a reevaluation. The south-eastern part of the region (the Svir block) could host undiscovered uranium deposits of this type.

Economic-grade vein-type uranium mineralization has not been discovered in the Ladoga region, but it can be presumed in some of the faults widespread there. The most interesting in this respect are the Ruskeala and Janisjarvi fault zones.

In general, uranium potential of the Ladoga region is estimated with moderate optimism. The general geological features of the region and the detailed characteristics of individual areas define the possibility for the discovery of economic-grade uranium deposits of different types, but large-tonnage objects are not expected. Most of the prospective areas are located in the Raahe-Ladoga zone.

GENERAL CONCLUSION

GENERAL CONCLUSION.

The Ladoga region is one of the most interesting areas of the Baltic Shield as in respect of geological structure as because of diversity of uranium mineralization.

The region is featured by location in crossing of two multiactivated transregional tectonic belts – the Raahe-Ladoga and Baltic-Mezen zone.

Generalized geological sequence of the region is composed of three principal structural levels:

1. AR-PR₁ crystalline basement;
2. Riphean protoplatform basin;
3. Upper Vend-Palaeozoic platform cover.

The basement was formed as a result of Palaeoproterozoic Svecofennian accretion of juvenile crust to the Archaean Karelian domain.

Aborted intracratonic riftogenesis of Riphean age occurred in the Ladoga region as a response of Sveconorwegian orogeny. It caused formation of large Pasha-Ladoga basin composed of sedimentary-volcanogenic formations.

Upper Vend-Palaeozoic platform sequence, preserved in southern part of the region, corresponds to succession of transgression-regression events occurred in stable cratonic environment.

Uranium ore mineralization occurs in all stratigraphic levels of geological sequence of the region. Structural, mineralogical-petrologic and geochemical characteristics of the occurrences are introduced in the thesis.

Diverse and numerous basement-hosted uranium occurrences have been discovered in the Northern Ladoga area of the Raahe-Ladoga zone. All of them are characterized by small resources with wide variation of uranium contents (up to few percent) and are below economic grade.

Unconformity-related Karku deposit and few unconformity-related and veined uranium ore-showings are located in Riphean formations of the Salmi depression of the Northern Ladoga area. The Karku deposit is considered as an analog of the Athabasca basin unconformity-type deposits, but significant differences from typical deposits have been revealed. They are

estimated as negative features and decreases perspectives of the Karku deposit and area in a whole.

Upper Vendian hosts sandstone-type deposits in the Southern Ladoga area. Uranium occurrences in Lower Ordovician black shales and phosphorites occur in south-eastern part of the region. Vend-Palaeozoic hosted occurrences have large total resource, but grade of uranium mineralization is very low and does not correspond to actual economic demands.

There is a gradual increase of the average uranium content through time in geological formations of the Ladoga region from Archaean to Palaeozoic.

Compilation of old and new age determinations of uranium mineralization allow to maintain three principal epoch of uranium deposition in the Ladoga region:

- I. 1.97-1.77 Ga Late Palaeoproterozoic;
- II. 1.6-1.2 Ga Lower-Middle Riphean;
- III. Ordovician-Devonian.

According to its economic potential uranium occurrences of the Ladoga region can be ranged in the following order:

1. Unconformity-type;
2. Sandstone-type;
3. Vein-type;
4. Black shale;
5. Anatexite-hosted;
6. Synmetamorphic;
7. Intrusive;
8. Phosporite;
9. Quartz-pebble conglomerate.

Only three first types – unconformity, sandstone and vein – considered as having potential economic importance.

Areas, perspective for economic deposits are marked in the Part 3 of the thesis. Most of them are related to the Raahe-Ladoga zone. The Southern Ladoga is presumably located on continuation of uraniumiferous South Finland migmatite belt and can be interesting as well.

Thus, the principal aim of the research – introducing of uranium potential of the Ladoga region – has been realized.

Nevertheless, several problems should be resolved by future researches for better understanding of uranium perspectives of the region.

As it was shown, there are many diverse types of uranium mineralization in the Ladoga region. Detail study of each one could be an object of a special study. That is why many questions could not be answered within the limits of a thesis. The most interesting one is a problem of uranium redistribution discovered in different type uranium occurrences. It has as fundamental interest as pragmatic importance, because the late vein-type uranium mineralization is one of the most concentrated and promising in the Ladoga region.

More certain correlation of late Svecofennian granites of the Ladoga region with those of the uraniferous Southern Finland Migmatite Belt has very important metallogenic sense. Following of this belt into the Ladoga region could help to definite areas the most promising for uranium mineralization of different types.

Research of parallelism of Ludicovian formations hosting numerous uranium occurrences in the Northern Ladoga with contemporary formations of adjacent Finish territory would allow to understand better the geological structure and uranium potential of crystalline basement on both sides from the frontier.

Uranium enrichment of the Ruskeala fault zone is ascertained and accurate following of this structure to adjacent territories is important prognostic task.

Subdivision of Riphean (Jotnian) sequence of the Pasha-Ladoga basin is controversial now. Resolving of this stratigraphic problem is necessary for correct modeling of process of the Mesoproterozoic sedimentation and uranium deposition at the unconformity.

These and other actual questions on geological-metallogenic characteristic of the Ladoga region deserve special complex researches.

REFERENCES

REFERENCES

- Afanasieva E.N., Mikhailov V.A., Kharlamov M.G., 2004. Geological Map of the Pre-Riphean formations of the Pasha-Ladoga area, scale 1:500 000. Report of ZAO Novaya Lekhta, (unpublished).
- Åhäll K.-I., Connelly J.N., Brewer T.S., 2000. Episodic rapakivi magmatism due to distal orogenesis: correlation of the 1.69-1.50 Ga orogenic and inboard “anorogenic” events in the Baltic Shield. *Geology*, v. 28 (9), pp. 823-826.
- Ahl M., Sundblad K., Schöberg H., 1999. Geology, geochemistry, age and geotectonic evolution of the Dala granitoids, central Sweden. *Precambrian Research* 95, pp. 147-166.
- Äikäs O., 1980. Uraniferous phosphorite and apatite-bearing gneisses in the Proterozoic of Finland. In: Uranium in the Pine Creek geosyncline, Proceedings of the international symposium on the Pine Creek geosyncline. IAEA, Vienna, pp. 675-681.
- Alm E., Sundblad K., Huhma H., 2005. Sm-Nd isotope determinations of low-temperature fluorite-calcite-galena mineralization in the margins of the Fennoscandian Shield. SKB Rapport R-05-66, November 2005, available at www.skb.se
- Altgauzen M.N., 1956. Causes of appearance of an epoch of accumulation of rare metals and phosphorus in the marine sediments of Lower Palaeozoic. Moscow, Gosgeolizdat. (In Russian: Альтгаузен М.Н., 1956. Причины возникновения эпохи накопления редких металлов и фосфора в морских осадках нижнего палеозоя, Москва, Госгеолиздат).
- Amantov A., Puura V., Raukas A., Spiridonov M., 1989. Geology and geomorphology of transition zone between Baltic Shield and Russian platform. In: Abstract of 28 IGS, Washington, vol.1, p. 38.
- Amantov A.V., 1992. Study of structure and estimation of possible metallogenic specialization of borderland of the Baltic Shield in the aquatories. In: N.V. Nikitin, D.A. Kirikov, K.A. Markov, L.V. Plotnikov (editors), Tectonic bases of the prognosis-metallogenic researches. St-Petersburg, VSEGEI, pp. 92-102 (In Russian: Амантов А.В., 1992. Изучение структуры и оценка возможной металлогенической специализации окраины Балтийского Щита в пределах акваторий, в: Никитин Н.В., Кириков Д.А., Марков К.А., Плотников Л.М. (ред.), Тектонические основы прогнозно-металлогенических исследований. Санкт-Петербург, ВСЕГЕИ, сс. 92-102).
- Amantov A.V., Voronov P.S., 1993. About age and genesis of present shapes of the Baltic and Canadian shields, *Regional geology and metallogeny*, 1, pp. 77-86 (In Russian: Амантов

- A.B., Воронов П.С. 1993, О возрасте и генезисе современных фигур Балтийского и Канадского щитов, Региональная геология и металлогения, сс. 77-86).
- Amantov A., Laitakari I., Poroshin Y., 1996. Jotnian and Postjotnian: Sandstones and diabases in the surrounding of the Gulf of Finland. Geological Survey of Finland, Special Paper 21, pp. 99-113.
- Amelin Y.V., Larin A.M., Tucker R.D., 1997. Chronology of multiphase emplacement of the Salmi rapakivi granite-anorthosite complex, Baltic Shield: Implication for magmatic evolution. *Contribution to the Mineralogy and Petrology*, 127, pp. 353-368.
- Anderson E.B., Nikitin S.A., Zaslavsky V.G., Lobickov A.F., Markova T.A., Drozdov P.A., 1990. Isotopic dating of uranium occurrences of eastern part of the Baltic Shield. In: *Abstracts of the all-Union meeting "Isotopic dating of endogen ore formations"*, Kiev, pp. 174-176 (In Russian: Андерсон Е.Б., Никитин С.А., Заславский В.Г., Лобиков А.Ф., Маркова Т.А., Дроздов П.А., 1990. Изотопное датирование проявлений урана восточной части Балтийского Щита, тезисы докладов Всесоюзного совещания "Изотопное датирование эндогенных рудных формаций", Киев, сс. 174-176).
- Anderson E.B. (scientific director), 1990. Studying of the processes of the uranium ore-genesis in the Central and Southern Karelia. Report of Radievyi institute of V.G. Хлопин (unpublished) (In Russian: Андерсон Е.Б. (научный руководитель), 1990. Изучение процессов уранового рудообразования Центральной и Южной Карелии, Радиевый институт имени В.Г. Хлопина).
- Andersson U.B., Eklund O., Fröjdö S., Konopelko D., 2006. 1.8 Ga magmatism in the Fennoscandian Shield; lateral variations in subcontinental mantle enrichment. *Lithos*, vol. 86, pp. 110-136.
- Artamonova N.A. (responsible executor), 1989. Report Geological structure and mineral resources of north-eastern Ladoga, Generalizing report on Impilakhti object 1984-89. "Nevskgeologia" (unpublished) (In Russian: Артамонова Н.А. (ответственный исполнитель), 1989. Геологическое строение и полезные ископаемые северо-восточного Приладожья, Объединенный отчет по Импилахтинскому объекту за 1984-89 г.г.).
- Baltybaev S.K., Glebovitsky V.A., Kozyreva I.V., Konopelko D.A., Levchenkov O.A., Sedova I.S., Shuldiner V.I., 2000. Geology and petrology of svecofennids of the Ladoga region, SPbGU, 200 p. (In Russian: Балтыбаев Ш.К., Глебовицкий В.А., Козырева И.В.,

- Левченков О.А., Седова И.В., Шульдинер В.И., 2000. Геология и петрология свекофеннид Приладожья, СПбГУ, 200 с.).
- Baltybaev S.K., Glebovitsky V.A., Levchenkov O.A., Berejnaya N.G., Levsky L.K., 2002. About age relations of provinces of potassic and sodium migmatites in svecofennids (Ladoga region, Baltic Shield), Reports of RAS, vol. 383, No 4, pp. 523-526 (In Russian: Балтыбаев Ш.К., Глебовицкий В. А., Левченков О.А., Бережная Н.Г., Левский Л.К., 2002. О возрастном соотношении провинций калиевых и натриевых мигматитов в свекофеннидах (Приладожье, Балтийский Щит), Доклады РАН, т. 383, № 4, сс. 523-526).
- Baltybaev S.K., Levchenkov O.A., Galankina O.L., 2004. First discovery of volcanites in the svecofennids of the Ladoga region and their age, Reports of RAS, 2004, vol. 395, No 3 (In Russian: Балтыбаев Ш.К., Левченков О.А., Галанкина О.Л., 2004. Первые находки вулканитов в свекофеннидах Приладожья и их возраст, Доклады РАН, т. 395, № 3).
- Bedrock Map of Finland, 1997. 1:1 000 000 scale, Geological Survey of Finland, Espoo.
- Berning, J., Cooke, R., Heimstra, S.A., Hoffman, U., 1976. The Rössing Uranium Deposit, South West Africa. Economic Geology, 71, pp. 351–368.
- Belyaev A.M., Bogdanov Y.B., Levchenkov O.A., 1998. Petrogenesis of the bimodal rapakivi-related volcanites of the Island of Hoagland, 1.64 Ga Wiborg batholith, Russia: insights to petrogenesis, In: International Field Conference: Proterozoic Granite System of the Penoken Terrane in Wisconsin, Madison, Wisconsin, USA, pp. 139-140.
- Bibikova E.V., Kirnozova T.I., Lazarev Yu.I., 1990. U-Pb isotopic age of the Vepsian of the Karelia, Reports of AS of the USSR, vol. 310, No 1, pp. 189-191 (In Russian: Бибикова Е. В., Кирнозова Т. И., Лазарев Ю.И., 1990. U-Pb – изотопный возраст вепсия Карелии, Доклады АН СССР, т. 310, № 1, сс.189-191).
- Bogachev V.A., Ivanikov V.V., Kozyreva I.V., 1999. U-Pb dating of synorogenic gabbro-diorite and granite intrusions of Northern Ladoga area, Vestnik of St-Petersburg State University, series 7, issue 3, pp. 23-33 (In Russian: Богачев В.А., Иваников В.В., Козырева И.В., 1999. U-Pb датирование синорогенных габбро-диоритовых и гранитных интрузий Северного Приладожья, Вестник Санкт-Петербургского Государственного Университета, серия 7, выпуск 3, сс. 23-33).
- Bogachev V.A. (responsible executor), 1999. Discrimination petrologic-geochemical etalons of magmatic complexes as indicators of Palaeogeodynamic conditions in Ladoga structural zone for the geodynamic analyses during additional geological study of areas of 200 000

- scale. Report of State specialized firm "Mineral", (unpublished) (In Russian: Богачев В.А. (ответственный исполнитель), 1999. Выделение петролого-геохимических эталонов магматических комплексов как индикаторов палеогеодинамических обстановок в Ладожской структурной зоне для геодинамического анализа при ГДП-200, Государственная специализированная фирма "Минерал", Санкт-Петербург).
- Bogdanov Yu. B. (chief editor), Akromovskii I.I., Astaf'ev B.Yu., Belyaev A.M., Voinov A.S., Voinova O.A., Guseva E.A., Egorov S.V., Zarrina E.P., Klushkin A.V., Legkova V.G., Petrov B.V., Nasonova L.D., Nahabtsev A.S., Nikolaev V.A., Nogina M.Yu., Rybalko A.E., Sammet E.Yu., Udachina O.N., Chuiko M.A., Yaduta V.A., Yakobson K.E., 2000. State Geological Map of the Russian Federation, 1:1 000 000 scale (new series), Sheets P-35, 36, 37 (In Russian: Богданов Ю.Б. (гл. ред.), Акромовский И.И., Астафьев Б.Ю., Беляев А.М., Воинов А.С., Воинова О.А., Гусева Е.А., Егоров С.В., Заррина Е.П., Ключкин А.В., Легкова В.Г., Петров Б.В., Насонова Л.Д., Нахабцев А.С., Николаев В.А., Ногина М.Ю., Рыбалко А.Е., Саммет Э.Ю., Удачина О.Н., Чуйко М.А., Ядута В.А., Якобсон К.Э., 2000. Государственная геологическая карта Российской Федерации, Масштаб 1:1 000 000 (новая серия), Листы P-35, 36, 37).
- Bogdanov Yu.B., Savatenkov V.V., Ivanikov V.V., Frank-Kamenetsky D.V., 2003. Isotopic age of volcanites of the Salmi suite of the Riphean. In: Materials of II Russian conference on isotopic geochronology "Isotopic geochronology for solution of problems of geodynamics and ore genesis", St-Petersburg, Center of the information culture, pp. 71-72 (In Russian: Богданов Ю.Б., Саватенков В.В., Иваников В.В., Франк-Каменецкий Д.В., 2003. Изотопный возраст вулканитов салминской свиты рифея. Материалы II Российской конференции по изотопной геохронологии "Изотопная геохронология в решении проблем геодинамики и рудогенеза", С-Петербург, Центр информационной культуры, с. 71-72).
- Bonhoure J., Kister P., Cuney M., Deloule E., 2005. Ion microprobe CAMECA IMS-3f REE and isotopic U-Pb analyses of uranium oxide. Proceedings of an international symposium "Uranium production and raw materials for the nuclear fuel cycle – Supply and demands, economics, the environment and energy security. Vienna, pp. 122-133.
- Bonhoure J., Kister P., Cuney M., Deloule E., 2007. Methodology for REE analyses of uranium oxides by ion microprobe. *Geostandard and geoanalysis research*, 31, 3, pp. 209-225.
- Bonhoure J., 2007. *Géochimie des terres rares et du plomb dans les oxygènes d'uranium naturels*. PhD thesis, UHP, Nancy.

- Boynton W. V., 1984. Geochemistry of the rare earth elements: meteorite studies. In: P.Henderson (editor), Rare Earth Element geochemistry. Elsevier, Amsterdam.
- Bruneton P., 1987. Geology of the Cigar Lake uranium deposit (Saskatchewan, Canada). Economic minerals of Canada. Saskatchewan Geological Society, Special Publication 8, pp. 99-119.
- Bruneton P., 1993. Geological environment of the Cigar Lake uranium deposit. Canadian Journal of Earth Sciences, Vol. 30, No 4, pp. 653-673.
- Bryzgalova M.V., Ivanova O.T., Lobanov I.N., Krivtsov N.E., Matveeva E.S., 1956. Reports on results of prospecting works carried out by the party No 12 in the Sortavala and Pitkjaranta districts of the KaSSR during 1954-55. "Nevskgeologia" (unpublished) (In Russian: Брызгалова М.В., Иванова О.Т., Лобанов И.Н., Кривцов Н.Е., Матвеева Э.С., 1956. Отчет о результатах поисково-разведочных работ проведенных партией № 12 в Сортавальском и Питкярантском районах КАССР в 1954-55 гг., «Невскгеология»).
- Bylinskaya L.V., Mikhailov V.A., Tolmacheva E.V., Demicheva L.A., 2004. Mineralogy and conditions of the formations of the uranium ores of the Karku deposit (Ladoga region). Materials on geology of deposits of uranium, rare and rare-earth metals, Issue 145, Moscow, pp. 71-80 (In Russian: Былинская Л.В., Михайлов В.А., Толмачева Е.В., Демичева Л.А., 2004. Минералогия и условия образования урановых руд месторождения Карку (Приладожье). Материалы по геологии месторождений урана, редких и редкоземельных металлов, Выпуск 145, Москва, сс. 71-80).
- Caillat C., Naumov S.S., Novikov G.I., Petrov O.V. (editors), 2002. Estimation of the Riphean Pasha-Ladoga depression for the possibility of discovering of economic uranium deposits of unconformity type (Expert conclusion). COGEMA-VSEGEI-"Nevskgeologia"-GEOLOGORAZVEDKA, St-Petersburg (unpublished).
- Calzia J.P, Rämö O.T., 2005. Miocene rapakivi granites in the southern Death Valley region, California, USA, Earth-Science Reviews 73, pp. 221-243.
- Chappel B.W., White A.J.R., 1974. Two contrasting granite types. Pacific Geology.
- Chuvardinsky V.G., 2000. Neotectonics of the Eastern part of the Baltic Shield, Apatity, KSC of RAS, 287 p. (In Russian: Чувардинский В.Г., Неотектоника Восточной части Балтийского Щита, 2000. Апатиты, КНЦ РАН, 287 с).
- Cumming G.L., Krstic D., Willson J.A., 1987. Age of the Athabasca Group, northern Alberta, Geological Association of Canada – Mineralogical Association of Canada, Program with Abstracts, v. 12, p. 35.

- Cuney M. 1980. Preliminary results on the petrology and fluid inclusions of the Rössing uraniferous alaskites. *Transactions of the Geolog. Society of South Africa*, 83, pp. 39-45.
- Cuney M.L., 1981. Comportement de l'uranium et du thorium au cours du métamorphisme. Rôle de l'anatexie dans la genèse des magmas riches en radioéléments. Thèse d'Etat, INPL, Nancy, 511 p.
- Cuney M.L., 1982. Processus de concentration de l'uranium et du thorium au cours de la fusion partielle et de la cristallisation des magmas granitiques. In: "Les méthodes de prospection de l'uranium", OCDE, Paris Edit., pp. 277-292.
- Cuney M.L., Barbey P., 1982. Mise en évidence de phénomènes de cristallisation fractionnée dans les migmatites. *C.R. Academy of Science*, 295, pp. 37-42.
- Cuney M.L., Brouand M., Derome D., Hecht L., Lorilleux G., Peiffert C., 2003. What parameters control the high-grade large tonnage of the Proterozoic unconformity related uranium deposits. In: Cuney (editor), *Uranium Geochemistry, International Conference Proceedings*, Nancy, pp. 123-126.
- Cuney M.L., 2005. World-class unconformity-related uranium deposits: key factors for their genesis. *Materials of SGA meeting*.
- Dahlkamp F.J., 1993. *Uranium ore deposits*. Springer-Verlag Berlin Heidelberg, 460 p.
- De Vivo B., Ippolito F., Capaldi G., Simpson P.R. (editors), 1988. *Uranium geochemistry, mineralogy, geology, exploration and resources*, Mir, Moscow (In Russian: Де Виво Б., Ипполито Ф., Капалди Г. и Симпсона П.Р. (ред.), 1988. Геология, геохимия, минералогия и методы оценки месторождений урана, Мир, Москва).
- Derome, D., M. Cuney M., Cathelineau M., Dubessy J., Bruneton P., 2003. A detailed fluid inclusion study in silicified breccias from the Komboldgie sandstones (Northern Territory, Australia): application to the genesis of Middle-Proterozoic unconformity type uranium deposits. *Journal of Exploration Geochemistry*, 80, pp. 259-275.
- Derome, D., Cuney M., Cathelineau M., Fabre C., Lhomme T., 2005. Evidences of brine mixings in the McArthur River unconformity-type uranium deposit (Saskatchewan, Canada). Implications on genetic models. *Economic Geology*.
- Dolgushina I.S., Kushnerenko V.K., 2004. Geochemical prognostic criteria of unconformity-type uranium deposits (by the example of the Karku deposit). *Materials on geology of deposits of uranium, rare and rare-earth metals*, Issue 146, Moscow, pp. 37-41 (In Russian: Долгушина И.С., Кушнеренко В.К., 2004. Геохимические критерии прогнозирования месторождений типа несогласия (на примере месторождения Карку). Материалы по

- геологии месторождений урана, редких и редкоземельных металлов, Выпуск 146, Москва, сс. 37-41).
- Dolgushina I.S., 2005. Geochemical criteria of the prognosis of the uranium deposits of “unconformity type” (by the example of the Karku deposit). In: Materials of the I International Scientific Conference “Geology, Geochemistry and Ecology of the North-West of the Russia”, pp. 19-22 (In Russian: Долгушина И.С., 2005. Геохимические критерии прогнозирования месторождений урана “типа несогласия” (на примере месторождения Карку). Материалы I Международной Научной Конференции “Геология, Геохимия и Экология Северо-Запада России”, сс. 19-22).
- Duhovinsky A.A., Artamonova, 1994. Space model and ore mineralization of gneiss-granite structures of the Baltic shield (by example of the Northern Ladoga area). Geology of ore deposits, No 6, pp. 554-564 (In Russian: Духовинский А.А., Артамонова Н.А., 1994. Объемная модель и рудоносность гнейсо-гранитовых структур Балтийского щита (на примере Северного Приладожья). Геология рудных месторождений, № 6, сс. 554-564).
- Elo S., Korja A., 1993. Geophysical interpretation of the crustal and upper mantle structure in the Wiborg rapakivi area, southeastern Finland. Precambrian Research, 64, pp. 273-288.
- Eskola P., 1925. On the petrology of Eastern Fennoscandia – Fennia, 45, No 19, 1-93.
- Eskola P.E., 1949. The problem of mantled gneiss domes. Geological Society London Quart. J.V. 104, pt. 4, pp. 461-476.
- Eklund O., Konopelko D., Rutanen H., Fröjdö S., Shebanov A.D., 1998. 1.8 Ga Svecofennian post-collision shoshonitic magmatism in the Fennoscandian shield. Lithos 45, pp. 87-108.
- Ekman J., Jlym V., 1991. Deglaciation, the Younger Dryas and moraines and their correlation in the Karelian ASSR and adjacent areas. Geological Survey of Finland Opus-guide 32, Espoo, pp. 73-101.
- Evensen N.M., Hamilton P.J. and O'Nions R.K., 1978. Rare-earth abundances in chondritic meteorites. Geochimica et Cosmochimica Acta, vol. 42, pp.1199-1212.
- Fouques J.P., Fowler M., Knipping H.D., Schimann K., 1986. The Cigar Lake uranium deposit: Discovery and general characteristics. In: Evans E.L. (editor), Uranium deposits of Canada. The Canadian Institute of Mining and Metallurgy, Special Volume 33, pp. 218-229.
- Frank-Kamenetsky D.A., 1996. Geology, geochemistry and petrology of Riphean basites of the Ladoga Region. Questions of geology of the Karelia-Cola region, pp. 12-14 (In Russian:

- Франк-Каменецкий Д.А., 1996, Геология, геохимия и петрология рифейских базитов Приладожья, Вопросы геологии Карело-Кольского региона, сс. 12-14).
- Frank-Kamenetsky D.A., 1998. Petrology of Riphean basites of the Ladoga Region, SPbSU, abstracts of PhD thesis, 16 p. (In Russian: Франк-Каменецкий Д.А., 1998. Петрология рифейских базитов Приладожья, СПбГУ, автореферат Диссертации на соискание учёной степени кандидата геолого-минералогических наук, 16 с.).
- Fuks V.Z. (responsible executor), 2007. Compilation of the map of uranium-bearing of European part of the Russian Federation, 1:5 000 000 scale, report of VSEGEI (unpublished) (In Russian: Фукс В.З. (ответственный исполнитель), 2007. Составление карты ураноносности европейской части Российской Федерации, масштаб 1:5 000 000, ВСЕГЕИ).
- Gaál G., Gorbatshev R., 1987, An outline of the Precambrian evolution of the BS, *Precambrian Research*, 35, pp. 15-52.
- Gavrilenko V.V., 1990. Geochemical evolution of the granite-gneiss domes (by the example of the Northern Ladoga). In: Rudnik V.A. (chief editor), *Petrochemical evolution of magmatic formations*, Moscow, Nauka, pp. 145-155 (In Russian: Гавриленко В.В., 1990, Геохимическая эволюция гранито-гнейсовых куполов (на примере Северного Приладожья), в: Рудник В.А. (гл. ред.). Петрохимическая эволюция магматических формаций, Москва, Наука, сс. 145-155)
- Gintov O.B., Orovetsky Y.P., Golub V.N., 1987. Sortavala deep magmatic diapir, In: IV regional petrographic meeting on European part of the USSR “Magmatism, metamorphism and geochronology of the Precambrian of the East-European Platform in connection with large scale mapping”, abstracts, Petrozavodsk, pp. 31-32 (In Russian: Гинтов О.Б., Оровецкий Ю.П., Голуб В.Н., 1987, Сортавальский глубинный магматический диапир, в: IV регионального петрографического совещания по европейской части СССР “Магматизм, метаморфизм и геохронология докембрия Восточно-Европейской платформы в связи с крупномасштабным картированием”, тезисы, Петрозаводск, сс. 31-32).
- Glebovitsky V.A., 2003. Connections of the metamorphism with tectonics, geodynamic consequences. In: *Metamorphism, granite forming and orogenesis (to 100 anniversary of N.G. Sudovicov)*, St-Petersburg, NIIZK SPbSU, pp. 56-60 (In Russian: Глебовицкий В. А., 2003, Связи метаморфизма с тектоникой, геодинамические следствия.

- Метаморфизм, гранитообразование и рудогенез (к 100-летию Н.Г. Судовикова), СПб., НИИЗК СПбГУ, сс. 56-60).
- Glebovitsky V.A (editor), 2005. The Early Precambrian of the Baltic Shield, St-Petersburg, Nauka, 711 p. (In Russian: Глебовицкий В.А. (редактор), 2005. Ранний докембрий Балтийского Щита, Санкт-Петербург, Наука).
- Glebovitsky V.A., Shemyakin V.M., 1996. Subdivision and correlation of the Early Precambrian. Regional geology and metallogeny, No 5, pp. 25-36 (In Russian: Глебовицкий В.А., Шемякин В.М., 1996, Расчленение и корреляция раннего докембрия. Региональная геология и металлогения, №5, сс. 25-36).
- Glebovitsky V.A., Baltybaev S.K, Levchenkov O.A., Berejnaya N.G., Levsky L.K., 2001. Main stage of pluton-magmatic activity in Ladoga area: results of isotopic age determinations, Reports of RAS, No 5. (In Russian: Глебовицкий В.А., Балтыбаев Ш.К., Левченков О.А., Бережная Н.Г., Левский Л.К., 2001. Главная стадия плутоно-магматической активности в Приладожье: результаты определения изотопного возраста, Доклады РАН, № 5).
- Gorbatshev R., Bogdanova S., 1993. Frontiers in the Baltic Shield. Precambrian Research, 64, pp. 3-21.
- Gortsevsky A.A., 1983. Main theses of the geological-genetic model of the unconformity-type uranium deposits, Materials on the geology of the deposits of uranium, rare and rare earth metals, issue 136, Moscow, pp. 75-85 (In Russian: Горцевский А.А., 1993, Основные положения геолого-генетической модели месторождений урана типа несогласия, Материалы по геологии месторождений урана, редких и редкоземельных металлов, вып. 136, Москва, сс. 75-85).
- Grigorieva L.V. (responsible executor), 1977. Estimation of perspectives of uranium mineralization of the Northern Ladoga and localization of individual structures for prospects of economic uranium mineralization, Report for theme 762, VSEGEI (unpublished) (In Russian: Григорьева Л.В. (ответственный исполнитель), 1977. Оценка перспектив ураноносности Северного Приладожья и локализация отдельных структур для поисков промышленного уранового оруденения, Отчёт по теме 762, ВСЕГЕИ).
- Grodnitsky L.L., 1982. Granite pegmatites of the Baltic Shield, Leningrad, 296 p. (In Russian: Гродницкий Л.Л., 1982. Гранитные пегматиты Балтийского щита, Ленинград, 296 с.).

- Gromov U.A., Andronenkov V.F., Bashkirtzev A.M., Sizov A.L., Stepanov I.V., Hasanov I.D., 1980. Report about results of prognosis-geological works of the Southern Karelia party No 7 in the Ruskeala-Leppesurye area (Northern Ladoga) during 1978-1979, Lyaskelya (unpublished) (In Russian: Громов Ю.А., Андроненков В.Ф., Башкирцев А.М., Сизов А.Л., Степанов И.В., Хасанов И.Д., 1980, Отчёт о результатах прогнозно-геологических работ Южно-Карельской партии № 7 на Рускеальско-Леппесюрской площади (Северное Приладожье) за 1978-1979 гг, Ляскеля).
- Gromov U.A., Andronenkov V.F., Bashkirtzev A.M., Stepanov I.V., Hasanov I.D., 1981. Report about results of prognosis-geological works of the Southern Karelia party No 7 in the Ruskeala and Leppesurye areas (Northern Ladoga) during 1978-1980, Lyaskelya (unpublished) (In Russian: Громов Ю.А., Андроненков В.Ф., Башкирцев А.М., Степанов И.В., Хасанов И.Д., 1981, Отчёт о результатах прогнозно-геологических работ Южно-Карельской партии № 7 на Рускеальской и Леппесюрской площадях (Северное Приладожье) за 1978-1980 гг, Ляскеля).
- Guptor E.B., Ufa B.J., 1953. Report on prospecting-exploration works carried out by Bolsheozerskaya party No 70 during period 1950-1952 at the Jalonvara deposit of copper pyrite. Oktyabrskaya expedition, Leningrad 1953 (unpublished) (In Russian: Отчёт о поисково-разведочных работах, проведённых партией № 70 за период с 1950 по 1952 г. на Ялонварском месторождении серного колчедана).
- Naapala I., Rämö O.T., 1992. Tectonic setting and origin of the Proterozoic rapakivi granites of southern Fennoscandia. *Transaction of the Royal Society of Edinburgh: Earth Sciences* 83, pp. 165-171.
- Naapala I., Rämö O.T., Frindt S., 2005. Comparison of Proterozoic and Phanerozoic rift-related basaltic-granitic magmatism, *Lithos*, 80, pp. 1-32.
- Heiskanen K.I., 1990. Palaeogeography of the Baltic Shield during the Karelian time. Petrozavodsk, Karelian Scientific Center of Academy of Science of USSR, 128 p. (In Russian: Хейсканен К.И., 1990, Палеогеография Балтийского щита в карельское время. Петрозаводск, КНЦ АН СССР, 128 с.).
- Hoeve J., Silbadd T., 1978. On the genesis of Rabbit Lake and other unconformity-type uranium deposits in northern Saskatchewan, Canada. *Economic Geology*, Vol. 73, pp. 1450-1473.
- Holliger P., 1988. Ages U-Pb definis in situ sur oxydes de uranium a la analyseur ionique: methodologie et consequences geochemiques. *Comptes rendus de l'Academie des Sciences de Paris*, v. 307(2), pp. 367-373.

- Huhma H., 1986. Sm-Nd, U-Pb and Pb-Pb isotopic evidence for the origin of early Proterozoic Svecokarelian crust in Finland. Geological Survey of Finland, Bulletin 343.
- Huhma H., Mutanen T, Whitehouse M, 2004. Oldest rocks of the Fennoscandian Shield; The 3.5 Ga Siuria trondhjemite gneiss of Pudasjärvi Granulite Belt, Finland, GFF 126, p. 17.
- Ibrahim A., 2007. Caractéristiques pétrographiques et géochimiques et évolution diagenétique des bassins silicoclastiques Mesoproterozoïques intracontinentaux. Implications sur la genèse des gisements d'uranium de type discordance. PhD thesis, UHP, Nancy.
- Ильин В.И. (ответственный исполнитель), 1984. Quantitative estimation of prognostic resources of the principal territory of activity of the Nevskoye PGO for 01.01.1984. Report of the "Nevskgeologia" (unpublished) (In Russian: Ильин В.И. (ответственный исполнитель) 1984. Количественная оценка прогнозных ресурсов урана основной территории деятельности Невского ПГО по состоянию на 01.01.1984).
- Isanina E.V., Bragin V.V., 1988. Report of party No 10 of the Central expedition No 2 for 1985-87. Researching of deep structure of the earth crust of Onega-Ladoga isthmus with method MOWZ for the geological assignment 2-38. "Nevskgeologia" (unpublished) (In Russian: Исанина Э.В., Брагин В.В., 1988 Отчёт партии №10 Центральной экспедиции №2 за 1985-87 г.г. Изучение глубинного строения земной коры Онежско-Ладожского перешейка методом МОВЗ по геол. заданию 2-38. Отчёт ГП "Невскгеология").
- Isanina E.V., Yujaninova S.I., Skorospelkin S.A., 2001. Specification of deep structure of southern slope of the Baltic shield and zone of joining of the shield and the Russian plate according to results of synthesizing of seismological and others data along the profile Voznesenie-Podporoje-Lodeynoye Pole-Novaya Ladoga. Report of "Nevskgeologia" (unpublished) (In Russian: Исанина Э.В., Южанинова С.И., Скорospelкин С.А., 2001. Уточнение глубинного строения южного склона Балтийского щита и зоны сочленения щита с Русской плитой по данным обобщения сейсмологических и других материалов по профилю Вознесенье-Подпорожье-Лодейное Поле-Новая Ладога. Отчёт ГП "Невскгеология").
- Ivanikov V.V., Popova V.A., Leonova V.A., Bogoleva I.T, Bogachev V.A., Belyaev A.M., 1984. Study of leucogranite formations of south-western Karelia and estimation of theirs ore productivity. Report of Leningrad State University, Leningrad (unpublished) (In Russian: Иваников В.В., Попова В.А., Леонова В.А., Боголева И.Т., Богачев В.А., Беляев А.М., 1984, Изучение лейкогранитовых формаций юго-западной Карелии и оценка их рудоносности, Отчет ЛГУ, Ленинград).

- Ivanikov V.V., Konopelko D.L., Pushkarev Y.D., Rublev A.G., Runtgenen G.I., 1996. Apatite-bearing potassic ultramafites-mafite of the Ladoga region – Riphean riftogenic or Palaeoproterozoic post-orogenic formations? *Vestnik of the St-Petersburg University, Series 7, Geology, geography, iss. 4* (In Russian: Иваников В.В., Конопелько Д.Л., Пушкарев Ю.Д., Рублев А.Г., Рюнгенен Г.И., 1996. Апатитоносные калиевые ультрамафит-мафиты Приладожья – рифейские рифтогенные или раннепротерозойские посторогенные образования?. *Вестник СПбГУ, Сер.7 Геология, география, Вып. 4*).
- Ivanikov V.V., Filippov N.B., Bogachev V.A., Muradymov G.S., 1999. Mineralogic-geochemic indications of ophiolite association in the Ladoga region, In: *Materials of International Conference “Riftogenesis, magmatism, metallogeny of Precambrian. Correlation of geological complexes of the Fennoscandia”*, Petrozavodsk (In Russian: Иваников В.В., Филиппов Н.Б., Богачев В.А., Мурадымов Г.Ш., 1999, Минералого-геохимические признаки офиолитовой ассоциации в Приладожье, в: *Материалы Международной конференции “Рифтогенез, магматизм, металлогения докембрия. Корреляция геологических комплексов Фенноскандии”*, Петрозаводск).
- Ivaschenko V.I., Ovchinnikova L.V., 1988. Age, geochemical types and ore bearing of granitoids of south-eastern border of the Baltic Shield, *Reports of AS of USSR, vol. 302, 6, 206-218* (In Russian: Иващенко В.И., Овчинникова Л.И., Возраст, геохимические типы и рудоносность гранитоидов юго-восточной окраины Балтийского Щита, *ДАН СССР, 1988, т. 302, № 6, 206-218*).
- Ivaschenko V.I., Lavrov O.B., 1994. Magmatogene-ore (Mo, W, Cu, Au) system of the Jalonvaara volcano-plutonic complex of the Archaean of the Karelia, *Petrozovodsk, 128 p.* (In Russian: Иващенко В.И., Лавров О.В., 1994. Магматогенно-рудная (Мо, W, Cu, Au) система Ялонварского вулканоплутонического комплекса Архея Карелии, *Петрозаводск, 128 с.*).
- Jefferson C.W., Thomas D., Quirt D., Mwenifumbo C.J., Brisbin D., 2007. Empirical models for unconformity-associated uranium deposits.
- Jdanov V.V., 1972. About connection of mafic and felsic magmatism of the Ladoga through. *Bulletin of Moscow Society of the Nature Exploitation, section Geology, vol. XLVII (4)* (In Russian: Жданов В.В. О связи основного и кислого магматизма Ладожского прогиба. *Бюллетень Московского Общества Использования Природы, отд. Геология, т. XLVII (4)*).

- Kahma A., 1973, The main metallogenic features of Finland. Geological Survey of Finland, Bulletin 265, pp. 1-28.
- Khazov R.A., Popov M.G., Biskae N.S., 1999. Riphean potassium alkaline magmatism of southern part of the Baltic Shield, St-Petersburg, Nauka (In Russian: Хазов Р.А., Попов М.Г., Бискэ Н.С., 1999. Рифейский калиевый щелочной магматизм южной части Балтийского Щита, СПб., Наука).
- Khazov R.A., Sharov N.V., Isaninana E.V., 2004. Deep structure and metallogeny of the Ladoga region, Geology and mineral resources of Karelia, Petrozavodsk, iss. N 7, pp. 55-74 (In Russian: Хазов Р.А., Шаров Н.В., Исанина Э.В. 2004. Глубинное строение и металлогения Приладожья, Геология и полезные ископаемые Карелии, Петрозаводск, вып. №7, сс. 55-74).
- Kakkuri J., 1997. Postglacial deformation of the Fennoscandian Crust, Geophysica, vol. 33, No 1, pp. 99-110.
- Kish, L., and Cuney, M., 1981. Uraninite-albite veins from Mistamisk Valley of the Labrador Trough, Quebec. Mineralogical Magazine, vol. 44, pp. 471-483.
- Kitsul V.I., 1963. Petrology of carbonate rocks of the Ladoga formation. Moscow (In Russian: Кицул В.И., 1963. Петрология карбонатных пород Ладожской формации. Москва).
- Kohonen J., Rämö O.T., 2002. Sedimentary Record and Magmatic Episodes Reflecting Mesoproterozoic-Phanerozoic Evolution of the Fennoscandian Shield. In: Lahtinen R., Korja A., Arhe K., Eklund O., Hjelt S.-E., Pesonen L.J. (editors). Lithosphere 2002: Second symposium on the structure, composition and evolution of the lithosphere in Finland, Espoo, Otaniemi, November 12-13, 2002, program and extended abstracts. Institute of Seismology, University of Helsinki, Reports S-42, pp. 23-32.
- Kolbantsev L.R., 1994. Mafic dyke complexes of riftogenic systems of eastern part of the Baltic Shield. Regional geology and metallogeny, No 2, pp. 13-25 (In Russian: Колбанцев Л.Р., 1994. Мафические дайковые комплексы рифтогенных систем восточной части Балтийского щита. Региональная геология и металлогения, № 2, сс. 13-25).
- Kondakov S.N., Afanasiev M.S., Dymsky Yu.A., Krivtsova E.B., Ipatov B.S., Ruvman A.S., Epstein E.S., Zolitokeylina E.E., 1963. Report about works of the Centralnaya party No 24, carried out in 1962, Leningrad (unpublished) (In Russian: Кондаков С.Н., Афанасьев М.С., Дымский Ю.А., Кривцов Е.Б., Ипатов Б.С., Рувман А.С., Эпштейн Е.С., Золотокрылова Е.Е., 1963. Отчёт о работах Центральной партии № 24, проведённых в 1962, Ленинград).

- Konopelko D., Eklund O., 2003. Timing and geochemistry of potassic magmatism in the eastern part of the Svecofennian domain, NW Ladoga Lake Region, Russian Karelia, *Precambrian Research*, vol. 120, pp. 37-53.
- Korotaev M.A., Andronenkov V.F., Gorjunov V.N., Grigorieva L.V., Belyaeva L.N., 1978. About prognostic-geological and prospecting works of the group N 7 in Sortavala-Pitkjaranta area (Northern Ladoga area) for 1975-1977, Leningrad, "Nevskgeologia" (In Russian: Коротаев М.А., Андроненков В.Ф., Горюнов В.Н., Григорьева Л.В., Беляева Л.Н., 1978. О прогнозно-геологических и поисковых работах партии № 7 на Сортавальско-Питкярантской площади (Северное Приладожье) за 1975-1977 гг., Ленинград, «Невскгеология»).
- Kotov A.B., Bibikova E.V., Neimark L.A., 1992. About duration of tectonic-magmatic circles (ТМС), In: *Structural analyses of metamorphic circles, (abstracts), Jakutiya*, pp. 15-21 (In Russian: Котов А.Б., Бибилова Е.В., Неймак Л.А., 1992, О продолжительности тектоно-метаморфических циклов (ТМЦ), Структурный анализ метаморфических комплексов, Якутия, сс. 15-21).
- Krats K.O., 1963, *Geology of karelides of the Karelia. Works of laboratory of Precambrian of AS USSR*, iss. 16, 211 p. (In Russian: Кратц О.Г., 1963, Геология карелид Карелии, Труды лаборатории докембрия АН СССР, вып. 16, 211 с.).
- Kushnerenko V.K., Kaizer V.A., Kostuchenko V.E., Filatov G.N., 1985. New data on uranium-bearing black shales of the Central Kazakhstan. *Materials on geology of uranium deposits. Issue 96, Moscow*, pp. 83-89 (In Russian: Кушнеренко В.К., Кайзер В.А., Костюченко В.Е., Филатов Г.Н., 1985. Новые данные по ураноносности чёрных сланцев Центрального Казахстана. Материалы по геологии урановых месторождений. Москва, Выпуск. 96., сс. 83-89).
- Kushnerenko V.K., Petrov Yu.V., Pichugin V.A., Gromov Yu.A., Shurilov A.V., Polekhovsky Yu.S., Tarasova I.P., Britvin S.N., 2004. Geological structure and succession of the epigenetic minerogenesis of the Karku uranium deposit (north-eastern Ladoga area). *Materials on geology of deposits of uranium, rare and rare-earth metals, Issue 146, Moscow*, pp. 11-22 (In Russian: Кушнеренко В.К., Петров Ю.В., Пичугин В.А., Громов Ю.А., Шурилов А.В., Полеховский Ю.С., Тарасова И.П., Бритвин С.Н., 2004. Геологическое строение и последовательность эпигенетического минералообразования уранового месторождения Карку (северо-восточное

- Приладожье). Материалы по геологии месторождений урана, редких и редкоземельных металлов. Москва, Выпуск 146., сс. 11-22).
- Landais, P., 1996. Organic geochemistry of sedimentary uranium ore deposits. *Ore Geology Review*, No 11, pp. 33-51.
- Larin A.M., Amelin Y.V., Neimark L.A., 1991. Age and genesis of complex skarn ores of the Pitkjaranta ore area. *Geology of ore deposits*, No 6, pp. 15-32. (in Russian: Ларин А.М., Амелин Ю.В., Неймарк Л.А., 1991. Возраст и генезис комплексных скарновых руд Питкярантского рудного района, *Геология рудных месторождений*, № 6, сс. 15-32).
- Larin A.M., Kutuyavin E.P., 1993. Age of Jotnian magmatism of the Northern Ladoga, *Stratigraphy. Geological correlation*, vol.1, No 5 (In Russian: Ларин А.М., Кутяин Э.П., 1993, Возраст иотнийского магматизма Северного Приладожья, *Стратиграфия. Геологическая корреляция*, Том 1, № 5).
- Larson S.Å., Tullborg E.-L., Cederbom C, Stiberg J.-P., 1999. Sveconorwegian and Caledonian foreland basins in the Baltic Shield revealed by fission-track thermochronology, *Terra Nova* 11 (5), pp. 210-215.
- Laverov N.P., Smilkstyn A.O., Shumilin M.V., 1983. Foreign deposits of uranium, Moscow, Nedra, 231 p. (In Russian: Лаверов Н.П., Смилкстын А.О., Шумилин М.В., 1983. Зарубежные месторождения урана, Москва, Недра, 231 с.).
- Le Maitre R.W., Bateman P., Dudek A., et al., 1989. A classification of igneous rocks and glossary of terms, Blackwell, Oxford.
- Lefebure D.V., 1996. Five-elements Veins Ag-Ni-Co-As+/--(Bi,U). In: Lefebure D.V., Höy T. (editors). *Selected British Columbia Mineral Deposits Profiles, Volume 2, Metallic deposits*. Ministry of Employment and Investment, Open file 1996-13, pp. 89-92.
- Lentz, D.R., 1996. U, Mo, and REE mineralization in the late-tectonic granitic pegmatites, southwestern Grenville Province, Canada. *Ore Geology Reviews*, vol. 11, pp. 197–227.
- Letnikov F.A., Balyshev S.O., Lashkevich V.V., 2000. Granite-gneiss domes as an example of self-organizing systems in the lithosphere. *Reports of Russian academy of science*, vol. 370, No 1, pp. 67-70 (In Russian: Летников Ф.А., Балышев С.О., Лашкевич В.В., 2000. Гранито-гнейсовые купола как пример самоорганизующихся систем в литосфере. *Доклады Академии Наук*, т. 370, №1, сс. 67-70).
- Lobaev V., 2005. Mineralogical and petrogeochemical characteristics of the Mesoproterozoic Pasha-Ladoga volcanic-sedimentary basin and its basement (Baltic shield, Russia).

- Inferences on the genesis of unconformity related uranium deposits. PhD thesis, UHP, Nancy.
- Lobanov I.N., Bryzgalova M.V., 1956. Brief description of uranium deposits and ore-showings of the Northern Ladoga area (Summary of prospect results from 1946 to 1955). Report of "Nevskgeologia" (unpublished) (In Russian: Лобанов И.Н., Брызгалова М.В., 1956. Краткое описание урановых месторождений и рудопроявлений Северного Приладожья (Сводка о результатах поисков с 1946 по 1955 гг), «Невскгеология»).
- Lobanov I.N., Kicul V.I., Ivanova O.T., 1956. Materials on geology of the Pjalkjarvi-Janisjarvi-Jalonvara area (party No 12, 1954-1955), Severnaya expedition, Leningrad (In Russian: Лобанов И.Н., Кицун В.И., Иванова О.Т., 1956. Материалы по геологии района Пялъярви-Янисъярви-Ялонвара (партия № 12, 1954-1955), Северная экспедиция, Ленинград).
- Lobanov I.N., Polikarpov V.I., 1981. Zone of deep fault between Karelian and Svecofennian blocks (South-Western Karelia), *Geotectonica*, No 5, pp. 34-40 (In Russian: Лобанов И.Н., Поликарпов В.И., 1981. Зона глубинного разлома между Карельским и Свеккофенским блоками (Юго-Западная Карелия), *Геотектоника*, № 5, сс. 34-40).
- Lokhov K.I., Verejnaya N.G., Matukov D.I., Presnyakov S.L., Halenev V.O., Rodionov N.I., Lepjekhina E.N., Lamberova S.B., Sergeev S.A., 2004. Phanerozoic age constrains for rocks of the Baltic shield with U-Pb method of zircons with help of the SHRIMP methodic: contamination or reality?, In: XVII Symposium on geochemistry of isotopes in the name of academic A.P. Vinogradov, 6-9th of December 2004, Moscow (abstracts) (In Russian: Лохов КИ, Бережная НГ, Матуков ДИ, Пресняков СЛ, Халенев ВО, Родионов НИ, Лепёхина ЕН, Ламберова СБ, Сергеев СА. Фанерозойские значения возраста в породах Балтийского щита по U-Pb методу по цирконам при помощи методики SHRIMP: контаминация проб или реальность?, в: XVII Симпозиум по геохимии изотопов имени академика АП Виноградова, 6-9 декабря 2004 Москва).
- Lorilleux, G, M. Cuney, M. Jebrak and J.C. Rippert, 2003. Hydrothermal processes in an unconformity type uranium deposit in the Eastern Athabasca basin (Canada). *Journal of Geochemical Explorations*, 80, pp 241-258.
- Ludwig K.R. 1999. Isoplot/ex version 2.10. A geochronological toolkit for Microsoft Excel. Special publication, № 1a, Berkeley Geochronological Center.
- Luosto U., 1997. Structure of the Earth's crust of the Fennoscandia as revealed from reflection and wide-angle reflection studies, *Geophysics*, vol. 128, pp. 183-208.

- Maniar P.D., Piccoli P.M., 1989. Tectonic discrimination of the granitoids. Geological Society of America. Bulletin 101, pp. 635-653.
- McMillan R.H., 1996. "Classical" U Veins. In: Lefebure D.V., Höy T. (editors). Selected British Columbia Mineral Deposits Profiles, Volume 2, Metallic deposits. Ministry of Employment and Investment, Open file 1996-13, pp. 93-96.
- McMillan R.H., 1998. Unconformity-associated U. In: Geological Fieldwork, British Columbia Ministry of Employment and Investment, Paper 1998-1, pp. 24G-1 - 24G-4.
- Miguta A.K., Ledeneva N.V., Ovsyannikov N.V., Petrov A.V., Rujnickii V.V., Sumin L.V., 2002. Uranium on the verge of the centuries: resources, production, demand, Works of the International uranium geological symposium (Moscow, 29.11.-01.12.2000) (In Russian: Мигута А.К., Леденёва Н.В., Овчинников Н.В., Петров А.В., Ружницкий В.В., Сумин Л.В., 2002. Условия формирования и преобразований урановых руд месторождения Карку в Северном Приладожье, Уран на рубеже веков: природные ресурсы, производство, потребление, Труды Международного симпозиума по геологии урана (Москва, 29.11.-01.12.2000)).
- Mikhailov V.A., Kluev N.K., Tikhomirov L.I., Harlamov M.G., Melnikov E.K., Petrov Y.V., Polikarpov V.I., Sharikov P.I., 1999. Metallogeny of uranium of Onega-Ladoga uranium ore province. Regional geology and metallogeny, 8, pp. 65-82, (In Russian: Михайлов В.А., Ключев, Н.К., Тихомиров Л.И., Харламов М.Г., Мельников Е.К., Петров Ю.В., Поликарпов В.И., Шариков П.И., 1999. Металлогения урана Онежско-Ладожского урановорудной провинции. Региональная геология и Металлогения, № 8, сс. 65-82).
- Mikhailov V.A., 2001. To the question of the genesis of ores of the unconformity-type deposits in the Karku deposit (Ladoga region), Materials on geology of deposits of uranium, rare and rare-earth metals, Issue 143, Moscow, pp. 30-39 (In Russian: Михайлов В.А., 2001. К вопросу о генезисе руд типа несогласий на месторождении Карку (Приладожье), Материалы по геологии месторождений урана, редких и редкоземельных металлов, Выпуск 143, Москва, сс. 30-39).
- Mikhailov V.A., Afanasieva E.N., 2004. Geological Map of the Middle Riphean formations of the Pasha-Ladoga area, 1:500 000 scale. Report of ZAO Novaya Lekhta (unpublished).
- Mikhailov V.A., Chernov V.J., Kushnerenko V.K., 2006. Dictyonema shales of the Pribaltic basin – a perspective object of industrial exploitation for uranium and other mineral resources. Materials on geology of deposits of uranium, rare and rare-earth metals, Issue 149, Moscow, pp. 92-98 (In Russian: Михайлов В.А., Чернов В.Я., Кушнеренко В.К.,

2006. Диктионемовые сланцы Прибалтийского бассейна – перспективный объект промышленного освоения на уран и другие полезные ископаемые. Материалы по геологии месторождений урана, редких и редкоземельных металлов, Выпуск 149, Москва, сс. 92-98).
- Mitrofanov F.P., Negrutsa V.Z. (editors), 2002. General stratigraphic scale of the Precambrian of Russia, Apatity, KSC of RAS (In Russian: Митрофанов Ф.Н., Негруца В.З., (редакторы), 2002. Общая стратиграфическая шкала нижнего докембрия России. Апатиты, КНЦ РАН).
- Nazimova Yu.V., 1986. Dolerite dyke of the northern Ladoga area. Operative informational materials of the Karelian branch of the AS USSR. Petrozavodsk, pp. 47-50 (In Russian: Назимова Ю.В., 1986. Долеритовая дайка северного Приладожья, Оперативные информационные материалы Карельского филиала АН СССР, Петрозаводск, сс. 47-50).
- Nemtsov S.N., Sukhanova O.S. et al, 1954. Report about results of prospecting-exploration works, carried out by party No 12 in the area of village Ruskeala city Sortavala (KFSSR) in 1951-53, "Nevskgeologia" (unpublished) (In Russian: Немцов С.Н., Суханова О.С. и др., 1954. Отчет о результатах поисково-разведочных работ, проведенных партией N12 в районе п. Рускеала - г. Сортавала (КФССР) в 1951-53 г.г., «Невскгеология»).
- Neruchev S.G., 1982. Uranium and life in the Earth history. Leningrad, Nedra, 208 p. (In Russian: Неручев С.Г., 1982, Уран и жизнь в истории Земли, Ленинград, Недра, 208 с.).
- Nex, P.A.M., Kinnaird, J.A., Oliver, G.J.H., 2001. Petrology, geochemistry and mineralization of post-collisional magmatism in the southern Central Zone, Damaran Orogen, Namibia. *Journal of African Earth Sciences* 33, pp. 481–502.
- Nikolskaya J.D., Gordienko L.I., 1977, Petrology and metallogeny of granitoid formations of Karelia, Moscow, Nedra, 152 p. (In Russian: Никольская Ж.Д., Гордиенко Л.И., 1977, Петрология и металлогения гранитоидных формаций Карелии, Москва, Недра, 152 с.).
- Nikishin A.M., Zeigler P.A., Stephenson R.A., Cloetingh S.A.P.L., Fure A.V., Fokin P.A., Ershov A.V., Bolotov S.N., Korotaev M.V., Alekseev A.S., Gorbachev V.I., Shipilov E.V., Lankreijer A., Bembinova E.Yu., Shalimov I.V., 1996. Late Precambrian to Triassic history of the East European Craton: dynamics of sedimentary basin evolution. *Tectonophysics*, 268, pp. 23-63.

- Nikolskaya J.D., Gordienko L.I., 1977. Petrology and metallogeny of granitoid formations of the Karelia, Moscow, Nedra, 152 p. (In Russian: Никольская Ж.Д., Гордиенко Л.И., 1977. Петрология и металлогения гранитоидных формаций Карелии, Недра, 152 с.).
- O'Brien H.E., Peltonen P., 1998. Comparison of diamondiferous kimberlites and lamproites of the Fennoscandian Shield, In: Svekalapko. Europrobe project Workshop Abstracts, Repino, Russia, 48 p.
- Ohlson L.G., 1979. Tungsten occurrences in Central Sweden // *Econ. Geol.* Vol. 74, No 5, pp. 1012-1034.
- Ojakangas R.W., Marmo J.S., Heiskanen K.I., 2001. Basin evolution of the Palaeoproterozoic Karelian Supergroup of the Fennoscandian (Baltic) Shield, *Sedimentary Geology*, No 141-142, pp. 255-285.
- Onjushko I.S. (responsible executors), 1979. Rules of location of uranium mineralization in the basal sediments of the Vendian Gdov horizon of the Baltic shield slopes. Report of VSEGEI (unpublished) (In Russian: Оношко И.С. (ответственный исполнитель), 1979. Закономерности размещения уранового оруденения в базальных отложениях гдовского горизонта венда склонов Балтийского щита. Отчет ВСЕГЕИ).
- Pearce J.A., 1983. Role of sub-continental lithosphere in magma genesis at active continental margins. In: Hawkesworth C.J., Hurry M.J. (editors) *Continental basalts and mantle xenoliths*, Shiva Publ., Nantwick.
- Pearce J.A., 1996. Source and setting of granitic rocks. *Episodes* 19, pp. 120-125.
- Pekkarinen L., 1979. The Karelian formations and the depositional basement in the Kiitelysvaarara-Värtisilä area, East Finland, Geological Survey of Finland, *Bulletin*, Volume 301.
- Peltonen P., Kontinen A., Huhma H., 1998. Petrogenesis of the mantle sequence of the Jormua Ophiolite (Finland): melt migration in the upper mantle during Palaeoproterozoic continental breakup. *Journal of Petrology*, 39, pp. 297-329.
- Petrov Yu.V. (responsible executor), 2006. Prospecting of the high-profitable uranium deposits of the unconformity-type in the limits of the Karkunlampi ore field (40 km²) and the Salmi area on the base of the drilling and complex of the advance geophysical works. Report of "Nevskgeologia", (unpublished) (In Russian: Петров Ю.В. (ответственный исполнитель), 2006. Поиски высокорентабельных месторождений урана «типа несогласия» в пределах рудного поля Каркунлампи (40 кв. км) и на Салминской

- площади на основе бурения и опережающих геофизических работ. Отчёт «Невскгеология», С.-Петербург).
- Polekhovsky Yu.S., Zolotarev A.A., Shurilov A.V., Narina N.A., 2002. Agates in the Riphean basaltoids in the rivere Tulemajoki (Ladoga region, Karelia). In: Mineralogical museums. St-Petersburg, pp. 330-331 (In Russian: Полеховский Ю.С., Золотарёв А.А., Шурилов А.В., Харина Н.А., 2002, Агаты в рифейских базальтоидах на р. Тулемайоки (Приладожье, Карелия). В сборнике: Минералогические музеи. С.-Петербург, сс. 330-331).
- Polekhovsky Yu.S., Bogdanov R.V., Krivitsky A.G., Yurchenko S.A., 2005. The valence condition of uranium in the ores of the Karku deposit (Karelia), Materials of the I International Scientific Conference “Geology, Geochemistry and Ecology of the North-West of the Russia”, pp. 68-71 (In Russian: Полеховский Ю.С., Богданов Р.В., Кривицкий А.Г., Юрченко С.А., 2005. Валентное состояние урана в рудах месторождения Карку (Карелия), Материалы I Международной Научной Конференции “Геология, Геохимия и Экология Северо-Запада России”, сс. 68-71).
- Polekhovsky Yu.S., Tarasova I.P., Britvin S.N., Kol'tsov A.B., Shurilov A.V., 2005 (2). Geology and mineral parageneses of Karku uranium deposit (North-Eastern Ladoga area, Karelia), Report of St-Petersburg State University (unpublished) (In Russian: Полеховский Ю.С., Тарасова И.П., Бритвин С.Н., Кольцов А.Б., Шурилов А.В., 2005. Геология и минеральные парагенезисы уранового месторождения Карку (Северо-восточное Приладожье, Карелия), Отчёт Санкт-Петербургского Государственного Университета, Санкт-Петербург).
- Polekhovsky Yu.S., Tarasova I.P., Shurilov A.V., 2007. Ore parageneses of radioactive mineralization of the Northern Ladoga area (Karelia). Report of the St.-Petersburg State University (unpublished).
- Polikarpov V.I., Ostanin G.H., Gorjunov E.N., Bogdanova V.G., Kovaliova Y.V., Belyaeva L.N., 1976. Reports about prospecting survey works of the Lesnaya party No 12 in the area of the Janisjarvi structure in the South-Western Karelia during 1973-75 (unpublished) (In Russian: Поликарпов В.И., Останин Г.Х., Горюнов Е.Н., Богданова В.Г., Ковалёва Ю.В., Беляева Л.Н., 1976. Отчёт о поисково-съёмочных работах Лесной партии № 12 на площади Янисъярвинской структуры в Юго-Западной Карелии в 1973-75 гг, Ленинград).

- Polikarpov V.I. (responsible executor), 1993. About results of the prognostic-geological works of 1:50000 scale, led by the Central expedition No 2 in the North-Eastern part of the Ladvinsky depression and its surrounding (Salminskaya area) in 1990-1993, Report of "Nevskgeologia" (unpublished) (In Russian: Поликарпов В.И., 1993 О результатах прогнозно-геологических работ масштаба 1:50000, проведенных Центральной экспедицией №2 в северо-восточной части Ладвинского прогиба и его обрамления (Салминская площадь) в 1990-1993 г.г. Геологическое задание 2-54, Отчёт «Невскгеология»).
- Puura V., Flodén T., 1999. Rapakivi-granite-anorthosite magmatism – a way of thinning and stabilization of the Svecofennian crust, Baltic Sea Basin, *Tectonophysics*, 305, pp. 75-92.
- Raffensperger J.P., Garven G., 1995. The formation of unconformity-type uranium-ore deposit, *American Journal of Science*, vol. 295, pp. 581-636.
- Rämö O.T., 1991. Petrogenesis of the Proterozoic rapakivi granites and related basic rocks of the southeastern Fennoscandia: Nd and Pb isotopic and general geochemical constrains. *Geological Survey of Finland, Bulletin 355*, 161 p.
- Rämö O.T., Haapala I., 1996. Rapakivi granite magmatism: a global review with emphasis on petrogenesis, In: Demaiffe D. (editor), *Petrology and Geochemistry of magmatic suites of rocks in the continental and oceanic crust*, ULB, Bruxelles, pp. 177-200.
- Rämö O.T., Korja A., 2000. Mid-Proterozoic evolution of the Fennoscandian Shield. Extended abstracts, 31st IGO, Rio de Janeiro.
- Rämö O.T., Korja A., Haapala I., Eklund O., Fröjjiö S., Vasjoki M., 2000. Evolution of the Fennoscandian lithosphere in the Mid-Proterozoic: the rapakivi magmatism. In: Pesonen L.J., Korja A., Hjelt S.-E. (editors), *Lithosphere 2000: a symposium on the structure, composition and evolution of the lithosphere in Finland*, Espoo, Otaniemi, October 4-5, 2000. Institute of Seismology, University of Helsinki, Reports S-41, pp.129-136.
- Rämö T., 2001. Isotopic composition of pyterlite in Vyborg (Viipuri), Wiborg batholith, Russia. *Bulletin of Geological Survey of Finland*, 73, Parts 1-2, pp. 111-115.
- Rämö T., Mänttiäri I., Vaasjoki M., Upton B.G.J., Sviridenko L.P., 2001. Age and significance of Mesoproterozoic CFB magmatism, Lake Ladoga region, NW Russia. *Geology Society of America*, 33 (6).
- Read D., Black S., Buckby T., Hellmuth K.-H., Marcos N., Siitari-Kauppi M., 2007. Secondary uranium mineralization in southern Finland and its relationship to recent glacial events, *Global and Planetary Change 2007*. Available at www.sciencedirect.com.

- Rehtijärvi P., Äikäs O., Mäkelä M., 1979. A Middle Precambrian uranium- and apatite-bearing horizon associated with the Vihanti zinc ore deposit, Western Finland. *Economic Geology*, volume 74, No 5, pp.1102-1117.
- Roman N.A., 2004. Epigenetic alterations of the Karku deposit hosting rocks by the example of the Ore body 3. *Materials on geology of deposits of uranium, rare and rare-earth metals*, Issue 146, Moscow, pp 41-44 (In Russian: Роман Н.А., 2004. Эпигенетические изменения вмещающих пород месторождения Карку на примере третьей рудной залежи. *Материалы по геологии месторождений урана, редких и редкоземельных металлов*, Выпуск 146, Москва, сс.41-44).
- Roy C., Halaburda J., Thomas D., Hersekorn D., 2005. Millenium Deposit – Basement-hosted derivative of the Unconformity Model. *International Symposium Uranium Production and Raw Materials for the Nuclear Fuel Cycle*. Vienna, Austria 20-24 June, pp. 42-45.
- Rumyantsev V.A. (responsible editor), 2002. *Lake Ladoga, an atlas*, St-Petersburg, 128 p. (In Russian: Румянцев В.А. (ответственный редактор), *Озеро Ладога, атлас*, 2002, Санкт-Петербург, 128 с.).
- Ruzicka V., 1993. Unconformity-type Uranium Deposits. In: R.V. Kilkham, W.D. Sinclair, R.I. Thorpe (Editors), *Mineral Deposit Modeling*, Geological Association of Canada, Special Paper 40, pp. 125-149.
- Rybakov S.I. and Golubev A.I. (editors), 1999. *Metallogeny of Karelia*. Petrozavodsk, KSC of RAS, 340 p. (In Russian: Рыбаков С.И. и Голубев А.И. (редакторы) 1999. *Металлогения Карелии*, Петрозаводск, КНЦ РАН, 340 с.).
- Saranchina G.M., 1972. *Granitoid magmatism, metamorphism and metasomatic of the Precambrian (by the example of the Ladoga region and other areas)*, Leningrad State University, 128 p. (In Russian: Саранчина Г.М., 1972. *Гранитоидный магматизм, метаморфизм и метасоматоз докембрия (на примере Приладожья и других областей)*, ЛГУ 128 с.).
- Sangely, Michels R., Chaussidon M., Brouand M., Cuney M., 2005. Abiotic macromolecular organic material in Proterozoic rocks. *Geochim Cosmochim Acta*, submitted.
- Scheglov A.D., Moskaleva V.N., Markovsky B.A., 1993. *Magmatism and metallogeny of riftogenic systems of eastern part of the Baltic Shield*, St-Petersburg, Nedra (In Russian: Щеглов А.Д., Москалева В.Н., Марковский Б.А., 1993. *Магматизм и металлогения рифтогенных систем восточной части Балтийского щита*, С-Петербург, Недра).

- Sergeev S.A., Bibikova E.V., Levchenkov O.A., Lobach-Juchenko S.B., Yakovleva S.Z., Ovchinnikova G.V., Neymark L.A., Komarov A.N., 1990. Isotope geochronology of vodlozero gneiss complex, *Geochemistry*, vol. 1, pp. 73-83 (In Russian: Сергеев С.А., Бибикина Е.В., Левченков О.А., Лобач-Жученко С.Б., Яковлева С.З., Овчинникова Г.В., Неймарк Л.А., Комаров А.Н., 1990. Изотопная геохронология водлозерского гнейсового комплекса, *Геохимия*, №1, сс. 73-83).
- Sergeev S.A., Lokhov K.I., Sergeev A.S., Polekhovsky Yu.S., 2001. An experience of $^{207}\text{Pb}/^{206}\text{Pb}$ age determination of accessory minerals with the multichannel mass-spectrometer with ionization in inducted-coupled plasma with local laser ablation. XVI Symposium on geochemistry of isotopes in the name of academic A.P. Vinogradov, Moscow, pp. 225-226 (In Russian: Сергеев С.А., Лохов К.И., Сергеев А.С., Полеховский Ю.С., 2001. Опыт определения $^{207}\text{Pb}/^{206}\text{Pb}$ возраста по аксессуарным минералам на многоканальном масс-спектрометре с ионизацией в индуктивно-связанной плазме с использованием локального лазерного пробоотбора. XVI симпозиум по геохимии изотопов им. акад. А.П. Виноградова. Москва, сс. 225-226).
- Sharikov P.I., Potapov K.I. (responsible executors), 1986. Evaluation of prospects of pre-Vendian and pre-Riphean unconformities in the Southern Ladoga area. Report of "Nevskgeologia" (unpublished) (In Russian: Шариков П.И., Потапов К.И. (ответственные исполнители), 1986. Оценка перспектив ураноносности предвендской и предрифейской поверхностей несогласия в Южном Приладожье. Отчет «Невскгеология»).
- Sharkov E.V., 1999. Intraplate magmatic systems of middle of the Proterozoic by the example of anorthosite-rapakivi-granite complexes of the Baltic and Ukraine Shields, *Russian journal of Earth science*, vol. 1, No 4, June, pp. 311-337 (In Russian: Шарков Е.В. 1999. Внутриплитные магматические системы середины протерозоя на примере анортозит-рапакивигранитных комплексов Балтийского и Украинского Щитов, *Российский журнал наук о Земле*. Том 1, № 4, июнь, сс. 311-337).
- Sharov N.V. (editor), 1993. Structure of the lithosphere of the Baltic shield, Moscow, RAS, National geophysical committee (In Russian: Н.В. Шарова (редактор), 1993. Строение литосферы Балтийского щита, РАН, Национальный геофизический комитет).
- Shinkarev N.F., Grigor'eva L.V., Ivanikov V.V., 1985. Granitoid magmatism and metallogeny of areas of late-Precambrian activity of the Baltic Shield. Patterns of concentrations of ore elements in the granitoid formations of the Karelia-Cola Shield, Apatity (In Russian:

- Шинкарев Н.Ф., Григорьева Л.В., Иваников В.В., 1985. Гранитоидный магматизм и металлогения областей позднедокембрийской активности Балтийского щита. Закономерности концентрации рудных элементов в гранитоидных формациях Карело-Кольского щита, Апатиты).
- Shuldiner V.I., Levchenkov O.A., Jakovleva S.Z., 1999. Upper Karelian in the stratigraphic scale of the Russia: choosing of lower limit and regional subdivisions of the stratotype domain. *Stratigraphy. Geological correlation*, Vol. 7, (In Russian: Шульдинер В.И., Левченков О.А., Яковлева С.З., 1999. Верхний Карелий в стратиграфической шкале России: выбор нижней границы и региональных подразделений стратотипической области, *Стратиграфия. Геологическая корреляция*, том 7).
- Shurilov A.V., Polekhovsky Yu.S., Petrov Yu.V., 2003. Geology and ore paragenesis of the Karku uranium deposit (North-Eastern Ladoga region), *Uranium Geochemistry. Uranium Deposits-Natural Analogs-Environment*, Nancy, 347-350.
- Shurilov A.V., Polekhovsky Yu.S., Tarasova I.P., Kister P., 2005. Karku uranium deposit: structural localization and ore mineralogy, Pasha – Ladoga basin, Russia. IAEA Tech., Doc., Vienna, pp. 206-209.
- Shustova L.E., 1997. Peculiarities of the Earth crust structure of main tectonotypes of the Baltic Shield, *Regional geology and Metallogeny*, No 6, pp. 54-63 (In Russian: Шустова Л.Е., 1997. Особенности строения земной коры основных тектонотипов Балтийского щита, *Региональная геология и металлогения*, № 6, сс. 54-63).
- Skorospelkin S.A., 1974. Granite-gneiss domes and uranium mineralization of median massifs. *Materials on geology of uranium deposits. Issue 35*, Moscow (In Russian: Скорospelкин С.А., 1974. Гранито-гнейсовые купола и урановое оруденение срединных массивов. /Мат. по геологии урановых месторождений, информ. сб., вып. 35, Москва).
- Skorospelkin S.A. (responsible executor), 2002. About results on estimation of prospects of discovering of uranium deposits near the pre-Riphean and pre-Palaeoproterozoic surfaces of the structural-stratigraphic unconformities on the base of compilation of geological-prognosis map of the 1:200 000 scale of Onega-Ladoga area, carrying out of specialized geological mapping of 1:50 000 scale in Svyr-Oyat and Ladva areas and reconnaissance drilling. Geological program 2-61. Report of “Nevskgeologia”(unpublished) (In Russian: Скорospelкин С.А. (ответственный исполнитель), 2002. О результатах работ по оценке перспектив выявления месторождений урана вблизи дорифейской и донижнепротерозойской поверхностей структурно-стратиграфических несогласий

- на основе составления геолого-прогнозной карты масштаба 1:200000 на Онежско-Ладожскую площадь, проведения специализированного геологического картирования масштаба 1:50000 на Свирско-Оятской и Ладвинской площадей и рекогносцировочного бурения. Геол. задание 2-61. Отчёт «Невскгеология»).
- Skorospelkin S.A., Dolgushina I.S., 2004. Map of the deep structure of the Pasha-Ladoga area, 1:500 000 scale. Report of ZAO Novaya Lekhta (unpublished).
- Sokolov V.A. (editor), 1984. Stratigraphy of Precambrian of Karelian ASSR (Archaean, Lower Proterozoic). Karelian branch of the Academy of Science of the USSR, 115 p. (In Russian: Соколов В.А. (отв. ред.), 1984. Стратиграфия докембрия Карельской АССР (Архей, Нижний Протерозой). Петрозаводск, Изд-во КарФАН СССР, 115 с.
- Sokolov Y.M. (editor), 1982. Data for the stratigraphic dictionary on the Precambrian of Karelia, Petrozavodsk, 136 p. (In Russian: Соколов Ю.М., 1982. Данные для стратиграфического словаря Карелии, Петрозаводск, 136 с.).
- Sorjonen-Ward, P., 1993. An overview of structural evolution and lithic units within and intruding the late Archean Hattu schist belt, Ilomantsi, eastern Finland. Geological Survey of Finland Special Paper, 17, 9-102.
- Spiridonov E.M., Ladygin V.M., Frolova Yu.V., 2001. When and how vesicular lavas transform into mandelstones, including agate-bearing ones. In: First All-Russia palaeovolcanogenic symposium. Petrozavodsk, pp. 123-124 (In Russian: Спиридонов Э.М., Ладыгин В.М., Фролова Ю.В., 2001. Когда и как пузыристые лавы превращаются в мандельштейны, в том числе агатоносные. В: Первый Всероссийский палеовулканоогический симпозиум. Петрозаводск, сс. 123-124).
- Stepanov K.I. (responsible executor) 2006. State Geological Map of the Russian Federation, 1:200 000 scale (Karelian series), Sheets P-35-XXIV, P-36-XIX, (In Russian: Степанов К.И. (ответственный исполнитель), 2006. Государственная геологическая карта Российской Федерации. Масштаб 1:200 000 (Карельская серия). Листы P-35-XXIV, P-36-XIX).
- Stepanov K.I., Sanina G.N., Bogachev V.A. 2006. Report on geological research of 1:200 000 scale of the Sortavala area, compilation and preparation to the publication of set of State Geological Map of the Russian Federation of 1:200 000 scale, sheets P-35-XXIV, P-36-XIX (unpublished) (In Russian: Степанов К.И. (ответственный исполнитель), 2006. По геологическому доизучению масштаба 1:200000 Сортавальской площади, составлению и подготовке к изданию комплекта Государственной геологической

- карты Российской Федерации масштаба 1:200000 листов P-35-XXIV, P-36-XIX (Карельская серия), Листы P-35-XXIV, P-36-XIX).
- Stem H.J., Markey R.J., 1996. Re-Os dating of molybdenites from Pitkjaranta, Russia. Reveals two temporary distinct periods of ore formation, a mask on late svecofennian Mo-W ores. In: Rapakivi granatites and related rocks, Helsinki, pp. 68-70.
- Sudovukov N.G., 1954. Tectonic, metamorphism, magmatization and granitization of rocks of Ladoga series. Works of laboratory of Precambrian of AS USSR, iss. 4, 199 p. (In Russian: Судовиков Н.Г., 1954. Тектоника, метаморфизм, магматизация и гранитизация пород Ладожской серии. Труды лаборатории докембрия АН СССР, вып. 4, 199).
- Sudovikov N.G., 1964. Regional metamorphism and some problems of the petrology, Leningrad University, Leningrad, 552 p. (In Russian: Судовиков Н.Г., 1964. Региональный метаморфизм и некоторые проблемы петрологии, Ленинградский Университет, Ленинград, 552 с.).
- Sukhanova O.S., 1952. Report about results of prospecting works carried out in the Pitkjaranta and Sortavala district by party No 4 of the KF SSR during 1949-51, "Nevskgeologia" (unpublished) (In Russian: Суханова О.С. 1952. Отчет о результатах поисково-разведочных работ, проведенных партией №4 в Питкярантском и Сортавальском районах КФ ССР в 1949-51 гг., "Невскгеология").
- Svetov A.P., 1979. Platform basalt volcanism of karelides of Karelia, Leningrad, 208 p. (In Russian: Светов А.П., 1979. Платформенный базальтовый вулканизм карелид Карелии, Ленинград, 208 с.).
- Svetov A.P., Sviridenko L.P., Ivaschenko V.I., 1990. volcano-plutonism of svecokareliides of the Baltic Shield, Petrozavodsk, Karelian Scientific Center of the Academy of Science of the USSR (In Russian: Светов А.П., Свириденко Л.П., Иващенко В.И., 1990. Вулкано-плутонизм свекокарелид Балтийского щита, Петрозаводск, КНЦ АН СССР).
- Svetov A.P., Sviridenko L.P., 1991. Magmatism of suture zones of the Baltic Shield, Leningrad, Nauka (In Russian: Светов А.П., Свириденко Л.П., 1991. Магматизм шовных зон Балтийского щита, Ленинград, Наука).
- Svetov S.A., 2004. Evolution of the magmatic systems in the ocean-continent transition zone in the Archaean Eastern part of the Fennoscandian Shield. Abstracts of the PhD thesis, SPbGU (In Russian: Светов С.А., 2004. Эволюция магматических систем в зоне перехода океан-континент в Архее Восточной части Фенноскандинавского Щита,

- СПбГУ, автореферат Диссертации на соискание учёной степени кандидата геолого-минералогических наук, 42 с.).
- Takahashi, Y., Yoshida, H., Sato, N., Hama, K., Yusa, Y., Shimizu, H., 2002. W- and M-type tetrad effects in REE patterns for water-rock systems in the Tono uranium deposit, central Japan. *Chemical Geology*, v. 184, pp. 311-335.
- Trustedt O., 1907. Arslagerstatten von Pitkaranta am Ladoga-zee Helsingfors, *Bulletin Committee Geologic of Finland*, N 19, pp. 333-334.
- Tugarinov A.I., Bibikova E.V., 1977. Geochronology of the Baltic Shield according to zirconometry data, Moscow, 142 p. (In Russian: Тугаринов А.И., Бибикина Е.В., 1977, Геохронология Балтийского Щита по данным цирконометрии, Москва, 142 с.)
- Vaasjoki M., Äikäs O., Rehtijärvi P., 1980. The age of mid-Proterozoic phosphatic metasediments in Finland as indicated by radiometric U-Pb dates. *Lithos*, vol. 13, No 3, pp. 257-262.
- Vaasjoki M., Sakko M., 1988. The evolution of the Raahe-Ladoga zone in Finland: isotopic constraints. *Geological Survey of Finland, Bulletin* 343.
- Vaasjoki M., Rämö O.T., Sakko M., 1991. New U-Pb ages from the Wiborg rapakivi area: constraints on the temporal evolution of the rapakivi granite-anorthosite-diabase dyke association of southeastern Finland. In: Haapala I., Condie K.S., (editors.), *Precambrian Granitoids-Petrogenesis, Geochemistry and Mineralogy, Precambrian Researches*, 51, pp. 227-243.
- Vaasjoki, M., Sorjonen-Ward, P. & Lavikainen, S., 1993. U-Pb age determinations and sulfide Pb-Pb characteristics from the late Archean Hattu schist belt, Ilomantsi, eastern Finland. *Geological Survey of Finland Special Paper*, 17, pp.103-131.
- Velichkin V.I. (responsible executor), 2001. Results of the complex geologic-mineralogical research of the Karku uranium deposit in the North-eastern Ladoga region and comparison of the ore districts of the Ladoga and Athabasca, Report of IGEM RAU (unpublished) (In Russian: Величкин В.И., 2001 Результаты комплексного геолого-минералогического изучения уранового месторождения Карку в Северо-Восточном Приладожье и сравнении рудных районов Приладожья и Атабаска, Отчёт ИГЕМ РАН).
- Velichkin V.I., Kushnerenko V.K., Tarasov N.N., Andreeva O.V., Kiselyova G.D., Krylova T.L., Doinikova O.A., Golubev V.N., Golovin V.A., 2005. Geology and Formation Conditions of the Karku Unconformity-Type Deposit in the Northern Ladoga Region (Russia). *Geology of Ore Deposits*, vol. 47, No 2, pp. 99-126 (In Russian: Величкин В.И.,

- Кушнеренко В.К., Тарасов Н.Н., Андреева О.В., Киселёва Г.Д., Крылова Т.Л., Дойникова О.А., Голубев В.Н., Головин В.А., 2005. Геология и условия формирования месторождения типа «несогласия» Карку в Северном Приладожье (Россия). Геология рудных месторождений, том 47, № 2, pp. 99-126).
- Velikoslavinsky D.A., Birkis A.P., Bogatkov O.A., 1978. Anorthosite-rapakivi granite formation. Leningrad, Nauka, 296 p. (In Russian: Великославинский Д.А., Биркис А.П., Богатиков О.А., 1978, Анортозит-рапакивигранитная формация, Ленинград, Наука, 296 с.).
- Voinov A.S., Polekhovsky Y.S., 1985. Quartz-feldspar metasomatites of eastern part of the Baltic shield (geological peculiarities and geochemical specialization), in: Vinogradov A.N. (editors), Regularities of concentration of ore elements in the granitoid formations of the Karelian-Cola region, Cola branch of AS of the USSR, pp. 53-61 (In Russian: Воинов А.С., Полеховский Ю.С., 1985. Кварц-полевошпатовые метасоматиты восточной части Балтийского щита (геологические особенности и геохимическая специализация). В: Виноградов А.Н. (редактор), Закономерности концентрации рудных элементов в гранитоидных формациях Карело-Кольского региона, Кольский филиал АН СССР, сс. 53-61).
- Ziegler P.A., 1981. Evolution of sedimentary basins in North-West Europe, In: Petroleum geology of the continental shelf of N-W Europe, London, pp. 3-39.

GENERAL APPENDIX 1

FIGURES

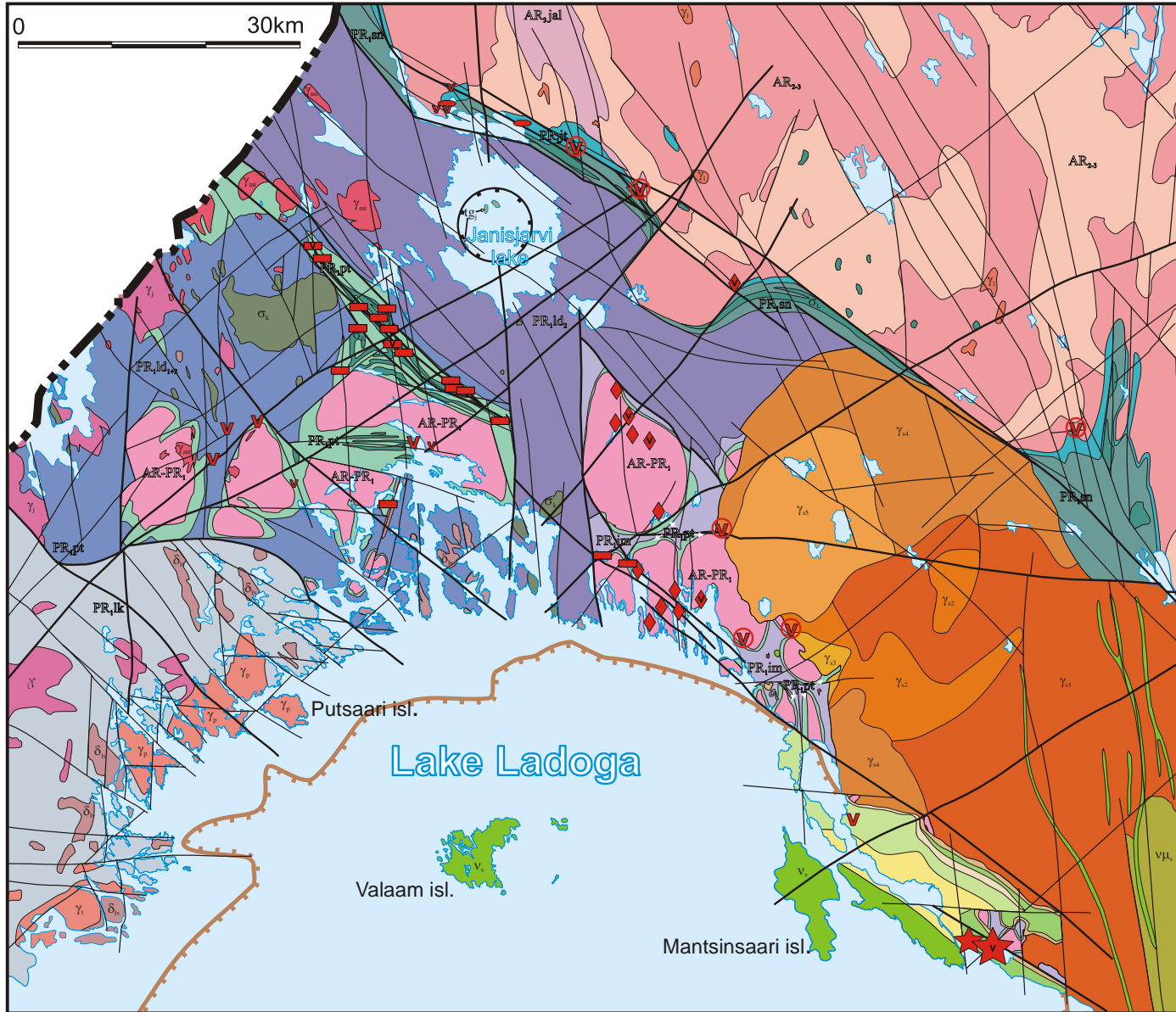


Figure 1.1. Geological map of the Northern Ladoga area.
 Compiled from “Nevskgeologia”, VSEGEI, “Mineral”, ZAO “NOVAYA LEKHTA” data and Amelin et al., 1997.

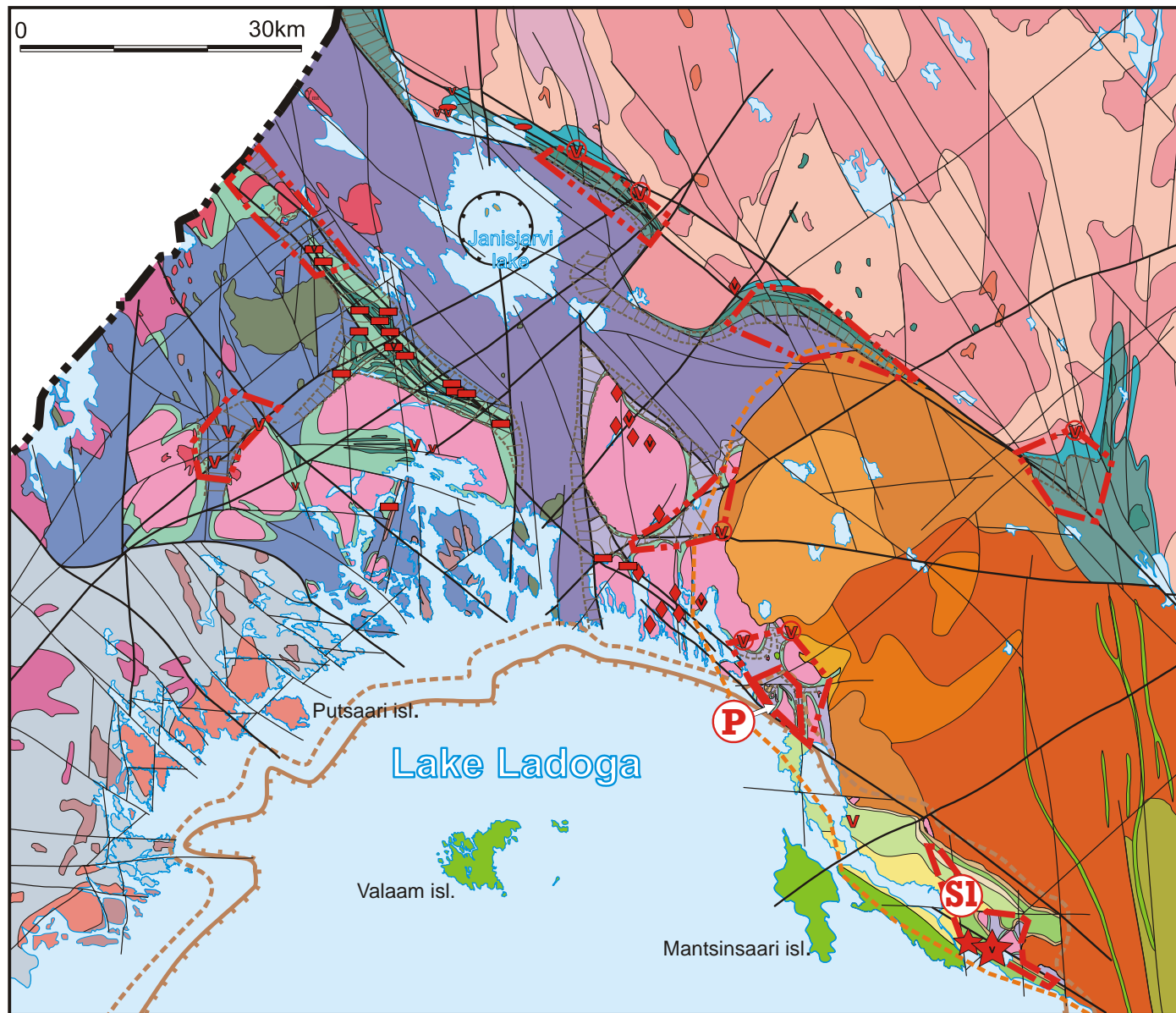


Figure 1.2. Prognostic geological map of the Northern Ladoga area.

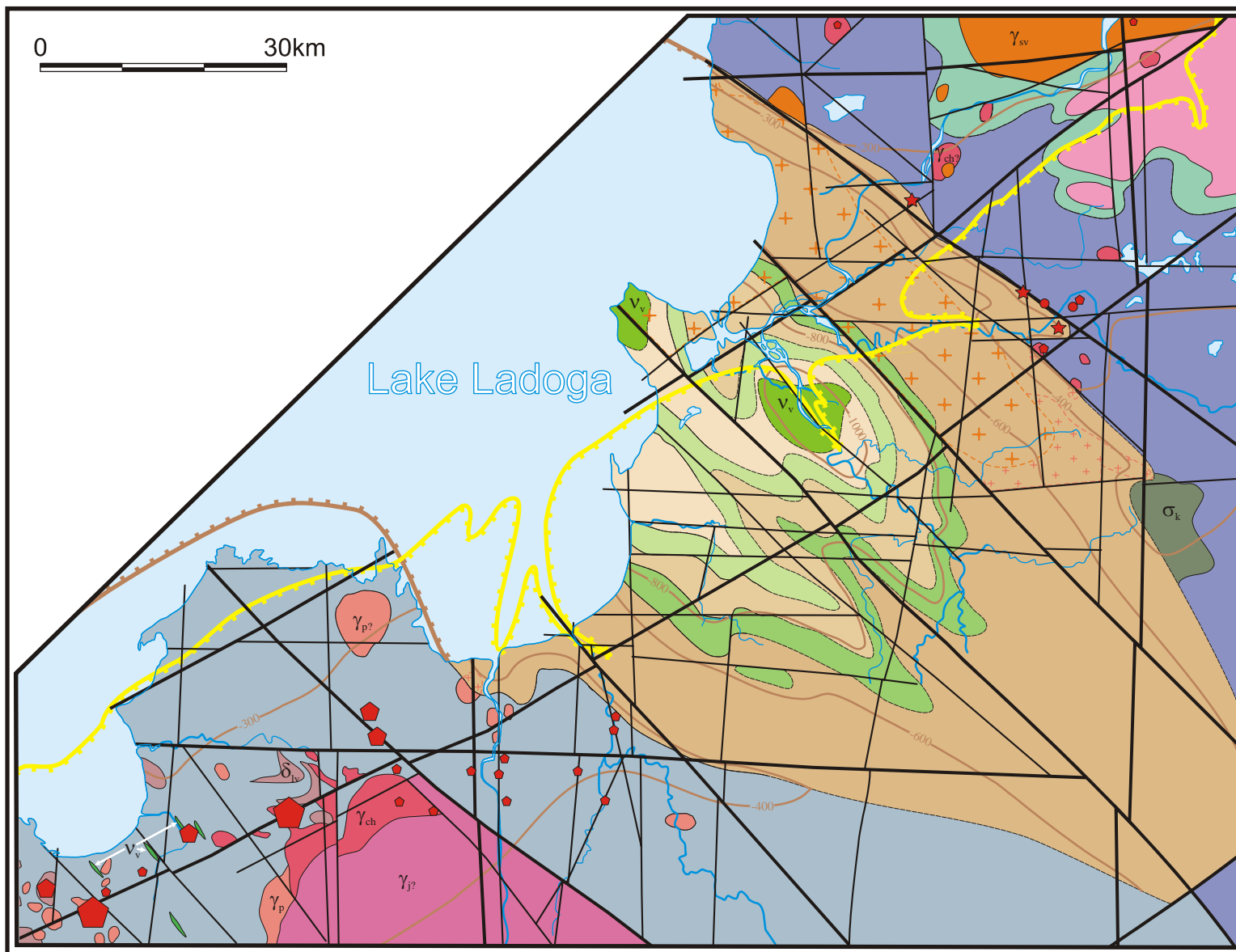


Figure 2.1. Geological map of the South-Eastern Ladoga area. Based on “Nevskgeologia” data.

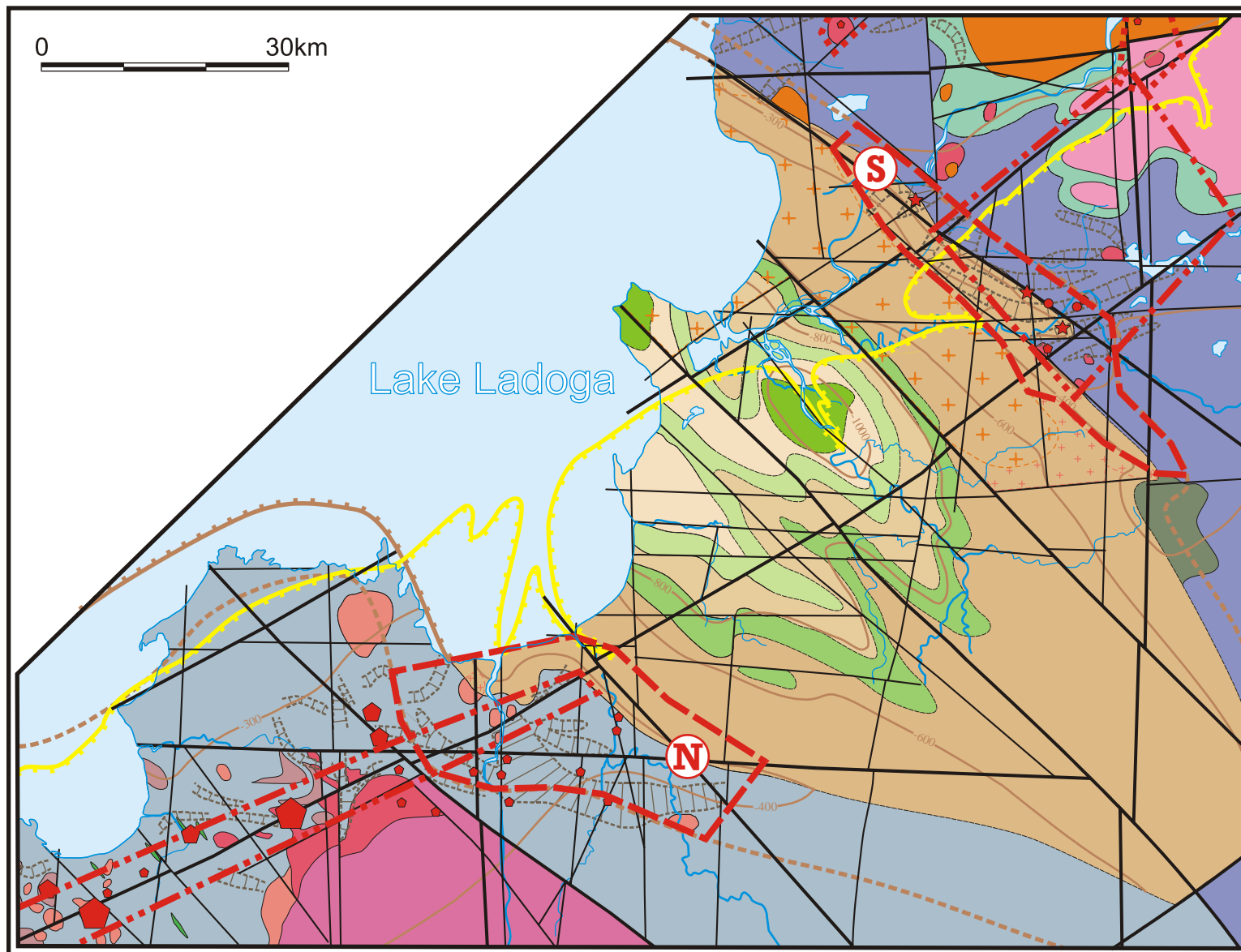


Figure 2.2. Prognostic geological map of the South-Eastern Ladoga area.

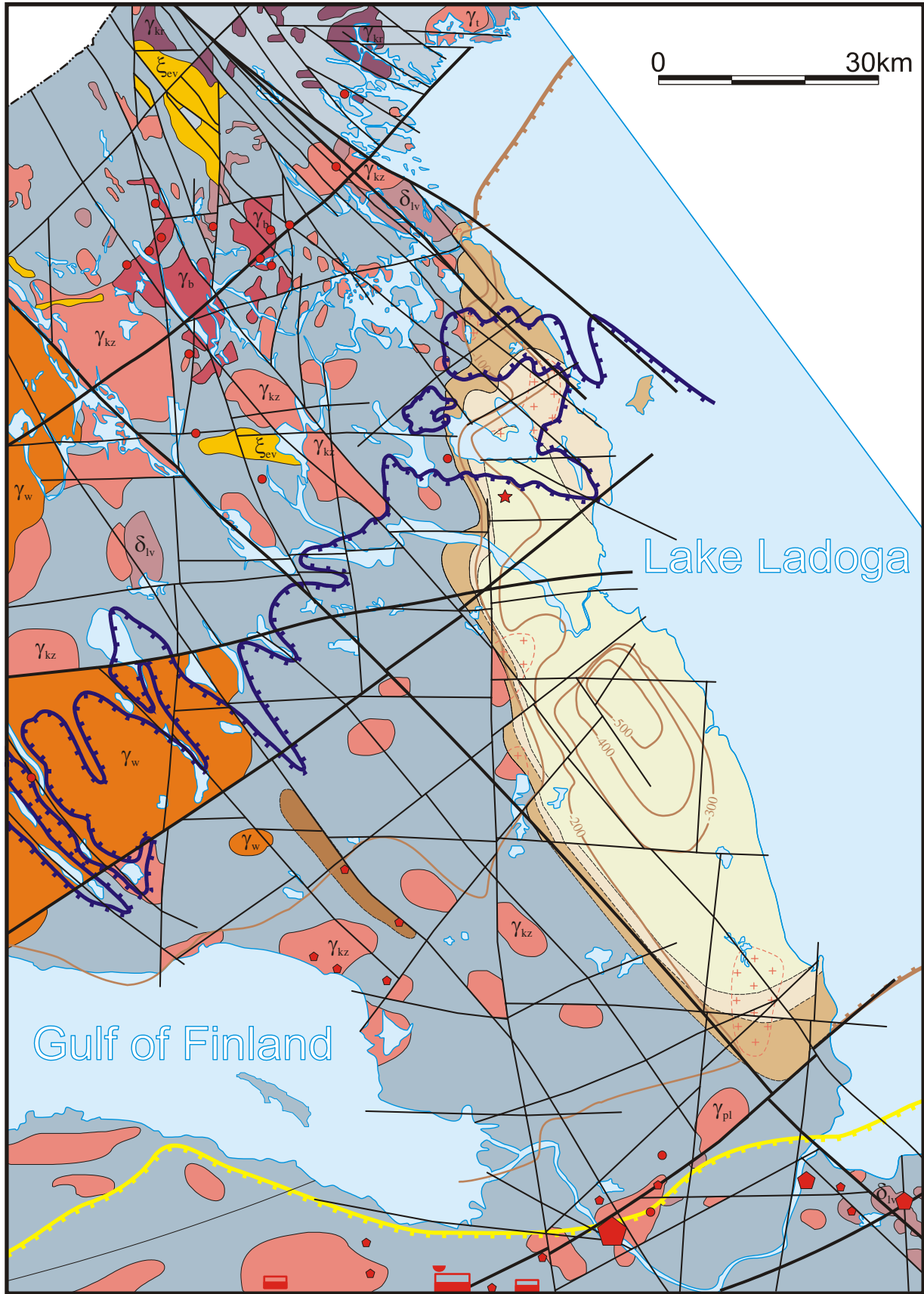


Figure 3.1. Geological map of the Western Ladoga area.
Based on “Nevskegeologia”, “Mineral”, VSEGEI and ZAO “Novaya Lekhta” data.

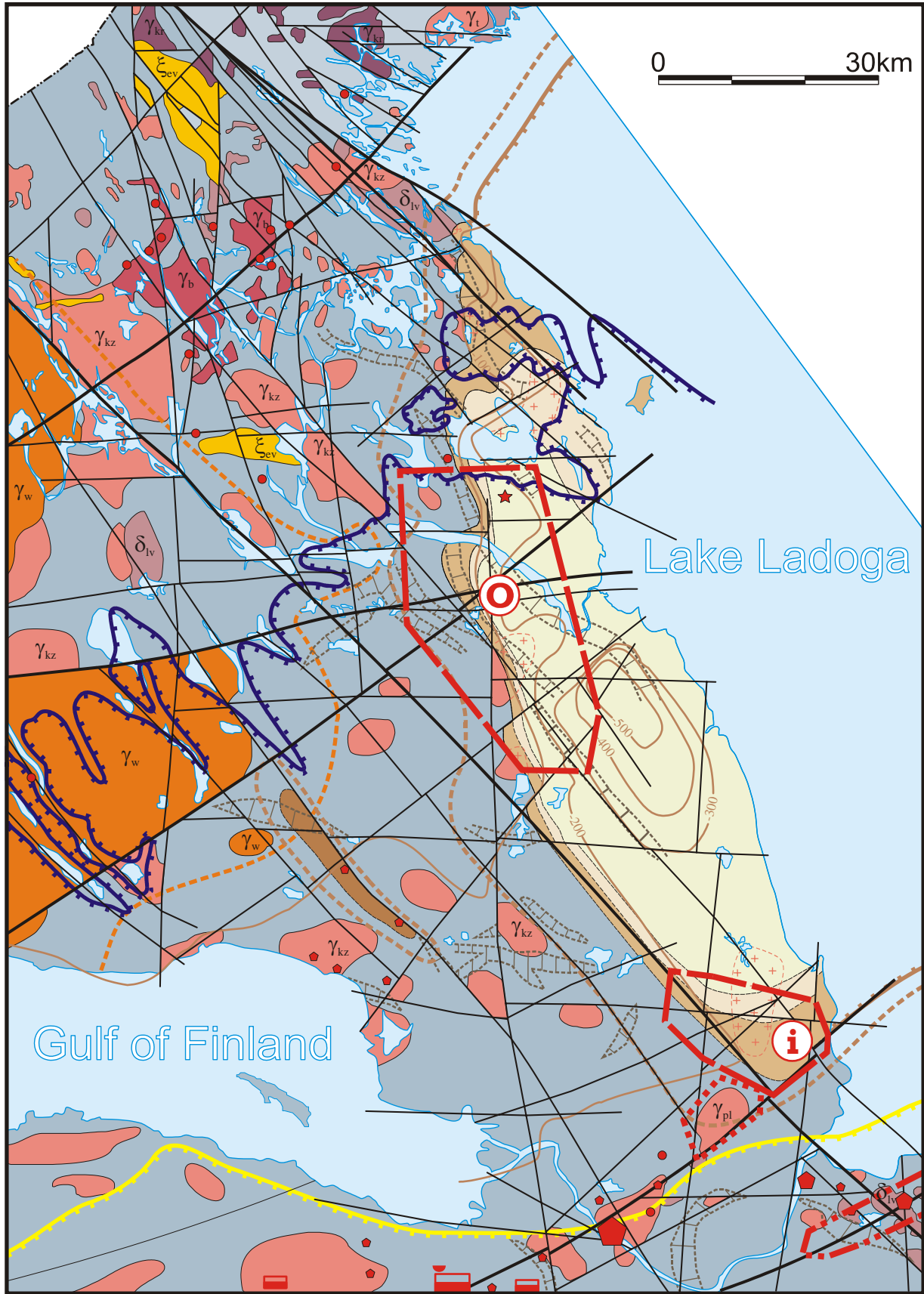

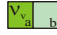




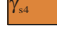
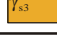


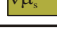

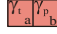
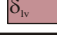

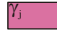










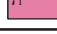















Figure 3.2. Prognostic geological map of the Western Ladoga area.

Figure. 4. Legend to geological and prognostic maps of the Northern, South-Eastern and Western Ladoga areas.


















Eontheme	Local subdivision	Isotopic age, Ma	Northern Ladoga				
Neoproterozoic	Lower Vendian						
	Upper Riphean	770-720		Janisjarvi impact complex: tagamaite, zuvite, andesite.			
Mesoproterozoic	Middle Riphean	1460-1250		Valaam complex: gabbro, dolerite; a-on land, b-under Lake Ladoga.			
				R,ph, Pasha suite: qtz-fsp sandstone, gritsone, siltstone.			
	Lower Riphean			R,s, Salmi suite: a - lower subsuite basalt, b - middle subsuite qu-fsp sandstone, gritsone, siltstone, c - upper subsuite basalt.			
				R,pr, Priozersk suite: qtz-fsp sandstone, gritstone, siltstone.			
			1535,4		Salmi massif, VI phase: porphyry biotite granite with fine-grained groundmass.		
			1538,4-1535		Salmi massif, VI phase: even-grained biotite granite.		
			1538		Salmi massif, V phase: albite-lithian siderophyllite granite.		
					Salmi massif, V phase: porphyric biotite-amphibole granite with fine-grained groundmass.		
			1540,6-1535,3		Salmi massif, IV phase: wiborgite, pyterlite.		
			1546,7		Salmi massif I and II phases: gabbro-norite, monzonite.		
			1640-1610?				
			1645-1615				
			Palaeoproterozoic	Kalevian	1810-1770		
					ca1800		Matkaselsky complex: bi-mica leucogranite.
1870-1860		Tervus (a) and Putsaari (b) complexes: bt granite, diorite, trondijemite.					
1880-1865		Lauvatsaari-Impiniemi complex tonalite, Qtz-diorite.					
1883							
1890-1880		Kaalamo complex: pyroxenite, gabbro, granodiorite, plagiogranite.					
1900-1890		Jakkima intrusive complex: tonalite and granodiorite.					
		PR _{ld} , Ladoga group, Kontiosaari, Naatselka, Pyalkjarvi, Hunuki, Velimyaki suites: quartzite, quartz-biotite, garnet-stavrolite, amphibole-biotite schist.					
		PR _{im} , Ladoga group, Impilakhti suite: biotite, garnet-biotite, cordierite gneiss and schist, migmatite.					
		PR _{ld,2,3} , Ladoga group undivided: sillimanite-muskovite-ortoclase gneiss, quartz-biotite schist, migmatite.					
Ludicovian-Kalevian				PR _{lk} , Lakhdenpohja group: garnet, sillimanite, staurolite gneiss.			
Ludicovian	2000-1940			PR _l , Ludicovian volcanite complex: metagabbro, metadolerite.			
				PR _{pt} , Sortavala group, Pitkjaranta suite: biotite-amphibole and carbonate schists, marble, skarn, migmatite.			
			PR _{sn} , Sortavala group, Soanlakhti suite: biotite-amphibole schist, dolomite, marble.				
Jatulian			PR _{jt} , Onega group, Jangozero and Tulomozero suites: quartzite, quartzite-sandstone, dolomite, limestone, phyllite, toleitic basalt.				
Sariolian			PR _{sl} , Seletskaya suite: quartz conglomerate.				
Archaean-Palaeoproterozoic				AR-PR ₁ , undivided, dome formations: granite-gneiss, gneiss-granite, migmatite, amphibolite.			
Neoarchaeic	Neolopian	ca. 2600		Jalonvara granite complex: diorite, granodiorite, granite.			
	Palaeolopian	2995-2865		AR _{3jal} , Jalonvaara suite: andesite, dacite, rhyolite, siliceous and carbonate schist.			
Mezo-Neoarchaeic	Saamian-Palaeolopian			AR _{2,3} , tonalite, granodiorite, diorite.			
				AR _{2,3} , migmatite, migmatite-granite, plagiogranite.			

NB: 1) Sariolian conglomerate is not shown because of its very local occurrence; 2) geological formations under the V-PZ cover are not surely identified.

Figure 4 (continued). Legend to geological and prognostic maps of the Northern Ladoga, South-Eastern Ladoga and Western Ladoga areas.

-  Offshore outline of the Pasha-Ladoga basin.
-  Supposed outline of the Riphean sediments under the Vendian cover.
-  Limit of Palaeozoic cover.
-  Limit of Upper Vendian cover.
-  Supposed location of Oyat rapakivi granite intrusions under the Riphean sediments.
-  Supposed location of Palaeoproterozoic granite intrusions under the Riphean sediments.
-  Major faults.
-  Second-grade faults.
-  Janisjarvi impact structure.
-  Isohypse of the Riphean unconformity.






Uranium and thorium occurrences

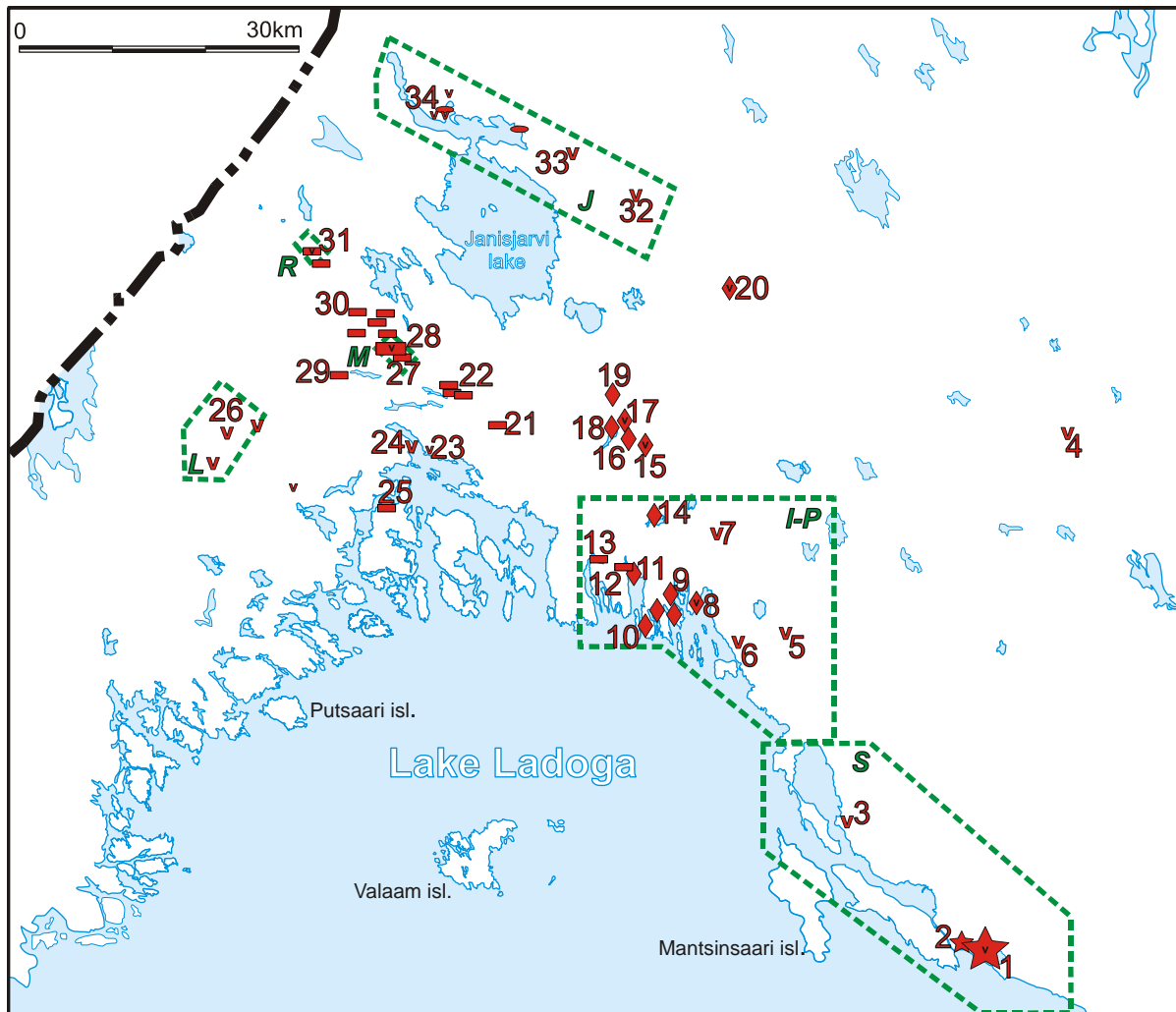
Grade of occurrence			Type of occurrence according to structural-lithological reference
deposit	ore-showing	anomaly	
			Related to Riphean unconformity
			Related to Upper Vendian sandstones
			Related to Lower Ordovician Dictyonema shale
			Related to anatectic granite
			Related to Ludicovian carbonate rocks
			Related to fracture zones (vein-type)
			Vein-type in occurrences of non-radioactive ores
			Vein-type mineralization in other type U occurrences
			Related to Jatulian quartzites
			Related to Lower Ordovician phosphorite
			Basement-hosted of uncertain nature

NB: 1) isohypse of the Riphean unconformity are not shown in the Northern Ladoga - see detailed map of the Salmi depression).
 2) for the Northern Ladoga area anomalies are not shown because of multiplicity.

Figure 4 (continued). Legend to geological and prognostic maps of the Northern Ladoga, South-Eastern Ladoga and Western Ladoga areas.

For the prognostic maps only:

-  Supposed outlines of areas where post-Riphean erosion level is less 200 m.
-  Zones of conductivity in the basement.
-  Areas promising for unconformity-type deposits:
P - Pitkjaranta; SI - Salmi; S - Svir-Oyat; O - Otradnensko-Vaskelovskaya;
i - Irinovskaya; N - Novoladogskaya.
-  Areas promising for sandstone-type deposits.
-  Areas promising for vein-type deposits.



Areas of detail consideration

L - Latvasurje, R - Ruskeala, J - Malpye Janisjarvi, M - Mramornaya Gora, I-P - Impilakhti-Pitkjaranta, S - Salmi.

1

U and Th occurrences mentioned in the text:

- 1 - Karku deposit; 2 - Matala ; 3 - Kotalakhti; 4 - Faddeyn-Kelya;
- 5 - Hopunvaara; 6 - Pitkjaranta; 7 - Kitelja; 8 - Korennoye; 9 - Mursula-Puttumyaki;
- 10 - Sjuskinsaari; 11 - Sumeria; 12 - Vostochno-Impilakhtinskoye;
- 13 - Centralno-Impilakhtinskoye; 14 - Vuorilampi; 15 - Maisunmyaki;
- 16 - Mustaoya; 17 - Sumukanmyaki; 18 - Kokkoya; 19 - Kokkoya Severnaya;
- 20 - Raskenjarvi; 21 - Harlu; 22 - Pitkajarvi; 23 - Kirjavalakhti; 24 - Varalakhti;
- 25 - Papinmyaki; 26 - Karinmyaki; 27 - Potkulampi; 28 - Maramornaya Gora;
- 29 Ruttu; 30 - Savinpuro; 31 - Ruskeala group; 32 - Jalonvara; 33 - Prolonvara;
- 34 - Kuhilaslampi area.

NB: for symbols for the occurrences see General Appendix 1 fig. 4.

GENERAL APPENDIX 2

TABLES

Table of radiogeochemical characteristics of the geological formations of the Ladoga region (after Mikhailov et al., 1999 and Bogachev, 1999).

Era	Selected geological formations (number in brackets is rate of U-enriched formation)	isotopic age, Ma	U, ppm			Rate of mobile U, %	Th, ppm	
			n	X	V, %			
Palaeozoic	D ₃	limstone, siltstone, sandstone		50	1.2	75		9
	O _{2kk+ld}	limestone, combustible shale		103	3.1	90		
	O _{1pk+lt}	clays, glauconitic sandstone, dictyonema shale (4 %), shell phosphorite		140	30	50		13
				15	13	35		16
				16	130	45		
			100	18	50			
C _{2sb-C_{3ld}}	sand, sandstone, clay, siltstone		143	2.1	27		12	
C _{1lm-ts}	sandstone		155	2.2	25		13	
Vendian	V _{2kt}	clays, sandstone		419	2.1	80		18
	V _{2rd}	mudstones, siltstones, carboniferous sandstones (5 %)		200	2.0	180		10
			80	5.2	120		9	
Riphean	R _{1-2vl}	trachydolerite	1450-1350	39	1	100	18	
	R _{1-2ph}	sandstone, mudstone (30 %)		136	3.6	45	10	14
				40	5.6	30		6
	R _{1-2sl}	sandstone, gritstone, tuffite		132	2.5	40		7
			20	4.0	30			
R _{1-2pr}	gritstone, conglomerate, apogranite weathering crust		322	3.5	65	58		
			34	4.2	60	20		
			48	3.8	55	16		

Table of radiogeochemical characteristics of the geological formations of the Ladoga region (continued).

Era	Selected geological formations (number in brackets is rate of U-enriched formation)	isotopic age, Ma	U, ppm			Rate of mobile U, %	Th, ppm
			<i>n</i>	<i>X</i>	<i>V</i> , %		
Lower Riphean	R ₁ gabbro-anorthosite-rapakivi granite (Wiborg Salmi, Ulalegi massifs): Li-F-bearing granite (5%), porphyraceous Bt-granite (20 %), ovoid granite (70 %), Qtz-monzonite, gabbro-norite	1538-1645	630	5.1	120	30	20
			55	7.6	120		28
			244	5.0	83	10	20
			91	3.6	37		20
			20	1.9	40	13	
			35	0.6	58	36	
Kalevian-Vepsian	PR _{1ev} gabbro-syenite-granite formation	1800-1785	80	2.1	45		22.3
Kalevian	PR _{1mt} leukogranite-granite formation	1800	114	9.5	102	40	4.6
	PR _{1kz,bd} granite formation	1870 - 1800	210	4.1	120	15	28
	PR _{1ms} granitoid, quartz-albite-microcline metasomatite	1880 - 1770	10 42	7 110	90 250		20
	PR _{1lv} plagiogranite-granodiorite formation	1880-1865	108	8	45		5
	PR _{1kl} gabbro-plagiogranite formation	1890-1880	59	1	60	25	5
	PR _{1nt,kn} mica schist, graphite- and sulphide-bearing schist (15 %)		309 45	2.6 4.8	80 40	50 40	11 7
	PR _{1vl,hn} sandstone - gritstones - dacite formation		194	2.4	80	12	9
Ludicovian	PR _{1pt} ampibol-carbonate schist, apatite-bearing dolomite marble (10 %)		700 79	2.1 8.0	290 80	22	8 7.7
	PR _{1snl} carboniferous carbonate schist, tuffite (20 %)		201	1.7	160	20	9
			60	1.3	120		11

Table of radiogeochemical characteristics of the geological formations of the Ladoga region (continued).

Era	Selected geological formations (number in brackets is rate of U-enriched formation)	isotopic age, Ma	U, ppm			Rate of mobile U, %	Th, ppm	
			<i>n</i>	<i>X</i>	<i>V</i> , %			
Jatulian	carboniferous dolomite (5 %)		142	1.4	70		2.5	
			50	2.3	130		3.0	
Lopian	granite, quartz-feldspar metasomatites (1%)	2600	312	4.8	77	35	30	
			12	12	40	10	60	
	migmatite-granite formation			550	2.1	110	18	6.8
	graphite/sulphide-bearing schists (1-3 %)	2900	146	1.1	50	4	6	
25			3.5	100	18	7		
migmatite-plagiogranite formation			355	1.3	90	10	3	
Saamian	micaceous and high-aluminous gneiss	3300	126	0.5	60		4.2	

Comment: *n* is amount of samples; *X* is average U content; *V* is variation coefficient.

General Appendix 2.2.

Table of U and Th contents in Svecofennian syn-, late- and post-orogenic intrusions of the Ladoga region, ppm (after Bogachev, 1999).

Complex	Intrusion	Type of intrusion	Rock	Th	U	
Lauvatsaari-Impiniemi	Impiniemi	massif	gabbro	2.9	1.2	
		-//-	bt diorite	3.71		
		-//-	granodiorite	4.3	1.4	
		-//-	qtz diorite	2.6	1.98	
		-//-	-//-	8.84	1.72	
Kuznechensky	Kuznechny	massif	granite	22.5	3.6	
		-//-	-//-	15	1.3	
		-//-	-//-	21	2.6	
		-//-	-//-	8	3.5	
		-//-	-//-	15	4.9	
		-//-	-//-	5	1.4	
	Lazurny	massif	granodiorite	19	2.1	
			-//-	-//-	25	1.4
			-//-	-//-	19	1.4
			-//-	-//-	20	0.6
			-//-	-//-	15	1.2
			-//-	-//-	20	1.7
			-//-	granite	14	1.2
			-//-	-//-	9.0	1
			-//-	-//-	10	1.2
			-//-	-//-	21	1.6
			-//-	-//-	23	1.2
			-//-	-//-	16	3.2
			-//-	-//-	16	1
			-//-	-//-	17.2	1.5
			-//-	-//-	16	1
			-//-	-//-	16	3
			-//-	-//-	30	2
			-//-	-//-	13	1.4
			-//-	-//-	13	1.2
			-//-	-//-	9.0	1.1
			-//-	-//-	13	0.6
-//-	-//-	11	1.5			
Borodinsky	Borodino	massif	granite	108	0.8	
		-//-	-//-	41	1.8	
		-//-	-//-	39	1.7	
		-//-	-//-	40	3	
		-//-	-//-	43	2	
		-//-	-//-	34	2.6	
		-//-	-//-	42	2.9	
		-//-	-//-	43	2.6	
		-//-	-//-	27	1.7	
		-//-	-//-	27.5	3.4	
		-//-	-//-	47.4	3.9	
		-//-	-//-	141	1.7	
		-//-	-//-	93		
		-//-	-//-	64	2.6	
-//-	-//-	12	1.8			

Table of U and Th contents in Svecofennian syn-, late- and post-orogenic intrusions of the Ladoga region, ppm (continued).

Complex	Intrusion	Type of intrusion	Rock	Th	U
Borodinsky	Zavetny	massif	granodiorite	31	3.5
		-//-	granite	52	2
		-//-	-//-	60	3.2
		-//-	-//-	24	1.4
		-//-	-//-	44	2.6
		-//-	-//-	57.4	2.8
		-//-	-//-	61	4.1
		-//-	-//-	43	1.7
		-//-	-//-	9	1.5
		-//-	-//-	18	1.4
	Gory	massif	granite	123	4.7
Tervussky	Tervus	massif	granite	12	3
		-//-	-//-	11	2
		-//-	-//-	12	3
		-//-	-//-	7	2.5
		-//-	-//-	18	3.2
		-//-	-//-	25	2.2
		-//-	-//-	12	4
		-//-	-//-	15	1.8
		-//-	-//-	11	2.2
		-//-	-//-	18	3
		-//-	-//-	17	3.8
		-//-	-//-	24	2.2
		-//-	-//-	18	3.9
		-//-	-//-	11	3.2
		-//-	-//-	18	3.6
		-//-	-//-	22	4.3
		-//-	-//-	20	2.3
		-//-	-//-	24	3
		-//-	-//-	13	4
		-//-	-//-	21	2.1
-//-	-//-	24	2.6		
Putsaarsky	Putsaari	massif	gabbro	13.1	5.54
		-//-	-//-	5.3	1.2
		-//-	-//-	1.89	0.78
		-//-	-//-	2	1
		-//-	-//-	2.4	1
		-//-	-//-	3.2	0.7
		-//-	-//-		0.96
		-//-	diorite	4.16	1.12
		-//-	-//-	1.6	1.1
		-//-	-//-	6	1
		-//-	-//-	2.1	0.78
		-//-	-//-	3.94	2.5
		-//-	-//-	5.1	1.3
		-//-	-//-	3	1
		-//-	-//-	4	1
-//-	qtz diorite	5.1	1.5		

Table of U and Th contents in Svecofennian syn-, late- and post-orogenic intrusions of the Ladoga region, ppm (continued).

Complex	Intrusion	Type of intrusion	Rock	Th	U	
Putsaarsky	Putsaari	massif	qtz diorite	1.5	2.2	
		-//-	-//-	1.5	0.7	
		-//-	-//-	8	1	
		-//-	-//-	4	1	
		-//-	-//-	2	1.7	
		-//-	granodiorite	10	3	
		-//-	granite	9.44	2.13	
		-//-	-//-	4.2	0.6	
		-//-	-//-	5	1	
		-//-	-//-	7	0.92	
		-//-	-//-	3	1.2	
		-//-	-//-	1.7	1.3	
		-//-	-//-	11	1	
		-//-	-//-	9	1.5	
		-//-	-//-	10	1	
		-//-	-//-	4.31	0.99	
		-//-	-//-	3	0.71	
-//-	-//-	3	0.6			
Matkaselsky	Jakkima	massif	ab leucogranite	4	1.7	
		-//-	-//-	5	2.5	
		-//-	-//-	3	2.3	
		-//-	leucoplagioaplite	3	1	
		-//-	-//-	2	1.1	
		pegmatite dyke	mcl leucogranite	5	2.6	
		-//-	-//-	5	3.5	
		-//-	-//-	21	4	
		-//-	-//-	5	2.3	
		-//-	ab leucogranite	2	1.5	
		-//-	-//-	1	6	
		-//-	-//-	3	3.5	
		-//-	leucoplagioaplite	5	5	
		-//-	-//-	1	3.5	
		-//-	pegmatite	5	4.1	
		-//-	-//-	3	2	
		-//-	-//-	3	6.6	
		-//-	-//-	1	4.4	
		-//-	-//-	1	5.5	
		-//-	-//-	2	3	
	Matkaselka	massif	mcl leucogranite	1	4.4	
			-//-	-//-	1	6.6
			-//-	-//-	0.5	2.6
			-//-	-//-	8	4.6
			-//-	ab leucogranite	1	10
			-//-	-//-	1	7.6
			-//-	-//-	2	18
			-//-	-//-	1	22
			-//-	-//-	4	40
-//-	-//-	1	10			

Table of U and Th contents in Svecofennian syn-, late- and post-orogenic intrusions of the Ladoga region, ppm (continued).

Complex	Intrusion	Type of intrusion	Rock	Th	U
Matkaselsky	Matkaselka	massif	ab leucogranite	2	4
		-//-	-//-	1	7.5
		-//-	-//-	4	16
		-//-	-//-	2	2.4
		-//-	-//-	1	2.6
		-//-	leucoplagioaplite	2	13
		-//-	-//-	1	28
		-//-	-//-	1	20
		-//-	-//-	1	1.8
		-//-	-//-	1	1.1
		-//-	-//-	1	8.6
		-//-	-//-	1	24
		-//-	-//-	1	32
		-//-	-//-	1	19
		-//-	pegmatite	1	1
		-//-	-//-	1	1.5
		-//-	-//-	6	1.2
		-//	-//	6	18
		-//-	-//-	6	14
		-//-	-//-	3	3
	-//-	-//-	2	6	
	-//-	-//-	4	6.5	
	-//-	-//-	4	8.5	
	Kurenlampi	massif	ab leucogranite	1	5
		-//-	-//-	2	3.1
		-//	-//	3	2.3
		-//-	-//-	2	65
		-//-	-//-	2	4
		-//-	-//-	1	4.7
		-//-	-//-	3	6.1
		-//-	-//-	3	14
		-//-	leucoplagioaplite	1	3.4
		pegmatite dyke	mcl leucogranite	1	3.3
		-//-	-//-	1	3.5
		-//-	ab leucogranite	3	7.5
		-//-	qtz-mus segregation	4	36.5
		-//-	-//-	3	2.7
	Pirtipohja pegmatite swarm	pegmatite dyke	leucoplagioaplite	8	16
		-//-	-//-	2	5.6
		-//	-//	1	9.5
		-//-	-//-	1	8.3
		-//-	-//-	1	3.5
		-//-	-//-	1	12
		-//-	-//-	1	8.5
		-//-	-//-	1	6.9
		-//-	ab leucogranite	1	14
	-//-	-//-	4	7.4	

Table of U and Th contents in Svecofennian syn-, late- and post-orogenic intrusions of the Ladoga region, ppm (continued).

Complex	Intrusion	Type of intrusion	Rock	Th	U
Matkaselsky	Pirtipohja pegmatite swarm	pegmatite dyke	ab leucogranite	1	2.7
		-//-	-//-	1	18
		-//-	-//-	2	3.4
		-//-	-//-	2	2.7
		-//-	-//-	2	2.3
		-//-	-//-	1	16
		-//-	pegmatite	3	7
		-//-	qtz-mus segregation	1	2.2
		-//-	-//-	3	30
		-//-	-//-	1	1.3
		-//-	-//-	4	6.4
		-//-	-//-	3	22
		-//-	-//-	1	11.5
		-//-	-//-	1	23
		-//-	-//-	1	2.7
		-//-	-//-	2	6.1
	Pitkjarantsky complex	pegmatite dyke	leucogranite	7	9.5
		-//-	-//-	16	9
		-//-	-//-	4	18
		-//-	-//-	19	19
		-//-	-//-	18	27
		-//-	-//-	24	17
		-//-	-//-	6	7
		-//-	-//-	6	8
		-//-	-//-	24	26
		-//-	-//-	13	16
		-//-	-//-	15	15
		-//-	-//-	26	6
		-//-	-//-	12	12
		-//-	-//-	16	16
		-//-	-//-	7	3.6
		-//-	-//-	4	2.4
		-//-	-//-	15	2.5
		-//-	-//-	14	4.3
	Latvasursky complex	pegmatite dyke	bt leucogranite	24	10
		-//-	mcl pegmatite	6	5
-//-		leucoplagiogranite	10	13.4	
Elisenvaarsko-Vuoksinsky	Vuoksa	massif	gabbroid	53	8.2
		-//-	-//-	16	2.6
		-//-	-//-	16	3.5
		-//-	-//-	20	
		-//-	-//-	9	1.5
		-//-	-//-	13	
		-//-	-//-	9	2.2
		-//-	-//-	15	
		-//-	-//-	35	6.3
-//-	diorite	8	1.8		

Table of U and Th contents in Svecofennian syn-, late- and post-orogenic intrusions of the Ladoga region, ppm (continued).

Complex	Intrusion	Type of intrusion	Rock	Th	U	
Elisenvaarsko-Vuoksinsky	Vuoksa	massif	monzonite	54	4	
		-//-	-//-	36		
		-//-	monzodiorite	6	1.2	
		-//-	-//-	8		
		-//-	-//-	16		
		-//-	-//-	23		
		-//-	-//-	9		
		-//-	-//-	26	1.4	
		-//-	-//-	20	1.2	
		-//-	-//-	18	1	
		-//-	-//-	12		
		-//-	qtz monzonite	28	1.8	
		-//-	-//-	34	3.6	
		-//-	-//-	42	1.4	
		-//-	-//-	36		
		Elisenvaara	massif	nevoit		30
	ladogalite				11	4
	-//-				11	2
	leucosyenite				12	2
	dyke			lamprophyr	23	8
	Oja-Jarvi	massif	gabbro		25	
			-//-	monzonite	32.5	7.5
			-//-	qtz monzodiorite-qtz monzonite	15	1.4
			-//-	-//-	45	0.8
			-//-	-//-	21	0.5
			-//-	-//-	29	1.1
			-//-	-//-	16	1.1
			-//-	-//-	15	0.6
			-//-	-//-	16	0.5
			-//-	-//-	14	1.4
			-//-	-//-	16	1
			-//-	-//-	15	0.9
			-//-	-//-	22	2.6
			-//-	-//-	17	1.7
			-//-	-//-	14	1.7
			-//-	-//-	13.5	2.6
			-//-	-//-	18	1.4
			-//-	-//-	24	1.5
			-//-	-//-	25	1.5
			-//-	-//-	21	1
			-//-	granodiorite	20	1
			-//-	-//-	31	0.9
-//-			-//-	22	0.6	
-//-	granite	67	4.6			

General Appendix 2.3.

Tables of chemical composition of uranium and thorium bearing mineral phases (wt. %).
Analyzed with ABT-55 Akashi electron microprobe, St-Petersburg (Polekhovsky et al., 2007).

Table 1. The Sjuskinsaari group of anomalies. Pegmatoid-hosted mineralization (Th was not analyzed).

No	Code	SiO ₂	Al ₂ O ₃	Fe ₂ O ₃	MnO	MgO	CaO	UO ₂	PbO	Y ₂ O ₃	BaO	Sum
URANINITE												
1	Sju-1-1	0.3					0.5	73.3	23.1	2.2		99.4
2	2	0.3		0.1		0.2	0.2	75.2	21.6	1.6		99.2
3	3	0.4	0.3	0.1			1.0	74.8	20.4	1.4		98.4
4	4	0.2	0.5	0.1			0.8	75.0	22.0	1.6		100.2
5	5	0.2	0.3	0.2		0.1	0.2	74.7	18.9	4.4		99.0
6	6	0.9	0.3	0.4			0.9	78.2	17.5	1.6		99.8
7	7	0.7	0.5	0.1	0.2	0.2	0.4	76.6	17.8	1.6	1.1	99.2
8	8	0.3	0.6	0.3		0.1	1.4	73.7	20.8	2.3	0.4	99.9
PITCHBLENDE												
9	Sju-1-9	2.5	0.4	0.1		0.3	3.3	60.7	7.4	1.1	0.2	76.0
10	10	2.2	0.6	0.4		0.3	3.5	65.2	9.1	1.5		82.8

Table 2. The Korennoye ore-showing. Migmatite-hosted mineralization.

No	Code	SiO ₂	TiO ₂	Al ₂ O ₃	Fe ₂ O ₃	MnO	MgO	CaO	UO ₂	PbO	Y ₂ O ₃	Ce ₂ O ₃	V ₂ O ₅	Sum
PITCHBLENDE - 1														
1	Ko-2-1	0.6		0.4			0.5	3.6	74.1	20.3	0.2			99.7
2	2	0.5		0.2			0.2	2.5	72.6	21.9	0.7	0.2		98.8
3	3	0.4		0.4				2.8	73.7	20.4	0.2	0.1		98.0
PITCHBLENDE - 2 (vein-type)														
4	Ko-1-1	3.8		1.0	4.0	1.2	0.3	3.8	79.3	5.9				99.3
5	2	4.1		1.0	3.9	1.3	0.3	3.7	79.3	7.1				100.7
6	3	4.0		1.2	4.0	1.2	0.4	3.8	79.9	5.5				100.0
7	10	5.5		0.8	2.0	1.4	0.2	2.6	81.1	3.1		2.1		98.8
8	11	5.3		0.9	1.7	1.3	0.5	2.4	81.8	3.9		2.0		99.8
9	12	5.1		0.5	2.1	1.3	0.1	2.4	82.5	3.9		2.2		100.1
10	13	5.5		0.7	2.0	1.1		2.5	82.5	3.2		2.6		100.1
11	14	4.9		0.9	2.0	1.3	0.3	2.2	80.5	5.0		2.3		99.4
PITCHBLENDE - 3 (vein-type)														
12	Ko-1-7	4.4		1.1	2.6	1.1	0.3	3.9	78.6	4.2		2.6		98.8
13	8	4.1		0.7	2.9	1.2	0.3	3.7	79.1	4.8	0.1	2.9		99.8
14	9	3.9		1.0	3.0	1.1	0.5	3.6	79.7	4.5		3.0		100.3
COFFINITE (vein-type)														
15	Ko-1-4	4.9		1.3	3.7	0.9	0.3	3.5	64.6	6.8				86.0
16	5	11.0	0.9	1.9	13.3	0.2	0.2	3.3	60.2	6.0	0.1	2.7	0.1	99.9
17	15	12.7	0.5	1.7	3.8	0.1	0.3	2.8	71.1	2.5		3.1	0.2	98.8
HEMATITE (vein-type)														
18	Ko-1-6	7.2		3.0	84.9	0.3	0.7	0.5	1.8	0.5	0.2		0.3	99.4

Table 3. The Hirsimyaki ore-showing. Migmatite-hosted pitchblende.

No	Code	SiO ₂	MgO	CaO	UO ₂	PbO	Y ₂ O ₃	Sum
1	Hm-1-8	0.4	0.4	0.3	74.7	23.1	1.9	100.8
2	9	0.4	0.1	0.3	74.2	21.8	1.6	98.4
3	10	0.1	0.2	0.3	75.5	22.5	1.2	99.8
4	12	0.3	0.3	0.3	76.0	23.6	1.4	101.9
5	13	0.4	0.2	0.2	74.3	22.0	1.5	98.6
6	14	0.4		0.7	74.1	21.5	1.3	98.0

Table 4. The Puttummyaki ore-showing. Migmatite-hosted mineralization.

No	Code	SiO ₂	TiO ₂	Al ₂ O ₃	Fe ₂ O ₃	MnO	MgO	CaO	UO ₂	PbO	CuO	ThO ₂	Y ₂ O ₃	ZrO ₂	HfO ₂	V ₂ O ₅	P ₂ O ₅	Sum
PITCHBLENDE - 1																		
1	Pt-1-1	0.3	0.2	0.3				1.2	73.8	22.2			2.0					100.0
2	2	0.2		0.3				1.5	73.8	21.7			1.9					99.4
3	3	0.3		0.4				1.4	73.9	21.2			2.2					99.4
4	6	0.4	0.1	0.2	0.1			1.9	74.8	19.5			2.2					99.2
5	Pt-2a-23				1.1				76.6	21.4	0.9							100.0
6	30				1.5		0.1		80.7	16.8	0.1							99.2
7	31				0.7		0.2	1.7	79.4	17.7								99.7
8	34				1.6		0.2	0.8	77.5	19.5	0.2							99.8
9	Pt-H6-1	0.5			0.3				75.7	21.3			2.8					100.6
10	2	0.2			0.1				76.0	21.0		0.4	2.1					99.8
11	13	0.7			0.3				75.8	20.1			2.3					99.2
12	17	0.6			0.3				81.1	16.1			2.3					100.4
COFFINITE																		
13	Pt-1-5	3.8		0.2	0.3			0.9	68.6	25.2			1.7					100.7
14	Pt-H6-14	15.9			2.6				61.6	2.3			4.7					87.1
15	16	16.8			2.2				59.5	2.9			4.3					85.7

Table 5. The Sumeria ore-showing. Migmatite-hosted mineralization.

No	Code	SiO ₂	Al ₂ O ₃	Fe ₂ O ₃	MgO	CaO	UO ₂	PbO	Y ₂ O ₃	Ce ₂ O ₃	P ₂ O ₅	Sum
PITCHBLENDE												
1	Su-3-1	1.3	0.6	0.1	0.1	1.0	74.8	19.4	2.2			99.5
2	3	0.1			0.3	1.0	75.9	20.5	2.3			100.1
3	4	0.3	0.2		0.1	0.9	77.1	19.7	2.5			100.8
4	7	0.5	0.6			1.6	73.2	21.2	1.8	0.8		99.7
5	8	0.3	0.3	0.1	0.2	1.1	75.3	19.3	2.3	0.7		99.6
6	9	0.3	0.3	0.2	0.1	2.4	79.7	13.7	2.6	0.7		100.0
7	15	3.0	0.5	0.1	0.1	1.3	69.4	23.8	2.1	0.9	0.3	101.5
COFFINITE												
8	Su-3-2	23.7	4.3	0.2	0.2	3.1	62.0	3.1	1.1			97.5
9	10	29.5	7.3	0.3	0.4	1.5	55.8	0.9	3.3	0.3	0.7	100.0
10	11	25.7	4.3		0.3	0.9	58.5	7.0	2.4		1.0	100.1

Table 6. The Pribrejny anomaly hosted by granitoid of the Kuhilaslampi area.

No	Code	SiO ₂	TiO ₂	Al ₂ O ₃	Fe ₂ O ₃	MnO	MgO	CaO	PbO	CuO	ThO ₂	Y ₂ O ₃	ZrO ₂	HfO ₂	BaO	Ce ₂ O ₃	La ₂ O ₃	Sum	
THORITE																			
1	Jn-1-5	17.5		1.1	3.4	2.0	0.3	1.7			42.6	1.3	8.3						78.2
2	6	18.6		1.6	3.4	2.8	0.8	1.4			41.5	1.1	8.0						79.2
3	7	21.2		4.2	2.6	1.7	2.7	2.9			30.8	1.3	8.0			2.5			77.9
4	8	19.1		2.5	1.0	1.0	0.9	2.9			35.9	1.9	9.4			2.1			76.7
5	12	16.5		1.1	4.1	2.8	0.3	1.7			48.5	2.7	1.3			2.9			81.9
6	15	20.6		1.3	0.2	7.2	0.3	2.2			30.9	1.4	11.2		0.2	1.3			76.8
7	23	16.9		0.9	0.7		0.1	2.0			55.7	2.6	1.7			6.5			87.1
ZIRCON																			
13	Jn-1-19	28.9		1.0	4.7	0.2	0.4	2.4			0.1	2.6	40.1	2.2		0.1			82.7
14	20	29.1		1.3	2.7	0.3	0.4	2.6				2.3	40.1	1.8		0.1			80.7
15	21	25.1	0.1	2.6	1.0	2.9	0.6	2.8			9.6	4.1	24.3	0.7	1.0	2.7			77.5
RUTILE																			
16	Jn-1-24		97.9		0.1	0.2	0.2	0.1			0.1			0.3		1.8			100.7
17	Jn-2-2a-1	0.3	99.1		0.3														99.7
ILMENITE																			
19	Jn-1-25	6.1	42.1	0.9	30.1	0.6	0.3	0.5			0.2	0.1	0.1			0.4			81.4
HOLLANDITE																			
23	Jn-1-3	1.0		1.3	0.6	66.4	0.4	0.4							6.7				76.8
24	4	1.1		1.0	0.5	62.2	0.3	0.4						10.7					76.2
25	13	6.9		4.8	27.4	29.9	2.9	0.4			0.2			4.0					76.5
26	17	25.4		9.9	1.0	43.7	0.5	0.6			0.2	0.2	0.1	10.9					92.5
27	18	7.2		4.2	3.6	51.8	1.6	0.3			0.4		0.1	13.9					83.1
28	22	1.2		0.9	0.5	59.3	0.5	0.5			0.4		0.1	16.1	0.1				79.6
HYDROHEMATITE																			
34	Jn-1-11	4.7	0.2	4.5	43.5	11.6	2.2	0.3				0.2	0.5			0.2			67.9
35	14	4.0		1.1	63.0	6.1	0.3	0.4							0.3				75.2
36	16	8.2		5.2	46.1	3.6	2.0	0.3			0.3				0.3				66.0
37	26	8.4	0.5	3.5	56.1	1.0	1.8	0.3											71.6

Table 7. Th-U anomalies hosted by the Jatulian quartzites of the Kuhilaslampi area.

No	Code	SiO ₂	TiO ₂	Al ₂ O ₃	Fe ₂ O ₃	MgO	CaO	UO ₂	ThO ₂	Nb ₂ O ₅	ZrO ₂	HfO ₂	Ce ₂ O ₃	La ₂ O ₃	V ₂ O ₅	P ₂ O ₅	Sum
MONAZITE																	
1	Jn-3-1-1	1.2			37.0		4.6	0.3	21.4				4.1	0.3		15.2	84.1
2	4	0.7			11.8		5.7	0.8	20.7				13.9	2.2		25.5	81.3
3	6	6.7			21.8		6.5	0.1	21.6				7.3	0.8		19.3	84.1
4	9	5.2		1.3	25.2	0.5	1.7		43.3				0.8	0.2		4.7	82.9
ZIRCON																	
5	Jn-3-1-2	33.7									65.5	2.4					101.6
6	3	13.5			2.0			0.8	24.9		38.9	2.4					82.5
RUTILE																	
7	Jn-3-1-7	1.8	91.0		1.6					2.1					1.2		97.7
8	8	14.0	33.6	0.4	26.9	0.1	0.4		14.9	0.1					0.4		90.8
HYDROHEMATITE																	
9	Jn-3-1-5	4.1			70.9				0.1				0.1				75.2

Table 8. The Mramornaya Gora ore-showing. Uranium mineralization hosted by Ludicovian carbonate rocks.

No	Code	SiO ₂	TiO ₂	Al ₂ O ₃	Fe ₂ O ₃	MnO	MgO	CaO	Cr ₂ O ₃	UO ₂	PbO	Y ₂ O ₃	ZrO ₂	BaO	SO ₃	Ce ₂ O ₃	P ₂ O ₅	Sum	
PITCHBLENDE - 1																			
1	MG-1-4-7	0.1			0.3		0.1			74.1	20.5	3.2							98.3
2	14	5.6			0.7		0.1	0.4		75.0	16.7								98.5
3	MG-4-1-3	1.5			0.5		0.5	3.4		70.8	20.6								97.3
4	9						0.1			76.8	22.1								99.0
PITCHBLENDE - 2																			
5	MG-5b-10	1.3	0.8	0.5	0.4			0.8	0.1	87.8	3.7		1.0		0.3				96.7
6	12	1.1	0.2	0.2	0.3			1.4		85.7	6.5		0.5		1.0				96.9
7	14	3.6	0.9	0.5	0.7			1.4		81.4	0.6							1.9	91.0
8	15	3.0	1.6	0.6	0.8			0.8		80.9	5.2				4.6			0.5	98.0
9	MG-6-5	1.4			0.2	0.2		2.7		84.6	5.0								94.1
10	5a	1.2			0.1			2.6		84.5	6.0								94.4
11	6	1.2			0.2	0.1		3.0		86.5	3.7								94.7
12	7	0.8			0.1			3.5		83.4	5.0								92.8
13	8	0.7			0.2	0.3		3.3		84.2	5.7								94.4
14	9	0.8				0.2		3.9		86.8	5.0								96.7
15	10	0.4			0.3	0.2		3.0		85.9	6.3								96.1
16	11	1.4			0.1			2.8		86.7	4.5								95.5
17	12	0.9			0.4			4.1		87.1	5.3								97.8
18	13	0.7			0.1			4.0		88.0	4.9								97.7
19	14	0.6						4.0		87.7	4.2								96.5
20	15	1.1			0.1	0.1		4.3		87.0	5.8								98.4
21	16	0.6				0.1		3.7		86.9	5.0								96.3
22	17	0.8			0.2	0.1		3.5		87.8	5.1								97.5
23	18	0.7				0.1		3.4		87.5	5.7								97.4
24	19	0.5				0.1		3.1		88.0	7.0								98.7
25	20	0.9			0.1	0.1		3.9		87.9	5.6								98.5
26	21	0.7			0.3	0.2		3.3		86.0	6.0								96.5
27	22	1.0			0.2	0.1		3.4		85.8	6.6								97.1
28	23	0.5			0.2	0.2		2.7		88.1	5.7								97.4
COFFINITE																			
29	MG-5b-20	14.0		2.1	0.4			1.0		72.9	3.7								94.1
TITANIUM-URANIUM PHASE																			
30	MG-5b-11	1.8	37.3	1.6	0.6			0.9		48.1			0.7	3.1	0.1			0.2	94.4
31	16	0.8	37.0	0.6	1.6			2.5	0.2	45.5	1.0			1.8				0.9	91.9
32	17	1.0	36.7	0.2	2.0			2.3		48.7	1.9			1.7				0.4	94.9
ZIRCON																			
33	MG-5b-9	25.2	0.6	2.2	4.9			1.7	0.2	0.8			28.7	5.3	8.8			1.1	79.5

Table 9. The Centralno-Impilakhtinskoye ore-showing. Pitchblende mineralization hosted by Ludicovian carbonate rocks.

No	Code	SiO ₂	TiO ₂	Al ₂ O ₃	Fe ₂ O ₃	MnO	MgO	CaO	Na ₂ O	K ₂ O	UO ₂	PbO	BaO	P ₂ O ₅	Sum
PITCHBLLENDE															
1	CI-1-1	3.9			1.9						74.2	19.9			99.9
2	2	4.3			1.7						74.9	19.0			99.9
3	10	2.2			1.0						76.8	19.7			99.7
4	11	3.6			2.5						74.6	19.3			100.0

Table 10. The Varalakhti ore-showing. Vein-type uranium mineralization.

No	Code	SiO ₂	TiO ₂	Al ₂ O ₃	Fe ₂ O ₃	MnO	MgO	CaO	Cr ₂ O ₃	UO ₂	PbO	CuO	Y ₂ O ₃	V ₂ O ₅	Sum
PITCHBLLENDE															
1	Va-1-1-5	0.5		0.4	0.8			4.6		77.4	16.2				99.9
2	6	0.4		0.2	0.7			4.3		76.0	18.3				99.9
3	12	0.6		0.4	0.7		0.1	4.5		76.3	17.2				99.8
4	20	0.1		0.3	0.5	0.1	0.2	3.0		77.2	18.2			0.4	100.0
5	Va-1-2-1	0.9			0.4	0.1		3.7		76.4	16.6		0.5	0.5	99.1
6	2	0.7			0.4	0.1		3.8		76.2	17.2		0.5	0.5	99.4
7	3	0.8			0.4	0.1		3.6		75.3	18.6		0.7	0.8	100.3
8	4	1.7	1.3		0.8	0.3		4.4		75.0	15.6		0.4	0.2	99.7
9	5	1.2	1.1		0.8			5.0		75.7	15.1		0.5	0.4	99.8
10	6	1.2	0.7		0.8	0.2		5.3		76.6	14.5		0.5	0.4	100.2
11	11	0.6	0.1	0.2	0.6	0.1	0.2	3.3	0.1	74.8	17.5		0.5	0.8	98.8
12	12	1.0	0.5	0.3	0.7	0.1		5.0	0.2	75.5	15.6		0.6	0.2	99.7
13	13	0.8		0.4	0.4		0.4	3.7	0.1	75.8	16.3		0.5	0.7	99.1
14	Va-1-5-20	1.2		0.5	0.3	0.1		3.5		75.8	17.2	0.4	0.8	0.3	100.1
COFFINITE															
15	Va-1-5-10	16.5			2.8		1.4	2.8		64.2	10.7	1.6			100.0
16	11	11.1			6.0		3.3	5.1		48.8	19.2	1.7	4.7	0.3	100.2
17	21	13.4		0.2	1.8	0.2	0.4	1.5		62.4	17.4	1.4	1.2		99.9
18	22	19.0		0.2	1.2	0.1	0.5	2.0		66.0	8.9	0.7	1.5		100.1

Table 11. The Karinmyaki ore-showing. Vein-type uranium mineralization.

No	Code	SiO ₂	Fe ₂ O ₃	MnO	CaO	UO ₂	PbO	Nd ₂ O ₃	SO ₃	SeO ₂	Ce ₂ O ₃	P ₂ O ₅	Sum
URANINITE													
1	La-1-1-1	9.0	0.3	1.7		81.3	5.0						97.3
2	2	8.6	0.2	1.7		83.0	5.5						99.0
3	7	8.5	0.4	1.7		80.1	5.6				0.5		96.8
4	9	8.5	0.2	0.8		80.4	5.7	1.5			1.4		98.5
5	22	8.9	0.4	1.8		82.0	4.6	1.0			0.9		99.6
PITCHBLENDE													
6	La-1-1-20	8.8	0.1	1.0		79.9	6.2	1.0			1.0		98.0
7	26	9.9	0.2	1.4		78.7	8.1						98.3
8	Ka-1-2-1	8.0	0.4	1.6	3.6	77.2	7.3						98.1
COFFINITE													
9	La-1-1-5	11.9		0.7		67.7	9.2	3.0	2.7	0.3	3.0		98.5
10	6	18.7	0.6			53.5	15.0	3.0	4.0	0.1	3.7		98.6
11	8	23.5	0.9	0.1		49.2	13.3		3.4		0.5		90.9
12	10	17.8				60.7	2.7	2.8	1.2		2.9		88.1
13	11	19.3	0.5	0.1		62.1	4.6	2.0	1.3		2.1		92.0
14	12	16.1	0.1			66.4	6.3	2.0	1.8		2.1		94.8
15	13	19.5	0.4			58.0	2.8	2.5	0.4	0.2	2.6		86.4
16	14	18.7	0.2	0.1		62.4	7.1	2.0	2.7		2.2		95.4
17	15	21.9	0.7			54.2	1.5	2.0	0.7		3.2		84.2
18	21	14.6	0.3	0.3		67.7	5.3		1.9	0.4	2.3		92.8
19	23	23.2	0.7			56.4	4.4	2.0	1.3	0.2	2.9		91.1
20	24	18.1	0.2	0.2		59.2	13.3	2.0	3.9	0.1	2.3		99.3
21	27	12.8	0.3	0.3		69.2	7.5	2.0	2.8	0.5	1.9		97.3
HYDROPITCHBLENDE													
22	Ka-1-2-2	2.8		0.2	1.6	66.1	17.7						88.4
23	2	2.9			1.4	66.1	13.4						83.8
CASOLITE													
24	Ka-1-2-4	10.5	0.2	0.1		48.3	38.2						97.3
25	5	8.3	0.2	0.3	0.7	59.0	26.5						95.0
26	6	9.5	0.1	0.1		45.9	35.6						91.2
27	7	6.7		0.2	0.1	58.1	28.0						93.1
28	8	11.6	0.1		5.3	58.5	12.5						88.0

Table 12. The Dyke anomaly. Vein-type thorite mineralization.

No	Code	SiO ₂	UO ₂	ThO ₂	Sum
1	Jn-8-1-5	23.5		76.5	100.0
2	6	25.4	1.0	73.5	99.9
3	7	22.7	2.1	75.2	100.0
4	9	23.7	0.7	75.6	100.0

Table 13. The Jalonvara complex ore deposit. Vein-type uranium mineralization.

No	Code	SiO ₂	TiO ₂	Al ₂ O ₃	Fe ₂ O ₃	MnO	MgO	UO ₂	PbO	ZrO ₂	SO ₃	Sum
ADMIXTURE No 1												
1	Jl-2-4	17.7		10.4	19.0	0.4	5.9	28.5	2.8			84.7
2	5	9.0	0.3	4.1	11.6	0.2	1.7	36.0	2.5			65.4
3	6	7.9		3.7	11.1	0.2	2.2	45.0	4.0			74.1
ADMIXTURE No 2												
4	Jl-1-5-2	11.8		3.0	23.9		0.3	22.7	0.9	13.3	8.0	83.9
5	3	10.6		3.2	29.4		0.4	18.0	0.4	11.4	9.0	82.4
6	4	7.2		4.9	35.5		0.5	11.4	0.7	6.2	7.7	74.1

Table 14. The Hopunvaara complex ore deposit. Vein-type ferrithorite.

No	Code	SiO ₂	Fe ₂ O ₃	ThO ₂	Y ₂ O ₃	P ₂ O ₅	Sum
1	BV-1-1-4	13.3	14.9	44.9	5.6	2.0	81.3
2	5	15.1	8.7	50.8	6.9	2.2	84.7

Table 15. The Karku area. Syn-sedimentary ferrithorite.

No	Code	SiO ₂	FeO	ThO ₂	Ce ₂ O ₃	P ₂ O ₅	Sum
1	838/264,4-1	12.7	27.9	38.9	2.2	2.5	84.2
2	838/264,4-2	14.1	27.1	38.2	4.0	4.5	89.1

Tables of chemical composition of uranium mineral phases (wt. %).

Analyzed with Cameca SX-100, Nancy.

Table 1. The Sjuskinsaari group of anomalies. Pegmatoid-hosted uraninite mineralization. Sample Sju-1.

No	SiO ₂	SO ₂	CaO	V ₂ O ₃	MnO	FeO	Y ₂ O ₃	Nd ₂ O ₃	Dy ₂ O ₃	PbO	UO ₂	ThO ₂	MgO	Total
1	0.037	0	1.195	0.094	0.08	0	1.524	0.129	0.331	17.79	66.285	5.081	0.02	92.565
2	0.036	0.06	0.783	0	0.007	0.054	2.084	0.257	0.535	18.447	64.818	5.35	0.023	92.454
3	0.054	0.158	1.051	0	0.018	0	1.46	0.291	0.399	19.415	68.086	4.659	0.035	95.627
4	0.064	0.015	0.351	0	0	0	1.953	0.183	0.447	19.556	65.612	5.678	0.01	93.869
5	0	0.001	0.829	0	0	0.016	2.422	0.286	0.616	19.473	64.976	5.204	0.019	93.843

Table 2. The Hirsimyaki ore-showing. Migmatite-hosted pitchblende mineralization. Sample Hm-1.

No	Al ₂ O ₃	SiO ₂	P ₂ O ₅	SO ₂	CaO	V ₂ O ₃	FeO	Y ₂ O ₃	Nd ₂ O ₃	Dy ₂ O ₃	PbO	UO ₂	ThO ₂	MgO	Total
1	0.002	0.002	0.034	0	0.562	0.04	0.091	1.239	0.244	0.335	17.467	62.95	0.01	0.03	83.005
2	0.049	0.032	0	0.065	0.671	0	0	1.282	0.219	0.499	19.049	72.076	0.064	0	94.007
3	0	0.113	0.051	0.076	0.942	0	0	1.531	0.251	0.531	18.441	70.532	0	0.003	92.472
4	0	0	0	0.025	0.491	0	0	1.55	0.775	0.491	19.276	69.958	0	0	92.564
5	0	0.018	0	0	0.38	0	0	1.407	0.372	0.505	20.492	70.299	0.111	0.02	93.605
6	0	0	0	0	0.565	0	0	1.451	0.24	0.607	19.457	70.861	0	0.008	93.188

Table 3. The Sumeria ore-showing. Migmatite-hosted pitchblende mineralization. Sample Su-3.

No	SiO ₂	P ₂ O ₅	SO ₂	CaO	V ₂ O ₃	MnO	FeO	Y ₂ O ₃	Nd ₂ O ₃	Dy ₂ O ₃	PbO	UO ₂	ThO ₂	MgO	Total
1	0	0.045	0.072	1.013	0	0	0.01	2.384	0.878	0.792	15.075	69.11	0	0	89.38
2	0.066	0	0.055	1.106	0.014	0	0.046	2.443	1.009	0.9	17.203	70.971	0.066	0.029	93.907
3	0	0.002	0.032	1.9	0.034	0.151	0.151	2.599	0.852	0.979	11.938	71.788	0	0.002	90.429
4	0	0	0.105	1.135	0	0	0	2.136	0.792	0.7	17.099	71.202	0	0.033	93.202
5	0	0	0	1.331	0	0	0	2.148	0.79	0.832	17.361	69.772	0.084	0.019	92.336
6	0.117	0	0	1.195	0.054	0	0.112	2.462	0.702	0.854	16.477	69.905	0	0	91.878

Table 4. The Mramornaya Gora ore-showing. Different types of pitchblende mineralization hosted by Ludicovian carbonate rocks. Session 1.

No	Sample	Mineral	Al ₂ O ₃	SiO ₂	SO ₂	CaO	V ₂ O ₃	FeO	Y ₂ O ₃	PbO	UO ₂	TiO ₂	MoO	NiO	CuO	AsO	BaO	Total
1	MG-1	Pbl-1	0	0.114	0.198	0.236	0.176	0.098	3.784	19.558	68.317	0.019	0	0.007	0.108	0	0	92.614
2	MG-5	Pbl-2	0	1.352	0.049	0.918	0.187	0.309	0.006	2.953	88.418	0.803	0	0.017	0.062	0.071	0	95.145
3	MG-5	Pbl-2	0.044	0.816	0.45	0.878	0.041	0.232	0.41	3.539	84.856	4.277	0.197	0	0.069	0.221	0	96.03
4	MG-5	Pbl-2	0	0.993	0.506	0.762	0.081	0.32	0	2.826	86.692	1.972	0.252	0	0	0.107	0	94.509
5	MG-5	Pbl-2	0.003	1.559	1.166	0.777	0	0.46	0	3.634	83.153	2.601	0.65	0.066	0.045	0.199	0	94.312
6	MG-5	Pbl-2	0	1.849	2.156	0.759	0	0.609	0	3.324	82.271	2.639	1.452	0	0	0.193	0	95.253
7	MG-5	Pbl-2	0.141	2.629	2.248	0.76	0.09	0.438	0.765	4.603	79.593	3.113	1.044	0	0.106	0.25	0	95.781
8	MG-5	Ti-U phase	0	0.893	0.148	2.172	0.107	1.146	0.448	1.118	48.489	34.116	0	0	0.003	0.048	1.851	90.539
9	MG-5	Ti-U phase	0	1.14	0.266	1.905	0.041	1.081	0	1.403	45.391	34.906	0.006	0	0.078	0.104	2.203	88.522

Table 5. The Mramornaya Gora ore-showing. Different types of pitchblende mineralization hosted by Ludicovian carbonate rocks. Session 2.

Sample MG-6.

No	Mineral	Al ₂ O ₃	SiO ₂	P ₂ O ₅	SO ₂	CaO	V ₂ O ₃	MnO	FeO	ZrO ₂	Nd ₂ O ₃	Dy ₂ O ₃	PbO	UO ₂	ThO ₂	MgO	Total
1	Pbl-2(?)*	0.283	0.866	0.108	3.049	2.651	0	0.128	0.291	0.946	0	0.117	19.003	68.776	0	0.016	96.235
2	Pbl-2	0	0.362	0.338	0.042	2.892	0.103	0.057	0.148	1.079	0	0.067	4.872	86.631	0	0.038	96.629
3	Pbl-2	0	0.21	0.2	0.581	2.793	0.119	0.15	0.024	1.466	0.029	0.027	6.426	84.768	0	0.023	96.815
4	Pbl-2	0.007	0.176	0.289	0.111	2.563	0	0	0.116	1.878	0	0.069	5.32	84.482	0.087	0.046	95.145
5	Pbl-2	0.055	0.309	0.31	0.055	3.193	0.085	0.139	0.093	1.006	0	0	4.551	85.763	0	0.038	95.596
6	Pbl-2	0.178	0.842	0.094	0.314	3.706	0	0	0.088	0.863	0	0.129	4.287	85.991	0	0.082	96.574
7	Pbl-2	0.022	0.476	0.345	0	3.361	0.084	0.022	0	1.003	0.008	0.029	4.637	86.503	0.049	0.031	96.57
8	Pbl-2	0.016	0.217	0.313	0.028	2.395	0.026	0	0	1.892	0	0.007	5.147	86.164	0	0.032	96.236
9	Pbl-2	0	0.608	0.244	0.007	3.549	0.042	0.072	0	1.158	0	0.039	3.695	86.962	0	0.022	96.397
10	Pbl-2	2.518	5.119	0.208	0.294	2.443	0	0.016	0.259	1.82	0	0.02	3.883	81.174	0	0.148	97.901
11	Pbl-2 (6)	0.031	0.457	0.261	0.131	3.27	0.063	0.073	0	1.326	0	0.029	4.089	87.505	0	0.053	97.289
12	Pbl-2 (6)	0.068	0.381	0.336	0.038	3.742	0	0.032	0	0.908	0	0.058	4.406	87.757	0	0.044	97.77
13	Pbl-2 (6)	0	0.53	0.291	0	3.403	0.028	0.021	0.063	1.326	0	0	4.141	86.419	0	0.004	96.228
14	Pbl-2 (6)	0.069	0.408	0.311	0.065	2.97	0.03	0	0	1.105	0.003	0.14	4.811	85.27	0.071	0.048	95.302
15	Pbl-2 (6)	0	0.516	0.417	0.072	3.371	0.105	0.035	0.136	0.656	0	0.017	4.817	86.633	0	0.032	96.805
16	Pbl-2 (6)	0.072	0.611	0.306	0	3.524	0	0.088	0.101	1.014	0	0	4.391	87.124	0	0.055	97.286

* Pbl-2(?) – a mineral phase optically similar to other Pbl-2, but relatively rich in PbO.

Table 6. The Varalakhti ore-showing. Vein-type pitchblende mineralization. Sample Va-1.

No	Al ₂ O ₃	SiO ₂	P ₂ O ₅	SO ₂	UO ₂	TiO ₂	FeO	Y ₂ O ₃	CaO	PbO	MoO	V ₂ O ₃	NiO	CuO	AsO	Cr ₂ O ₃	Total
1	0.008	0.308	0.36	0.12	72.97	0.069	0.276	1.054	3.2	17.893	0.102	0.606	0	0.239	0.127	0.076	97.41
2	0.02	0.575	2.544	0.002	72.516	0.279	0.679	0.553	4.009	16.886	0.024	0.447	0.063	0.159	0.012	0.192	98.96
3	0.019	0.366	0.398	0.04	72.967	0.118	0.331	0.648	3.404	16.448	0	0.696	0.03	0.071	0.082	0.063	95.68
4	0.082	0.854	0.09	0.041	73.103	0.407	0.742	0.709	4.443	14.693	0.024	0.503	0.129	0	0.028	0.159	96.01
5	0.008	0.219	0.46	0.548	70.846	0.253	0.471	0.381	2.777	17.048	0	0.613	0.01	0.809	0.127	0.111	94.68

Table of chemical composition of pitchblendes from the Karku deposit (wt. %).

Analyzed with ABT-55 Akashi electron microprobe, St-Petersburg (Polekhovsky et al., 2005).

No	DDH	SiO ₂	TiO ₂	A ₂ O ₃	FeO	MnO	MgO	CaO	K ₂ O	Cr ₂ O ₃	UO ₂	PbO	ThO ₂	Y ₂ O ₃	BaO	SrO	SO ₃	Sum
PITCH BLENDE - 1																		
1	625	-	-	-	-	1.83	-	-	-	-	82.51	11.1	-	-	-	-	1.1	87.15
2	-/-	-	-	-	-	1.51	-	-	-	-	79.39	15.07	-	-	-	-	2.75	98.72
3	-/-	3.2	-	0.4	0.3	-	-	2.2	-	-	82.7	5.3	2.1	-	-	-	-	96.2
4	627	5.4	0.3	0.7	0.4	-	-	1.2	-	-	80.6	5.3	2.5	-	-	-	-	96.4
5	-/-	5.8	0.6	1.1	0.5	0.4	1.1	1.2	-	-	77.1	4.8	2.2	-	-	-	-	94.8
6	-/-	5.3	0.2	0.5	-	0.8	-	1.1	-	-	82.3	3.8	2.2	-	-	-	-	96.2
7	-/-	5.5	0.2	0.6	0.3	0.9	-	1.1	-	-	78.5	4.5	3.9	-	-	-	-	95.5
8	-/-	4.4	-	0.6	0.3	0.7	-	4.4	-	-	77.4	6.6	2.8	-	-	-	-	97.2
9	-/-	3.6	-	0.5	0.4	0.7	-	1.7	-	-	78.9	7.4	3.7	-	-	-	-	96.9
10	-/-	4.8	0.2	0.3	0.4	0.4	0.2	1.3	-	-	77.5	5.8	4.6	-	-	-	-	95.5
11	-/-	4.3	0.5	0.4	0.4	0.8	0.3	1.5	-	-	79.6	5.9	3.0	-	-	-	-	96.7
12	-/-	12.2	-	0.8	0.3	0.4	0.3	1.5	-	-	76.0	2.1	1.6	-	-	-	-	95.2
13	-/-	7.4	0.3	0.5	0.5	0.5	-	1.5	-	-	77.2	3.8	4.1	-	-	-	-	95.8
14	-/-	9.1	-	0.6	0.3	0.4	-	1.7	-	-	77.1	3.1	3.6	-	-	-	-	95.9
15	-/-	5.0	0.2	0.5	0.4	0.8	-	1.8	-	-	81.1	1.4	3.4	-	-	-	-	94.6
16	-/-	5.0	-	0.4	0.3	0.5	-	1.3	-	-	80.9	6.8	2.2	-	-	-	-	97.4
17	-/-	4.1	0.2	0.3	0.4	0.8	-	1.6	-	-	78.7	6.2	4.1	-	-	-	-	96.4
18	-/-	2.0	0.2	0.2	0.3	0.7	0.2	1.8	-	-	80.3	6.8	3.2	-	-	-	-	95.7
19	-/-	5.3	0.2	0.6	1.1	0.8	0.7	1.5	-	-	78.8	4.2	4.1	-	-	-	-	97.3
20	-/-	4.9	0.2	0.5	0.5	0.9	-	1.4	-	-	78.6	4.2	5.0	-	-	-	-	96.2
21	-/-	4.8	-	0.5	0.4	0.8	-	1.4	-	-	78.7	5.5	3.5	-	-	-	-	95.6
22	-/-	4.0	0.2	0.5	0.5	0.7	-	2.2	-	-	79.5	6.3	3.8	-	-	-	-	97.7

Table of chemical composition of pitchblendes from the Karku deposit (wt. %).

No	DDH	SiO ₂	TiO ₂	Al ₂ O ₃	FeO	MnO	MgO	CaO	K ₂ O	Cr ₂ O ₃	UO ₂	PbO	ThO ₂	Y ₂ O ₃	BaO	SrO	SO ₃	Sum
PITCH BLENDE - 1																		
23	627	4.2	0.2	0.4	0.3	0.7	-	1.5	-	-	77.7	5.7	5.4	-	-	-	-	96.1
24	-/-	4.6	-	0.4	-	0.8	-	1.4	-	-	79.1	5.6	4.0	-	-	-	-	95.9
25	-/-	4.2	-	0.5	-	0.7	-	1.3	-	-	79.6	5.3	3.9	-	-	-	-	95.5
26	-/-	8.3	0.2	0.6	0.4	-	0.2	1.1	-	-	77.7	4.2	3.1	-	-	-	-	95.8
27	656	1.6	-	-	0.5	0.6	-	3.8	-	-	84.2	7.6	0.4	-	-	-	-	98.7
28	-/-	1.6	-	-	0.5	0.8	-	3.4	-	-	84.0	7.5	0.1	-	-	-	-	97.9
29	-/-	1.8	-	-	0.5	0.8	-	3.1	-	-	86.4	6.8	-	-	-	-	-	99.4
30	-/-	3.4	1.9	0.5	0.4	0.5	-	2.1	0.5	-	77.9	9.4	-	0.4	-	0.5	-	97.5
31	671	6.2	0.3	0.7	0.9	0.3	0.5	2.1	-	0.1	82.7	1.5	-	-	-	-	-	95.3
PITCH BLENDE - 2																		
32	625	7.88	-	-	-	1.9	-	-	-	-	80.72	6.38	-	-	-	-	1.06	97.93
33	-/-	8.94	-	-	-	1.75	-	-	-	-	82.92	6.22	-	-	-	-	1.56	101.38
34	-/-	8.66	-	-	-	1.6	-	-	-	-	80.42	10.05	-	-	-	-	1.75	102.48
35	-/-	9.12	-	-	-	1.38	-	-	-	-	82.24	6.38	-	-	-	-	0.93	100.04
36	-/-	4.3	-	0.4	0.2	-	-	1.6	-	-	74.6	13.0	-	-	-	-	-	94.1
37	-/-	6.9	-	0.3	0.5	-	0.3	1.5	-	-	75.3	7.9	1.7	-	-	-	-	94.4
38	627	6.0	-	0.5	0.6	-	-	1.5	-	-	75.0	8.9	2.3	-	-	-	-	94.8
39	-/-	6.5	-	0.7	2.2	-	0.5	1.4	-	-	75.9	4.5	2.5	-	-	-	-	94.2
40	-/-	10.2	-	1.3	2.4	-	1.5	1.6	-	-	66.6	9.5	1.9	-	-	-	-	95.0
41	656	12.3	3.6	1.6	0.2	-	-	1.9	0.2	-	75.7	0.7	0.3	-	-	-	-	96.5
42	-/-	12.8	3.1	1.6	0.2	-	-	1.9	0.2	-	72.8	0.7	0.3	1.5	1.1	0.9	-	97.1
43	-/-	11.8	0.2	1.3	-	-	-	0.4	0.1	-	68.3	8.6	-	3.9	0.9	0.8	-	96.3
44	-/-	12.0	5.9	1.0	0.1	-	-	1.1	0.2	-	63.8	9.3	0.2	1.6	1.3	0.6	-	97.1
45	-/-	10.0	7.2	1.2	0.1	0.1	-	1.6	-	-	68.0	6.0	0.7	0.8	0.5	1.0	-	97.2

Table of chemical composition of pitchblende from the Karku deposit and the Kotalakhti ore-showing (wt. %).

Analyzed with Cameca SX-100, Nancy.

No	Occurrence	DDH	Al ₂ O ₃	SiO ₂	P ₂ O ₅	SO ₂	TiO ₂	CaO	FeO	YO ₂	PbO	ThO ₂	UO ₂	Total
PITCH BLENDE - 1														
1	Karku	625	0	2.661	0	0.559	0	4.555	0.492	0	9.631	0	77.73	96.046
2		625	0	2.88	0	0.927	0	4.12	0.331	0	12.926	0	76.252	97.648
3		625	0	2.914	0	0.579	0	4.427	0.491	0	10.156	0	76.279	95.042
4		625	0	2.411	0	0.229	0	5.386	0.486	0	9.517	0	74.728	93.099
5		625	0	3.404	0	1.281	0	3.75	0.407	0	10.268	0	75.47	94.914
6		625	0	1.89	0	0.314	0	5.431	0.461	0	16.529	0	68.263	93.213
PITCH BLENDE - 3														
7	Kotalakhti	1001	0.389	5.101	0	0	0	2.604	2.084	0	4.097	0	79.492	94.291
COFFINITE														
8	Karku	674	0.944	14.513	0.282	0.103	1.985	0.108		4.004	0.777	0	65.207	88.02
9		674	1.007	17.476	0.776	0.132	2.3	0.11	0.323	6.586	0	0	58.289	87.28
10		674	0.887	18.212	1.588	0	1.801	0	0.364	9.65	0	0	54.178	86.958
11		674	1.038	17.598	1.423	0	2.548	0	0.791	9.503	0.787	0.451	55.079	89.309

Tables of chondrite-normalized REE and Y content in the uranium oxides.

Table 1. The Sjuskinsaari group of anomalies. Pegmatoid-hosted uraninite mineralization. Sample Sju-1.

No	La	Ce	Pr	Nd	Sm	Eu	Tb	Dy	Ho	Er	Tm	Lu	Y
1	2377.55	3468.57	8865.49	8588.99	11936.47	3167.29	19601.99	19423.28	24130.05	21619.15	25817.19	7174.24	35419.84
2	3236.03	5757.33	13407.76	11864.13	15573.61	5127.80	25147.89	24287.00	30015.43	24909.92	33819.84	10743.23	55431.13

Table 2. The Korennoye ore-showing. Late vein-type pitchblende from the anatectite-hosted occurrence. Sample Ko-1. Gd and Yb contents are calculated as an arithmetic mean value of Eu and Tb, Tm and Lu (interpretation of Bonhoure, 2007).

No	La	Ce	Pr	Nd	Sm	Eu	Gd	Tb	Dy	Ho	Er	Tm	Yb	Lu
1	494158.78	72926.76	12540.74	12512.72	-3340.05	770.77	2188.19	3605.62	257.10	267.37	309.17	295.91	160.31	24.71
2	323228.02	56231.43	12147.74	6728.99	246.27	413.37	918.35	1423.33	133.10	104.59	133.83	131.26	68.73	6.21
3	228363.45	41938.56	7531.54	4304.77	346.81	257.28	833.61	1409.94	102.70	79.01	113.51	104.99	55.39	5.78
4	228562.52	41404.07	7288.67	4172.61	321.57	257.17	792.97	1328.76	92.03	79.33	109.99	95.22	50.71	6.21
5	192763.55	36106.96	8458.33	4388.23	390.64	298.37	785.52	1272.66	111.55	85.04	144.25	109.49	57.91	6.32

Table 3. The Mramornaya Gora ore-showing. Late vein-type pitchblende hosted by Ludicovian carbonate rocks. Sample MG-6.

No	La	Ce	Pr	Nd	Sm	Eu	Tb	Dy	Ho	Er	Tm	Lu	Y
1	1132.54	184.88	231.70	161.21	330.26	566.43	454.63	458.06	655.42	537.26	677.06	184.52	3266.03
2	314.60	105.69	171.81	173.84	540.05	676.08	706.54	786.79	987.87	778.22	967.13	252.53	2557.39